QUATERNARY GEOLOGY AND STRATIGRAPHY OF NORTH WESTLAND, SOUTH ISLAND, NEW ZEALAND

A thesis submitted in partial fulfilment of the requirements for the

Degree of

Doctor of Philosophy
in Geology

in the University of Canterbury

by

Robert V. Rose

October 2011

CONTENTS

LIST OF FIGURES

Chapter 1

Chapter 3

Chapter 4

Chapter 5

Chapter 6

Chapter 7

Chapter 8

LIST OF TABLES

Chapter 1

Chapter 3

Chapter 4

Chapter 5

Chapter 6

Chapter 7

Chapter 8

Appendix Four

LIST OF MAPS (ON DVD)

ABSTRACT

Infrared stimulated luminescence ages are presented from the North Westland region, West Coast, South Island, New Zealand. These ages span much of the last interglacial-glacial cycle from 123.3 ± 12.7 ka to 33.6 ± 3.6 ka. Coverage is extended to c. 14 ka via cosmogenic isotope dating.

A new Quaternary stratigraphy and Marine Isotope Stage correlation is proposed for the on-shore glacial-interglacial fluvioglacial, fluvial and marine terrace sequence. The new model incorporates previously published luminescence and radiocarbon ages. It necessitates reinterpretation of the evolution of the climate in North Westland for the period from 123 ka to 14 ka. Reinterpretation of fossil pollen and plant macrofossil records implies a period of probable near-interglacial climate in North Westland during the early to middle portion of Marine Isotope Stage 3. It also implies the presence in North Westland of raised marine terraces dating from this Isotope Stage.

In addition it is concluded that during the period from c.60 ka to c.50 ka podocarp dominated forest was widespread in the lowland portion of Westland. Between Okarito and Westport *Dacrydium cupressinum* and *Nestegis* were ubiquitous components of this forest. This finding aligns the Marine Isotope Stage 3 climate of North Westland nicely with that of other parts of New Zealand where good records exist for this period.

Acknowledgements

This thesis has only been possible due to the forbearance/tolerance of my partner Karen Hamilton and my children Jordan and Oliver who put up with my frequent absence from regular family activities over a long period.

My supervisors Professors Steve Weaver and Jamie Shulmeister have been exceedingly patient particularly in terms of the duration of this project, which has been conducted on a part-time basis. Professor Shulmeister has dedicated considerable time to directing the research down fruitful lines of inquiry.

The luminescence dating project undertaken as a core part of the research was funded by the Mason Trust and this assistance is gratefully acknowledged. The luminescence samples were dated by Dr Uwe Rieser of the Victoria University of Wellington. This assistance was vital to the outcome of the project. The cosmogenic isotope dating project was carried out in conjunction with Dr Tim Barrows.

The PhD project was initiated shortly after the commencement of another related project that was undertaken for the West Coast Commercial Gold Miners Association. This prior project set the basic scene for my subsequent research. It was funded by the West Coast Commercial Gold Miners Association, Technology New Zealand, the Grey District Council, the Buller District Council and the Westland District Council.

The PhD project has benefited from discussions with West Coast based geologists John Wood and Anthony Jury. It has also been assisted by discussions and field excursions with Dr R.P. Suggate.

A number of land owners gave consent to access to their private land. In this respect special thanks is given to Mr Fred Phelps of Hokitika for access to his opencast goldmine.

CHAPTER ONE: INTRODUCTION

1.1 SCOPE AND OBJECTIVES

This project was initiated as a study of the evolution of Quaternary alluvial gold deposits in North Westland. During the early phase of this project it was found that a paucity of reliable numerical ages meant it was not possible to verify the existing model of the deposition of Late Quaternary deposits in this region. So the scope of the project was altered to encompass a programme of dating by infrared stimulated luminescence (IRSL). This leads into a detailed analysis of the depositional history of Quaternary fluvial, glacial, and marine strandline deposits, of the soil profiles on these surfaces and of changes in climate and vegetation. These issues appeared to present a more significant and fundamental problem than the description of gold deposit evolution that the project initially sought to address.

The existing model of glacial/interglacial climate history for North Westland is based in large part of the work of Dr RP Suggate. This model contains a variety of assumptions that are based on a rather limited body of numerical ages. The primary matter addressed in this dissertation is the age of the Quaternary deposits of North Westland. Previously these fluvial, glacial, lacustrine and marginal marine deposits have proved too old to be dated reliably using the radiocarbon method. So they have been dated primarily by correlation with eustatic sea level events and global climate events. The reference sea level curve has been that derived from the raised terrace sequence from the Huon Peninsula of Papua New Guinea. Local climate and sea level events have been correlated with the glacial-interglacial pattern revealed by the standard marine oxygen isotope curves (e.g. Imbrie et al 1984; Martinson et al 1987, Chappell & Shackleton 1986).

In the existing stratigraphic framework for North Westland glacial and interglacial events in North Westland are correlated with those in and the Northern Hemisphere, but the assumption that these events are more or less synchronous has never been proven. It could be true for some major global climate events but there is increasingly evidence that at other times climate events in the middle to high latitudes of the Northern and Southern Hemispheres have not always been synchronous. In fact some of the interstadial events may have been asynchronous, as proposed in relation to Greenland and Antarctica by Ahn & Brook (2008). Similar asynchronous behaviour has been proposed in relation to events in South Westland by Sutherland et al (2007). The possibility that this could also be so in North Westland is investigated in this dissertation.

The core purpose of this dissertation is an examination of the assumptions underling the existing Quaternary stratigraphic model for North Westland. It is not so much that there is any particular individual problem that needs to be fixed but rather that the entire model rests on a raft of unproven assumptions that have not previously been examined in detail. In examining the stratigraphic framework for North Westland the writer seeks to link the timing of glacial advance and retreat with changes in regional climate. This activity requires examination of local sedimentology, geomorphology, and the relevant numerical dating carried out within the region. It has also involved new numerical dating using the infrared stimulated luminescence method on subsurface materials and the cosmogenic isotope method on surficial materials.

Chapters three to five summarise a variety of data that has a bearing on the interpretation of the timing of events in North Westland. Chapter 6 describes the stratigraphic relationships in detail. Chapter 7 examines the altitudes of the various raised marine terraces and discusses implications for the tectonic

uplift rate in North Westland. This chapter also summarises an alternative model of the climatic, vegetational and glacial history of North Westland.

1.2 GENERAL SETTING

1.2.1 Location of the Study Area

This has not been a mapping project and as such so there are no clearly defined boundaries to the land area covered by this thesis. As a generalisation fieldwork that has contributed directly to the text of the thesis has been carried within the West Coast region, mainly north of Ross, south of Punakaiki and west of the Alpine Fault. This area is outlined in figure 1.1 below. Broadly speaking the study area comprises the northern portion of Westland District, and the Grey District and can be referred to as North Westland.

A number of maps were prepared during the thesis project. These are included as appendices to the thesis. Selected areas were chosen for detailed geomorphological evaluation relating to support for the project by the West Coast Commercial Gold Miners Association Incorporated. Except in relation to a small number of specific matters these maps are not described or discussed in detail in the main text of the thesis.

1.2.2 Physiography

The West Coast is a long narrow region that includes steep mountain ranges, dissected foothills, glaciated and terraced river valleys, raised marine terraces, a narrow coastal plain, and the continental shelf under the Tasman Sea. The eastern boundary of the region is defined by the main divide of the Southern Alps. On land its western boundary is defined by the eastern shore of the Tasman Sea. The topographic relief is considerable, varying from sea level at the coast to around 2620 metres at Mt Evans in the Whitcombe Valley.

A large proportion of the region has been glaciated in the recent geological past. The most extensive source areas for glacial ice are the Southern Alps between the main divide and the Alpine Fault, the Paparoa Range, the Victoria Range and the Hohonu Range. There are still numerous small glaciers situated on the high peaks in the vicinity of the main divide. These areas of permanent ice are mostly situated to the South of the Taramakau Valley.

In times of full glaciation the ice advanced onto the lowlands and coalesced to form Piedmont glaciers. Lowland landforms that provide evidence for this include terminal and lateral moraines, erratic boulders, meltwater channels, terraces composed of glacial outwash, glacial lake beds, kame terraces, and moraine dammed lakes.

1.2.3 Plate Tectonics and Continental Collision

The landforms that have evolved in Westland reflect a dynamic geological environment that includes rapidly uplifting mountain ranges, active faulting and folding (figure 1), and an active boundary between the Australian and Pacific tectonic plates.

Detailed descriptions of the pre-Quaternary history of the region can be found elsewhere (e.g. Nathan et al 1986, Kamp, 1986). There are a number of long-lived structural features within the region that

have been inherited from orogenic events during Cretaceous and early to middle Tertiary times. Some of these are still active so modern patterns of faulting and folding at least in part reflect an inheritance from older times. The region has been subject to at least three periods of continental scale rifting / crustal extension. These events formed large, deep sedimentary basins bounded by normal faults.

More recently a transformation from a generally extensional to a collisional environment has seen a reversal in the sense of movement on some of the older structures such that some northerly striking normal faults have become reverse faults. Some areas that were formerly deep basins have become mountain ranges. In the Paparoa Ranges this has involved as much as 4 kilometres of uplift, mainly in Plio-Pleistocene times. Other areas that were formerly structural highs are now within regional scale depressions, for instance much of the Grey Valley depression.

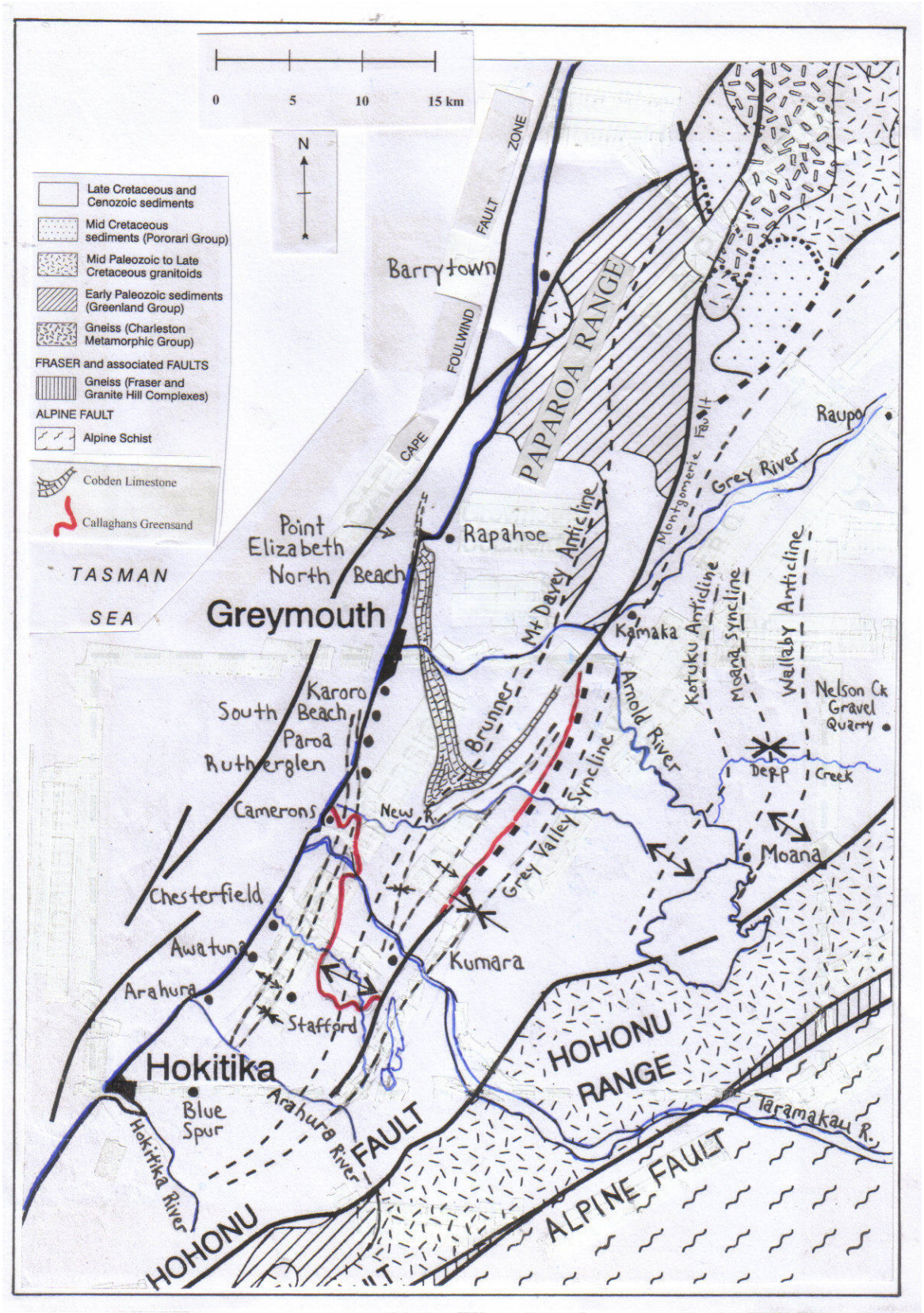

Figure 1.1 General location map for the study area.

1.2.3a First Order

The primary tectonic feature within the West Coast region is the Alpine Fault, named by Wellman & Willet (1942). This is the single largest active fault within the New Zealand section of the modern Australian-Pacific Plate Boundary. Carter & Norris (1976) proposed that a strike-slip or transtensional plate boundary regime was operative in the South Island from the Oligocene period onward. The plate boundary is a broad zone running the length of the South Island. Much of the displacement within the Plate Boundary has occurred at the Alpine Fault. In addition a significant proportion of the modern deformation is distributed/partitioned across the Southern Alps (Norris & Cooper 2001). The Alpine Fault divides of the North Westland into two areas underlain by basement rock of contrasting character. It also separates the region into contrasting physiographic zones being the Southern Alps (to the east) and the West Coast lowlands and foothills (to the west). In this region the Alpine Fault has been active as a right-lateral transcurrent feature since Miocene times. Investigation of the provenance of conglomerates in sedimentary basins adjacent to the Alpine Fault (e.g. Cutten 1979) indicates that substantial transcurrent displacement commenced at this fault no earlier than 18 million years ago (Rose 1996).

Prior to the dominantly transcurrent relative motion at the plate boundary (prior to the inception of the Alpine fault) North Westland was located close to the axis of a right-lateral transtensional plate boundary known as the Challenger rift system (Kamp, 1986). The axis of this Mid-Tertiary system passed through the region on a North-South trend. During its evolution 10's of kilometres of horizontal extension are likely to have been accommodated normal to the rift axis. Much of the extension has since been reversed as a result of the increasingly collisional nature of the modern plate boundary. Analysis of the plate tectonic context of the South Island by Cox & Sutherland (2007) indicates that plate boundary evolved gradually from almost purely extensional, to transtensional to transcurrent. In the South Island prior to about 18 ma the transcurrent component may have been accommodated within the Challenger Rift Zone rather than at the (yet to be initiated) Alpine Fault. In this context it is notable that Randall et al (2011) demonstrated commencement of block rotation between the various "Marlborough Faults" at the southern end of the Hikurangi margin at ~ 20 Ma, which may date the commencement of subduction of oceanic crust adjacent to Marlborough at the northern end of the Alpine Fault.

Continental collision within the modern plate boundary zone produces a combination of horizontal and vertical movement. Sibson et al (1981) demonstrated that the SW-NE striking Alpine Fault dips to the southeast under the Southern Alps. Modern displacement at the fault is right lateral reverse slip with relative uplift on the eastern side. Tippett & Kamp (1993) have demonstrated that adjacent to North Westland, for at least 5 to 6 million years, rock on the Southern Alps (SE) side of the fault has been uplifted continuously. This is a result of west-southwest oriented reverse motion at an oblique angle across the fault plane.

Uplift of basement rock between the Alpine Fault and the Main Divide of the Southern Alps amounts to at least 15 kilometres over the last 5-6 million years. In some places uplift could be as great as 16 to 20 kilometres (figure 2, Garver & Kamp 2002). This is balanced by a similar amount of surface erosion. The Southern Alps represent the difference between total uplift and total erosion. As illustrated by Wellman (1979) the uplift rate is greatest in the Mt Cook area where it is probably around 10-12 millimetres per year (~ one kilometre per 100,000 years).

The modern rate of horizontal displacement varies along the length of the Alpine Fault. For the area between Milford Sound and Hokitika Norris & Cooper (1995) estimated the slip rate to be 27±5

millimetres per year. At Inchbonnie in North Westland the modern right-lateral slip rate at the Alpine Fault has been estimated to be 13.6±1.8 by Randall et al (2009). Here lateral displacement is accompanied by reverse slip and uplift of 2.9 ± 0.4, and 3.4 ± 0.6 mm/yr respectively. The displacement rate across the plate boundary zone as a whole is around 35 to 40 mm/yr. Commencing no later than 18 million years ago there has been at least 420 kilometres (Cutten 1979) of right lateral displacement at the Alpine Fault. Additional lateral displacement has occurred within the plate boundary zone as well as substantial contraction normal to the plate boundary.

The primary influences of the Plate Boundary Zone on Quaternary geology include:

- Its role over several million years in the uplift and exposure of basement rocks. This includes the Alpine Schist in the Southern Alps and the Greenland Group and various granitoid rocks west of the Alpine Fault). Uplift has provided sources for coarse clastic sediment that has been deposited in West Coast sedimentary basins. The clastic sediment is relatively resistant to weathering and is capable of being recycled within fluvial systems.

- Its indirect effect on Regional climate by uplifting the Southern Alps. This mountain belt is a continental-scale barrier to weather systems. It intercepts the moist westerly airflow, causing orographic precipitation which is concentrated to the west of the main divide of the mountain belt. Flow in all the major rivers west of the main divide is to the Tasman Sea.

- During glacial periods the Southern Alps provide a regional scale source for glacial ice, an efficient means of liberating clastic material and heavy minerals from the bedrock. The ice provides a conveyor like transport system for the delivery of clastic material to the lowlands. During interglacial periods these mountains provide source catchments for heavy mineral transporting rivers in the West Coast region.

- Its role in governing large scale aspects of the underlying structure and geomorphology of the region, for instance the positions of the Paparoa Range, the Brunner-Mt Davy Anticline and the Grey-Inangahua Depression.

- Its role (west of the Alpine Fault) in the uplift (and subsequent recycling) of relatively young clastic deposits. This has caused repeated re-concentration of the heavy minerals within Quaternary alluvial materials.

1.2.3b Second Order

Although the bulk of the plate tectonic displacement occurs at and near the Alpine and Hope Faults a lesser proportion is distributed on other structures including the Hohonu Fault, the Grey Valley syncline and the Paparoa Anticline. The proportion of plate boundary deformation occurring within the West Coast lowlands and in offshore areas is small relative to that in the Southern Alps. Nevertheless this deformation plays a critical role in the evolution of the landscape to the west of the Alpine Fault.

1.2.3c Horizontal Displacement West of the Alpine Fault

At this stage it is not clear precisely how much of the relative plate motion is distributed as horizontal displacement to the West of the Alpine Fault. To date the rate of strain accumulation has been

assumed to be relatively small. Geophysical studies, including analysis of the distortion of survey networks, have suggested that stress accumulation contributing to right lateral plate boundary movement is relatively low to the west of the Alpine Fault. This does not mean that stain accumulation is low, but rather, as demonstrated by Pearson et al (1995), that the rate of right-lateral shear is low compared to the area east of the Alpine Fault. In the Westland lowlands crustal shortening is occurring normal to the Alpine Fault. The mechanisms have not been examined in detail to date but may include strain accumulating on deep-seated low angle faults (e.g. blind thrusts), faults that are situated offshore, or regional-scale folds with axes normal to the direction of shortening.

West of the Alpine Fault few northeast striking faults have been demonstrated to have had relatively recent right lateral movement. Some northerly striking faults in the Inangahua to Murchison area have a reverse and/or left lateral style of displacement. This includes the White Creek Fault (Berryman 1980). It may be the case that strain is partitioned to a certain extent, the Alpine Fault marking a modern westward limit to predominantly right lateral displacement, while west of the Alpine Fault faulting, folding and rotation in Tertiary and Quaternary deposits is a response to the nature of the compressional stress system and the orientation of deep seated structures in the older basement rocks.

1.2.3d Uplift and Folding

West of the Alpine Fault in North Westland part of the relative plate motion is being taken up in shortening and crustal thickening. The entire on-land area within North Westland is subject to tectonic uplift. In a compressional environment long term uplift generally requires crustal thickening. Quaternary crustal thickening and this is typically accompanied by horizontal shortening, as demonstrated in Westland by Beavan et al (1999). In the lowlands of Westland, both the measured and modeled contraction normal to the Alpine Fault are greater than in the Southern Alps (figure 7 in Pearson et al 1995). Modern crustal thickening in North Westland is essentially the reverse of the extreme crustal thinning that occurred in mid-Tertiary times while the Challenger rift zone (Kamp 1986) was active. Many faults that previously evolved to accommodate crustal extension now have a broadly reversed sense of displacement.

In a study of basin evolution in Westland, Kamp et al (1992) estimated that there has been as much as 12 km of crustal shortening in North Westland west of the Alpine Fault. This includes the area between Ross and Greymouth. They suggest much of the deformation was located to the east of the Hohonu Fault and that the shortening was accommodated largely by uplift and erosion.

Kamp et al (1999) used zircon fission-track cooling ages to show that the Greymouth coalfield, at the Southern end of the Paparoa Range had been uplifted in three stages during the Late Tertiary period. These uplift phases occurred at 20-15 Ma, 12-7 Ma, and 2 Ma to present. The amounts of uplift are c.2.5, c.1.2 and c.1.4 m respectively. For the axis of the Brunner-Mt Davey anticline within the Greymouth coalfield they calculated (their table 5) an average uplift rate of c. 0.61 to 1.04 mm/yr for the last 2 million years. On the basis of apatite and zircon fission track dating Seward and White (1992) concluded that the onset of uplift at the northern end of the Paparoa Range occurred at < 20 Ma, and coincided with a change from extensional to compressional tectonics.

Active folding is widespread or perhaps ubiquitous in North Westland and may be accompanied by "blind" faults at depth. Some of the folds are of regional scale notably those associated with the growth of the Paparoa and Victoria Ranges. These structures extend southward into lowland areas (figure 4.17 in Suggate & Waight 1999) and have been active through the Pliocene and Quaternary periods. The Hohonu Fault (approximately parallel to the Alpine Fault) has been active during the

Quaternary and is associated with strong folding in Tertiary strata situated immediately to the west (figure 4.24 in Suggate & Waight 1999).

Differential tilting has produced some variation in the elevation of Late Quaternary marine strandline deposits which reflects the long-standing pattern of folding. This topic has previously been assessed by Suggate (1987, 1992). The uplift rate is highest in the vicinity of anticlinal hinge zones and lowest in the vicinity of synclinal hinge zones. In the vicinity of some of the range bounding faults late Quaternary surfaces are tilted and in some cases displaced by surface ruptures. Older surfaces are tilted more than younger surfaces. There are good examples at Blackball (Young 1968, Nicol & Nathan 2001) and at Ross (Gage 1945).

To the west of the Alpine Fault in Westland uplift occurs at a rate that is thought to be considerably slower than in the Southern Alps. Based on the existing Quaternary stratigraphic model for North Westland (Suggate and Waight 1999) the uplift rate in the lowlands is thought to be no greater than 0.45 millimetres per year (Suggate 1992). At the crests of the Paparoa and Victoria Ranges modern uplift rates could be as high as 2 millimetres per year (Wellman 1979). One problem with all previous calculations of the uplift rate for the lowlands is that they are based on a series of unproven assumptions inherent in the Quaternary stratigraphic model. The marine and fluvial terrace sequences have been dated primarily on the basis correlation with Late Quaternary global sea level maxima and Northern Hemisphere glacial events. This is an issue that is discussed in further in the body of the thesis.

It is not entirely clear how long uplift has been occurring in lowland areas. There is stratigraphic evidence that suggests the modern cycle of uplift in the Paparoa Range extends back at least 3 million years. In lower lying areas the widespread accumulation of thick Torlesse Greywacke dominated conglomerates and sandstones of the Plio-Pleistocene Old Man Group suggests either subsidence or at least exceedingly slow uplift probably until the middle Pleistocene. This was followed by a change in patterns of sedimentation. Accumulation of fluvioglacial sediment became more localized as relatively incised valley systems evolved. This may imply the commencement of a more regionally widespread phase of uplift that has persisted through the middle to late Pleistocene.

The rate of uplift is one of the main controls on the evolution of the landscape, for instance the way in which local rivers behave on their floodplains. The activity of river systems is an important contributing factor to the overall evolution of Quaternary alluvial deposits within the region. So obtaining good control on the uplift rate is seen as an essential component of this research project.

As a result of research undertaken during this project it is proposed that the tectonic uplift rate in the coastal portion of North Westland is in the range 1.0 to 1.4 mm/yr. This is approximately 3 times the previous (Suggate (1992)) estimate. It is as much as 10% of the maximum rate in the Mount Cook area. This implies that the rate of NE-SW shortening west of the Alpine Fault is at least as great as the uplift rate. There could be some clockwise rotation in the lowlands in sympathy with the general plate tectonic motion.

1.3 CLIMATE

1.3.1 Introduction

The climate of North Westland is a topic that is central to this project. Climate change is a major driver in variability of rates of clastic sediment production and transport. It is also a major driver in patterns of vegetative cover and colonisation/decolonisation by various plant species.

Changes in solar insolation and climate influence the accumulation and ablation of glacial ice in the mountain ranges of the South Island. This subject is addressed in detail in Chapter 4. Ice accumulation can impact on local sea level histories through the isostatic response to changes in ice volume. Isostatic subsidence and uplift influence erosional base levels within the fluvial system. A complete analysis local sea level histories in the South Island is likely to require that consideration is given to ice volume and climate fluctuation. This is a topic that is beyond the scope of this project.

Understanding the timing of climate change is a key component to unravelling the late Quaternary erosional and depositional history and geomorphic evolution of the North Westland lowlands. In this thesis a new model for the Quaternary climate history of North Westland is proposed. It is entwined with a new stratigraphic model, a new sea level history and a new "timeline".

1.3.2 Timing of Climate Change

At the orbital or astronomical scale climate undergoes cyclical change and some of these changes have been shown to be of global scale. Major periods of interglacial climate tend to occur more or less synchronously throughout the globe, as do some major periods of glacial climate. There are some differences between the Northern and Southern Hemisphere in terms of the onset of changes to climate and these are more pronounced on "suborbital" timescales.

For climatic events at the millennial timescale there are some clear differences in timing between events in the Northern Hemisphere and those of at least some parts of the Southern Hemisphere. For instance Blunier & Brook (2001) used gas contents measured from ice cores to show that within Marine isotope stages 2, 3, and 4 interstadial events in Antarctica tend to be in anti-phase to comparable events in Greenland. With regard to millennial scale climate change in Westland it is not yet entirely clear whether the timing of events more closely matches that in Antarctica or that of events in the Northern Hemisphere.

In Westland the expansion of glaciers is controlled to a considerable degree by wind strength and direction. Wind direction is a major control on humidity, cloud cover, temperature, temperature of precipitation, quantity of precipitation and equilibrium line altitude. Wind direction in Westland is strongly related to hemispheric scale climate events. These have a component of control originating in Antarctica and the Southern Ocean. So it is possible that on the millennial timescale local (North Westland) the timing of glacial maxima reflects the timing and magnitude of temperature minima in Antarctica and the timing of local maxima for wind from westerly and southwesterly directions. This combination produces large amounts of cold precipitation and a low elevation for the equilibrium line altitude. (ELA).

In previous assessments of the ranking and timing of glacial events in Westland (e.g. Suggate 1992, Suggate and Waight 1999) it has been assumed that large changes local ice volume and ice extent approximately match the timing of similar fluctuations in Northern Hemisphere ice sheets. Given that

the various controls on ice accumulation here probably not the same as those in the Northern Hemisphere the logic of this argument is debatable. In global terms the glacial ice volume in Westland is trivial (less than 0.05 % of the LGM total). In a high precipitation climate such as that of Westland the time required to produce a local ice volume maxima is quite short (probably no more than a few thousands of years) particularly if the starting point is interstadial (potentially partially glaciated) rather than full interglacial conditions.

In this document some of these issues are further discussed in the context of the stratigraphic framework for Westland.

1.3.3 Modern Climate

1.3.3a Temperature and Precipitation

Due to the prevailing moist westerly air flow off the Tasman Sea, the West Coast has a relatively wet, mild climate. The main mountain ranges form a barrier to the prevailing winds, forcing weather systems to produce orographic precipitation. The areas that receive the greatest annual precipitation are situated on the western flanks of the main ranges.

There is a strong seasonal contrast in surface temperature. Temperature is moderated by the proximity of the Tasman Sea and the fact that the prevailing winds generally come off the sea.

In this region at the present time the bushline or timberline is situated at around 1200 to 1300 metres. The elevation at which permanent snow and ice can accumulate varies with slope aspect and latitude being higher in the north. So there is substantial variation in the equilibrium line defining a balance between accumulation and ablation. At present in North and Central Westland few areas below 1700 metres elevation collect substantial permanent ice cover. It is notable that snow can fall to elevations below the bushline at any time of the year, though it is relatively uncommon from January to March.

The following tables and graphs provide a characterization of mean climate, by month, for the Western sector of the South Island. Climate stations from outside of the primary area of study are included to give a broad context to discussion of variability in North Westland. The data are compiled from tables in the NIWA cliflo database.

Figure 1.2 charts the mean surface temperature by month for the western South Island. From figure 1.2a the climate stations at Westport, Greymouth, Hokitika, Milford Sound and Invercargill are situated at the local airport. With the exception of Franz Josef (which is several kilometres inland) and Hokitika (39 m AMSL) these stations are essentially coastal sites at an elevation of 2 to 8 m above sea level.

From table 1.1a it appears that the mean annual temperature along the coast at the foot of the Paparoa Range is greater than that just a few kilometres away as the mean temperatures at Punakaiki (13.5°C) and Barrytown (13.1°C) are greater than those of Westport (12.47°C) and Greymouth (12.3°C). Clearly the local microclimate can have a significant impact on the mean annual temperature and this will be significant in terms of the viability of floristic refugia during glacial periods.

Table 1.1a Monthly and Annual Mean Temperatures, Western South Island, New Zealand

Location	Jan	Feb	March	Apr	May	June	July	Aug	Sept	Oct	Nov	Dec	Mean
Cape Farewell	17.2	17.6	16.7	14.5	11.8	9.75	8.9	9.7	11.3	13.1	14.2	15.9	13.4
Cobb Dam	13.3	13.6	12.2	9.5	6.4	4.1	3.2	4	5.8	7.8	9.7	11.7	8.44
Motueka	17.4	17.4	16	13	10	7.6	7	8.1	10.2	12.3	14.3	16.3	12.47
Westport	16.2	16.4	15.6	13.3	11	9.1	8.5	9.2	10.5	11.7	13.2	15	12.47
Lake Rotoiti	14.6	14.6	13	9.6	6.2	3.8	3.2	4.6	6.6	8.8	11	13.1	9.09
Reefton NZFS	16.6	16.7	15.1	11.7	8.1	5.3	4.9	6.8	9.2	11.3	13.2	15.2	11.17
Punakaiki Rocks	17.2	17.4	16.4	14.4	12.5	10.7	10	10.5	11.4	12.4	13.6	15.1	13.5
Barrytown	16.4	16.7	16	13.9	11.8	10.5	9.7	10.3	11.2	12.3	13.7	14.4	13.1
Totara Flat	16.3	16.3	15	11.8	8.6	6.1	5.7	7.3	9.5	11.3	13.3	15.2	11.37
Greymouth	16.1	16.3	15.4	13.1	10.6	8.7	8.1	9.1	10.4	11.7	13.2	15	12.31
Otira	14.8	15	13.8	10.9	7.6	5.3	4.7	5.9	7.4	9.7	11.4	13.2	9.98
Arthur's Pass	13	13	10.9	8.2	5.4	2.9	1.9	3.2	5.5	7.2	9.2	11.3	7.6
Hokitika	15.4	15.8	15	12.6	9.8	7.9	7.3	8.3	9.8	11.1	12.8	14.4	11.68
Craigieburn Forest	13.4	13.7	12	8.9	5.3	2.7	2	3.4	5.7	7.7	9.8	11.9	8.04
Pukekura	14.8	15.1	13.4	11.3	8.7	6.8	6.2	7.5	8.9	10.4	12	14.8	10.8
Harihari NZFS	15.4	15.8	14.9	12	8.7	6.4	6.1	7.4	9.2	10.7	12.5	14.5	11.13
Okarito	15.7	16	14.6	12.4	10.5	8.1	7.5	8.5	10.1	11.3	12.7	14.4	11.8
Franz Josef	15	15.4	14.5	12.1	9.3	7.1	6.6	7.5	9	10.5	11.9	14	11.07
The Hermitage	14.3	14.6	12.6	9.4	5.8	3	2.1	3.7	6.5	8.9	10.8	12.8	8.71
Milford Sound	14.6	14.9	13.8	11.3	8.2	5.7	5.5	6.9	8.5	10.1	11.7	13.6	10.4
Manapouri West Arm	14	14.1	12.4	9.5	6.5	4.2	3.7	4.8	6.9	9.1	11.2	12.9	9.11
Puysegar Point	13.8	13.9	13	11.7	10.3	8.5	8.1	8.5	9.5	10	10.9	12.4	10.9
Invercargill	14	13.7	12.6	10.3	7.7	5.5	5.3	6.4	8.3	9.9	11.4	13	9.84

Figure 1.2 Mean Surface Temperature by Month, Western South Island, New Zealand.

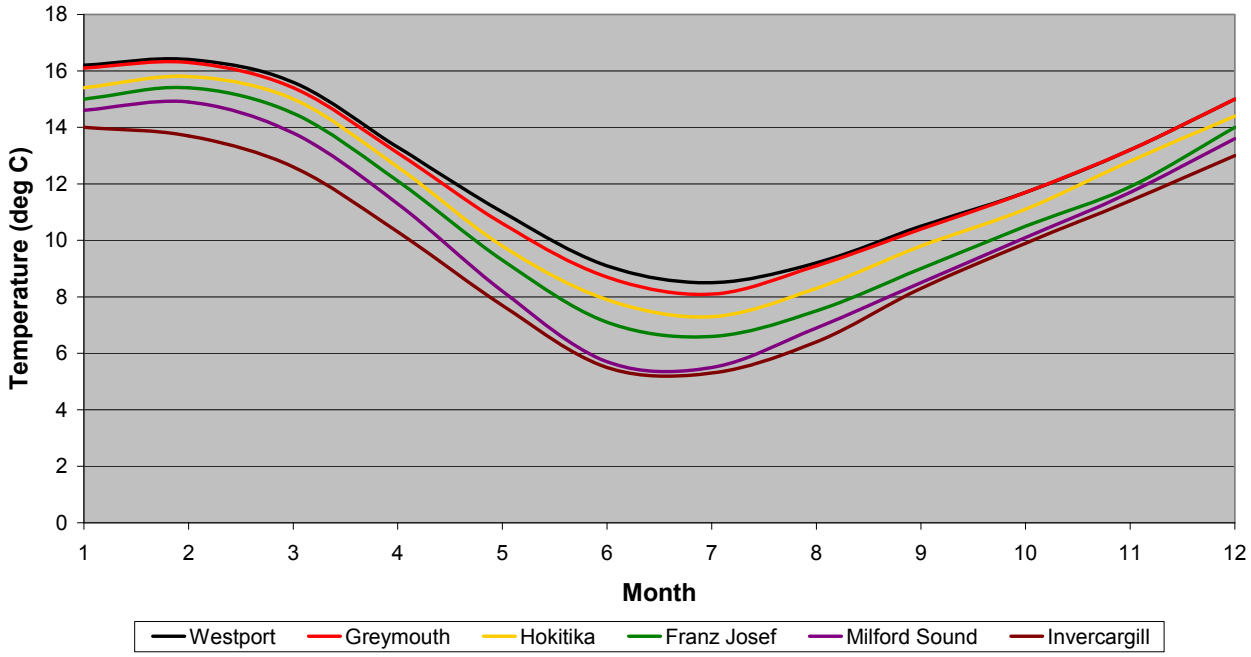

Figures 1.3a and 1.3b display the mean monthly precipitation for various climate stations situated on the western side of the South Island. Grid references for these stations can be found in table 1.1c. Of particular note is that the general monthly minimum for precipitation occurs during February at each of the climate stations. The precipitation maximum occurs during the September to November (spring to early summer) at most of the climate stations. A secondary maximum is present during April-May at most of the climate stations situated between Ross and Karamea. South of Ross the early maximum occurs during the March-April period. Through most of the western side of the South Island the winter months of June, July and August represent a precipitation minimum. With the exception of Bainham the spring precipitation maximum appears to be absent in the Nelson Region. Bainham is the closest of the Nelson stations to the West Coast. The winter period is not a precipitation minimum in the Nelson region.

The West Coast winter precipitation minimum is most pronounced at the following climate stations: Arnold Power Station, Dobson, Blackball, Grey/Robinson River, Rotomanu, Inchbonnie, Lake Kaniere, Arthur's Pass, Kowhiterangi, Lower Whataroa, Whataroa 2, Mahitahi, The Hermitage (Mt Cook), Paringa, Haast Pass, and Milford Sound. With the exception of the Arnold Power Station, these sites are all either within the Southern Alps, immediately adjacent to the Southern Alps, or immediately adjacent to the Paparoa Range. Sites that are more distant from the range-front, for instance Hokitika and Greymouth, display less variability in mean monthly rainfall. The Southern Alps have a strong orographic impact on precipitation. This effect is clearly strongest in the late-summer-autumn and spring-early summer periods and probably relates to seasonal variation in the frequency of strong westerly winds.

Figure 1.3a Mean Monthly Precipitation, Westport To Greymouth

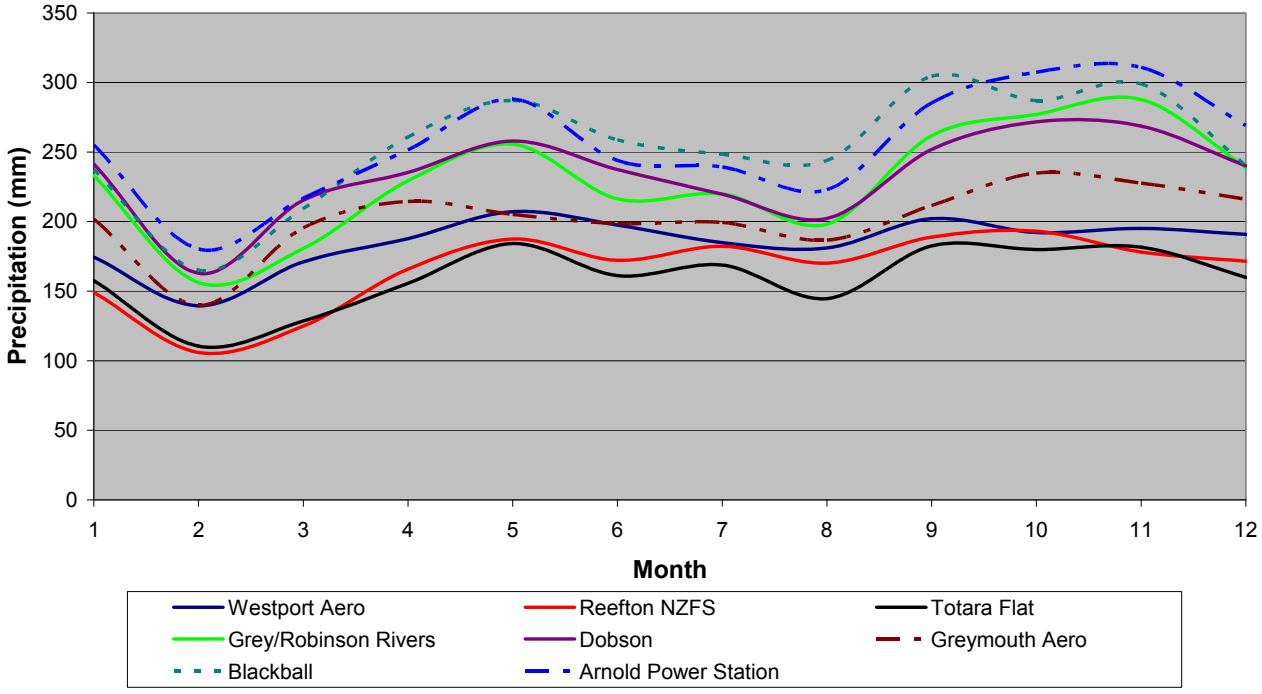

Figure 1.3b Mean Monthly Precipitation, Rotomanu To Ross

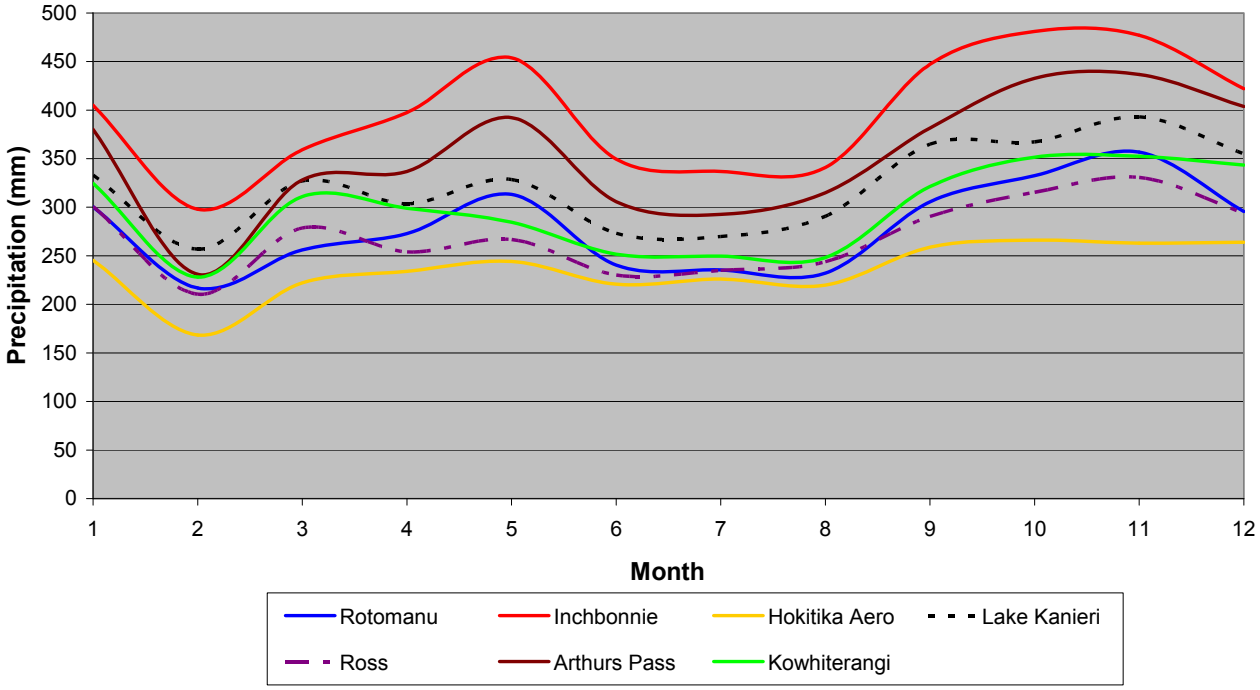

Table 1.1b Western South Island Monthly Precipitation (mm)

	Jan	Feb	March	Apr	May	June	July	Aug	Sept	Oct	Nov	Dec	Total
Patarau	133.8	94.6	137.6	155.7	155.1	175.1	182.2	169.8	154.6	182.8	161	145.6	1847.9
Bainham (Golden Bay)	261.8	200.6	294.9	314.8	343.2	339.9	372	382.6	359.6	390.5	381.3	307.5	3948.7
Uruwhenua (Golden Bay)	144.9	110.9	151.8	202.1	201.6	193.3	237.8	262.7	199.1	231.1	190.2	152.4	2277.9
Motueka	86.8	79.8	102.8	119.2	125.8	131	158.2	164	119.5	125.4	110.3	95.4	1418.2
Cobb Dam	131.4	106.4	163.5	174.9	212.2	197.4	242.3	229.6	210.5	216.3	198.8	164.5	2247.8
Karamea	148.4	101.8	131.1	161.5	175.7	172.4	154.2	138	194.2	169.3	185.3	162.5	1894.4
Murchison	118.2	82.7	94.1	135.2	142.9	135.8	143.1	128.4	153.7	153.4	147	129.3	1563.8
Lake Rotoiti	133.7	95.9	114.4	130.7	138.6	125.2	125.3	118.4	142.4	160	148.8	147.2	1580.6
Westport Aero	174.5	139.4	171.1	187.8	207.2	197.6	184.9	181.1	202.1	192.2	195.1	190.8	2223.8
Reefton NZFS	149.1	105.9	125	165.9	187.4	172.2	182.3	170.2	188.8	193.1	178.1	171.5	1989.5
Totara Flat	157.7	110.6	128.6	155.7	184.2	161.2	168.8	144.6	182.6	179.9	181.6	160	1915.5
Grey/Robinson Rivers	233.1	156.2	180.8	229.3	255.7	216.3	219.9	198.1	261.8	277.1	287.7	239	2755
Dobson	241.4	162.8	215.5	235.3	257.9	237.4	219.8	202.3	251.8	271.7	268.7	240.1	2804.7
Greymouth Aero	201.8	139.8	195.5	214.5	205.2	198.6	199.4	186.7	211.5	234.8	227.6	216	2431.4
Blackball	237.3	165.2	209.3	260.9	287.1	258.7	248.5	243.9	304.4	287	298.9	240.5	3041.7
Arnold Power Station	255	180.2	216.8	251.6	288.1	243.9	239.3	223	285.3	307.4	310.8	269.1	3070.5
Rotomanu	300.3	216.9	256	272.9	313.2	240.5	235.4	232.2	305.6	332.4	356.7	295.7	3357.8
Inchbonnie	405	297.9	359.1	397.4	453.7	349.6	336.8	341	447.3	481	477.1	422.1	4768
Hokitika Aero	245.3	168.4	222	233.8	244.1	220.7	226.1	219.8	258.8	266.1	263.1	263.9	2832.1
Lake Kanieri	332.9	257	327	303.5	328.6	273.1	269.8	290.6	364.8	367.3	393.1	355.1	3862.8
Ross	300.6	210.4	278.5	254	266.7	230.1	235.1	243.8	290.5	315.4	330.6	293.9	3249.6

Arthurs Pass	380.2	230.9	328.1	336.9	392.2	305.7	292.5	315	381.5	432.7	436.6	403.7	4236
Kowhiterangi	324.6	227.9	311.1	298.9	284.4	251.6	249.7	248.2	321.3	351.6	352.3	343.3	3564.9
Lower Whataroa	331.7	258	346.5	301.5	296.2	250.6	260	287.1	332.3	360.7	338.6	347.3	3710.5
Whataroa 2	425	292	444.1	351.8	363	297.4	292.7	331.1	404.8	439	413.1	435.5	4489.5
Mahitahi	332.9	257	327	303.5	328.6	273.1	269.8	290.6	364.8	367.3	393.1	355.1	3862.8
The Hermitage	417.6	257.1	436.3	336.2	351.5	268.6	259.8	287.9	343.4	415.3	385.3	434.9	4193.9
Paringa	494.5	378.2	617.8	427.6	421.1	369.7	392.7	414.3	493.2	546.1	493.3	471.1	5519.6
Haast Pass	398.5	260.7	398.4	351.8	377.1	301.8	299.9	331.3	451.1	458.8	403.6	378.7	4411.7
Makarora Station	186.4	134	230.3	176.5	193.5	180.4	195.1	207.1	233.1	247.1	198.8	210.7	2393
Wanaka	60	40.2	69	54.7	62.2	58.3	57.9	57.6	63.8	71.1	52.7	56.2	703.7
Milford Sound	651.9	472	669.7	562.1	556	404.7	383.3	408.7	563.7	639	548.7	642	6501.8
Puysegur Point	206.9	158	190.8	206.9	204.2	190	165.9	152.2	174.4	173.3	163.3	184.1	2170
Total	8603	6149	8445	8265	8804	7622	7701	7802	9216	9836	9471	8925	

Table 1.1c Location and Station ID

	Mean Monthly Precipitation	Elevation (m)	Latitude	Longitude	NOAA Station ID NZ9300000…..
Paturau	154	30	40° 40'	172° 24'	F026410
Bainham (Golden Bay)	329.1	79	40° 46'	172° 33'	F027510
Uruwhenua (Golden Bay)	189.8	91	40° 58'	172° 49'	F029910
Motueka	118.2	8	41° 06'	172° 58'	G121910
Cobb Dam	187.3	823	41° 06'	172° 40'	F121620
Karamea	157.9	4	41° 15'	172° 07'	F122110
Murchison	130.3	160	41° 48'	172° 19'	F128310
Lake Rotoiti	131.7	634	41° 48'	172° 51'	F128520
Westport Aero	185.3	2	41° 43'	171° 34'	NZ9351500F117520
Reefton NZFS	165.8	198	42° 07'	171° 34'	F211820
Totara Flat	159.6	77	42° 18'	171° 37'	F213610
Grey/Robinson Rivers	229.6	368	42° 27'	172° 01	F224010
Dobson	233.7	14	42° 27'	171° 18'	F214310
Greymouth Aero	202.6	4	42° 27'	171° 10'	F214220
Blackball	253.5	107	42° 22'	171° 25'	F213410
Arnold Power Station	255.9	75	42° 31'	171° 25'	F215410
Rotomanu	279.8	107	42° 39'	171° 34'	F216530
Inchbonnie	397.3	116	42° 40'	171° 27'	F216410
Hokitika Aero	236	39	42° 43'	170° 58'	NZ9361400F207930
Lake Kanieri	321.9	133	42° 48'	171° 07'	F218120
Ross	270.8	15	42° 54'	170° 48'	F209810
Arthurs Pass	353	738	42° 57'	171° 34'	H307110
Kowhiterangi	297.1	30	42° 57'	171° 01'	F218101
Lower Whataroa	309.2	30	43° 12'	170° 22'	F396620
Whataroa 2	374.1	64	43° 16'	170° 22'	F302330
Mahitahi	321.9	30	43° 37'	169° 27'	F396620
The Hermitage	349.5	765	43° 43'	170° 06'	NZ9373300H307110
Paringa	460	43	43° 43'	169° 27'	F497110
Haast Pass	367.6	524	44° 06'	169° 22'	F491320
Makarora Station	199.4	320	44° 15'	169° 13'	I492220

Wanaka	58.6	314	44° 42'	169° 07'	I497110
Milford Sound	541.8	3	44° 40'	169° 22'	NZ9372000F476910
Puysegur Point	180.8	43	46° 09'	166° 37'	F661610
NIWA Location and Site ID details					
Otira Substation		383	42.833°	171.563°	4001
Lake Rotoroa		445	41.797°	172.59°	3862
Hanmer Forest		387	42.522°	172.854°	4458, 11234
Boyle River		600	42.519°	172.386°	4455

Table 1.2 NIWA "Alpine" Climate Stations, West Coast Region

Site	Site Number	Map NZMS260	Grid Ref	Altitude (m)	Mean Annual Rainfall (mm)
Ford Creek (Paparoa Range)	213303	K31	744707	517	1800
Butchers Creek (Lake Kanieri)	218117	J33	547220	140	3800
Taipo River (State Highway 6 Bridge)	217411	K33	794266	130	4834
Arthurs Pass (~ Main Divide)	219506	K33	926064	738	4250
Colliers Creek (Middle Hokitika Valley)	209910	J33	465001	95	7202
Rapid Creek (Middle Hokitika Valley)	310010	J34	482975	152	7506
Prices Flat (Upper Hokitika Valley	311010	J34	480870	427	7540
Cropp Hut (Trib, Whitcombe Valley)	301913	J34	459900	860	10510
Cropp Waterfall (Trib, Whitcombe Valley)	311015	J34	439907	975	11516
Tuke Hut (Tuke Valley)	301910	J34	382888	975	10438
Mathaias (East of Main Divide)	312110	J34	582785	670	4444
Rakaia (Lake Ramsay, Easy of Mn Divide)	303911	J35	411673	945	4815
Douglas Hut (Waiho Valley)	304210	H35	809500	250	6546
Whataroa (State Highway Bridge)	303411	I35	992657	90	5591
Cron Creek (Haast Valley)	399210	F37	021862	58	7856
Roaring Billy (Haast Valley)	399213	G37	129895	60?	5341
Moa Creek (Haast Valley)	399410	G37	216842	105	3969

Ford Creek- near the Roa Coal Mine
Moa Creek- near Haast River / Landsbrough River confluence
Cron Creek- inland (east) from Southern Alps range-front
Roaring Billy-up valley from Cron Creek
Colliers Creek- near DoC Hut, Hokitika Valley, just inland from Southern Alps range-front
Rapid Creek- near DoC Hut 3 km up valley from Colliers Creek
Cropp Hut- In the Cropp Valley, a tributary of the Whitcombe Valley in the upper Hokitika River catchment area.
Mathaias- NZ Deer Stalkers Association Hut
Whataroa- Southern Alps Range Front, just south of State Highway Bridge
Tuke River- Mikonui River tributary

With regard to temperature it can be seen from figure 1.2 that the warmest mean monthly temperature at almost all the West Coast climate stations occurs during February. There are a few exceptions where January and February are of approximately equal warmth. Throughout the western side of the South Island the coldest months are June, July and August.

February is also generally the driest month along the western half of the South Island. The annual February precipitation minimum corresponds to a minimum in the strength/frequency of southwesterly winds. Westerly winds tend to be stronger and more persistent in "El Nino" periods during which the

rainfall also tends to be greater than average. These same periods also tend to be slightly colder than average at sea level.

As can be seen from figure 1.3 and table 1.1b there is a large variation in rainfall across the region. The modern precipitation maximum of ~11500 mm occurs at an elevation above 900 m about mid-way between the Southern Alps range-front and the "main divide". The annual precipitation drops below 4500 mm just a few km to the east of the main divide. Near the coast the annual precipitation varies from about 3860 mm at Mahitahi (Jacobs River) in the south to 1895 mm at Karamea in the north. In part the difference is due to a more abrupt transition from coastal lowland to alpine topography in the south.

The extremely high rainfall in the Southern Alps between the range-front and the main divide is important in terms of ice accumulation. The spring precipitation maximum also tends to correspond to the maximum in snowfall.

1.3.3b Modern Environmental Lapse Rates

Along the western side of the South Island the environmental lapse rate (ELR) is much greater during the winter months than during the summer months. ELRs are estimated in table 1.3 by measuring the difference in mean temperature between climate stations that have a large contrast in altitude. For these calculations the stations are paired on the basis that they share similar latitude. In most individual examples the ELR represents the difference between an open, level relatively coastal site, and a confined inland valley. The most obvious exceptions are the pairings Omarama- Mt John, Mt Hutt-Highbank Power Station, and Blenheim Aero—Black Birch Range, where one of the stations is at or near the top of a mountain. During the winter the mean cross-surface ELR is around 7.5°C/km. During the summer it is around 2.5°C/km. The annual mean in cross-surface ELR is approximately 4.9°C/km. These measurements are relatively crude and the error range is unknown.

As a comparison the average annual cross-surface ELR calculated by Anderson et al (2006) across several temporary surface stations at the Franz Josef glacier was 4.8°C/km. They found that there was an additional glacier-proximal cooling effect of about 1.35°C which may be due at least partially to the reflection of solar radiation by the ice.

Table 1.3 Modern Environmental Lapse Rate (Surface) based on temperature measurements from surface climate stations

Location	Diff in Elevation (m)	Diff in January Temp (°C)	January Lapse Rate (°C/km)	Diff in July Temp (°C)	July Lapse Rate (°C/km)	Diff in Mean Temp (°C)	Annual Lapse Rate (°C/km)
Cobb Dam - Motueka	815	4.1	5.03	3.8	4.7	4.04	4.94
Westport - Lake Rotoiti	632	1.6	2.5	5.3	8.4	3.38	5.35
Westport - Lake Rotoroa	441	1.2	2.71	4.3	9.75	2.7	6.1
Hokitika - Craigieburn Forest	875	2	2.3	5.3	6.1	3.64	4.16
Hokitika - Otira	379	0.6	1.74	2.6	6.9	1.7	4.5
Hokitika - Arthurs Pass	734	2.4	3.43	5.4	7.4	4.1	5.6
Greymouth - Boyle River	596	0.5	0.84	4.3	7.2	2.6	4.4
Greymouth- Hanmer	383	0.4	1.04	4.18	10.9	2.2	5.7
Franz Josef - The Hermitage	543	0.3	0.55	4.5	8.3	2.36	4.3

Invercargill - Manapouri (West Arm)	232	0	0	1.6	6.9	0.73	3.1
Omarama-Mt John	539	0.13	0.24	2.95	5.47	1.69	3.14
Palmerston-Naseby	586	1.05	1.79	3.33	5.68	2	3.4
Kaikoura-Hanmer	279	0.8	2.87	4	14.6	2.1	7.53
Molesworth-Cape Campbell	887	3	3.38	7.45	8.4	5	5.6
Mt Hut-Highbank Power Station	1370	6.9	5.04	7.2	5.25	7	5.11
Arapito-Cobb Dam	805	3.3	4.1	5.3	6.6	4.21	5.09
Blenheim Aero-Black Birch Range	1356	7.25	4.8	6.5	4.8	6.8	5.01
Total		35.53	42.36	78.01	127.35	56.25	83.03
Mean		**2.09**	**2.49**	**4.59**	**7.49**	**3.31**	**4.88**

Another strategy contrasts the mean annual sea-level temperature across a series of coastal climate stations and compares it with the mean elevation-adjusted" temperature across a series of climate stations at inland mountainous sites. For the South Island the annual mean surface temperature at an altitude of 500 metres over the recorded historic period to 2010 (see figure 1.4) is estimated to be 9.3°C. This estimate is sensitive to the choice of climate stations and particularly to the latitudinal spread of the sites. The sites shown in figure 1.2 yield an average annual sea-level surface temperature of approximately 12°C.

The fact that the mean cross-surface altitudinal environmental lapse rate is greater during winter than during summer is rather interesting. Colder temperatures appear to correspond to a greater lapse rate so is the summer lapse rate greater during a cold summer than during a hot summer? Is the summer lapse rate constant at a millennial timescale? At this scale mean summer insolation is not constant. Nor is the angle of incidence for incoming solar radiation. So it might be expected that under cyclically reduced summer insolation there will be a cyclically increased summer lapse rate. This is likely to have a climatic impact, including an impact on summer snow ablation.

It is proposed here that the modern seasonal variability in ELR also applied throughout the Quaternary period. During the Quaternary the summer ELR would therefore vary with orbital scale variations in summer insolation. At 40°S mean summer and mean winter insolation each vary by as much as 8% through the precessional cycle. In terms of alpine ice ablation summer is the period where melting is most rapid. So one could reasonably expect:

1. That a lower mean summer temperature throughout the Southern Alps (due to reduced summer insolation) during glacial periods will produce an increase in the summer ELR.
2. That a greater summer ELR will lower the equilibrium line for ice accumulation/ablation.
3. This would increase the area available for ice accumulation, and the average reflectivity of the ground surface which would further reduce summer temperatures over the Southern Alps.

1.3.4 Climate during glacial periods

The first point to make here is that regardless of timing within an orbital or millennial scale climate cycle the "local" mean annual precipitation is always relatively high. The region always intercepts a relatively moist air stream, wind being dominantly from the west off the Tasman Sea. The strength of the air-flow may vary and its average direction may become more southerly (colder) or more northerly (warmer). The position of the region within the overall belt of westerly air flow may vary as well (Shulmeister et al 2004) making surface temperatures in the West Coast Region either warmer or

colder. North-south changes in the position of the westerly wind belt also impact directly on the sea surface temperature in the South Tasman Sea.

The extent of glacial ice in Westland is dependent on the elevation of the ELA (equilibrium line for ice accumulation). During periods of severe glaciation the ELA in Westland falls from ~ 1800 m to around 1000 m on north facing slopes. On south facing slopes the ELA falls from a modern interglacial elevation around 1600 m to a "stadial" elevation as low as 800 metres (relative to modern sea level). The glacial-interglacial difference is as much as 800 m. Using the estimated modern surface environmental lapse rate from table 1.3 of c. 4.8°C/km this ELA lowering would imply a minimum change in mean annual temperature of around 3.8 to 4°C. It is not clear that the surface environmental lapse rate is stationary through time though and it may be greater during glacial periods.

Lowering of the ELA by c.800m causes a massive increase in the land area capable of accumulating permanent snow and ice. Rapid infilling of mountain valleys by glaciers is inevitable if the ELA drops substantially. The ice can then accumulate in areas where the rock surface is below the nominal ELA, raising the average elevation of the landscape and thereby further increasing the total surface area situated above the ELA. The geomorphology of south facing slopes in Westland indicates that during the most recent glaciations cirque and small valley glaciers have accumulated on or immediately under any area at a modern elevation of about 1050 to 1200 metres. Currently the requirement is more like 1850 metres to 2000 metres. At glacial maxima, in areas west of the Main Divide of the Southern Alps, substantial glaciers accumulate on south facing slopes where there are significant accumulation areas above a modern elevation of 1200 metres. Presently this requires significant accumulation areas above 2100 metres.

The question of climate during glacial periods in Westland has been addressed directly by Burge (2007) who studied changes in beetle and vegetative assemblages in the Westport area. During the LGM it was found that winter mean-minimum temperatures were depressed by 4.5 to 6 °C and mean summer temperatures by 0 to 5 °C.

The climate stations used in the construction of the South Island inland temperature index (figure 1.4 below) include: Hanmer Forest, Hanmer Forest Ews, Arthurs Pass Ews, Cromwell Ews, Lake Rotoiti, Lake Rotoiti Ews, Cobb Dam, Lake Rotoroa, Reefton Ews, Otira Substation, Golden Downs Forest, Boyle River Lodge, Molesworth, Mt Cook Ews, Mt Cook (The Hermitage), Craigieburn Forest, Harper River, Lake Colleridge, Winchmore Mixed Farm, Winchmore Ews, Lake Tekapo & Air Safaris, Fairlie, Fairlie (Riverview Tce), Twizel, Omarama, Tara Hills, Lake Hawea, Mt Luxmore, Manapouri Aero Aws, Queenstown Aero Aws, Cromwell M.W.D., Cromwell 2, Ophir 2, Mahinerangi Dam, and Nugget Point Aws.

From figure 1.4 the modern inter-annual to inter-decadal variation in the annual air temperature in coastal and inland parts of the South Island is estimated to be of the order of 1.0 to 1.5°C. The temperature series presented here have been adjusted for variation in mean altitude across the component climate stations and for variation in mean latitude.

Figure 1.4: Altitude adjusted historic mean temperature index, South Island (NZ) using inland climate stations (non-coastal, non-urban), an ELR of 4.4 °C per km and a reference elevation of 500 m amsl.

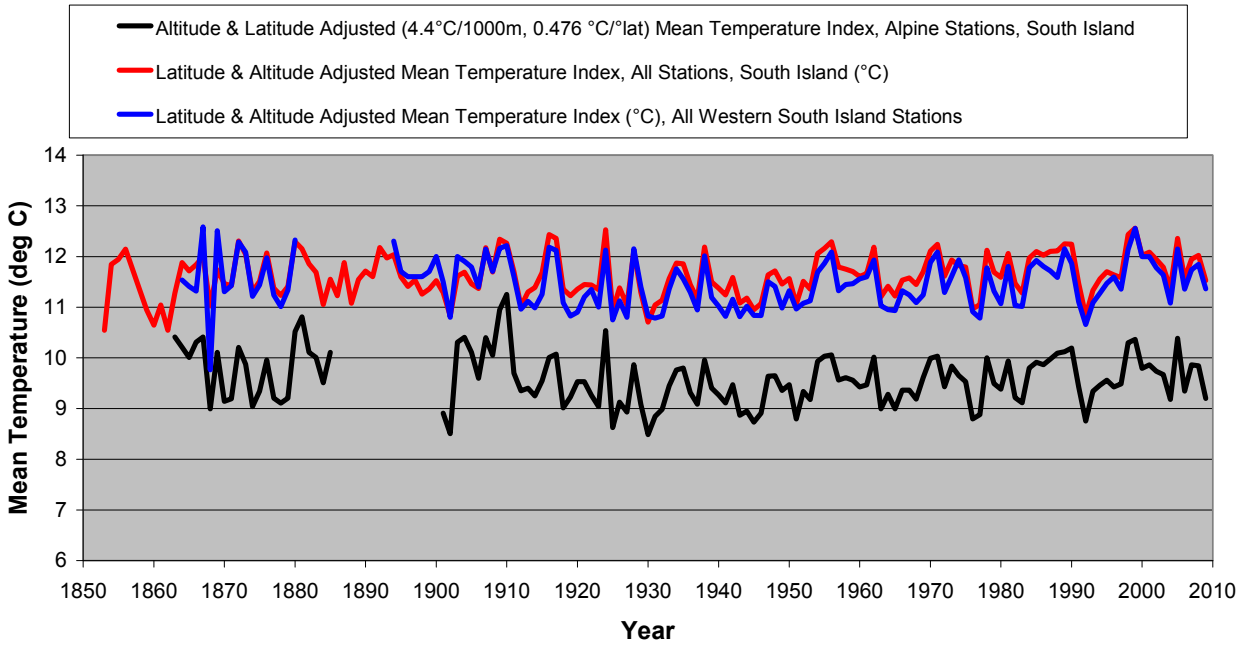

1.3.5 Sediment Production

High annual precipitation and in particular high-intensity rainfall events contribute to the generally high modern rates of erosion and sediment transport within the region. Production of new clastic sediment is more rapid in the Southern Alps than elsewhere in the region. There are additional important sources of fresh, hard clastic sediment including the Paparoa, Victoria and Hohonu Ranges and other areas of outcropping crystalline basement rock. In the modern setting new clastic sediment is generated mainly in Mountainous areas. During episodes of widespread glaciation there are additional sources of new sediment because glaciers scour areas that (interglacial) rivers cannot reach.

Changes in the regional climate strongly influence rates of sediment production, and types of erosion and deposition. Such long-term climate fluctuations (over thousands to 10's of thousands of years) have caused alternation between temperate (modern) and sub arctic (ice age) extremes in this region. Colder climates lead to accelerated rates of physical weathering, particularly in mountainous areas. During cold climate periods the area and volume of glacial ice in the Southern Alps increases substantially and vastly exceeds the area of modern glacial remnants. Icefields feed numerous valley glaciers that are generally larger than the biggest of the presently surviving glaciers in the Mt Cook area. The Taramakau Glacier, for instance, reached as far west as Kumara Township as recently as 16,000 years ago. At that time the locality now known as Jackson's was buried by hundreds of metres of glacial ice.

The geomorphology of the main valley systems between the Alpine Fault and the Main Divide is suggestive of formation by a large number of glaciers of various sizes and variable basal ice velocity. The large steep-sided, deeply incised valleys are the former positions large glaciers. Many of the higher surfaces on the intervening ranges are ice scoured but almost plateau-like sloping at moderate

angles toward the main and/or smaller feeder valleys. It is likely that in the middle to upper reaches of the main valley systems what appear to be trim-lines might be better characterized as the margins of deep ice flowing at a faster velocity than the immediately adjacent ice. The ice surface could be well have been above the "trim-line".

1.4 Previous Work on Quaternary Geology and Climate in North Westland

1.4.1 Brief Introduction to the Key Research

In this thesis the relevant information from key historic publications is referred to within the body of the report where those studies have a direct bearing of the matters under discussion. The key papers that have influenced or defined historical thinking in relation to the Quaternary Geology of North Westland are described briefly here.

The first detailed study was that of McKay (1893, 1894). McKay summarised a variety of reports by workers including himself, Hochstetter, Haast, Hector, and Hutton. Much of the early work consisted of descriptions of fluvial and glacial deposits exposed in alluvial gold mines situated throughout the region. The fact that there are widespread glacial deposits in North Westland was broadly understood by the alluvial gold miners, officials of the goldfields administration, and others, including scientists like Haast and Hochstetter. McKay noted that many of the valleys were sculpted by glacial ice, that Lake Kaniere was formed by a glacier, and that many of the low hills of the region are belts of moraine.

Subsequent to the work of McKay further reference to the glacial origin of Quaternary deposits was made by Bell & Fraser (1906) and Morgan (1911). In both volumes the glacial deposits were recognized as being older than the Holocene deposits, and younger than the underlying Tertiary strata. But no attempt was made to further subdivide the glacial deposits.

Classification of the fluvial and glacial deposits on the basis of multiple glacial events commenced with Gage & Suggate (1958) and Gage (1961a, b). The work by Gage (1961b) was primarily in relation to the Plio-Pleistocene geology of the Ross area and described the oldest glacial till so far identified in New Zealand. Bowen (1965) extended the work of Gage (1961) describing the distribution of Plio-Pleistocene fluvioglacial deposits throughout North Westland. These early ideas were subsequently refined by Suggate (1965) particularly in relation to the Late Quaternary period. The key contribution was the identification of four successive glacial advances in the Kumara area. These were defined as the Hohonu, Kumara 1, Kumara 2, and Kumara 3 advances. These four advances were assigned to three glaciations being the Waimaunga, Waimea, and Otira Glaciations. Gage (1985) is a useful summary of the early research on glacial on glaciation New Zealand. Subsequently Suggate (1985a, 1992) further subdivided the moraine belts, outwash terraces, and raised marine strandlines now defining 4 Late Quaternary glaciations some containing multiple advances, most notably the Otira Glaciation. The newly identified glaciation was the Nemona Glaciation. Suggate & Waight (1999) identified an additional glaciation being the Kawhaka Glaciation raising the total number to five. This is the status quo at present.

The sequence of raised marine strandlines is discussed briefly by Gage (1952), who recognized "terraces" near Greymouth at elevations of approximately 3 m, 24 m, 55 m, 76 m, and 152 m. The sequence is also discussed by Nathan (1975, 1976, 1978), Suggate (1985, 1991 1992), and Suggate &

Waight (1999). Nathan mapped the marine terrace sequence in the Westport-Cape Foulwind, Cape Foulwind-Charleston, and Greymouth areas at 1:63360 scale. The raised marine terraces of the Westport area were also mapped by MacPherson (1978). The content of each Late Quaternary Formation in North Westland outlined by Suggate (1985) and Suggate and Waight (1999) as well as the stratigraphic relationships between the various marine and fluvioglacial deposits.

In a parallel line of research Dickson (1972); Moar & Suggate (1969, 1979, 1996), Burrows (1997), Moar & McKellar (2001), Vandergoes et al (2005); Newnham et al (2007) and Moar et al (2008) have collated a series of records of past vegetation for substantial number of localities. The primary data in these records consists mostly of pollen diagrams. The study by Vandergoes et al (2005) is discussed in detail in Chapter 5. Some of the studies incorporate radiocarbon and/or luminescence dating of the sediments. One of the key references summarizing the older radiocarbon data is Grant-Taylor and Rafter (1971). Substantial numbers of radiocarbon ages have also been reported by Hormes et al (2003) and Denton et al (1999).

A number of studies have been carried out on the structure, chemistry and age of Quaternary soil and loess from various parts of the region. These include reports by Mew et al: (1986, 1988); Berger et al (2001); Neall et al (2001); Almond (1996) and Almond et al (2001). The work of Almond et al (2001) is particularly interesting as it tends to challenge some aspects of the hitherto generally accepted climate and glacial history in Westland. They find evidence for widespread glaciation during MIS3 in South/Central Westland whereas none had been noted previously in North Westland.

Fitzsimons et al (1996) studied the palaeomagnetic character of glacial deposits in the northern South Island, including a number of sites in North Westland. The implications of the results are that all 5 middle to late Quaternary glaciations defined for this region have normal polarity and therefore are likely to be younger than the Bruhnes-Jaramillo transition at around 0.78 Ma.

There are also a large number of mineral exploration reports held at the Crown Minerals (Ministry of Economic Development) library, for instance Jury & Hancock (1989) and Cavaney (1968) that make reference to multiple glaciations in North Westland. Another significant study with an economic slant is Henley & Adams 1979.

Quaternary studies that have made use of luminescence dating include Hormes et al (2003); Preusser et al (2005); Preusser et al (2006); Vandergoes et al (2005); Almond et al (2001); Berger et al (1994, 2001) and Burge et al (2007). The results have been rather mixed. It is clear that the selection of suitable material for dating is critical in achieving sensible results. This is a topic addressed in detail by Preusser et al (2006). Generally speaking the ages have raised some questions with respect to the isotope stage correlations proposed by Suggate (1985). This will be discussed in more detail in chapter 4.

During the most recent 10 year period there has been a substantial quantity of new information published on the Quaternary deposits of Westland. Studies include those of Suggate & Waight (1999) which was a regional mapping exercise; Hormes (2001); Denton et al (1999); Suggate and Almond (2005); Pelejero et al (2006); Sutherland et al (2007); Barrows (2007); Burge (2007); Burge & Shulmeister (2007a, 2007b) and Moar et al (2008).

1.5 The Existing Model of Climate and Glaciation for North Westland

As indicated by the publication record discussed above an enormous amount of effort has been put into definition of the Quaternary stratigraphy of North Westland by Dr RP Suggate. The basic default model for the climate and glacial history of the region has been assembled by Dr Suggate. This body of knowledge is hereafter referred to as the "Suggate Model". But note that there have been a number of additional contributors. This model could be termed the "orthodox account" of the local Quaternary history. For several decades the Suggate model has underpinned "onshore" glacial/interglacial" history for the entire South Island. It has operated as the "gold standard".

As indicated in part 1.4 above early ideas on the history of glaciation in Westland were summarised and extended in Suggate (1965). Evidence for multiple glaciation was presented and discussed. This was followed by more comprehensive accounts in Suggate & Moar (1970), Suggate (1987) and Suggate (1990) where evidence for alternating glacial and interglacial climate is discussed along with a discussion of the stratigraphic relationships between glacial and interglacial deposits. In particular Suggate linked the raised marine deposits to episodes of relatively warm climate and high sealevel. The eustatic sea level curve of Chappell & Shackleton (1986) was used by Suggate (1992) to define sea level for each of the raised marine terraces. Using the elevation above sea level for succeeding terraces on several coast-normal profiles average uplift rates were calculated and range from 0.225 to 0.48 mm/yr. Some alterations were made to the stratigraphy, for instance by Suggate & Mildenhall (1991). The stratigraphic model is summarised in Suggate & Waight (1999), which describes the geology of much of the relevant area via a large 1:50,000 scale map sheet.

Note that five main Middle to Late Quaternary glaciations have been identified in North Westland by Dr Suggate. Multiple moraine/glacial till features have been identified for several of the main glacial events, most notably the Otira Glaciation. The older deposits of the Porika Formation are not included here as they lie outside the study area. The deposits of the even older Ross Glaciation are also excluded though there are outcrops within the study area.

In terms of individual glacial formations these consist of all the deposits of one major ice advance. This includes till, lake beds, fluvial outwash and loess/soil that collects on the surface. Interglacial/interstadial formations consist of coastal marine and estuarine deposits and coeval fluvial deposits. Most of the interglacial fluvial deposits in the main valleys seem to be destroyed or buried during subsequent glacial periods, those of the Holocene period being the primary exception.

In its initial conception, developed largely through the 1960's to the late 1980's the Suggate model included three glaciations. This was amended to a five glaciation model by Suggate & Waight (1999) with the mapping and definition of the Mudgie Ridge Formation. Some modifications were made to the timing of events in the latter portion of the Otira Glaciation by Suggate & Almond (2005). The Suggate model was developed for North Westland with minimal explicit reference to or reliance on correlation with similar sequences in other parts of the South Island. In terms of this thesis a similar policy applies.

The Suggate model is the orthodox definition for the glacial/interglacial history of North Westland so it is treated as if it were the null hypothesis for a scientific experiment. Given that the model is effectively a theory or collection of hypotheses it must by definition be available for testing. Clearly there is potential for the falsification of parts of the model through the collection and analysis of new data and observations and through reinterpretation of past observations. If the model is found wanting then alternative hypotheses can be formulated and evaluated. This project has proceeded on the basis

that we should prefer those models or theories that lead to successful predictions but require the least number of auxiliary hypotheses or assumptions.

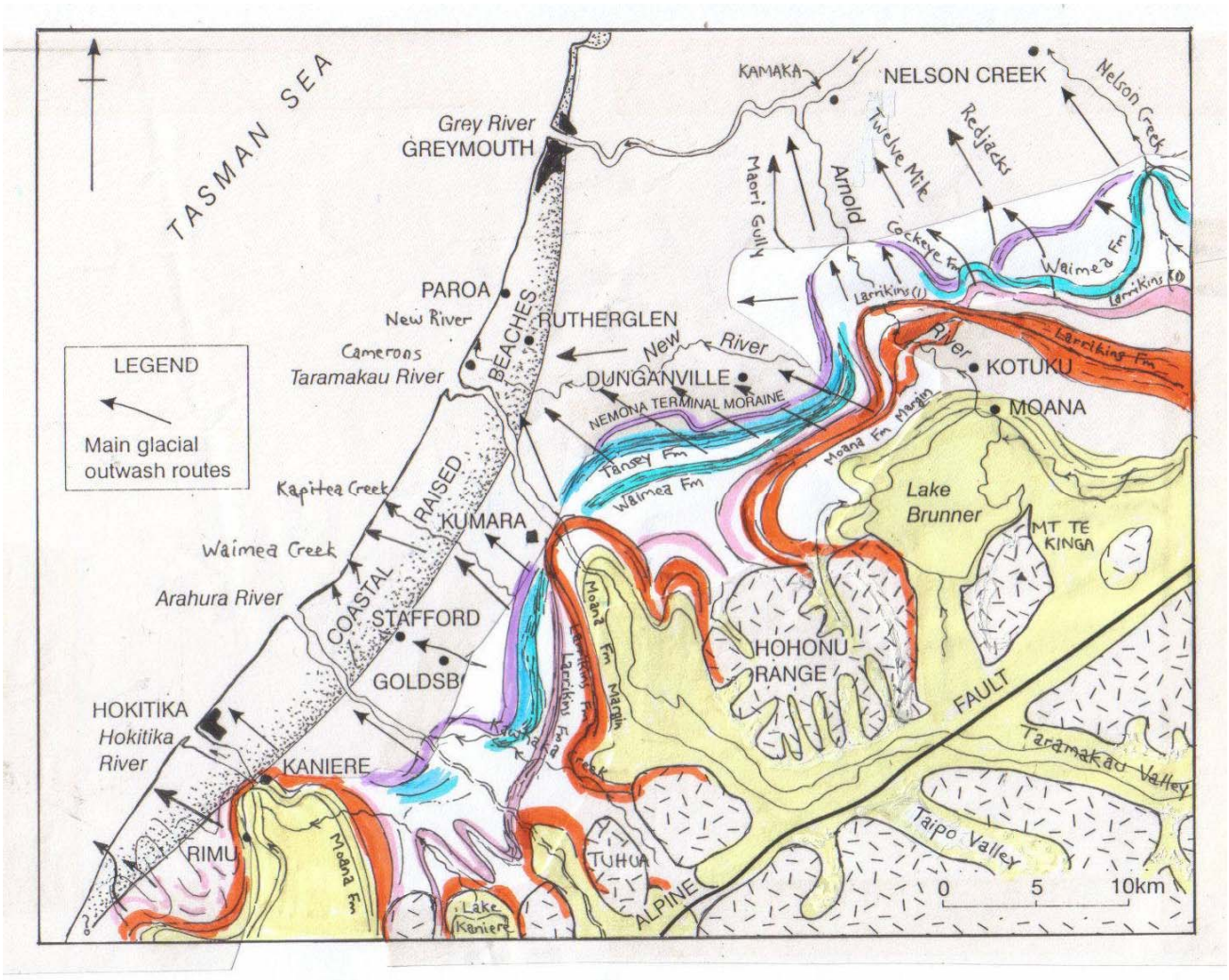

Figure 1.5 General distribution of terminal moraine belts in North Westland [adapted from figure 1 of Suggate (1996)].

Assumptions inherent in the Suggate model include:

1. Radiocarbon ages that do not fit with the correlation are generally assumed to be incorrect, usually due to contamination by younger carbon.

2. Widespread tall canopy forest cover is assumed to be present during interglacial periods and during those "stadial periods" of considerable duration that approach Holocene warmth. However, it has been assumed that such forest is not present during stadial and transitional climates. Further the model also assumes that brief episodes of near interglacial climate associated with interstadials do not coincide with widespread development of tall canopy forest, or at least do not result in widespread synchronous deposition of the pollen of such a forest in the underlying soil.

3. In the model it is assumed that a full forest flora automatically equals a full or near-full interglacial climate and that the lack of such a flora implies conditions were significantly colder than those of an interglacial. This has been questioned by work on beetle assemblages near Westport by Burge (2007). In fact it is not clear that pollen is always well preserved in soil that is coeval with immediately adjacent forest growth. Nor is it clear that changes is vegetative species composition keep pace with rapid changes in climate.

4. It assumes that significant periods of near-interglacial climate in North Westland are approximately synchronous with interglacial periods in the Northern Hemisphere.

5. It assumes that full-scale glaciation occurs in North Westland more-or-less in synchronisation with Northern Hemisphere glaciations. It makes no explicit allowance for major glacial advances in North Westland that might coincide with sub-orbital scale stadial events in Antarctica and which might be out of phase with Northern Hemisphere climate or eustatic sea level minima.

6. It assumes that the raised marine strandlines of North Westland were deposited during 1st order eustatic sea level maxima. The eustatic maxima of isotope stages 5a and 5c are included in this category. It assumes the raised marine strandlines were formed when sea level was within about 10 to 20 metres of the modern eustatic level. It also assumes little or no lasting isostatic impacts from the loading of glacial ice on the Southern Alps and so little isostatic impact on local sea level.

7. It assumes that minor to moderate (or 2nd order) sea level maxima are not represented in the on-shore marine strandline sequence.

8. It relies heavily on correlation with Northern Hemisphere glacial events and eustatic sea level events in defining the age of most of the Quaternary Formations.

9. In North Westland a flight of raised marine strandlines provide convenient markers for the calculation of tectonic uplift rates. In the Suggate model the strandlines are dated by an assumed correlation with eustatic sea level and Northern Hemisphere climate (Suggate 1992). The uplift rate will be subject to error if it turns out the original correlation was wrong.

10. The Suggate model assumes that ice volume fluctuations and glacial advances in North Westland reflect astronomical scale changes in global (largely Northern Hemisphere) ice volume. Therefore local fluvioglacial outwash deposits are correlated in the Suggate model only with the main expansions of the Northern Hemisphere ice sheets. The corollary is that periods of intermediate ice volume in the Northern Hemisphere (e.g. MIS 3, 5b, 5d, 7b and 7d) are not represented by substantial fluvioglacial deposits in North Westland.

11. It assumes that extensive local cold climate deposits (e.g. glacial till and fluvioglacial outwash) were deposited during periods when eustatic sea level was relatively low.

12. It assumes that the flora represented by pollen near the base of soils deposited immediately on raised marine strandlines necessarily reflects the climate that was current when the underlying sandy marine unit was being deposited, rather than the climate during accumulation that significantly post-dates the sea level maxima.

During the early part of marine isotope stage 3 (MIS 3) there was a significant period of near interglacial climate in the New Zealand region. The various assumptions inherent in the Suggate

model make it very difficult to fit such an episode into the climate and vegetation history of North Westland.

Questions can be raised in terms of each of the assumptions listed above but there is no doubt about the comprehensive nature of most of the mapping of Quaternary deposits carried out by Dr Suggate in North Westland. As discussed in Chapter 4 the model ties the Quaternary Stratigraphy of North Westland logically into a coherent series of events and defines the relative ages of the various formations.

So overall the model correlates both glacial and interglacial events between North Westland and the Northern Hemisphere and implies these events are more or less synchronous. This may be true for some major global climate events but it is becoming increasingly clear that at other times climate events in the middle to high latitudes of the Southern Hemisphere have not always been synchronous with similar events in the mid to high latitudes of the Northern Hemisphere. Rather they are out of phase, potentially by some thousands of years as demonstrated by Blunier & Brook (2001), Raynaud et al (2000), EPICA Community Members (2006) and Ahn & Brook (2008). Could this asynchronous relationship be a significant factor in the climate history of North Westland? This has already been suggested by Sutherland et al (2007) in terms of the exposure ages of boulders on moraines on the Cascade Plateau in South Westland.

In terms of a detailed understanding of the Quaternary geological, climatic and vegetation history of North Westland it is essential that that the Suggate model be examined in detail. Chapters three to five summarise a variety of data that has a bearing on the interpretation of the timing of events in North Westland. The implications are discussed as well.

So the core of this dissertation is dedicated to an examination of the assumptions underling the Suggate model. It's not so much that there was a clear problem that needed to be fixed but rather that the entire model seemed to be resting on a raft of unproven assumptions. A more in-depth discussion of the detail of the Suggate model can be found in chapters three and five. An alternative model for the Quaternary climate history of North Westland is proposed as a result of the analysis carried out here.

The basic stratigraphic nomenclature is presented in the following table:

Table 1.4 Existing Quaternary Stratigraphy and Marine Isotope Stage Correlation for North Westland (as proposed by Suggate and Waight 1999)

Isotope Stage	**Formation** **Glacial**	**Interglacial**	Climate	Glacial Advance
1		Nine Mile 2 Nine Mile 1	Aranui Interglacial	
2	Moana (minor interval) Larrikins 2 Larrikins 1		Otira Glaciation	Kumara 3 Kumara 2_2
3	None (important interval)			
4	Loopline			Kumara 2_1
5a		Craig?	Kaihinu Interglacial	
5b	None			
5c		Awatuna		
5d	None			

5e	Rutherglen		
6	Waimea	Waimea Glaciation	Kumara 1
7	Karoro Scandinavia	Karoro Interglacial	
8	Tansey	Waimaunga Glaciation	Tansey 2 Re-advance Tansey 1
9	Caledonian		
10	Cockeye	Nemona Glaciation	
11	Whiskey Candlelight		
12	Mudgie Ridge Fm	Kawhaka Glaciation	

CHAPTER TWO: METHODS

2.1 GENERAL METHODOLOGY

2.1.1 Literature Review

During the course of this project large number of published scientific papers and unpublished reports have been collected and studied. In the introductory chapter the key literature relevant to this geochronology project is briefly summarized. The published research is abundant and quite diverse and is discussed in more depth within the body of this dissertation in the context in which it is appropriate. Topics covered in the literature review include: West Coast stratigraphy, geochronology, tectonics, geomorphology, regional and global climate, global sea level, fluvial and marine sedimentary processes, local mineral resources and exploration/mining history.

2.1.2 A Testable Model and a Null Hypothesis

As discussed in Chapter One the "Suggate model" relies on a large number of assumptions relating to the timing of climate and sea level events in North Westland. Beyond about 40 to 45 ka the model has minimal age control other than global correlation. Even in the interval between about 30 and 40 ka the available ^{14}C ages are really only relied upon when they are congenial to the preconceived or desired age. There are multiple examples of rejected radiometric ages and several of these are discussed in chapter six. This strategy of rejecting ages is understandable but risks being labeled as special pleading. The writers' opinion is that the ages should not be cast aside unless there is a particularly good reason for doing so.

The "Suggate model" assembles the glacial, fluvial, lacustrine and littoral sediments of North Westland into an organized stratigraphy. Various formations are assigned classified as having been deposited in glacial, interglacial or interstadial climatic conditions. These climatic events are then correlated with events of global scale. In the model all of the recognized raised marine beach deposits are considered to be older than 90 ka. One relatively low elevation raised beach deposit situated south of Hokitika, just outside the area mapped by Suggate & Waight (1999), was considered by Suggate (pers com) to be slightly younger at about 80 ka (MIS5a). This means that other than Holocene deposits all the raised marine deposits were thought to be too old to be dated directly by the radiocarbon method.

In this dissertation the conceptual model that has guided the rejection of ^{14}C ages is reexamined. This is a valid endeavor even in the absence of new numerical ages. There may be other ways of correlating observed factual data with regional and/or global climate events that would enable us to accept many of the offending radiometric ages.

It is possible to define a null hypothesis and an alternative hypothesis for this project. With regard to this project the "default" model is the "Suggate model" which constitutes the "null hypothesis" (H_o). The purpose of the thesis is to test the null hypothesis to see if it can be proven to be incorrect. Generally a null hypothesis cannot be proven to be correct, nor can an alternative hypothesis be proven to be correct. Even if there are no apparent defects in the null hypothesis it is still valid to test that hypothesis. A failure to find fault with the null hypothesis simply means that one fails to reject it. One of the prime ways that science progresses is by repeated testing of ideas. This process is not

disrespectful to the originator(s) of a hypothesis or model. It can identify areas where the hypothesis/model being tested is indeed incorrect or lacking in some way.

It is also possible to define an alternative hypothesis (H_1). In this case the detail of the alternative hypothesis is formed after careful evaluation of the various types of evidence that are presented. The alternative hypothesis is simply the alternative model proposed in this thesis. It includes a new isotope-stage correlation for the fluvioglacial and marine terraces of North Westland. The effect of this new correlation is to decrease the previously assumed ages for most of the older Quaternary landforms and deposits by as much as a factor of 2. The merits of the two competing hypotheses are discussed. This does not mean that either hypothesis is dismissed in the end, but there may be a preference for one over the other. A failure to reject the null hypothesis, if that were to occur, can not be regarded as a poor result or as a failure for the project. The process of hypotheses testing is perfectly valid and standard procedure in many scientific fields. It involves the usual experimental, observational, inductive and deductive methods used for interrogating abstract ideas. It includes the collection of relevant factual data and the subsequent creation of an informed opinion. These methods are used in analysis of the assumptions listed in section 1.5 of chapter 1.

The IRSL and cosmogenic isotope dating programmes outlined below were designed to help test the null and help create the alternative hypothesis.

A general model of the formation of large fluvial gold placers in North Westland is advanced as part of this dissertation. The model (Rose 2000b) is presented as appendix five. It was developed through adsorption of large quantities of information about gold exploration (drilling and trenching results, observations of gravel exposures in active mines, road cuttings etc), mine production records, mining methods etc, in association with developing knowledge of the stratigraphy, geochronology and climate of the region. This model is a refinement of ideas promoted by Jury and Hancock (1989). The model of gold placer formation is not critical to stratigraphic modeling issues that are the main focus of the thesis. The creation of a placer model was the initial focus of the project and was accompanied by a substantial amount of geomorphological mapping referred to in 3.1.3 below. However, it was found that the placer model could not be completed satisfactorily until the writer had examined the timing of fluvial, glacial and marine deposition, its relation to eustatic and local sealevel, and the evolution of the climate in North Westland. The placer model is included as a statement of progress on that portion of the overall project. It is clearly a "work in progress". The underpinning observational data and exploration data are voluminous and non-digital. Presentation of this material would be a distraction from the main purpose of the thesis. It is not necessary in relation to the discussion of the Quaternary stratigraphy. However, the work serves to introduce the reader to some of the complexity of fluvioglacial deposits in North Westland and this is a valid reason for including it in the thesis.

The process of creating the placer formation model involved the writer in intimate familiarization with the Quaternary geology of North Westland and this can considered as part of the methodology of the full project. Some of the exposures and glacial boulders selected for luminescence and cosmogenic isotope dating were discovered during the fieldwork associated with the gold placer work.

2.1.3 Geomorphology/Mapping/Correlation

At the commencement of this project the writer had many years of experience in dealing with aspects of the Quaternary geology of this region as it applies to the placer gold mining industry. Rather than producing regional maps the focus is placed on a few particular issues and at particular sites.

The study area is almost fully covered by a published 1:50,000 scale geological map (Suggate and Waight 1999). This map and the accompanying bulletin are important documents in the context of the dissertation. Together, they form a solid base line of geological information. Given that the area had already been mapped it was decided that while there would be mapping elements to this PhD project a mapping project as such. Rather, the objective was to look at individual localities and areas in more detail to tease out aspects of the depositional environment, climate, and geomorphic history of the region. For instance a considerable amount of time was spent in the field with an ABNEY level and a handheld GPS unit establishing marine terrace elevations at Point Elizabeth and elsewhere. The survey at Point Elizabeth involved clambering though the thick undergrowth looking at the remains of old alluvial gold workings situated in otherwise undisturbed marine beachsand/gravel.

A considerable amount of air photo and field based geological mapping was carried out in the early stages of the project, partly as a cross-check on the published 1:50,000 mapping, but mainly as part of the initial study of gold placer formation referred to above. These geomorphological maps are included as appendices to the thesis. The original purpose of the mapping was to identify potential economic placer deposits. On the basis of landform types, sedimentary environment, sedimentology and assumed age (based on the Suggate model), targets were proposed for exploration by members of the West Coast Commercial Gold Miners Association. As a result several exploration projects were carried out with poor to marginal economic success. This contributed to the writers decision to examine the Suggate model in more detail. Towards the end of this early portion of the project it was becoming apparent that some of the fluvial deposits underlying what were clearly well-defined meltwater channels may have been rather sort-lived and might not have the significance implied from previous mapping presented in Suggate & Waight (1999).

2.1.4 Stratigraphy

The writer had many years of experience working as a specialist in Quaternary geology in the Placer Mining Industry in North Westland prior to commencing the PhD project. This necessarily required familiarity with the work of Dr RP Suggate. Prior to the commencement of this project the writer considered that mapping and the Quaternary stratigraphy defined by Suggate and Waight (1999) was internally consistent. This opinion was built on consideration of the field evidence underpinning the model, as the same evidence underpins the geological reporting of gold placer deposits. The view that most of the stratigraphic relationships are broadly correct still holds on completion of the project though a number of reservations are discussed in chapter 6. The issues that most urgently seemed to need testing were related to the timing of climatic, erosional and depositional events and the correlation of these events both at inter-regional and hemispheric scales, rather than the general order of events. Impetus for the change in focus was also imparted by recognition that the internal architecture of several of the large glacial outwash terraces was more complex than indicated in Suggate and Waight (1999).

In the early portion of the project a large amount of time was spent studying the geomorphology and subsurface geology both in the field and via topographic and geological maps, cross-sections etc, considering various permutations of terrace correlations and age correlation, uplift rate, terrace elevation, sea level, etc. and the impact on channel shapes, dimensions and gradients etc. This included reaching an understanding of the local correlations between various terrace surfaces, and the potential correlations between sub-surface materials.

2.1.5 Sampling

Much of the work was site specific and relates to the sites chosen for infrared stimulated luminescence (IRSL) sampling and to a lesser extent cosmogenic isotope dating. The IRSL sites are discussed in detail individually. In general terms sites were selected where there were good exposures of materials that might be suitable for dating. For instance road cuttings and faces in quarries and opencast goldmines. The work included recording general details of the site, cleaning parts of the outcrop prior to sampling, recording details of the cleaned face, carrying out the sampling and forwarding the samples to the dating laboratory. This work is discussed further in 2.2 below.

2.1.6 Dating Methods

The methods for relative and numerical dating used during this project are:

- Infrared and optical luminescence dating.
- Cosmogenic isotope dating.
- Compilation and reassessment of published luminescence ages.
- Compilation and reassessment of existing radiocarbon ages Use of basic stratigraphic methods for determining relative ages of materials in the field.
- Correlation of various surfaces using elevations and gradients.
- Correlation of various surfaces and deposits with events in other regions or parts of New Zealand.

Collectively these methods are used to create a chronology for the deposits in question.

2.2 INFRARED STIMULATED LUMINESCENCE DATING, HOKITIKA-GREYMOUTH AREA, NORTH WESTLAND, SOUTH ISLAND

2.2.1 Why Use Luminescence Dating in North Westland?

One of the main focuses of the project has been to collect samples for luminescence dating from suitable sites and materials. The ages obtained from these samples are used in correlation between localities inside the region and with events in other regions.

There are numerous question marks over the age of Late Quaternary deposits in North Westland. This is because many of the dated deposits are near or past the limit of conventional ^{14}C dating. Because there is uncertainty in the numerical age of the youngest of pre Holocene raised marine terraces there are issues with the marine isotope stage correlation of the entire sequence. This makes it doubly difficult to understand the evolution of the local vegetation and the (gold bearing) fluvial and fluvioglacial deposits in North Westland. The depositional processes in fluvioglacial systems are strongly influenced by local base level and so by relative sea level change. Local deposits can't be matched against a eustatic sea level curve unless the age of the deposits is known with reasonable certainty. So the dating uncertainty does not help when one is trying to understand the evolution of the placer deposits.

One of the issues of interest is whether or not MIS 3 glacial, fluvial and littoral deposits are present in this region. If MIS 3 moraines and fluvioglacial outwash are present (not identified to date but certainly possible) then this may go a long way to explaining the paucity of alluvial gold in some parts of the region. Glacial events during MIS 3 are likely to have been of relatively short duration (c.f. MIS

2, MIS 4, and MIS 6). A short duration reduces the likelihood of prolonged gold accumulation in proximal deposits. It would certainly be very useful to have some solid evidence about the age of the Loopline Formation (MIS 4 in the Suggate model) and the underlying Awatuna Formation (MIS 5c in the Suggate model). In order to constrain the evolution of the Quaternary terrace sequence it was proposed that samples would be taken from raised marine terraces as well.

The main reason for trialing luminescence dating was is the perceived difficulty in finding material either suitable for or young enough for radiometric dating (^{14}C). Luminescence was initially proposed primarily because it can be carried out on non-organic (crystalline) materials that dominate the relevant deposits. The method has been applied successfully elsewhere to the types of material that are available in North Westland.

2.2.2 Field Sampling for Infrared and Optical Luminescence Dating.

Thirty two (32) samples (laboratory code listed in table 3.1) were submitted for luminescence dating the writer. These were derived from two sampling campaigns.

The sampling process starts with the fieldwork required for selection of a suitable site that is likely to contain materials suitable for dating. Most sites required preparation prior to sampling. This basically consisted of digging a fresh upright face sufficient deeply into the candidate medium that it would be free from any historic penetration by visible light and free from penetration by roots, cracks and burrowing invertebrates. For the luminescence dating programme there were two rounds of sampling.

After preparation of the site a suitable horizon is selected for sampling. A strong metal cylinder measuring about 120 x 60 mm is hammered carefully into the face. Care is taken to keep the sample isolated as much as is practicable from visible light during and after this process. Immediately after the cylinder has been hammered in it is extracted from the face and quickly wrapped in several layers of thick black plastic.

2.3 LABORATORY METHOD FOR LUMINESCENCE DATING

2.3.1 Multiple aliquot additive dose IRSL dating

For this study the multiple aliquot additive dose (MAA) IRSL method was used was used to date samples from several sedimentary environments. This method that is used principally on the fine-grained polymineral or the quartz fractions that are extracted from the sediment. The procedure involves application of additional doses (beta or gamma) to the natural luminescence on separate aliquots of the sample. This allows the building a dose response curve, simulating future dose and allows interpolation of an equivalent dose to the solar reset level. The basic method was developed for thermoluminescence (TL) dating. It is used in largely unaltered form for IRSL and OSL analysis. The method has proved to be robust as it has yielded ages in agreement with other chronologic control for at least the past c. 100 ka at many locations and in many environments. A review of the general application of the method is beyond the scope of this project.

2.3.2 Sample Preparation

The laboratory work was undertaken by Dr. Uwe Rieser and Mrs Ningsheng Wang, Luminescence Dating Laboratory, School of Geography, Environment and Earth Sciences, Victoria University of Wellington.

The laboratory procedures used for the two sets of samples were the same. Sample preparation was done under extremely subdued safe orange light in a darkroom. The outer surfaces of the samples, which may have seen light during sampling, were removed and discarded. The water content and water saturation of the samples were measured using 'fresh' inside material.

The samples were treated with 10% HCl to remove carbonates until the reaction stopped, then carefully rinsed with distilled water. Thereafter, all organic matter was destroyed with 10% H_2O_2 until the reaction stopped, then carefully rinsed with distilled water. By treatment with a solution of sodium citrate, sodium bicarbonate and sodium dithionate iron oxide coatings were removed from the mineral grains and then the sample was carefully rinsed again.

The grain size 4-11μm was extracted from the samples in a water-filled (with added dispersing agent to deflocculate clay) measuring cylinder using Stokes' Law. The other fractions were discarded. The samples then are brought into suspension in pure acetone and deposited evenly in a thin layer on 70 aluminum discs (1cm diameter).

All depositional ages have been determined using the silt fraction.

2.3.3 Palaeodose measurement and doserate estimation

The palaeodose, i.e. the radiation dose accumulated in the sample after the last light exposure (assumed at deposition), was determined by measuring the blue luminescence output during infrared optical stimulation (which selectively stimulates the feldspar fraction). Luminescence measurements were done using a standard Riso TL-DA15 measurement system, equipped with Kopp 5-58 and Schott BG39 optical filters to select the luminescence blue band. Stimulation was done at about 30mW/cm^2 with infrared diodes at 880Δ80nm. β-irradiations were done on a Daybreak 801E ^{90}Sr, ^{90}Y β-irradiator, calibrated against SFU, Vancouver, Canada to about 3% accuracy. α-irradiations were done on a ^{241}Am irradiator supplied and calibrated by ELSEC, Littlemore, UK.

The palaeodoses were estimated by use of the multiple aliquot additive-dose method (with late-light subtraction). After an initial test-measurement, 30 aliquots were β-irradiated in six groups up to six times of the dose result taken from the test. 9 aliquots were α-irradiated in three groups up to three times of the dose result taken from the test.

The 39 disks were stored in the dark for four weeks to relax the crystal lattice after irradiation. After storage, these 39 disks and 9 unirradiated disks were preheated for 5min at 220C to remove unstable signal components, and then measured for 100sec each, resulting in 39 shinedown curves. These curves were then normalized for their luminescence response, using 0.1s shortshine measurements taken before irradiation from all aliquots.

The luminescence growth curve (β-induced luminescence intensity vs added dose) is then constructed by using the initial 10 seconds of the shine down curves and subtracting the average of the last 20 sec, the so called late light which is thought to be a mixture of background and hardly bleachable components. The shine plateau was checked to be flat after this manipulation. Extrapolation of this

growth curve to the dose-axis gives the equivalent dose D_e, which is used as an estimate of the Paleodose.

A similar plot for the alpha-irradiated discs allows an estimate of the α-efficiency, the a-value (Luminescence/dose generated by the α-source divided by the luminescence/dose generated by the β-source).

The doserate was estimated on the basis of a low level gamma spectrometry measurement.

2.3.4 Gamma spectrometry procedure

The gamma spectrometry measurements on samples RR1 to RR19 were carried out by Riitta Pilvio at the National Radiation Laboratory in Christchurch. The sample preparation methodology for all samples (RR1 to RR34) is outlined below.

The dry, ground and homogenised soil samples were encapsuled in airtight perspex containers and stored for at least 4 weeks. This procedure minimizes the loss of the short-lived noble gas ^{222}Rn and allows ^{226}Ra to reach equilibrium with its daughters ^{214}Pb and ^{214}Bi.

The samples were counted using high resolution gamma spectrometry with a broad energy Ge detector for a minimum time of 24h. The spectra were analysed using GENIE2000 software. The doserate calculation is based on the activity concentration of the nuclides ^{40}K, ^{208}Tl, ^{212}Pb, ^{228}Ac, ^{214}Bi, ^{214}Pb, ^{226}Ra.

All gamma spectrometry measurements on samples RR20 to RR34 were done at the Victoria University Dating Laboratory. The laboratory is calibrated against the National Radiation Laboratory (Christchurch), the Max-Planck-Institute Nuclear Physics Heidelberg and IAEA (International Atomic Agency) in Vienna. This includes the calibration of the spectrometer used in measurements on the samples from this project. Given this calibration there is no reason to suggest that the dose rates measured on the samples taken during this project is in any way incorrect.

As discussed in chapter 5 the dose rate that contributes to the measured palaeodose depends primarily on the radioactivity of the sampled material. This in turn is dependent on the mineralogy of the samples. Overall as a group the samples taken from North Westland to date are more radioactive than the average New Zealand sample. One of the reasons for this is that the sediment simply contains more radioactive minerals by weight than that from many other regions. Rates of sediment production are very high in the widespread areas of crystalline basement exposed in this region. Potassium, uranium and thorium bearing minerals are ubiquitous in the granites and schists here. Fresh bedrock samples yield similar levels of radioactivity (see Herman et al 2009). Therefore it is not surprising that some sedimentary deposits that have been subject to secondary concentration by gravity and grainsize sorting produce unusually high levels of radioactivity. Sand and silt samples collected during this thesis are not the most radioactive ever collected in this region. This title is held by the heavy-mineral rich beachsand deposits situated under the coastal plain at Barrytown. Samples from this area are discussed by Roberts & Whitehead (1991) and Whitehead & Roberts (1991). The thorium and uranium contents are up to an order of magnitude greater than the typical levels measured during this project.

The amount of radioactivity in a sample is generally not a limiting factor in luminescence dating except for very old samples. Intense radioactivity can be a problem if it has an inhomogeneous distribution in a sediment, i.e. the radioactivity is concentrated in a few heavy mineral grains leading exposure of

some quartz/feldspar grains to extremely high doses [those adjacent to the hot grains] and others to low doses. Because the radiation field can't be reconstructed individually for each grain one must use an average doserate. In this respect fine grain dating is more resilient than coarse grain dating. This is because the De determination already utilizes the average dose. Abundant highly radioactive heavy minerals tend to cause a massively scattered De distribution in coarse grained samples and this can be very difficult to interpret. Notably, quartz or feldspar grains with high De may have a high dose either due to burial next to a zircon (for instance), or because it was not bleached at deposition. In the former case the grain should be included in the age calculation, but in the latter case not. However we have no way of distinguishing between these two possibilities unless we know for certain that the sediment contains few highly radioactive minerals. This is one of the reasons why during this project coarse grained fluvial deposits were avoided.

In terms of measurement options Gammaspectrometry is by far the best method. Beta dosimetry only makes sense when doing coarse grain feldspar samples (to determine the percentage of K-Feldspar in a feldspar separate). This percentage is included in the doserate calculation as the so-called internal potassium doserate. Beta dosimetry is not useful when working with fine grain feldspars or sand-sized quartz. ICP-MS on silt is also pointless, as it requires very small sample sizes. One would have to homogenise the sample first to get representative data, which is not a trivial exercise. ICP-MS is expensive and many ICP-MS machines don't analyse for K (as its mass is close Ar which is the counting gas they use), or U and Th, which are at the high mass end. ICP-MS cannot detect radioactive disequilibria, which almost rules it out for OSL dating. ICP-MS could be of use to people doing single grain dating, as they have to make sure they know the composition of every single grain they date. This is one reason why single grain dating is rarely practiced.

In contrast, gammaspectrometry is a well-established method that uses large samples (some tens of grams, which are indeed representative for the OSL sample), and it is relatively inexpensive. All good OSL dating labs use this method. Other methods in use include alpha-counting for U, Th (not as good as gammaspectrometry, but even cheaper and inherently somewhat corrects for disequilibria), delayed neutron analysis for U and Th (doesn't detect disequilibria, which makes it inferior), Atomic Absorption Spectroscopy for K (only used in laboratories that can source cheap labour, as it is time consuming).

2.4 COSMOGENIC ISOTOPE DATING

A number of samples were taken for cosmogenic isotope dating as a joint project between the writer and Dr T Barrows of the Australian National University, Canberra. The purpose of the work was to assess the age of glacial erratic boulders in the Kumara Reservoir-Kapitea Reservoir area near Dillmanstown, and to compare these ages with that proposed for moraines in this area via the Suggate model. Samples were also taken in the vicinity of Moana (Arnold River and Nelson Creek Valleys).

The method involved identifying boulders that were suitable for dating in areas already known to contain large erratic boulders. Suitable samples were chiseled from the upper surfaces of 6 very large erratic boulders near the Kumara Reservoir. A total of 41 samples were taken in the Moana-Aratika-Bell Hill area.

The sampled boulders all project more than 1 metre above the general land surface. Observations were also made in relation to the likely thickness of vegetation and root-mat cover on the boulders. The average declination to the horizon was measured at each sample site.

The laboratory analysis was carried out by Dr Barrows at ANU, Canberra. The fundamentals of the laboratory method are outlined in detail in Barrows et al (2002) as follows:

> "We extracted ^{10}Be and ^{36}Cl from separated quartz and whole-rock dolerite samples, respectively, using standard methods (e.g., Kohl and Nishiizumi, 1992, Stone et al., 1996a). Isotopic ratios were measured by accelerator mass spectrometry on the 14UD accelerator at the Australian National University (ANU) (Fifield et al., 1994). Target element concentrations and the neutron production and capture properties of samples analysed for ^{36}Cl are based on X-ray fluorescence analyses of major elements and inductively coupled plasma mass-spectrometric analyses of trace B, Gd, U and Th. We determined chlorine content by isotope dilution on ~0.5 g splits of the leached rock samples analysed for ^{36}Cl. Full chemical data are given in Appendix 1. Appendices can be obtained from the Australian Quaternary Data Archive (http://rses.anu.edu.au/enproc/AQUADATA/archive.html) or the WDC-A for Paleoclimatology (http://www.ngdc.noaa.gov/paleo/paleo.html).
>
> Exposure ages were calculated following conventional procedures (cf. Cerling and Craig, 1994). Beryllium-10 ages are based on a production rate of 5.02±0.27 atom $g^{-1}a^{-1}$ at 1013 mbar pressure (sea level) and high latitude, scaled for altitude and latitude assuming 3% of ^{10}Be production at sea-level is due to muon reactions. This production rate is derived from calibration measurements on glacially abraded bedrock samples from Scotland (Stone et al., 1998a), corrected by 7% to account for a standardization error in the original measurements. The value is close to the sea-level production rate of ~5.1 atom $g^{-1}a^{-1}$ derived from rescaling the results of all published ^{10}Be calibration measurements, after correcting for overestimation of ^{10}Be production by muon reactions in the original studies (Gosse and Stone, 2001).
>
> Chlorine-36 ages are based primarily on production rates derived at the ANU, using the same laboratory procedures and standards used in this study. For ^{36}Cl production from calcium we use the spallation and muon capture production rates of Stone et al. (1996a, 1998b). For ^{36}Cl production from potassium we use the total production rate given by Stone et al. (1996b), scaled assuming 5% of production at sea-level is due to muon capture (Evans, unpublished data). To ensure our results are comparable with ^{36}Cl exposure ages based on other production rate calibrations (e.g. Swanson et al., 1994; Phillips et al., 1996b) we have included production of ^{36}Cl by spallation of titanium and iron, assuming the theoretical production rates calculated by Masarik and Reedy (1996). Chlorine-36 produced by these reactions is included in calibrations based on whole-rock samples, but not in ANU production rate calibrations based on separated, iron and titanium free minerals. Pending calibration of these minor reactions, we assigned an uncertainty of 750% to the production rate values used.
>
> To calculate ^{36}Cl production by neutron capture on ^{35}Cl and ^{39}K, we used the method of Liu et al. (1994), coupled with a value of 586±40 fast $n\ g^{-1}\ a^{-1}$ for the sea-level secondary neutron production rate in air (Phillips et al., 1996b). We reduced the altitude scaling factor for neutron capture production slightly, based on the assumption that 20% of the fast secondary neutrons are produced by muon capture reactions (Stone et al., 1998b). Due to the low chlorine contents of most of our samples, our results are insensitive to the treatment of neutron capture, which is responsible for an average of 5% of total ^{36}Cl production."

2.5 CLASSIFICATION AND NOMENCLATURE

2.5.1 Subdivision of the deposits

The deposits are subdivided on the basis of:

- Type of sediment e.g. marine; fluvial; glacial; lacustrine
- Relative elevations of the upper surfaces of the various terraces
- Climatic implications of pollen from soil deposits on or within clastic sediments
- Numerical age data
- Contact relationships
- Weathering

2.5.2 Deposits from Glacial/stadial episodes

The key characteristics of deposits produced during glacial/stadial episodes in this region are:

- In the main valleys they tend to contain voluminous sandy fluvial gravel derived mainly from a glacial source. The deposits are aggradational in character, bouldery near the glacial source but maximum clast size decreases down valley.
- The fluvial deposits tend to backfill previously incised channels.
- The surface of accumulation is unbroken across the width of the valley at the completion of aggradation.
- Even when partially destroyed by subsequent incision the aggradational surface can typically be traced for substantial distances up-valley to a glacial moraine. The fluvial gravel underlying an aggradational outwash terrace normally has a clear genetic relationship the glacial till beneath the moraine.
- It has been assumed that each major outwash event can be correlated from valley to valley.
- It has been assumed that each major outwash event has an associated loess sheet that is deposited on older surfaces.
- Inland from the modern coastline the fluvioglacial outwash deposits do not grade down to and interfinger with any coeval marine strandline deposits (at least no such relationships are observed on land today).

2.5.3 Deposits from Interglacial/Interstadial episodes

The key characteristics of formations produced during interglacial/interstadial episodes in this region are:

- Widespread organic soil/peat accumulation, typically with the preservation of abundant wood. These deposits usually contain pollen that is indicative of relatively warm climate, whereas underlying or overlying loess generally contains pollen that is indicative of cooler climate.
- Holocene fluvial deposits in the main valley systems have clearly undergone an episode of aggradation in response to a change in base level (rising sea level in this region).
- The aggradational fluvial deposits typically overlie a basal lag deposit that was formed at a time when then base level was much lower. This lag deposit postdates the previous orbital scale glacial event, forming soon after the glacial maximum while sea level is still very low.
- In the lower portions of the main valley systems interglacial fluvial surfaces have a much lower surface gradient than fluvioglacial deposits.

- Interglacial fluvial deposits are mainly either buried or destroyed by erosional sedimentary processes during subsequent glacial episodes.
- Eustatic sea level is high during orbital scale warm events so heavy mineral rich marine

Reconstruction of the history of local climate and vegetation change, sedimentation, sea level, tectonics and landscape development is based on the stratigraphic model and the correlation of local with global events. The existing marine isotope stage correlation has been somewhat conjectural, as the stratigraphic model is not supported by good numerical age control. It is based on:

- Comparison of the local raised marine terrace sequence with that from the Huon Peninsula, Papua New Guinea. This includes an attempt to apply palaeo sea levels (derived from PNG) to the local sequence. The eustatic sea level maxima have been correlated with the turning points on marine isotope curves developed by the likes of Martinson et al (1987) and Imbrie et al (1984).
- Rather sparse numerical age data of unknown quality and reliability. Until recently most of the ages were obtained via the radiocarbon method. Contamination by young carbon has been shown to be a problem at some sites in this region.
- Estimates of local uplift rates based on assumed palaeo sea levels and assumed ages for the various terraces. Uplift rates have been assigned at different points based on coast parallel correlation of marine terrace fragments.
- Modeling of palaeoclimate from pollen sequences in local soils and noting the various stratigraphic relationships with fluvioglacial and marine sediments.
- An assumption that at the astronomical-scale local climate broadly mirrors Northern Hemisphere climate. This enables a simple correlation between local events and climate proxies including marine isotope curves (proxy sea level/ice volume curves).
- An assumption that the various raised marine strandlines were deposited only during the most prominent eustatic sea level maxima and so can be correlated in a straight forward way with a eustatic sea level curve.
- An assumption that ice volume fluctuations in North Westland reflect astronomical scale changes in global ice volume. Local fluvioglacial outwash deposits are correlated with the main expansions of the Northern Hemisphere ice sheets. The corollary is that periods of intermediate ice volume in the Northern Hemisphere (e.g. MIS 3, 5b, 5d, 7b and 7d) are not represented by substantial fluvioglacial deposits in North Westland.
- An assumption that local cold climate deposits should be correlated with periods when eustatic sea level was low (due mainly to the large volume of the Northern Hemisphere ice sheets).

CHAPTER THREE: RESULTS OF LUMINESCENCE AND COSMOGENIC ISOTOPE DATING AND PREVIOUS NUMERICAL AGE CONTROL

3.1 SUMMARY OF RESULTS FROM THE LUMINECENCE DATING PROGRAMME

In the following tables the IRSL dating results from this project are summarized. The multiple aliquot additive dose (MAA) method for $IRSL_{(blue)}$ dating of K-feldspar is outlined in chapter two. Dating was conducted at the Victoria University of Wellington luminescence dating laboratory. All of the samples were analysed by Dr U Rieser. Ages were obtained from samples that were composed of silt or soil, or where the sand contained a significant silt fraction. Optical luminescence measurements were attempted on quartz from the sand samples where there was minimal silt. The quartz did not give satisfactory results and Dr Rieser considered this to be a failed method on these samples.

Table 3.1 IRSL Sample Locations and dating method

Sample number	Field Code	Grid Reference & Map Sheet (NZMS260)	Location	Dating Method
WLL216	RR1	N 582780 E 234230 J33	Southside, Hokitka	NA
WLL169	RR2	N 2780 E 4230 J33	Southside, Hokitka	Multiple aliquot additive dose
WLL170	RR3	N 2805 E 4340 J33	Southside, Hokitka	Multiple aliquot additive dose
WLL217	RR4	N 2795 E 4260 J33	Southside, Hokitka	NA
WLL147	RR5	N 2805 E 4280 J33	Southside, Hokitka	NA
WLL218	RR6	N 3640 E 5340 J32	Scandinavian Hill, Stafford	Multiple aliquot additive dose
WLL148	RR7	N 3640 E 5340 J32	Scandinavian Hill, Stafford	NA
WLL219	RR8	N 4030 E 5490 J32	Sunday Creek, Chesterfield	Single aliquot regenerative & Multiple aliquot additive dose
WLL220	RR9	N 4025 E 5480 J32	Sunday Creek, Chesterfield	Single aliquot regenerative & Multiple aliquot additive dose
WLL149	RR10	N 6620 E 6330 J31	North Beach, Greymouth	NA
WLL171	RR11	N 6625 E 6320 J31	North Beach, Greymouth	Multiple aliquot additive dose
WLL296	RR12	N 6780 E 6350 J31	Point Elizabeth, Greymouth	Multiple aliquot additive dose
WLL150	RR13	N 6690 E 6345 J31	Point Elizabeth, Greymouth	Single (bad dataset) & Multiple aliquot additive dose
WLL277	RR14	N 5520 E 6060 J32	South Beach, Greymouth	NA
WLL297	RR15	N 5530 E 6060 J32	South Beach, Greymouth	Single aliquot regenerative dose
WLL278	RR16	N 5530 E 6060 J32	South Beach, Greymouth	NA
WLL172	RR17	N 5700 E 6130 J32	Power Road, Karoro	Multiple aliquot additive dose
WLL151	RR18	N 5700 E 6130 J32	Power Road, Karoro	NA
WLL173	RR19	N 6845 E 6480 J31	Rapahoe Beach	NA
WLL524	RR20*	N 7425 E 6730 J31	Schulz Creek, SH6, 12 Mile	Multiple aliquot additive dose
WLL526	RR21	N 6305 E 7760 K31	SH7, Kamaka, Grey Valley	Multiple aliquot additive dose
WLL527	RR22*	N 5450 E 6610 J32	South Beach, Greymouth	Multiple aliquot additive dose
WLL528	RR23	N 5450 E 6610 J32	South Beach, Greymouth	Multiple aliquot additive dose
WLL529	RR24	N 4070 E 5525 J32	Chesterfield Rd, Chesterfield	Multiple aliquot additive dose
WLL530	RR25**	N 3890 E 5555 J32	Upper Sunday Creek	Multiple aliquot additive dose
WLL531	RR26*	N 4700 E 5950 J32	Candle Light, Camerons	Multiple aliquot additive dose
WLL532	RR27	N 4700 E 5950 J32	Candle Light, Camerons	Multiple aliquot additive dose
WLL533	RR28	N 3370 E 6125 J32	Kapitea Reservoir	Multiple aliquot additive dose
WLL534	RR29**	N 4005 E 5220 J32	Blakes Terrace, Awatuna	Multiple aliquot additive dose
WLL535	RR30	N 4005 E 5275 J32	Blakes Terrace, Awatuna	Multiple aliquot additive dose

WLL536	RR33	N 5490 E 6065 J32	South Beach, Greymouth	Multiple aliquot additive dose
WLL537	RR34*	N 5490 E 6095 J32	South Beach, Greymouth	Multiple aliquot additive dose

The geology of the various IRSL sample sites is discussed in chapter 6 where the context of the local stratigraphy and other available numerical dates is evaluated. The details of the sampled exposures are presented in appendix 1. The location of each of the sample sites is presented in appendix 2 on (satellite) photographic images obtained from the google-earth website.

The third column in table 3.2 indicates the designation of the surface or formation at that site as defined or mapped previously, commonly by Suggate & Waight (1999). As discussed in chapter 6, in several cases these designations are likely to be incorrect.

3.2 SUMMARY OF THE DETAILS FOR INDIVIDUAL LUMINESCENCE SAMPLES

In the initial sampling round, conducted over two days, 19 samples were collected from soil horizons and marine sand layers at 14 individual sites. It was hoped that quartz within the sand would yield stable OSL ages. This turned out not to be the case. The initial sampling round was a trial conducted by RV Rose, James Schulmeister, and Uwe Rieser. The sites had previously been identified and prepared by RV Rose. Of the 19 samples taken (RR1 to RR19), 10 produced ages, and 9 failed to produce ages.

Lab Code	Field Code	Formation	Mineral Dated	Size Range Dated	General Nature of Sample
WLL216	RR1	Craig	Unsuitable	-	Beachsand containing minimal silt
WLL169	RR2	Craig	Silt	4–11 μm	Wood bearing basal organic soil on beach sand
WLL170	RR3	Loopline	Silt	4–11 μm	Silt from fine-grained layer between two fluvioglacial gravel units
WLL217	RR4	Blake	Unsuitable	-	Beachsand from long tunnel. Sand contains minimal silt.
WLL147	RR5	Blake	Unsuitable	-	Beachsand from short tunnel. Sand contains minimal silt.
WLL218	RR6	Scandinavia	Silt	4–11 μm	Silt from soil on beachsand
WLL148	RR7	Scandinavia	Unsuitable	-	Beachsand from roadside exposure, Sand contains minimal silt.
WLL219	RR8	Awatuna	Silt	4–11 μm	Wood-bearing organic soil on thin (1m) fluvial gravel above beachsand at Awatuna type-section. Above RR9
WLL220	RR9	Awatuna	Silt	4–11 μm	Beachsand with bands of imbricated pebbles.
WLL149	RR10	Rutherglen	Unsuitable	-	Clean fine-medium beachsand containing minimal silt
WLL171	RR11	Awatuna	Silt	4–11 μm	Basal silty clay immediately above imbricated beach pebbles and below wood bearing organic-rich soil
WLL296	RR12	Blake	Silt	4–11 μm	Interlayered sand and discoidal pebbly beach gravel
WLL150	RR13	Caledonian	Silt	4–11 μm	Silty shallow marine sand
WLL277	RR14	Rutherglen	Unsuitable	-	Shallow marine sand containing minimal silt
WLL297	RR15	Rutherglen	Silt	4–11 μm	Silty shallow marine sand
WLL278	RR16	Rutherglen	Unsuitable	-	Clean shallow-marine fine-medium sand containing minimal silt
WLL172	RR17	Rutherglen	Silt	4–11 μm	Shallow marine samdy silt situated above RR18
WLL151	RR18	Rutherglen	Unsuitable	-	Beach or marine fine to medium sand containing minimal silt
WLL173	RR19	Nine Mile	Unsuitable	-	Early Holocene beachsand containing minimal silt
WLL524	RR20	Awatuna	Silt	4-11μm	Wood bearing basal organic soil on beach sand
WLL526	RR21	Larrikins	Silt	4-11μm	Silt unit within fluvioglacial gravel
WLL527	RR22	Karoro	Silt	4-11μm	Silt with organic layers situated above RR23
WLL528	RR23	Karoro	Silt	4-11μm	Sandy silt resting directly on marine Sand
WLL529	RR24	Loopline	Silt	4-11μm	Silt on fluvioglacial outwash
WLL530	RR25	Waimea	Silt	4-11μm	Soil on fluvioglacial outwash
WLL531	RR26	Rutherglen	Silt	4-11μm	Basal laminated silt resting directly on marine sand
WLL532	RR27	Rutherglen	Silt	4-11μm	Laminated silt and clay on marine sand

WLL533	RR28	Pre-Loopline	Silt	4-11μm	Very hard laminated silt on glacial till, the silt situated below Holocene and buried Late Quaternary organic soils (both wood-bearing)
WLL534	RR29	Pre-Loopline	Silt	4-11μm	Silt between two fluvioglacial gravel units
WLL535	RR30	Blake	Silt	4-11μm	Basal organic soil on marine sand
WLL536	RR33	Rutherglen	Silt	4-11μm	Basal wood-bearing organic soil on marine sand
WLL537	RR34	Karoro	Silt	4-11μm	Basal wood-bearing organic soil on marine sand

Table 3.2 (above) Summary of luminescence sample materials

For the second round sampling was undertaken by RV Rose. The target materials were silts and organic soils. This type of material was chosen because samples from the first sampling round returned ages from the silt fraction rather than the sand fraction. Second time round there was an advantage in that the "clean sands" that were shown not to work well in the first round were avoided.

In the second sampling programme all 13 samples gave an age result by IRSL dating. Nevertheless Dr Rieser's confidence in the luminescence ages varied from sample to sample. The dating procedure is covered in section 2.4 of this dissertation.

Table 3.2 (above) summarises the nature of the individual luminescence samples collected during this project. More detailed geological information on the sample sites is presented in Appendix One.

Table 3.3: Dose-rate contribution of cosmic radiation

Sample no.	**Field code**	**Depth below surface (m)**	**dD_e/dt (Gy/ka)[1]**	**Sample no.**	**Field code**	**Depth below surface (m)**	**dD_e/dt (Gy/ka)[1]**
WLL216	RR-1	22.5	0.0239±0.0012	WLL172	RR-17	3	0.1386±0.0069
WLL169	RR-2	22.5	0.0239±0.0012	WLL151	RR-18	4	0.1221±0.0061
WLL170	RR-3	10	0.0633±0.0032	WLL173	RR-19	1.5	0.1692±0.0085
WLL217	RR-4	17.5	0.0337±0.0017	WLL524	RR20	4.75	0.1104±0.0055
WLL147	RR-5	20	0.0282±0.0014	WLL526	RR21	4.5	0.1138±0.0057
WLL218	RR-6	8	0.0774±0.0039	WLL527	RR22	3	0.1373±0.0069
WLL148	RR-7	8	0.0774±0.0039	WLL528	RR23	4.5	0.1138±0.0057
WLL219	RR-8	15	0.0408±0.0020	WLL529	RR24	0.95	0.1807±0.0090
WLL220	RR-9	17	0.0350±0.0017	WLL530	RR25	3.5	0.1288±0.0064
WLL149	RR-10	5	0.1082±0.0054	WLL531	RR26	5	0.1072±0.0054
WLL171	RR-11	3.5	0.1300±0.0065	WLL532	RR27	7.5	0.0808±0.0040
WLL296	RR-12	2	0.1581±0.0079	WLL533	RR28	1.2	0.1746±0.0087
WLL150	RR-13	6	0.0963±0.0048	WLL534	RR29	14.5	0.0421±0.0021
WLL277	RR-14	1.5	0.1692±0.0085	WLL535	RR30	1.3	0.1722±0.0086
WLL297	RR-15	7.5	0.0816±0.0041	WLL536	RR33	1.1	0.1770±0.0089
WLL278	RR-16	8.5	0.0735±0.0037	WLL537	RR34	2.2	0.1525±0.0076

[1] Contribution of cosmic radiation to the total doserate, calculated as proposed by Prescott & Hutton (1994), Radiation Measurements, Vol. 23.

Table 3.4: Radionuclide and water contents

Sample No.	Field code	Water content d[1]	U (mg/g) from ^{234}Th	U (mg/g)[2] from ^{226}Ra, ^{214}Pb, ^{214}Bi	U (mg/g) from ^{210}Pb	Th (mg/g)[2] from ^{208}Tl, ^{212}Pb, ^{228}Ac	K (%)
WLL216	RR1	1.139	1.86±0.44	2.43±0.13	2.83±0.44	10.4±0.4	1.37±0.05
WLL169	RR2	1.296	3.64±0.40	4.10±0.34	3.80±0.49	16.2±0.7	1.25±0.05
WLL170	RR3	1.305	3.74±0.39	3.21±0.14	3.40±0.49	11.6±0.5	1.89±0.11
WLL217	RR4	1.182	2.26±0.49	2.73±0.08	2.67±0.44	10.8±0.4	1.83±0.07
WLL147	RR5	1.201	4.93±0.53	4.79±0.24	4.37±0.61	26.4±0.7	1.93±0.11
WLL218	RR6	1.297	2.83±0.53	3.67±0.10	3.24±0.53	12.0±0.5	2.29±0.08
WLL148	RR7	1.177	2.73±0.39	3.26±0.26	2.83±0.49	15.4±0.5	2.11±0.11
WLL219	RR8	1.383	2.59±0.77	3.30±0.09	3.64±0.49	8.2±0.4	1.27±0.05
WLL220	RR9	1.215	5.10±0.81	6.97±0.15	5.74±0.69	28.4±0.8	0.86±0.04
WLL149	RR10	1.183	2.79±0.36	3.05±0.30	3.88±0.49	11.0±0.4	1.92±0.07
WLL171*	RR11	1.602	2.82±0.37	4.07±0.39	4.61±0.53	9.79±0.42	1.46±0.10
WLL296*	RR12	1.141	3.00±0.34	2.22±0.04	2.52±0.33	8.22±0.12	1.56±0.03
WLL150	RR13	1.196	2.80±0.35	2.62±0.26	2.35±0.44	10.8±0.4	2.25±0.11
WLL277	RR14	1.067					
WLL297	RR15	1.208	4.43±0.46	3.75±0.06	4.44±0.44	15.7±0.2	1.64±0.04
WLL278	RR16	1.148					
WLL172	RR17	1.336	3.80±0.44	4.23±0.27	4.77±0.61	15.2±0.5	3.26±0.14
WLL151	RR18	1.175	2.79±0.37	3.08±0.21	3.40±0.49	12.1±0.5	1.97±0.12
WLL173	RR19	1.198	6.71±0.65	6.74±0.24	6.23±0.73	45.0±1.0	1.38±0.11
WLL524	RR20	1.306	3.34±0.24	3.16±0.16	3.70±0.23	11.29±0.14	1.67±0.04
WLL526	RR21	1.307	3.70±0.24	3.63±0.17	3.95±0.23	14.18±0.16	2.09±0.04
WLL527	RR22	1.375	2.65±0.25	2.73±0.17	2.99±0.24	10.06±0.14	2.90±0.06
WLL528	RR23	1.257	3.08±0.24	3.21±0.16	3.43±0.22	14.08±0.17	2.01±0.04
WLL529	RR24	1.215	3.27±0.20	3.03±0.13	3.48±0.18	13.45±0.14	1.82±0.04
WLL530	RR25	1.306	4.08±0.32	4.02±0.21	4.19±0.29	13.72±0.18	1.97±0.04
WLL531	RR26	1.229	4.35±0.29	3.72±0.18	4.11±0.25	15.08±0.18	2.05±0.04
WLL532	RR27	1.307	4.13±0.28	3.20±0.18	3.66±0.25	13.11±0.16	2.58±0.05
WLL533	RR28	1.299	3.95±0.26	3.71±0.17	3.92±0.24	12.27±0.15	1.60±0.03
WLL534	RR29	1.183	3.34±0.34	3.10±0.25	3.73±0.30	12.85±0.19	1.96±0.05
WLL535	RR30	1.259	3.53±0.35	3.13±0.23	3.29±0.30	21.75±0.27	0.80±0.02
WLL536	RR33	1.392	3.92±0.28	2.88±0.17	3.28±0.24	13.43±0.17	1.39±0.03
WLL537	RR34	1.3	3.77±0.33	3.20±0.21	3.17±0.27	17.21±0.22	1.59±0.04

[1] Ratio wet sample to dry sample weight. Errors assumed 50% of (δ-1).
[2] U and Th-content is calculated from the error weighted mean of the isotope equivalent contents

Table 3.5: Measured a-value and equivalent dose, dose-rate and luminescence age

Sample no.	Field code	a-value	D_e (Gy)	dD/dt (Gy/ka)	IRSL-age (ka)
WLL216	RR1	N/A		2.44±0.13	**None**
WLL169	RR2	0.052±0.011	116.6±5.8	3.47±0.32	**33.6±3.6**
WLL170	RR3	0.061±0.005	196.3±10.3	3.46±0.31	**56.8±5.9**
WLL217	RR4	N/A		2.83±0.19	**None**
WLL147	RR5	N/A		4.23±0.31	**None**
WLL218	RR6	0.051±0.013	477.0±20.7	3.87±0.36	**123.3±12.7**
WLL148	RR7	N/A		3.53±0.24	**None**
WLL219	RR8	0.084±0.007	93.6±2.0	2.69±0.27	**34.8±3.5**
WLL220	RR9	N/A	229.6±13.8 (259.4±29.2)	3.84±0.28	**47.8 ± 6.6 (54.0 ± 7.3)**
WLL149	RR10	N/A		3.06±0.21	**None**
WLL171[1]	RR11		140.3±4.7	2.60±0.35 (2.73±0.35)	**53.9±7.6 (51.5±6.9)**
WLL296	RR12		120.4±3.6	3.05±0.15 (2.97±0.15)	**39.5±2.4 (40.6±2.4)**
WLL150	RR13	N/A	331.5±8.3	3.19±0.23	**87.1±8.3**
WLL277	RR14	N/A			**None**
WLL297	RR15	0.058±0.015	270.1±4.0	4.10±0.33	**65.9±5.4**
WLL278	RR16	N/A			**None**
WLL172	RR17	0.057±0.008	319.3±43.0	5.02±0.48	**63.6±10.5**
WLL151	RR18	N/A		3.21±0.22	**None**
WLL173	RR19	N/A		5.47±0.37	**None**
WLL524	RR20**	0.123±0.021	165.4±21.0	3.89±0.38	**42.5±6.8**
WLL526	RR21	0.090±0.007	152.9±5.3	4.34±0.37	**35.3±3.2**
WLL527	RR22**	0.154±0.011	384.8±11.9	4.56±0.45	**84.3±8.7**
WLL528	RR23	0.096±0.010	288.4±11.8	4.39±0.34	**65.7±5.7**
WLL529	RR24	0.086±0.012	227.2±8.4	4.22±0.30	**53.8±4.3**
WLL530	RR25*	0.095±0.008	334.2±18.1	4.41±0.37	**75.9±7.6**
WLL531	RR26**	0.081±0.034	332.0±11.0	4.63±0.55	**71.7±8.8**
WLL532	RR27	0.08±0.02*	418.5±15.5	4.34±0.43	**96.5±10.2**
WLL533	RR28	0.062±0.004	278.7±9.7	3.57±0.29	**78.1±6.8**
WLL534	RR29*	0.076±0.020	355.3±8.6	4.18±0.34	**84.9±7.2**
WLL535	RR30	0.069±0.011	243.5±19.8	3.83±0.31	**63.6±7.4**
WLL536	RR33	0.087±0.019	183.6±12.1	3.26±0.35	**56.3±7.1**
WLL537	RR34**	0.048±0.006	337.2±19.8	3.64±0.30	**92.5±9.4**

* a-value estimated (sample was saturated)

[1] The doserate and age for this sample was corrected for a radioactive disequilibrium (in brackets is the uncorrected age, i.e. it was calculated using the U-equivalent of the isotope 226-Ra only). As the level of disequilibrium over time is unknown, this age is only a better estimate and cannot be seen as the 'true' age.

Dr Rieser commented that owing to high doserates (even in a NZ context) some of the older samples close to saturation.

Table 3.6 Summary of Sample Elevations, Depths and Luminescence Ages

Sample number	**Field Code**	**Approximate Elevation (m amsl)**	**Depth Below Original Surface (m)**	**IRSL Age (Ka)**
WLL216	RR1	8-10	20-25	None (Not suitable)
WLL169	RR2	9-11	20-25	33.6 ± 3.6#
WLL170	RR3	25	10	56.8 ± 5.9#
WLL217	RR4	15-18	15-20	None (Not suitable)
WLL147	RR5	20	20	None (Not suitable)
WLL218	RR6	110-115	8	*123.3 ± 12.7#
WLL148	RR7	110-115	8	None (Not suitable)
WLL219	RR8	50	15	*34.8 ± 3.5, 37.8 ± 3.8#
WLL220	RR9	48	17	(47.8 ± 6.6*) 54.0 ± 7.3
WLL149	RR10	65-70	5	None (Not suitable)
WLL171	RR11	44-45	2-5	53.9 ± 7.6
WLL296	RR12	30-33	2	*39.5 ± 2.4
WLL150	RR13	115-120	5-7	(87 ± 8.3) 98.6 ± 24.4
WLL277	RR14	60	1-2	None (Not suitable)
WLL297	RR15	52-55	7-8	*65.9 ± 5.4
WLL278	RR16	52-55	8-9	None (Not suitable)
WLL172	RR17	75-80	3	63.6 ± 10.5 #
WLL151	RR18	75-80	4	None (Not suitable)
WLL173	RR19	6-7	1-2	None (Not suitable)
WLL524	RR20	45	4.5-5	42.5±6.8**
WLL526	RR21	30	4-5	35.3±3.2**
WLL527	RR22	75	3	84.3±8.7**
WLL528	RR23	73	4.5	65.7±5.7**
WLL529	RR24	65	0.9-1.0	53.8±4.3**
WLL530	RR25	100	3.5	75.9±7.6**
WLL531	RR26	62	5	71.7±8.8**
WLL532	RR27	62-64	7.5	96.5±10.2**
WLL533	RR28	165	1.2	78.1±6.8**
WLL534	RR29	18-22	13-16	84.9±7.2**
WLL535	RR30	30	1.3	63.6±7.4**
WLL536	RR33	65-70	1.1	56.3±7.1**
WLL537	RR34	75	2.2	92.5±9.4**

= ages supplied by Dr Rieser during 2002

* = ages supplied by Dr Rieser during 2004
** = ages supplied by Dr Rieser during 2008
( ) = single aliquot fine grain-IRSL, the other ages are by multiple aliquot fine-grain IRSL

In terms of the underlying data for the calculation of (feldspar) ages, for most of the samples taken during this project there are no "equivalent dose (ED) distributions". Such distributions relate to the single aliquot method rather than the multiple aliquot method. Attempts were made to date quartz but the results were unsatisfactory so no ages were produced. ED distributions exist for these experiments on quartz but they are not presented here.

For this project shine-down data from five (RR15, RR21, RR25, RR28, and RR33) of the thirty two individual luminescence samples have been selected for display. These samples are representative of the general range of depositional environments from which material was collected. The underlying data are presented graphically in appendix four. All of the digital data is archived at the dating laboratory. In each case the shinecurves shown are representative for the sample. For each sample results are displayed for an unirradiated disc ('natural') and a disc irradiated with the highest dose. During the dating process a very large quantity of data is produced. Overall, a MAAD age is based on 48 shinedown curves, plus 58 normalisation measurements, plus 10 shinedown curves for the fading test. It is not particularly informative or practical to present all of the data. In terms of this data the writer is not directly accountable for its production and played no part in the laboratory analysis. The analysis was done independently at the laboratory which minimises the chance that prior expectations might influence the resulting ages.

3.3 SUMMARY OF THE AGE AND ELEVATION OF THE IRSL SAMPLES

In figures 3.1 and 3.2 (below) a number of the new IRSL ages are plotted against elevation. These are the samples that come from:

1. Strandline or marine sediments that were at or very close to sea level (within ~5 m) during deposition
2. Silt deposits resting immediately on the upper surface of the strandline deposits that were very close to sea level (within ~5 m).

Part of the scatter in figures 3.1 and 3.2 is due to variation in the uplift rate parallel to the coastline in North Westland. Part of the scatter is due to the certainty that the different strandlines were formed at under different eustatic sealevel conditions and potentially under different local crustal isostatic conditions. Part of the scatter relates to the fact that some samples were from the marine/littoral deposits in question and some are derived from the silt/soil coverbeds. In addition, as discussed in chapter five (part 5.7) the samples are impacted to a variable extent by partial bleaching, which impacts on the luminescence signal measured during the dating process and so on the quoted age.

In figure 3.1 the samples are colour coded with respect to the formation from which they were taken. Despite the scatter it is reasonably clear that the older samples have been subjected to more tectonic uplift than the younger samples.

Figure 3.1: IRSL(Blue) sample age, elevation and formation for samples that are either marine/littoral or resting directly on marine/littoral sediments,

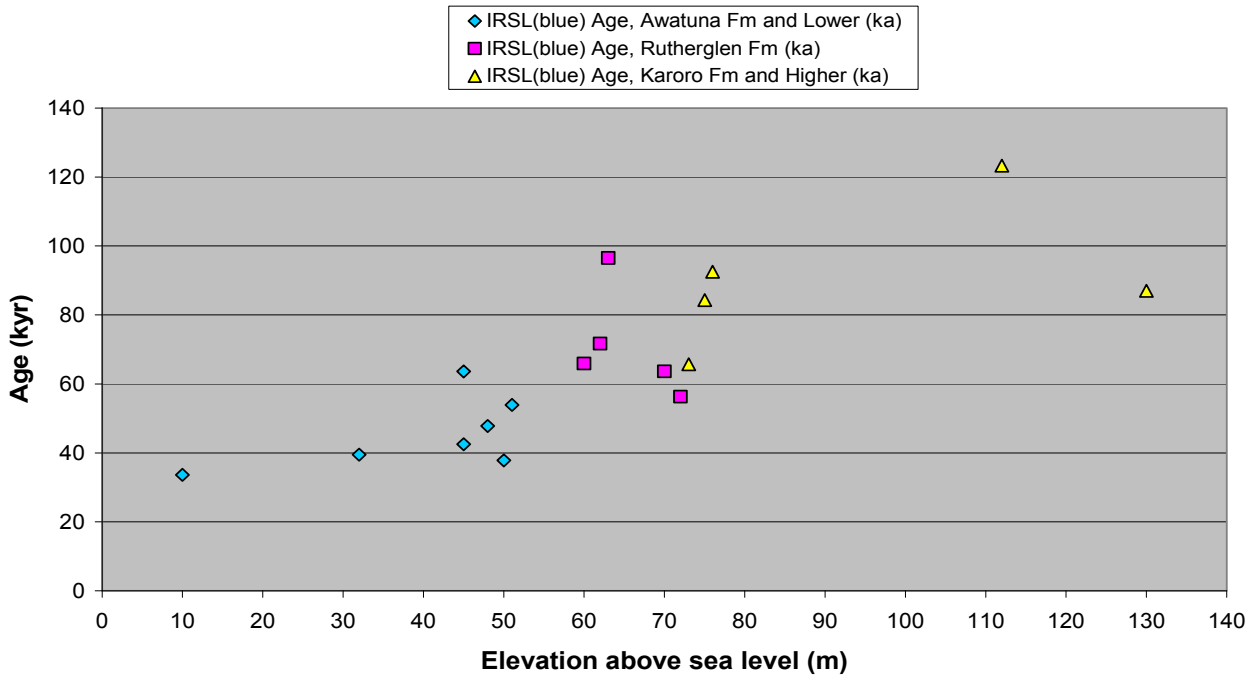

Figure 3.2: $IRSL_{(blue)}$ age (this study) with 1SD errors vs elevation above mean sea level for marine/littoral samples and samples from on-shore silt resting on marine/littoral sediments

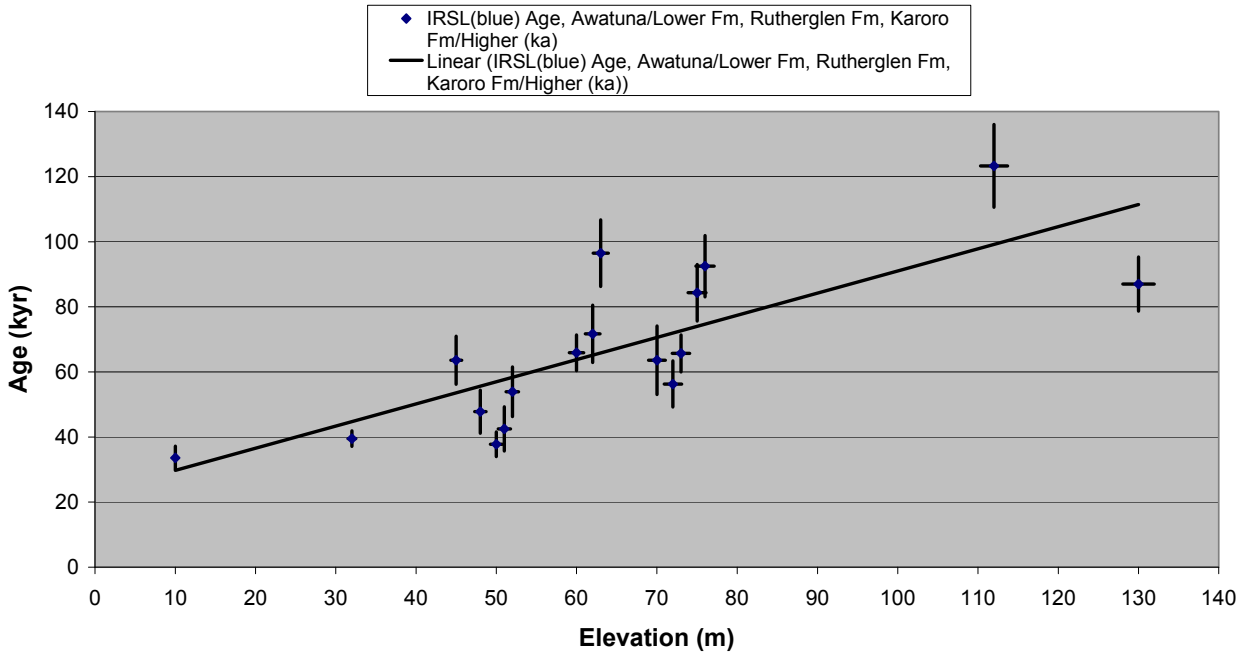

3.4 NON-SUITABILITY FOR OSL DATING OF QUARTZ IN SAND AND GRAVEL FROM NORTH WESTLAND

The quartz recovered from the mainly sandy samples taken during the first sampling campaign (Rose, Shulmeister, and Rieser) was not suitable for OSL dating. The quartz OSL was extremely dim under green light stimulation, and the quartz showed high sensitivity change which leads to extreme scatter in the dataset. In attempting to purify the quartz, complete removal of contamination by other minerals was not possible. The main problem was feldspar which is of a very similar density to quartz. It is likely that feldspars are ingrown within many of the quartz grains, making attempts to remove them by etching futile. As the feldspars give much brighter OSL compared to NZ quartz, even a tiny contamination dominates the OSL signal. Most of our quartz aliquots displayed OSL of dubious origin. De values scattered over orders of magnitude [further enhanced by an inhomogenous radiation field caused by heavy minerals], and negative De was not uncommon (i.e. implying that the sample would be deposited in the future). Clearly it would be imprudent to simply average these De values to obtain an age. Virtually all of the aliquots suffered from one or the other detrimental effect.

Subsequent to the collection of samples for this project Preusser et al (2006) published a commentary on the luminescence dating of quartz sand from Westland. They also found quartz from this region to be unsuitable for luminescence dating. They report that the quartz suffers from 3 problems:

1. The OSL intensity of samples is low because most of the quartz grains are “dim”.
2. The samples were affected by thermal transfer that had an effect on equivalent dose determination.
3. The samples showed poor performance in the SAR protocol

In addition Preusser et al (2006) speculated that the quartz grains appeared to have had a short sedimentary history resulting in a lack of repeated irradiation/bleaching cycles. This contributes to a paucity of defects/traps many of which are created by repeated natural cycles of irradiation and readout.

Given the difficulty experienced with dating quartz from sand samples in the first sampling campaign, this type of material was avoided in the second round of sampling. In the second sampling campaign soil/silt horizons were targeted exclusively for IRSL dating. This has resulted in a suite of ages that place limits on the commencement or completion of deposition, but which do not define the timing of deposition of either the marine sand or alluvial/glacial gravel directly.

The results of the IRSL sampling carried out for this project are discussed further in Chapters five and six. The writer has a number of concerns about dating carried out by luminescence methods in North Westland and these are discussed in chapter five. Broadly speaking the conclusion is that for North Westland the IRSL method commonly overestimates the sample ages, particularly when conducted on the sand-sized K-feldspar component of fluvial and littoral sediments.

3.5 COSMOGENIC ISOTOPE DATING IN THE KUMARA RESERVOIR AND MOANA AREAS

3.5.1 Kumara Reservoir

During 2003 sampling for surface exposure dating was carried out by Dr Tim Barrows of ANU (Canberra) and the writer near Kumara. During 2004 further sampling was carried out near Moana

(summarised below). In the Kumara area samples were taken from 6 large glacial erratic boulders in the vicinity of Loopline Road and the Kumara and Kapitea Reservoirs. Sample processing and age calculations were carried out by Dr Barrows. The boulders are situated in an areas mapped as terminal and recessional moraine by Suggate & Waight (1999).

Kumara reservoir is situated between Dillmanstown and Stafford. Sample locations are indicated in figure 3.1. Other notable features include Loopline Road, which crosses the narrow neck between the two lakes and the neck itself, which is probably a recessional moraine. The most prominent of the terminal moraines in this area run NNE-SW just west of the two lakes. The position of the highest of these is defined by the (electricity) pylon track that also runs SSW-NNE just to the west of the two lakes.

At the time of writing four of the samples (LL-02, LL-04, LL-05, LL-06) had been fully processed. The samples were taken from an area mapped as "Loopline Formation" (by Suggate & Waight 1999) and are listed at the top of table 3.7. This general area has been considered to be part of the type section for the Loopline Formation.

These Loopline Road sample ages indicate potential boulder deposition around 20 to 24 ka with an outlier at around 14 ka. The immediate suspicion is that the exceedingly prominent moraine ridges situated adjacent and just west of the Kumara and Kapitea Reservoirs are, at least on the surface, features that formed during MIS 2. The Loopline Formation is correlated with MIS 4 in the Suggate model, so it was anticipated that it would produce exposure ages of around 65 ka. These results are discussed in more detail in Chapter 5.

It should be noted that the two relatively shallow lakes visible in figure 3.3 are part of a hydroelectric scheme. At the time of sampling the water level was lower than depicted in the figure, and consequently the lake edges had retreated at that time.

Note that in table 3.4 the samples are grouped by area and geological formation. The classification by formation adopted here was taken directly from the 1:50,000 scale map sheet by Suggate & Waight (1999) at the time of sampling. It does not represent an interpretation of the ages that were produced.

Four areas that had been mapped as Loopline Formation have been sampled for cosmogenic isotope dating. One of these areas is situated at Loopline Road. The other three are in the Moana area. At the time of writing 11 ages had been produced from 17 samples. None of the ages fall within MIS4 which is the mapped age. The oldest of this broad group (LPL-08) is dated at 35.3 ± 3.0 ka.

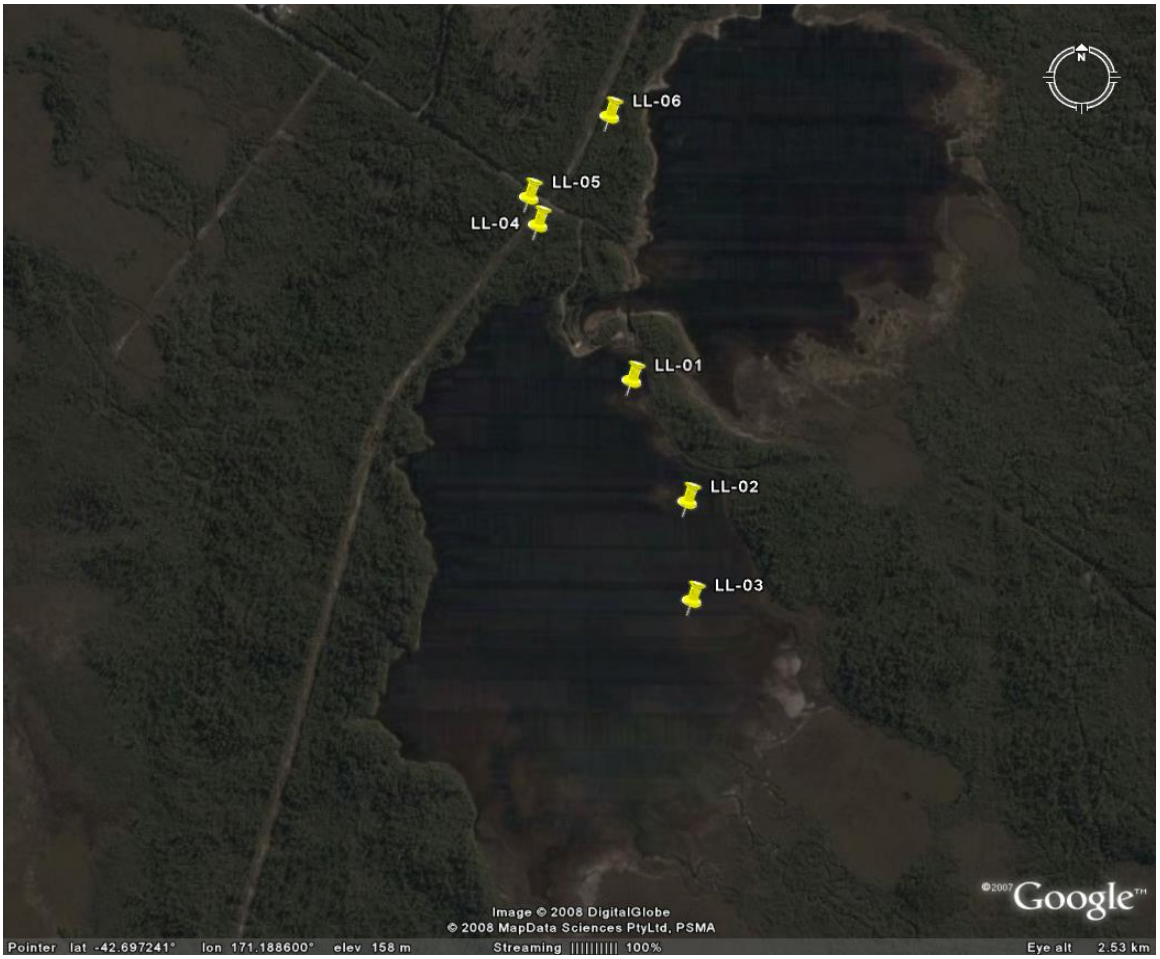

Figure 3.3. Location of cosmogenic isotope sample sites adjacent to the Kumara Reservoir.

Table 3.7 Be-10 Exposure ages

Sample	Lab code	Grid Reference (NZMS 260 J32)	$[^{10}Be]_c$ (x10^4 g^{-1})	Σ Production rate (atoms $g^{-1}.yr^{-1}$)	Exposure age (ka)
Loopline Formation (Loop Line Road, Kumara)					
LL-02	ANU-M347-29	N327 E819	12.5 ± 0.56	5.473 ± 0.382	23.0 ± 1.9
LL-04	ANU-M347-24	N334 E814	12.3 ± 0.55	5.513 ± 0.384	22.4 ± 1.9
LL-05	ANU-M347-24	N335 E814	7.67 ± 0.56	5.415 ± 0.378	14.2 ± 1.4
LL-06	ANU-M347-26	N338 E816	10.8 ± 0.66	5.517 ± 0.385	19.7 ± 1.8
Loopline Formation (Arnold River valley)					
LPL-02	ANU-M392-22		11.3 ± 0.75	5.507 ± 0.384	20.7 ± 2.0
LPL-04	ANU-M392-10		6.92 ± 0.48	5.357 ± 0.374	13.0 ± 1.3
LPL-05	ANU-M392-24		10.1 ± 0.43	5.297 ± 0.369	19.2 ± 1.6
Loopline Formation (Molloys Lookout)					
LPL-06	ANU-M392-25		17.1 ± 0.80	5.836 ± 0.407	29.4 ± 2.5

LPL-07	ANU-M430-27	11.6 ± 0.75	5.799 ± 0.404	20.1 ± 1.9
Loopline Formation (Bell Hill Farm)				
LPL-08	ANU-M392-26	20.9 ± 1.00	5.979 ± 0.417	35.3 ± 3.0
LPL-11	ANU-M392-27	14.9 ± 0.67	5.999 ± 0.418	25.0 ± 2.1
Moana Formation (Lake Brunner)				
MNA-03	ANU-M422-03	3.78 ± 0.35	5.152 ± 0.359	7.3 ± 0.8
MNA-04	ANU-M421-19	4.97 ± 0.24	5.247 ± 0.366	9.5 ± 0.8
MNA-05	Not run			
MNA-06	ANU-M422-04	7.64 ± 0.41	5.414 ± 0.377	14.1 ± 1.2
MNA-07	ANU-M421-20	7.63 ± 0.37	5.442 ± 0.379	14.1 ± 1.2
MNA-08	ANU-M422-05	7.68 ± 0.41	5.403 ± 0.377	14.3 ± 1.3
MNA-09	Not finalised			
MNA-10	ANU-M430-21	4.97 ± 0.36	5.377 ± 0.375	9.3 ± 0.9
LAR-09	ANU-M392-21	7.95 ± 0.59	5.554 ± 0.387	14.4 ± 1.5
Larrikins Formation (Lake Brunner)				
LAR-01B	ANU-M422-06	9.45 ± 0.47	5.844 ± 0.407	16.2 ± 1.4
LAR-02	ANU-M392-19	9.33 ± 0.97	5.774 ± 0.403	16.2 ± 2.0
LAR-03	ANU-M392-20	11.7 ± 0.68	5.805 ± 0.405	20.3 ± 1.8
LAR-04	ANU-M422-07	9.51 ± 0.42	5.778 ± 0.403	16.5 ± 1.4
LAR-05	ANU-M422-08	9.93 ± 0.75	5.777 ± 0.403	17.2 ± 1.8
LAR-06	ANU-M430-22	9.54 ± 0.55	5.852 ± 0.408	16.4 ± 1.5
LAR-07	ANU-M422-10	11.6 ± 0.55	5.577 ± 0.389	20.9 ± 1.8
LAR-08	ANU-M422-11	9.38 ± 0.40	5.579 ± 0.389	16.9 ± 1.4
LAR-10	ANU-M422-12	9.20 ± 0.37	5.774 ± 0.403	16.0 ± 1.3
LAR-11	ANU-M392-22	11.2 ± 0.61	5.585 ± 0.389	20.1 ± 1.8
LAR-12	ANU-M422-13	10.3 ± 0.69	5.758 ± 0.401	18.0 ± 1.7
LAR-14	ANU-M430-23	8.99 ± 0.56	5.664 ± 0.395	15.9 ± 1.5
LAR-15	Not precipitated			
LAR-16	Not finalised			
LAR-17	ANU-M422-14	9.48 ± 0.48	5.396 ± 0.376	17.6 ± 1.5
LAR-18	Not finalised			
LAR-19	ANU-M422-15	8.67 ± 0.52	5.412 ± 0.377	16.1 ± 1.5
LAR-20	ANU-M430-26	9.35 ± 0.60	5.420 ± 0.378	17.3 ± 1.6

Data are normalised to NIST SRM 4325 assuming $^{10}Be/^{9}Be = 3.00 \times 10^{-11}$ Carrier $^{10}Be/^{9}Be = <1 \times 10^{-15}$. ^{10}Be decay constant = 4.62×10^{-7} yr^{-1}. Site data for the exposure ages are given in Table A4.4h (Appendix 4).

3.5.2 Moana

A total of 41 cosmogenic isotope dating samples were taken from glacial erratic boulders in the Moana area. Ten samples were taken from moraines thought to be of the Moana Formation. Twenty samples were taken from moraines mapped as Larrikins (2) and Larrikins (1) Formations by Suggate & Waight (1999). Eleven samples were taken from moraines mapped as Loopline Formation by Suggate & Waight (1999). The sample locations are displayed in figures 3.4, 3.5, 3.6, and 3.7.

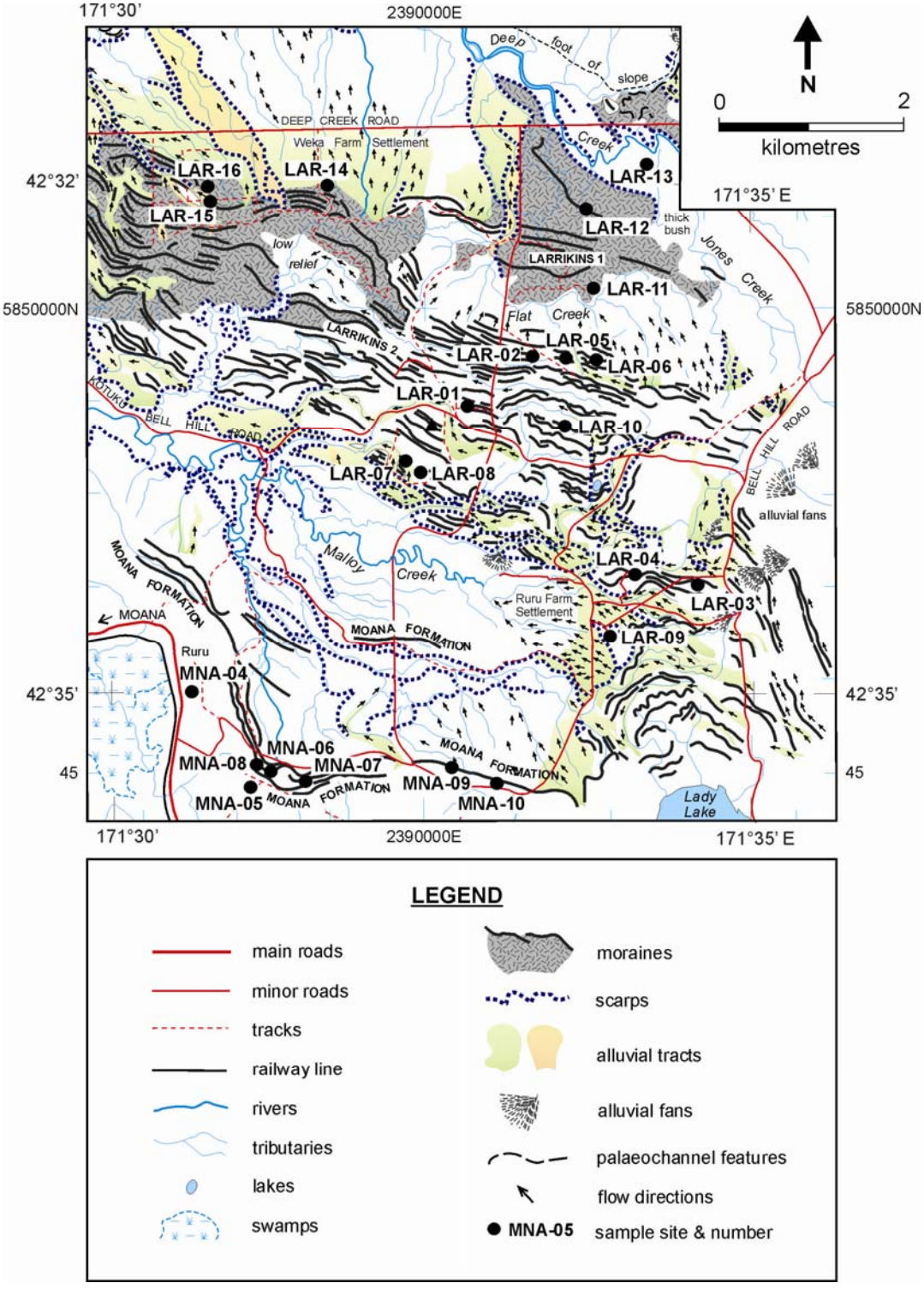

Figure 3.4 (above) Cosmogenic Isotope sample sites in the Deep Creek - Molloy Creek area.

On geomorphic, elevation and dating grounds it appears that the Loopline till and outwash may be the result of two separate glacial advances. Boulders sampled at the Nelson Creek Farm Settlement (figure 3.3) and just east of Molloys Lookout (figure 3.3) have ages ranging from 20.1±1.9 to 35.3±3.0 ka. Boulders sampled from the Blair Farm Settlement in the Arnold Valley gave ages ranging from

13.0±1.3 to 20.7±2.0 ka and may be from a significantly younger surface. This terrace, located just west of Molloys Lookout is significantly lower than the terrace sampled on the east side of the lookout. It may be more appropriate to define the till and outwash to the west of Mollys Lookout as Larrikins(1) Formation rather than Loopline.

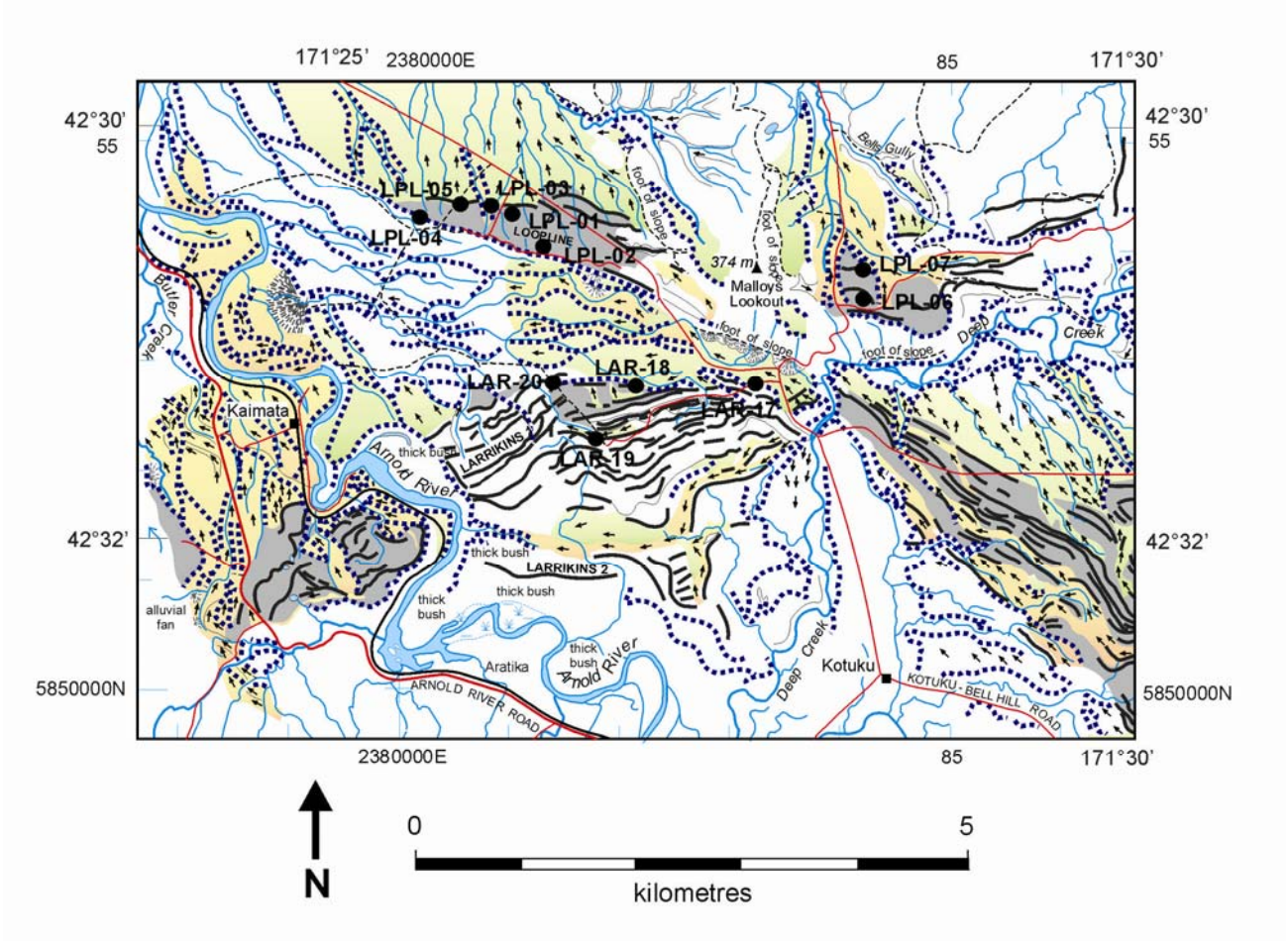

Figure 3.5 Cosmogenic Isotope sample sites in the Kotuku-Aratika area.

Re-assignment of the Loopline Formation at the Blair Farm Settlement to the Larrikins(1) Formation provides an opportunity for separate Larrikins(1) and Larrikins(2) meltwater flow paths. Separate discharge routes might have been expected if the two Larrikins moraine belts relate to different ice advances within the Otira Glaciation.

Dating of the Larrikins and Moana Formations was not one of the primary focuses of this project. However, the opportunity arose after the commencement of the project. Due to funding constraints the processing of the samples was rather slow. The ages were made available vey late during the final production of the thesis.

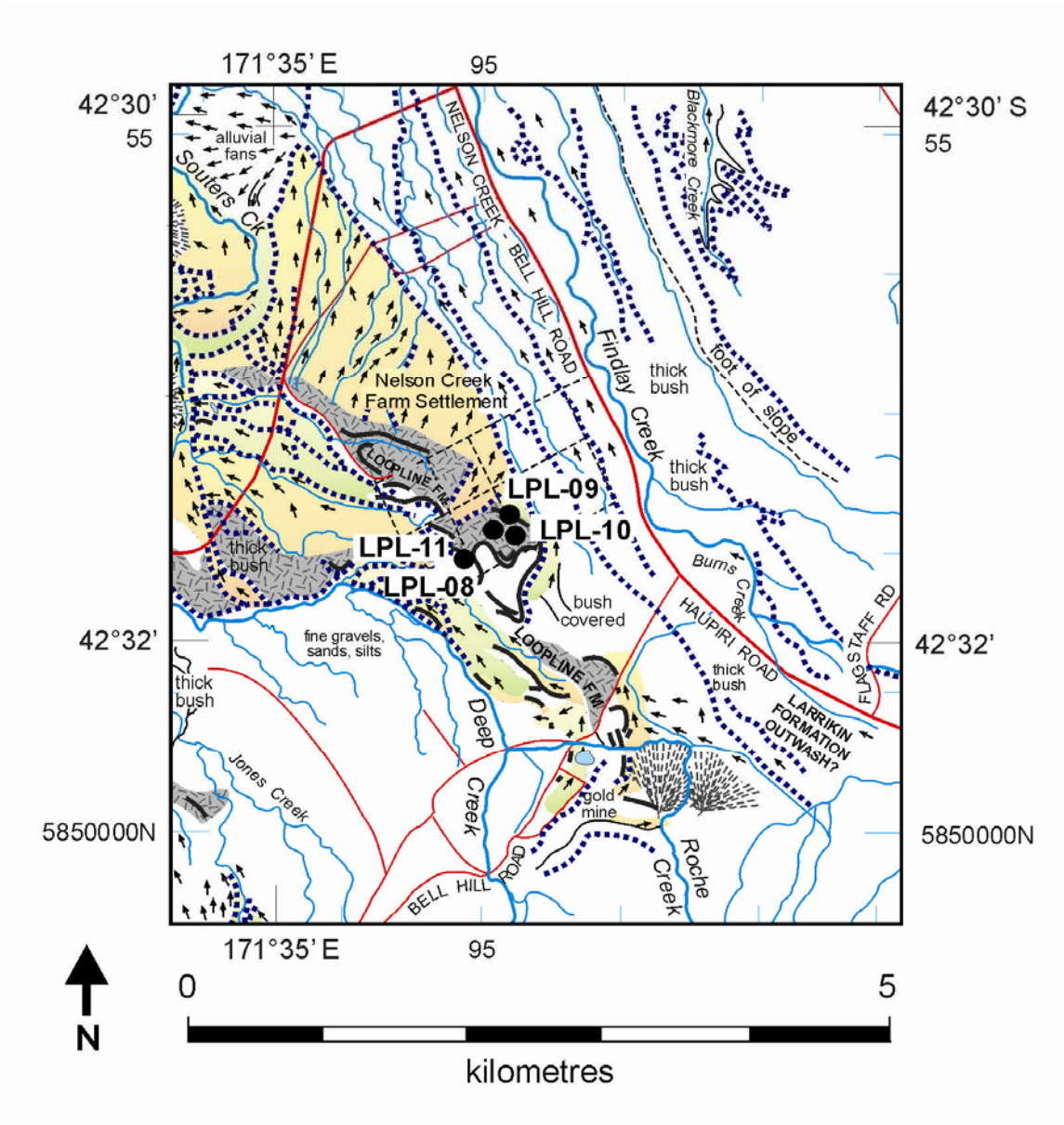

Figure 3.6 Cosmogenic Isotope sample sites in the Nelson Creek Farm Settlement area.

The cosmogenic isotope ages from the Nelson Creek Farm Settlement are important in the context of numerical dating carried out nearby. A number of IRSL ages were produced from the genetically linked outwash terrace just to the NNW by Preusser et al (2005). These ages are discussed in chapters 5 and 6 of this thesis in relation to partial bleaching and the utility of IRSL dating on feldspar in sand from proximal fluvioglacial gravel and to the age of the Loopline Formation.

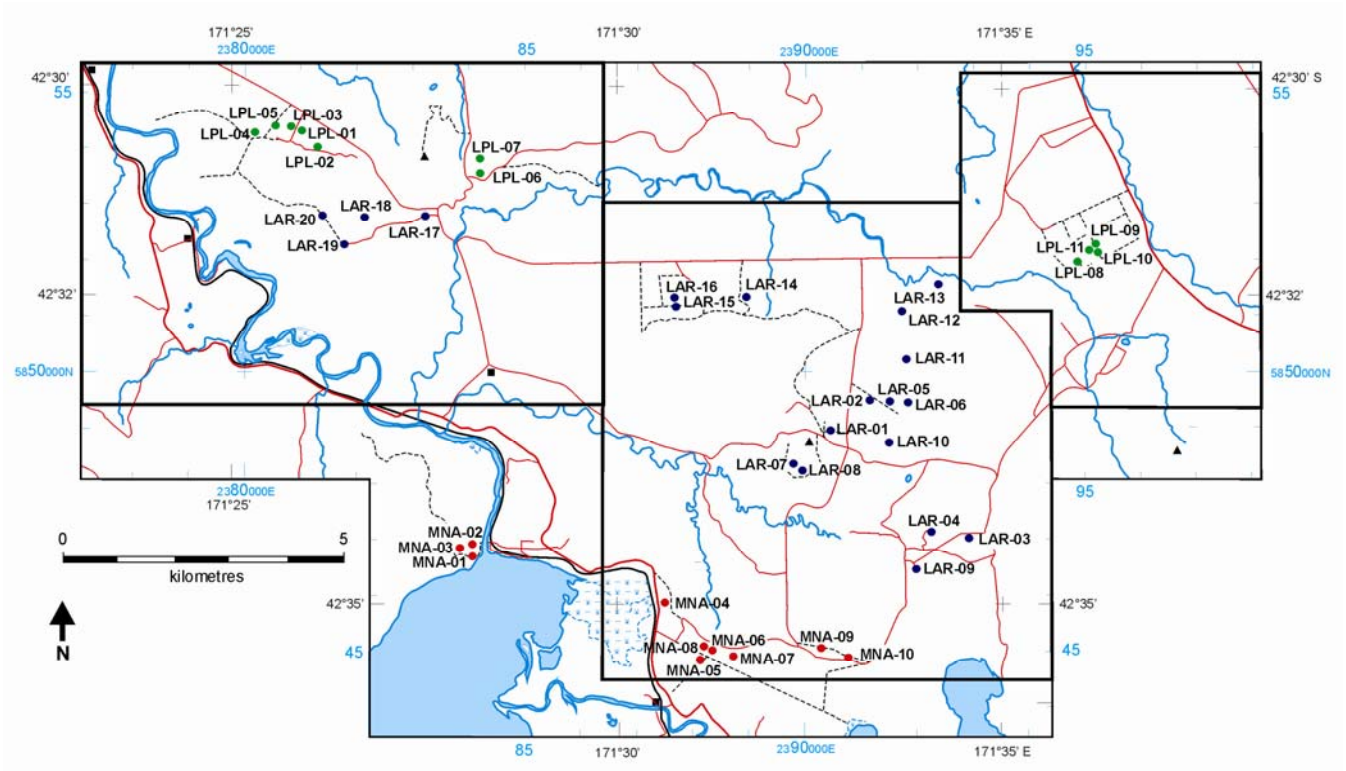

Figure 3.7 Summary map for numerical dating in the Moana-Kotuku-Bell Hill area. The large lake is Brunner (*Moana*). The outlet river running to the northwest is the Arnold River. The major tributary is Deep Creek. The Nelson Creek Farm Settlement is in the NE corner and Lady Lake is in the SE corner.

3.6 PREVIOUS NUMERICAL AGE CONTROL

3.6.1 Introduction

The following is a discussion of some issues surrounding the application and interpretation of numerical dating in North Westland. Numerical dating methods that have been applied in Quaternary studies in Westland include:

i) Thermoluminescence (TL), Optical and Infrared luminescence (OSL & IRSL)
ii) Radiocarbon
iii) Amino Acid Racemisation (AAR)
iv) Tephrochronology

Luminescence dating is discussed in detail in Chapter two, above in parts 3.1 to 3.3, in Chapter 5 and in Appendix 1.

3.6.2 Radiocarbon

Historically the most widely applied numerical dating method in North Westland is radiocarbon dating. This work commenced in the 1950's and has continued to the present.

The Suggate model is based on a selective interpretation of the existing database of numerical ages. The internal justification hinges in part around an assumption that in this region radiocarbon dating is unreliable. It has been demonstrated by Hammond et al (1991) that at one site on Grahams Terrace near Nelson Creek

(discussed in relation to the Waimea Formation in Chapter 6) sampled carbonaceous material was been significantly contaminated by younger carbon. It has also been demonstrated by Newnham et al (2007a) for a site in South Westland. But in the Suggate model numerous ^{14}C ages have been rejected at other sites without hard evidence for significant contamination having been presented. On the other hand there are several sites where the dating by ^{14}C appears to have given repeatable, internally consistent results and there does not appear to be any problem with contamination. For instance at Kamaka by Denton et al (1999) and Gage & Suggate (1958). Until recently the absence of widespread numerical dating by another method has made the existing isotope stage correlation virtually unfalsifiable and has created substantial scope for the development of circular arguments. Potentially the introduction of only a few numerical ages from well-chosen pre-MIS 2 sites could cause the collapse of the isotope stage correlation defined by the Suggate model.

The sites where significant contamination appears to be genuine are in relatively young material (post 30 ka) and have several things in common. First they are in soil deposits dominated by loess. Second, although the loess may be thick at these sites, it is not buried by younger fluvial or marine deposits. So the dated material has always been close to the ground surface over periods of 10's of thousands of years. The loess has always been subject to the percolation of abundant groundwater. This is a high rainfall region so podzolised soils are almost always damp, if not saturated. Carbon and aluminium complexes can be mobilised and transported by organic acids then redeposited within the profile. For some sites it has also been proposed that the soils have been reduced in mass and thickness by weathering and preferential leaching of some components. The effect of mobilization of iron and manganese is visible in soil profiles on many West Coast fluvioglacial terraces. Transport of organic matter is discussed b Hammond et al (1991). The transport of aluminium complexes in North Westland soils is discussed by Mew et al (1983), Mew & Lee (1988) and Knuepfer (1988). Many of the features of soils on the Quaternary terraces of North Westland are described by Mew (1983).

Horizons where ^{14}C dating has been shown to give good results, backed up by luminescence dating, are from sites where the dated material has been buried by younger fluvial or dune material. The depth of burial is multiple metres. The burial was rapid and followed not long after accumulation of the target soil. The upper surface of the cover is also a soil, which then limits the percolation down to the sample target by meteoric water. Ideally the sample materials are situated above any long-term groundwater table, particularly groundwater situated at or close to the basal contact of the Quaternary Formation in question. This set of circumstances limits the extent of carbon mobilization in the target soil. There are two such dated sites in the Grey Valley, one at Kamaka, and one at Raupo.

Other sites where buried soils have been sampled for ^{14}C dating include one near Cape Foulwind (Waites Formation), one at Wilsons Lead Road (Waites Formation), one at Chesterfield (Awatuna Formation) and one at Schulz Creek (Awatuna Formation). They have returned a mixture of finite and infinite ages. The context was thought to be marine transgression/regression followed immediately by soil deposition around 100 ka. The assumption is this means the lower portion of the soil would be too old for successful radiocarbon dating and that finite ages imply that contamination had occurred. However, at these sites there is a thick cover sequence that was potentially deposited soon after formation of the organic-rich soil and peat. At these sites the dated material is not loess, it is organic soil and peat.

3.6.3 Amino Acid Racemisation

In this region amino acid racemisation (AAR) has been used at a single locality. This is situated near Mill Creek at South Beach, Greymouth. The site (at grid ref J32 610555450) is referred to as "Ferguson's Pond" by Moar and Suggate (1996). Two wood samples were dated and the results are presented by Pillans (1990). The original mapping of the site by Nathan (1978) indicated the site was on Karoro Formation. Suggate and Waight (1999) remapped the area and the sample site was redefined as Rutherglen Formation. The AAR ages are 120 ka ± 30% for sample BJP-153A (identified as Pittosporum) and 140 ka ± 30% for sample BJP-153B

(identified as Libocedrus). Although 1σ errors are not normally quoted in terms of a percentage of the preferred age this is the way they are presented by Pillans (1990). These AAR ages could be quoted as 120±36 ka and 140±42 ka respectively. Initially the ages invite a coverbed correlation with MIS 5e. A correlation with MIS 5c is also within the 1σ errors for both samples.

Fergusons Pond was a water supply for an exotic forestry block. The locality was mapped by Suggate & Waight (1999). When the area was carried out the area was occupied by mature pine forest. Suggate & Waight defined the pond site as a very small area of Rutherglen Formation at the end of a long narrow spur occupied largely by Karoro Formation. During the logging of the area around the time of commencement of this project the pond was destroyed, making way for a logging skid-site. At that time a new exposure was created through the full thickness of the coverbeds across about half of the width of the spur. During this project both the pond site and the surrounding area have been reexamined. Reexamination of the area indicates the spur is entirely Karoro Formation. The Rutherglen strandline is at least 50 m to the west (beyond the end of the spur at Fergusons Pond). Previously the Karoro Formation had been assigned to MIS 7. If the AAR ages are correct then this correlation may need to be changed.

3.6.4 The Kawakawa Tephra

A rhyolitic tephra has been found at a number of localities in the West Coast region, putting an age limit on some parts of the landscape. An assumption has universally been made that it can be correlated with the Kawakawa tephra (22.59 ± 0.23 ka ^{14}C yrs or numerical ages of c. 26.5 ka by Wilson et al (1988) and 27.097 ± 0.957 ka by Lowe et al (2008). This tephra is sourced from the Lake Taupo volcano in located in Taupo Volcanic Zone in the North Island of New Zealand.

The Kawakawa tephra is present in loess at:

- A number of profiles from both the Loopline and Waimea Formations near Chesterfield (Mew et. al. 1988).
- The Loopline Formation adjacent to the Kapitea reservoir near Dillmanstown and near Kumara.
- The Waimea Formation near Kumara (Neall et al 2001).
- The Waimea Formation at Blue Spur near Hokitika (Berger et al 2001).
- The Waimea Formation at Grahams Terrace near Nelson Creek in the Grey Valley (Mew et al 1986, Hammond et al 1991).
- The Cockeye Formation near Callaghans. (Neall et al 2000)
- Several moraines in the Saltwater Forest area in South Westland (Berger et al 2001).
- At Maimai, Flagstaff, Hukarere, Charleston, and Okarito (Robertson and Mew 1982).
- The Okarito Pakihi bog (Vandergoes et al 2005).

Because loess on the Loopline surface contains abundant glass shards the underlying outwash gravel presumably cannot be younger than 27 ka. Loess on the Larrikins(2) surface only contains scattered glass shards (probably reworked according to Neall et al 2001) so this Formation has been assumed to be younger than 27 ka. Although the Loopline Formation has been correlated with MIS 4 the presence of the tephra near the base of the overlying loess does not rule out a correlation with MIS 3 or a correlation with the MIS 3/2 transition.

3.7 GEOMORPHOLOGICAL MAPPING

As indicated in chapter two a significant amount of geomorphological mapping was undertaken during this project. The mapping was conducted in two main areas:

- An bounded by the Hokitika and Totara Rivers and by coastline between Hokitika and Ross.
- An area approximately bounded by the Arnold River, Lake Brunner, Lady Lake, Deep Creek and Findlay Creek. Figures 3.4 to 3.7 summarise this work.
- A third area covered in less detail near Waipuna in the Upper Grey Valley.

The detailed maps are appended to the thesis and the map legend is presented below as figure 3.8.

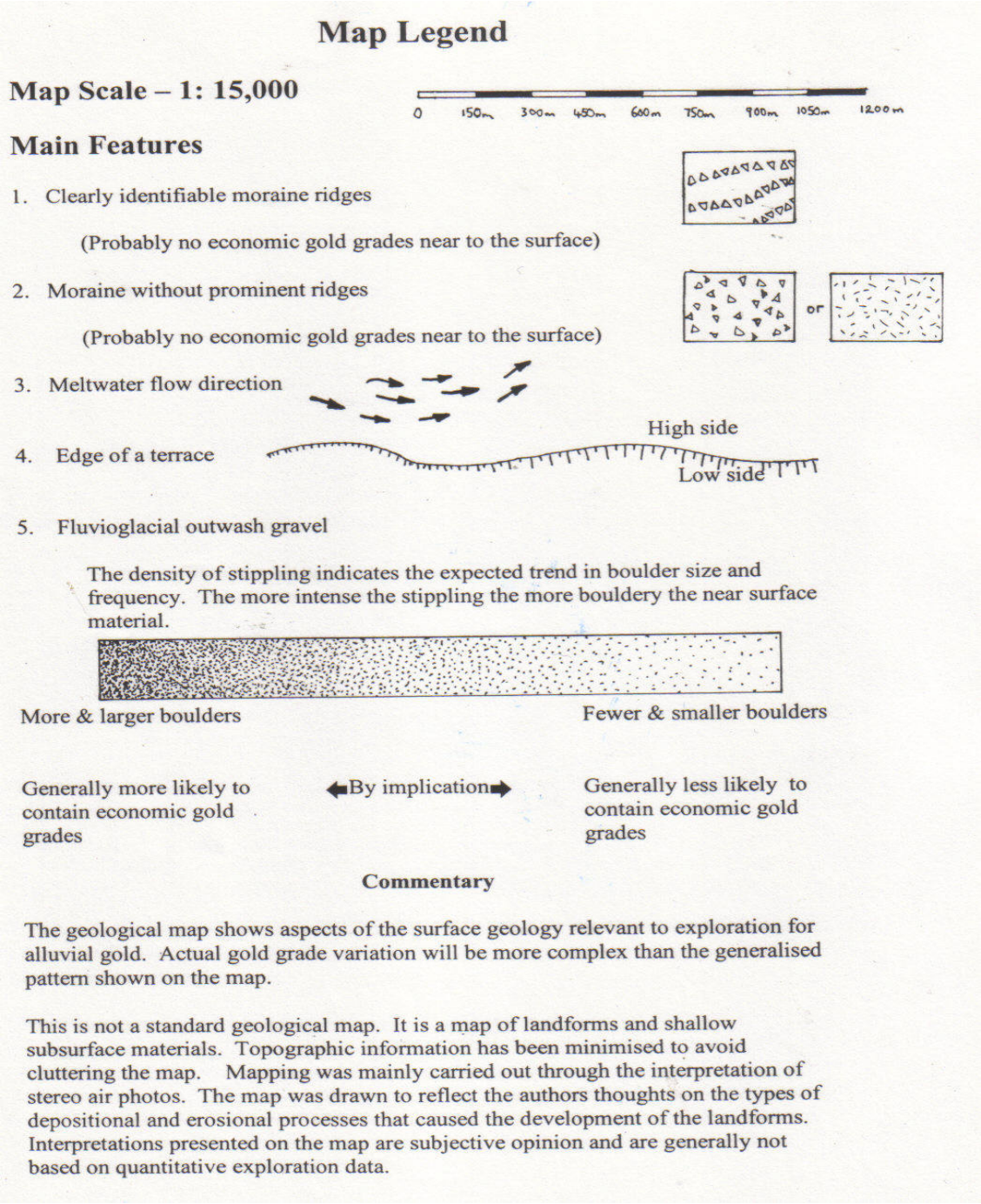

Figure 3.8: Key to the detailed geomorphological maps appended to this thesis. This is also the key to a number of geomorphological illustrations appearing elsewhere in the thesis.

CHAPTER FOUR: GLOBAL AND REGIONAL CONTEXT

4.1 INTRODUCTION

In New Zealand most terrestrial-marine correlations (e.g. Suggate & Waight 1999 & Pillans 1990a, 1990b) have historically been compiled under the assumption that glacial events here should correspond in time with those in the Northern Hemisphere. In chapter six an alternative stratigraphy is proposed for North Westland. The implied climatic correlations do not require a strictly in-phase relationship between Northern and Southern Hemisphere climate events. The aim for chapter 4 is to provide some general context in terms of recent research on climate related matters that is relevant to the timing and magnitude of climate events in Westland. In this chapter climate forcing mechanisms are examined and discussed to provide a framework for the timing of glaciation in Westland.

The position adopted here is that we should not expect sub-orbital scale climate events in Westland to mirror directly the broad climatic trends observed in the Northern Hemisphere. Temperature and precipitation in this region are at least partially controlled by sea surface temperature and prevailing wind direction/strength in the Southern Tasman Sea and the Southern Ocean. The climate of Westland is linked to climate change in the Southern Ocean and Antarctica as suggested for the New Zealand region by Fink et al (2009). For the last 90 kyr many sub-orbital scale climate events in Antarctica have been shown by Ahn & Brook (2008) to be out of phase with those in the Northern Hemisphere. In addition, at the orbital or astronomical scale Southern Hemisphere summer insolation maxima (see figure 4.3a, 4.3b) are precisely out of phase with Northern Hemisphere summer insolation. In this chapter the possibility of an in-phase relationship between New Zealand (and North Westland) and Antarctic climate change is considered.

Another issue worthy of consideration is the relative extent of successive glaciations in North Westland. At present we can not be absolutely sure of the prior (Suggate & Waight 1999) correlation of local deposits with the marine isotope stage system. So can we be sure that assigning ages to glaciations partly on the basis of ice extent is a valid procedure? For instance, if we consider climatic factors that apply directly to local climate, is there any particular reason why a glaciation on the West Coast of the South Island during MIS3 needs to be any smaller in extent than a glaciation in stages 2, 4, or 6? The possibility that glaciation in the Southern Alps will be driven partly by the relative prevalence of a cool but moist south-westerly air stream should be considered. In other words air temperature is not the sole determinant of the local ELA and the timing of expansion and contraction of local glaciers is not inevitably the same as occurs at the Northern Hemisphere ice sheets.

The modern volume of glacial ice in the Southern Alps is subject to significant change on a decadal timescale. A recent (perhaps temporary) increase in mass balance has occurred throughout the Southern Alps. This change, identified by Chinn et al (2005), is coincident with a change in the Interdecadal Pacific Oscillation and an associated increase in El-Nino/Southern Oscillation events. This set of circumstances commenced around 1976/77. It has affected precipitation, wind and temperature patterns throughout the Southern Alps. One outcome has been a modest glacial advance of up to 1.5 km for the terminus face of the Franz Josef glacier in the Waiho Valley between 1985 and 2000 (Anderson et al 2006). The response has been rapid with a switch from retreat to advance within about 5 years of the change in the regional climate. Chinn et al (2005) note that the increased mass balance occurred on both sides of the main divide and includes the Tasman Glacier. Here the initial impact has been restricted to zones of accumulation. They indicate that the main trunk of the Tasman glacier had not responded. However, they also noted that the Tasman and Hooker Glaciers were still

adjusting to the post-Little Ice Age mass balance and that response times were not the same for glaciers in different climatic zones. It appears that to the east of the main divide large glaciers respond more slowly to decadal scale climate change than those to the west. It is assumed here that the response time is several decades or more.

Chinn et al (2005) make the following statement in relation to modern glacier expansion and contraction in New Zealand:

> *"Hooker and Fitzharris (1999) concluded that during the period of glacier expansion the atmospheric circulation pattern favours higher accumulation as well as reduced ablation. The Southern Hemisphere westerly wind belt was further north in the New Zealand region. There were anomalous southwesterly winds over the country, especially during the accumulation season. Stronger westerlies generate higher precipitation and melt is retarded because of cooler temperatures and increased cloudiness (Hay and Fitzharris 1988). Increased albedo from more frequent summer snowfalls also limits melt (Fitzharris et al. 1992). Atmospheric circulation during periods of glacier retreat favoured both lower accumulation and increased ablation losses."*

So the modern pattern of glacial advance and retreat can be traced to hemispheric scale changes in atmospheric circulation patterns. This could be completely disconnected from global changes in mean surface temperature.

4.1.1 Events in the Northern Hemisphere

There is an increasing body of evidence (e.g. Blunier & Brook 2001; Pahnke et al 2003; Oppo et al 2003; Spotl & Mangini 2002, Shackleton et al 2004) from numerous localities worldwide that there were several warm interstadial periods during MIS3. The Fennoscandian Ice Sheet varied hugely in volume and shape during MIS3, as summarised in figure 4.1. Episodes of greatly reduced volume occurred between 60 ka & 55 ka, between 50 ka & 43 ka and between 40 ka and 33 ka. The variable ice volume in this region contributed to eustatic sea-level change during MIS3.

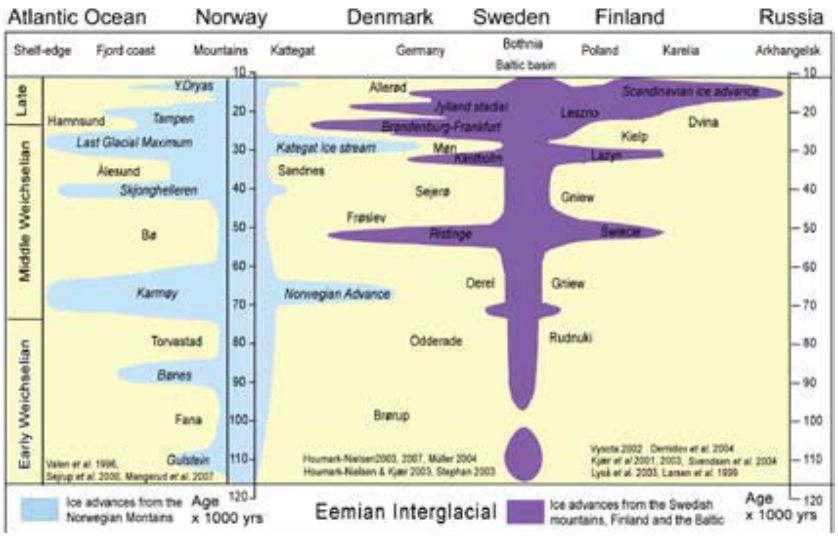

Figure 4.1 (Figure 3-1 of Wohlfarth 2009). Time-distance diagram showing the advance and retreat of the Fennoscandian ice sheet margin during the Weichselian. This reconstruction assumes more or less continuous ice cover over the Norwegian Mountains, the Baltic basin and central and northern Sweden during the entire Weichselian. See also Figures 3-2 to 3-4. Figure courtesy of Michael Houmark-Nielsen

There is also evidence from Canada that the Laurentide Ice Cap may have undergone partial deglaciation to a significantly reduced size at least once during MIS3 (Klemen et al 2010), for example dated evidence for ice free conditions in Hudson Bay (Berger & Nielsen 1991) and marine episodes in Hudson Strait (Laymon 1991). Mechanisms for repeated partial collapse of the MIS3 Laurentide Ice Sheet are discussed by MacAyeal (1993) and Clarke & Marshall (1999).

A study of "marine oxygen isotopes" in foraminifera from the Sulu Sea by Linsley (1996) hints at a combination of fluctuating interstadial sea level and local sea surface salinity variability during MIS3. This implies substantial fluctuation in Northern Hemisphere ice sheet volume at this time. The history of sea level change is covered in more detail in section 4.1 below.

Table 4.1 has been assembled from U series dated speleothem isotopic records, marine ^{14}C age records and ice-core $\delta^{18}O$ records. The sources of the data by column are: (i) Genty et al (2002); (ii) Wang et al (2001); (iii) Bar-Mattews et al (2000); (iv) Spotl & Mangini (2002); (v) Shackleton et al (2004); (vi) Svensson et al (2008); (vii) Johnsen et al (2001) [SS09 timescale]; and (viii) Rohling et al (2003). This table defines the ages of the sudden climate transitions in these records. The final column is a summary of the findings of an investigation into event timing in isotopic records from marine cores. The objective in assembling table 4.1 has been to provide independent confirmation of the likely timing of peak warming during Antarctic Interstadials A1 to A6. As demonstrated by Ahn & Brook (2008) peak warming in Antarctica coincides with the abrupt commencement of Greenland interstadials 8, 12, 14, 17, 19 and 20. It is probably no coincidence that these particular Greenland interstadials, which immediately follow strong Antarctic warming, represent the strongest of the North Atlantic MIS3/4 Dansgaard-Oeschger (DO) events. On the basis of the timing of DO events in the Northern Hemisphere the predicted timing for peak Antarctic warmth is: A1 at 37-39 ka, A2 at 45-48 ka, A3 at 53-55.5 ka, A4 at 58.5-61 ka, A5 at 68-70 ka and A6 at 72-73 ka.

During MIS3 and MIS4 there were a series of global sea level maxima. Sea level maxima are assumed to coincide with the terminations of Heinrich Events (the transition to the subsequent DO event) as discussed by Chappell (1992), Siddall et al (2008b) and Rohling et al (2008). The end of a Heinrich event marks the end of a period of (approximately synchronous) massive ice discharge from the Northern Hemisphere ice sheets. It also marks the onset of an interstadial period and of net ice accumulation under a relatively warm climate in the Northern Hemisphere (probably lowering the global sea level).

4.1.2 Events in the Southern Hemisphere

At a millennial scale an anti-phase relationship between Northern and Southern Hemisphere climate means that sudden transitions to warmer climate in the north correspond approximately to the peak of interstadial warmth in the south (Blunier & Brook 2001; Ahn & Brook 2008; Barker et al 2009; Schmittner et al 2003, 2007, Longworth & Bryden 2007).

Table 4.1: Timing of Northern Hemisphere Climate Events

Event/Event Transition	**(i) Villar's Cave, France (ka)**	**(ii) Hulu Cave, China (ka)**	**(iii) Soreq Cave, Israel (ka)**	**(iv) Klee-gruben Cave, Austria (ka)**	**(v) Marine Core MD95 -2042 (ka)**	**(vi) North GRIP (ka)**	**(vii) SS09 Time Scale (ka)**	**(viii) ^{14}C dated Marine Cores Calibrated ^{14}C ages**
Trans to DO 20	75	75 – 76	78 – 77?	-	74.5		77.12	
A6								
Trans to DO 19(2)	71	72?	73	-		67?		
A5								
Trans to DO 19(1)	67.5	70	-	-				
Trans to DO 18		65	-	-				
H E 6; A4	60	61 – 58.5	-	-				60 – 58
Trans to DO 17	60-59	58.5	59	-	59	59.44	60.24	
Trans to DO 16	58-57.5	57.5	-	57.5		58.28		
Trans to DO 15	-	55.5	56.5	55.5	55.66	55.8	56.58	
HE 5(2); A3	-	55 – 54	55.5 – 54	55.3 – 54				53 – 52
Trans to DO 14	52	53.5	54	54	54.29	54.22	55.08	
Trans to DO 13	48	~49.5 – 49	49.5	49.5	49.45	49.28	49.78	
HE 5(1); A2	47 – 45.5	48.5 – 47.5	47 – 45	48 – 47				47 – 45
Trans to DO 12	45.5	~47.5 – 47	47	47	47.2	46.86	47.36	
Trans to DO 11	42.5	43			43.9	43.34	43.68	
Trans to DO 10	41.5 – 41	41.5			42.1	41.46	41.74	
Trans to DO 9	40	40.5			40.8	40.16	40.34	
HE 4; A1	39 – 37	39.5 – 38						40 – 38
Trans to DO 8	37-36	37			39.0	38.22	38.34	
Trans to DO 7	34.5	35			36.29	35.48	35.38	
Trans to DO 6	33.5	~34 – 33.5			34.64	33.74	33.58	
Trans to DO 5	32	32.5			33.4	32.5	32.26	
HE 3		31 – 30						31 – 29
Trans to DO 4		29.5			30.06	28.9	28.56	
Trans to DO 3		28			29.0	27.78	27.4	
HE 2		24.5 – 23.5						26 – 24

Northern Hemisphere grounded ice volume decreases during the most severe Northern Hemisphere MIS3 stadial events which correspond with Heinrich Events. These events are associated with massive discharge of ice from the Laurentide Ice Sheet. The causes and timing of ice discharge are discussed by MacAyeal (1993) and Clarke et al (1999) and Clark (2007). It has been proposed (Chappell 2002; Clark 2007; Rohling et al 2008) that these ice discharge events are of sufficient magnitude to cause significant changes in sea level, a topic that is discussed in section 4.3 below. In addition is has been proposed by Rohling et al (2008) that the timing of MIS3 sealevel maxima is similar to that of peak warmth during Antarctic interstadial events, global sea level mimicking the Antarctic surface temperature curve.

There is now a large body of information concerning inter-hemispheric linkages in oceanic circulation an atmospheric climate. In terms of timing cooling, of SST in the North Atlantic appears generally to coincide with warming of SST in the Southern Ocean. Warming of SST in the Southern Ocean then propagates quickly northward to the equatorial Pacific Ocean as discussed by Longworth and Bryden (2007).

There is evidence for near-interglacial conditions during MIS3 in and near to the South Island. This includes:

- The pollen record from marine core DSDP 594 reported by Nelson et al (1993)
- The faunal and alkenone based SST records from marine core SO136-GC3 by Barrows et al (2007). The faunal SST record is shown in figure 5.5 (Chapter five).
- The SST record from marine core MD06-2986 by which is shown in figures 4.7, 4.12 and 5.1 of Kolodziej (2010).
- The alkenone based SST record from marine core MD97-2120 by Pahnke & Sachs (2006) which is presented here in figure 4.15a.

The SST recorded at marine cores MD06-2986 and SO136-GC3 indicates average SST during the early portion of MIS3 between about 50 ka and 60 ka comfortably reached and possibly exceeded 14°C. This is an increase from typical full glacial values of ~10.5 to 11.5°C. Both cores are situated in the Tasman Sea on the continental shelf adjacent to North Westland. At these cores the SST off North Westland during the warmest Late Quaternary full interglacial (MIS5e) may have reached 18°C but the evidence from these cores is that the average SST during the Holocene interglacial has been close to 15°C. Exactly what this means for surface temperature on-shore is difficult to say. The mean modern (last 100 years) annual sea-level temperature at climate stations on the western side of the South Island (see figure 1.4) ranges from about 11°C to 12°C, the average at Greymouth being approximately 12.25°C between 1948 and 2009 (annual mean temperature from the cliflo database managed by NIWA). This onshore mean is substantially lower than the Holocene mean SST from cores MD06-2986 and SO136-GC3. On the Southern Flank of the Chatham Rise the alkenone based SST record for core MD97-2120 shows strong warming during the early portion of MIS3. At this site early MIS3 warming approaches the average temperature of the later portion of the Holocene. Warming of SST during the early portion of MIS3 appears to be of regional scale but the magnitude varies. For instance at marine core MD97-2120 on the northern flank of the Chatham Rise the early MIS3 warming recorded in alkenone-based SST is relatively muted in comparison to core MD97-2120.

There is published evidence for a rather muted vegetative response to long-term climate change during MIS3 in South Westland. This comes from a long pollen record from the Okarito Pakihi reported by Vandergoes et al (2005). However, the age control in that study is open to question and is discussed extensively in Chapter 5.

The following summary of glacial activity is for the South Westland area from Almond et al (2001) and Suggate and Almond (2005).

Time (ka)	Loess sheet	Glacial Moraine/ advance	MIS Stage (RVR)
0 to 14	none		1/2
19-20.5	-	M6	2
21.5 to 24.5	L1a	M5(2)	2
28 to 34	L1b	M5(1)	2/3
45 to c. 50	L2	M4a	3
>50 to <80	L3, L4	M2, M3	4, 4/5a
>120 to <200	L5	M1	6

Suggate and Almond (2005) contains an excellent summary of ^{14}C dating covering the last glacial maximum for the Westland region. Their analysis centers on the LGM. There is essentially no

discussion of the M4 event that was assigned to MIS3 by Almond et al (2001). It does appear from the text of Suggate and Almond (2005) that there is some doubt with respect to the existence of the 40-50 ka glacial advance in South Westland. In the past there seems to have been an assumption that in climate of Westland was "cool-interstadial" during MIS3 but not cold enough for a glacial event of sufficient magnitude that surficial till or fluvioglacial outwash deposits have been preserved. In the "Suggate model" there was either no MIS3 glaciation, or any such deposits were destroyed by more extensive glaciation during MIS2. Later in this chapter the sea surface temperature of the Southern Ocean is discussed at length and it is shown that conditions were cold enough to have sustained an extensive glaciation in the Southern Alps at c.50 to 40 ka.

With respect to table 4.2a (below) the ages for events in Antarctic ice cores are derived from Ahn & Brook (2008), Blunier & Brook (2001), Brook et al (2005), Epica Team Members (2006), Raynaud et al (2000) and Shackleton et al (2004). Ages for South Westland stadials are from Berger et al (2001), Almond et al (2001) and Suggate & Almond (2005). Ages for sea surface temperate (SST) events are from Pahnke et al (2003) for MD97-2120, Kaiser et al (2005) for ODP 1233, Cortese et al (2002, 2007) for ODP 1089. Ice rafted detritus events are by Kanfoush et al (2000) for the Southern Atlantic and Carter et al (2002) for the Campbell Plateau.

Although there clearly is some uncertainty no attempt has been made to specify the 1σ errors for the various ages assembled in Table 4.2a. Nevertheless one could claim there is some coherence in the timing of climate events, relatively warm climate in mid-latitude regions of the Southern Hemisphere coinciding with Antarctic interstadials and relatively cool events at mid-latitudes coinciding with Antarctic stadial events. Study of the various temperature and proxy temperature datasets reveals that the major fluctuations are common to most sites. This implies a common or at least related cause that acts more-or-less simultaneously throughout Antarctica and the Southern Ocean.

Table 4.2b is a comparison of the timing and intensity of climatic events in the middle to high latitudes of the Southern Hemisphere. This illustration is intended to be qualitative rather than quantitative, highlighting the main climatic events in the mid to high latitudes of the Southern Hemisphere.

The sources for timing of sea surface temperature events in table 4.2b are Pahnke et al (2003) for MD97-2120, Kaiser et al (2005) for ODP 1233, Cortese et al (2002, 2007) for ODP 1089. The sources for ages of surface temperature fluctuations at Antarctic ice core sites are Kawamura et al (2007) for Dome Fuji, Jouzel et al (2007) for Dome C and Petit et al (1999) for Vostok. The sources for $\delta^{18}O$ at the Byrd and Taylor Dome sites are Blunier & Brook (2001), Steig et al (2000) and Steig (2006).

During the last 85 kyr there appear to have been several cold phases that are potentially of similar amplitude but differing duration. The amplitude of temperature change varies from site to site. A different selection of site may reveal a similar timing but different average amplitude. So no attempt has been made to extract meaning through calculating an average amplitude. The underlying time-series summarised in table 4.2b are compiled using different age-depth models. This means that variation is inevitable in the precise timing for individual events. Bearing this in mind it is apparent from that there is substantial coherence in terms of event timing at the various locations. The comparison is continued and strengthened using a large number of marine cores in Tables 4.5 and 4.6 below.

Table 4.2a: Timing of mid-latitude climate events in the Southern Hemisphere

Antarctic Ice Cores (references listed above)		Fiordland Stadial/ Inter-stadial (Williams 1996)	South Westland Stadial Events (Almond et al 2001)	Ice Rafted Detritus events (Kanfoush et al 2000; Carter et al 2002)		Tasmanian Speleothem $\delta^{18}O$ (Geode 1994)		Marine Core ODP 1089 (Cortese 2007)	
Interstadial	Stadial			Southern Atlantic	Campbell Plateau	Inter-stadial	Stadial	Inter-stadial	Stadial
	20-22	21<	19-20.5						
22-24 (HE2 23-24.5)									23-25
			21.5-24.5	23-26					
	24-26	21-39			27			25-27	
(HE3 29-31)									27-29.5
		Inter-stadial	28 - 34	30-32	29			30-35	
35-36.5									35-37
	36-37.0				36				
A1 37.7-39.6 (HE4 38-40)				36-38					
								38-39	
	40-42	40-41							39-40.6
		41-45 Inter-stadial		40.5 - 44	41			40.6-43	
A1(2) 42-43									
	43-45								43-44
A2 45.5-48.1 ($HE5_1$ 45-46.5)			45-c.50					44-46	
		46-48							46-48.6
	47-51.5				49-51			48.6-50	
A3 51.5-54.4 ($HE5_2$ 52-53)		49-66 Inter-stadial	Btw 50 & 80	51-52					50-51
					53-54			51-52	
	55-57			55-59				53-56	
A4 57.2-61.5 (HE6 58.5-62)						56-60			56-57
								57-61	
							60-65		61-62.5
	62-67							62.5-65	
		66+				65-67.5			65-66
A5 68-70								67-68	
	71-72						67.5-71		68-69
A6 72-74						71-76		69-76	
	74-79						76-78		76-81
A7 79.5-86.5						78-86		81-86	
							86-88		86-92

It has been suggested by Tyson et al (1997) in connection with the climate of the 20th century that there were teleconnections between enhanced precipitation in the west of the South Island of New Zealand and periods of drought in Southern Africa. This is an out-of phase relationship related to the Southern Oscillation Index. On longer timescales it has been suggested by Rother & Shulmeister (2006) and Zech et al (2008) that shifts in the location of the zonal westerly winds of the mid to high southern latitudes have a major influence on temperature, precipitation and ice accumulation in the South Island of New Zealand and in Southern Andes mountain chain of South America. Although climatic teleconnections of a certain type may have existed through the 20th century there is not guarantee that such connections persist or are stable though time. The issue of potential stationarity though time is discussed below in with reference to tables 4.8 and 4.9.

Table 4.2 b: Late Quaternary Climate events in Antarctica and the Southern Ocean

Dronning Maud Land $\delta^{18}O$	Vostok Temp °C	Dome C Temp °C	Byrd $\delta^{18}O$	Dome Fuji Temp °C	MD97-2120 SST (Mg/Ca)	ODP 1233 SST	ODP1089 SST
c.17.3	c.17-0	17.5-0	c.18-0	18-0	18.3-0	18-0	17-0
			21.5-18	21-18	23-18.3	23-18	20.5-17
			23.5-21.5	23.5-21	24-23	24-23	
					25.1-24		25.5-20.5
		27.5-17.5	26.5-23.5		26.6-25.1		27-25.5
			27.5-26.5	27-23	28.5-26.6	28-24	29.5-27
30-28.5	31.5-17		28.7-27.5	30-27	29.5-28.5	31-28	
			29.3-28.7		31.1-29.5	32-31	33-29.5
32-28.5		27.5-35	31.3-28.7	33-30	32.2-31.1		34-33
	34.5-31.5		32.3-31.3	34.1-33	34-32.2	37.5-32	35-34
34.8-32			34-32.3	36.6-34.1	35.4-34		
36-34.8	36-34.5	35.5-35	35-34				
37.7-36	38-36	37.2-35.5	36-35		37.7-35.4	38.5-37.5	
39.6-37.7	39-38	38.7-37.2	37.5-36	38.9-36.6	40.6-37.7	40-38.5	39.5-35
			40-37.5				
42.5-39.6	41-39	42.8-38.7	42-40	41.6-38.9		41-40	41-39.5
43.5-42.5	43.5-41	42-42.8	43.1-42	43-41.6	43.4-40.6	43.5-41	43.5-41
45.1-43.5	44.5-43.5	44.9-42	44.6-43.1	44.1-43	45.1-43.4	46-43.5	44.5-43.5
48.0-45.1	47-44.5	47.5-44.9	47.4-44.6	47.1-44.1	46.5-45.1	48-46	45.6-44.5
50-48	49-47	49.5-47.5		49.6-47.1			48.6-45.6
51.3-50		51.8-49.5	51.2-47.5		51.5-46.5	51-48	50-48.6
	53-49						53.6-50
54.6-51.3		54.5-51.8	54.8-51.2	54.6-49.6	54.5-51.5	55-51	56-53.6
55.8-54.6	55-53	56.5-54.5	56.7-54.8	55.8-54.6	57.4-54.5	57-55	58-56
56.9-55.8							
61-56.9	59-55	60.4-56.5	61.1-56.7	60.6-55.8	61.6-57.4	62-57	61-58
62.3-61	62-59	62-60.4	62-61.1	62.4-60.6			
	63-62	63.5-62		63-62.4		65-62	62.5-61
64.3-62.3	64.5-63	64-63.5	64.8-64.1		65.8-61.6	66-65	65-62.5
68.6-64.3	68.5-64.5	68-64					66.5-65
69.3-68.6	69.5-68.5	68.5-68	68.2-64.8		68-65.8		67.5-66.5
70-69.3	70.6-69.5	69.5-68.5		69.8-65.8		68.5-66	70-67.5
72.2-70	73-70.6	72-69.5	71.5-68	71.5-68	71.5-68	70-68.5	
73.5-72.2	74.5-73	73.5-72	71.5-70.5	73.6-72.1	73.8-71.5		
75.8-73.5	77.6-74.5	75.5-73.5	74.3-71.5	76-73.6	76.4-73.8		76.7-70
77-75.8	78.7-77.6	78-75.5	78-74.3	78.1-76	79-74		81-76.7
87-77	88-78.7	86-78	87-78	86.5-78.1	86.5-79		87-81

Key to table 4.2b

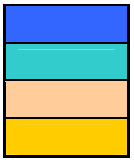

It is clear that from tables 4.2a, 4.2b and figures 4.15a, 4.15b, 4.16, and 4.17 that a solid case can be made for relatively warm climate in the mid latitudes of the Southern Hemisphere at around 36-39 ka. This fits nicely with the findings of Burge (2007) relating to vegetation, temperature and precipitation in the Westport area on the West Coast of the South Island.

4.2 MID TO HIGH LATITUDE SOLAR FORCING IN THE SOUTHERN HEMISPHERE

4.2.1 Introduction

A number of widespread depositional events in North Westland are discussed in Chapter 6. These include the deposition of the Karoro, Waimea, Rutherglen and Awatuna Formations. As mentioned elsewhere the ages implied by dating carried out during this project are younger than would be expected in light of prior theory. This raises the question of whether or not these Late Quaternary Formations represent globally recognized "climatic events" as per the Suggate model, or whether they could be reinterpreted and reassigned based on a model incorporating mid-latitude Southern Hemisphere climate forcing mechanisms. As discussed in chapter one the "Suggate model" is reliant on a number of assumptions. These include:

- The assumption that significant periods of near-interglacial climate in North Westland are approximately synchronous with interglacial periods in the Northern Hemisphere.

- The assumption that full-scale glaciation occurs in North Westland more-or-less in synchronisation with Northern Hemisphere glaciations. The model makes no explicit allowance for major glacial advances in North Westland that might coincide with sub-orbital scale stadial events in Antarctica and which might be out of phase with Northern Hemisphere climate or change in eustatic sea level.

- The assumption that ice volume fluctuations and glacial advances in North Westland reflect astronomical scale changes in global (largely Northern Hemisphere) ice volume. In the Suggate model local fluvioglacial outwash deposits are correlated with the main expansions of the Northern Hemisphere ice sheets. The corollary is that periods of intermediate ice volume in the Northern Hemisphere (e.g. MIS 3, 5b, 5d, 7b and 7d) are not represented by substantial fluvioglacial deposits in North Westland.

These assumptions may be largely correct but should not be taken on faith and discussion is warranted, particularly given the fact that potential correlations with antipodean orbital and millennial scale climate events of potentially hemispheric scale has not previously been considered in relation to the Late Quaternary sequence of North Westland

.

Before examining this issue further attention is turned to long-term variations in solar energy input into the regional climate system and how this might influence local climate at orbital to millennial timescales in the Southern Hemisphere.

4.2.2 Summer Ice Accumulation/Ablation and Glaciation in the Southern Alps

The hypothesis proposed here relates to the accumulation of ice in the Southern Alps on an annual basis. At the orbital-timescale fluctuations in summer and spring insolation in Westland directly influences the accumulation/ablation of new (< 1 year old) snow and older ice in the Southern Alps. If less ice melts and/or more snow falls during the warmer portion of the year then this influences the glacial mass balance in this region. A positive mass balance is more likely if:

- Summer/spring insolation is at a minimum causing lessened direct ablation (weaker sunshine).
- The summer/spring mean cross latitudinal temperature gradient is conducive to the supply of frequent cold/cloudy weather.
- The annual mean cross latitudinal temperature gradient is also conducive to the supply of frequent cold/cloudy weather.
- Millennial-scale cycles in patterns of oceanic heat transport are at that time creating very cold conditions in the Southern Ocean and over Antarctica.

The "reduced ablation" hypothesis is not unusual in terms of theories of glaciation and ice sheet inception. It is the primary underlying assumption of most published versions of "Milankovitch style" glacial inception and icesheet growth for the Northern Hemisphere. These assume a need for reduced summer insolation at around 60°N to 65°N (e.g. Imbrie et al 1984, Martinson et al 1987, Imbrie et al 1993 and many others since then). Reduced summer insolation and/or summer duration allows at least some ice to survive during each summer period in upland regions at this latitude.

4.2.3 The effect of Northern Hemisphere Ice-sheets on Southern Hemisphere Climate

The weight of evidence from sea surface temperatures and marine oxygen isotope ratios (e.g. Martinson et al 1987) makes it reasonably clear that climate in the mid-latitudes of the Southern Hemisphere is substantially influenced by Northern Hemisphere driving mechanisms. The global climate is influenced by expansion and contraction of the Northern Hemisphere continental ice sheets and the associated changes in seasonal snow cover, sea-ice extent, eustatic sea level, and land-area. The atmospheric climate is also influenced by vegetative patterns on land, marine productivity, global cloud cover, atmospheric humidity, wind blown dust, sea surface temperature, and oceanic circulation. Collectively these various factors impact on the global energy budget, most notably by altering the global albedo. Albedo changes probably have a greater significance in the Northern Hemisphere than in the Southern Hemisphere, given the differences in percentage of land and sea-ice area versus ocean area. Overall, cooling of the Earth during major glacial events is driven primarily by an increase in the average reflectivity of the surface and an accompanying decrease in tropospheric humidity. In the case of major expansion of continental scale ice-sheets the primary albedo change occurs in the Northern Hemisphere causing increased reflection of solar energy directly to space. When the Northern Hemisphere ice sheets expand significantly the average surface temperature in the Northern Hemisphere tends to decline. This decline is recorded in many long temperature sensitive archives including speleothem and ice core $\delta^{18}O$ (e.g. Winograd et al 1997) pollen from sediment cores and changes in planktonic foraminiferal abundance and oxygen isotope ratios in marine cores (e.g.

Martinson et al 1987). As discussed by Toggweiler & Lea (2010) changes in atmospheric and oceanic circulation almost certainly allow northward export of excess heat from the Southern Hemisphere (to the Northern Hemisphere), thereby enabling simultaneous cooling in both Hemispheres. This effect has been termed "inter-hemispheric heat piracy" by Seidov et al (2001). It is operative at millennial and orbital timescales. The basic idea is that one hemisphere can warm, at the expense of relative cooling in the other, by the transfer of heat across the equator. Even though there may be net transfer from the exporting to the importing hemisphere it does not mean that the exporting hemisphere is actually warmer than the importing hemisphere. This transfer can occur via the atmosphere, via the movement of surface waters or via the movement of intermediate and deep waters. Hemispheric and global scale oceanic circulation patterns that enable such heat piracy are modeled by Keeling and Stephens (2001).

As demonstrated by the deep ice-core isotopic records from Antarctica and Greenland (e.g. Ahn & Brook 2008), at the millennial scale there is significant evidence for asynchronous and even antiphase climatic behaviour between the high latitudes of the two Hemispheres. As discussed by Clark et al (2007) this behaviour is facilitated in part by changes in circulation patterns within the deep ocean which influence the absorption, storage, transport and emission of heat within the climate system including the ocean, land and atmosphere.

One of the goals here is to examine whether or not the millennial-scale climatic fluctuations observed in Westland are in phase with Northern Hemispheric events, potentially implying a northern driving mechanism, or whether these events are in phase with mid to high latitude Southern Hemisphere (Antarctic and Southern Ocean) events. If the latter then a set of Southern Hemisphere driving mechanisms could be largely responsible for climate change in Westland.

One of the oddities of the luminescence dating programme carried out for this PhD project, that by Preusser et al (2005), and the cosmogenic isotope dating by Sutherland et al (2007), is that these projects tend to point to deposition of the glacial Waimea Formation around 75 to 80 ka. The evidence is discussed in detail in chapter 6. One immediate question is whether the dating evidence should be considered strictly on its own merits or whether it should be considered to be rather approximate, allowing the events to be pigeon-holed in the traditional manner into a Northern Hemisphere type model. Is there a significant Southern Hemisphere response to changes in local summer insolation? Is the Waimea Formation an outcome of a glaciation associated with the southern solar insolation minimum at c. 82 to 80 ka (see figure 4.3). A slightly lagged climate response places the Waimea Formation comfortably into this event, allowing a literal interpretation of the numerical ages discussed in chapter 6. This could be seen as a time of low heat input into the ocean in summer, a high summer insolation gradient across the mid latitudes, and relatively strong westerly airflow along and across the middle latitudes. The summer insolation minimum at 80-82 ka is more pronounced than any of the 4 subsequent minimum (including the 25 ka minimum during the LGM). Could reduced summer insolation at this time have had a direct impact on ice ablation/accumulation in the Southern Alps? (figures 4.3 and 4.4 below). In terms of insolation received at the top of the atmosphere at 40°S the difference between 0 ka (492 w/m^2) and 80 ka (449 w/m^2) is 43 w/m^2. At the top of the atmosphere this is a direct difference in blackbody heating potential of (305.2 - 298.3 K) = 6.9°C. Naturally this figure does not account for a host of other relevant climatic influences. Nor does it account for losses directly to space due to reflection by the surface and by clouds, or in other words that part of the incoming radiation that does not contribute to surface climate.

4.2.4 Long-term trends in Solar Insolation in the Southern Hemisphere

At an orbital/Milankovitch timescale there is substantial seasonal variation in the direct incidence of delivery of solar energy in low to mid latitude oceanic areas in the Southern Hemisphere. The very high percentage of ocean surface in this region potentially makes it rather susceptible to changes in sea-surface temperature forced directly by changes in the timing of variation in seasonal insolation. In terms of local climate this then has a significant influence on surface air temperature in maritime areas. Changes in solar insolation impact on air pressure and temperature gradients, heat content, humidity and wind speed. In terms of the Late Quaternary period in the Southern Hemisphere the influence of these factors is not particularly well understood and they will not be modeled in detail here. The purpose here is to briefly point out some of the bounding conditions and emphasize that strict adherence to a dominant Northern Hemisphere climate forcing paradigm could be of limited value for Quaternary climate studies in Westland.

In figures 4.2a and 4.2b long-term changes in the three primary variables governing mean monthly and annual solar insolation values are defined. The variables are the eccentricity of the Earth's orbit around the sun, the obliquity of the earths rotational axis (to the plane of the orbit), and the precession (wobble) of the rotational axis. The impact of these variables on Southern Hemisphere summer insolation is displayed in figure 4.3.

Figure 4.2a Obliquity of the Earth's rotational axis.

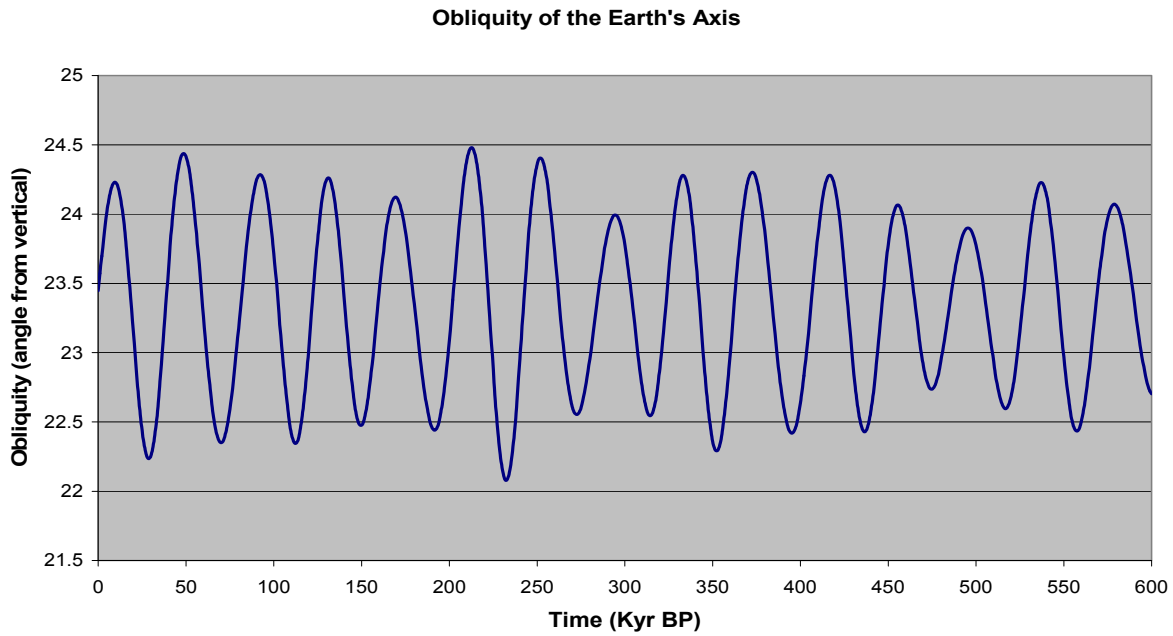

Peaks (+ve) in the precession values in figure 4.2b correspond to decreased summer insolation at mid to high latitudes in the Northern Hemisphere. Conversely these peaks correspond to increased summer insolation at mid to high latitudes of the Southern Hemisphere. In figure 4.2a larger values of obliquity (greater axial tilt) correspond to summer warming at mid to high southern latitudes.

Figure 4.2b Eccentricity of the Earth's orbit around the Sun and precession of the Earth's rotational axis.

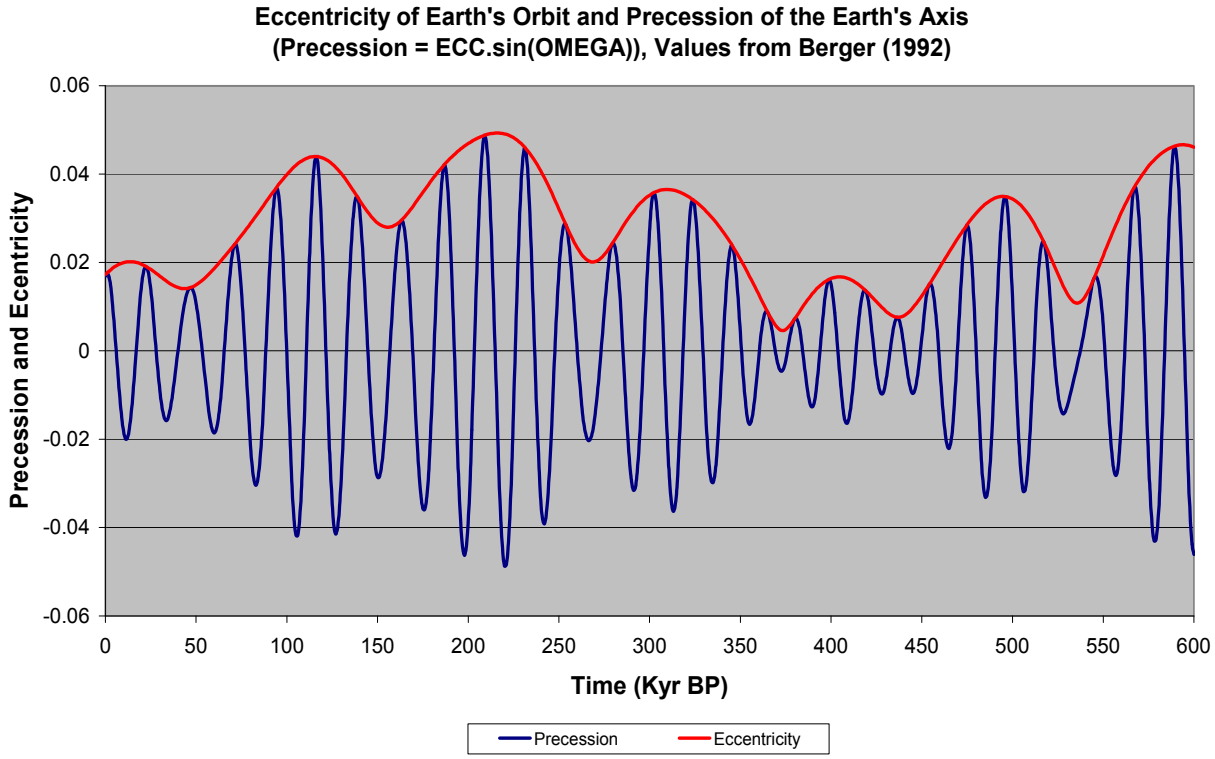

As can be seen from figure 4.2b and figure 4.3 the eccentricity cycle modulates the strength of the precessional signal but has less impact on the obliquity signal.

4.2.5 Top of Atmosphere Insolation and Temperature

Berger (1992) & Berger & Loutre (1991) have calculated the mean monthly insolation at one thousand year intervals for the last 10 million years for various latitudes. This is the source for the data presented in figures 4.2, 4.3 and 4.4. The insolation data as presented by Berger & Loutre are essentially the solar irradiation received at the top of the atmosphere (TOA), prior to any loss by reflection, transformation by absorption or transport by advection. So these figures are not equivalent to the energy received at the ground surface. The monthly mean data are presented on a per-unit-area (per m^2) basis at each latitude for a surface oriented parallel to the surface of the Earth.

In figure 4.7 the monthly mean "top of atmosphere insolation" has been converted to a "top of atmosphere temperature". This is the expected mean temperature of emission to interplanetary space of a blackbody object in response to the continuous incidence of that quantity of solar insolation. The altitude at which this temperature is measured is that where all of the outward emission of energy occurs by radiation and none occurs by convection (transfer of kinetic energy and latent heat) or conduction. It is assumed here that:

- At each latitude the TOA temperature of emission will respond directly to seasonal changes in insolation at that particular latitude (this response is modulated by factors internal to the Earth's climate system).
- At each latitude the TOA temperature of emission will respond directly to orbital-scale changes in insolation at that particular latitude (this response is modulated by factors internal to the Earth's climate system).
- Broadly speaking, each latitude has its own characteristic TOA temperature of emission and this impacts directly on the surface temperature.

For the purposes of this discussion it is assumed that the TOA temperature of emission responds fully and immediately to seasonal changes in the incident solar insolation. In the real world, on a seasonal basis, trends in temperature will parallel but slightly lag trends in insolation as demonstrated in figures 1.1a and 1.1b. In the real-world the TOA temperature response is affected by atmospheric and oceanic processes that allow accumulation, advection and delayed emission of heat within the climate system. For simplicity it is assumed that the scale of these effects is stationary through time.

In the illustrations that follow the focus is on the potential impact of variation in summer and annual insolation on the climate in the New Zealand region. The latitudinal insolation data most relevant to climate in Westland during the last 222 kyr are displayed in 4.3. At each latitude summer insolation varies with time. Note the strong influence of the precessional cycle which imparts a periodicity of approximately 21 kyr.

Figure 4.3 The variation in top-of-atmosphere mean summer (January) solar insolation from 30°S to 80°S.

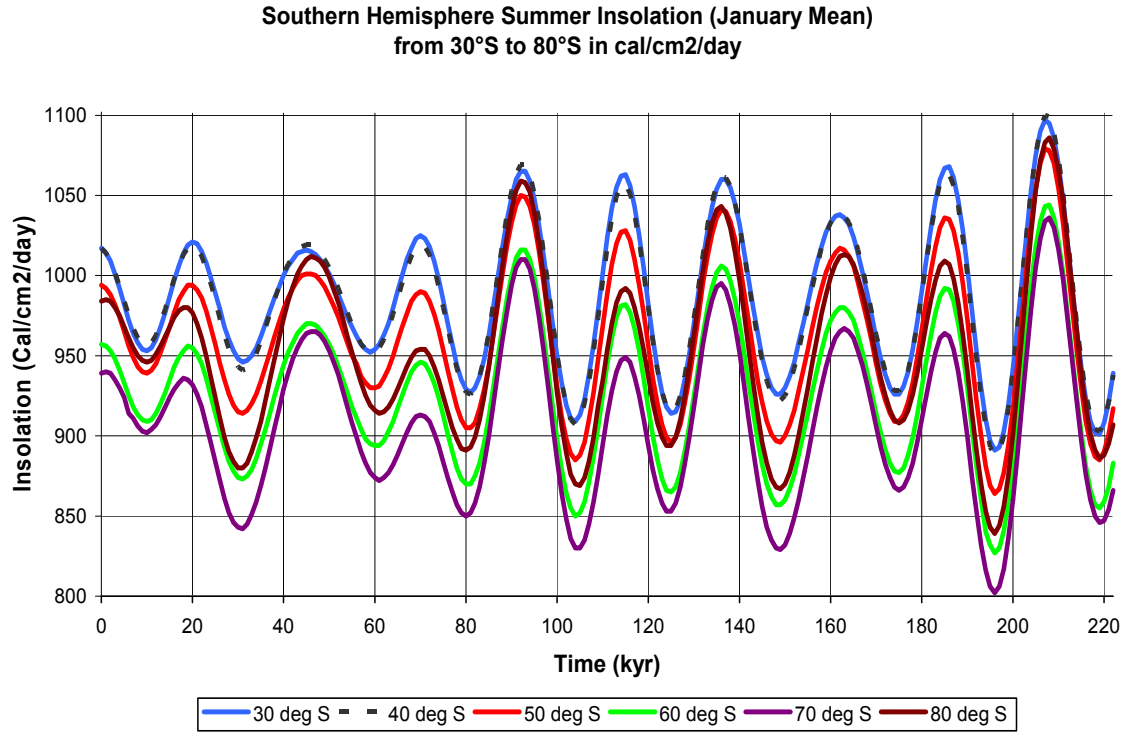

Note that a number of the prominent precessional peaks evident in figures 4.3 ands 4.4 are absent from a number of the figures that follow. It is worth bearing in mind that summer insolation maxima in the c.20 kyr precessional cycle in mid-latitudes of the Southern Hemisphere are precisely in anti-phase with those at the same latitude in the Northern Hemisphere. Given the strong variation (up to ~15%) in summer insolation over the southern polar region one might expect to see this expressed in long continuous climate archives from Antarctica. However as can be seen in figure 4.3b annual average surface temperature at the Dome Fuji ice core site is generally in an antiphase relationship with summer insolation at 60°S. The temperature data are from Kawamura et al (2007).

Figure 4.3b Surface temperature anomaly at Dome Fuji, Antarctica contrasted with mean January insolation at 60°S

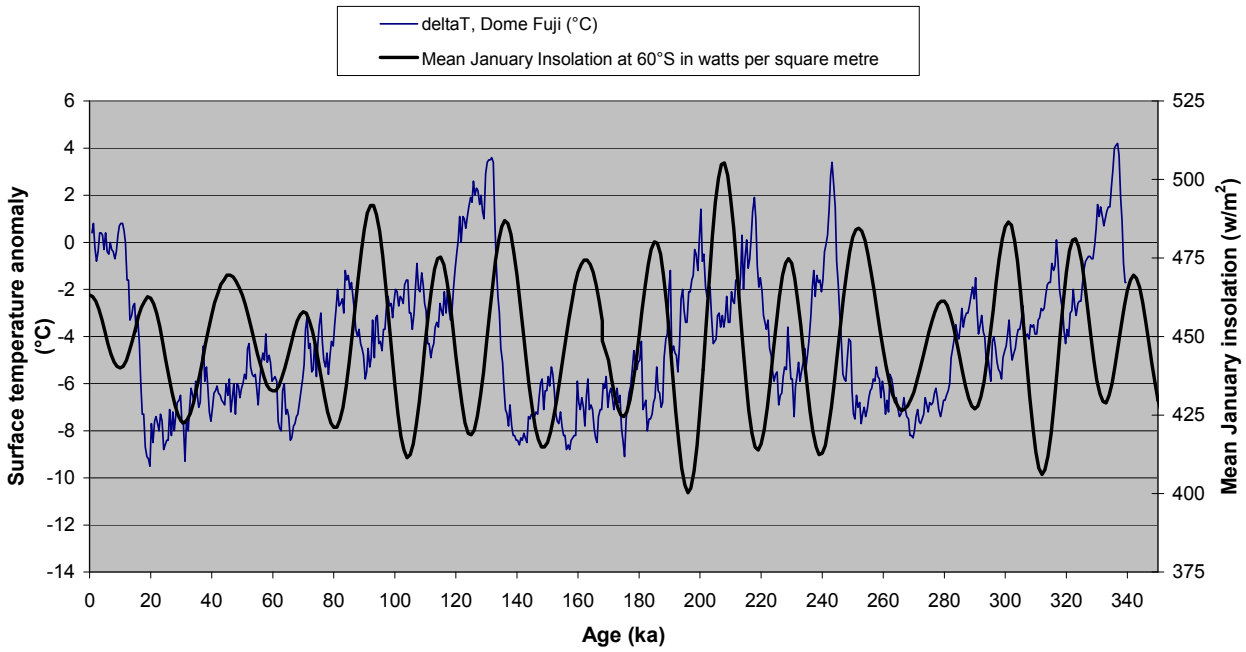

Clearly something other than local summer insolation must be the primary driver of surface temperature at Dome Fuji. There is essentially zero winter insolation here (see figure 4.4). So regardless of the influence of precession and obliquity on insolation, variation in the local input of solar energy at 70°S to 90°S must be dominated by the summer precessional curve. This precessional cycle is displayed in the N_2/O_2 ratio from air trapped in the ice at Dome Fuji (and Vostok) but not in the annual mean surface temperature. The N_2/O_2 ratio that forms the basis for the Dome Fuji ice-core age-depth relationship (Kawamura et al (2007) and the Vostok timescale (Suwa et al 2008). Does this antiphase relationship indicate that at an orbital-scale temperature variation at Dome Fuji is broadly controlled by Northern Hemisphere forcing mechanisms? Is there an alternative Southern orbital-scale forcing that can be correlated directly with air temperatures over Antarctica, and by extension to other Southern regions? These questions are relevant to the analysis of the Suggate model which broadly assumes that major climate-change in North Westland follows a Northern Hemisphere rhythm.

Dome Fuji is not the only Antarctic ice-core site that exhibits this rather muted direct response of surface temperature to local insolation change. Similar patterns can be observed in the long temperature records from Vostok Station (Petit et al 2001) and Dome Concordia (Parrenin et al 2007)

and in the isotopic records from the Dronning Maud Land (EPICA team members 2006) and Taylor Dome (Steig et al 2006) cores. These patterns are illustrated in figure 4.15c and figure 4.16.

Figure 4.4 Top-of-Atmosphere Winter (July Mean) Insolation, Southern Hemisphere from 40°S to 70°S in cal/cm2/day

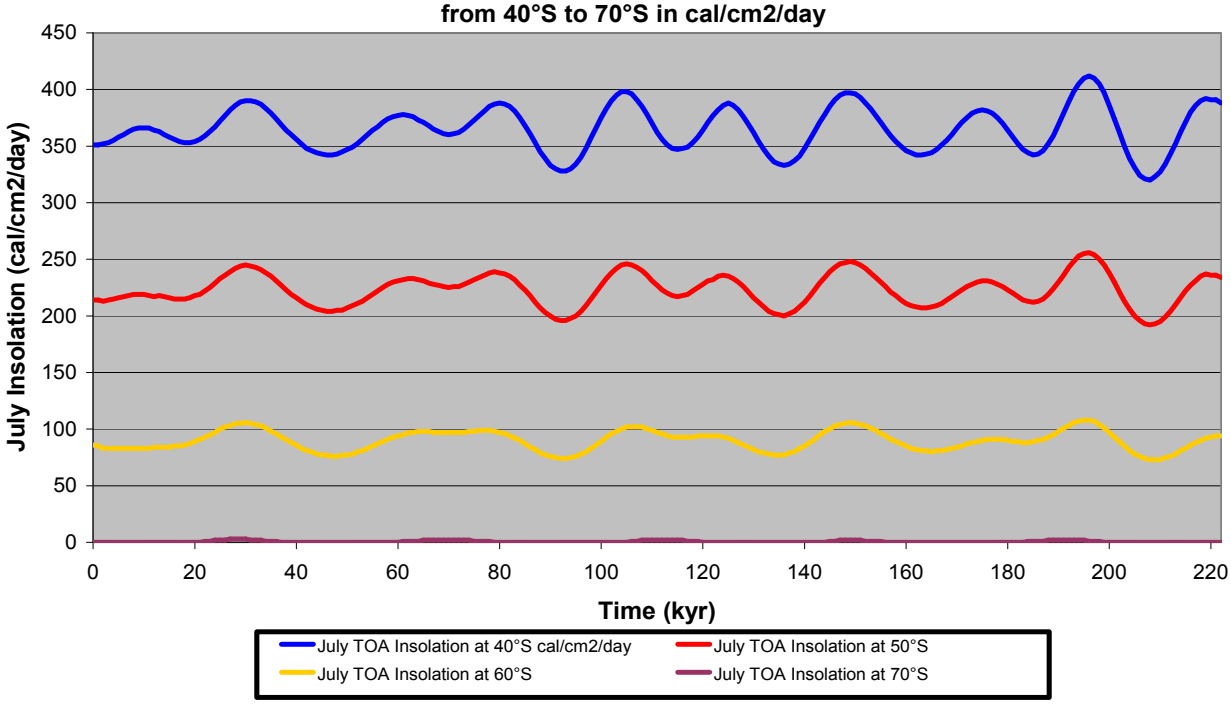

4.2.6 Cross-latitudinal Insolation and Temperature Gradients of the Southern Hemisphere

The following discussion focuses on the cross-latitudinal (or meridianal) transport of heat within the climate system of the Southern Hemisphere, which is in part driven by variation in the cross-latitudinal theoretical top of atmosphere blackbody temperature gradient. This temperature gradient, which clearly has an analogous gradient at the Earth's surface, impacts on the lateral advection of heat within the climate system. On an annual basis this temperature gradient influences the development and position of strong circumpolar westerly winds. At an orbital timescale changes in this gradient may impact on the strength and position of the circumpolar westerly wind belt. In a North Westland context this is significant because such changes could influence the annual mean surface temperature, mean annual precipitation, mean wind direction and cloud cover. As discussed in part 4.1 above, temperature, precipitation and cloud cover all impact on ice accumulation in the Southern Alps.

Figure 4.5 (below) was compiled as a continuation of the summary of climate station data presented in Chapter 1. It illustrates the mean annual surface temperature from various climate stations situated within New Zealand, Antarctica and Chile and on islands within the Pacific Ocean, Tasman Sea and Southern Ocean. The meridional pattern has a clearly discernable trend. North Westland is situated at approximately 41°S to 43°S and fits neatly into the trend, which is slightly spiky due to a significant latitudinal spread among the climate stations that define the trend. Spikiness is also imparted by local effects from station specific microclimates, and variations in the local influence of oceanic and atmospheric circulation patterns. Across the Antarctic continent the trend includes an adjustment for

surface elevation. Most other stations are either at or close to sea level and no correction was applied. Over millennial to orbital timescales relative heating or cooling at various points along the meridional trend may have the capacity to alter its gradient. This could impact other sites along the meridian including North Westland.

In the analysis presented here, rather than using insolation gradients, theoretical top of atmosphere temperature gradients are used as a proxy for heat transport. While the top of atmosphere (TOA) insolation is a measure of the input of heat into the climate system it is not equivalent to the heat input at the Earth's surface. The combined effects of lateral advection of heat and local downward radiative heat input at the surface controls the accumulation/ablation of snow and ice and by extension glacial advance and retreat. However, there is no simple way to construct a reliable long-term record of heat flux at the Earth's surface. Changes in the theoretical TOA temperature and insolation for each latitude are used here as a bounding condition.

For simplicity it is assumed that for Southern Hemisphere middle latitudes the greybody (surface) temperature response to orbital-scale fluctuations in insolation is generally proportional to the TOA blackbody temperature response. This requires a simplifying assumption that on a regional basis the seasonally averaged albedo, humidity and air pressure are more or less constant through time. There will be times when these and other factors temporarily overwhelm or reverse the impact of changes in the meridional TOA temperature gradient. That does not imply that orbital scale forcing at the TOA ceases to have an impact on climate. For evidence of the effect of changes in the temperature forced by the TOA insolation gradient one would need to apply a filter to remove other variables. As discussed below this has effectively been carried out for one climatic archive by Vimeaux et al (2002).

Figure 4.5 The cross-latitudinal temperature gradient across New Zealand and adjacent regions.

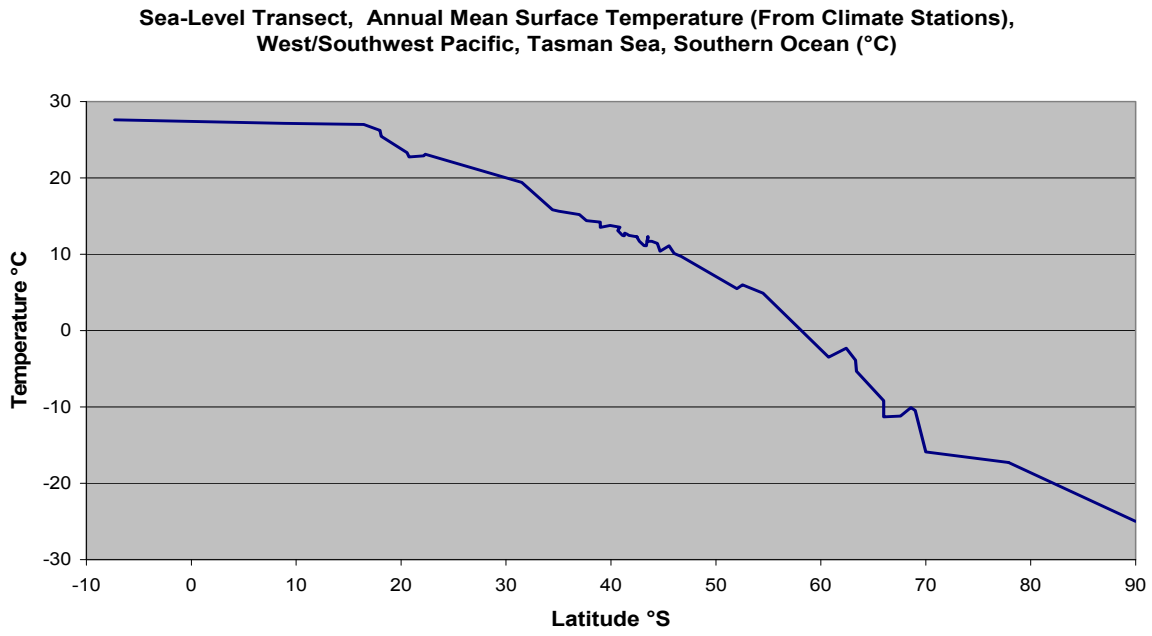

The modern cross-latitudinal temperature trend in annual mean sea-level temperature illustrated here is not stationary through time. In the following discussion a number of the factors that influence this trend are examined. The questions that drive the investigation include:

- Is the difference in solar input at the TOA at two points in the same hemisphere situated on a single meridian approximately the same through time, or does the difference change significantly in a predictable manner?
- If we take the same two localities and calculate the TOA blackbody temperature at each at regular intervals through the Quaternary period what is the pattern of relative temperature difference?
- If there is a pattern to the temperature difference how is this related to orbital scale control on insolation?
- Is the pattern the same for all seasons?
- Can any trends in meridional temperature difference be identified in palaeoclimatic records.

The literature on this subject is not particularly extensive. Relevant studies include Davis & Brewer (2009, 2011). Davis & Brewer (2009) examine the subject from a largely Northern Hemisphere perspective and document the impact of cross-latitudinal temperature contrasts in continuous Holocene pollen series. Davis & Brewer (2011) review the topic, again primarily from a Northern Hemisphere perspective and describe differences in the orbital components between the winter and summer seasons.

Figures 4.6a and 4.6b below chart the relationship between incoming solar radiation and the blackbody temperature of a spherical body that intercepts that radiation. This relationship is based on the Stefan-Boltzmann equation:

$\mathbf{T = \sqrt[4]{(E/\sigma)}}$ where:

σ = Stefan's constant {= 5.67×10^{-8} $W/m^2/deg^4$},
E = solar irradiation in w/m^2, and
T = the "Blackbody temperature" (in degrees Kelvin) of the irradiated object assuming zero reflection

This equation is used to derive the expected mean top of atmosphere (TOA) temperature for any particular month and latitude by adopting the mean insolation for that month. The underlying data are from Berger & Loutre (1991) who provide mean values at latitudes separated by 10° from the North Pole to the South Pole for each month at 1 kyr intervals over the last 10 Ma. They report insolation in units of $cal/cm^2/day$. In order to use the data in the Stefan-Boltzmann equation a conversion is applied to give energy in w/m^2(watts per square metre). The relationship is:

$1 w/m^2 = 2.066$ $cal/cm^2/day$

The orbitally controlled insolation values archived by Berger & Loutre (1991) provide an important and continuous external driver to the long-term climate at regional and hemispheric scales. There are many other factors that influence the climate system. These include external forcings like the variation of solar output at source and internal forcings within the Earth's climate system. Some may have regular cycles (for instance the slight variation in solar irradiance that accompanies the ~ 11 yr sunspot

cycle) and some may be somewhat chaotic. The theoretical orbital control on TOA blackbody temperature of emission for several different latitudes is illustrated in figures 4.7, 4.8, 4.10, and 4.11.

Figure 4.6a Blackbody temperature (K) in response to solar irradiance (w/m^2).

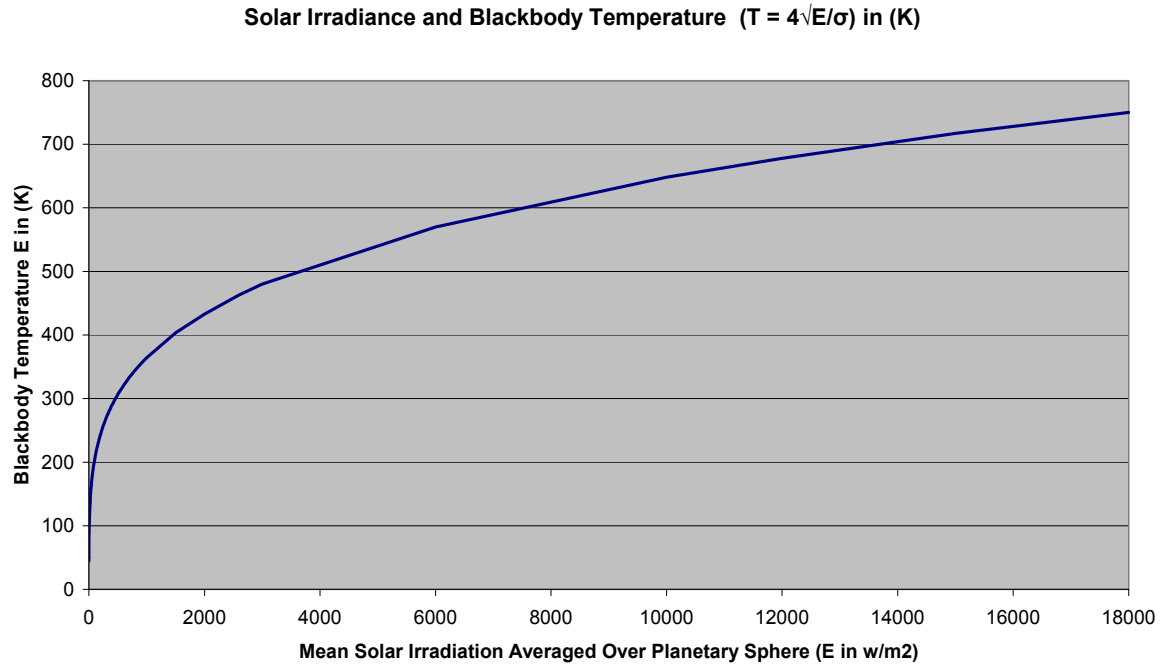

Figure 4.6b Blackbody temperature (K) in response to solar irradiance (w/m^2).

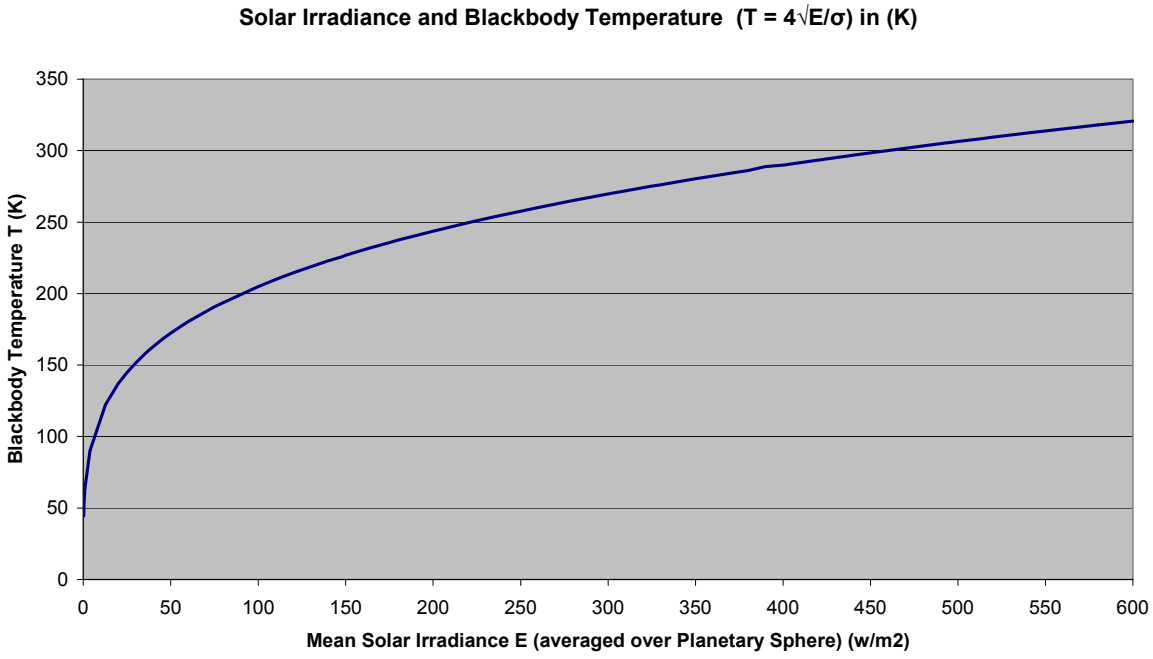

Figure 4.7 Potential summer "Blackbody" temperature response to changing insolation from 40°S to 70°S, ignoring lateral advection of heat through the climate system.

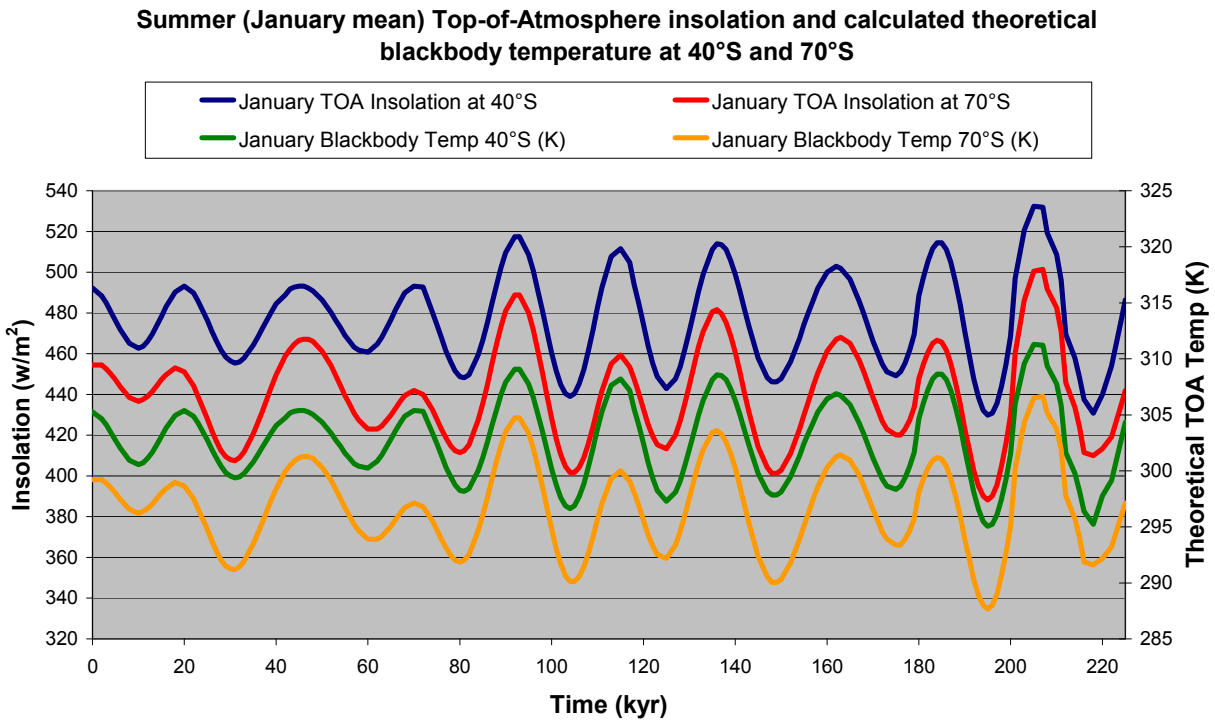

As discussed in Chapter 1 the extent of glacial ice in the Westland region is dependent on the elevation of the ELA (equilibrium line for ice accumulation). Fundamentally for individual localities changes in seasonal insolation are important in terms of climatic evolution. Similarly changes in the insolation gradient between locations are likely to have a significant impact on climatic evolution. However, changes in insolation measured in w/m^2 are not particularly informative in terms of the potential influence they exert on the ELA. This is one reason why it is useful to look at the effect that changes in insolation may have on the TOA blackbody temperature. While this is not the same as the effect of insolation on surface temperature it does inform us of the potential magnitude of temperature change or at least one component of such change. Temperature is more easily related to potential for change in the ELA than insolation. In addition we tend to be conditioned by life-experience to think in terms of temperature rather than heat/energy. So consideration of the impact of insolation on temperature may make the magnitude of "orbital-scale" fluctuation of insolation more meaningful.

4.2.7 Relative Impacts of Precession and Obliquity

The latitude of Westland is approximately 41°S to 44°S. Here the peak values for summer and winter insolation (see figures 4.3, 4.4, and 4.7) occur cyclically with a period of approximately 20 kyr. The obvious periodicity in these curves is imparted primarily by the precessional and obliquity cycles. Visually the most striking feature is the impact of the Earth's precessional cycle. One question raised here is whether local air temperatures, precipitation and ice accumulation are controlled primarily by local solar forcing via the combined precessional and obliquity cycles, or by the mean air-pressure and temperature gradients across the southern mid latitudes as a whole? The pressure and temperature gradients together control seasonal wind patterns, heat transport (advection from other regions) and

moisture transport. The air-pressure and temperature gradients are strongly influenced by the regional gradient in solar forcing.

Figure 4.7 demonstrates that the trends in the theoretical top-of-atmosphere summer (mean January) insolation from 40°S to 70°S are almost exactly in-phase and likewise for the theoretical TOA blackbody temperature. However, close inspection reveals that the difference or relative anomaly between and two summer (or winter) insolation curves is not a constant value. Figures 4.9 and 4.10 illustrate the substantial variation in the summer and spring (mean January and mean October) insolation and TOA blackbody temperature gradients between 40°S to 70°S. The "first difference" in values between the two latitudes is cyclical and has a period of approximately 40 kyr. This cycle is driven almost exclusively by variation in the obliquity (or tilt) of the Earth's spin axis. A similar cycle occurs in the Northern Hemisphere. These two hemispheric cycles are slightly out of phase both with each other and with the obliquity cycle. This is illustrated in figure 4.11c. The two corresponding (Northern and Southern Hemisphere 1st difference) curves can be summed to give a combined curve that follows the cycle in the Earth's obliquity precisely. There have been five maxima and six minima within the Southern Hemisphere cycle over the last 220 kyr. The minimum in Southern Hemisphere cross-latitudinal summer insolation gradient corresponds to the maximum tilt of the Earth's axis. At the present time the West Coast region is approximately midway between the extreme low and high points of this cycle.

Figures 4.9, 4.10, 4.11a, and 4.11b also demonstrate that the Earth's precessional cycle has little impact on middle to high-latitude seasonal temperature ($\Delta T_{40S} - \Delta T_{70S}$) gradients. For any particular month axial precession does change the intensity of seasonal insolation but these changes are synchronous and have more-or-less equal magnitude across the middle to high southern latitudes. In the Southern Hemisphere meridional differences in the value of seasonal or monthly insolation between any two particular latitudes (figure 4.8 for instance) do not change substantially in response to the precessional cycle. This is significant because the vigour of weather systems is controlled primarily by meridional energy and pressure gradients rather than by the absolute temperature (which is influenced by the precessional cycle). One would expect a tendency for more vigorous circulation (storminess) and lateral heat transport when the energy/temperature gradient is at a maximum. For summer this corresponds precisely to obliquity minima i.e. periods when the rotational axis is more "upright". Similarly there is an expectation that less vigorous summer circulation (with more local summer heating) will occur when the energy gradient is at a minimum (which corresponds to global obliquity maxima). But note from figure 4.11a and figure 4.11b that the summer and winter cycles in meridional TOA blackbody temperature gradient have an antiphase relationship.

The precessional cycle is probably less significant in terms of forcing of regional climate in the New Zealand region than it is over the northern half of North America. In New Zealand there is minimal opportunity for the development of truly continental-scale ice sheets that impact in a major fashion on climate and atmospheric circulation at the hemispheric and global scales.
Figures 4.9 and 4.10 (below) display the cycles in the summer (January mean) and spring (October mean) top-of-atmosphere blackbody temperature gradient between latitudes 40°S and at 70°S. The first differences are calculated at 1000 year intervals. This is done for each latitude by taking the January mean values for insolation provided by Berger & Loutre (1991), converting the mean insolation to a theoretical TOA blackbody temperature, taking the difference between these two values, and averaging this over the 30° latitude band. From figure 4.10 it can be seen that there are similar cycles in the summer and spring cross-latitudinal TOA blackbody temperature gradient. See table 4.3 for a comparison of the timing between these two cycles. There is a similar winter pattern which has an antiphase relationship to the summer curve (figure 4.11a and figure 4.11b).

Figure 4.8: Potential summer (January mean) TOA blackbody temperature response to changing summer insolation at 40°S and 70°S

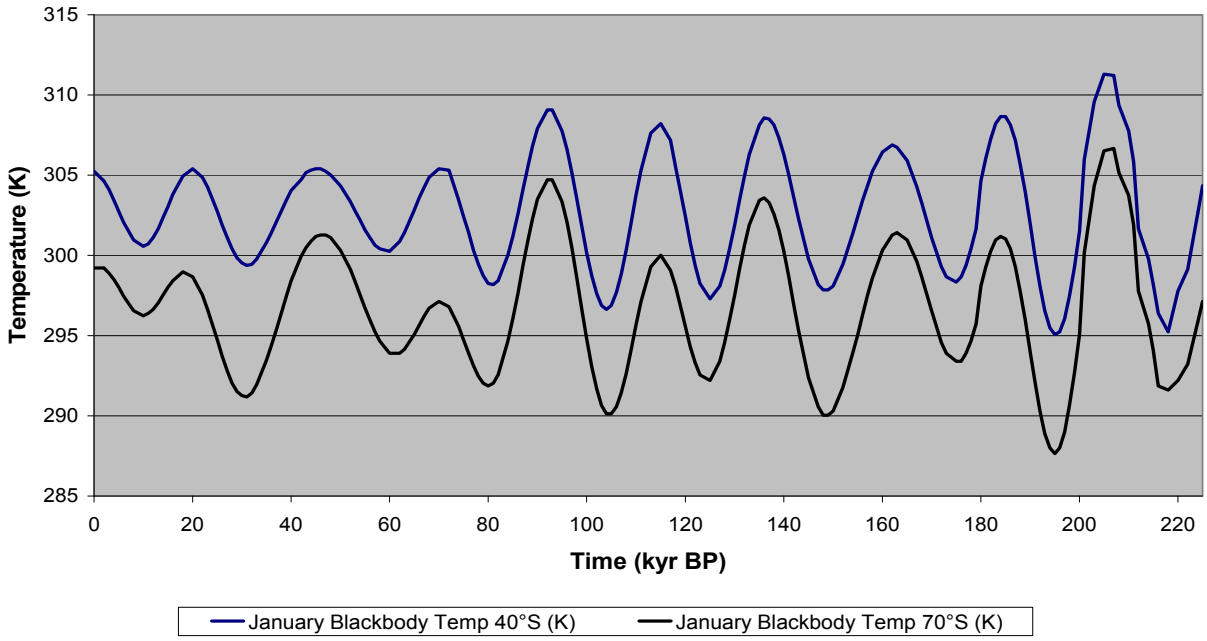

In figure 4.9 the dips represent smaller values for the summer cross-latitudinal TOA blackbody gradient. From figures 4.10, 4.11a and 4.11b it can be seen that there is a similar cycle in the spring (October mean) cross-latitudinal TOA blackbody temperature gradient, peaks and troughs having a similar timing to those of the summer cycle. See table 4.3 for a comparison of the timing between these two cycles.

Figure 4.9: Variation in meridional summer (January mean) TOA insolation gradient from 40°S to 70°S across the New Zealand region caused largely by changes in the obliquity of the Earth's axis

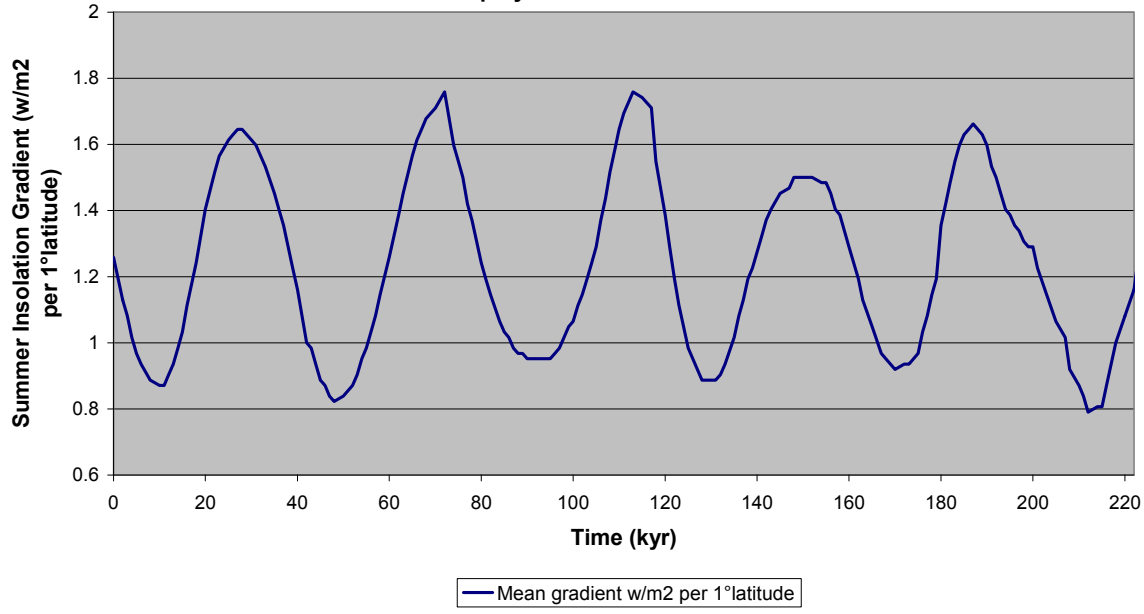

In the New Zealand region there may be a tendency towards increased meridional (north to south) heat transport at obliquity maxima. These coincide more-or-less with minima in the cross-latitudinal spring and summer meridional insolation gradients and maxima in the winter meridional insolation gradient. Periods of maximum mean temperature in Antarctica appear to coincide with periods of maximum winter meridional insolation gradient which coincide with the maxima top of atmosphere (TOA) theoretical blackbody temperature gradient (figures 4.11a, 4.11b, 4.11c, 4.11d. 4.12b, 4.14)

In Antarctica regional cooling tends to correlate with obliquity minima (figure 4.11d, 4.14). At such times the annual index of meridional temperature difference between 40°S and at 70°S (black curve in figures 4.11a and 4.11b) is at a minima and this corresponds to the minimum mid to high latitude TOA blackbody temperature difference during the winter season. In other words the mean annual surface temperature in Antarctica (see figure 4.14) is at a minimum when the winter TOA mid to high latitude temperature gradient is at a minimum. At such times the lateral advection of heat into the Antarctic interior appears to be reduced.

The winter TOA blackbody temperature gradient is always high across the mid to high-latitudes (see figure 4.10 above). So there is always strong meridional energy transfer (across the Southern Ocean) during the winter to early spring period. But the magnitude of this effect is variable. From figures 4.11a and 4.11b it can be seen that the variability of winter TOA meridional temperature gradient (amplitude of the cycle) is greater than the variability in the summer TOA meridional temperature gradient. When these effects are summed to give an annual index the winter trend tends to dominate the result (figures 4.11a, 4.11b, 4.11c).

In terms of modern climatic patterns, precipitation peaks during the spring season. Monthly mean precipitation at western South Island recording stations is displayed in figures 1.2a to1.2e and tables 1.1a, 1.1b and 1.2. The springtime peak in precipitation is accompanied by an abundance of snowfall in the Southern Alps. There is a long-term cycle in the spring-time cross-latitudinal temperature gradient between 40°S and 70°S as shown in figure 4.10. This c. 40 kyr cycle is controlled by the obliquity of the Earth's spin axis rather than by its precession. It is likely to impact on spring-time temperature, precipitation and snow ablation in the Southern Alps.

If long-term changes in the mean climatic state in Westland are driven to a significant extent by external processes the there should be some an imprint on long-term climate proxies including sea surface temperature in the New Zealand region. Rates of heat transport within the climate system may vary with time and the trends may have opposite sign between the summer and the winter. The question of which seasonal effect is dominant may be hard to answer. The simplest approach may be to integrate the meridional gradients over the full year and see whether this corresponds to long records of sea surface temperature. This comparison is made in figures 4.15a, 4.15b and 4.15c. From these figures it is reasonably clear that SST maxima in the New Zealand region correlate very strongly with periods of maximum TOA meridional blackbody temperature gradient across the mid to high southern latitudes. Similarly broad SST minima tend to correspond to periods of minimum TOA meridional blackbody temperature gradient. There is likely to be an impact on ice accumulation and ablation in Alpine regions of the South Island and potentially an impact on glacial advance and retreat.

The precessional cycle is significant in a local sense in that it strongly influences the absolute value of solar energy received at the ground surface. In terms of glaciation in the Southern Alps it impacts directly on spring, summer and autumn ice ablation. This is particularly important in the summer months. Along the West Coast of the South Island the regional mean air temperature is strongly influenced by the adjacent sea surface temperature. Nevertheless the local effects on air temperature

and ELA from changes in direct summer insolation are likely to be significant. This could affect the overall rates of accumulation and ablation of glacial ice in the Southern Alps, but the effect could also be partially masked by other factors including nearby sea surface temperature, and changes in annual mean precipitation.

Figure 4.10 Potential evolution of the meridinal summer (January mean) and spring (October mean) TOA "Blackbody" temperature gradient ($\Delta T_{40°S} - \Delta T_{70°S}$) between 40°S & 70°S caused largely by changes in the obliquity of the Earth's axis.

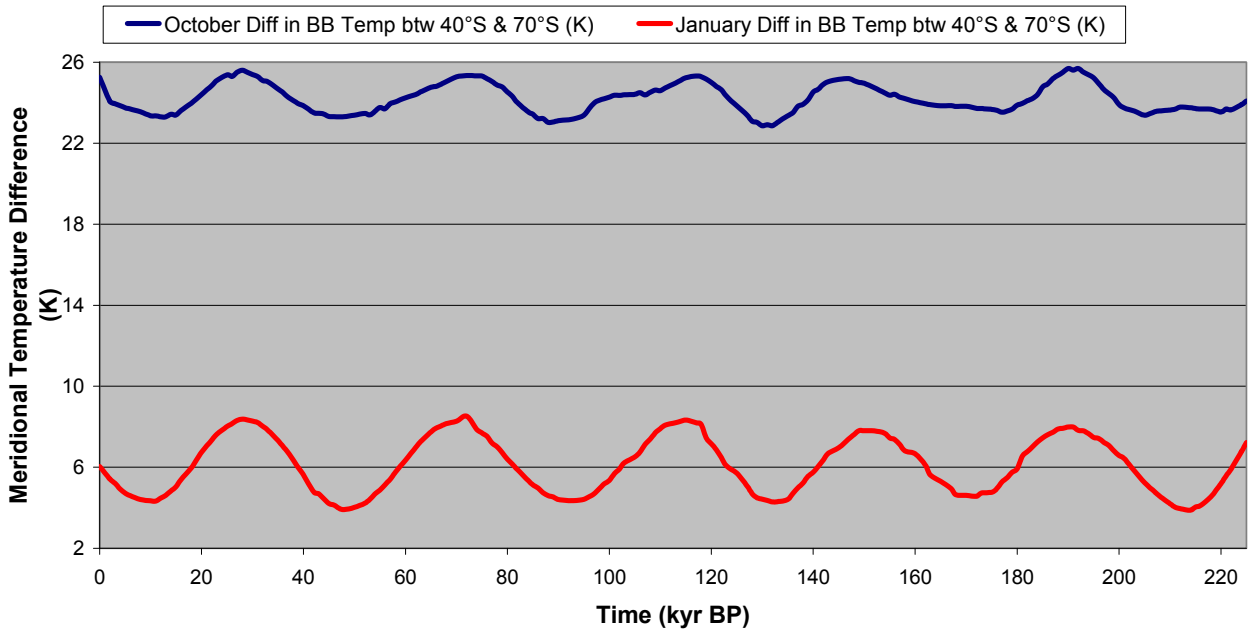

The eccentricity cycle is readily identifiable in figure 4.3, 4.11a, 4.11b, 4.11c, and 4.12a. This cycle will have an effect on surface temperature and so on spring and summer ablation but the impact will be difficult to extract from long proxy climate records. Examination of figures 4.9 and 4.10 indicates that the c.100 kyr cycle in the eccentricity of the Earth's orbit does not have a particularly strong impact on the meridional summer and spring insolation and TOA blackbody temperature gradients between 40°S and 70°S. In calculating these meridional gradients the full (combined effect of obliquity, precession and eccentricity) values for mean-spring and mean-summer insolation were used. The absence of a clear eccentricity signal in summer and spring output implies that there is a high degree of meridional stationarity in this input. In other words eccentricity does not impact substantially on meridional differences in spring or summer insolation between 40°S and 70°S. Both latitudes are impacted by eccentricity approximately the same amount at the same time.

In contrast to spring and summer the eccentricity cycle is readily visible in the winter meridional TOA blackbody temperature gradient (figure 4.11a). It is also visible in the summed annual index of monthly anomalies (figures 4.11a, 4.11b).

There is support for the view that the obliquity cycle exerts a substantial influence on middle latitude climate. The five quotes that follow come from Kukla & Gavin (2005):

> "The change of obliquity (axial tilt) affects the insolation reaching polar caps and the equatorial belt in summer and winter. The effect is symmetrical in both hemispheres. The impact on middle latitudes and in transitional seasons is minor. At low obliquity, less energy is received at the poles and more at the equator. The meridional insolation

gradient increases. The potential cooling effect of low obliquity is particularly pronounced near the summer solstice (late spring and early summer) in the high northern latitudes. There the difference between radiation at the top of the atmosphere (TOA) and that reaching the surface is especially large."

This is more significant than just the impact on insolation at the top of the atmosphere. The radiation which reaches the surface depends on the thickness of atmosphere through which it must pass and this is impacted by the axial tilt (obliquity).

"As illustrated by observations made at arctic drifting stations, the radiation reaching the surface decreases exponentially with decreasing solar elevation above the horizon *(Marshunova 1961*). This is due to the relatively long pathway of the solar beam through the atmosphere and by the disproportionally higher reflection from clouds and snow at low solar elevations *(Taylor & Snow 1984*). The snow begins to melt when the sun is 15° - 20° above the horizon."

"We propose that with obliquity substantially lower than today, the summers in the Northern Hemisphere would become considerably cooler and more variable. Polar air outbreaks into the middle northern latitudes would become commonplace throughout the year."

"The insolation increase at the equator is relatively small. It is largest around the solstices and negligible in transitional seasons. Zonally averaged sea surface temperature (SST) in the equatorial region changes by about 2.5°C during the year. The ocean warms between August and April and increases most rapidly in March. It cools fastest between May and July. Dynamic effects, in particular the seasonal shift of the intertropical convergence zone, probably influences the seasonal SST cycle more strongly than direct solar heating. Nevertheless, one would expect that under present climate conditions, the increased energy income between October and February due to low obliquity and a stronger winter solar beam, would enhance the ocean heating. Increased insolation between May and July would reduce the summer cooling. The change would bring the tropical oceans to a warmer state (Fig. 2). The direct radiative impact of low obliquity on the middle latitudes of both hemispheres is minor, but the indirect effect of increased equator-to-pole insolation contrast is large. It would intensify circulation vigor and increase the amplitude of waves bringing arctic air equator-ward and warm, moist air northward."

"The impact of the changed insolation cycle is dominated by the Northern Hemisphere because the annual amplitudes of SST, water vapor greenhouse forcing and snow extent are considerably smaller in the ocean dominated Southern Hemisphere. We therefore suggest that a stronger solar beam in January, February and March, compensated by a relatively weak one in July, August and September, enhances warming of the oceans in the low and middle northern latitudes, while at the same time facilitating earlier establishment of snow cover on northern continents. In combination this leads to an increased equator-to-pole temperature gradient and enhanced moisture transport to polar lands *(Vettoretti & Peltier 2003)*."

The role of the obliquity cycle in global climate change has also been discussed by Huybers (2006) who comments in relation to obliquity as follows:

"In agreement with earlier results (Huybers & Wunch 2005), terminations occur at intervals of about two (80-kyr) or three (120-kyr) obliquity cycles, on average giving the ~100-kyr variability."

"Long-term variations in Northern Hemisphere summer insolation are generally thought to control glaciation. But the intensity of summer insolation is primarily controlled by the 20,000-year cycles in the precession of the equinoxes, whereas the early Pleistocene glacial cycles occur at 40,000-year intervals, matching the period of changes in Earth's obliquity. The resolution of this 40,000-year problem is that glaciers are sensitive to insolation integrated over the duration of the summer. The integrated summer insolation is primarily controlled by obliquity and not precession because, by Kepler's second law, the duration of the summer is inversely proportional to the Earth's distance from the sun."

"One possibility is that the latitudinal gradient in insolation, which enhances obliquity over precession, is more important than local insolation (Raymo & Nisancioglu 2003). However, models used to explore the effects of changes in the insolation gradient have found that the local insolation is the more important control on glacial mass balance (Nisancioglu 2004)."

The final quote from Huybers (2007) tends to imply that the local effect of precession on ice mass-balance is very important. The argument advanced here is that the effects of obliquity and precession are not the same. Obliquity simply impacts on climate in ways that precession cannot. Further the impacts of these two variables might not be the same in the two hemispheres. In the South the polar region is occupied by a massive land based ice sheet extending to an average latitude of approximately 70°S. In the North the polar region is occupied by ocean to an average latitude of approximately 75°N. In the South there is zero possibility of the development of a major continental ice sheet at about 70°S to 50°S. However in the North two major land-based ice sheets develop during full glacial periods. These ice sheets must have substantial impacts on surface temperature, air pressure and surface albedo.

Figure 4.11 displays orbital-scale cycles in the first difference for the mean TOA blackbody temperatures at latitudes 40°S and at 70°S. These are presented for each month and on an annual basis. The values for each month are calculated as an anomaly relative to the mean long-term value for that month. The annual curve is the sum of the twelve individual monthly anomalies. The first-difference is calculated at 1000 year intervals. The mean values for insolation at each latitude are provided on a monthly basis by Berger & Loutre (1991) for each latitude. These are converted monthly theoretical mean TOA blackbody temperatures for each latitude. The major peaks and troughs in the cycles that emerge are caused primarily by change in the Earth's obliquity rather than by precession. In figure 4.11 (below) peaks correspond to a high meridional insolation gradient and probably to enhanced cross latitudinal heat transport. These peaks may also correlate with strong circum-Antarctic wind strength and strong westerly to southwesterly winds along the West Coast of the South Island.

Figure 4.11a: Monthly theoretical meridional TOA blackbody temperature differences between 40°S and 70°S and annual sum of monthly temperature differences

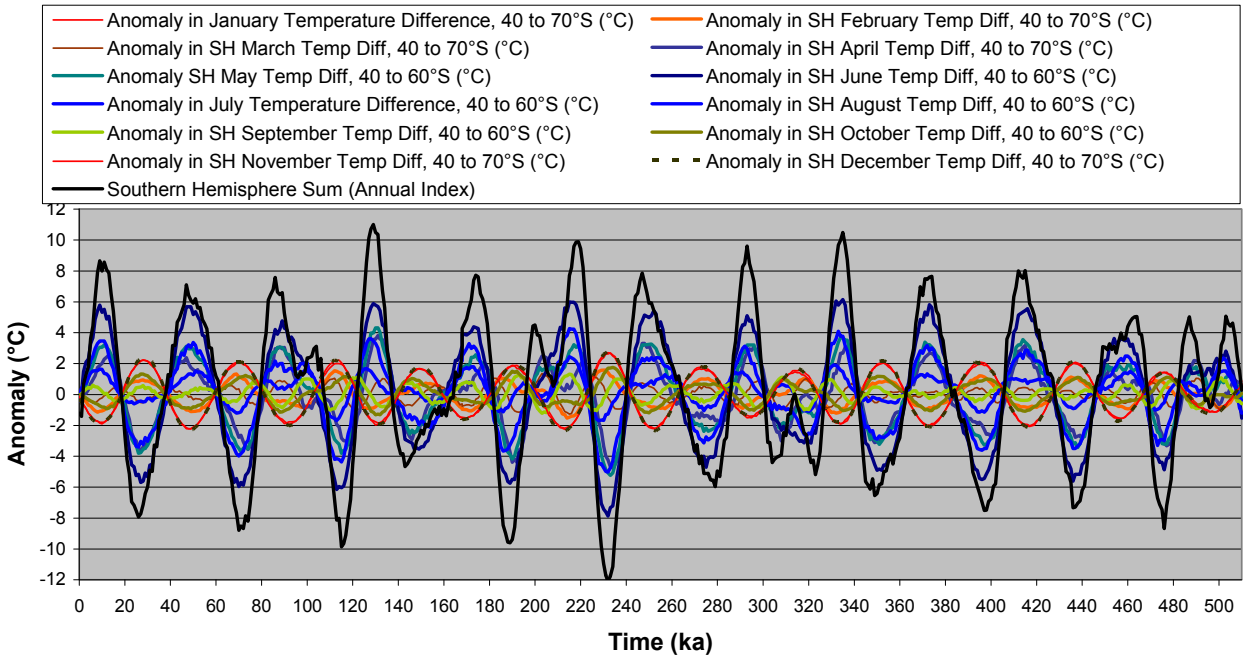

On a month by month basis the difference in theoretical TOA blackbody temperature between 40°S and at 70°S is substantially larger during the winter than during the summer. The maxima and minima of the winter and summer cycles are in antiphase. When summed to produce an annual index the timing of the maxima and minima are constrained to follow those of the mid-winter months. When this exercise is conducted for the Northern Hemisphere the result is similar. In the Southern Hemisphere

changes in obliquity are the primary cause of fluctuation in the theoretical annual and monthly meridional TOA blackbody temperature gradients. It can be seen in figure 4.12 that this is also the case in the Northern Hemisphere. In both cases subsidiary peaks on the annual (summed) index curve are the result of an interference pattern between the curves for summer and winter months.

Figure 4.11b: Detailed illustration of monthly theoretical meridional TOA blackbody temperature differences between 40°S & 70°S and annual sum of temperature differences

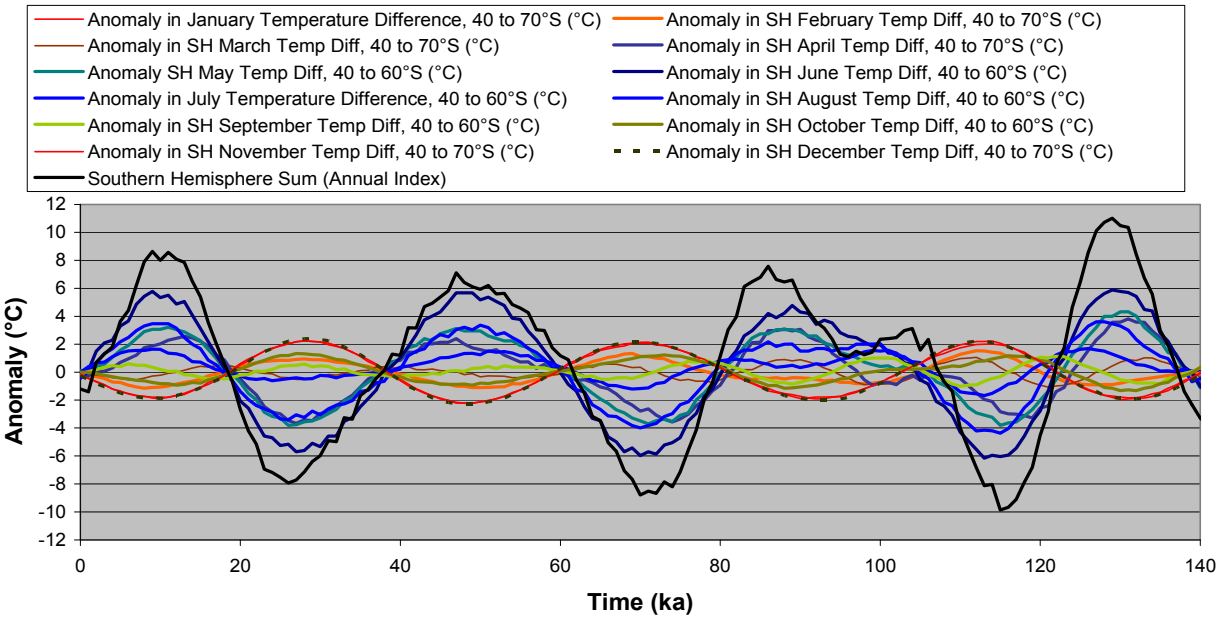

Figure 4.11c: Annual anomaly in theoretical meridional TOA blackbody temperature difference between latitudes 40° & 70°, Northern and Southern Hemispheres

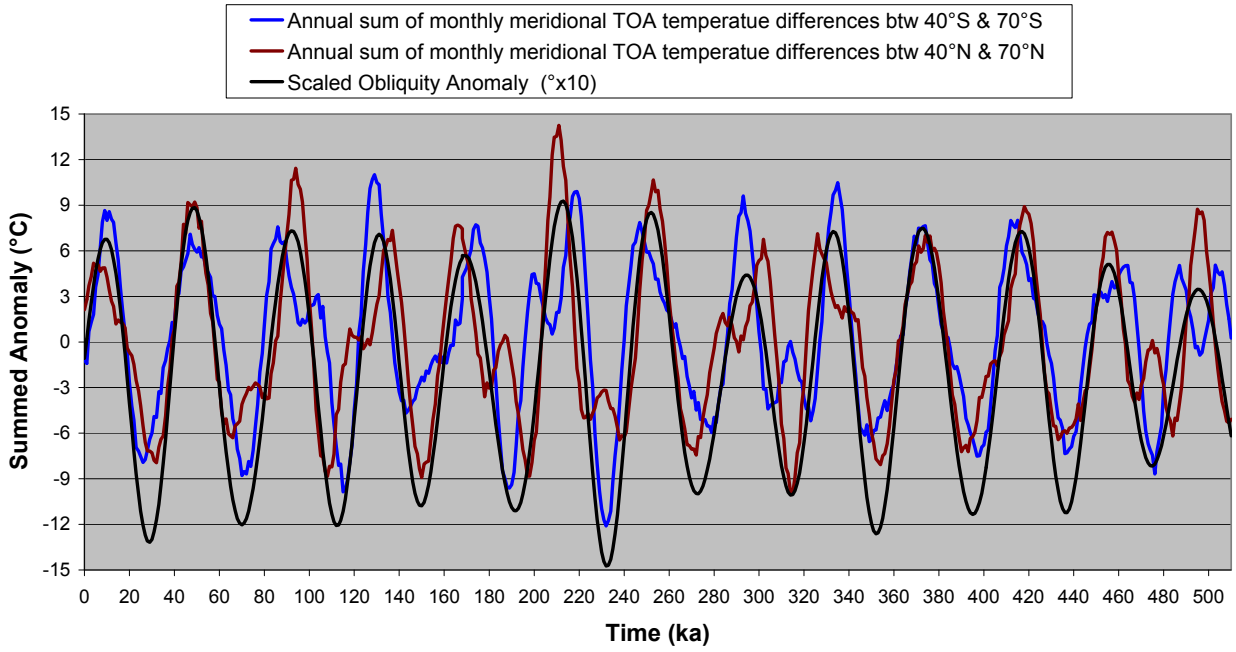

In figure 4.11c above the mid to high latitude annual indices for meridional TOA temperature difference are displayed. In both hemispheres the index is closely correlated with the obliquity of the

Earths axis. In the Southern Hemisphere this index shows only a minor influence from changes in eccentricity and precession. In both hemispheres the timing of the cycle in the temperature difference anomaly is clearly controlled by the obliquity of the Earths axis.

Figure 4.11d: Annual sum of monthly meridional TOA blackbody temperature differences btw 40°S and 70°S contrasted with $\delta^{18}O$(ice) from the Dome Fuji ice core and $\delta^{18}O$(air) from the Vostok ice core.

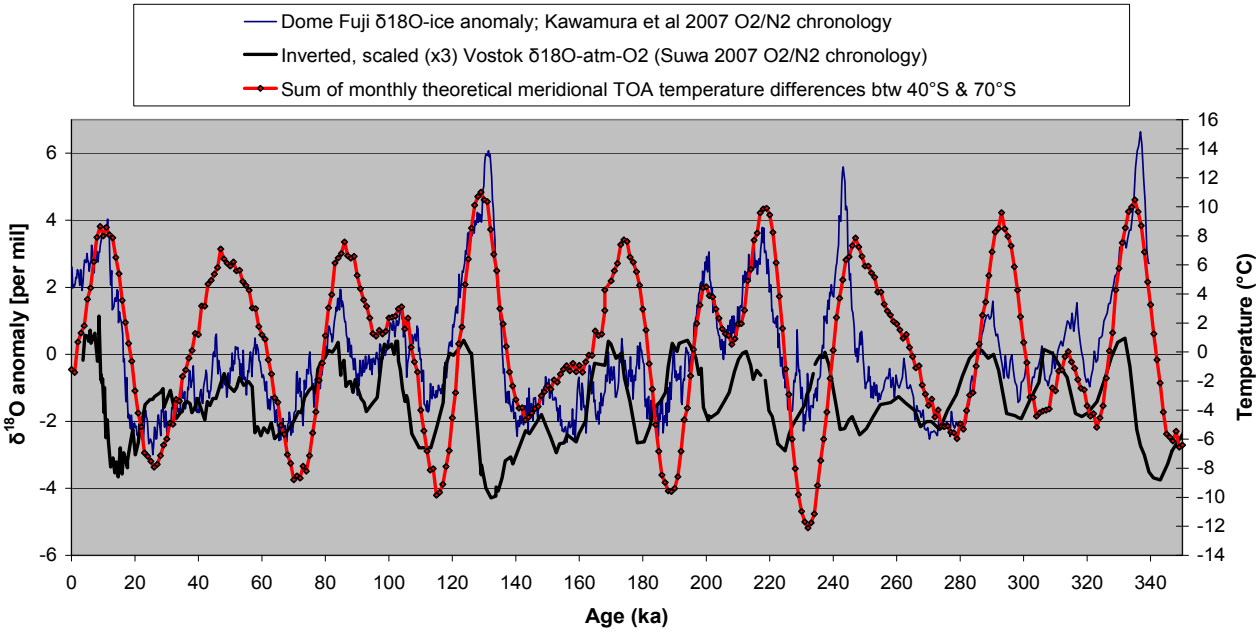

Figure 4.12a: First difference in the annual indices of Southern and Northern Hemisphere monthly meridional TOA blackbody temperature difference (between 40° & 70°)

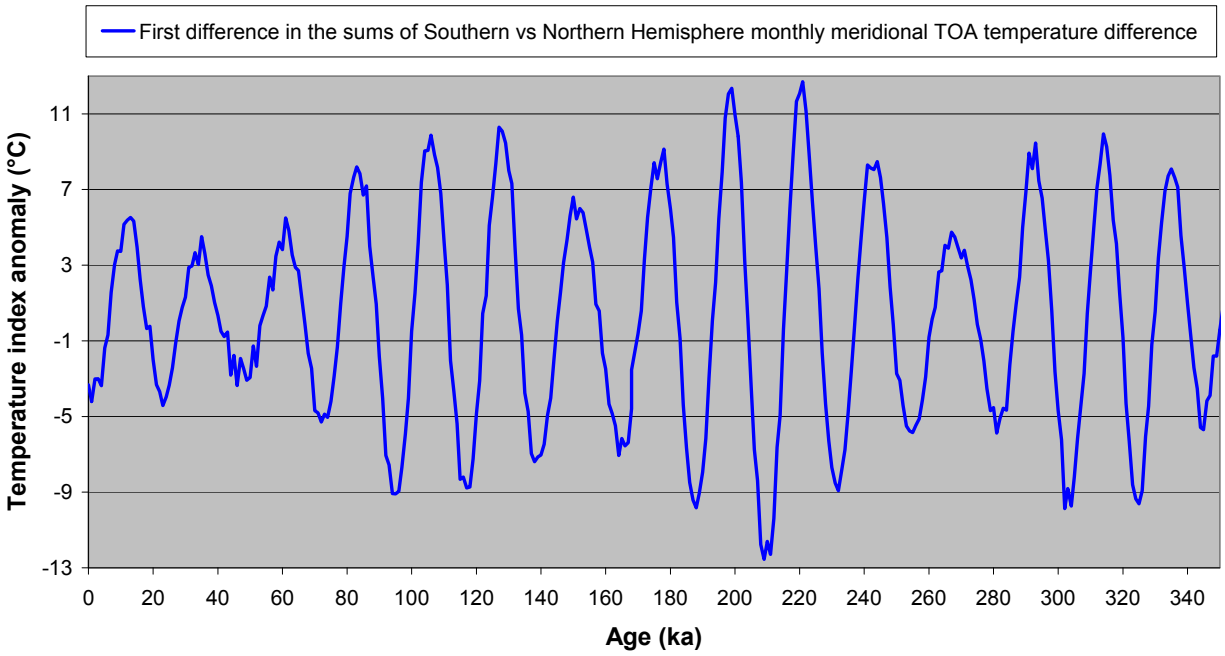

There are slight differences in the timing of the annual indices of mid to high latitude meridional TOA blackbody temperature difference. These are displayed in figure 4.11c (above). These differences are specified in figure 4.12a. Here the value of the Northern Hemisphere index has been subtracted from that of the Southern Hemisphere. When contrasted with figure 4.3a it is immediately clear that cycle in this first-difference curve matches the timing of the precession of the Earths axis. The trend in magnitude of peaks and troughs mirrors the eccentricity of the Earths orbit around the sun. Clearly the relative magnitude of the meridional TOA blackbody temperature difference changes with time. From figure 4.12a it can be seen that the annual TOA mid to high latitude temperature gradient is stronger in the Southern Hemisphere when the anomaly in the index of 1st differences is positive. It is stronger in the Northern Hemisphere when this anomaly is negative. In figure 4.13 the index first difference (Southern minus Northern Hemisphere) is contrasted with summer (mean January) insolation at 60°N. It can be seen that the annual mid to high latitude theoretical blackbody temperature gradient in the Southern Hemisphere is stronger than that of the Northern Hemisphere precisely at each precessional peak in summer insolation at 60°N. Likewise it can be seen that this gradient in the Southern Hemisphere is weaker than that of the Northern Hemisphere at precisely each precessional minimum in summer insolation at 60°N.

The first difference in the Southern and Northern Hemisphere annual meridional indices is plotted against the well-dated $\delta^{18}O$ record from the Dome Fuji (Antarctic) ice core in figure 4.12b and against Dome Fuji surface temperature in figure 4.14. The $\delta^{18}O$ and surface temperature data are from Parrenin et al (2007). It can be seen that the annual mid to high latitude temperature gradient in the Southern Hemisphere is stronger than that of the Northern Hemisphere precisely at each precessional peak in $\delta^{18}O$ at Dome Fuji. Likewise it can be seen that the annual gradient in the Southern Hemisphere is weaker than that of the Northern Hemisphere precisely at each precessional minimum in summer insolation at 60°N. It can also be seen that there is a tendency for the orbital scale temperature maxima at Dome Fuji to be weaker during minima in the eccentricity cycle.

Figure 4.12b: First difference in Northern and Southern Hemisphere indices of summed theoretical meridional temperature difference (between 40 & 70°) compared with Dome Fuji d18O (O2/N2 based Sthn Hem orbital timescale)

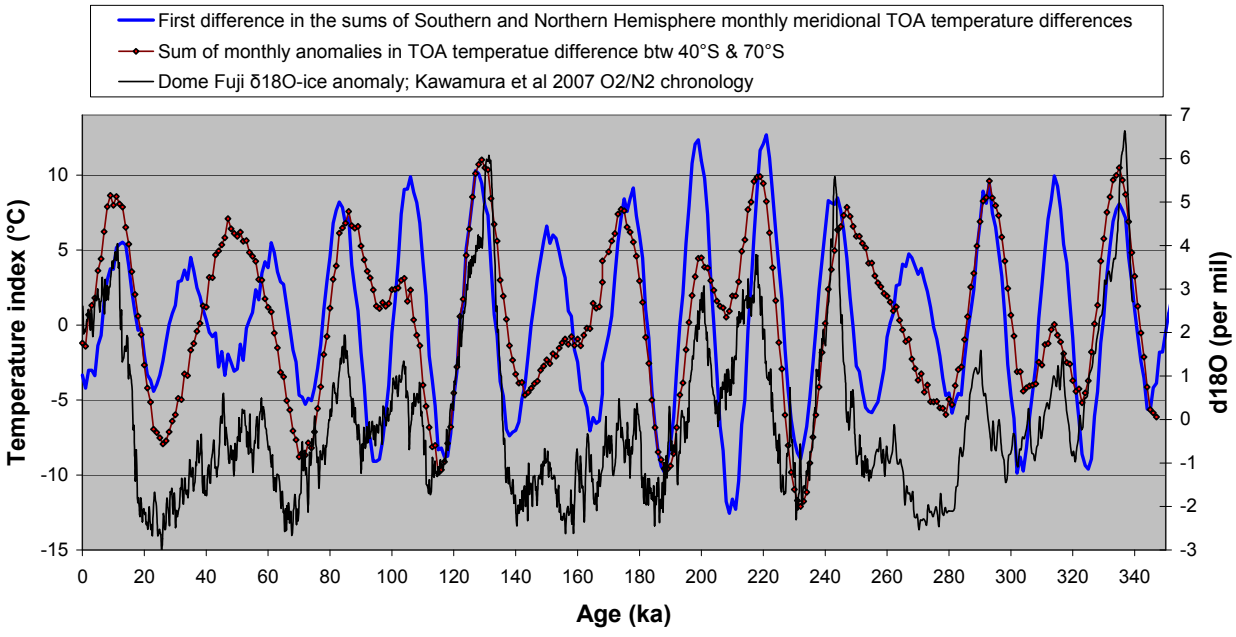

Figure 4.13: Summer (mean January) insolation at 60°N and 60°S contrasted with the 1st difference in the annual indices of middle to high latitude meridional TOA blackbody temperature difference

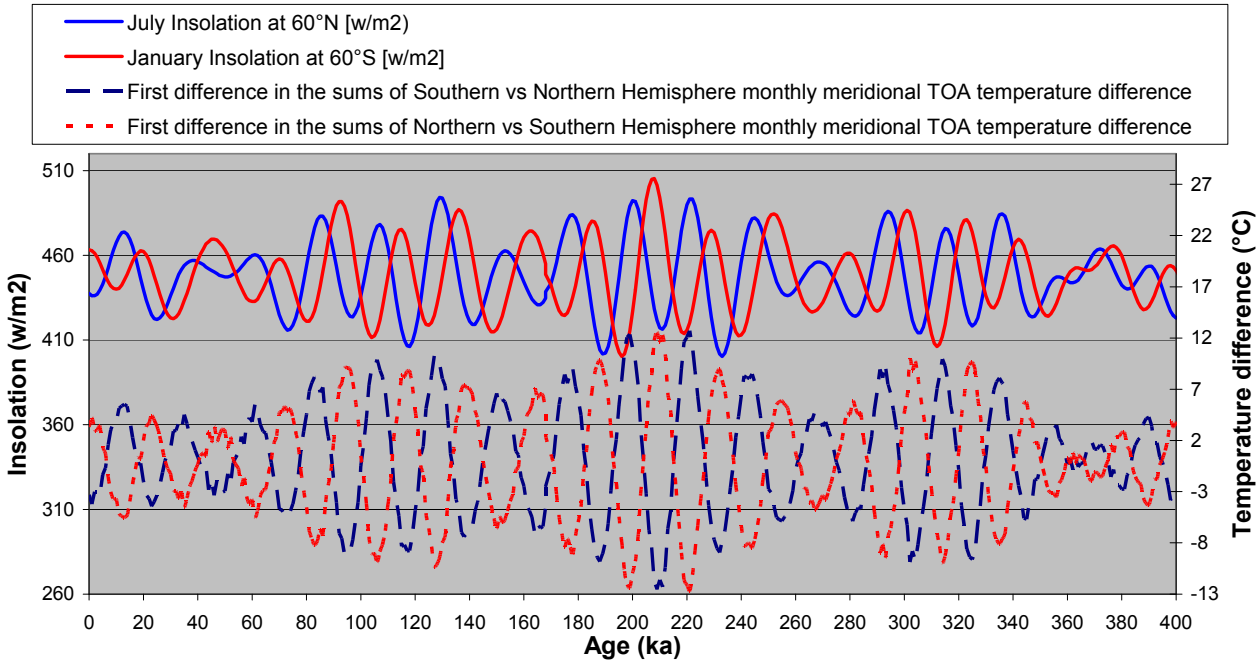

Figure 4.14: First difference between the Northern and Southern Hemisphere annual meridional TOA blackbody temperature indices (diff btw 40° and 70°) contrasted with surface temperature at the Dome Fuji ice core.

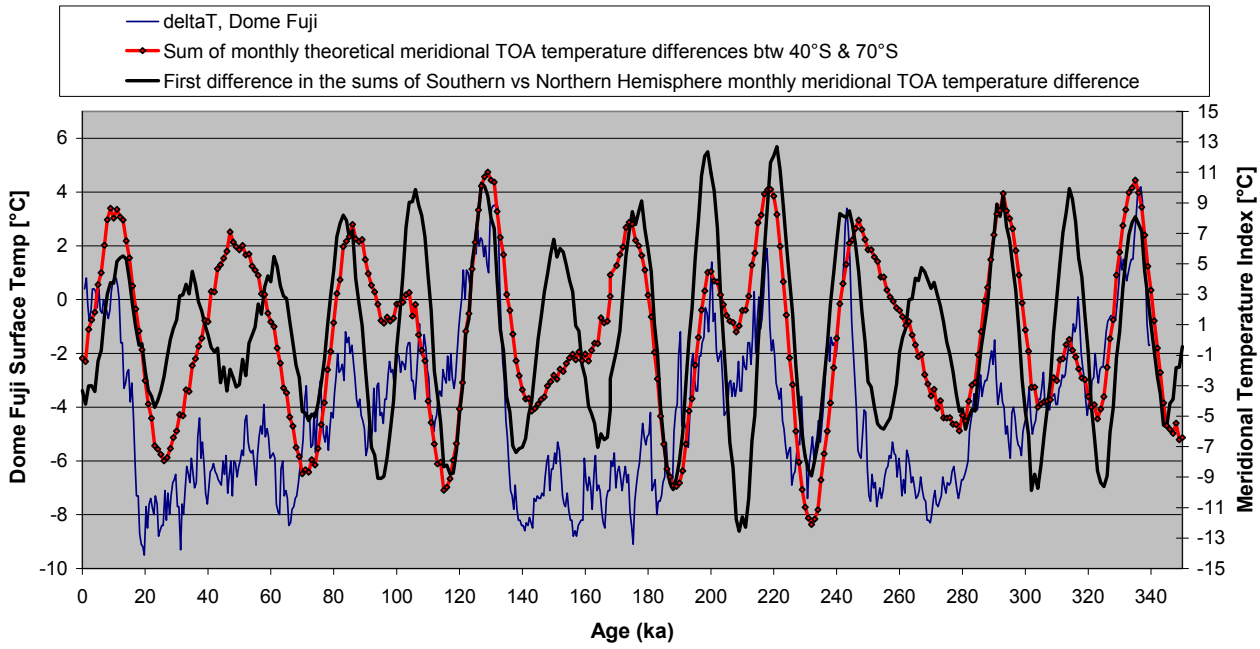

In terms of the mid-latitude to high-latitude meridional theoretical TOA blackbody temperature gradient (forced by meridional variation in insolation) it is proposed here that when this gradient is stronger in one hemisphere than the other there may be a tendency for one hemisphere to gain heat at the expense of the other. Heat is likely to be transported, by various mechanisms, across the equator toward the hemisphere with the steeper mid to high latitude meridional TOA temperature gradient. In relation to the long surface temperature record from Dome Fuji (Kawamura et al 2007) there are times when the TOA temperature gradient favours heat transport into Antarctica. Referring back to the monthly anomalies this would appear to be dominated by the maximum meridional contrast which occurs during the winter months. In terms of radiative properties, heat transport (in an equivalent number of Joules) has its greatest impact on the radiative temperature of the surface when the temperature of emission is at its lowest point (being winter). In other words, following the blackbody curves shown in figures 4.6a and 4.6b, the lateral advection into Antarctica of a quantum of heat has a substantially greater impact on surface temperature during the winter than during the summer. This may be one of the reasons why the mean annual temperature fluctuates so strongly at the Dome Fuji, Dome Concordia, and Vostok ice core sites on an orbital timescale. The amplitude of the variation in mean annual temperature is up to 10°C at Dome Fuji (figure 4.14).

The close correspondence of temperature change at Dome Fuji (figure 4.14) and SST at marine cores MD97-2120 and MD97-2121 (figures 4.15a, 4.15c, 4.15c) with the relative difference between the annual indices of TOA meridional blackbody temperature difference is remarkable. There are times when the correlation is very strong and other times when the correlation is weaker. In the later case correlation is weak precisely when the Northern Hemisphere land-based ice sheets reach maximum volume, in other words during late MIS3/MIS2, MIS6 and MIS8. The explanation may be relatively straight forward. At these times there is a massive heat deficit in the Northern Hemisphere and this is probably associated with long-term cross-equatorial heat piracy from south to north. There are a number of contributing effects that are probably dominated by large changes in the average albedo of the Northern Hemisphere. The albedo change is synchronous with change in the combined area of the northern ice sheets and accompanying changes in atmospheric dust greenhouse gas content. In this context it should be noted that Bielefeld (1997) calculated a reduction in global radiation budget of 7 to 10% relative to today at the last glacial maximum as a result of changes in surface albedo.

Heat loss (to space) over the northern ice sheets probably sets up an additional temperature and energy transport gradient that temporarily mutes the mid to high latitude orbital-scale gradient in the Southern Hemisphere. Solar heat gained in the low latitudes of the Southern Hemisphere is likely to be exported more strongly to the north when solar heat gain in the northern hemisphere is reduced due to reflection (to space) off the huge northern ice sheets and similarly off any accompanying increase in the area of northern sea ice and winter land-based snow cover.

Radiation of Heat to Space

The entire surface are of the globe is available for the radiation of heat to space. A substantial portion of the global surface area is located in the high Southern latitudes. As discussed above there are times when the insolation/temperature gradient is such that delivery of heat to high Southern latitudes is likely to be enhanced. As pointed out by Pahnke & Sachs (2006) [see the quotes below] at high Southern latitudes these periods are suited to enhanced cross-latitudinal winds and southward transport of moisture and latent heat. This transport increases the surface area available for the radiation to space of "subtropical and temperate" heat. Even though heat is radiated more quickly from a warm (tropical/subtropical) surface (due to a lower rate of longwave emission at a lower blackbody temperature) the total radiative area is also important. The high Southern latitudes can be thought of as

robbing atmospheric heat and moisture from low latitudes. At such times a larger proportion of the annual emission of heat to space occurs at high latitudes. This could result in a relative cooling of the average surface temperature of the entire hemisphere.

4.2.8 Application of Changes in Seasonal Insolation to Southern Mid-latitude Climate

Do the cyclical changes in Southern Hemisphere solar forcing described above have an impact on surface temperature in the Southern Hemisphere? Inevitably they must, but in terms of attribution for local changes, Southern Hemispheric forcing has typically been overlooked in favour of a Northern Hemispheric driver.

Table 4.3 Timing of maxima and minima for the Earth's obliquity and the Southern Hemisphere summer and spring cross latitudinal temperature gradients between 40° and 70° South.

Annual TOA Blackbody Temp Differential		Sthn Hem Summer BB temp differential	Sthn Hem Spring BB temp differential	Sthn Hem meridional temp gradient from Vimeux et al (2002)	Obliquity	Precessional extremes
Nthn Hem (ka)	Sthn Hem (ka)	(ka)	(ka)	Broad Maxima & Minima (ka)	(ka)	(ka)
10-11 ka min	4 min	10 min	11 min	8-15 min	9-10 max	12 -ve
25-26 ka max	31 max	28 max	28 max	18-35 max	29 min	23 +ve
	41 min					35 –ve
50-51 ka min		47 min	47 min	38-60 min	49 max	48 +ve
	64 max					61 –ve
71-72 ka max	73 min	67-74 max	75 max	62-80 max	70 min	72 +ve
84 ka min	81 max					84 –ve
95 ka max	94 min	93-95 min	89 min	85-103 min	92-93 max	95 +ve
104 ka min	107 max					106 –ve
116-117 ka max	118 min	113-115 max	118 max	103-116 max	112-113 min	116 +ve
128-129 ka min	126 max	131 min	132 min	120-135 min	131 max	127 –ve
141-142 ka max	137 min			135+ max		139 +ve
	150 max	149-150 max	145 max		150 min	151 –ve
	165 min					164 +ve
		168-172 min	177 min		170 max	
	178 max					176 –ve
	187 min					187 +ve
		190 max	191 max		193 min	
	196 max					198 –ve
						209 +ve
		212 min	205 min		214 max	
						221 –ve
					233 min	232 +ve

Figures 4.15a and 4.15b contain climatic information from two high-resolution marine cores, being MD97-2120 and MD97-2121 from the Chatham Rise. These cores are located at (45°32.060'S, 174°55.850'E) and (40°22.80S, 177°59.40'E) respectively. The alkenone based SST maxima at marine cores MD97-2120 and MD97-2121 (Pahnke & Sachs 2006) appears to cycle in a manner similar to that of index of annual mean TOA blackbody temperature difference between 40°S and 70°S. The correspondence with the first difference between the northern and southern hemisphere coindices is even more striking, particularly for MD97-2120. So at least at the Chatham rise, and particularly on the southern flank of the Chatham Rise SST changes coincide with this aspect of (Southern

Hemisphere) orbital forcing, as noted by Pahnke & Sachs (2006). The normal practice is to make an assumption that a Northern Hemisphere forcing mechanism is driving mid-latitude SW Pacific SST.

The alkenone based SST minima at MD97-2120 (figure 4.15a) and MD97-2120 (figure 4.15b) occur more-or-less in-phase with maxima in the theoretical annual cross-latitudinal TOA blackbody temperature gradient. This also applies to the SST at MD94-103 (Sicre et al 2005). The maximum in TOA blackbody temperature-gradient should correspond to a tendency for vigorous atmospheric circulation and accelerated cross-latitudinal heat flux. This is a situation that is ideally suited for enhanced delivery of moisture to Antarctica and the radiation of heat to space from high latitudes, which has the potential to cool most of the Southern Hemisphere. It is also ideal for northwards circulation of bitterly cold polar air to the southern mid-latitudes and this could have a cooling effect on middle latitude sea-surface-temperatures particularly during spring and summer.

Figure 4.15a: Alkenone-based sea-surface-temperature anomaly (°C) for marine core MD97-2120 situated on the southern flank of the Chatham Rise to the east of New Zealand. The SST data are from Pahnke & Sachs (2006)

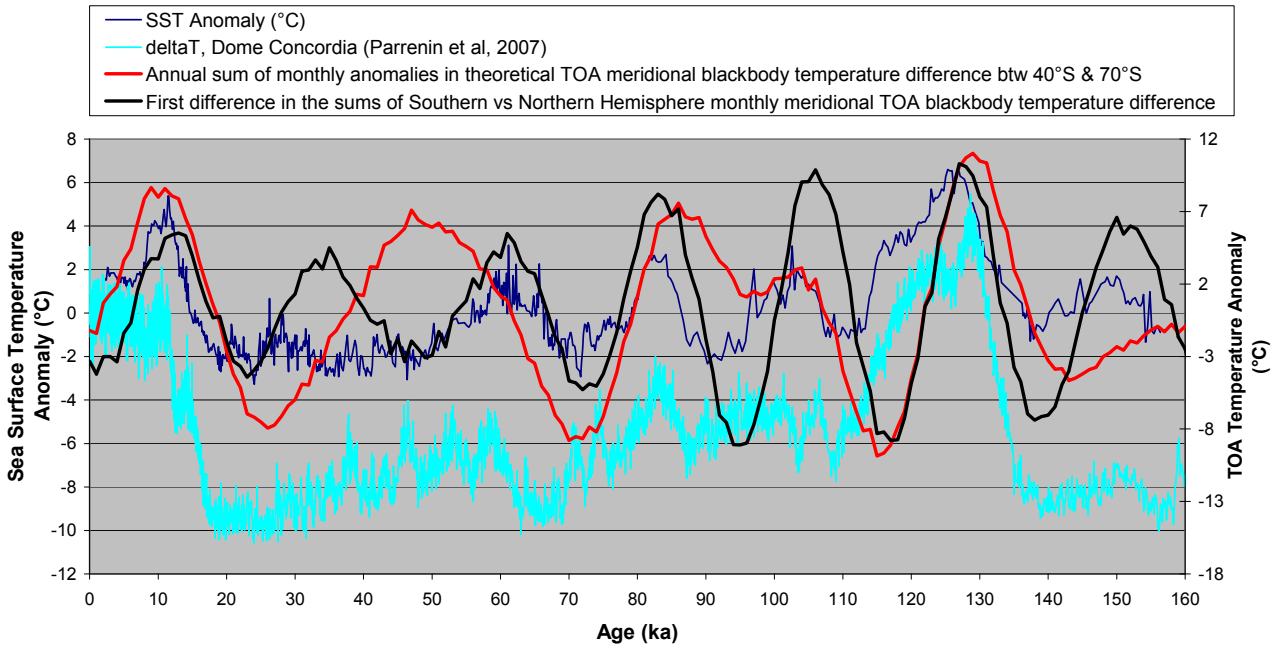

Figure 4.15a displays the alkenone based SST record by Pahnke & Sachs (2006) from core MD97-2120. Clearly there are differences in the SST history between marine cores MD97-2120 and MD97-2120 (figure 5.15b). These cores are situated either side of the Chatham Rise and either side of the modern subtropical-convergence, which is likely to have shifted position significantly and repeatedly over time. A similar high-resolution SST record was generated by Pahnke (2003) using Mg/Ca ratios on foraminifera from core MD97-2120. The dating carried out for MD97-2120 is among the most comprehensive for any Southern Hemisphere marine core. The data used include at least 10 ^{14}C ages and high resolution alkenone and Mg/Ca based SST and benthic $\delta^{18}O$ records. This produces a number of very good ties points with Antarctic ice-core isotopic records, and similarly good tie points with benthic $\delta^{18}O$ records from North Atlantic cores.

The alkenone-based temperature is particularly interesting in terms of conditions during the early portion of MIS3. At this time the SST appears to have been only slightly cooler than during MIS5a, equivalent to that of MIS5c and similar to that of the Late Holocene. The pronounced warmth

registered at MD97-2120 during MIS3 (figure 4.15a) is similar to that from marine core SO136-GC3 (figure 5.8, data from Barrows et al 2007) situated just to the NE of Hokitika on the West Coast of the South Island. This part of the SST record from both cores bears a striking resemblance to the supposed MIS5 pollen record from the Okarito Pakihi Bog (figure 5.3) situated in South Westland. The pollen profile and numerical dating from this site are discussed in detail in Chapter 5.

The sharp drop off in SST from c.51 ka at MD97-2120 is mirrored at numerous mid-latitude marine cores in the Southern Hemisphere. This point is discussed below in relation to table 4.5.

Figure 4.15b: Alkenone-based sea-surface-temperature anomaly (°C) for marine core MD97-2120 situated on the northern flank of the Chatham Rise to the east of New Zealand. The SST data are from Pahnke & Sachs (2006)

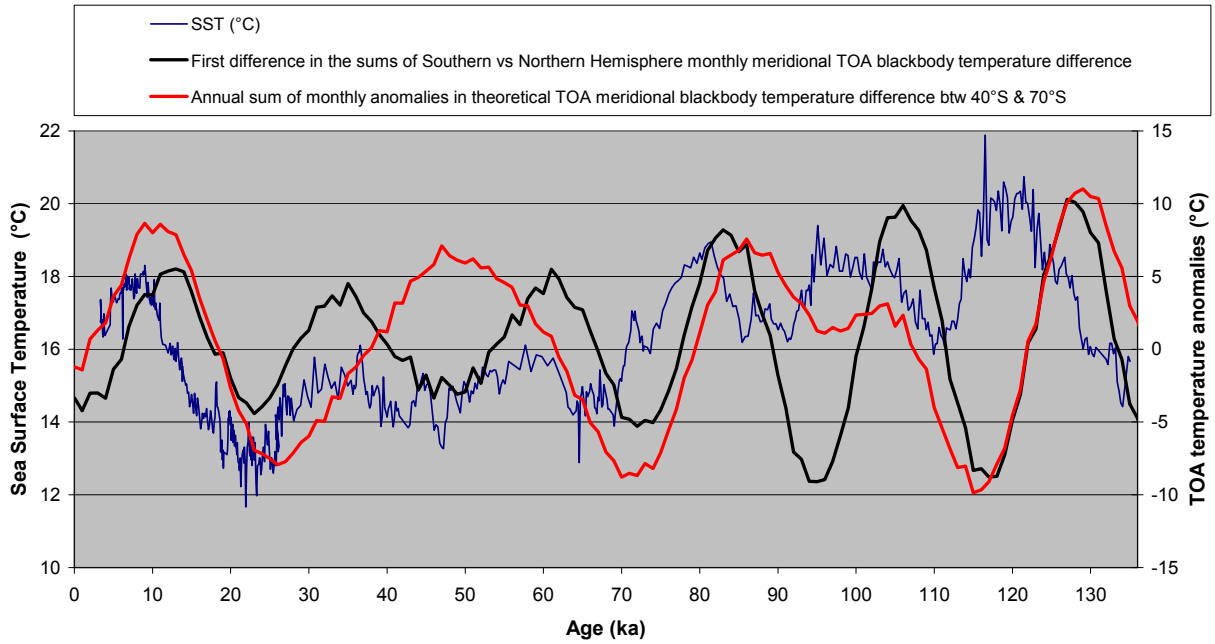

In relation to the impact of the meridional temperature gradient on the strength of westerly circulation in the Southern Ocean Pahnke & Sachs (2006) comment as follows:

> "The distribution of paleo-SST records with contrasting temperature patterns indicates differential heating between low/mid and high latitudes (their figures 4, 5, and 6) and suggests an increase in the meridional thermal gradient at 47–23 kyr B.P. For such conditions, the thermal wind balance predicts stronger winds [Peixoto and Oort, 1992] and thus enhanced atmospheric transport of heat and moisture from low to high latitudes. Momentum conservation requires an increase in westerly wind strength and zonal surface ocean circulation in response to increased poleward atmospheric and ocean transport. A resulting sharpening of thermal oceanic fronts at the subtropical-subpolar boundary has been shown to have a positive feedback on atmospheric temperature gradients [Cessi, 2000] and may have reinforced the disparate SST pattern at the end of MIS3.
>
> Using an ocean-atmosphere coupled model, Khodri et al. [2001] simulated climate conditions at the last glacial inception (115 kyr B.P.) and suggested that enhanced equator-to-pole thermal gradients induced by seasonal perturbations in insolation forcing led to an increase in northward heat and moisture transport. Similar dynamics may have been active just prior to the LGM owing to differential heating of high and low/mid latitudes.
>
> With Milankovitch forcing incorporated into the model, mid-latitude atmospheric and ocean temperatures directly respond to insolation changes, while high-latitude climate variables rather respond to changes in ice mass balance [Gildor and Tziperman, 2000]. Our SST observations would be in line with such scenario in that **low- to mid-latitude temperatures follow obliquity-driven mean annual insolation changes** and precession-modulated

Northern Hemisphere summer insolation, while high-latitude temperatures decreased in concert with increasing global ice volume."

Figure 4.15c: Comparison of Mg/Ca based sea surface temperature at the Chatham Rise (Pahnke et al 2003) with surface temperature at Dome Fuji and Dome Concordia (Antarctic) ice core sites

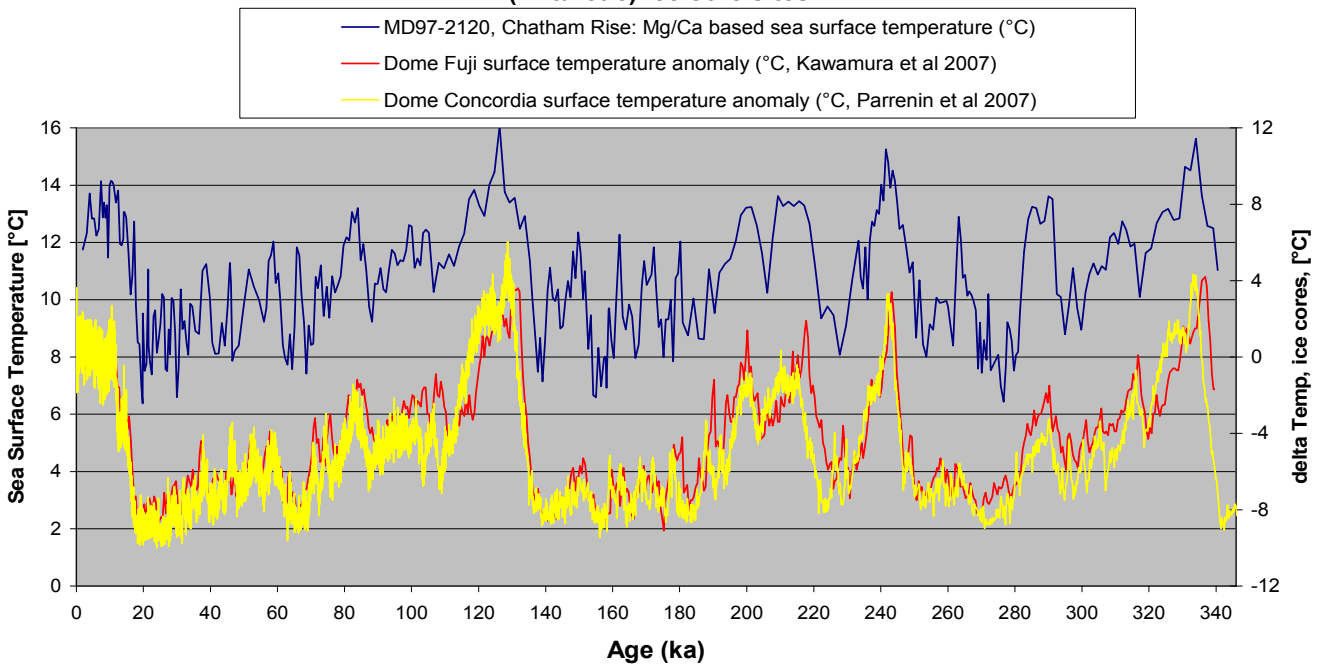

Is there any observational evidence supporting the view of hemispheric-scale heat transport presented above? Potentially the best long and continuous archive of heat transport at this scale is the isotopic record from Antarctica. Vimeux et al (2002) have produced a continuous 420 kyr long record of the meridional (cross latitudinal) temperature gradient $\{\Delta T_{source} - \Delta T_{site}\}$ between Vostok Station (78.4667˚S, 106.80˚E) and the oceans surrounding Antarctica. The meridional temperature gradient is derived from isotopic ratios in precipitation preserved as ice in a deep core from this site. Vimeux et al (2002) modeled the moisture source temperature (SST), local depositional temperature (Vostok), and oceanic isotopic composition. In their figures 5 & 7 they present this measured temperature contrast in graphical form. The temperature contrast varies in time more-or-less synchronously with the earth's obliquity cycle, rather that the precessional cycle. Peaks in the cross-latitudinal temperature gradient cycle $\{\Delta T_{source} - \Delta T_{site}\}$ recorded at Vostok Station (see table 4.3) coincide with the maximum in summer ($\Delta T_{40°S} - \Delta T_{70°S}$) from the anomaly study described above. Minima in $\{\Delta T_{source} - \Delta T_{site}\}$ coincide with minima in ($\Delta T_{40S} - \Delta T_{70S}$). In other words a lower TOA blackbody temperature differential between 40°S and 70°S corresponds to a lower differential between Southern Hemisphere sea-surface-temperature (temperature of the moisture source) and the surface temperature at Vostok station.

In the analysis presented here the amplitude of the summer TOA temperature difference ($\Delta T_{40°S} - \Delta T_{70°S}$) between 40°S and 70°S is 4.0 K to 8.6 K (Kelvin). The minimum amplitude of $\Delta\{T_{source} - T_{site}\}$ for Vostok Station is c. 5.0 K and the maximum is c. 10.0 K. In terms of the source region Vimeux et al (2002) compiled a composite seawater temperature and isotopic profile for 11 marine cores, five from 0°S to 20°S and six from 40°S to 50°S. The northern set is composed of cores MD85-668, GeoB-1028, GeoB-1016, GeoB-1008 and GeoB-1710. The southern set is composed of cores MD84-527, MD84-551, MD88-770, MD88-769, MD94-101 and MD94-102. So the (polar) Vostok isotopic record was contrasted with oceanic source areas as far north as latitude 0°S (the equator). This

means Vimeux et al (2002) considered a wider latitudinal band than considered here but with a similar result.

Long-term insolation driven temperature contrasts are not the only influence on local temperature trends and heat transport. There are shorter-term changes in wind-strength, atmospheric heat transport, oceanic heat transport, and oceanic upwelling that act within the Southern Hemisphere. There is also substantial cross-equatorial transport of heat as modeled by Seidov et al 2001, particularly by oceanic currents, and particularly during major Northern Hemisphere glacial periods. This means that the heat can be either lost or gained from the global climate system affecting both hemispheres simultaneously. So it is possible for the Southern Hemisphere to cool overall, while simultaneously undergoing a reduction in mid-latitude to polar temperature differential. But this is not equivalent to universal Northern forcing of all cyclical changes in Southern climate.

The study by Vimeux et al (2002) in connection with source site/temperatures for the Vostok ice core has been emulated by Stenni et al (2004). This more recent work focuses on the Byrd ice core from West Antarctica. It has greater resolution but covers a much shorter period being the window from 15 ka to 45 ka. Key findings from this work include synchronous changes in temperature of similar magnitude and direction at the marine source and ice core site. The result is strikingly similar to that by Vimeux et al for the 15 ka to 45 ka interval. In terms of this PhD thesis the most important finding by Stenni et al (2004) is that a period of extreme cooling of sea surface temperature occurred at c. 45-39 ka and this precisely matched very low air temperature at the ice core site. The sea surface temperature of the oceanic source region is estimated to be 1.5 K colder at 41 ka than it was during the coldest part of the LGM at c. 21-18 ka. The surface air temperature at the site is estimated to be almost as cold at 41 ka (within c. 1 K) as during the two LGM thermal minima here at 26 ka and 20 ka. The Vostok record of Vimeux et al (2002) contains evidence of an abrupt increase in the temperature of the source relative to that of the site (warmer sea surface source and colder depositional site) from c. 50 to 45 ka, followed by a sharp reduction at c. 45-39 ka. These events are of sufficient magnitude (c. 1.5 K) to have a substantial impact on wind strength and the transfer of heat within the climate system. The event begins with a thermal anomaly that encourages strong atmospheric circulation bringing cold air out of the high latitude region into the middle latitude region, probably enhancing precipitation over the western side of the Southern Alps. At Byrd Station this is followed by a potentially hemisphere-wide decline in sea surface temperature from c. 45-39 ka and a substantial recovery (warming) from c. 39-35 ka peaking at 38 ka for both source and site.

The cooling event at 45-39 ka doesn't appear to have a simple explanation in terms of forcing by changes in (local) Southern Hemisphere insolation or TOA blackbody temperature gradient. But there may be a correspondence with the potential for heat piracy by the Northern Hemisphere at this time. The general mid-MIS3 SST minimal exhibited in figure 4.15b coincides with a minimal in the first-difference between the mid-high latitude meridional TOA blackbody temperature gradients. There is independent observational evidence for a widespread thermal (cooling) event in the surface waters of the Southern Ocean between about 50 ka and 39 ka. Hemispheric-scale cooling is indicated in numerous proxy climate records many of which are listed in tables 4.4 and 4.5. These include sea surface temperature records from the following marine cores:

GeoB1016-3, GeoB1706-2, GeoB1028-5, GeoB1117-2, GeoB1008-3, GeoB1710-3, GeoB1711-4, GeoB1712-4, GeoB3005 GeoB3007, GeoB3375-1, GeoB3910-2, ODP1089, ODP1233, ODP1123, ODP 1172, ODP1145, MD84-527, MD88-769, MD88-770, MD90-963, MD94-103, MD96-2087, MD97-2120, MD97-2121, MD01-2421, MD01-2378, MD02-2575, RC-11-120, RC13-228, SO136-

GC3, DSDP594, PS1756-5, PS2082-1, PC12, E11-2, GC-07, SR1, WIND28K, V22-176, V25-56, V30-40.

From this widely distributed collection of cores (for lat/long see table 4.4 below) it appears that on average the Southern Ocean reached its coldest average SST from about 45 - 40 ka. This event was of lesser duration than the local effect (in the Southern Hemisphere) of the LGM but may have been of greater intensity. This has a bearing on climate in the New Zealand region where there is increasing evidence that the local "LGM" did not coincide with that in the Northern Hemisphere in terms of air temperature, SST and ice volume. As suggested by Suggate & Almond (2005) the local ice-area maximum in New Zealand probably occurred some time prior to 27 ka. This is supported by cosmogenic isotope dating on glacial erractic boulders from Loopline Formation moraines (this thesis).

So do any of the seasonal orbital-scale trends in insolation coincide with generally low SST during the 50-40 ka period? There is a prominent mean-June/July insolation minimum centered at c. 47-45 ka. This minimum is present everywhere from 40°S to 80°S. North of 40°S this minimum is less prominent. Perhaps the impact of this June/July insolation minimum overwhelms other factors during this period.

4.2.8a The 28-30 ka Summer Insolation Minimum

The following discussion is focused on the potential impact of orbital-scale or Milankovitch-type forcing on climate at middle to high latitudes in the Southern Hemisphere. There is high probability that global oceanic circulation is strongly impacted by sea surface salinity and SST in the North Atlantic and Nordic Seas and by atmospheric heat transport in the Northern Hemisphere. So there are likely to be global impacts on atmospheric climate that are caused by events in the Northern Hemisphere. Consequently there is no implication here that atmospheric climate at mid Southern Hemisphere latitudes responds solely to local insolation changes or to the theoretical TOA blackbody temperature gradients described above. Such potential gradients are likely to be a component of the climate system. They may act at some times to accentuate trends in the Southern climate and at other times to moderate such trends.

In terms of potential impact on climate in Westland there are events from the TOA blackbody temperature gradient analysis and from the summer insolation cycle that bear close examination. The minimum in southern mid-latitude summer solar insolation at 28-30 ka is quite striking for a number of reasons.

In terms of **summer** (mean January top-of-atmosphere) insolation:

- The 28-30 ka summer insolation minimum essentially coincides with the MIS3/2 transition.
- At 40°S the 28-30 ka precessional minimum in summer insolation was the deepest since 80 kyr. This may have caused a reduction in direct summer ablation of ice in mountainous regions at mid-latitudes of the Southern Hemisphere as suggested by Vandergoes et al (2005). Vandergoes et al (2005) also suggest an early onset for the LGM in South Westland.
- The TOA blackbody temperature difference (Summer $\Delta T_{40S} - \Delta T_{70S}$) between 40°S and 70°S was at a maximum, favouring strong mid latitude westerly atmospheric circulation and high precipitation on the west side of the Southern Alps. This would have produced a tendency for the regular delivery of exceedingly cold but moist air to the West Coast region during spring

and summer (fig 4.10), a situation suitable for ice accumulation rather than ablation in alpine areas.
- The 28-30 ka obliquity minimum coincided with a major minimum in calculated TOA summer (mean January) insolation everywhere from 30°S to 80°S. At 70°S this was the deepest minimum since 110 ka. This favours both atmospheric and oceanic cooling.

In terms of mean **annual** top-of-atmosphere cross-latitudinal blackbody temperature gradient (fig 11):

- At 28-30 ka the annual index of Southern Hemisphere monthly meridional TOA theoretical blackbody temperature differences between 40°S and 70°S is declining rapidly towards the minimum value. This strong annual gradient would have favoured vigorous westerly to southwesterly atmospheric circulation across the New Zealand region at 28-30 ka.

These orbital-scale patterns have an uncertain impact on climate in the West Coast region, which is strongly affected by millennial-scale events emanating from the Southern Ocean (as recorded by various proxy measurements from Antarctic ice-cores). However, at ~ 28-30 the West Coast region would have been particularly susceptible to rapid accumulation of glacial ice (in the main Mountain ranges) and an earlier than otherwise expected decline into the local LGM. This proposal is consistent with the finding by Burge (2007) that in the Westport area the period from 34 ka to 28 ka correlates with mean winter temperatures c. 5°C colder than the modern winter mean. This is colder than the mean winter temperature during the more recent glacial advance at c. 24 ka to 22 ka which had a temperature depression of c. 3°C in the Westport area.

It is worth noting here that Suggate and Almond (2005) identified a major glacial advance in Westland at c. 34-28 ka. In South Westland this advance constituted the furthest down-valley extension of glacial ice during the local LGM. This is consistent with the finding by Williams et al (2009) of maximal ice extent in the South Island at approximately 28 ka and SE Australia at 32 ± 2.5 ka. It is also consistent with recent finding by Doughty et al (2009) of major ice advances at Mary Burn, Lake Pukaki in South Canterbury at ~35 ka and 27 ka by exposure dating. Similarly Putnam et al (2009) have reported the commencement of the local LGM by 31 ka using exposure ages on terminal moraine at the Lake Ohau in South Canterbury.

4.2.8b The 46-50 ka Summer Insolation Maximum

The maximum in southern latitude summer (mean January) top-of-atmosphere solar insolation at 46-50 ka is quite striking for a number of reasons.

In terms of summer (mean January top-of-atmosphere) blackbody temperature and insolation:

- This insolation maximum coincides with a minimum in the theoretical summer top-of-atmosphere blackbody temperature gradient between 40°S and 70°S. This theoretical gradient was at a 200 kyr minimum at 46-50 ka.
- The extreme summer insolation gradient minimum is caused by the 70°S summer (mean January) insolation being 11.8 w/m^2 greater than the modern level.
- The precession and obliquity curves are precisely in-phase at 48 ka.

So all-up the Southern Hemisphere orbital/solar forcing was conducive to a warm summer climate in the New Zealand region, more so than during the Holocene period. However at the same time climate

in the NZ region would have been modulated by millennial scale events such as those identified in Antarctic ice cores and by global climate forcing originating in the Northern Hemisphere. In this interval there was a substantial and probably growing ice sheet in Canada and potentially a modest ice sheet in the Fennoscandia/Barrents Sea region of northern Europe. Sea level was lower than at present exposing significant areas of continental shelf. Together these conditions translate to a change in global albedo and so overall less energy was being trapped in the global atmospheric and oceanic climate system.

In terms of the theoretical mean annual top-of-atmosphere cross-latitudinal blackbody temperature gradient (fig 4.11a, 4.11b):

- At 55-40 ka the annual index of Southern Hemisphere monthly meridional TOA theoretical blackbody temperature differences between 40°S and 70°S (figure 4.11a, 4.11b) is at the maximum value which would tend to favour advection of heat across the mid-latitudes. But at approximately the same time, from 52 to 44 ka (figure 4.12a) the first difference in the Northern and Southern Hemisphere mid to high latitude meridional temperature indices is at a minimum which favours heat piracy by the Northern Hemisphere. Inter-hemispheric heat piracy across the mid-high Southern latitudes is favoured from about 67 to 57 ka (figure 4.12a).

Overall "orbital forcing" of summer and annual mean mid-southern latitude TOA blackbody temperature is consistent with a relatively sustained episode of warm climate in the early part of MIS3. This has potential implications for climate studies throughout New Zealand. A primary role for "local orbital forcing" during this time period is not recognized in the Suggate model for the climate of North Westland, and doesn't appear to have been considered in relation to the evolution of vegetative cover (e.g. Moar & Suggate 1996) through this period.

However, a number of SST records indicate that the MIS3 thermal maximum is likely to have occurred from c.61 ka to c.51 ka in the Southern Ocean, including Cores E11-2 (Mashiota et al 1999), RC11-120 (Martinson et al (1987), MD02-2488 (Govin et al 2009), ODP1233 (Kaiser et al 2007). The timing of this event is similar at marine cores in the NZ region including SO136-GC3 (Barrows et al 2007), MD97-2120 (Pahnke & Sachs 2006), MD06-2986 (Kolodziej 2010), DSDP594 (Marret et al 2001) and ODP1123 (Crundwell et al 2008), and is shown in figure 4.15a. As discussed above, in relation to the same to marine cores, cooler temperatures register in the New Zealand region for the period from about 51 ka to 39 ka. Similarly deep ice cores from Antarctica indicate relatively cold temperatures from c.51 ka to c.41 ka as discussed in detail below.

The potential for warm climate during the early to middle portion of MIS3 is particularly relevant to the discussion in chapter five regarding the age of peat and organic silt in a series drill-cores recovered from the Okarito Pakihi by Vandergoes et al (2005). It is also relevant to the age/dating of organic-rich deposits at a number of other localities in Westland including but not limited to: The Phelps Goldmine, the Awatuna Formation type section, the Rutherglen Formation at Candlelight, the Awatuna Formation at Schulz Creek, the Waites Formation at Martins Quarry, the Awatuna Formation at Bullock Creek, and the Waimea Formation at Blue Spur, Kumara, Chesterfield Road and Grahams Terrace.

4.2.8c The 63-56 ka Summer Insolation Minimum

In terms of solar forcing of local climate the 63-56 ka period corresponds to a TOA summer (January mean) insolation minimum. The summer cross-latitudinal summer insolation gradient was not at a maximum. The annual index of Southern Hemisphere monthly meridional TOA theoretical blackbody

temperature differences between 40°S and 70°S (figure 4.11a, 4.11b) is at intermediate values during this period. Overall the solar/orbital component of local climate forcing in Westland was not at a continuous extreme at this time. But this would not have precluded episodes of strong westerly atmospheric circulation.

From 67 to 53 ka (figure 4.12a) the first difference in the Northern and Southern Hemisphere mid to high latitude meridional temperature indices is at a maximum which favours heat piracy by the Southern Hemisphere. This curve coincides with the maxima in SST at MD97-2120 and MD97-2121 (figures 4.15a, 4.15b) at this time.

4.2.8d The 84-78 ka Summer Insolation Minimum

In terms of summer (mean January) top-of-atmosphere blackbody temperature gradient:

- At 40°S the 84-78 ka summer insolation minimum was very deep, the deepest since 105 ka, despite the fact that the precessional and obliquity cycles were out of phase.
- The 78-84 ka precessional extreme caused very low summer and spring insolation across the entire region between 30°S and 80°S.

In terms of the theoretical mean annual top-of-atmosphere blackbody cross-latitudinal temperature gradient (fig 4.11a, 4.11b):

- From 84-78 ka the annual index of Southern Hemisphere monthly meridional TOA theoretical blackbody temperature differences between 40°S and 70°S (figure 4.11a, 4.11b) is at intermediate to high values which would tend to favour advection of heat across the mid-latitudes. These gradients would have been capable of promoting vigorous westerly atmospheric circulation. In Westland this could have produced a tendency for the regular delivery of exceedingly cold air from the deep south during spring and summer, coupled with regular delivery of moist air from the north. When coupled with rather low spring/summer insolation this situation may favour high precipitation and reduced snow/ice ablation.

Considering mid-latitude Southern Hemisphere solar forcing of climate (in isolation from other aspects of the behaviour of the climate system) cooling would be an expectation rather than a surprise from about 82 to 75 ka. This is relevant to the causes of the glacial advance that produced the Waimea Formation. A literal interpretation of the luminescence dating and cosmogenic isotope dating in Westland is that it provides evidence for pronounced cooling between 80 ka and 75 ka. This is discussed in relation to the Waimea Formation in chapter 6. If the luminescence ages have been overestimated (due to partial bleaching) then the Waimea Formation could easily be correlated with MIS4. If the literal interpretation is correct the glacial advance is more-or-less in anti-phase with general warmth in the Northern Hemisphere. In terms of sea surface temperatures in the Southern Ocean there is evidence for a modest minimum at this time. Crosta et al (2004) used a modern analogue technique applied to fossil diatoms at marine core SO136-111 (56°40'S, 160°14'E) to estimate the SST. Minima occurred at 83-80 ka and 78-74 ka with a brief recovery between. Pichon et al (1992) report on diatom based summer SST from core MD884-527 (53°19.6'S, 75°48'E). At this site there is a pronounced temperature minimum at c.86-80 ka which follows a pronounced summer maximum from 94-88 ka. Sowers et al (1993) discuss the long diatom based SST record from core MD88-770 (46.022°S, 96.4606°E). At this site there is an abrupt SST cooling at 79-77 ka. Cortese et al (2007) report on a high-resolution radiolarian based summer SST record from core ODP177-1089

(40°56'S, 9°54'E). This shows a pronounced SST minimum from 81-76 ka. Sikes et al (2002) present alkenone based summer SST's for cores U938 (45°4.5'S, 179°30'E) and U939 (44°32'S, 179°30'E) from the south side of the Chatham Rise. This is south of the subtropical convergence. At both sites there is a noticeable summer SST minimum at c.80-75 ka. The evidence for cooling at this time is discussed further below in relation to sites listed in section 4.10.

4.2.9 Southern Hemisphere Thermal Minimum from c.51 ka to c.39 ka

As discussed above in relation to the isotopic temperature of precipitation at the Byrd Station ice core there is evidence for a period of unusually cold air temperature and SST at high Southern latitudes during the middle of MIS3. As discussed clearly and explicitly by Pahnke and Sachs (2006) this episode is clearly displayed in the Vostok deuterium excess record (of Vimeux et al 2002) and in the SST record at the following marine cores: SO90-136 (23°N); TY93-929 (13°N); ODP999 (12°N); VM28-122 (11°N); MD90-963 (5°N); GeoB-1105 (1.7°S); GeoB-1008-3 (6.6°S); ODP-1089/TN057-21 (41°S); MD97-2121 (40°S) and MD97-2120 (45°S). It is also present in the SST record at marine core GeoB-3007 (16°N); TR163-22 (0.5°N); ODP1145 (19.5°N); MD01-2421 (36°N) and GIK17961/17964 (8.5°N) references for which can be found in table 4.4. The various marine records are of a proxy-temperature nature and there are almost certainly dating inconsistencies between the different cores. Nevertheless there is a reasonable reproducibility in terms of timing and magnitude. The broad timing of this SST minimum as described by Pahnke and Sachs (2006) occurs around 48-44 ka (see their figure 4). This "event" appears to have been almost ubiquitous in terms of moderate to high resolution SST records from the Southern Hemisphere and as noted above is common at low latitude marine cores in the Northern Hemisphere.

As a group the marine cores listed in table 4.4 indicate the occurrence of a Hemispheric-scale minimum in SST for the middle portion of MIS3. Table 4.4 is a summary of the timing of this cold-event. Thirty two of these moderate to high resolution SST records are from the Southern Hemisphere. There is some between-core variability in the timing and total duration of the cold-event. A significant portion of the variation in timing for the intra-MIS3 cold-event in the marine cores is likely an artifact introduced by the time-scales and dating procedures applied.

This is to be expected given the range of sedimentation rate assumptions made in the dating of the cores and the range in sample spacing. A variety of different temperature proxies are listed in table 4.5. These do not all react to climate change in precisely the same way or with the same timing. The cores also have a wide geographic spread and there is a variable availability of ^{14}C ages. The year(s) in which the drilling/sampling occurred is also significant. Some cores, particularly the lower resolution ones, are dated almost exclusively using the SPECMAP age model, which is an indirect method relying on correlation of marine oxygen isotope curves. This is most common for published SST histories that pre-date the paper by Petit et al (1999) relating to the Vostok ice core. Others, particularly those published post 1999 are typically dated using a combination of ^{14}C ages and direct comparison with isotopic records from high-resolution Antarctic ice cores. Some of these marine cores, for instance MD97-2120 (Pahnke et al 2003, 2008), have SST records that exhibit a remarkable degree of coherence with the temperature records from the Antarctic ice cores.

During the late Quaternary in the Southern Ocean the SST almost certainly varied in synchronization with the air temperature as measured at the EPICA Dome-C, Vostok Station, Taylor Dome, Byrd Station, Dome Fuji, and Siple Dome localities in continental Antarctica. This interpretation is supported by the foraminiferal Mg/Ca based SST record from marine core MD97-2120 by Pahnke et al

(2003). In fact the evolution of SST in the circum-Antarctic Southern Ocean probably exerts considerable control over the air temperature recorded in the various Antarctic ice cores.

The middle-MIS3 cold-event was severe and lasted for about 10 to 12 kyr. For the purposes of this PhD project great precision in estimation (from the marine cores) of the age of the cold-event is not necessary. It appears to have occurred at c. 51-39 ka. The commencement of this event coincided with the end of Antarctic Interstadial A3. It continued until the beginning of Antarctic Interstadial A1 and contained least one modest short-term recovery (during Antarctic Interstadial A2). Tables 4.5 and 4.7 summarize the timing of the intra-MIS3 cold-event in deep Antarctic ice cores. There is some variation between the age-scales for these cores so it is assumed for the purposes of this PhD thesis that a global average across the cores gives a reasonable estimate of the timing of the event. The limiting ages appear to be approximately 51 ka and 39 ka.

Table 4.4 Summary of Sea Surface Temperature Minima During MIS3: Cores with a prominent minimum at c. 50-40 ka

Core	Latitude and Longitude	Timing of SST Minimum	SST measurement method	Location	Reference
GeoB 3910-2	-4.2450˚S -26.3450˚	c. 48-39 ka	Alkenone	Northeast Brazilian margin	Jaeschke et al 2007
GeoB 1711-4	23.32˚S, 12.3˚E	52-42 ka 47-44 ka	Alkenone, Wind max, cold water planktonic forams	African margin, SE Atlantic off Walvis Bay	Shi et al 2001 Kirst et al 1999
GeoB 1710-3	23.4317˚S 11.6983 E	52- 42 ka	Alkenone	As above	Kirst et al 1999
GeoB 1712-4	23.26˚S, 12.81˚E	48-42 ka	Alkenone	As above	Kirst et al 1999
GeoB 1028-5	20˚ 06.2'S, 9˚11.1'E		Alkenone	Walvis Ridge	Schneider et al 1995
GeoB 3910-2	-4.245˚, -26.345˚	c. 48-39 ka	Alkenone	Equatorial Atlantic Ocean	Jaeschke et al 2007
PGPC12	22˚16.0S, 12˚32.3E	c. 55-45 ka	Alkenone	African margin, SE Atlantic off Walvis Bay	Summerhayes et al 1995
MD96-2087	25.6˚S, 13.38˚E	48-38 ka	Alkenone	SE Atlantic off South Africa	Pichevin et al 2005
PS 1756-5	48˚ 53.9'S, 11˚44.3'E	45-35 ka	MAT on dinoflagellate cysts	Southern Ocean south of South Africa	Esper et al 2007
PS 2082-1	43˚13.2'S, 11˚44.3'E	47-38 ka	MAT on dinoflagellate cysts	As above	Esper et al 2007
ODP 1089	40˚56'S, 9˚54'E	50-40 ka	Mg/Ca on Radiolaria	As above	Cortese et al 2004, 2007
Pretoria salt pan	40 km NNW of Pretoria, Sth Africa	48-37 ka	Precipitation minimum	Pretoria, South Africa	Partridge et al 1997
MD90-963	5˚04'N, 73˚53'E	50-40 ka	Alkenone	Nth Indian Ocean	Budziak 2000
WIND-28K	10.1538˚S, 51.0128˚E	c. 50-40 ka	Mg/Ca ratios	Mascarene Basin, Eastern Indian Ocean	Kiefer et al 2006
Stalagmite Bt2	27˚13'24"S, 49˚9'20"E	47-38 ka	Growth rate minimum	Southern Brazil	Cruz et al 2007
GeoB 3007	16˚10.2'N, 59˚45.3'E	c. 50-40 ka	Alkenone	Arabian Sea	Budziak 2004
MD01-2378	13˚4.95'S, 121˚47.27E	46-39 ka	Mg/Ca ratio on planktonic forams	South Timor Sea	Durkop et al 2008
MD84-527	55˚S 73˚E	c. 47-42 ka	Diatom transfer function	Southern Indian Ocean	Pichon et al 1992
MD84-551	44˚S 51˚E	c. 46-38 ka	Diatom transfer	Southern Indian	Pichon et al 1992

			function	Ocean	
MD94-103	42˚32'S, 86˚32'E	50-35 ka	Alkenone	Southern Indian Ocean	Sicre et al 2005
MD88-770	46˚01'S, 96˚28'E	49-39 ka	Foraminiferal summer SST	Southern Indian Ocean	Labeyrie et al 1996
MD88-769	46˚04'S, 90˚06'E	45-40 ka	Alkenone	Southern Indian Ocean	Kim et al 2009
TR163-22	0˚30.9'N, 92˚23.9'W	c. 44-38 ka	Mg/Ca ratio	Equatorial Pacific	Lea et al 2006
ODP 1233	41˚47.17'S, 74˚26.19E	51 ka onwards	Alkenone	E Pacific, Chilean Margin	Kaiser et al 2007
GeoB 3375-1	27˚28'S, 71˚15'W	52-38 ka	high humidity (from sedimentology)	Northern Chilean Margin	Stuut et al 2004
E11-2	56˚04'S, 115˚05'W	50 ka onward	Mg/Ca ratio	Subantarctic Pacific Ocean	Mashiota et al 1999
RS147GC-07	45˚09'S, 146˚17'E	c. 53-44 ka	Alkenone	Sth Tasman Rise	Sikes et al 2008
ODP 1172A	43˚57.585'S, 149˚55.696'E	c. 50-42 ka	Mg/Ca Ratios	East Tasman Rise	Nurnberg & Groeneveld 2006
ODP 1123	41˚47.17'S, 171˚29.94'W	c.50-40 ka	MAT Foraminifera ANN	North Flank, Chatham Rise	Hayward et al 2008; Crundwell et al 2008
MD97-2120	45˚32'S, 174˚55'E	50 ka onward	Alkenone	Western Bounty Trough/ South Flank, Chatham Rise	Pahnke & Sachs 2006
		50-40 ka	Mg/Ca ratio		Pahnke et al 2003, 2008
MD97-2121	40˚22.8'S, 177˚59.4'E	50-40 ka	Alkenone	East Coast, Nth I, NZ @ northern margin of Chatham Rise	Pahnke & Sachs 2006
SO136-GC3	42˚18'S, 169˚53'E	50 ka onward?	Faunal based SST & Alkenone	Continental shelf, West Coast, South Island, NZ	Barrows et al 2007, Pelejero et al 2006
DSDP-594	45˚31.41S, 174˚56.88'E	50-38 ka	Summer & winter SST by Dinoflagellate Cyst assemblages.	South flank, Chatham Rise	Marrett et al 2001
DSDP-594		49.2-44.4 ka	MAT Plankt Forams		Schaefer et al 2005
SO136-111	56˚40'S, 160˚14"E	c. 50-40 ka	MAT on diatom assemblages	Southern Ocean south of NZ	Crosta et al 2004
RC11-120	43.52˚S 79.867˚E	54-47	MAT on Radiolaria	Subantarctic Indian Ocean	Martinson et al 1987
ODP 1145	19˚35'N, 117˚38'E	50-46 ka	Mg/Ca Ratios	South China Sea	Oppo & Sun 2005
MD01-2421	36˚02'N, 141˚47'E	48-39 ka	Alkenone	NW Pacific off Japan	Yamamoto et al 2004, fig 3
GIK 17961/17964	8˚30.4'N, 112˚19.9'E	48-38 ka	Alkenone	South China Sea	Pelejero et al 1999
V30-40	-0.2000, -23.1500	45-40 ka	"Calculated"		Imbrie & McIntyre 2006
Byrd Station	80˚01'S, 119˚31' W	c. 52-40 ka	Precipitation source mean SST	Ice Core Antarctica	Brook et al 2005
Vostok	78.4667˚S, 106.80˚E	c. 50-38 ka	Large surface temp depression relative to modern	Ice Core Antarctica	Petit et al 1999
			Large source temp (SST) depression rel. modern.		Vimeux et al 2002
EPICA Dome-C	75˚06S, 123˚24'E	51-38 ka	Minima in atm CH_4, maxima in	Ice Core Antarctica	Loulergue et al 2007

		52-39 ka	dust. Minima in surface temperature		
Dronning Maud Land	75˚S, 0E	c. 46-39 ka	$\delta^{18}O$ ice	Ice Core, Antarctica	EPICA Community Members 2006
Taylor Dome	-77.6667, 158.0000	c. 45-39 ka	$\delta^{18}O$ ice	Ice Core Antarctica	Steig 2006
Dome Fuji	77°9'S, 39°42'E	50-38.5 ka	Surface Temperature Minima	Ice Core Antarctica	Kawamura et al 2007
Dome C	75˚06S, 123˚24'E	42-39 ka	Surface temp and source temp minima	Ice core Antarctica	Stenni et al 2004
RC13-228	22.33˚S, 11.198˚W	c. 45-38 ka	"Calculated"		Imbrie & McIntyre 2006
V25-56	-3.5500˚S -35.2300˚	c. 45-40 ka	"Calculated"		Imbrie & McIntyre 2006

In general at middle to high latitudes the impact of the middle-MIS3 thermal minimum on SST's appears to have of comparable intensity to that of stadial events from MIS2 and MIS4. This is illustrated in a qualitative manner in table 4.5 where various Southern Hemisphere SST records are listed. At low latitudes (closer to the equator) the MIS3 SST minimum tends to be more intense (colder) than the stadial events from MIS2 and MIS4, a pattern noted by Pahnke & Sachs (2006). The MIS3 thermal minimum was associated with the northwards migration of oceanic fronts like the "subtropical convergence" and with some oceanic circulation patterns including the Benguela - Angola Current.

Table 4.5 Relative intensity of stadial events in terms of sea surface temperature during the last glaciation (MIS2, MIS3 & MIS4)

Marine Sediment Core	**Coldest part of MIS3**	**Intensity of mid-MIS3 cooling relative to MIS2 stadial events**	**Intensity of mid-MIS3 cooling relative to MIS4 stadial events**	**Reference**
DSDP594	5m to 4m	Equal for summer Equal for winter	Equal for summer Equal for winter	Marret et al 2001
MD97-2120	c. 51-40 ka	Approaches MIS2 (on Alkenone based SST). Equal based on Mg/Ca ratios	Equal to MIS4 (on Alkenone based SST). Equal based on Mg/Ca ratios	Pahnke et al 2008 Pahnke & Sachs 2006
MD97-2121	c. 51-39 ka	Generally colder than MIS2 from Alkenone based SST	Colder than MIS4 from Alkenone based SST	Pahnke & Sachs 2006
SO136-GC3	c. 50-40 ka	As cold as MIS2 (using revised analogue technique)	As cold as MIS4 (using revised analogue technique)	Barrows et al 2007
SO136-111	c. 50-40 ka	As cold as MIS2 (using Feb SST. MAT on fossil diatom assemblages)	As cold as MIS2 (using Feb SST; MAT on fossil diatom assemblages)	Crosta et al 2004
RS147-GC07	51-45 ka	As cold as MIS2. (Alkenone based SST)		Sikes et al 2008
ODP1123	c. 50-45 ka	Almost as cold as MIS2	Almost as cold as MIS4	Crundwell et al 2008
ODP1172	c.50-40 ka	Equal to MIS2	Almost as cold as MIS4	Nurnberg & Groeneveld 2006
ODP1089	c.50-40 ka	Colder than MIS2	Colder than MIS4	Cortese et al 1989
ODP 1232	41-39 ka	Colder than MIS2 (based on Planktonic Foram $\delta^{18}O$)	Colder than MIS4 (based on Planktonic Foram $\delta^{18}O$)	Blumberg et al 2008
ODP1233	51-48 ka	As cold as MIS2 (Alkenone based SST)	Equal to MIS4	Kaiser et al 2005

	46-43.5 ka 41-40 ka	Colder than MIS2 As cold as MIS2	Equal to MIS4 Equal to MIS4	
RC11-120		As cold as MIS2 (Mg/Ca on G. rubber) As cold as MIS2 (radiolarian SST)	As cold as MIS4 (Mg/Ca on G. rubber) As cold as MIS4 (radiolarian SST)	Mashiota et al 1999 Martinson et al 1987
MD84-527	c. 48-42 ka	Colder than MIS2 (Diatom transfer function)	Colder than MIS4, (Diatom transfer function)	Pichon et al 1992
MD84-551	c. 45-38 ka	Almost as cold as MIS2 (Diatom transfer function)	Colder than MIS4 (Diatom transfer function)	Pichon et al 1992
MD88-770	c. 50-38 ka	As cold as MIS2	As cold as MIS4	Labeyrie et al 1996
MD94-101	MIS3 stadials	Colder than MIS2 (RAM on planktonic foraminifera)	Colder than MIS4	Waelbroeck 1999
MD88-769	c. 50-37 ka	Colder than MIS2 (Alkenone based SST)		Kim et al 2009
E11-12	MIS3 stadials	As cold as MIS2 (Mg/Ca ratios on *N. pachyderma)*	As cold as MIS4 (Mg/Ca ratios on *N. pachyderma)*	Mashiota et al 1999
ODP806B		SST flat-lines from c. 70 ka to c. 17 ka (Mg/Ca ratios on *G. ruber*)		Lea et al 2002
TR163-22	c. 44-38 ka	As cold as MIS2	As cold as MIS4	Lea et al 2006
PS1756-5	MIS3 stadials	As cold as MIS2 (summer SST; MAT on dinoflagellate cysts)		Esper et al 2007
PS2082-1	MIS3 stadials	As cold as MIS2	As cold as MIS4	Esper et al 2007
PS1768-8	MIS3 stadials	As cold as MIS2	As cold as MIS4	Esper et al 2007
GeoB 3007-1	50-38 ka	Colder than MIS2 (Alkenone based SST)	Colder than MIS4	Buzdiak 2004
WIND-28K		Colder than MIS2 (Mg/Ca ratio, planktonic foraminifera)	As cold as MIS4	Kiefer et al 2006
RC13-228	45-38 ka	As cold as MIS2	As cold as MIS4	Imbrie 2006
V25-56	47-40	Winter SST as cold as MIS2	Winter SST colder than MIS4	Imbrie 2006
V30-40	MIS3 stadials	As cold as MIS2	As cold as MIS4	McIntyre et al 1989
GeoB 1710-3	MIS3 stadials	As cold as MIS2, (Alkenone based SST)	Almost as cold as MIS4	Kirst et al 2001
GeoB 1711-4	50-36 ka	Colder than MIS2 (Alkenone based SST)	Colder than MIS4	Kirst et al 2001
GeoB 1712-4	MIS3 stadial	Colder than MIS2	Colder than MIS4	Kirst et al 2001
GeoB 1016-3	50-45 ka	As cold as MIS2 (Alkenone based SST)	As cold as MIS4	Schneider et al 1995
ODP1145	MIS3 stadials	Almost as cold as MIS2	Almost as cold as MIS4	Oppo & Sun 2005
MD97-2142	MIS3 stadial	Almost as cold as MIS2	Colder than MIS4	Yu et al 2003
MD07-2575	45-41 ka	Almost as cold as MIS2	As cold as MIS4	Ziegler et al 2008
MD01-2378	45-39 ka	Colder than MIS2	----	Zuraida et al 2009

A number of the marine cores listed in table 4.5 are particularly relevant to North Westland including cores SO136-GC3; SO136-111; MD97-2120; MD97-2121; DSDP594; ODP1123; and RS147-GC07. The timing of the middle MIS3 cold period is reasonably well constrained in these cores to c.51-39 ka. This is equivalent to the period between Antarctic Interstadials A3 and A1 as defined in the isotopic

record from Antarctic ice cores (see tables 4.2a, 4.2b, & 4.7). The Mg/Ca SST record from this period at MD97-2120 contains a modest warm event that probably correlates with Antarctic Interstadial A2.

As discussed below the SST records from the marine cores listed in table 4.5 indicate this event was preceded by a period of relative warmth in the ocean surrounding the South Island.

The oceans are the major repository of heat in the hemispheric-scale climate system. The surface air temperature in immediately adjacent coastal areas can be expected to respond quickly to changes in the mean state of the sea surface temperature. The climate in Westland obviously is not isolated from that of the rest of the Southern Hemisphere. It must respond to the broad evolution of prevailing wind strength, cloud cover and precipitation, adjacent sea surface temperature, cross-latitudinal heat transfer and local changes in insolation. As demonstrated by Vandergoes et al (2005) in relation to the pollen record from the Okarito Pakihi Bog which implies a major middle MIS3 contraction of *Podocarp* dominated forest and possible expansion or at least retention of *Nothofagus* dominated forest. The evolution of vegetative cover here during MIS3 may have been controlled to a significant extent by is may be changes in the climate. In Chapter 5 the dating of this record is discussed in detail. The dating is compatible with evidence from Williams (1996) and Berger et al (2001) for significant glacial advances in Westland and Fiordland between c.51 ka and c.39 ka.

Table 4.6 Prominent Late Quaternary cold events defined in isotopic records from Antarctic ice cores

Dome Concordia	Taylor Dome	Vostok Station	Dome Fuji	Dronning Maud Land
Parrenin et al 2007 (kyr BP) Duration	Steig et al 2000 (kyr BP)	Petit et al 1999 (kyr BP)	Kawamura et al 2007 (kyr BP)	EPICA Team 2006 (kyr BP)
135.1+	134+	133.4+	134.5+	133+
113.5-107.5 (6.0)	115.2-107.8 (7.4)	114.8-107.3 (7.5)	114.5-110.5 (4.0)	115-107.5 (7.5)
104.9-102.4 (2.5)	105.6-104.1 (1.5)	105.8-104 (1.8)	106.5-104.5 (2.0)	105.5-103.3 (2.2)
92.6-91.1 (1.5)	91.5-90.3 (1.2)	91.5-88 (3.5)	92.5-88.5 (4.0)	93-86.5 (6.5)
80-75.5 (4.5)	80.4-76.6 (3.8)	80-77 (3.0)	80-76 (4.0)	80-75.6 (4.4)
73.8-71.2 (2.6)	74.5-70.4 (4.1)	74.5-72.8 (1.7)	74-72 (2.0)	73.6-72.1 (1.5)
70.1-61.5 (8.6)	69.5-58.9 (10.6)	71-59.5 (11.5)	69.5-61.5 (8.0)	70.9-61.8 (9.1)
56.4-54.4 (2.0)	54.6-53.9 (0.7)	55.2-52.8 (2.4)	55.5-54.5 (1.1)	56.9-55.7 (1.2)
51.3-48.4 (2.5)	49.6-48.2 (1.4)	49.6-43.3 (6.3)	50.0-38.5 (11.5)	49.9-48.1 (1.8)
45.6-39.0 (6.6)	45.3-39.3 (6.0)	41.2-36.8 (4.4)		45.1-39.2 (5.9)
36.9-16.4 (20.5)	36.2-14.9 (21.3)	35.1-16.1 (19)	36.5-16.5 (20)	37.6-16.5 (21)
(30.2-27.7) warm	(29.7-27) warm	(29.3-28.1) warm	(30-27) warm	(30.6-27.8) warm

4.2.10 Southern Hemisphere Thermal Maximum from c.61 ka to c.51 ka

The transition from MIS4 to MIS3 was accompanied throughout the Southern Hemisphere by a substantial increase in SST and generally by warming in continental areas. The early portion of MIS3 appears generally to have been warmer than the middle to later portion and is defined here as the intra-MIS3 thermal maximum or "climatic optimum". Antarctic ice core evidence (see table 4.6) suggests warming into the thermal maximum commenced no later than 61 ka. The thermal maximum lasted to about 51 ka and contained a modest cool episode at from c.55.5 to c.54.5 ka. The Southern Hemisphere MIS3 thermal maximum encompassed Antarctic Interstadials A4 and A3 and had a total duration of approximately 10 kyr. In terms of marine cores this warming appears to be more pronounced in low latitude regions than in high latitude regions. These temperature trends are most

obvious in the higher-resolution cores. The sea surface temperature record for MIS3 is important with regard to this (PhD) project. The broad features of climate in Westland almost inevitably reflect conditions across the Southern Ocean as a whole, given that Westland is very exposed to westerly winds derived from that oceanic region. So naturally discovery of on-land evidence for relative warmth in the early portion of MIS3 shouldn't be unexpected. The same holds for the discovery of episodes of cold climate in the middle of MIS3. Confirmation of a period of relatively mild climatic conditions in the Westport area between about 39 ka and 35 ka by Burge (2007) is in harmony with trends in SST in the Southern Ocean and Antarctica from that time.

Table 4.7 South African precipitation. Precipitation is broadly in-phase with Southern Hemisphere summer insolation cycles, dry phases tending to coincide with summer minima.

Pretoria Saltpan, South Africa (~26.5°S, 28°E), Partridge et al (1997)		Lake Tswaing (25°24'30'' S, 28°04'59'' E), Kristen et al (2007)	
Wet (green)	Dry	Wet	Dry
	28-6 ka		26-5 ka
37-28ka		35-26	
	48-37		37-35
55-48		41-37	
	70-55		46-41
75-70		55-46	
	87-75		66-55
98-87		72-66	
	108-98		85-72
119-108		100-85	
	132-119		106-100
145-132		120-106	
	155-145		132-120
168-155		142-132	
			155-142
		165-155	

During the MIS3 thermal maximum the climate in the South Island and surrounding areas probably was not as stable as that of the Holocene and was probably slightly cooler overall. By comparison the Holocene period commenced at c. 11.5 ka and so has only been slightly longer than the MIS3 thermal maximum. It is likely that in areas such as North Westland the floristic recovery from the MIS4 thermal minimum was more rapid than the recovery from the MIS2 thermal minimum. Overall MIS2 appears to have been the more prolonged and severe event. It has been suggested by Williams et al (2009) and Fink et al (2009) that in terms of maximum ice extent the LGM in New Zealand may have occurred during MIS4 rather than MIS2. MIS2 appears to have been a longer-lived event (see table 4.6), and was preceded by a series of severe MIS3 stadial events. MIS4 was probably not preceded by such a long/drawn-out period of climatic cooling.

The MIS3 thermal maximum is well defined at each of the marine cores that are particularly relevant to the West Coast of the South Island. These cores (also listed above in connection with the intra-MIS3 thermal minimum) are: SO136-GC3; SO136-111; MD97-2120; MD97-2121; DSDP594; ODP1123;

and RS147-GC07. The timing of the warm period is reasonably well constrained in these cores to c.61-51 ka. Evidence for a sustained period of relatively warm climate in Westland during the MIS3 thermal maximum, particularly in connection with the pollen archive from the Okarito Pakihi Bog, is discussed in more detail in Chapter 5.

Table 4.8 Synchronous high and low latitude climate events in the Southern Hemisphere, climate-proxy data from Bolivia and Antarctica

Age of ^{14}C & U/Th dated Borehole Gamma events and stratigraphic horizons, Salar de Uyuni, Bolivia, Fritz et al (2004)		Dust from Antarctic Ice Cores Lambert et al (2008): Dome C core Petit et al (1999): Vostok core		
Age (ka) down-hole gamma events (counts per second) High gamma = blue Low gamma = brown	Interpretation: High gamma = wet (usually with perennial lake conditions) Low gamma = relatively dry	Age of event (ka)		Nature of event
		Dome C	Vostok	
14.5-13.5	Drier/less windy	ACR		
26-16	Wetter/windier		28.4-17.5	Cold, dusty
28-26	Drier/less windy	29-27	29.3-28.4	Warm, dust min.
32-28	Wetter/windier	32-29	35-29.3	Cold, dusty
37-32	Drier/less windy	39-32	37-35	Warm, dust min.
48-46	Drier/less windy	48-45		Warm, dust min.
49-48	Wetter/windier	50-48	49-45	Cold, dusty
55-49	Drier/less windy	54-50	57-49	Warm, dust min.
59-55	Wetter/windier	56.5-54	59-58	Cold, dusty
67-59	Drier/less windy	60-56.5	63.5-59	Warm, dust min.
		70-60	72-63.5	Cold, dusty
70-67	Wetter/windier			
72-70	Drier/less windy	72-70	72-70.5	Warm, dust min.
74-72	Wetter/windier	73.5-72	75-72	Cold, dusty
78-74	Drier/less windy	75.5-73.5	79-75	Warm, dust min.
81.5-78	Wetter/windier	80-75.5	82.3-79	Cold, dusty
85-81.5	Drier/less windy	86.5-80	88-82.3	Warm, dust min.
87-85	Wetter/Windier	88-86	90-88	Cold, dusty
93-87	Drier/less windy	103-88	92-90 95-92 dust 102-95	Warm, dust min Warm, dust min
96-93	Wetter/Windier			
107-96	Drier/less windy	105-103	105-102	Cold, dusty
		107-105	133-105	Warm, dust min.
111-107	Wetter/windier	112-107		Cold, dusty
114-111	Drier/less windy	133-112		Warm, dust min.
116-114	Wetter/windier			
133-116	Drier/less windy			
138-133	Wetter/windier	133+	133+	Cold, dusty

Table 4.8 (above) is presented as an example of stationarity in climatic teleconnections between the Bolivian Andes and two Antarctic ice cores (Vostok and Dome Concordia). There is a consistent relationship between these sites such that wetter/windier episodes at Salar de Uyuni (Bolivia) correlate with cold/dusty episodes at Vostok/Dome C. The South American wind speed-relationship/Antarctic temperature relationship displayed in table 4.8 is discussed in detail by Rothlisberger et al (2008). It appears to be a persistent feature of Southern Hemisphere climate. The relationship becomes stronger

as Antarctic temperatures decrease. These authors report that in terms of nssCa flux to the Dome C ice core there is a threshold at 2°C below the modern value where a stable level is reached and further warming does not change the flux.

4.2.11 Southern Hemisphere Surface Temperatures from c.82 to c.75 ka

From Westland there is evidence for a substantial glacial advance between 82 ka and 75 ka, including luminescence dating from this (PhD) project, luminescence dating by Preusser et al (2005), and cosmogenic isotope dating by Sutherland et al (2007). Glaciation at this time would be consistent with reduced ice ablation during summer in the Southern Alps coincident with the local summer (mean January) insolation minimum that occurred at c.80-82 ka. This timing does not fall neatly into a Milankovitch-style Northern Hemisphere forcing model. It is not obvious in terms of global sea-level expectations generated by the SPECMAP stacked marine isotope record of Martinson et al (1987). However, potential alpine glaciation in the South Island of New Zealand, the Tasmanian Highlands, and Southern South America would have a negligible impact on global sea level as the ice volume is small relative to the large Northern Hemisphere ice sheets.

So is there evidence for a substantial and widespread cooling during the 80-82 ka Southern Hemisphere insolation minimum? High resolution records of dust deposition in Antarctica are available for deep ice cores from Dronning Maud Land, Vostok, and Dome Concordia (Antarctica). The Dome C record of Lambert et al (2008) is displayed in figure 4.18 below. Collectively these ice cores indicate that a dust deposition event from c. 80-75 ka is more pronounced than any other deposition event between 130 ka and 75 ka. The record of dust deposition is discussed in detail by Delmonte et al (2004), Fischer et al (2007) and Lambert et al (2008) who propose that the primary dust source is the Pampas region (dust source) of South America and that increased dust deposition correlates strongly with lower surface temperatures and higher mean wind speeds.

The timing of the most prominent surface temperature maxima and minima at the various Antarctic ice cores is summarised in table 4.9. Three prominent minima are present. These occurred at c. 74-77 ka, c.87-91 ka, and c. 108-111 ka. Two particularly prominent maxima are present most likely correlating with MIS5a and MIS5e. In Antarctica these maxima occurred at c.83.5-86 ka and c.128-133 ka. MIS5c is not represented by such a clear-cut surface temperature maximum in the Antarctic ice cores when taken as a group. The Antarctic cold event at 77-74 ka occurs between Antarctic interstadials A6 and A7 as defined by Blunier and Brook (2001).

So there is clearly evidence for a general cooling of surface temperatures at high southern latitudes (Antarctica) reaching a regional minimum at c.77-74 ka. Is this matched by a cooling of SST particularly in the Southern Ocean and in the South Pacific? An SST stadial event that probably coincides with that in Antarctica between interstadials A6 and A7 can be ascertained at the marine cores listed in table 4.10. The grid references for the marine cores listed below are given in table 4.4.

Figure 4.16: Climate anomalies at five Antarctic ice core sites

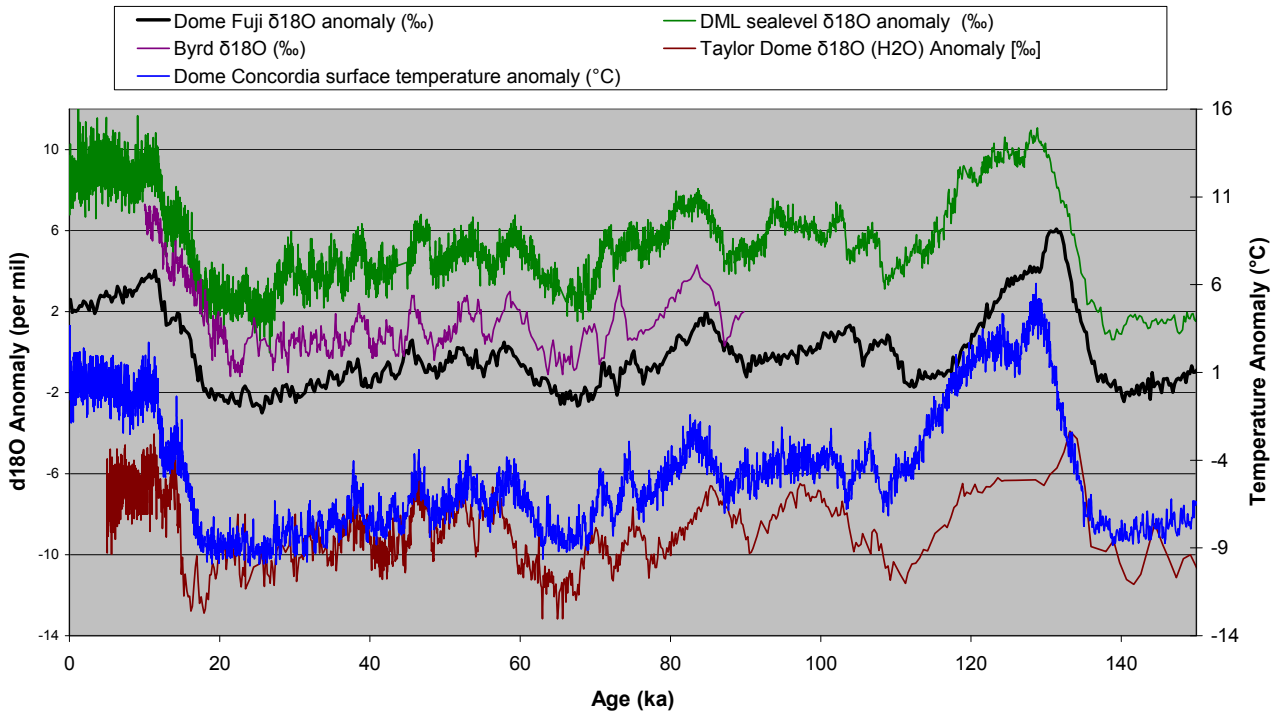

Table 4.9 Timing of Maximum and Minimum Surface Temperature Events (ka)						
Location	**MIS4/5a Minimum btw A6 and A7**	**MIS5a Max**	**MIS5b Min**	**MIS5c Max**	**MIS5d Min**	**MIS5e Max**
DML Core, $\delta^{18}O$, EPICA Team Members (2006)	76	83.8	88-91	94	109	128
Taylor Dome, $\delta^{18}O$, Steig (2006)	77	85.7	91	97	111	133
Dome Fuji, Temp, Kawamura et al (2007)	77	84	90	107	111	131
Vostok, Temp. Waelbroeck et al (2002)	77	84.5	90	102	108	128
Vostok, d2H, Petit et al (1999)	77.3	85.6	90.5	96/102	108	129
Dome C, Temp Parrenin et al (2007)	76	83.8	88	95	108	128-129
Dome C, Dust, Lambert et al (2008)	76.3	84.8	88	95.7	108	132
Byrd Station, $\delta^{18}O$, Blunier & Brook (2001)	74.6	83.5-84	87.2	---	---	---
SO136-GC3 $\delta^{18}O$, G.bulloides, Barrows et al (2007)	c. 76	84	88	95	106-110	120-12
MD97-2120, Mg/Ca SST, Pahnke & Sachs (2008)	72-76	80-84	87	---	108	126
MD02-2488, SST, Govin et al (2008)	75-79	84	87	100	103/ 108	130
MD95-2041 Cayre et al (1999) SST	80-82	88-84	92-89	105-103	110-113	125

The list of moderate and high resolution marine proxy climate records in table 4.10 provides support for the view that sea surface temperatures over the middle to lower latitudes of the Southern Hemisphere cooled steadily and substantially from about 82 ka to about 75 ka.

Table 4.10 Timing of the stadial event between Antarctic Interstadials A6 and A7 from marine cores located in the Pacific and Southern Oceans			
Marine Core	**Timing of stadial**	**Method**	**Reference**
DSDP594	82-78 ka	Dinoflagellate based SST	Barrows et al 2007, Marret et al 2001
DSDP594	82-78 ka	MAT based SST	Wells & Okada 1997
MD91-2121	79-74 ka	Alkenone based SST.	Pahnke & Sachs 2006
MD97-2120	81-74 ka	Alkenone based SST, Nth Flank, Chatham Rise	Pahnke & Zahn 2008; Pahnke & Sachs 2006
MD97-2120	c.80-75 ka	MG/Ca based SST (fig 5.4 this PhD)	Pahnke et al 2003
U939, U938	c.85-75 ka	Alkenone based SST minimum, southern flank, Sthn flank, Chatham Rise	Sikes et al 2002
ODP1123	83-80 ka	Mean annual faunal-based SST	Crundwell et al 2008
RS147- GC07	c.90-75 ka	Alkenone-based SST, Sth Tasman Rise	Sikes et al 2008
ODP1172A	c.80 ka	Commencement of decline in Mg/Ca ratio on G. bulloides	Nurnberg & Groeneveld 2006
MD02-2488	c.80-75 ka	SST base on foraminiferal abundance/percentages	Govin et al 2009
MD88-770	79-77 ka	Faunal based SST	Barrows et al 2007
RC11-120	80 ka	Mg/Ca based SST	Mashiota et al 1999
E11-2	80 ka	Commencement of decline, Mg/Ca based SST	Mashiota et al 1999
PS1756-5	c.80-74 ka	Dinoflagellate cyst based summer SST	Esper & Zonneveld 2007
PS2082-1	c.80-75 ka	Dinoflagellate cyst based summer SST	Esper & Zonneveld 2007
TR163-22	81-76 ka	Mg/Ca based SST	Lea et al 2000
GeoB3375	~80-78 ka	Commencement of high humidity, Nthn Chile (sedimentology)	Stuut et al 2004
ODP806B	80 ka	Commencement of decline, Mg/Ca based SST	Lea et al 2000
TR163-19	80 ka	Commencement of decline, Mg/Ca based SST	Lea et al 2000
ODP1145	80-77 ka	Mg/Ca based SST, South China Sea	Oppo & Sun 2005
GIK 17964	82-75 ka	Alkenone based SST, South China Sea	Pelejero et al 1999
SR1	80-77 ka	Mg/Ca based SST, western North-Pacific	Itou et al
MD97-2151	78-74 ka	Rapid SST decline, South China Sea	Zhao et al 2006
GIK 17964	82-75 ka	Rapid SST decline, South China Sea	Pelejero et al 1999

On land there is also evidence for cool climate approximately coincident with the stadial event between Antarctic interstadials A6 and A7. Fink et al (2000) report exposure ages of c.80 ka on glaciated surfaces from Cradle Valley, Tasmania. Sutherland et al (2007) produced exposure ages of C.80-75 ka on glacial erratic boulders from the Cascade Valley, Northwest Fiordland, New Zealand. Geode et al (1998) dated speleothem trace element and $\delta^{18}O$ from Frankcombe Cave, Florentine Valley, south-central Tasmania at C.77-72 ka. Fritz et al (2004) document the development of Perennial lakes at Solar de Uyuni, Bolivia at ~82-78 ka. Partridge et al (1997) document a major precipitation minimum at the Pretoria salt pan, South Africa at 85-74 ka. So evidence for relatively cool and/or dry climate is present for most of the major Southern Hemisphere landmasses, though the number of well-dated records is modest.

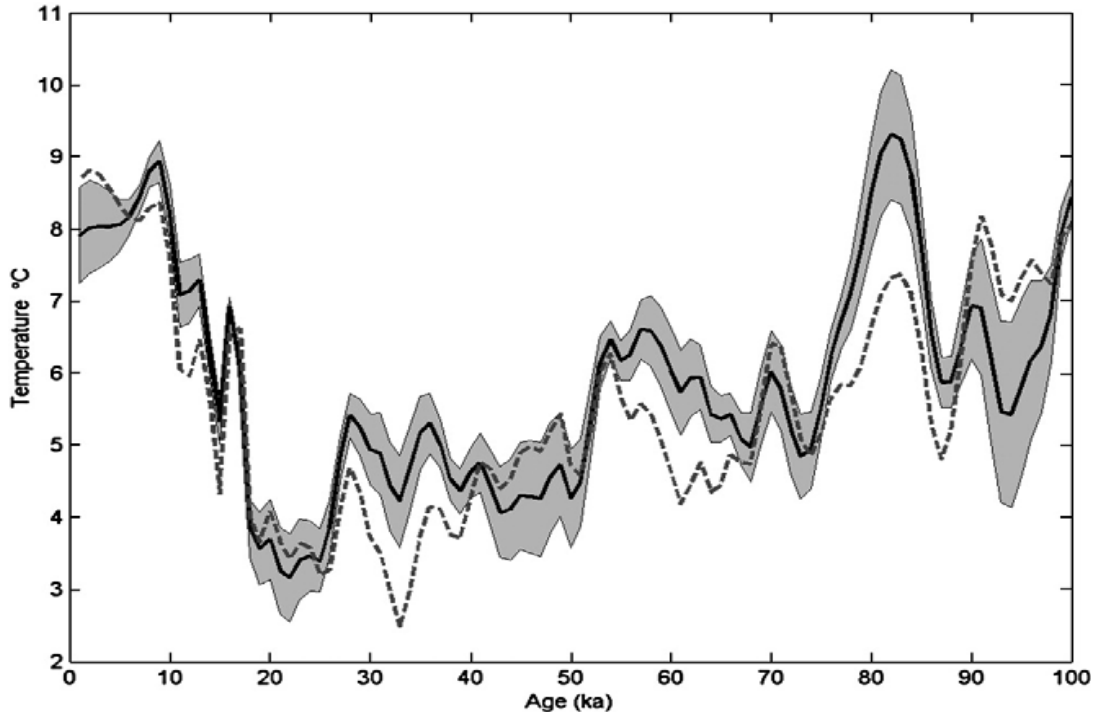

Figure 4.17 Speleothem growth history derived from Ersek et al (2009) from stalagmites at the Oregon Caves National Monument.

Figure 4.17 displays the results of cave temperature modeling for the last 100 ka on U-series dated stalagmites from Oregon Caves National Monument. The continuous line shows the average temperature of the model runs that produced modern cave temperatures of 7 to 8.8 °C. The stippled line represents the adjusted SST record (see text for explanation). The shaded gray area represents one standard deviation of the average modeled temperatures. Points worth particular attention in fig 4.16 include the abrupt decline in modeled temperature at c.52 ka, which mirrors the widespread Pacific SST results discussed in this chapter, and the decline in temperature to a minimum at c. 74-73 ka. This MIS5/4a transition event mirrors the SST evolution in the Southern Ocean, South Pacific Ocean and Antarctica. Although the MIS5a/4 event appears slightly delayed in Oregon the difference in timing is barely discernable and probably within the measurement error. Also worth noting is the significant early MIS3 warming from c.64 ka to c.52 ka.

4.2.12 Potential MIS5a Glacial Advance in the Southern Alps

The overall scenario constructed from the references listed above is that the period from around 82 ka to 75 ka in the high to mid southern latitudes included:

- Steady decline in SST throughout the Southern Ocean
- Steady decline in surface temperature over Antarctica
- Steady decline in SST at marine sites surrounding the South Island of New Zealand
- Increased dust deposition at three deep ice core sites in Antarctica
- A minimum in summer (mean January) solar insolation at 83 to 78 ka which was significantly lower than at any time since.
- A minimum in mid to high latitude meridional annual TOA blackbody temperature gradient at c. from about 73 ka.

- A minimum in the first difference between the Southern and Northern hemisphere mid to high latitude meridional TOA blackbody temperature gradient at 76 to 70 ka. As discussed above this is consistent with northwards heat piracy in favour of the Northern Hemisphere at the expense of the Southern Hemisphere.
- A sharp drop in alkenone based SST at marine core MD97-2120 on the southern flank of the Chatham rise, completed by ~78 ka (fig 4.15a)
- Increased wind, humidity and precipitation in the Bolivian Altiplano region
- Clear-cut mid-latitude Southern Hemisphere insolation control of precipitation over Southern Africa.

Collectively this set of circumstances is an ideal scenario for rapid accumulation of ice in the Southern Alps.

Prior to about 82 ka it is generally acknowledged that the mean global sea surface temperature and lower tropospheric temperature were both relatively high, though globally not quite in a full interglacial state, as the Laurentide ice sheet failed to melt away completely. Temperature adjusted marine $\delta^{18}O$ records (Shackleton 2000; Waelbroeck et al 2002) indicate eustatic sea level peaked at around -10 to -20 metres during MIS5a.

In the Southern Alps how long would it take to go from near full-interglacial climate at c.83-86 ka (table 4.9) to a major glaciation? Is there time for this to occur by 79-75 ka? It should be noted that a precessional scale summer insolation minimum occurred in the Southern Hemisphere mid-latitudes at 81-80 ka. So the direct local contribution of summer insolation to ice ablation was at a minimum at this time in the Southern Alps. In addition it appears from a large number of long marine records that during MIS5a the mean SST was generally slightly lower than the Holocene mean. Westland is a maritime region that is strongly affected by the adjacent surface temperature of the Tasman Sea. The SST reported by Barrows et al (2007) for marine core SO136-GC3 indicates surface temperatures were similar during the Holocene and MIS5a. So it is likely on the basis of adjacent oceanic heat that the ELA for permanent snow accumulation was no higher through most of MIS5a than during the Holocene. The timing of the decline in SST into MIS4 is highly dependent on assumptions relating to the phasing of local SST with planktic foraminiferal $\delta^{18}O$ (this core) and on phasing of planktic $\delta^{18}O$ with $\delta^{18}O_{seawater}$.

Several assumptions are made as follows:

- Strengthened westerly circulation at about 82-75 ka was almost certainly accompanied by increased cloudiness in Westland. Shading the surface in the Southern Alps and decreases the mean surface temperature. Increased wind strength is indicated by increased dust deposition in Antarctica at this time.
- At the millennial-scale, periods of high dust deposition in Antarctica (fig 4.16) coincide with periods of strong westerly wind over southern South America (Lambert et al 2008; Rothlisberger et al 2008, Fischer et al 2007 and Delmonte et al 2004). It is assumed here that this correlation holds for strong westerly winds over the South Island of New Zealand. In Antarctica these periods of rapid dust deposition coincide with colder surface temperature (isotopic temperature of precipitation).
- A high resolution precipitation history has derived from oxygen and carbon isotopic ratios in a speleothem from Hollywood Cave near Charleston (41°57'S; 171°28'E) on the West Coast by

Whittaker et al (2011). MIS 4 is a period of high precipitation in Westland and this coincides with periods of relatively low SST in the Tasman Sea and the Chatham Rise region .

- In the modern era (last 100 years) El-Nino like conditions in the Central/North Pacific correlate well with episodes of increased annual precipitation and strong Westerly circulation in Westland. It is assumed, using modern experience as an analogue, that millennial-scale episodes of strong westerly circulation are also characterized by relatively high mean annual precipitation in Westland. In areas above 1000 m elevation west of the main divide of the Southern Alps this is likely to mean an annual precipitation in the 6 to 12 metre range and precipitation of 3.5 to 4.5 m along the foot of the range front (at the Alpine Fault).
- From straightforward calculation of the theoretical change in temperature due to changing insolation in the mid-latitudes of the Southern Hemisphere, the difference between the modern summer (January mean) top of atmosphere blackbody temperature (305.2 K) and that at the 80 ka insolation minimum (298.2 K) is 7.0 °C. This does not coincide precisely with the SST minimum in the Southern Ocean. Averaged over the full year at 80 ka the theoretical TOA blackbody temperature was 1.6°C lower then than now. It is assumed that this translates to a genuine reduction in solar energy input in the Southern Alps. So ablation of snow/ice is reduced. This is equivalent to the effect of increasing the mean cloudiness. It is separate to the effect of a reduction in adjacent sea surface temperature caused by changes in wind direction and speed.
- The SST minimum at c.76–75 ka was accompanied by a summer theoretical TOA blackbody temperature depression of c. 2.7°C to 3.7°C.

A selection of estimates for the temperature depression during the 82-75 ka event is given in table 4.11 below.

Table 4.11 Maximum temperature depression during the first MIS5/4a cooling episode at c. 82-75 ka (relative to the MIS5a thermal maximum)

Location/Core	**Temperature depression**	**Source**
Vostok Station, Antarctic	= c. 4 to 5°C	Waelbroeck et al (2002)
Dome Fuji, Antarctica	= c. 4 to 4.5°C	Kawamura et al (2007)
Dome C, Antarctica	= c. 4.5 to 5°C	Parrenin et al (2007)
MD02-2488	= c. 3.5 to 4°C	Govin et al (2008)
SO136-GC3 East Tasman Sea	= c. 2°C	Barrows et al (2007)
MD97-2120 Chatham Rise	= c. 3 to 3.5°C	Pahnke & Sachs (2006)
MD97-2121 Chatham Rise	= c. 2 to 2.5°C	Pahnke & Sachs (2006)
DSDP594 Chatham Rise	= c. 2 to 4°C	Marret et al (2001)
MD88-770 Southern Ocean	= c. 3°C	Barrows et al (2007)
GC07, South Tasman Rise	= c. 4°C	Sikes et al (2008)

Environmental lapse rate in Westland

In Chapter One the modern mean-annual environmental lapse rate (ELR) in the South Island is estimated at 4.88°C/km (The lapse rate adopted by Anderson et al (2006) in a study of the mass balance of the Franz Josef glacier was 4.8°C/km, over an elevation range from about 300 to 2300 m, with an additional 1.35°C downward step off the ice as there is an abrupt change in temperature in comparison

with the long-term record at Franz Josef). It is noted there that the modern ELR is greater during the winter than during the summer. It is not clear that this mean ELR is constant through time. Through the year the ELR appears to be rather sensitive to the mean monthly solar irradiance, increasing as irradiance decreases. This relationship may also hold for the summer season through time. That is, through the orbital (precession and obliquity) cycle, reduced summer solar irradiance is likely to correspond to an increased summer ELR. So at summer insolation minima surface temperature falls faster with increasing altitude than it does during summer insolation maxima. Logically therefore one might predict that the cooling of summer temperature with decreasing summer insolation is more exaggerated at higher altitudes than at sea level. This is potentially important because summer is still the warmest time of the year and the ELA (equilibrium altitude for ablation/accumulation) is controlled primarily by the summer temperature.

At 40°S the summer-winter insolation difference is as follows:

> At 0 ka the mean January to mean July difference is 666 cal/cm^2/day.
> At 81 ka the mean January to mean July difference is 539 cal/cm^2/day.
> The cyclical variation in the January-July insolation difference is as much as c. 127 cal/cm^2/day
> The cyclical variation is as much as 19% of the modern annual summer-winter insolation difference.

At 40°S the modern summer and winter ELRs (from chapter 1) are 2.49°C/km and 7.49°C/km, a difference of 5°C/km. So it would not be unreasonable to speculate that the summer ELR could vary by as much as 1°C/km, which could have a significant impact on the ELA. The ELA could be lowered by as much as 100 to 300 m as consequence during insolation minima. This is a cyclical effect that is generally not accounted for in discussions of the causes of glaciation. It is particularly relevant in the South Island because glaciation here is occurs in an alpine region from about 41°S to 46°S. This is in the relatively warm middle latitudes whereas Northern Hemisphere glaciation tends to centre around 60°N to 65°N in areas of relatively low altitude where the lapse rate may be less important.

There is direct evidence for glaciation during the MIS5a/4 transition and evidence for high humidity and strong westerly atmospheric circulation. So how quickly could a full-scale glaciation be established in the Southern Alps? Lets speculate in relation to a mean ELA of say 1000 m elevation that above this elevation no less than ½ of the annual precipitation accumulates, initially as snow and ultimately is compressed to become ice. Also that a substantial portion does not avalanche immediately to the lowest possible point. Further, lets speculate that this was a period of cooling when humidity was similar to the present time. In the main zone of ice accumulation between the range front and the main divide the mean annual precipitation is likely to be >6 m (The modern minimum is >4 m at the range front, while the maximum is as high as 12 m at high elevation. See Chapter 1 for climate station data). If initially 30% of the land surface is above 1000 metres then this area could accumulate over 3000 m of ice within 1 kyr. Naturally there would be a spill-over effect to adjacent areas at slightly lower elevations Accumulation of ice increases the surface elevation and increases the area with a surface elevation greater than 1000 m. Within as little as 2000 to 3000 years it would be possible for the accumulation of sufficient ice to fill all the major alpine valleys on the western side of the Southern Alps. The process would almost certainly accelerate as the glaciers expanded. So there is no particular reason to assume a major glaciation is either unlikely or not possible for the Southern Alps at 82-75 ka. It is notable in this connection that Sutherland et al (2007) found the extent of ice in the Cascade Valley in South Westland at 79.0 ± 3.9 ka was greater than that during the LGM.

Southern Alps ice accumulation has been modeled by Rother & Shulmeister (2006). They find that rapid conversion of precipitation from rainfall to snowfall drives massive ice accumulation at small thermal changes (1–4°C) sufficient to cause extensive glaciation and that such moderate cooling could be generated by changes in synoptic climatology, specifically through enhanced regional flow of moist westerly air masses.

This leads to an important question that has a bearing on the Quaternary stratigraphy of Westland. That is, why is there currently little hard evidence for a major glaciation in Westland during the MIS4 thermal minimum? The evidence from Antarctic ice cores confirms a major prolonged dust accumulation episode during MIS4 and surface temperatures that were as cold as those during MIS2. Indications from the work of Partridge et al (1996) and Kristen et al (2007) are that MIS4 was a period of relative aridity over much of southern Africa. The growth rate proposed for the Bt2 speleothem from Botuverá cave in Southern Brazil by Cruz et al (2007) was very low (slowest during the last 120 kyr) during the core portion of MIS4, potentially indicating relative aridity at that site.

Stuut et al (2004) concluded on the basis of mineralogy and grainsize at GeoB-3355 (27˚28'S, 71˚15'W), a marine core off the northern coast of Chile, that from c. 66 ka to 52 ka climate over the adjacent continental landmass was very arid. They found that climate during MIS2 from about 29 to 17 ka was very humid at that site and that the humidity during the period from c. 80-74 ka was substantially greater than during the coldest portion of MIS4.

Figure 4.18: Laser dust mass (ng/g) EPICA Dome Concodia ice core (75˚06'S, 123˚24'E) , Antarctica. Data from Lambert et al (2008)

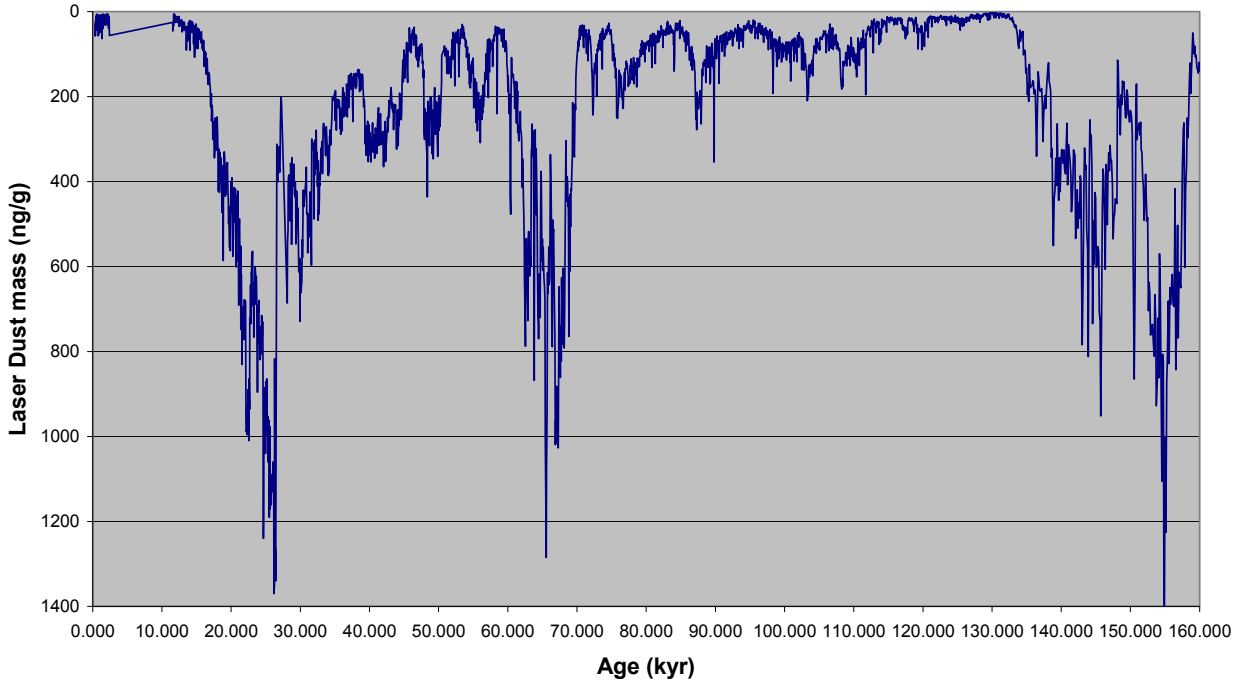

It is evident from the temperature records of a large number of marine cores examined during this study (tables 4.5 & 4.6) that the mean (Southern) Hemispheric sea surface temperature was probably no lower during MIS4 than it was during the middle portion of MIS3 or during MIS2. So why are the MIS3 and MIS5a dust spikes in the Antarctic ice cores rather subdued relative to that of MIS4? The solution may relate sea level and possibly humidity rather than temperature. MIS4 was a period of rapid ice-sheet growth in the Northern Hemisphere resulting in a drop in eustatic sea level. The

Argentine lowlands in the lee of the Andes mountain chain across the has been proposed as the dominant source of Antarctic ice core dust by Lambert et al (2008), Rothlisberger et al (2008) and Delmonte et al (2004). This Andes chain may have produced a strong rain-shadow effect during MIS4 (as it continues to do in the modern era). A substantial fall in sealevel dramatically expands the Argentine lowlands on the large area of shallow continental shelf to the east of southern Argentina. This increases the aerial extent of the dust sources, most notably during MIS2, MIS4, and MIS6 and result in increased dust deposition in Antarctic that might not be related directly to temperature in the middle to high latitudes of the Southern Hemisphere.

The preceding discussion indicates that one should not assume MIS4 produced glaciation in Westland with an extent comparable to MIS2, MIS3 or to the MIS5a/4 transition. It is notable that Sutherland et al (2007) did not produce any clear-cut MIS4 cosmogenic isotope ages from glacial erratic boulders in the Cascade Valley, whereas they did procure a number of MIS5a and MIS3 ages. The MIS3 ages were then "shoe-horned" into MIS2 and MIS4 with no genuine justification. This introduces a distinct possibility that glaciation in the Cascade Valley was more extensive than during MIS3 than during MIS4. It is interesting that there were episodes during MIS3 when the surface of the Southern Ocean was as-cold or colder than it was during MIS4 and that at those times the mid-latitudes of the Southern Hemisphere appear to have been more humid than during MIS4. Once again these circumstances favour more rapid ice accumulation in the Southern Alps during MIS3 than during MIS4.

In terms of understanding the stratigraphy, climate and vegetation history of Westland there is little value in assuming one can apply a 65°N orbital forcing (Northern Hemisphere ice volume) model in Westland without solid support from numerical dating of local deposits. The numerical of potential MIS3/4 deposits is discussed in detail in Chapter 6 of this thesis.

4.3 EUSTATIC SEALEVEL DURING MIS3

4.3.1 Global Sealevel

The global eustatic sea level history for MIS3 has long been a controversial subject. Early studies of oxygen isotope ratios in marine carbonate tended to imply that sea level was relatively low through the entire MIS4 to MIS2 period and that the world was gripped in a more or less unrelenting ice age. This view is not universal though. At the time of writing there is no general consensus with respect to the precise level attained during individual MIS3 eustatic sea level maxima. This is because a range of related issues concerning glacio-isostasy, uplift rates, $\delta^{18}O$ of the global ocean, oceanic temperature and global ice volume have yet to be fully resolved. There are numerous well dated examples of relatively high sea level and proxy sea level for the early to middle portion of MIS3 including:

The Calabrian Coast of Italy	Dumas et al (2005); Balescu et al (1997)
The Ionian Coast, Calabria, Italy	Santoro et al (2009)
Carnegie ridge (core V19-30)	Cutler et al (2003)
Global curve- $\delta^{18}O$ atmospheric oxygen	Shackleton (2000)
Temp-corrected marine $\delta^{18}O$ (proxy)	Waelbroeck et al (2002); Labeyrie et al (1987)
Crotone Peninsula, Italy	Mauz & Hassler (2000)
The Texas coast, Gulf of Mexico	Rodriguez et al (2000)
Northwestern Gulf of Mexico	Simms et al (2009)
U.S. Atlantic Shelf	Blackwelder et al (1979)

New Jersey margin, USA	Wright et al (2009)
Gulf of St Vincent, Australia	Cann et al (1988, 1993)
Gippsland Lakes, Australia	Bryant & Price (1997)
Strait of Gibraltar	Gracia et al (2008)
Persian Gulf	Uchupi et al (1999)
South Hokaido, Japan	Ota & Machida (1987)
Kikai Island, Japan	Sasaki et al (2004)
SE coast, South Korea	Choi et al (2003a, 2003b)
Red River delta, Vietnam	Hanebuth et al (2006)
Malakula, Vanuatu	Cabioch & Ayliffe (2001)
Point Dombo, Sthn Rote, Indonesia	Merritts et al (1998)
Ben Lomond, Santa Cruz, California	(Perg et al (2001)
Isla Vista terrace, California	Trecker et al (1998)
Huon Peninsula, PNG	Chappell (1978), Bloom et al (1974), Chappell (2002)
Red Sea region	Rohling et al (2008), Siddall et al (2008a, b)
Global Ocean	Jouzel et al 2002; Waelbroek et al 2002; Lea et al 2002
Sulu Sea, Philippines	Linsley 1996; Oppo et al 2003

4.3.2 Cause of MIS3 Sea Level Fluctuation

Relatively high MIS 3 sea level maxima are believed to have resulted from a combination of the long-distance isostatic effects of continental scale ice sheets and fluctuations in the global eustatic sea level as discussed by Chappell (2002). Interpretation of the eustatic sea level at the various coastal transects is dependent on assumptions regarding uplift rates. In the case of the exceptionally well preserved and well dated coral terrace sequence at the Huon Peninsula of Papua New Guinea preservation is due largely to a relatively rapid tectonic uplift rate. This sequence has been a key database for the development of models of Late Quaternary eustatic sea level fluctuation. Studies relevant to the dating and interpretation of the reefs, associated sea level fluctuations, and tectonic uplift include: Bloom et al (1974); Chappell (2002); Chappell et al (1996); Esat et al (1999); Esat & Yokoyama (2006, 2008); Lambeck et al (2002); McCulloch et al (1999) McCulloch & Esat (2000); Ota & Chappell (1996); Siddall et al (2008a,b); Rohling et al (2008); Stein et al (2003); Yokoyama et al (2000, 2001a, 2001b); Yokoyama & Esat (2004); Yoshida & Brumby (1999) and Zhu et al (1994).

The dating of Huon Peninsula corals shows that MIS3 sea level fluctuated repeatedly and rapidly. Chappell (2002) proposed that the more substantial rising trends in sea level occurred in-time with "massive ice breakout from North America". Further it was noted that the timing of rising sea level coincides with well-documented and well-dated widespread deposition of ice rafted detritus (IRD) in the North Atlantic Ocean. These IRD bearing layers, many of which have been defined as "Heinrich Events" have been dated in a multitude of independent studies, for instance Cacho et al (1999). Well dated correlative events have been identified in the isotopic record from Greenland ice cores and continental speleothems (see table 4.5). Heinrich events influence the atmospheric climate on a hemispheric scale. In the mid to high latitudes of the Northern Hemisphere atmospheric climate is relatively cold during Heinrich events, particularly over the Greenland icesheet as revealed in $\delta^{18}O_{(ice)}$ from a number of deep ice-cores in the summit region (see for instance Svensson et al 2008) . Rising sea level is not caused primarily by rapid melting of the surface or margins of the ice sheets. Cold atmospheric temperatures correlate with low rates of mass accumulation over the ice sheets (reduced precipitation) as demonstrated by the annual layer thickness at the North GRIP core site (Svensson et al 2008). Cold atmospheric temperatures in the Northern Hemisphere also correlate with accelerated and

synchronized ice discharge from the large outlet glaciers (Clark et al 2007) and reduced salinity of surface waters in the North Atlantic and Nordic Seas, increased permanent sea-ice cover, and a sharp reduction in the rate of formation of North Atlantic Deep Water (NADW) (see MacAyeal 1993). Klemen et al (2010) summarise the evidence for variability in the size of the Laurentide ice sheet during the last glacial period. They suggest that this ice sheet varied significantly in area and volume during MIS3 being reduced to "residual ice centres with uncertain margins" during interstadial conditions. The precise timing of these events is uncertain. Mechanisms for the self destruction of ice sheets are discussed by Hughes (2011).

Conversely during MIS3 falling eustatic sea level correlates with warm/interstadial conditions in the Northern Hemisphere (Sidall et al 2008). The initiation of each of the main periods of falling sea level occurs at the termination of a Heinrich event, coincident with reduced ice discharge rates from the main ice-sheets, a sharp decline in deposition of ice rafted detritus, increased surface salinity in the North Atlantic, reduced permanent sea-ice cover, and the resumption of NADW formation. These all correlate with changes in $\delta^{18}O_{(ice)}$ from the deep Greenland ice-cores and an immediate increase in mass accumulation rates on the main ice sheets due to sharply increased precipitation.

In addition to changes in ocean volume and grounded ice mass during glacial-interglacial cycles there are other effects on sea level. It can't be assumed that eustatic sea level changes are distributed evenly around the globe during these cycles. The global mass redistribution causes the Earth's rotational pole to wander, which has the effect of redistributing water in the oceans due to changes in centripetal acceleration, the effect being as much as 4 metres for some mid-latitude localities over a full glacial-interglacial cycle (Vermeersen & Sabadini 1999). In addition the Earth's crust and mantle are sufficiently inhomogeneous that there will be different coastal responses to the redistribution of ice and water loads. So it is likely that some far-field localities will demonstrate sea level changes that are greater than the global average.

For North Westland the situation is further complicated by the potential for regional isostatic effects from growth and shrinkage of glacial ice volume in the Southern Alps. These effects were discussed briefly by Mathews (1965) in relation to ice loading at the LGM. From Mathews figure 6 the estimated LGM isostatic depression at the modern coast adjacent to Mt Cook National Park is approximately 60 feet or 18 metres. This is significant in relation to other glacial events here in the Late Quaternary, for instance those leading to the deposition of the Loopline, Waimea 1 and Waimea 2 Formations. The extent of glaciation during these events was similar to that of the LGM. As with the LGM the isostatic impact on local sealevel is potentially similar in magnitude to millennial-scale eustatic sea level fluctuations during MIS4 and MIS3.

As demonstrated by Rohling et al (2008) and Clark et al (2007), during MIS4/3 the timing of eustatic sea-level maxima probably coincides with maximum warmth during Antarctic interstadials, while sea level minima to correspond with minimum warmth during Antarctic stadials. Rohling et al (2008) also illustrate rising level rising during Heinrich events reaching a maximum at the abrupt termination of each Heinrich event. In other words sealevel rise stops when the surge in the rate of ice discharge from the Northern Hemisphere ice sheets comes to an end. Ice accumulation, as measured for instance by layer thickness at the North GRIP ice core site in Greenland (Svensson et al 2008), is at a maximum during the early phase of each of the main interstadial phases during MIS3. This corresponds with falling eustatic sea level. Siddall et al (2008b) review the evidence for the timing and magnitude of MIS3 sealevel change. They suggest that Antarctic ice volume increases and decreases in time with that of the main northern hemisphere ice sheets implying that ice volume reduction in Antarctica during MIS3 corresponds to a warming climate and ice gain corresponds to a cooling climate. However,

Antarctic air temperature has minor relevance to this cycle. Siddall et al (2008) suggest there is a substantial contribution to MIS3 sea level fluctuation from the Antarctic ice sheet. If this is correct then this contribution to eustatic sealevel change is likely to be a passive response to sea level change forced by ice loss from North America and Eurasia during Heinrich events in the North Atlantic. Rising sea level changes the ice grounding line on the Antarctic continental shelf which has a direct effect on the stability of the ice sheet. This process, and its effect on Antarctic ice volume, has been modeled by Bye et al (2006) who found that ice loss due to increased ice calving exceeded the increased snow deposition due to increased atmospheric transport of moisture. There is also potential in Antarctica for glacio-isostatic effects to contribute to the local sea level and position of the ice-grounding line and this may have an impact on ice sheet stability as discussed by Nakada et al (2000). It is suggested here that rapid calving of formerly grounded ice during warming phases on the Antarctic continental shelf could lead to widespread deposition of ice-rafted-detritus deposition in the Southern Ocean during MIS3.

4.3.3 Magnitude of MIS3 Sea Level Fluctuation

One current estimate of the maximum level achieved during MIS3 is that of Simms et al (2009). They suggest a maximum eustatic high-stand of -42.8 ± 6 m. This is similar to the MIS3 eustatic level maximum of ~ -35 to -40 m estimated on the basis of oceanic bottom water temperature and benthic foraminiferal $\delta^{18}O$ by Waelbroeck et al (2002) and Labeyrie et al (1987) A similar estimate was made by Shackleton (2000) on the basis of the $\delta^{18}O$ of O_2 in ice core air bubbles. The MIS3 estimate by from Lea et al (2002) has a maximum at about -50 m based on temperature corrected foraminiferal $\delta^{18}O$. However, even at the relatively stable continental margin of South Australia, which is distant from the glacio-isostatic effects of continental ice sheets, the MIS3 sea level peaked at -22 to -29 m (Cann et al 1993). MIS3 sea level estimated from temperature corrected foraminiferal $\delta^{18}O$ in the Sulu Sea is also high (Linsley 1996, Oppo et al 2003) but possibly compounded by the effects of surface salinity variability. Similar salinity issues are discussed by Pahnke et al (2003) in relation to temperature corrected foraminiferal $\delta^{18}O$ at core MD97-2120; by Mashiota et al (1999) at cores E11-2 and RC11-120, and by Ijiri et al (2005) for core MD98-2195 in the East China Sea.

It was inferred by Chappell (2002) that the magnitude of MIS3 sea level fluctuations at the Huon Peninsula was from 10 m to 25 m. The highest eustatic sea level during the period 30 ka to 65 ka was estimated to be c. -45 metres, though this is sensitive to the estimated local tectonic uplift rate.

The magnitude of intra-MIS3 sea level fluctuations has been estimated at 15 to 35 metres by Esat & Yokoyama (2006) and Chappell (2002) based on dating of uplifted coral at the Huon Peninsula. The duration from minimum to maximum is as short as 2 to 3 thousand years. As noted in 4.3.2 above the main MIS3 eustatic sea-level high-stands each reach their maximum level at the completion of a "Heinrich Event". These events involved massive discharge of ice and meltwater from the Laurentide icesheet. The initial change in sealevel impacts on the ice-grounding line on continental shelves around the Fennoscandian and Antarctic icesheets, potentially initiating discharges of a similar magnitude from these icesheets and a cycle of positive feedback. This may be important in the context of North Westland. If the timing of climatic events here corresponds with that in Antarctica then brief but warm interstadial episodes could coincide almost exactly with the peak eustatic sealevel during millennial scale events.

Interstadial sea level fluctuations of this scale could leave an imprint in the Quaternary stratigraphy of North Westland. Preservation on-land simply requires tectonic uplift at a rate that prevents complete destruction of unconsolidated deposits by subsequent sea level maxima. On the basis of the

luminescence dating carried out for this PhD project the early MIS3 sea level maxima for North Westland is estimate to be in the -20 to -35 m range. This is within 10 metres of a number of estimates for global eustatic sea level.

4.3.4 Timing of MIS3 Sea Level Fluctuation

The primary rise in sea level of c. 60 m following MIS4 occurred at ~62-57 ka (Siddall et al 2008b) and there were at least 4 sea level maxima during MIS3. At present there is no uniform consensus with regard to the precise timing of eustatic sea level maxima during the MIS5a to MIS3 period. Potential sea level maxima revealed by fluctuations in benthic foraminiferal $\delta^{18}O$ in the marine core stack by Lisieke & Raymo (2005) occur at 38 ka, 45 ka, 52 ka, 55 ka, 64 ka, 68 ka, 72 ka, 75 ka, and 82 ka. Arz et al (2007) suggest eustatic peaks occurred at 37-38 ka, 43 ka, 45-46 ka, 51 ka, 55-58 ka, 62 ka and 65 ka based on benthic $\delta^{18}O$ from the northern part of the Red Sea. At the Huon Peninsula Chappell (2002) identified eustatic sea level maxima at approximately 33 ka, 38 ka, 44.5 ka, 48 ka, 52 ka, and 58-60 ka. Lea et al 2002 proposed a eustatic sea level curve derived from temperature detrended $\delta^{18}O$ (marine core TR163-19) from foraminiferal calcite. They proposed MIS3 sealevel maxima at approximately 32 ka, 40 ka, 45 ka and 55ka. Based on "Dole-effect corrected" $\delta^{18}O$ of atmospheric O_2 in air bubbles trapped in the Vostok ice core Jouzel et al (2002) proposed that MIS3 eustatic sea level maxima occurred at approximately 40 ka, 53 ka and 61 ka. Rohling et al (2008) proposed eustatic MIS3 sealevel peaks at approximately 38-40 ka, 42.5 ka (minor), 44 ka (minor), 46-47 ka, 50-55 ka, and 57-61 ka in the Red Sea. Much of the modern literature on MIS3 sealevel is summarised by Siddall et al (2008b). They discuss evidence for at least 4 separate sea level maxima during MIS3 with peak to trough amplitude of 20 to 40 metres.

The timing of sea level maxima and minima as revealed by radiometric dating of corals at the Huon Peninsula is supported by studies from the Red Sea by Rohling et al (2008) and Siddall et al (2008a). Much of the recent literature on MIS3 sea level is summarised by Siddall et al (2008b). Siddall et al (2008b) propose that there was a similar contribution to these eustatic events from Northern and Southern Hemisphere (Antarctic) sources.

Sasaki et al (2004) integrate dating work on coral terraces from Kikai Island, Japan and the event timing from the Huon Peninsula. They record three hemicycles from transgression to highstand at ~66, ~62, and ~52 ka associated with the drowning of the reefs. From the Calabrian Coast of Italy Dumas et al (2005) report substantial sea-level rise events at 72 ka and 58 ka.

At present it may be premature to infer a unified global eustatic sea level curve from these various studies. The significant observation is that sea level variation occurred during MIS3, that these events are preserved in the geological record at multiple localities, and that the peak levels were relatively high at some localities.

In this context Carter et al (2002) report on the deposition of ice rafted detritus (IRD) on the Campbell Plateau in the Southwest Pacific Ocean. There were significant IRD events at c.54-53 ka, 51-49 ka, 41 ka, and 36 ka. These may relate to sea level maxima causing the break-up of grounded ice shelves around Antarctica, rather than by glacial advance during cold climate events. This is the interpretation made for a similar IRD record from the Southern South Atlantic Ocean by Kanfoush et al (2000) who suggested sea level rise during MIS3 and MIS4 may have resulted in periodic destabilization of grounded ice sheets in the Weddell Sea region of West Antarctica. The timing of these IRD events is noted in table 4.7 above. Note that Chappell (2002) also suggests MIS 3 sea level change may have triggered ice break-outs from Antarctica.

A number of estimates regarding the timing of various sea level maxima are listed in table 4.12 which can be compared with the timing of Antarctic climatic events displayed in figure 4.19.

Table 4.12 Timing of sea level maxima during the last glacial period. Ages are in kyr BP.

Antarctic ice-core Interstadial Events (kyr BP)	Benthic $\delta^{18}O$ minima Lisieke & Raymo (2005)	Sea level maxima from benthic $\delta^{18}O$ by Arz et al (2007)	Sea level maxima from coral reefs by Chappell (2002)	Sea level maxima from $\delta^{18}O$, Red Sea. Rohling et al (2008)	Southern Atlantic IRD Events, Kanfoush et al (2000)	Planktonic $\delta^{18}O$, SO136-GC3 Barrows et al (2007)	Benthic $\delta^{18}O$ minima MD97-2120 Barrows et al (2007)
			33		30-32		
37.5-39.5 (A1)	38	37-38	37-38	37-39	36-38	34-40	34-40
42-43		43		42-42.5	40.5-44		
45-47 (A2)	45	45-46	44-45	44, 46-47		44-46	45-47
			48				
51.5-54 (A3)	52	51	51-53	51-54	51-52	50-54	50-54
	55	55-58					
57-61 (A4)		62	60	57-61	55-59	57-60	57-60
	64	65				63-64	64-66
68-70.5 (A5)	68					69-70	
72-74 (A6)	72, 75		72				72-74
79-86 (A7)	82					76-84	80-84

Figure 4.19 Source for the timing of Antarctic events listed in the first column of table 4.10. This figure is in turn derived from Ahn & Brook (2008)

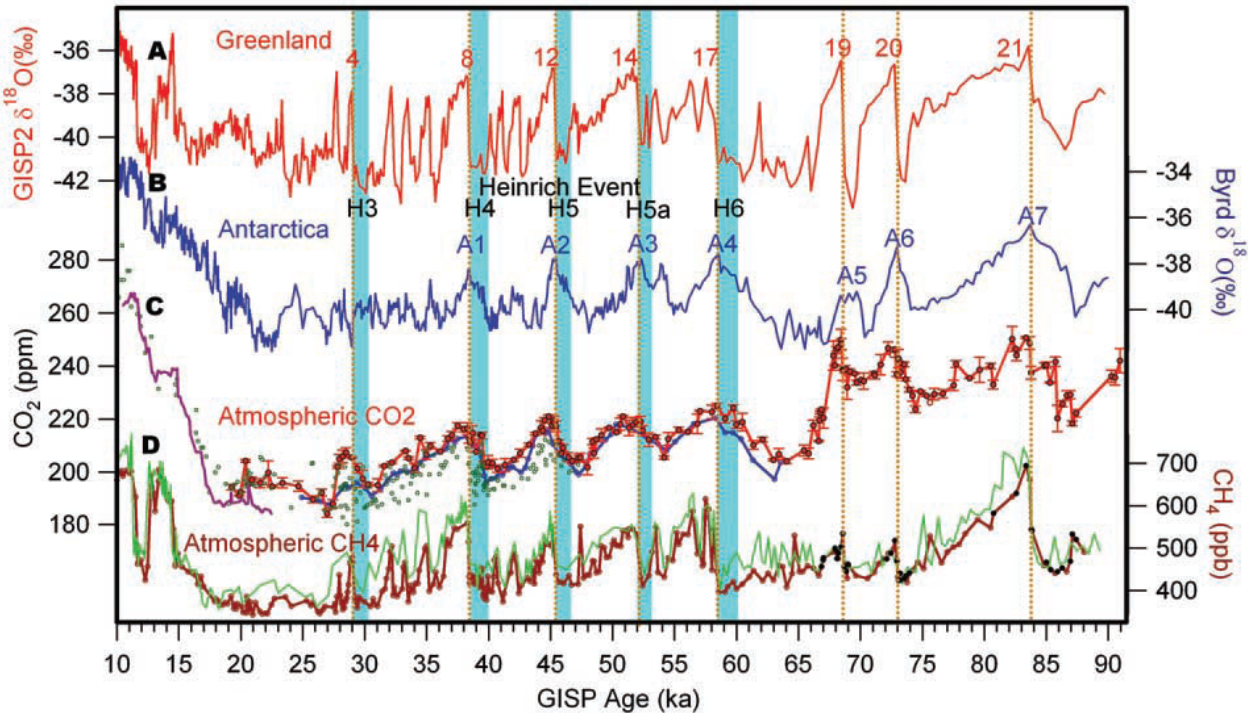

4.3.5 MIS3 Sealevel in New Zealand

How likely is it that an MIS3 sea-level high-stand would leave an imprint in the on-land sedimentary record of North Westland? This depends to a large extent on the tectonic uplift rate, the calculation of which depends on the age assigned to the marine various strandlines, raising the possibility of a circular argument with regard to palaeo sea level. With respect to this PhD project it is significant that several localities in NZ appear to provide evidence for anomalously high MIS3 sea level maxima which may act as precedents for similar events in North Westland. These include:

Wanganui Coast, North Island, NZ (Pillans 1990b)
Mahia Peninsula, North Island, NZ (Berryman 1993)
Kaikoura, South Island, NZ (Ota et al 1996)

The key feature that these three areas share is a relatively rapid uplift rate. Confirmation of one or more MIS3 strandlines in North Westland requires that the available numerical dating is compatible with that interpretation and that climatic information, for instance as revealed by pollen and beetle remains in overlying soils, can be reconciled with an MIS3 correlation. Other evidence that needs to be accounted for includes long continuous climate records from nearby areas, for instance the vegetation history from Okarito Bog in South Westland. The conclusions of Vandergoes et al (2005) and Newnham et al (2007b) in relation to the Okarito pollen profile tends to contradict the new interpretation of the regional climate history presented in this thesis. In fact the palynology and numerical dating from the Okarito Bog are discussed in detail in Chapter 5. In the form presented by Vandergoes e al (2005) it is the only long continuous paleoecological record from the region. In the interpretation presented here it may be matched by the paleoecological record from Schulz Creek by Moar et al (2008). The age-depth model for the Okarito record of Vandergoes et al (2005) is challenged in Chapter 5. The age-depth model for the Schulz Creek record of Moar et al (2008) is challenged in Chapter 6.

If the relatively brief MIS3/4 sea level maxima coincide with Antarctic warm events and local (North Westland) interstadial events then they may also coincide with glacial minima in the Southern Alps. Soil might not begin to deposit on the marine strandline sediment until the commencement of seaward migration of the coastline as sea level falls. In that case the soil that initially accumulates on the exposed marine deposits may reflect a rapidly cooling climate rather than the climate that existed during the sea level maxima. So the base of the soil that collects on an MIS3 raised marine terrace might correlate with the following stadial event. In that case the base of the soil will contain a relatively cold-climate pollen assemblage. A sequence of events of this nature is recorded on the Rutherglen Formation at Candle Light (pollen zone CL1, profiles 74/19/1 & 74/19/2, fig 4a, Moar & Suggate (1996)).

CHAPTER FIVE: NUMERCIAL DATING OF NORTH WESTLAND QUATERNARY SEDIMENTS USING OPTICAL AND INFRARED STIMULATED LUMINSCENCE FROM QUARTZ AND K-FELDSPAR

5.1 POTENTIAL ISSUES IN THE USE OF OSL AND IRSL DATING IN NORTH WESTLAND

In the North Westland context the primary advantage of luminescence dating over other dating methods is its ability date the deposition of aeolian, fluvial and marine silt directly. During deposition the luminescence 'clock' is reset if quartz or feldspar mineral grains are fully exposed to daylight. The sample ages produced can be used to date the deposition of the sampled material or place constraints on the age of underlying and/or overlying materials.

There are a number of issues that could potentially confound the interpretation of infrared stimulated luminescence (IRSL) and optically stimulated luminescence (OSL) ages derived from sediments in North Westland. These relate to "anomalous fading" (leading to age underestimates) and to "incomplete bleaching" (leading to age overestimates). As fading tests have shown, anomalous fading does not appear to have a significant influence on sample ages here. However, partial bleaching does impact on sample ages, particularly at sites where sediment deposition has been rapid or where conditions have limited direct exposure to daylight. In the following discussion several groups of samples will be discussed in order to show the potential impact of partial bleaching on the derived numerical ages. The geology and general context of these sites will be discussed in more detail in Chapter Six.

5.2 ANOMALOUS FADING

Certain feldspar varieties in some regions can show anomalous fading of the IRSL signal, such that the age of samples is underestimated. Laboratory tests are routinely applied to determine the potential severity of this effect. According to Preusser et al (2005) the issue tends to affect the luminescence signal only over part of the emissions wavelength range, most particularly the ultraviolet portion of it

The instability of the UV emission, and its likely connection to the phenomenon called anomalous fading, was proven independently by two spectrometry groups back in the 90s, being Krbetschek et al (1996) and Clark et al (1997). It should be noted that Dr Uwe Rieser, who conducted the IRSL dating for this project was a co-author in the former of these two studies.

Preusser et al (2005) tested samples from North Westland by 12 hour sample storage after which no fading was detected. At Raupo and Kamaka it proved possible to replicate the ages of ^{14}C dated horizons in the 20 to 28 ka year age range using IRSL. Similarly Vandergoes et al (2005) were able to replicate of ^{14}C dated silt horizons from Okarito in South Westland using IRSL dating indicating that anomalous fading was unimportant. In relation to the Okarito Pakihi Newnham et al (2007b) state:

> *"Although optical dating of feldspar from some regions seems to systematically **underestimate** the known age of a sample due to fading of the luminescence signal, previous experience with luminescence dating in Westland indicated that feldspars from there apparently were not affected by this phenomenon (Almond et al.,*

> *2001; Hormes et al., 2003; Preusser et al., 2005). General agreement with the radiocarbon chronology at this site (*Okarito*), and with the age for Kawakawa Tephra (Fig. 2), also gives confidence in the chronology derived from luminescence dating."*

All samples within this PhD project (RR) were routinely tested for anomalous fading by storing some sample aliquots for six months after irradiation. None of the samples showed signs of anomalous fading, using a 5% threshold criterion to test for signal loss.

5.3 OSL DATING OF QUARTZ IN NORTH WESTLAND

Quartz recovered from the mainly sandy samples taken during the first sampling campaign for this PhD project was not suitable for OSL dating. Due to the likelihood of erroneous results, and severe scatter, Dr Rieser was not prepared to calculate ages from the data produced during attempted dating of quartz. Numerous samples were affected. The reasons for this are not entirely clear but are likely similar to some of the issues discussed by Preusser et al (2006). Subsequent to the collection of samples for this project Preusser et al (2006) published a commentary on the luminescence dating of quartz sand from Westland. They found that quartz from this region is unsuitable for luminescence dating and reported that it suffers from 3 problems:

1. The majority of grains have extremely low OSL intensity. Few are bright and most of the signal comes from low-intensity grains.
2. The quartz is affected by thermal transfer and this has an effect on equivalent dose determination.
3. The samples showed poor performance in the SAR protocol by generally failing to give an accurate equivalent dose with poor sensitivity correction as well.

In addition Preusser et al (2006) speculated that the quartz grains appeared to have had a short sedimentary history resulting in a lack of repeated irradiation/bleaching cycles. This contributes to a paucity of defects/traps, many of which are created by repeated natural cycles of irradiation and readout. There is little doubt that they are correct in relation to the relatively short sedimentary history of sand grains in the deposits in question.

Given the difficulty experienced with dating quartz from sand samples in the first sampling campaign, for this PhD project, clean sand was avoided in the second round of sampling. On the recommendation of Dr Uwe Rieser gravel deposits were not sampled as they tend to be dominated by first depositional cycle materials. In addition the presence of large clasts, particularly of granite, can create a variable internal doserate within the sediment. In the second sampling campaign soil/silt horizons were targeted exclusively. Ages were obtained by $IRSL_{(blue)}$ dating on K-feldspar. This has resulted in a suite of ages that generally place limits on the commencement or completion of deposition, but which might not directly define the timing of deposition of either the underlying or overlying marine sand or alluvial/glacial gravel.

After briefly discussing the heavy-liquid separation of quartz and feldspar Preusser et al (2005) make the following statement in relation to luminescence dating of quartz in North Westland:

> "However, according to our experience, quartz from North Westland is not very suitable for luminescence dating. It is usually very dim and shows large changes in sensitivity during

measurements. Ages for sand sized grains reported here were all determined using K-rich feldspar separates."

This statement nicely anticipates similar more detailed findings from Preusser et al (2006) referred to above. But if quartz sand is unsuitable for luminescence dating then it is likely that quartz in the silt size-range will also be unsuitable. The quartz in the silt fraction of a sampled fluvial deposit is likely to be of a similar age to the sand from that environment, with similar natural radioactivity, chemistry, mineral lattice structure and density of potential luminescence traps. It will also have a similar provenance to the quartz sand rejected as unsuitable by Preusser et al (2006). So one might anticipate that any ages derived from quartz luminescence would be announced as such, given that non-specialists might be interested in the results.

After the above statement from Preusser et al (2005) the word quartz barely appears (just once) in the remainder of the paper. However, they dated numerous samples of quartz in polymineral finegrained material, 14 samples by $OSL_{(UV)}$ and an additional 17 by $_{Post\text{-}IR}OSL$. These are part of the overall database used in the assessing the age of materials at a number of sites. For instance at the combined Phelps Mine and Pine Creek locality 23 ages are used in the age model, 12 IRSL ages on feldspar and 11 OSL ages on quartz. Three additional quartz results were not used in the age model here due to partial bleaching. With regard to thermoluminescence (TL) ages a total of 13 $TL_{(blue)}$ and $TL_{(UV)}$ ages from this locality are not used by Pruesser et al (2005) because these ages are rather erratic, several as a clear result of partial bleaching. Although they warn against the use of optical luminescence dating on North Westland quartz, at this locality they use many of the quartz ages regardless. In addition they prefer 2 quartz (Post-IR OSL) ages over 2 feldspar ($IRSL_{(UV)}$) ages at Upper Chesterfield road.

- In discussion with Uwe Rieser regarding dating in North Westland he had several relevant suggestions. First when conducting optical dating, even though $IRSL_{(UV)}$ measurements might be taken, the ages should not be used, as they are likely underestimates (see below). $OSL_{(UV)}$ and Post-IR OSL on feldspar bearing fractions both are very likely to date the feldspars, not quartz. As Preusser et al (2006) have shown quartz from North Westland is very dim, so OSL can easily be dominated by the brighter feldspars and because of the UV filter still have underestimation problems.

Quite apart from the dimness and poor SAR performance issues identified by Preusser et al (2006) in respect of Westland Quartz, there are additional issues with $_{Post\text{-}IR}OSL$ and $OSL_{(UV)}$ performed on $IRSL_{(blue)}$ samples. The method of Banerjee et al (2001) was applied to polymineral finegrain samples containing both quartz and feldspar. In stimulating the sample to obtain luminescence from quartz, luminescence is also stimulated by K-feldspars at wavelengths similar to that of quartz (Mauz & Lang 2004). This OSL is concentrated in the blue portion of the spectrum. Cross-contamination is difficult to avoid unless the feldspar is removed entirely.

The writer has a number of concerns about dating carried out by luminescence methods in North Westland. Specific localities where these concerns apply are discussed below and in Chapter Six.

5.4 $IRSL_{(UV)}$ DATING OF K-FELDSPAR

Feldspars are the only minerals commonly dated by IRSL. In personal communication with Dr Uwe Rieser from the luminescence dating laboratory at Victoria University of Wellington he has indicated that the $IRSL_{(UV)}$ dating of K-feldspar is problematic. The Hoya filters that are generally used for dating quartz in polymineral fine-grained materials are also used in the $IRSL_{(UV)}$ dating of K-feldspar from the same samples. Unfortunately this filter is wide enough to pass 290 nm emissions which impact on readings from K-feldspar. Dr Rieser expressed the opinion that $IRSL_{UV}$ ages derived from K-feldspar are likely to be underestimated as shown by Krbetschek et al (1996) and Clarke & Rendell (1997).

Preusser et al (2005) report a number of $IRSL_{(UV)}$ ages from North Westland, including 7 from the Phelps gold mine, all of which are used in the age model for this site. Five of these samples are from a grey coloured relatively inorganic silt bed that Preusser et al (2005) claim to be an "overbank deposit". This is a reasonable suggestion given that the silt is sandwiched between two aggradational fluvioglacial gravel units, each more than 7 m thick. But if this material is fluvial silt, rather than loess, then it may have been deposited quite quickly. The unit is known to have minimal pollen content (pers com RP Suggate, results not published).

Geomorphological mapping carried out for this project indicates the site is located only 2 km from the nearest moraine associated with the overlying outwash gravel. See figure 6.6a for this portion of the map (Map 2). The silt is therefore quite likely to have been deposited in an ice-proximal fluvioglacial setting. The average gradient on the upper surface is approximately 16 m/km. This is quite steep (common in proximal fluvioglacial settings) and provides the potential for very rapid delivery of fine sediment in highly turbid flows. Flow velocities in the vicinity of 5 km/hour can be expected in such an environment which could mean delivery of silt from a glacial source in 30 minutes or less. The potential for zero to partial IRSL bleaching during deposition of K-feldspar is discussed below in relation to the Nelson Creek Farm Settlement gravel quarry, and in relation to silt deposits at Kamaka and the Phelps goldmine. Given that sediment of silt size can is carried quickly as suspended rather than bedload in a meltwater river, the issue could be as severe at the Phelps Mine as at the Nelson Creek quarry. This situation could also impact on the bleaching of quartz. The samples dated by $IRSL_{(UV)}$ at the Phelps Mine were also dated by $_{post\text{-}IR}$OSL. Two of the OSL ages (PGM5 & PGM7) were rejected by Preusser et al (2005) on the basis of partial bleaching. Another (PGM8) has $IRSL_{(UV)}$ and $_{post\text{-}IR}$OSL ages that do not overlap at 1δ, the quartz age being older by 22 kyr, and approaching the upper age considered acceptable for this site by Preusser et al (2005). Field and experimental evidence indicates that quartz bleaches more quickly than feldspar (Klasen et al 2007, Rendell et al 1994). Given the potential issues with partial bleaching and with dating methodology these observations do not bode well for the feldspar $IRSL_{(UV)}$ ages at the sites considered below.

5.5 PARTIAL BLEACHING OF IRSL AND OSL DURING SEDIMENT DEPOSITION

There has been a substantial amount of investigation carried out on IRSL dating of K-feldspar worldwide. The method has been most successful on relatively fine-grained (sand and silt) derived from texturally mature sediments that have been well bleached during and/or immediately before deposition. But for coarse grained fluvial deposits, proximal fluvioglacial outwash gravels, glacial till, and ice proximal lacustrine deposits IRSL dating routinely gives results that are difficult to interpret. One of the problems faced in dating fluvial and glacial deposits by IRSL is the tendency for rapid sediment transport and rapid rates of deposition. This can result in incomplete bleaching of quartz and K-feldspar, an issue that is discussed in detail by Wallinga (2002), Fuchs & Owen (2008) and Lukas et al (2007). Relevant studies of Quaternary fluvial and fluvioglacial deposits where luminescence dating on K-feldspar has proved to be problematic include Alexanderson et al (2008), Berger et al (2010), Clarke (1996), Clarke et al (1999), Ditlefsen (1992), Duller (1994, 2006), Fuchs et al (2005), Fuchs et al (2007), Forman & Ennis (1992), Forman (2009), Houmark-Nielsen (2008), Hutt & Junger (1992), Lamothe (1996), Lamothe & Auclair (1997), Lang (1994), Rhodes & Pownall (1994), Bonnet et al (2009), Spencer & Owen (2004), and Stokes et al (2001). Incomplete bleaching has been shown in natural modern fluvial and proximal glacial settings (Rieser et al 2010, Gemmell 1999). In laboratory experiments (Rendell et al 1994, Ditlefsen 1992, Gemmell 1988) it has been shown that the TL and IRSL signals from K-feldspar can be poorly bleached in turbid water under full daylight conditions.

Conditions adverse to natural bleaching of K-feldspar derived from proximal glacial environments centre on exposure to light. Under some conditions the expectation that bleaching should occur at all may be unwarranted. Modern meltwater in a proximal glacial environment within 2 km of the Triolet and Pre de Bar Glaciers (Italian Alps) is described by Gemmell (1999) and provides a striking example. Here the diurnal cycle in natural D_e from suspended silt was measured. D_e values were generally less than 20 Gy during daylight but averaged around 100 to 120 Gy during the hours of darkness. Gemmell concluded:

> *"Treating individual samples as aliquots of a single sample of suspended sediment has shown that two types of sediment bleaching are represented in a 24 h period: a) a mixture of fully zeroed and partially zeroed sediment during the day; and (b) unzeroed sediment at night. If the samples collected in this study are typical of glacifluvial materials, then when the unzeroed "night" samples are mixed in with "daylight" material a sediment with complex luminescence characteristics is produced."*

The samples were collected during June 1996 (Northern Hemisphere summer). The measured dose vs time graphic shows abrupt changes. It would be interesting to see such a study extended to cover seasonal variation as the issue is likely to be more severe when there are fewer daylight hours and when direct sunlight has a lower angle on incidence promoting greater surface reflection. Dose rates were not described. In a North Westland context doses of 100 to 120 Gy would potentially imply an inherited age of 25 to 60 ka at typical dose rates of 2 to 4 Gy/ka for the part of the sediment deposited at night. That is as long as the deposited sediment is not re-exposed before long-term concealment.

The Rangitikei River is both a modern and post-LGM example from a non-glacial region where age overestimation has been clearly demonstrated. This is described by Rieser et al (2009). Samples of river sediment deposited in 1984 during flood conditions returned OSL ages of 37.4±3.1 and 55.1±3.5 ka. Post-LGM river terraces at elevations of 20 and 30 m yielded sample ages of 106±7.6 and

104.4±7.7 ka. Rieser et al (2009) suggest that the age given by any particular sample depends on the proportion of mixing between bleached and non-bleached grains.

In a study remnant D_e in newly deposited silt from a major flood on the Elbe and Rote Weißeritz Rivers in Saxony, Germany, Fuchs et al (2005) determined that both feldspar and quartz suffered from partial bleaching. Feldspar returned remnant D_e of up to 16 Gy, equivalent to an age of several thousand years. Hu et al (2010) studied remnant D_e in modern silt and fine sand from the extremely turbid middle reaches of the Yellow River in China. They found a wide range of values for D_e for multigrain aliquots and single grains of quartz. Multigrain aliquots commonly returned D_e of zero to 15 Gy. Vandenberghe et al (2007) also found significant remnant D_e in flood deposits in Belgium.

Review of the relevant literature indicates that there should be no expectation of thorough zeroing of IRSL, OSL, or TL for fluvial sediment deposited in ice proximal environments, particularly where deposition occurs in turbid meltwater. The problem is difficult to detect and difficult to overcome. Duller (2006) has suggested that the best approach might be to date large numbers of single grains from each sample and use statistical methods to extract the most likely depositional age. Duller suggests that even very small aliquots of less than ten grains are insufficiently precise to provide excellent ages where partial bleaching has occurred. In this context it is notable that unpublished quartz single grain dating on Holocene Rangitikei sediments mentioned above was a complete failure as the quartz was unsuitable (pers. com. U Rieser).

5.6 IRSL DATING OF SAND AND SILT SIZED K-FELDSPAR IN NORTH WESTLAND

As well as known issues with luminescence dating of sedimentary quartz grains in Westland there are other general matters that need to be addressed. One of the main methods applied in this region by Preusser et al (2005) was single aliquot regenerative (SAR) $IRSL_{(blue)}$ dating on the sand fraction of fluvioglacial gravel, marine strandline deposits, and fluvial silt. This dating was carried out primarily on the K-feldspar component of the sand and silt. With respect to the fluvial deposits a number of samples were taken from sandy horizons situated in coarse gravel deposits dominated by pebbles, cobbles and boulders. The gravel deposits each represent an extremely high energy depositional environment. Sample locations include:

- The Upper Chesterfield Road gravel quarry (sample UCS1),
- The Stafford Loop Road gravel quarry (sample LOL1),
- The Raupo gravel quarry (samples RUG1, RUG2, RUG3),
- The Hokitika gravel quarry (samples BSG1, BSG2, BSG3),
- The Nelson Creek Farm Settlement gravel quarry (samples NCL1, NCL2),
- A roadside exposure adjacent to State Highway 7 at Kamaka (samples KMK5b, KMK8b),
- Sunday Creek near Chesterfield (sandy marine gravel).
- The Phelps mine where two main silt beds sampled by Preusser et al (2005) were described as a fluvial "overbank" deposit and an estuarine deposit.

Several of these localities are proximal to substantial terminal moraines. At four of these sites (Nelson Creek, Hokitika, and Chesterfield Road and the Phelps Mine) the overlying loessic beds were sampled. This material was dated by $IRSL_{(blue)}$ and OSL on polymineral finegrains. In two cases the ages, at face value, indicate either a very long depositional hiatus at the base of the silt (about 65 kyr at Hokitika and about 90-100 kyr at Nelson Creek), or an erosional episode. At Chesterfield road the loess ages, at face

value, may indicate greater continuity of deposition. These localities are discussed below and in chapter six.

5.6.1 Nelson Creek Farm Settlement gravel quarry

The Nelson Creek Farm Settlement Gravel Quarry has been dated by Preusser et al (2005). The site is discussed here in terms of the potential for partial bleaching of IRSL during deposition and therefore possible age overestimation. The Quarry is situated at the northern tip of an extensive fluvioglacial outwash terrace. The terrace gravel has been assumed to be Loopline Formation. This formation here consists of fluvioglacial outwash under a thin loessic soil. As shown in figure 5.1 the Nelson Creek Quarry is less than 1.5 km down the depositional gradient or meltwater flow-path from the relevant terminal moraine. Sand in the gravel deposit has been transported under the following general conditions:

- A very high surface gradient. This is about 15 m/km across the intervening ground between the moraine and the quarry.
- High meltwater flow velocities which could have been in the 5 to 10 km/hr range during high-flow conditions. Rapid flow is indicated by the coarse grainsize (boulders and cobbles) exposed throughout the quarry and elsewhere on the outwash terrace. The stratified gravel is relatively free from silt and clay so substantial sorting occurred during its deposition.
- The deposit is clearly constructional and is likely to have been deposited quickly.
- The bouldery nature of the sediment is such that one could expect new sand and silt grains to be created and released by grinding due to stone on stone impacts during high-flow conditions.
- Water discharging from the ice could comfortably have reached the quarry within a travel time of about 8 to 15 minutes. This is particularly the case under high-flow (flood) conditions due to rapid melting when relatively warm rain has fallen on extensive (many 10's of km^2) glacial ice. Rainfall events of several hundred mm/day are not uncommon in this area today. Nearby rain gauges at Rotomanu, Inchbonnie, Grey/Robinson Rivers, Taipo River (State Highway bridge) and the Arnold Power Station (table 1.1b) have measured annual average total precipitation of 3357, 4768, 2755, 4834 and 3070 mm respectively. These stations are at similar elevations to the quarry site. Modern precipitation is as high or higher in the adjacent mountainous areas. The first 3 sites listed were formerly under the glacier feeding meltwater to the Nelson Creek quarry site.
- Given the high turbidity of modern meltwater flow off the Franz Josef and Fox glaciers (South Westland) it is inevitable that under high flow conditions meltwater reaching the quarry site would also have been rather turbid and therefore close to impenetrable by daylight in depths of more than a few centimetres.
- During depositional events at the quarry water depths of at least several 10's of cm would be required to roll the cobbles and boulders into position.
- Sand transport from the glacial terminus to the quarry is likely to have taken place mainly by saltation along the sediment-water interface in a position shielded from daylight by moderate to extreme turbidity.
- Transport times for individual grains would vary greatly, some arriving in a single flood event, and some being remobilized by scouring in fluvial channels on multiple occasions. But the scouring would occur in turbid conditions. At least a portion of the sand could be delivered within about ½ to several hours of release from the glacier.
- According to Zhang (2001) different weather conditions during fluvial transport and deposition can affect the degree of bleaching in grains of feldspar. Rendell et al (1994) demonstrated that

under some clear-water conditions the rate of IRSL bleaching of feldspar in daylight is slower than the rate of OSL bleaching for quartz. Experiments discussed by Klasen et al (2007) also indicate that quartz bleaches more quickly than feldspar.

Many of these points also apply to the fluvioglacial sites sampled by Preusser et al (2005) at Upper Chesterfield Road (about 5 km from the position of the glacial terminus and a surface gradient of about 10 m/km), the Stafford Loop Road Quarry (about 1 km from the ice margin and a surface gradient of ~ 20 m km), and the Hokitika Gravel Quarry (a maximum of 2.5 km from the ice margin).

For the Hokitika quarry site Preusser et al (2005) suggest sand from the fluvial gravel, dated by $IRSL_{(blue)}$, was fully bleached at deposition because:

- The three sample ages are similar (BSG1 = 82±8, BSG2 = 85±6 , BSG3 = 88±8 ka).
- Individual small aliquots from each of the samples do not have a skewed distribution of equivalent doses.
- All other samples from similar sedimentary settings in North Westland appear to be completely bleached prior to deposition.

The complete bleaching of "all other samples" from Preusser et al (2005) is not entirely correct. Preusser et al (2005) demonstrate wildly inaccurate TL ages on several of the silt samples from the Phelps Gold Mine. Several of the quartz OSL ages from this locality are doubtful and are not used in age modeling by Preusser et al (2005). As discussed below they also demonstrate that 3 samples from a 60 cm thick distal fluvial silt bed at Kamaka dated by $IRSL_{(blue)}$, (polymineral finegrains) suffered from partial bleaching giving ages up to double the ^{14}C age of Denton et al (1999). One sample (RR21) taken by the writer from the same locality is also likely to suffer from incomplete bleaching.

All seven $TL_{(blue)}$ ages on silt from the Phelps goldmine were rejected on the basis of insufficient bleaching [TL as a method is not normally suitable for fluvial deposits, as TL signals bleach much more slowly compared with IRSL and OSL, i.e. over hours rather than minutes- per com Uwe Rieser]. In addition 2 post IR-OSL ages from this locality were rejected based on potential partial bleaching. Three of these samples had the $IRSL_{(blue)}$ age removed from consideration for the age model here due to potential bleaching issues. At least two more samples from the Phelps goldmine are borderline under the same criteria.

With regard to the gravel deposit at Nelson Creek quarry there are additional problems. In terms of the extent of bleaching by visible light it can safely be assumed that a significant proportion of the meltwater was released from subglacial flow paths. Inevitably a substantial portion of the contained sediment will have been released by melting from within and under the ice during low to zero light conditions and/or from beneath a debris mantle situated on the ice.

The outwash delivered to the Nelson Creek quarry is composed of sediment from a number of likely sources. These include Late Tertiary siltstones, sandstones and conglomerates, low-rank metagreywacke (Torlesse Supergroup, Rakaia Terrane), biotite to garnet grade quartzofeldspathic schist, Cretaceaous granites, and redeposited Late Quaternary fluvioglacial deposits. Each source will provide sediment containing significant remnant D_e that was still present at the time of release from the glacial ice near to the terminal moraine. Quartz taken from 13 samples of in-situ metagreywacke/schist in the Whataroa Valley by Herman et al (2010) yielded mean OSL D_e and age of 251 Gy and 81.6 ± 13.5 ka respectively. This is effectively the mean cooling age for the samples at a closure temperature

of 30 to 35°C. If the K-feldspar component of these rocks exhibits a similar behaviour then this mineral will also contain a variety of relict cooling ages from schist and granite sources in the glacial catchment. It should be noted that uplift rates are thought to be slower in the Southern Alps within the catchments of the glaciers contributing to the Moana ice lobe than is the case in the Whataroa Valley. So one might expect average cooling ages in the Southern Alps near Moana to be greater than those near Whataroa. This has not been demonstrated so far via by OSL thermochronology but it has been demonstrated by Tippett & Kamp (1993) with respect to the Alpine Schist belt using zircon and apatite fission track dating.

- With respect to the relatively low mean De of 251Gy from Herman et al (2009) this could be an artifact of sensitivity changes inherent in the OSL dating process. These changes are enormous in NZ quartz, and our protocol does not properly correct for them so OSL thermochronology is somewhat speculative. So the feldspar in these rocks may give a contrasting result to that of the quartz. (pers. com. U Rieser).

At the Nelson Creek quarry site a substantial portion of the gravel and sand has a granitic provenance. This material contains abundant K-feldspar whereas the Alpine Schist has a lower K-Feldspar content. So if K-feldspar sand grains here have an inherited age it is likely primarily a reflection either of the cooling age of the granite, or more likely its IRSL saturation limit. Sand sized K-feldspar grains liberated from the granite by glacial rasping will have been subject to much slower cooling than similar grains derived from Alpine Schist. As discussed in Chapter One there is a discontinuity in the uplift rate across the Alpine Fault. The uplift rate in the granite-bearing area to the NW of the fault is slower than that to the SE of the fault. As discussed in Chapter One fission track dating of apatite and zircon from the schists and granites demonstrates that the cooling rate in the granites has been much slower than that in the schists.

In summary it is almost inevitable that sand-sized K-feldspar in proximal fluvioglacial outwash at the Nelson Creek quarry contains significant remnant IRSL D_e. The remnant D_e must contribute to the total D_e. But there does not appear to be a distinguishable impact in the dose-response curves for sample NCL1 from the Nelson Creek quarry or sample KMK6 from Kamaka.

Preusser et al (2005) obtained two samples (NCL1, NCL2) taken from fluvial sediment in the Nelson Creek Farm Settlement gravel quarry. These were dated by IRSL on K-Feldspar from the sand fraction. The grainsizes were 150-200 and 250-300 μm respectively. Final ages of 109 ± 8 and 113 ± 8 ka were obtained. Is any evidence presented by Preusser et al (2005) to confirm complete bleaching of sand in the gravel at Nelson Creek prior to deposition? They make the following statement in relation to these samples from Nelson Creek:

> *"The consistency of ages determined for samples from the same stratigraphic position and the non-skewed ED distribution are interpreted to indicate complete bleaching of the IRSL signal prior to deposition (see Section 5)."*

Then in section 5:

> *"Are the luminescence ages reported here reliable? Two major potential error sources have to be considered. First, ages could be overestimated due to incomplete bleaching of the luminescence signal prior to deposition."*

The other main issue is anomalous fading which will not be discussed further here.

Further they state:

> *"There are several methods to investigate if a sediment sample was completely or partially bleached prior to deposition (cf. Wallinga, 2002a). The first approach is to compare luminescence signals that show different bleaching rates."*

This can't be done for the Nelson Creek samples as they were dated by a single method (K-Feldspar IRSL on the sand fraction), or at least this is how the results were reported.

Preusser et al then state:

> *"Another method is to analyse the form of the optical decay curve. Huntley et al. (1985) proposed that a rise in equivalent dose as a function of illumination time is likely to reflect incomplete bleaching at deposition. This assumption is based on the idea that the optical signal measured with longer illumination time originates from traps that are more difficult to empty optically. Recent work has demonstrated that analysing the shape of the decay curve can give valuable information about partial bleaching of quartz grains."*

However, it was K-feldspar that was dated at Nelson Creek rather than quartz. So this test (called a plateau test) might not apply. If the plateau rises, i.e. the tail of the shinedown curves gives higher ages, this is an indication of partial bleaching. However, this test only picks up partial bleaching if individual grains have been partially bleached. It does not detect a mixture of well-bleached and unbleached grains (pers com U Rieser).

Preusser et al (2005) then state:

> *"The scatter of replicate ED determinations for the same sample is another indicator for incomplete bleaching. However, microdosimetry also significantly contributes to the observed scatter (Murray and Roberts, 1997; Nathan et al., 2003). Partially bleached samples show typically a distribution with a tail towards high ED values (Olley et al., 1998, 1999). Samples showing a non-skewed distribution are interpreted to be completely bleached. A typical dose distribution from North Westland is shown in Fig. 11 for sample LOL 1, which is the most proximal sample investigated in the present study and, therefore, has the highest potential for incomplete bleaching prior to deposition. The histogram plot displays a relatively broad but non skewed dose distribution, which is interpreted to indicate complete bleaching of the IRSL signal prior to deposition. The board scatter is attributed to the small aliquot size (a few dozens of grains) from which only a few grains will contribute to the IRSL signal (cf. Wallinga, 2002b; Duller et al., 2003)."*

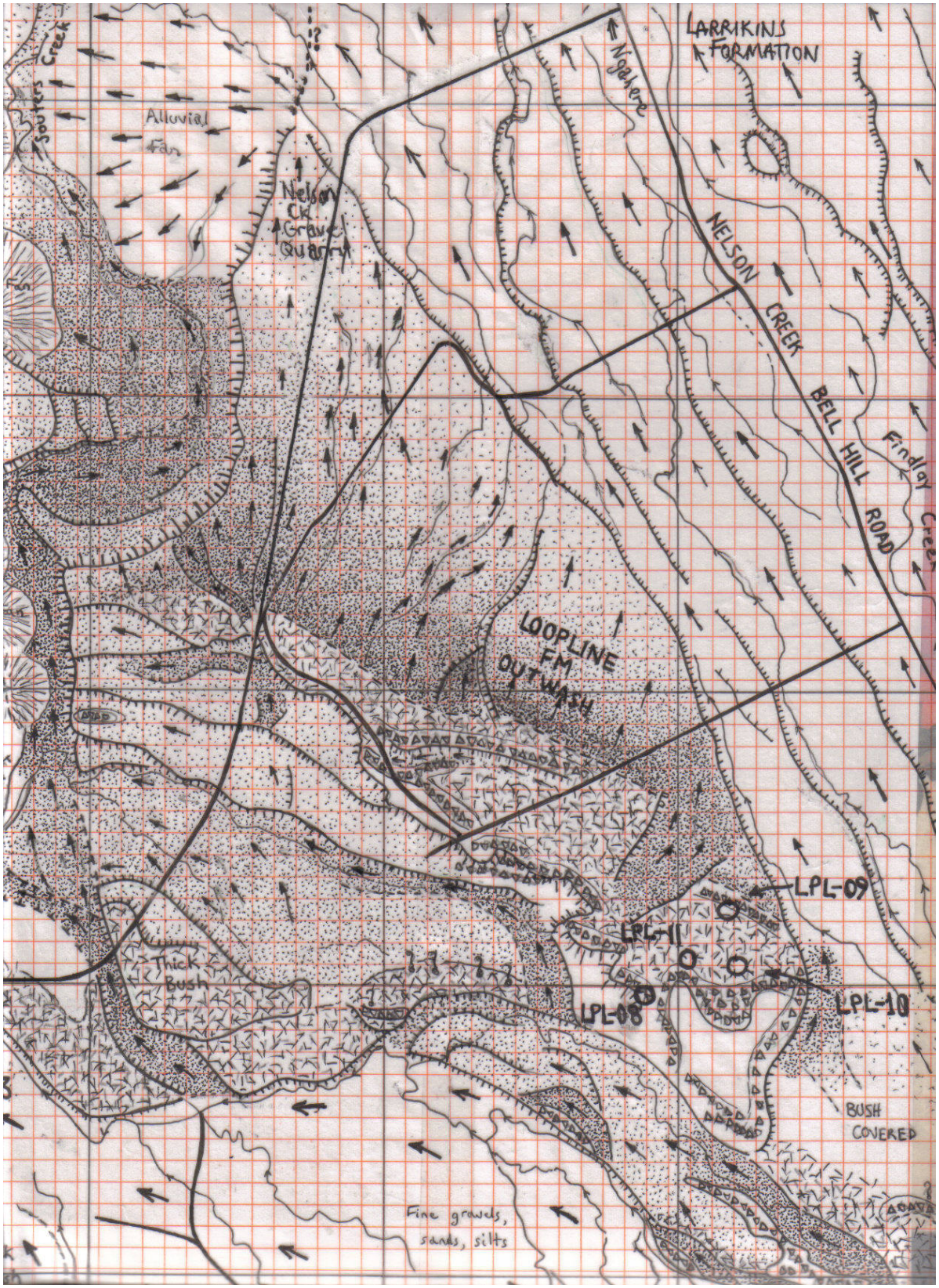

Figure 5.1 Geomorphological map of the Nelson Creek Farm Settlement area.

Unfortunately, as discussed in relation to this site in Chapter Six of this thesis, sample LOL1 may be Loopline Formation but it is not genetically related to the nearby terminal moraine. Though mapped as Loopline by Suggate & Waight (1999), this moraine is Larrikins(1) Formation and is substantially younger than the Loopline Formation. There is an unconformity at the sample site and LOL1 was almost certainly taken from below it. The geology of this area is discussed further in chapter six. Cosmogenic isotope dating carried out on the relevant terminal moraine provides surface exposure ages of 20 to 24 ka and is also discussed in chapter six. The only D_e-frequency plot shown in Preusser et al (2005) is that for LOL1. If the sample was from above the unconformity then the partial bleaching test has certainly failed for this sample as the sample age is 64±5 ka.

Preusser et al (2005) state further that:

> *"Another important indicator for complete bleaching is the consistency of ages determined for different samples from the same geological unit. As the spatial and temporal dynamics vary within fluvial systems it is rather unlikely that different incompletely beached samples are overestimated to a similar or even to the same degree. A broad consistency of IRSL and OSL ages determined for different samples taken from the same geological unit, with the exception of a few presumably incompletely bleached samples (e.g. KMK2-4), is demonstrated for several of the sites investigated in the present study (Figs. 4–7, Table 4). In conclusion, it appears that partial bleaching is restricted to a few samples only and that the majority of IRSL and OSL ages are not overestimated"*

But at Nelson Creek there are only two samples. These are similar in general nature, were deposited during the same glacial event and are very close to the same sediment source. They could give a similar result purely by chance or based on similar inherited/pre-depositional D_e. It is likely that if the sediment supply contained a substantial non-bleached component, then both samples could be similarly afflicted. Preusser et al (2005) did not provide D_e frequency plots for the SAR IRSL data on the sand samples dated from Nelson Creek quarry. A single D_e frequency plot is provided for 21 aliquots from LOL1 which is from the Stafford Loop Road quarry near Kumara. It was claimed that the distribution is not skewed. However, it is certainly rather broad (from about 120 to 300 Gy). Visually skewness is difficult to diagnose from a small number of sub-samples on a single dated sample (and, as was pointed out, may have other causes than partial bleaching).

Preusser et al (2005) indicate that the typical aliquot size used measured a few dozens of grains. What type of D_e distribution would one expect to see from a large number of SAR aliquots of small size taken from material sampled at a site like the Nelson Creek Quarry if:

- The dated sand was actually deposited somewhere between 25 ka and 35 ka.
- The dated sand was mainly derived dominantly from a small range of basement lithologies, dominated by schist, metagreywacke and granite, and the K-feldspar IRSL D_e is controlled by passage through the closure temperature at an average of around 80 to 100 kyr earlier (say 105 to 132 ka).
- Poor bleaching of the inherited IRSL D_e during deposition at the quarry site.

How would the test of non-skewness hold up under these general circumstances? Wouldn't one expect multiple small aliquots to display a broad distribution of D_e with rather subdued skewness? The prior studies cited in the extracts from by Preusser et al (2005) might not have been dealing with a partial

bleaching that potentially has a rather uniform or non-skewed character. The issue is prominent in a study by Lukas et al (2007) that is discussed briefly below.

In the context of the above discussion of the Nelson Creek quarry site two new cosmogenic isotope ages are now available from large glacial erratic boulders on the "Loopline" terminal moraine about 2.5 km SE of the quarry. The moraine and outwash surfaces are genetically linked (see figure 5.1). The exposure ages for samples LPL-08 and LPL-11 are 35.3 ± 3.0 ka and 25.0 ± 2.1 ka. So the first of the three preconditions listed above is likely to have been satisfied. The study by Herman et al (2009) discussed above hints that the second of these pre-conditions is could easily apply here. Are there studies that collectively demonstrate almost ubiquitously poorly bleached feldspar IRSL D_e in similar environments (given that quartz OSL is even more sensitive to zeroing under daylight conditions, examples of poorly bleached fluvioglacial quartz would also qualify)? In terms of this question the following studies are particularly relevant: Alexanderson et al (2008), Berger et al (2010), Clarke (1996), Clarke et al (1999), Ditlefsen (1992), Duller (1994, 2006), Fuchs et al (2005), Fuchs et al (2005, 2007), Forman & Ennis (1992), Gemmell (1999), Houmark-Nielsen (2008), Lamothe (1996), Lamothe & Auclair (1997), Lang (1994), Lukas et al (2007), Rhodes & Pownall (1994), Rieser et al (2009), Spencer & Owen (2004), and Stokes et al (2001). Collectively these studies indicate that in ice-proximal fluvioglacial environments great care is needed in assessing the results of SAR IRSL on K-feldspar from the sand fraction. Much of this work is summarised by Fuchs & Owen (2008). In their figure 8 they illustrate the increasing potential for bleaching with increasing distance from the proximity of the glacial terminus.

It was demonstrated by Fuchs et al (2007) that the production of non-skewed D_e distributions does not rule out partial bleaching. Lukas et al (2007) dated glacial sediments from the NW Scottish Highlands using feldspar IRSL (and quartz OSL). For 3mm feldspar SAR aliquots of small (~200 grain) size "excellent data" was produced but the D_e was an order of magnitude larger than expected from independent (^{14}C) age control. Reduction of aliquot size limited but did not eliminate the problem. Aliquots of one to eight grains yielded D_e at 2 to 3 times that expected. It was concluded that non-zeroing of feldspar luminescence during deposition of the dated sediment was due to the ice-proximal environment and to sediment derivation via subglacial erosion from older glacial sediments. Similar problems were encountered by Duller (2006) in dating ice proximal sediments in Scotland, one sample age being overestimated by as much as 80 kyr. For glacial environments Duller (2006) concluded that although (OSL) ages based on multigrain aliquots can be correct:

> *"one can only be confident of the age determined when additional single grain measurements are made to investigate the completeness of bleaching at deposition."* And *"Comparison with independent ages based on cosmogenic ^{10}Be, ^{14}C on organic material, and relative age control support the accuracy of these single grain optical ages."*

At Nelson Creek two ^{10}Be ages directly contradict the IRSL ages. There are no relevant ^{14}C ages here.

In a review of luminescence age overestimation Wallinga (2002) found that during SAR OSL, when the aliquot size is large, the signal is averaged over many grains so incomplete bleaching averages out. Therefore different aliquots can show similar D_e even where there has been partial bleaching and so the absence of scatter in D_e is not a sufficient criteria for good bleaching. It was also found that contaminating grains can act to decrease the scatter in D_e. Further it was found that there is no universal agreement as to the number of individual grains in a "small aliquot". The definition of "small" appeared to vary among different laboratories.

The issue of proximity to ice margins has largely been avoided in the IRSL sampling carried out for this thesis. One single sample (RR28) of silt was taken by the writer from an area mapped as Loopline Formation terminal moraine by Suggate & Waight (1999). Several other silt samples taken by the writer may have been deposited by fluvial action. So care is needed in interpretation.

In North Westland loessic (wind-blown) material derived from surficial coverbeds does not appear to have been systematically affected by partial bleaching. From Preusser et al (2005) samples that fit this category include NCL3, NCL4, BSG4, BSG5, PGM10, PGM11, UCS2 and UCS3. Loessic material probably has a reasonable chance to become fully bleached after deposition, even if it is not bleached prior to or during deposition. Bleaching can occur in-situ on the depositional surface while more aeolian silt slowly collects at the site, eventually resulting in burial. Therefore it is not surprising that there can be an apparent age discontinuity between the slowly deposited loessic cover beds and rapidly deposited underlying gravel.

6.6.2 Kamaka

The exposure at Kamaka is a road cutting adjacent to SH7. The sequence is described in Gage & Suggate (1958), Suggate (1965), Denton et al (1999), Preusser et al (2005), Suggate & Moar (2004) and in this thesis.

The sediments in the road cutting consist of fluvial silt, sand and gravel. Some of the fine-grained material could be lacustrine, as suggested by Suggate (1965). The position of the site is on the margin of the Grey Valley at the confluence of Twelve Mile Creek (Ongionui River) and the Grey River. Suggate (1965) suggests that the fine sediments here were deposited by the Grey River in response to "damming" of the valley several kilometres downstream by a gravel fan produced by the Arnold River. But the fine grained sediments wedge out quickly into fluvial gravel in a down valley direction towards Stillwater township and the Arnold River. The fine grained beds thicken towards the valley margin, towards the Ongionui Valley and potentially upslope into the Ongionui Valley. An equally likely scenario is that the ponding referred to by Suggate (1965) was caused by rapid Grey River aggradation blocking the mouth of the Ongionui Valley. The Ongionui River is relatively small and if forced to aggrade in response to the Grey River, it would not be capable of transporting gravel in its lowermost section.

The first dating for this site is reported in Gage & Suggate (1958). A ^{14}C age of 22.3 ± 0.35 ka was supplemented by numerous additional fourteen ^{14}C ages reported in Denton et al (1999). The mean of these 14 ages is 22.46 ka or a calibrated age of ~ 25 ka as suggested by Denton et al. This may be closer to 27 ka if the newest INTCAL is used. At Kamaka the sediments were clearly being deposited during MIS2. The pollen analysis reported by Suggate (1965) is indicative of a cold climate. It contained 2% tree, 10 % herbs and 82 % grass pollen.

Preusser et al (2005) obtained 8 samples from Kamaka for luminescence dating, being KMK1 to KMK8. The writer obtained a single sample being RR21. The exposure sampled for this project is described in appendix 1. Four of the luminescence samples (RR21, KMK2, 3, 4, &7) appear to significantly overestimate the age of the silt.

Sample	IRSL(blue) age (ka)	OSL(UV) age (ka)	TL (blue) age (ka)	TL(UV) age (ka)
KMK7	28.5±3.2		71±20	
KMK6	23.4±3.6	38±4	26.1±2.9	25.8±2.6
RR1	35.3±3.2			
KMK4	39±5	35±6	75±13	36±10
KMK3	45±4	29±4	83±16	35±4
KMK2	41±5	38±5	84±35	84±8

Table 5.1 Ages of selected samples from the SH7 road cutting at Kamaka.

Only one of the 13 luminescence ages (samples RR1, KMK2, KMK3, KMK4) from the ^{14}C dated silt is within 1δ of the mean ^{14}C age, and then only just. It is reasonably clear that none of the luminescence samples were fully bleached prior to deposition. This is recognized by Preusser et al (2005). They do not discuss the reasons for this except to say that this is unusual in fine grained fluvial sediments. As discussed above in relation to a number of recent studies of D_e in modern and Quaternary environments this point is debatable for regions in which the fluvial silt is derived from proximal glacial sources or where the majority of fluvial deposition occurs under conditions of extreme turbidity.

At this site the IRSL ages for RR1, KMK2, KMK3 and KMK4 are about 8 to 20 kyr too old while the OSL ages are around 4 to 13 kyr too old. This is a finding that should be kept in mind during the discussion of fluvial sand and silt at other localities in North Westland. The age overestimation is likely due to residual D_e that was not zeroed at the time of deposition.

Note that the two silt samples dated from higher up the exposure at Kamaka also produced erratic ages. The IRSL age for KMK7 is close to the expected age but TL age about 3 times the expected age. The OSL age for KMK6 is about 13 kyr older than expected, while the IRSL and TL ages are within the expected range. Clearly it is possible for several luminescence methods to give erratic results on fluvial/lacustrine silt. At Kamaka IRSL, OSL and TL all gave one or more ages close to the ^{14}C age. On this evidence it seems that TL gave the worst performance. For Kamaka the evidence is insufficient to allow a preference between the IRSL and OSL methods. Similar dating exercises by Preusser et al (2005) at the Sunday Creek Phelps goldmine sites are examined in the light of the Kamaka example.

It should also be noted that the Kamaka site is more distant from glacial ice and glacial till than any other site discussed by Preusser et al (2005). Fluvial silt sampled at the Phelps Mine and at Sunday Creek is more ice-proximal. Sediments sampled at the Nelson Creek, Stafford Loop Road, Chesterfield Road, Raupo and Hokitika gravel quarries is also more ice-proximal. Another study to have revealed partial bleaching issues in this region is Hormes et al (2003). They managed to get reasonable correspondence between ^{14}C and OSL ages at the Raupo gravel quarry. But they detected systematically poor bleaching of TL at deposition.

At the time of silt deposition at Kamaka there were substantial glaciers in the Paparoa Range on the NW flank of the Grey Valley, in the Arnold Valley, at the head of Nelson Creek (Haupiri Valley), the Ahaura Valley and the Big Grey Valley, all feeding meltwater laden with rock-flour into the Grey River. The terminus of the large Ahaura Glacier was about 30 to 35 km up valley from Kamaka. This glacier was of similar proportions to the large Taramakau and Hokitika Glaciers. Abundant silt, freshly derived from bedrock sources and recycled Quaternary deposits by glaciers of this size, is likely to be

very poorly bleached on release. In this system, at the modern day, floodwaters from the Ahaura-Grey confluence (about 30 km) can reach the sea in about 5 hours at an average speed of around 6 km per hour. The travel time for suspended silt to cover the distance from the Ahaura glacial terminus to Kamaka time is likely to have been similar. During high flow conditions, when most of the sediment transport occurs abundant poorly bleached silt would have been available for deposition at Kamaka. The silt was transported in extremely turbid waters both during and outside of daylight hours, so poor bleaching of prior D_e should be anticipated. The best modern local analogues are the extremely turbid discharges from the Fox and Franz Josef Glaciers in South Westland.

In comparison with most other sites dated by luminescence methods in North Westland to date, Kamaka is well dated by an alternative method. The likelihood that other dated sites in North Westland contain materials that have similar luminescence properties is high but this will be difficult to demonstrate until more ages are available via dating by other methods.

5.6.3 Pine Creek/Phelps Mine

This site is situated to the south of the Hokitika River near Hokitika and is of particular interest to the writer, who carried out an exploration project here during the late 1980's for the then landowner, Mr Ray Tinsley. Dr R.P. Suggate was first introduced to the Phelps Mine site by the writer on 12/2/95. Dr Suggate obtained two silt samples for pollen analysis during that visit, one from the silt horizon separating two thick fluvioglacial gravel units and one from the organic silt that rests on the deeply buried marine strandline sediments. Correlation of two separate and distinctive buried marine units situated beneath the property with similar deposits north of the Hokitika River was discussed during the visit. Dr Suggate was of the opinion that the lower of the two marine units had not previously been identified in North Westland, being at an altitude too low for ready correlation with other known deposits. This unit would therefore need to be named. It was suggested that as the property was known as "Craigs Freehold" when the buried gold-bearing beach sand was first discovered and mined (by tunneling around 1900) that the name "Craigs Formation" would be suitable.

Strata	Depositional Environment Preusser et al (2005)		Depositional Environment This study
Surficial Loess	Aeolian		Aeolian ---------- RL 35-36 m
Fluvioglacial gravel	Fluvial	7 m	Fluvioglacial gravel
Upper buried silt	Fluvial overbank	1 m	Fluvial?
Fluvioglacial gravel	Fluvial	9 m	Fluvioglacial gravel
Silt	Estuarine	{1.2 m	Fluvial
Lower buried peaty organic silt	Fluvial?	{	Fluvial ---------- RL 10-12 m
Sand and sandy gravel	Littoral	{5 to 10 m	Littoral
Plio-Pleistocene pebbly sandstone	Fluvial		Fluvial

The geology of this site is discussed in Chapter Six. The general geomorphic context of the site is shown in figure 6.6a. A sequence containing two extensive buried silt horizons has been exposed in two gold mines, one on the south side of Pine Creek and one between Pine Creek and the Hokitika Valley. The stratigraphy is essentially the same at both mine sites. The two mines are separated by a small valley drained by Pine Creek. The valley is relatively young (probably post-LGM) and is incised into a substantial terrace which is around 30-35 m higher than the nearby floodplain of the Hokitika River. For the purpose of this discussion the two mines which are about 200 to 300 m apart are treated as a single locality.

The dated units are the surficial loess, the fluvial overbank silt, the estuarine silt and the organic soil.

The uppermost surface at the mine (assumed to be Larrikins Formation by Preusser et al 2005) is situated about 1.5 km down-gradient from the nearest terminal moraine. The surface gradient is about 12.5 m/km. So during fluvial aggradation meltwater flows are likely to have been at a high velocity, with very short travel times for silt and fine sand. As at the Nelson Creek quarry the potential for partial bleaching of natural D_e is high. Is there evidence for partial bleaching in the various Phelps Mine samples?

Upper buried grey silt	Lower buried silt	These 21 polymineral fine-grain ages are used by Preusser et al (2005) in the age model		Rejected by Preusser as an outlier on the basis of likely incomplete OSL bleaching	Not used or rejected by Preusser et al (2005) on suspicion of partial bleaching	Incomplete TL bleaching specifically mentioned Preusser et al (2005)	
Sample	**K-Feldspar IRSL (blue) age**	**K-feldspar IRSL(UV) age (ka)**	**Quartz OSL(UV) age**	**Quartz Post-IR-OSL age**	**TL(UV) age (ka)**	**TL(blue) age**	**Grainsize dated**
PGM9 (SAR)		76±8		85±8			Silt
PGM8 (SAR)		61±6		83±8			Silt
RR3 (MAA)	**56.8±5.9**						Silt
PGM7 (SAR)		69±6		103±10			Silt
PGM6 (SAR)		58±5		69±7			Silt
PIC1 (MAA)	74±15		66 ± 5		68 ± 15	87±10	Silt
PIC2 (MAA)	78±14		63 ± 9		66 ± 11	70±10	Silt
PGM5 (SAR)		63±6		102±10			Silt
PIC3 (MAA)	76±11		80 ± 13		78 ± 12	114±17	Silt
PGM4 (MAA)	74±8		101 ± 25			261±48	Silt
PGM3 (MAA)	66±8		84 ± 9		89 ± 17	67±10	Silt
PGM2 (MAA)	76±18		65 ± 12		107 ± 13	204±40	Silt
PGM1 (MAA)	67±8		72 ± 12		70 ± 12	72±9	Silt
RR2 (MAA)	33.6±3.6						Silt

Sand bed in gravel

Organic soil

Table 5.2: Ages of samples from the Phelps Gold Mine and Pine Creek Quarry.

As at Kamaka there is significant scatter in the ages at the Phelps Mine. The scatter is most prominent in the TL ages, but it is also present in the OSL and IRSL ages. None of the TL ages were considered by Preusser et al (2005) for the age model for this site due to clear-cut partial bleaching issues. However PGM1, PGM3, PIC1, & PIC2 were said to be showing depositional ages by TL. Three of the OSL ages were not considered in the age model due to suspected partial bleaching. In discussion of the sample ages for this site they do not refer to their earlier comments on the very dim luminescence observed in quartz, the sensitivity issues, or the generally poor SAR performance of quartz from this region.

Observations in relation to the above dataset:

- All of the IRSL ages are centered on values less than 80 ka
- The OSL ages are more erratic than the IRSL ages
- The TL ages are more erratic than both the IRSL and the OSL ages
- The IRSL ages should be treated as maximum ages given the proximity of this site to moraines created by the Hokitika Glacier. The average IRSL ages for the upper (67.6 ka) and lower (65.1 ka) buried silt horizons might not represent the depositional age as the sediments may contain remnant (non-bleached at deposition) D_e.
- The presence or absence of partial bleaching of IRSL in these samples may be very difficult to detect.
- The issue of anomalous fading of IRSL was addressed by Preusser et al (2005). It was found that there was no evidence for fading. The same conclusion was reached by Hormes et al (2003) in relation to IRSL at Raupo in the Grey Valley, and by Vandergoes et al (2005) in relation to IRSL at Okarito in South Westland.

The known issues with the TL ages here centre on incomplete bleaching so only the youngest of these ages have relevance to the age of the deposits. Six of the thirteen TL ages come in at 72 ka or less. The average of these ages is 68 ka for the upper silt and 70 ka for the lower silt.

Given the known issues with OSL dating on quartz in Westland all of these ages should probably be rejected, or at the very least any such age outside of the central tendency of the IRSL ages should be treated with suspicion particularly given that several of these ages were rejected on the basis of partial bleaching. In addition to the three OSL ages rejected by Preusser et al (2005) there are an additional three that do not overlap with the corresponding IRSL age at 1δ. These are PGM3, PGM8, PGM9. [though according to the definition of 1sigma one would expect 68.3% of ages to be within 1sigma, and 31.7% outside. So, of the 12 IRSL ages one might expect that several would be outside 1sigma]. The remaining OSL ages on the upper and lower buried silts give mean ages of 66 ka and 72 ka respectively, which should also be regarded as maximum mean ages.

As discussed above, where independent age control is available the measured D_e for polymineral finegrain samples in proximal glacial environments (e.g. Fuchs & Owen 2008; Lukas et al 2007; Duller, 2006) can be several times that expected from the true depositional age where independent numerical ages are available. The only independent age control at this site is a group of ^{14}C ages which are reported to come from the upper buried silt. These gave ages of >50 ka, which could set a minimum age for this unit.

At the Phelps Mine the two samples (RR2, RR3) from this project dated by MAA IRSL on polymineral finegrains are both younger than the equivalent samples from Preusser et al (2005). The IRSL age for RR3 from the upper buried silt, at 56.8±5.9 ka, is regarded as a maximum by the writer. The position (between two thick aggradational fluvioglacial gravel units), the thickness of the silt (~ 1m) and the paucity of organic remains tend to indicate relatively rapid silt accumulation during a hiatus in gravel deposition. That may mean no more than a temporary migration of a meltwater river to another position on the floodplain. If this unit is an "overbank silt" as suggested by Preusser et al (2005) then the likelihood of partial bleaching for IRSL is relatively high.

With regard to the lower buried silt the writer has not observed evidence for an estuarine depositional environment. The base of the silt is peaty with in-situ tree stumps. It grades up into silt with a lower organic content, then into fluvial gravel. The sand on which the soil rests is gold-bearing and heavy-mineral rich. It was deposited in an upper shore-face or near shore aeolian dune setting. Modern analogues are abundant in this region and indicate the upper surface of the sand was probably formed between 3 and 6 metres above mean sea level. The upward transition into aggradational fluvial gravel is from a moderate-energy fluvial environment into a high energy fluvioglacial environment. Partial bleaching of quartz OSL and TL have been demonstrated. So the potential for partial IRSL bleaching through this transition is very high. Even a modest degree of partial bleaching would potentially put the Preusser et al (2005) late MIS5-MIS4 assignment for the lower silt in doubt. For the "younger samples" an inherited D_e corresponding to 30 to 40 kyr would bring the Preusser et al (2005) results into line with RR2 (33.6±3.6 ka). But this would be difficult to reconcile with the ^{14}C ages reported in figure 7 of Preusser et al (2005) which are reported to be on wood remains found in the overbank deposits.

The general context of the site, its situation in respect of proximity to nearby terminal moraines and the likely turbid nature of meltwater discharging over the site invite care in the interpretation of the luminescence ages. Given clear evidence for incomplete bleaching here it would be prudent to base the age model on the samples least likely to be affected by partial bleaching. Note that similarity in several ages by different methods on the same sample does not guarantee a good result. As demonstrated at Kamaka multiple samples from an individual site can carry similar remnant IRSL, OSL and TL D_e.

5.6.4 Sunday Creek

The stratigraphy at the Sunday Creek site is similar to that at the Phelps Mine and is discussed in chapter six. The general sequence is:

Strata	Depositional Environment	Thickness
Surficial Loess	Aeolian/fluvial	~ 1 m
Fluvioglacial gravel	Fluvial	~15 m
Silt	Fluvial	~ 1 m
Peaty organic silt	Fluvial/Aeolian	~ 0.5 m
Pebbly sand and gravel	Fluvial	~ 0-1 m
Sand and sandy gravel	Littoral	~ 2-5 m
Gravel	Fluvial	2^+ m
Eight Mile Fm (fine sandstone)		

This is the type section for the Awatuna Formation, which consists of the littoral sand and gravel and the overlying peat/silt deposits. Samples have been for luminescence dating from the littoral sand and from the overlying silt. There is a wide range in the sample ages. IRSL dating on samples from the silt and peat gave generally younger ages than those on sand from the littoral deposits. Assessment of the depositional age of the littoral unit requires discussion of the potential for partial for bleaching.

Preusser et al (2005) state that most of the OSL-MAA, TL and MAA-IRSL ages on the same samples are similar. This was "interpreted to indicate zeroing of most of the different signals before deposition." But given the type of environment is the answer so simple? It may indicate no more than a similar proportion of non zeroed grains in each sample and a consistent pattern of sediment supply

and deposition within the environment in question. In contradiction to this claim by Preusser et al (2005) their own OSL and IRSL ages for several samples at Kamaka are also similar and this clearly gives zero support to any claim those samples were well bleached. Because the deposits at Sunday Creek are beyond the reliable range of ^{14}C it is not possible to verify the claim that the IRSL and OSL signals were fully bleached at deposition.

Buried silt	Buried beach deposit	These ages used by Preusser et al (2005) in the age model			
Sample	**K-Feldspar IRSL (blue) age (ka)**	**Quartz OSL (UV) age (ka)**	**TL(blue) age**	**TL(UV) age**	
SDC5 MAA	58±8	64±10	66±10	94±14	Polymineral silt
SDC8 MAA	58±7			78±9	Polymineral silt
SDC7 MAA	71±10	77±11	86±17	81±9	Polymineral silt
SDC4 MAA	61±8	86±9	89±14	77±10	Polymineral silt
RR8 MAA	**34.8±3.5**				Polymineral silt
SDC3 MAA	64± 5				Fine sand
RR9 MAA	**47.8 ± 6.6**				Polymineral silt
SDC2 MAA	81±11				Fine sand
SDC1 MAA	118±28				Fine sand
SDC6 MAA	71±8				Fine sand
Mean for silt	62±8	75.6±11		82.5±10	
Organic soil					

Table 5.3 (above): Ages from the Awatuna Formation at Sunday Creek.

In terms of the primary outliers in the age distribution these are SDC1 and SDC2. SDC1 in particular is at the base of the unit in a position that would imply deposition in deeper water, potentially with less exposure to light.

The sediments have been deposited at the foot of a prominent marine cliff. At the time of deposition the cliff had a height of approximately 30 m. Marine erosion had exposed the thick textually immature fluvioglacial outwash gravel of the Waimea Formation in the cliff face. This is a potential local source of poorly bleached sand and silt. Immediately underlying the littoral deposits there is an older fluvial conglomerate which could have supplied poorly bleached sediment from basal erosion. A little further along the coastline to the SW the same littoral unit rests directly on local bedrock. This is the poorly indurated Mio-Pliocene Eight Mile Formation which is a potential local source of poorly bleached silt and sand. Silt and sand with potential bleaching issues is also likely to have been widespread in the nearshore marine environment.

For this coastline the modern analogue for the Awatuna strandline is an extremely high-energy one. Sediment moves year-round in large volumes in the near-shore environment and can be both deposited

and eroded quickly. The water in near-shore areas is typically rather turbid, silts and clays being disturbed frequently by wave action, particularly in stormy conditions. The water clarity can be very poor and is also affected by the introduction of turbid flow from local rivers and streams. So there is potential at Sunday Creek for the deposition of poorly bleached marine sediment. Complete bleaching at deposition has been assumed by Preusser et al (2005) rather than demonstrated.

Feldspar is a relatively low-SG mineral that is easily transported once liberated and it can move through a sedimentary system quickly. So it can potentially be incorporated quickly into sediment in which the other components are better bleached due to exposure in the depositional environment over a longer timeframe. OSL dating of zircon might be a better approach as this mineral accumulates in strandline deposits over considerable periods of time, bleaches readily and tends to have a substantially higher internal dose rate.

The position adopted in this analysis is that the $IRSL_{(blue)}$ ages on K-feldspar in marine sand at Sunday Creek give a maximum age. Additionally the age SDC1 is regarded here as an outlier.

The $IRSL_{(blue)}$ ages for silt samples taken at Sunday Ck are all younger than the corresponding OSL ages. With respect to the OSL ages this is not promising as OSL is supposed to bleach more readily than IRSL. The mean of $TL_{(UV)}$ ages does not overlap with mean of IRSL ages at 1δ. This is not promising with regard to the TL ages here. TL does not appear to have been fully bleached here.

Four of the silt/peat samples have TL ages. Comparison with the IRSL ages points to poor TL bleaching in all four cases. Three of these samples were also dated by OSL. For each sample the OSL age is greater than the IRSL age. One of the OSL ages is greater than the matching TL age. In the general context of this site, Kamaka, and the Phelps Mine site this is not promising. At 1δ another OSL age (SDC4) does not overlap the IRSL age for the same sample. For all 4 silt samples the IRSL age is the youngest available. This is notable given that IRSL is generally thought to bleach less readily than OSL. If the OSL signal has not bleached, what chance is there that IRSL will have? It is the IRSL ages that Preusser et al highlight for the age model at this site, possibly because of the acknowledged issues with quartz in North Westland but this is not given as a reason by them in this case.

Preparation of the Quartz $OSL_{(UV)}$ samples from this site (and other sites dated by Pruesser et al 2005) involves digestion of the non-quartz component in HF. The aim is to produce a sample that is more-or-less uncontaminated by other (less resistant) minerals (particularly K Feldspar) that might contaminate the optically stimulated emission from the quartz. One issue that was not addressed was the potential presence of residual acid-resistant non-coloured translucent minerals that have a similar visual appearance to quartz. In samples from North Westland the presence or absence of zircon, monazite and uranothorite should be assessed. If present these will contribute to the dosimetry within the sample as a whole. They will also discharge luminescence when the quartz is stimulated, potentially contributing to an age overestimate. An outcome of this type might cause $OSL_{(UV)}$ ages to exceed $IRSL_{(blue)}$ ages from the same sample.

There is a wide spread of sample ages for the littoral samples. Preusser et al (2005) suggest this may be due to post depositional bleaching by reworking/mixing/bleaching of the sediment. No evidence is produced in support of the claim. In this environment disturbance of the sediment would inevitably mix silt and clay into the clean beach sand. Such disturbance would also destroy the fine-scale shore-face lamination visible throughout the littoral unit and it would destroy the prominent pebble imbrication imparted by wave action on a sloping beach surface. There is no evidence at the site that this has occurred.

In a stratigraphic sense Preusser et al (2005) need the littoral deposits at Sunday Creek to be older than about 80-90 ka. The equivalent unit near Hokitika is buried by fluvial gravel, the surface of which was dated by Preusser et al (2005) at the Hokitika gravel quarry. The gravel, mapped as Loopline Formation by Suggate & Waight (1999) spreads out as an alluvial fan in the Hokitika Airport area. Here it overlies what have been mapped as the Rutherglen and Awatuna Formations. The average luminescence age for sand in 3 shallow samples taken from the quarry is ~85 ka (mean of 3 samples). The much younger IRSL samples at Sunday Creek are rather inconvenient in this light.

At Sunday Creek the average age of 3 samples from the silt resting on the littoral sand is ~59±8 ka without 1 outlier or ~62 ka for 4 samples including one outlier. The age for the uppermost marine sand sample is 64±5 ka. This is indistinguishable from the average age of the overlying silt samples. So, taken at face value these samples do not indicate a significant hiatus between sand and silt deposition.

Based on IRSL dating at Sunday Creek by Preusser et al (2005) a simple interpretation is that the maximum age for the organic silt is c. 62±8 ka as this is where the ages for the silt and the shallowest sand sample tend to cluster. Given the potential for non-zeroing at deposition the age could easily be younger. One of the two IRSL ages from the base of the underlying littoral sand could be as young as 63 ka (at 1δ from 71±8 ka). That leaves two outliers at 81±11 and 118±18 ka. Samples RR8 at 34.8±3.5 ka from the organic silt and RR9 at 47.8 ± 6.6 ka from the littoral sand lower the overall average age to ~56 ka providing support for the proposal that the two older sand samples (SDC1, SDC2) are outliers influenced by incomplete bleaching. If that is the case then the overlying fluvioglacial outwash gravel is unlikely to have been deposited during MIS4.

5.6.5 Hokitika Gravel Quarry

As mentioned above the Hokitika gravel quarry is situated in a fluvioglacial outwash terrace mapped as Loopline Formation by Suggate & Waight (1999). The same mapping demonstrates that the Loopline Formation rests on two pre-Holocene marine strandlines. The geology of the Phelps goldmine indicates there is probably a third (younger) pre-Holocene strandline that must also be situated under the Loopline Formation east of the Hokitika airport. Basic stratigraphic principles require that the Loopline Formation, as mapped here, is younger than the Rutherglen, Awatuna, and Craigs Formations. The mean $IRSL_{(blue)}$ age for 3 sand samples taken from a sand horizon near the top of the gravel in the Hokitika quarry is 85±8 ka (BSG1 = 82±8, BSG2 = 85±6 , BSG3 = 88±8 ka).

As discussed above the central tendency for IRSL ages by Preusser et al (2005) from silt resting on the Craigs Formation is ~ 65 ka and a case can be made that this is the maximum age for this silt. The Loopline gravel at the Hokitika Quarry on the opposite (north) side of the Hokitika River should be younger than this.

As discussed above a case can be made from dating by Preusser et al (2005) for a maximum age of ~ 62 ka for silt resting on the Awatuna Formation at Sunday Creek. The Loopline gravel at the Hokitika Quarry should be younger than this.

In addition the uppermost gravel at the Hokitika gravel quarry must be younger than samples RR2 (33.6±3.6 ka for silt on the Craigs Formation), RR8 (34.8 ± 3.5 for silt on the Awatuna Formation at Awatuna), RR9 (47.8 ± 6.6 ka for silt from the littoral sand of the Awatuna Formation) and RR30 (63.6±7.4 ka for soil on the Blake Formation at Blakes Terrace). The base of the silt resting on the Loopline Formation at Chesterfield Road, near the Awatuna Formation type section, was dated (RR24)

at 53.8±4.3 ka (an age that could also be an overestimate). Until shown otherwise there is no particular reason to assume that the Loopline Formation at Chesterfield is different in age to that at Hokitika, so RR24 is highly relevant. In addition the upper gravel at the Phelps Mine has not been shown to be a different unit to that in the Hokitika Quarry. The elevations of the two terraces, either side of the Hokitika River are close to the same. RR3 was taken from silt at the base of the upper gravel at the Phelps mine. The age is 56.8±5.9 ka and under the general logic outlined above it could be an overestimate. This age also forms part of the limiting dataset. The average of 11 ages from the Preusser et al (2005) data at this horizon is 71 ka, which is also younger than the mean of the Hokitika quarry ages. All other luminescence ages from this project on Awatuna Formation terraces, or lower terraces, further to the north are < 60 ka.

Therefore even though there are 3 similar $IRSL_{(blue)}$ ages from sand in the Hokitika Quarry the likelihood that they reflect the actual depositional age is probably not high. The reason is likely to be incomplete bleaching though this proposal can not be proven at present. The general context of the quarry site bears a striking similarity to the Nelson Creek gravel quarry which is discussed above. Common factors include:

- The nature of the sediment.
- The relatively high slope on the upper surface.
- The proximity to terminal moraine (opposite side of the Hokitika River) that is likely to be genetically linked.
- The youthfulness of the overlying loessic soil.

As discussed above the glacial environment that prevailed at the time of deposition of the gravel in this quarry is precisely the type of environment from which one would expect the deposition of voluminous quantities of poorly bleached silt and sand. Partial bleaching should be assumed until proven otherwise. The correlation made for this surface by Suggate & Waight (1999) has not been overturned by the luminescence ages from the Hokitika Quarry. On basic stratigraphic grounds the gravel from this quarry could be assigned almost any age from around 22 ka to 70 ka (older than the overlying loess and younger than the underlying marine strandline deposits).

Comment on TL, IRSL(UV), OSL(UV), and post-IR(UV) ages:

For the reasons discussed above in section 5.6 a number of previously published ages probably should not have been released to an unsuspecting audience. These include the TL(blue), TL(UV), IRSL(UV), OSL(UV) [on quartz] and, to some degree, post-IR(UV) [on quartz] ages from North Westland. In this thesis serious discussion of the age of the various Late Quaternary formations centers around the IRSL(blue) data [both fine and coarse grained samples] from this PhD dissertation, and other projects.

5.7 PARTIAL BLEACHING ISSUES FOR IRSL SAMPLES DATED DURING THIS PROJECT

During this PhD project the sampling budget was quite small. There were a large number of potential datable sites. An early decision was made to obtain numerical age coverage across a range of deposits of differing type and altitude, rather than collecting large numbers of samples from just a few sites. This limits the extent to which an average age can be calculated for a particular horizon. However, it gives a different regional perspective. It also means that a number of new sites were sampled, rather than just sites that were already well known.

All of the samples taken for OSL and IRSL dating during this project come from in-situ materials. There is no evidence at any of the sampled localities that any of the sampled materials have been remobilized or redeposited except that colluvial processes may have contributed to the deposition the material from which RR11 was sampled.

The sampled sites are described in table 5.4 (below) in relation for the potential for partial bleaching (and consequent age overestimation) and in light of the general discussion relating to partial bleaching of IRSL, OSL and TL above. It should be considered as an indication that some individual sample ages may be affected by partial bleaching. The extent of partial bleaching is likely to vary from site to site. The fact that bleaching might be an issue at some sites or for some samples is not an indication that any of the results are failures. It simply alerts us to environmental factors that might not otherwise have been considered.

With regard to luminescence dating (or any numerical dating method) there is no particular need to defend individual ages as being a true record of the number of years that have lapsed since sample deposition. Because the potential for partial bleaching is both site-specific and bed-specific one should not expect that all ages for a particular formation or horizon will be the same, or even that they will neatly overlap at 1δ. Nor should it be expected that several ages from one formation, taken from different localities, will necessarily average to the true depositional age. If there is age variation within the cohort for a particular formation, and that variation relates to partial bleaching, then the most likely depositional age is best defined by the youngest age or youngest group of ages, rather than by the mean of all samples. For this project there was an opportunity to obtain numerical ages across each of a number of formations. But the number of samples for each formation is not large. Any of those samples could be impacted by partial bleaching. So the most appropriate age for a formation is not just a simple average of the dated samples. Such an average could generate inconsistencies across the different formations. Other relevant stratigraphic, climatic and numerical dating evidence may be assembled and discussed and may contribute to the final age assignment.

For the purposes of discussion of the age of various Late Quaternary formations in North Westland the mineral species that gives the most consistent ages is K-feldspar. The ages are most consistent when the dating method is IRSL(blue) and when the dated material is silt that has been deposited in an environment that favours complete pre-depositional bleaching of the luminescence signal. For localities where quartz OSL ages have been produced and published these will be noted and discussed but the samples will not be used in the assessment of the age of the deposit.

Given the small number of IRSL(blue) sample ages at of the sites sampled during this project it is not possible to form a solid opinion regarding the precise extent of partial bleaching. The general assumption made is that the dating expert (Uwe Rieser) has made a best estimate of the depositional age, given the laboratory performance of the sampled material, and taking account of any observed

tendency for anomalous fading. In fact there was no anomalous fading and this was also the case for luminescence dating by Preusser et al (2005). The numerical age that has been delivered is then the assumed maximum age, given that partial bleaching can be rather difficult to detect. The real age (and error bands) could be centered on a numerical value lower than that supplied from the dating laboratory. The extent of the difference will vary from zero (full bleaching at deposition) to substantial (poor bleaching at deposition).

Table 5.4: Classification of luminescence dating samples from this project in terms of the potential for complete bleaching during or immediately prior to deposition.

Field Code	Formation	Location	Dating Method and Grain-size dated (silt = 4-11 μm)	Type of Sediment	Potential for complete bleaching of IRSL in the silt during deposition	Comments
RR1	Craig	Southside, Hokitka	NA	Beachsand, minimal silt	Moderate	Energetic littoral environment but multiple potential sources of very immature sediment. Mainly marine sediment transport.
RR2	Craig	Southside, Hokitka	MAA, silt	Wood bearing organic soil on beach sand	Moderate	Low energy environment with a potentially fluvial component. Deposition from turbid water possible. Directly overlain by fluvial silt and fluvial gravel. Close to multiple sources of very immature sediment. Possible ponding of turbid floodwater behind beach ridges.
RR3	Loopline	Southside, Hokitka	MAA, silt	Silt layer between two fluvioglacial gravels	Poor to very poor	Probable fluvial overbank silt resting directly on and under outwash gravel, potentially in an ice- proximal setting. Deposition from very turbid meltwater water probable, loessic component possible.
RR4	Blake	Southside, Hokitka	NA	Beachsand, minimal silt.	Moderate	Energetic littoral environment but multiple local potential sources of very immature sediment. Mainly marine sediment transport.
RR5	Blake	Southside, Hokitka	NA	Beachsand, minimal silt.	Moderate	Energetic littoral environment but multiple local potential sources of very immature sediment. Mainly marine sediment transport.
RR6	Scandinavia	Scandinavian Hill, Stafford	MAA, silt	Silt from soil on beachsand	Moderate	Possible low energy environment but deposition from turbid water possible. Very close (10's of m) to Scandinavia strandline (and a seacliff) and the mouth of Waimea Creek. Immediately overlain by fluvial gravel. Sample site close to multiple sources of very immature sediment.
RR7	Scandinavia	Scandinavian Hill, Stafford	NA	Beachsand, minimal silt.	Moderate to good	Energetic littoral environment but multiple potential sources of very immature sediment. Situated at the Scandinavia strandline (and a seacliff) and close to the mouth of Waimea Creek. Mainly marine sediment transport.
RR8	Awatuna	Sunday Creek, Chesterfield	SAR & MAA, silt	Wood-bearing organic soil on thin (1m) fluvial gravel above beachsand	Moderate	Highly organic but underlain and overlain by fluvial gravel, and located very close (< 25 m) to a substantial marine cliff cut into very immature outwash gravel. Organic deposition with potential fluvial and aeolian components. Close to the mouths of Kapitea and Sunday Creeks.
RR9	Awatuna	Sunday Creek, Chesterfield	SAR & MAA, silt	Pebbly beachsand	Moderate	Energetic littoral environment but multiple potential sources of very immature sediment inland from the adjacent seacliff. Close to the mouths of Kapitea and Sunday Creeks. Mainly marine sediment transport.
RR10	Rutherglen	North Beach, Greymouth	NA	Beachsand, minimal silt	Moderate to good	Energetic littoral environment. Potential of fresh immature sediment but these sources more distant than for the sample

						sites south of Greymouth. Mainly marine sediment transport.
RR11	Awatuna	North Beach, Greymouth	MAA, silt	Grey silty clay. Above imbricated beach pebbles & below wood bearing organic-rich silt	Moderate	Deposition on a narrow shore platform with a steep hill immediately (< 30m) inland. Clay contains some coarse limestone debris from the hill behind. Potentially deposited by turbid water.
RR12	Blake	Point Elizabeth, Greymouth	MAA, silt	Beachsand from inter-layered sand and discoidal gravel	Moderate	Energetic littoral environment. Potential for fresh immature sediment but these sources more distant than for the sample sites south of Greymouth. Mainly marine sediment transport.
RR13	Caledonian	Point Elizabeth, Greymouth	SAR & MAA, silt	Silty shallow marine sand	Moderate to good	Energetic littoral environment. Potential for fresh immature sediment but these sources more distant than for the sample sites south of Greymouth. Mainly marine sediment transport.
RR14	Rutherglen	South Beach, Greymouth	NA	Shallow marine sand, minimal silt	Moderate to good	Energetic littoral environment. Potential for fresh immature sediment but these sources more distant than for the samples situated south of Camerons. Mainly marine sediment transport.
RR15	Rutherglen	South Beach, Greymouth	MAA, silt	Silty shallow marine sand	Moderate to good	Energetic littoral environment. Potential for fresh immature sediment but these sources more distant than for the samples situated south of Camerons. Mainly marine sediment transport.
RR16	Rutherglen	South Beach, Greymouth	NA	Shallow marine sand, minimal silt	Moderate to good	Energetic littoral environment. Potential for fresh immature sediment but these sources more distant than for the samples situated south of Camerons. Mainly marine sediment transport.
RR17	Rutherglen	Power Road, Karoro	MAA, silt	Shallow marine silt	Good to very good	Energetic littoral environment. Potential for fresh immature sediment but these sources more distant than for the samples situated south of Camerons. Mainly marine sediment transport.
RR18	Rutherglen	Power Road, Karoro	NA	Beach or marine sand, minimal silt	Good to very good to good	Energetic littoral environment. Potential for fresh immature sediment but these sources more distant than for the samples situated south of Camerons. Mainly marine sediment transport.
RR19	Nine Mile	Rapahoe Beach	NA	Holocene beachsand, minimal silt	Good to very good	Energetic littoral environment. Potential for fresh immature sediment but these sources more distant than for the samples situated south of Greymouth. Mainly marine sediment transport.
RR20	Awatuna	Schulz Creek, SH6, 12 Mile	MAA, silt	Wood bearing organic silt	Moderate to good	Relatively low energy environment. Potential sources of immature fluvial silt from small streams draining off the sea-cliff situated ~ 50 m to the east. Sampled organic soil situated beneath 5 m+ of interbedded fluvial silt, sand, and pebbly gravel.
RR21	Larrikins	SH7, Kamaka, Grey Valley	MAA, silt	Silt bed within fluvioglacial gravel	Very poor	Fluvial silt probably deposited by the Grey River (very large). Silt situated between two fluvioglacial gravel units. Water probably very turbid during deposition here. Clear-cut partial bleaching identified in this unit at this locality
RR22	Karoro	South Beach, Greymouth	MAA, silt	Silt with organic layers	Good to very good	Low energy environment, Thick silt coverbeds could be fluvial and/or aeolian, > 100 m from seacliff.
RR23	Karoro	South Beach, Greymouth	MAA, silt	Sandy silt	Good to very good	Low energy environment. Thick silt coverbeds could be fluvial and/or aeolian, > 100 m from seacliff.
RR24	Loopline	Chesterfield Rd, Chesterfield	MAA, silt	Base of silt on fluvioglacial outwash	Poor to moderate	Probable fluvial overbank silt resting directly on outwash gravel. High gradient on outwash surface and potentially rapid sediment transport.
RR25	Waimea	Upper Sunday Creek	MAA, silt	Silt on fluvioglacial outwash	Poor to moderate	Probable relatively high-energy fluvial environment. Overbank silt resting directly on fluvioglacial outwash gravel. Possible

						deposition from turbid floodwater. Buried by interlayered fluvial silt and gravel and loessic beds. High gradient on outwash surface and potentially rapid sediment transport.
RR26	Rutherglen	Candle Light, Camerons	MAA, silt	Grey inorganic laminated silt above marine sand	Poor to moderate	Probable low energy environment during deposition. Close (< 30 m) to marine cliff. Thick (>4m) fluvial fan deposits overlie the sampled level. Fan deposits include numerous wood bearing soils interlayered with channelized and lensoidal fluvial gravel beds deposited by local streams eroding very immature outwash gravel and Pliocene siltstone. Potentially close to the mouths of New River and the Taramakau River. Possible ponding of turbid floodwater.
RR27	Rutherglen	Candle Light, Camerons	MAA, silt	Grey inorganic laminated silt and clay above marine sand	Poor to moderate	Probable low energy environment during deposition. Close (< 30 m) to marine cliff. Thick (>4m) fluvial fan deposits overlie the sampled level. Fan deposits include numerous wood bearing soils interlayered with channelized and lensoidal fluvial gravel beds deposited by local streams eroding very immature outwash gravel and Pliocene siltstone. Potentially close to the mouths of New River and the Taramakau River. Possible ponding of turbid floodwater.
RR28	Pre-Loopline	Kapitea Reservoir	MAA, silt	Very hard laminated silt on glacial till, the silt situated below Holocene and buried Late Quaternary organic soils (both wood-bearing)	Very poor	Ice proximal locality. Potentially subglacial origin for the sampled silt at this site. Sample from a few 10's of cm above glacial till. Extreme sediment immaturity. Source of poorly bleached till within metres laterally from the sampled material.
RR29	Pre-Loopline	Blakes Terrace, Awatuna	MAA, silt	Silt between two outwash gravels	Poor to very poor	Thick silt bed (2 m plus) situated between two fluvioglacial gravel units. Clearly deposited rapidly over a large area (this bed appears to be continuous over several km). Probably deposited by a substantial river carrying very turbid water.
RR30	Blake	Blakes Terrace, Awatuna	MAA, silt	Organic silt on marine sand	Moderate	Low energy environment. Sampled organic silt rests on thin grey sandy silt that thickens laterally into fluvial sand then fluvial gravel. So fluvial content cannot be ruled out (especially by mixing due to bioturbation) . Close to a large expanse of fluvial terraces. Sample contains organic and potentially aeolian and fluvial components.
RR33	Rutherglen	South Beach, Greymouth	MAA, silt	Wood-bearing organic soil on marine sand	Good to very good	Low energy environment. No discernable fluvial influence. Close to low (~2m) terrace riser at strandline between Rutherglen and Karoro Formation. Potential aeolian and organic deposition for the sampled material.
RR34	Karoro	South Beach, Greymouth	MAA, silt	Wood-bearing organic soil on marine sand	Good	Low energy environment. No discernable fluvial influence. Close (< 50m) to seacliff at inner margin of Karoro Formation. Mio-Pliocene siltstone and immature fluvial gravel exposed in the seacliff and the adjacent higher terraces. Potential aeolian and organic deposition for the sampled material.

In the group of samples dated for this project there are a number that should be assessed with particular caution. These are samples of rapidly deposited fluvial silt and one sample taken from an ice-proximal position including as follows:

- RR3 (intra Loopline Formation, Phelps Mine). The sampled material is described as overbank silt (this study and Preusser et al 2005). Its fluvial nature and proximity to glacial moraines make it likely to suffer from partial bleaching and age overestimation.
- RR21 (Larrikins Formation, Kamaka). As discussed above in relation to the Kamaka sample site RR21 almost certainly suffers from partial bleaching.
- RR24 (Loopline surface, Chesterfield Road). The sample consists of fluvial overbank silt resting immediately on fluvioglacial outwash gravel and underlying loess deposits. The loess unit contains Kawakawa tephra near the base. The sample could suffer from partial bleaching. Two younger sample ages (RR8, RR9) were obtained nearby at the Awatuna Formation type section, which is stratigraphically below the RR24 sample site.
- RR25 (Waimea Formation, terrace above Sunday Creek). The sampled material is fluvial silt resting directly on fluvioglacial outwash. The thick coverbeds above the sample include thin lenses of fluvial gravel. There is potential for partial bleaching so the sample age is considered to be a maximum.
- RR28 (Larrikins or Loopline Formation, Kapitea Reservoir). RR28 was taken from silt that rests directly on glacial till. The age and context is discussed in Chapter Six. Given the general discussion above in relation to IRSL dating on ice-proximal deposits the sample age is probably an overestimate.
- RR29 (pre-Loopline at Blakes terrace). The sampled material is fluvial and was almost certainly deposited from very turbid water. The climatic affinity is unknown. The resulting age is considered as a maximum for the site as there is clear potential for partial bleaching.

A number of the samples taken for luminescence dating during this project are from material situated just above marine strandline deposits. It is assumed that the sealevel was at a maximum at the time of deposition of the inner strandline during that marine transgression. So any deposit situated on the marine strandline was probably also formed significantly above mean sea level. This is particularly clear in situations where there has been economic extraction of alluvial gold from the beach material. In the modern analogue such gold and heavy mineral deposits do not form below mean sea level. For the fossil examples referred to here this is confirmed by the presence of shore-face deposits. Samples taken from silt situated above the strandline sediments include: RR3, RR6, RR8, RR11, RR20, RR22, RR23, RR26, RR27, RR30, RR33 and RR34. In each case the deposition was either by fluvial or aeolian processes or by a combination of these processes.

In the modern analogy fluvial silt deposits can accumulate rapidly over substantial areas immediately inland from a coeval shoreline. Streams tend to flow parallel to the coast on a low gradient and the stream outlets are frequently blocked by the coast-parallel propagation of sand and gravel bars. Flooding is common at such times. The environment is suitable for the development of swampy forest (often Kahikatea dominated in modern examples). The deposited sediments can take on a wood bearing and somewhat estuarine appearance but typically the environment would be described more accurately as fluvial-lacustrine. In this environment there is potential for partial bleaching during deposition. This potential likely decreases with distance from sources of fresh glacial silt. Sediments that are highly organic are likely to have been deposited more slowly than those that are inorganic. A case could be made for a lower likelihood of partial bleaching in organic than non-organic fluvial

deposits but this is somewhat speculative. The number of samples taken at each locality prevents determination of the relative degree of bleaching in different sediment types in this general environment. Organic-rich materials were targeted during the sampling campaign where these were located close to the upper surface of the beach deposits. The samples that were organic-rich are: RR2, RR8, RR20, RR23, RR30, RR33, and RR34. Samples that were relatively non-organic are: RR6, RR11, RR26 and RR27. There was no deliberate effort to collect samples of contrasting character (organic and inorganic). At the time of sampling the aim was to minimise the potential difference in age between the sampled silt and the underlying strandline deposits so the samples were collected as close to the beach-soil transition as was feasible.

Samples RR2, RR8, RR6, RR26, RR27 and RR30 were each taken from outcrops in close proximity to fluvioglacial gravel deposits. In each case there is a to moderate to high chance that the age is affected by partial bleaching. Therefore the reported age is regarded as the maximum age. Samples RR11, RR20, RR23, RR30, RR33 and RR34 were taken from outcrops that are not in close proximity to fluvioglacial gravel deposits. The sample ages place limits on the age of the underlying marine/littoral deposits. In each case there is a minor to moderate chance that the age is affected by partial bleaching. Therefore the reported age is regarded as the maximum age.

Of the relatively non-organic samples situated above beach deposits, RR11 was the closest to a marine cliff. The sampled horizon contained contains blocks of relatively angular, locally derived limestone greater than 10 cm in diameter. This material could have accumulated quickly from local streams or due to colluvial processes on the nearby limestone/siltstone dip-slope. So the depositional environment could result in delivery of partially bleached sediment.

Samples RR1, RR4, RR5, RR7, RR9, RR10, RR14, RR16, RR18 and RR19 were taken directly from beachsand or near-shore (shallow marine) sand. These samples contained insufficient silt for polymineral finegrain IRSL dating. No attempt was made to date K-feldspar in the sand size fraction by IRSL.

Samples RR12, RR13, RR15, and RR17 consist of beachsand and shallow marine sand/silt. In each case sufficient silt was present for polymineral finegrain IRSL dating. None of the sample sites are from outcrops that are in close proximity to fluvioglacial gravel deposits. In each case there is minor potential for the deposition of poorly bleached K-feldspar transported by longshore drift. So the ages should be reasonably accurate and should directly reflect the timing of deposition in a marine/littoral environment.

In terms of the precision of dating there are two primary issues impacting on accuracy. The first is relates to the dating process. The final age produced from the laboratory is assigned a 1 sigma error. The error varies between samples. It covers all quantifiable analytical factors including those that may occur during the measurement radionuclide abundance, the extent of radioactive disequilibrium, the percentage of potassium in feldspars etc. With regard to IRSL dating the 1 sigma error is typically around ± 10%. Errors quoted in connection with ages received from the laboratory do not exclude the fact that there may be external factors not considered in the analysis. These could include variation of coverbed thickness through time, changes in the level of the water table and changes in degree of saturation of the sampled material where it was always above the water table. The quoted error does not cover the potential for partial bleaching of the sediment. In dating using a polymineral finegrained sample it is not possible to detect the precise impact of partial IRSL bleaching as the effect can't be quantified. As discussed above, in relation to the proximal fluvioglacial environment it is difficult to

determine the impact of partial bleaching even in small aliquots of sand-sized K-feldspar grains. Detection requires a realization that the effect may be pervasive.

In light of the above discussion the stance taken in relation to luminescence ages on samples from North Westland is that one should neither put too much trust in the data nor be overly skeptical. More weight is placed on samples that are likely to be better bleached. Samples that are likely to be less well bleached (and thus overestimate the age) still put upper limits on the depositional age.

5.8 ADDITIONAL LUMINESCENCE DATING ISSUES IN OKARITO

5.8.1 Background

The dating programme for this PhD project produced a substantial number of MIS4/3 luminescence ages. In light of the prior (Suggate) model for the Late Quaternary history of North Westland these ages were unexpected. There are some notable differences between ages produced in this study and luminescence ages reported from several of the same localities by Preusser et al (2005). This raised questions with respect to the utility of this dating method in Westland and necessitated a detailed examination of previously published luminescence ages from Preusser et al (2005), Vandergoes et al (2005), Hormes et al (2003), Berger et al (1994) and Berger et al (2001). One question that needed to be resolved is whether or not the various luminescence ages can be reconciled. Another is whether or not the body of luminescence ages can be reconciled with dating by the radiocarbon method and with previous marine isotope stage correlations.

In this chapter 5 a number of common assumptions with regard to the climate history of Westland and marine isotope stage correlations for the Late Quaternary stratigraphy are examined. Discussion extends to:

- Validation of luminescence dating in Westland by other dating methods.
- Assessing whether luminescence ages reported in previous studies reflect the true depositional age of the sediments and whether the sample ages justify the published interpretation of the age of the sediments?
- Examination of dose rate measurements and an assessment of what is revealed in terms of the dating procedures.
- The impact of reassessment of previous numerical dating on the timing of climate change and vegetative response as revealed in pollen diagrams.

If it can be demonstrated that the previous interpretation of a substantial number of the published luminescence ages is likely to be incorrect then this creates an opportunity to revise and improve the understanding of the climate history of the entire region. In section 5.8 the discussion focuses on luminescence and radiocarbon dating carried out at Okarito in South Westland. Strictly speaking this locality is outside the thesis study area. However the dating carried out there is highly relevant to the climate history of the entire West Coast region, particularly during marine isotope stages 3 and 4. This is particularly important in terms of further discussion of the stratigraphy of North Westland carried out in chapter 6.

Vandergoes et al (2005) and Newnham et al (2007b) report a large number of radiocarbon and luminescence ages for cores taken from the Okarito Pakihi Bog. Cores from this site were also sampled intensively for pollen. The number of radiocarbon and luminescence ages obtained from this locality means this site has potentially yielded one of the best dated on-shore Late Quaternary proxy climate records in New Zealand to date, particularly for the period from 12 to 70 ka.

One of the primary issues discussed here is whether the lower of two organic silt layers at the Okarito Pakihi Bog was deposited primarily during MIS5 as claimed by Vandergoes et al (2005) or whether this unit was deposited primarily during MIS3. This distinction is critical because if it can be shown that the lower organic unit dates from MIS3 then several assumptions that underpin the "Suggate model" are more or less invalidated. More particularly if the lower organic silt is an early to middle

MIS3 deposit containing significant pollen from the *Nestegis* genus, then the presence of *Nestegis* pollen in late Quaternary soils cannot be taken to be evidence of fully interglacial conditions. Before discussing the palynology of the Okarito deposits a detailed examination of the dating of these deposits is required.

5.8.2 Use of Radiocarbon Dating in Validation of Luminescence Dating at the Okarito Pakihi, South Westland

The first point considered here is whether or not any of the luminescence dating methods listed above have been validated against any other non-luminescence numerical dating method in Westland. Full validation requires comparison against another well tested method, preferably over a period of several tens of thousands of years. Radiocarbon dating is the only radiometric method that has regularly been applied to Quaternary sediments in North Westland. This method has its own issues, in particular the potential for post depositional contamination by younger carbon and/or the potential for re-deposition of old carbon (e.g. wood fragments) in a younger sediment. So in Westland the validation of luminescence dating requires testing against a stratigraphic sequence that has been dated by radiocarbon and that the radiocarbon dating can also be validated. The location that comes closest to achieving this is the Okarito Pakihi. The primary studies are Vandergoes et al (2005) and Newnham et al (2007a, b).

Vandergoes et al (2005) and Newnham et al (2007b) describe a high-resolution record of pollen deposition in sediment cores taken from a basin near Okarito in South Westland. This work is summarised in figures 5.2 and 5.3 and is discussed here because it is highly relevant to the validation of luminescence dating and ^{14}C dating in Westland and because it reveals significant information on the timing of climate and vegetative change in this region. The Okarito site is situated at 43°14' 30"S, 170° 13'E and is 70m above sea level. Vandergoes et al (2005) discuss a single composite core with a depth of about 9.7 metres. This composite is assembled from a total of 13 individual cores. A large number of luminescence and ^{14}C ages are described in supplementary information published along with the main paper. The composite core can be divided approximately as follows:

Unit	Marine Isotope Stage Correlation Vandergoes et al (2005)	Environment
Upper organic silt/peat	Holocene	Pakihi/swamp
Upper largely inorganic grey silt with minimal tree pollen	MIS2, 3 &4	Lacustrine
Lower organic silt/peat	MIS5	Lacustrine
Lower largely inorganic grey silt	MIS6.	Lacustrine

This discussion proceeds on the basis of an assumption that there are two organic silt/peat units and two inorganic silt units as proposed by Vandergoes et al (2005). They suggest that from MIS6 to the end of MIS4 the Okarito Pakihi contained a lake at the position of the cores. In their interpretation this period covers the deposition of the lower inorganic silt, the lower organic silt and the lower part of the upper inorganic silt. So the lower organic silt is presumed to be a lacustrine deposit. Newnham et al (2007a) extend the duration of lacustrine sedimentation at Okarito Pakihi to the early Holocene, or in other words to the base of the upper organic silt/peat. This is interesting in light of the discussion of partial bleaching issues in relation to late Quaternary sediments from North Westland (sections 5.3 to

5.6 above). A fully lacustrine environment should promote slow deposition and potentially complete bleaching of silt during deposition.

Newnham et al (2007b) conducted a detailed study of ^{14}C dating procedures at several sites near Okarito. One of these sites, Galway Tarn (43°24'30" S, 169°52'24" E), was a lake from MIS2 to the present. The second is Skiffington Swamp (43°25' S, 169°59'30 E). The third is the Okarito Pakihi (43°14'30"S, 170°13'E). They report that Skiffington Swamp and the Okarito Pakihi were probably lakes until the Holocene period. MIS2 sediments deposited at Galway Tarn and the Okarito Pakihi did not suffer contamination (by younger carbon) to the extent found at Skiffington Swamp. Contamination appears to correlate strongly with depth of burial at these sites and probably with the extent of root penetration from above.

At the Okarito Pakihi one critical feature is the presence of the Kawakawa Tephra which has a known calibrated ^{14}C age of c. 27.09 ka (Lowe et al 2008). Under the assumption that this age is correct Vandergoes et al (2005) established that organic carbon in core samples from Okarito contains contamination by younger carbon. But note that on the basis of luminescence dating Grapes et al (2009) have contested the previously accepted age for the Kawakawa tephra and that the issues raised remain to be solved.

It is notable that the sample cleaning procedures adopted by Newnham et al (2007b) were sufficient to remove enough of the contamination from the Okarito samples to replicate the known ^{14}C age of the Kawakawa tephra. Cleaned pollen concentrates from samples taken a few cm either side of the Kawakawa Tephra match the known age of the tephra. This was also achieved in the same study for samples taken from Galway Tarn but not from those taken from Skiffington Swamp.

Newnham et al (2007b) found that root penetration was probably not an issue for the samples from the Okarito site. This is particularly relevant to ^{14}C dating by Vandergoes et al (2005) in the deeper portions of the various Okarito Cores, notably the upper portion of the lower organic silt and the lower portion of the upper non-organic silt. These sediments were submerged for most of their older history, buried initially by relatively impervious lake silt and then buried further by substantial organic rich overburden from the Holocene period.

The extent of contamination by young carbon at these three sites appears to be depth related. Newnham et al (2007b) hypothesised that root penetration from vegetation could be responsible for providing pathways for downward penetration of carbon. Samples from the Okarito Pakihi and Galway Tarn sites appeared to be currently beyond the depth of significant root penetration whereas the Skiffington Swamp site probably is not. These sites also have the potential advantage that they were lakes until the early Holocene so for c. 10 kyr or more following deposition of the Kawakawa Tephra there was minimal chance for root penetration.

The depth issue is likely to be very important in relation to ^{14}C dating in general in Westland. Pre-Holocene sites that are capable of yielding robust finite and/or "background" ages all share a common characteristic being considerable depth of burial of the dated horizons and typically burial beneath at least one relatively impervious layer. This is the case at Kamaka, Raupo, Sunday Creek, Cape Foulwind, Schulz Creek, Wilson's Lead Road, Bullock Creek and the Phelps Mine all of which are discussed in Chapter 6.

The classic site where rather intractable contamination by young ^{14}C has been studied in detail is Grahams Terrace in the Grey Valley (Hammond et al 1991) which shares one important characteristic

with Skiffington Swamp, being the relatively shallow depth of the Kawakawa Tephra marker horizon. The difficulties encountered at sites like these, where the young(er) carbon content can be as high as 35% of the sample (Skiffington Swamp, Newnham et al 2007b), have tended to give ^{14}C dating a poor reputation with respect to its use in Westland. Finite ages on samples thought (on other grounds) to have depositional ages greater than 50 ka have almost always been rejected as contaminated. This rejection tends to be applied regardless of the apparent success or failure of cleaning processes for carbon contamination.

In Westland, according to the published record, luminescence dating has not been fully tested in any stratigraphic sequence with a well-sampled ^{14}C dated record that covers a span of several tens of thousands of years. This might be possible at the Okarito Pakihi where a large number of ^{14}C and luminescence ages were reported by Vandergoes et al (2005). Although they went to considerable lengths to prepare contamination-free samples for dating by ^{14}C, Vandergoes et al (2005) were not prepared to use ^{14}C ages older than about 18 ka in the final age model. A substantial number of ages were generated with ages in the 18 to 49 ka window. Their reluctance to discuss potential implications of these ^{14}C results seems to have several causes as follows:

- An interpretation of the stratigraphy which leads them to assume an isotope stage correlation that might not be supported by the ^{14}C and luminescence ages.
- A lack of confidence in ^{14}C due to potential contamination of samples by younger carbon.
- The way in which they have assembled the composite age model for the composite pollen record (discussed at length below).

Validation of luminescence dating on "polymineral fine-grains" by Vandergoes et al (2005) {see the supplementary information for that paper} at Okarito relies on a simple regression of the two methods used ($IRSL_{(blue)}$ v $TL_{(UV)}$). This is shown in figures 5.4a and 5.4b below. The detailed sample results are presented in table 5.5a, 5.5b & 5.5c below. For the Okarito samples there appears to be a strong correlation between these methods, but that might mean no more than that both are subject to similar errors or biases. The regression seems to indicate that for this locality $IRSL_{(blue)}$ dating might be giving a reasonable estimate of the sample ages, potentially back as far as 75 kyr BP. For the next older sample (96 ka by $IRSL_{(blue)}$) the tight relationship breaks down with the TL age being far older (208 ka). Unfortunately the 3 samples that gave still older $IRSL_{(blue)}$ ages were not dated by $TL_{(UV)}$ and the 1σ errors for these samples are rather large. One additional sample had reached sample saturation.

In the Vandergoes et al (2005) study the contribution from cosmic rays to the total luminescence dose rate was calculated using the modern depth and this could result in a minor overestimation of the depositional age. No results were reported for anomalous fading tests. Dose rates were determined using the present sediment moisture content.

The majority of the samples that were dated by Vandergoes et al (2005) using luminescence methods had ages <75 ka. Generally the $TL_{(UV)}$ age is slightly greater than the $IRSL_{(blue)}$ age. Solely on the basis of the regression there is no particular reason why some samples should make it into the age model while others are rejected. The choice of samples used in the age model appears to be largely a matter of preference by Vandergoes et al (2005). There is no discussion of the reasons why several inconvenient ages failed to make it into the age model.

No infinite ages were produced by Vandergoes et al (2005) from materials that are stratigraphically above the lower organic silt. Two ^{14}C samples taken from positions within the lower organic silt were "beyond detection". Both are within the top 0.88 metres of this unit. A total of 7 ^{14}C results were

obtained for this interval, but the precise depths are not reported. The luminescence results from this horizon imply that one would expect to see some "infinite" or "background" ^{14}C ages here so the fact that such ages were obtained is not surprising.

The Vandergoes et al (2005) dating programme registered 13 ^{14}C dated samples with ages > 40 ka. Two were listed as "wood" (WK-6981 @ 42.1 ± 2.39 ka, WK-6982 @ 41.09 ± 3.7 ka) which came from the upper grey silt. This silt contains only a very small quantity of "tree" pollen. Both samples gave ^{14}C ages that are much older than the ^{14}C age of the surrounding sediment. One could ask: is the wood essentially in "growth position" or was it transported in? Is the wood genuinely older than the encasing sediment? The 11 adjacent samples were treated by an acid-base-acid wash method to remove potential contamination. These samples are listed in table 5.5. They display a nice progression of increasing age (no significant age reversals) with increasing depth. The age at the base of this sequence is 32.65 ± 0.75 ^{14}C ka. This appears to be approximately mid-way down the grey silt by comparison with nearby cores. Unfortunately the particular core from which this sequence of ages is derived (core 860) was not deep enough to penetrate the lower peat unit. If the sedimentation rate had been approximately constant through the deposition of the grey silt then a basal age of around 45 ka would not be particularly remarkable.

5.8.3 Age of the Upper Inorganic Silt at Okarito Pakihi

In order to come to grips with the radiocarbon dating at Okarito a digression into the luminescence dating is required at this point. One of the problems in understanding the Vandergoes et al (2005) age model is that the dated samples are spread across 13 different cores. Numerous core to core correlation assumptions were made and these influence the assembly of the final age/stratigraphic model. There is also the potential for unconscious "preference" of ages to fit a preconceived pattern, and selective exclusion to achieve the same result.

The most critical site in terms of the age model by Vandergoes et al (2005) is core 0004. Before discussing the luminescence dating for core 0004 the other luminescence ages from two other cores that penetrate the upper grey silt need to be discussed.

Cores 0212 and 0212b

These cores are illustrated in figure 5.1 below. The strata and luminescence samples in cores 0212 and 0212a are as follows:

Horizon	Core 0212	Core 0212b
Upper peat		
(Upper) Grey silt	}← Samples OBC1-OBC5	}← Samples OBD1-OBD16
Lower Peat		}← Samples OBC17, OBD18

Core 0212b penetrated the full thickness of the upper grey inorganic silt at Okarito. A total of 16 luminescence dating samples were taken from this unit in this individual core. The results are shown in table 5.5a They appear to have recovered close to a full profile though the upper grey silt in this is core,

except perhaps at the very top. The contact with the overlying peat is not illustrated in their supplementary figure 1 which includes graphic logs of all the holes drilled for the project.

Table 5.5a The sequence of luminescence ages in stratigraphic order from Core 0212b, Okarito Pakihi, Vandergoes et al (2005).

Site	Sample	IRSL(blue)	Post IR-OSL	Unit
101	OBD-1	13.2 ± 1.1	13.1 ± 1.2	Upper grey silt
102	OBD-2	13.3 ± 1.2	12.4 ± 1.3	Upper grey silt
103	OBD-3	16.2 ± 1.4	15.8 ± 1.4	Upper grey silt
104	OBD-4	18.4 ± 1.6	16.8 ± 1.4	Upper grey silt
105	OBD-5	24.4 ± 2.1	24.3 ± 2.2	Upper grey silt
106	OBD-6	30.6 ± 2.5	32.3 ± 2.7	Upper grey silt
107	OBD-7	25.5 ± 2.1	25.6 ± 2.2	Upper grey silt
108	OBD-8	34.1 ± 2.8	34.5 ± 2.9	Upper grey silt
109	OBD-9	33.7 ± 2.9	34.3 ± 3.1	Upper grey silt
110	OBD-10	31.8 ± 2.8	34.3 ± 3.2	Upper grey silt
111	OBD-11	34.7 ± 2.9	37.0 ± 3.2	Upper grey silt
112	OBD-12	31.9 ± 2.6	32.6 ± 2.7	Upper grey silt
113	OBD-13	44.9 ± 3.8	46.3 ± 4.3	Upper grey silt
114	OBD-14	43.2 ± 3.7	42.4 ± 3.6	Upper grey silt
115	OBD-15	48.4 ± 4.2	51.8 ± 5.0	Upper grey silt
116	OBD-16	50.1 ± 4.3	53.0 ± 4.6	Upper grey silt
117	OBD-17	54.6 ± 4.6	59.3 ± 5.7	Lower Organic Silt
118	OBD-18	66.4 ± 5.4	68.5 ± 5.8	Lower Organic Silt

In core 0212b the $IRSL_{blue}$ age at the transition from the lower organic silt upward into the upper grey silt is c. 50.1 ± 4.3 ka. For the purposes of this PhD thesis, $IRSL_{blue}$ is considered to produce more consistent ages than Post-IR-OSL in Westland (discussed in more detail later in this chapter). At core 0212b this certainly appears to be the case, with substantially less variance in sample ages and a more consistent progression of ages down the core. There is a rapid upward change in the percentage of tree pollen in the Okarito composite at the transition from organic-silt to grey-silt. This transition is from an interstadial assemblage to a stadial assemblage. At face-value the timing is consistent with the age of the ice maximum for the Aurora 5 glacial advance (48-46ka) in Fiordland from Williams (1996). It is also consistent with the timing of the glacial advance that produced the L2 loess and M4a moraine in the Saltwater Forest area of South Westland which has been assigned limiting ages of 45 to 50 ka by Almond et al (2001).

It should be noted that none of the 16 luminescence ages from the upper grey silt unit in core 0212b is from the early portion of MIS3 and none is from MIS4. All these samples are early-mid MIS3 to early Holocene in age. Strangely none of these excellent concordant ages make it into the age model for the composite pollen record of Vandergoes et al (2005). The ages listed table 5.5a are taken here as confirmation that no part of the upper inorganic grey silt can be readily correlated with MIS4.

Vandergoes et al (2005) dated cores 0212 (samples OBC1 to OBC5) and 0212a (samples OBD1 to OBD18) from Okarito intensively by luminescence methods. The $IRSL_{(blue)}$ results for the upper grey inorganic silt span the period from 12.6 ± 1.2 ka to 50.1 ± 4.3 ka with no significant age reversals. Unfortunately the upper grey inorganic silt wasn't dated by both radiocarbon and luminescence methods in the same individual core. Nevertheless, it can be argued that radiocarbon and luminescence

dating appear to converge to similar ages for what appears to be the same stratigraphic unit at the Okarito Pakihi.

Core 0212a does not contain the transition from the upper peat to the upper grey silt. However, core 0212 does contain this transition. The luminescence samples from core 0212 begin just below the contact between these units. So the transition is not dated securely. Nevertheless, the sample ages indicate that the transition occurred close to 12.6 ± 1.2 ka. This core appears to have penetrated the top portion of the upper inorganic silt but not the lower portion. The ages are listed in stratigraphic order in table 5.5b below.

Table 5.5b The sequence of luminescence ages in stratigraphic order from Core 0212, Okarito Pakihi, Vandergoes et al (2005).

Site	Sample	IRSL(blue)	Post IR-OSL	Unit
101	OBC-1	13.3 ± 1.3	11.7 ± 1.3	Upper grey silt
102	OBC-2	12.6 ± 1.2	12.5 ± 1.2	Upper grey silt
103	OBC-3	16.0 ± 1.4	15.6± 1.5	Upper grey silt
104	OBC-4	15.2 ± 1.2	15.6 ± 1.5	Upper grey silt
105	OBC-5	22.7 ± 1.9	21.3 ± 1.9	Upper grey silt

Collectively the luminescence ages from cores 0212 and 0121a span the full thickness of the upper grey silt. These two cores contain 21 concordant luminescence ages from samples in the upper grey silt. None of these ages give the slightest indication that any part of this silt ages from MIS4 or from the MIS4/5 transition.

Core 0004

Core 0004 is a short core with a potentially condensed sequence. Correlation of the lithological boundaries in this core with those in the other cores is open to question. A number of the absolutely key ages for the final composite age model are from this core as well as one of the key excluded ages. The strata in core 0004 are as follows:

Upper peat

(Upper) Grey silt ← Sample BPB1 (c.26 ka)

Lower Peat

Lower Grey silt ← Samples BPB2, BPB3, BPB4, & BPB5

In relation to core 0004 it appears that Vandergoes et al (2005) have lumped the two peats together as one. This means they consider that the lower grey silt in core 0004 matches with the upper grey silt from the other cores. The presence/absence of internal lamination seems to have an impact on this correlation.

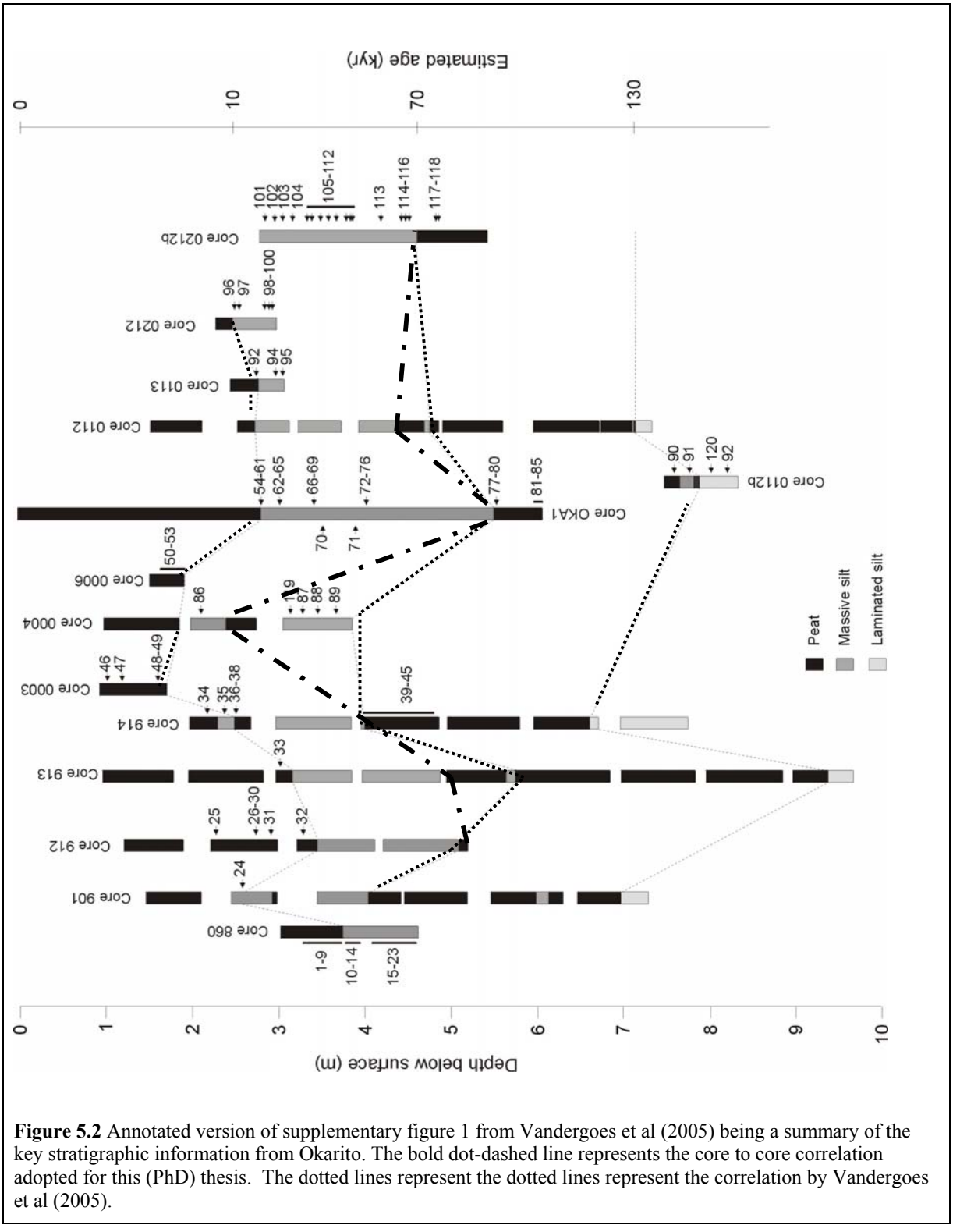

Figure 5.2 Annotated version of supplementary figure 1 from Vandergoes et al (2005) being a summary of the key stratigraphic information from Okarito. The bold dot-dashed line represents the core to core correlation adopted for this (PhD) thesis. The dotted lines represent the dotted lines represent the correlation by Vandergoes et al (2005).

Let us briefly treat core 0004 on its own merits. Luminescence sample BPB1 was taken from the highest grey silt bed in this core. This sample is situated about 1/3 of the way down the upper grey silt. The two luminescence ages for this sample are 28 ± 3 ($IRSL_{blue}$) and 24 ± 3 (TL_{UV}) and are nicely concordant with a mean of 26 ka. In terms of proportionality within the upper silt unit this sample is at

the depth that we might expect for the Kawakawa Tephra. Preusser et al (2005) claim that IRSL dating tends to underestimate depositional ages in Westland so there would be no reason to assume this particular sample overestimates the age of this grey silt.

Four luminescence samples were taken from the lower grey silt in core 0004. In stratigraphic order the luminescence ages from core 0004 are:

Code	Sample	$IRSL_{(blue)}$	$TL_{(UV)}$	Mean	Stratigraphic unit
86	BPB1	28±3	24±3	26±3	upper grey silt
119	BPB2	97±12	208±58	------	lower grey silt
87	BPB3	57±12	60±20	58.5±16	lower grey silt
88	BPB4	48±6	48±6	48±6	lower grey silt
89	BPB5	75±10	75±10	75±10	lower grey silt

Sample BPB2 from the lowermost grey silt in core 0004 at Okarito gave $IRSL_{blue}$ and TL_{UV} ages of 92 ± 12 and 208 ± 58 ka respectively. These ages don't overlap. Either the dating results for sample BPB2 grossly overestimate the true depositional age or the sample was incompletely bleached. BPB2 is not part of the final age model in Vandergoes et al (2005) and will not be considered further here.

The lower organic silt in this core was not dated directly. However, logic suggests that if BPB1 is correct then the lower organic silt is older than 26 ka. In that case it can't be part of the upper (Holocene) peat which has been demonstrated to have a basal age of c.13-15 kyr in several of the other cores from the Okarito Pakihi. In other words the upper grey silt in this core is not just a lens inside a thick upper peat. But that is effectively what Vandergoes et al are implying in the final age model. The luminescence ages for BPB1 very strongly suggest that the lower (deeper) peat in core 0004 should be correlated laterally with the lower peat in the other Okarito cores. Supplementary figure 1, (figure 5.2 above) from Vandergoes et al (2005) illustrates lateral correlations between the various cores and appears to indicate that the base of the upper (Holocene) peat is situated above BPB1. That means that the lower peat is probably not part of the deglacial/Holocene record. But they do not carry interpretation into supplementary figure 2 which is the age/stratigraphic model resulting in a stratigraphic contradiction between their figures 1 and 2. Another interpretation of supplementary figure 1 from is that the lower peat in this core is a separate unit, being neither the upper nor the lower peat recorded in the other cores. That would mean this unit is an intra-MIS3 organic silt, but this is not discussed by Vandergoes et al (2005).

The two luminescence two methods used are nicely concordant for samples BPB3, BPB4 &BPB5. The ages for these samples make it into the final age model. The mean of the ages is approximately 61±12 ka. On balance these ages imply that the lower grey silt in this core is likely to have been deposited during MIS4. So logically the transition between the lower grey silt and the lower organic silt two units in this core would appear to correlate with the MIS4/3 transition. This interpretation of sample ages for the strata in core 0004 does not make it into the final overall age-model for the composite core of Vandergoes et al (2005). They place BPB2, BPB3, BPB4, and BPB5 above the lower organic silt. This placement is not discussed or justified by them in the supplementary information and not mentioned in the main paper. It is suggested here that this is a fundamental weakness in their age model. The assumption must have been that core 0004 did not penetrate into the (main) lower organic silt.

Looking laterally across the other Okarito cores, and setting core 0004 aside briefly, it is clear that there are no other MIS4 numerical samples ages from the upper grey silt. But there are abundant MIS2 and MIS3 ^{14}C and luminescence ages from samples this unit. The oldest remaining $IRSL_{blue}$ age from the upper grey silt is 50.1 ± 4.3 ka (OBD 16 from core 0212b). This sample is situated at the transition between the upper grey silt and the lower organic silt and places firm constraints on the timing of the transition.

In figure 5.5a below the ages of all the Okarito luminescence samples are plotted against sample depth. It can be seen that most of these ages form a linear trend that could be interpreted as a more-or-less constant sedimentation rate. The samples that do not fall on this trend all come from core 0004. If one were to correlate core 0004 with the other cores (212, 0212b and 0112b) by simply doubling the sedimentation rate then all the samples would fall into the same general age-depth pattern.

Table 5.5c: Radiocarbon ages in stratigraphic order from core 860 at Okarito. The data are from Vandergoes et al (2005)

Core	Depth (cm)	Pretreatment	^{14}C Lab #	^{14}C Age	+/-1σ	Calibrated age range 2σ	Unit
860	373-379	wood	Wk-6984	10,060	100	12,284-11,226	Upper grey silt
	380-385	Acid-Base-Acid (ABA)	Wk-6809	10,630	200	13,108-11,927	Upper grey silt
	385-391	ABA	Wk-6808	17,760	170	21,912-20,371	Upper grey silt
	391-397	ABA	Wk-6807	20,550	180	-	Upper grey silt
	391-397	wood	Wk-6982	41,090	3730	-	Upper grey silt
	416-422	ABA	Wk-6806	25,130	190	-	Upper grey silt
	416-422	wood	Wk-6981	42,100	2910	-	Upper grey silt
	422-428	ABA	Wk-6805	27,770	270	-	Upper grey silt
	428-434	ABA	Wk-6804	27,660	270	-	Upper grey silt
	434-440	ABA	Wk-6803	29,390	340	-	Upper grey silt
	440-446	ABA	Wk-6802	29,060	310	-	Upper grey silt
	446-452	ABA	Wk-6801	29,230	330	-	Upper grey silt
	452-458	ABA	Wk-6534	29,650	820	-	Upper grey silt
	458-465	ABA	Wk-6533	32,650	750	-	Upper grey silt

If we take an approach that moves BPB2, BPB3, BPB4, and BPB5 out of the upper silt and places them into the lower silt (and into an alternative composite age model) then the host of ^{14}C ages that are provided and then ignored by Vandergoes et al (2005) take on an entirely new meaning. All the remaining ^{14}C and luminescence ages in the upper silt fall into MIS2 and MIS3. There are finite ^{14}C ages all the way down the upper silt. There are no infinite ^{14}C ages in the upper silt. There are finite and infinite ^{14}C ages in the top part of the lower organic silt, exactly as one would expect if it was deposited in the middle to early portion of MIS3. Note that Vandergoes et al (2005) went to great lengths to remove potential contamination from these samples so the ^{14}C ages look quite good. In core 860 (see figure 5.5c) there is a nice sequence of ^{14}C ages in the upper grey silt. The samples are situated at the same or greater depth than those reported from Okarito by Newnham et al (2007b). In the case of Newnham et al the cleaning of contamination by young carbon was probably more thorough but this is not sufficient reason to dismiss the Vandergoes et al (2005) ages listed in table 5.5c

Depth in Core OKA1 (cm)	Pretreatment	^{14}C Lab Code	^{14}C Age (+/-1σ)	Calibrated age range 2σ	Stratigraphic location/code (for Fig.1, Vandergoes Suppl info)	Position in upper inorganic silt
281-282	Wood	NZA 10085	10,267±70	**12,741-11,674**	54	
283	Bulk sediment (organics)	NZA 10991	9692±65	**11,209-10,760**	55	Samples all from the organic/inorganic transition at the top of the upper grey silt
283	Bulk sediment (organics)	NZA 11103	9758±70	**11,248-10,878**	56	
283	Leaf: *H. bidwillii*	NZA 11605	9553±60	**11,157-10,643**	57 Ψ	
283	Leaf: *Leptospermum*	NZA 11606	9591±60	**11,167-10,692**	58 Ψ	
283	Organic residue (density separate)	NZA 11633	9565±60	11,160-10,679	59 Ψ	
283	Organic residue (density separate)	NZA 11634	9627±60	11,178-10,701	60 Ψ	
283	Pollen concentrate	NZA 11635	9903±65	11,551-11,185	61 Ψ	
283	**Pooled weighted mean**		**9640±27**	**10,762-11,167**	**10,964**	
300-301	Organic residue >125 µm	NZA 11200	11,215±65	13,431-12,920	62	
300-301	Pollen concentrate	NZA 11076	11,975±65	15,297-13,647	63 Ψ	About 10% of the distance down the upper grey silt
300-301	Pollen concentrate	NZA 11075	11,802±65	15,188-13,470	64 Ψ	
300-301	Pooled weighted mean		**11,888**±46	**13,611-15,191**	**14,401**	
302-303	Organic residue <125 µm	NZA 11105	12,231±60	15,425-13,876	65	
340-342	Pollen concentrate	NZA 11199	14,504±70	17,917-16,874	66 Ψ	
340-342	Pollen concentrate	NZA 11197	14,302±70	17,672-16,650	67 Ψ	About 20% of the distance down the upper grey silt
340-342	**Pooled weighted mean**		**14,403**±49	**16,769-17,774**	**17,271**	
340-342	Organic residue (density separate)	NZA 11198	13,340±110	16,552-15,082	68	
342-343	Organic residue <125 µm	NZA 11104	14,445±70	17,844-16,809	69	
349-350	Bulk sediment (organics)	NZA 10082	12,069±60	15,144-13,671	70	About 25% of the way dn
390-391	Bulk sediment (organics)	NZA 10090	11,228±90	13,763-12,913	71	About 40% of the way dn
400-403	Organic residue (density separate)	NZA 11201	9053±85	10,400-9917	72	Samples all from just above the mid-point within the upper grey silt
400-403	Organic residue (density separate)	NZA 11077	14,689±85	18,137-17,065	73	
400-403	Pollen concentrate	NZA 11106	19,330±120	23,696-22,193	74	
400-403	Pollen concentrate	NZA 11107	20,110±120	24,532-23,053	75	
400-403	Pollen concentrate	NZA 11108	19,500±170	23,948-22,331	76	
553-554	Bulk sediment (organics)	NZA 10091	31,080±490	-	77	Samples all from just below the basal transition from the upper grey silt to the lower organic silt
554-555	Pollen concentrate	NZA 11202	42,200±1200	-	78	
554-555	Pollen concentrate	NZA 11203	43,900±1500	-	79	
556-557	Organic residue <125 µm	NZA 11109	>45,200	-	80	
596-597	Organic residue (density separate)	NZA 11204	>45,900	-	81	Samples within the lower organic silt aproximately 40 cm below the base of the upper grey inorganic silt
596-597	Organic residue (density separate)	NZA 11205	>45,300	-	82	
598-599	Organic residue <125	NZA 11110	45,400±1800	-	83	
598-599	Organic residue >125 µm	NZA 11206	36,770±620	-	84	
599-600	Bulk sediment (organics)	NZA 8199	35,630±430	-	85	

Table 5.5d: List of ^{14}C ages from core OKA1 of Vandergoes et al (2005).

The wood samples from core 860 are generally substantially older than adjacent samples but the ages are not necessarily caused by contamination. These wood fragments may be a component of the

sediment that was washed into the lake basin after being eroded from older deposits. Given that eroded/transported wood fragments are likely to have had a specific gravity not much greater than 1.0 (coal has an SG of about 1.2 to 1.3) it would not be surprising to find such material being deposited in association silty sediment in a shallow lake environment. This is particularly likely if the surrounding landscape has been partially denuded of forest and has become more vulnerable to soil erosion. Note that the modern mean annual rainfall near the coast in South Westland is > 3.5 metres (3.71 m at Lower Whataroa, 3.86 metres at Mahitahi [Jacobs River]) so scouring of shallow deposits slopes near the Okarito Pakihi (former lake) during frequent heavy rain would not be unexpected.

With the exception of the wood samples the other ^{14}C ages in core 860 become progressively older with increasing depth and there are no significant age reversals. Interestingly, the ^{14}C ages in this part of the core span the latter portion of MIS3. There is no hint of the early MIS3 to MIS4/5a age distribution claimed by Vandergoes et al (2005) for the lower part of this unit. The counter argument is that the core did not penetrate to the base of the grey silt. If the suggestion of "foreign" origin for the wood fragments seems far fetched then consider the following quotes from Newnham et al (2007a) which is a study of ^{14}C contamination in the Quaternary sediments of South Westland:

> "it has been demonstrated that catchment disturbance can result in inwashing of old carbon into lakes while peat sites can be unaffected".
>
> "lake sites, or other depositional settings where root penetration can be discounted, would seem to pose a much lower risk of contamination by younger carbon. At the two sites not seriously affected by contamination, ages on both pollen concentrates and organic residues are generally in line with, or slightly younger than, the established age of the tephra benchmark, suggesting that, with careful site selection, reliable chronologies can be achieved in this region."

Only two of the 13 cores at Okarito contain abundant ^{14}C ages in the upper grey inorganic silt. These are cores 860 and OKA1. There is clearly evidence for contamination by young carbon at the base of the upper grey silt in core OKA1. However, this is not strong evidence that the age at the base of this unit is greater than 45 ka. Note that the same transition is dated by $IRSL_{(blue)}$ at ~50.1 ± 4.3 ka (sample OBD-16). This is well short of the MIS5a/4 transition (say 75-70 ka) suggested by Vandergoes et al (2005). At this point it is pertinent to note that there are a number of fundamental issues raised in this thesis with respect to dose rates for luminescence dating. Dose rates measured for samples taken for luminescence dating for this PhD project appear to be systematically greater than those measured for the Okarito study by Vandergoes et al (2005) and those measured for another study in North Westland by the Preusser et al (2005). This issue is discussed at length below.

Core	Depth	Pretreatment	^{14}C Lab Code	^{14}C Age (+/-1σ)	Calibrated age range 2σ	Stratigraphic location/code (for Fig.1, Vandergoes Suppl info)	Code	Position (this PhD)
914	217-222	ABA	Wk-7642	9490	100	11,163-10,429	34	Upper organic silt
914	240	wood	Wk-7641	9800	230	12,110-10,556	35	Inorganic lens
914	250-263	organic silt (whole)	Wk-8697	10,310	100	12,806-11,643	36	Upper organic silt
914	250-263	organic silt (organics)	Wk-8698	10,320	100	12,811-11,659	37	Upper organic silt
914	250-263	organic silt (silt)	Wk-8699	10,770	140	13,127-12,352	38	Upper organic silt

Table 5.5e: List of ^{14}C ages from core 914 Vandergoes et al (2005).

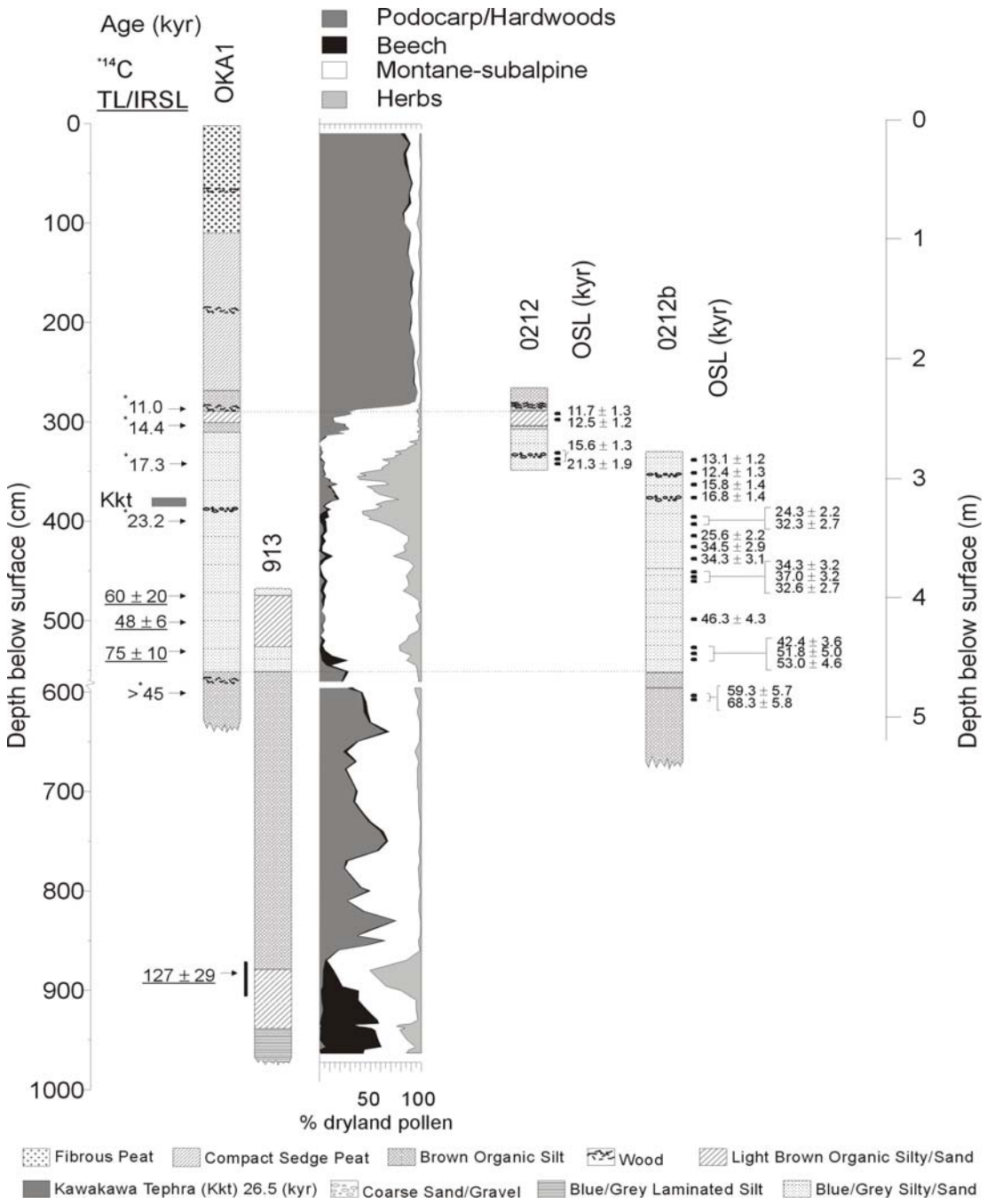

Figure 5.3 Reproduction of supplementary Figure 2 from Vandergoes et al (2005) which positions luminescence ages against the stratigraphy for cores 0212 and 0212b and the summary pollen diagram developed from cores OKA1 and 913. According to Vandergoes et al (2005) "Radiocarbon ages above the Kawakawa Tephra represent a pooled weighted mean of the age results indicated by Ψ in Supplementary Table 1, at 2 σ level, in calibrated kyr. Underlined luminescence ages are TL and IRSL ages correlated from cores 0004, 0112b and 0113 (see Supplementary Fig 1, Table 2). A pooled weighted mean age of 127 ± 29 kyr is derived from IRSL ages from core 0112b, Supplementary Table 2." Note the disconnection between the luminescence ages "correlated" onto core OKA1 on the left and those reliably positioned in cores 0212 and 0212b on the right.

5.8.4 Age of the upper inorganic silt at Okarito Pakihi

In figure 4 of their supplementary information Vandergoes et al (2005) produce a nice regression of IRSL age versus post IR-OSL age for samples from Okarito. This result is reproduced in figure 5.3 below. This linear regression demonstrates some consistency between the two luminescence dating methods. So regardless of whether the dating results are meaningful at least the two methods are likely to be in error by a similar amount. The regression provides no justification for preference in terms of the particular sample ages that should be used in an age-depth model. So why are the luminescence ages that appear to be best, i.e. those younger than 55 ka, largely not used in the age-depth model? Why are samples BPB5 and BPB3 preferred in the age model when they do not constitute part of the validation of the dating method (the linear regression)? These two samples are critical to the model but were not dated by multiple methods and additionally suffer from relatively large 1σ errors.

Collectively the 26 excluded numerical ages from middle MIS3 to early MIS2 span the bulk of the upper "blue-grey inorganic silt" that contains only minor tree pollen. Most of these ages are from middle to late MIS3 rather than early MIS3. By not using these ages Vandergoes et al (2005) avoid having to discuss a potential warm phase in the early portion of MIS3.

From figure 5.2 it can be seen that an upper grey silt is dated by luminescence methods in 3 cores being core 0004, core 0212, and core 212b. The luminescence ages from cores 0212 and 0212b span the full thickness of the upper grey silt. They produced a large number of concordant luminescence ages. As discussed above one sample was taken from the upper grey silt in Core 0004. This sample (BPB1) produced a concordant age as well. So the upper grey silt in core 0004 can be correlated with the upper grey silt in cores 0212 and 212b. Collectively the luminescence ages imply unequivocally that the upper grey silt in these cores was largely deposited during middle MIS3 to MIS2 and has a basal IRSL age of approximately 50 ka (OBD-16).

Core 0004 also contains a lower organic silt. In the age/stratigraphic model preferred by Vandergoes et al (2005) this organic silt, which must be older than 26 ka (mean age for BPB1), does not extend laterally into the other cores dated by luminescence methods. This interpretation is rather tenuous.

As can be seen in figure 2 (or figure 1 of the Vandergoes et al supplementary information) they show the uppermost grey silt unit in core 0004 merging into the upper organic silt/peat at core 914, where there is a thin lens of grey silt. The grey silt bed in core 914 is bounded by 14C sample imply an age at the top no younger than 10 ka and an age at the base no older than 13 ka. The grey silt bed in core 914 was also sampled directly for 14C dating. At 1δ the resulting age limits for this sample are 10.5 ka and 12.1 ka. Yet they wish readers to accept correlation across to a grey silt bed in core 0004 that, near to the top, has a concordant luminescence age (BPB1) of c.26 ka. No matter how appealing it may appear, on the basis of ^{14}C dating (see table 5.5e) and luminescence dating this lateral stratigraphic interpretation is unlikely to be correct.

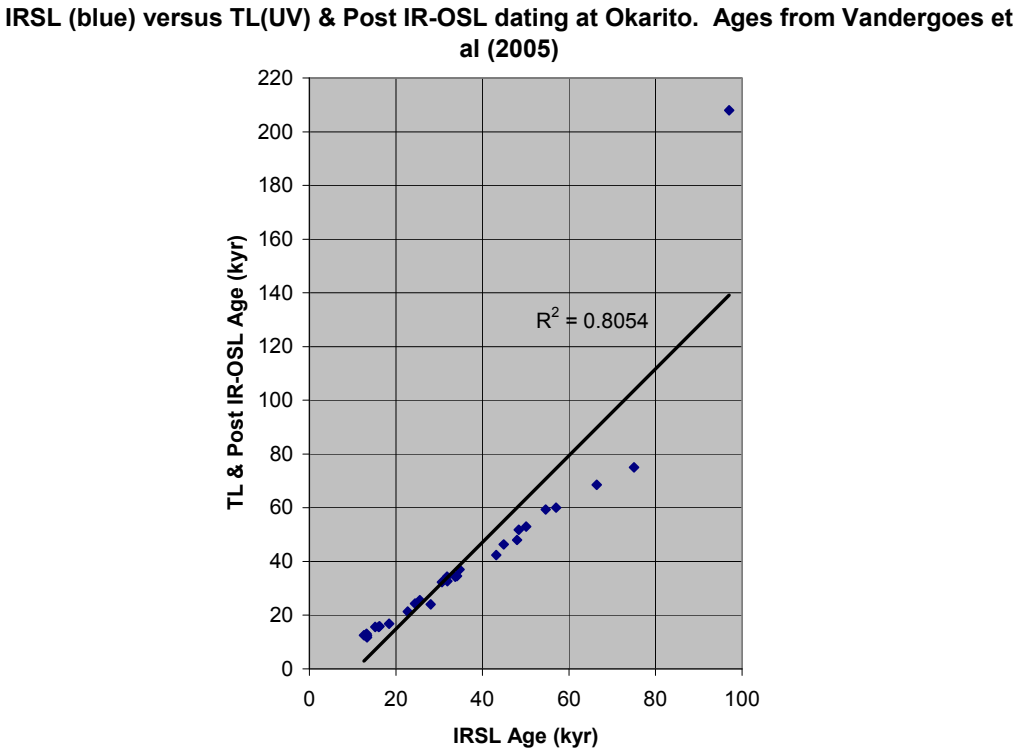

Figure 5.4a Linear regression for luminescence ages from the Okarito Pakihi

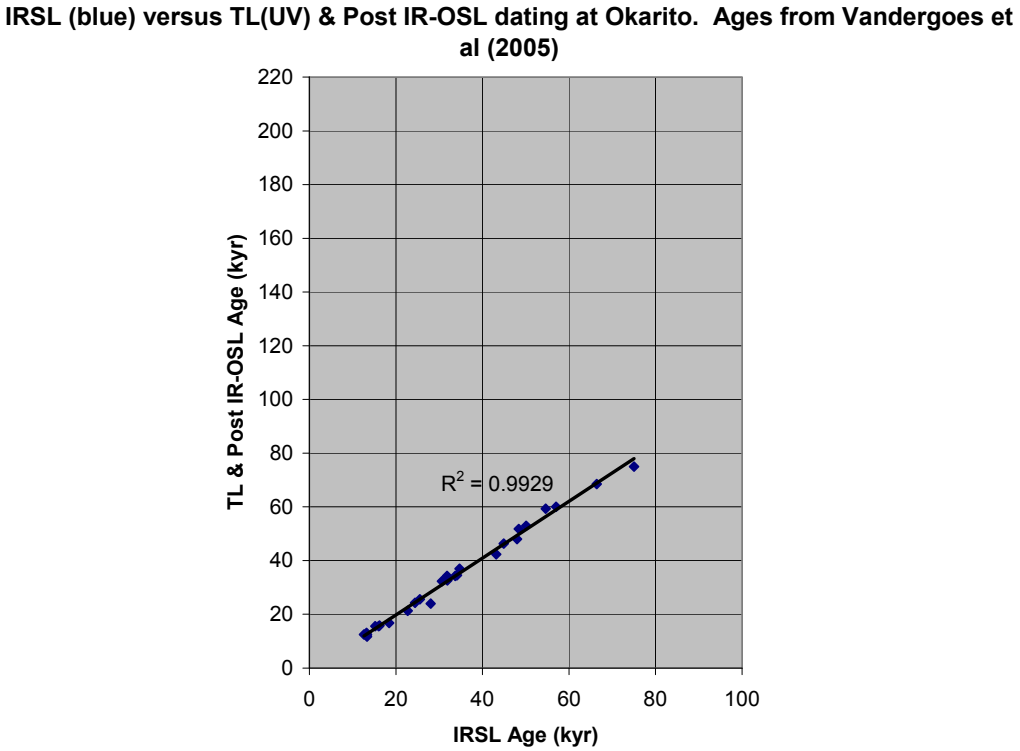

Figure 5.4b Linear regression for luminescence ages from the Okarito Pakihi, but varying from Fig 5.4a by omitting the "oldest" sample.

As can be seen in figure 2 Vandergoes et al (2005) have matched the lower grey silt from core 0004 with the upper grey silt from cores 0212 and 212b. They do not discuss this correlation or the contradictions created by it. There are three concordant $IRSL_{(blue)}$ sample ages from this unit in core 0004. The average age for these samples is c. 60 ka. Under the logic of the Vandergoes et al correlation the lowermost grey silt in core 0004 spans the interval from about 15 ka to 75 ka. It must be so because, as noted above, they illustrate the uppermost grey silt in this core as a sub-unit within the Holocene organic silt. So the physical core above BPB3 (which is dated by $IRSL_{(blue)}$ at 57± 12ka and code = 87) upward to the base of the overlying organic silt (supposedly Holocene but containing BPB1 at 26 ka high up the unit) which is around 40 cm in thickness (see figure 5.2) spans c. 40 kyr of supposedly continuous deposition. The likelihood that this is correct is modest. This thin interval in core 0004 is supposedly located tightly against the base of the Holocene also contains BPB2 which had saturation and/or partial bleaching issues as discussed above. In figure 5.3 (this PhD) Vandergoes et al (2005) have positioned BPB3 such that there is an *apparent* distance of about 180 cm to the base of the Holocene.

5.8.5 Age of the lower organic silt at Okarito

As discussed above there are ^{14}C ages within the top 1 m of the lower organic layer that are essentially "infinite". These can't really be used in an age model except that they tend to indicate the upward transition from the lower organic silt to the upper grey silt is probably no younger than about 43 ka.

Vandergoes et al (2005) avoided discussion of the ages for samples OBD 17 (IRSL, 54.6 ± 4.6 ka) and OBD 18 (IRSL, 66.4 ± 5.4 ka), both of which were taken from the lower organic silt. These are the only luminescence samples that are **clearly** demonstrated to have come from this unit and they are not MIS5a ages. One sample (OBD 17) has an MIS3 age.

The local MIS4/3 transition probably occurred from 63 to 60 ka. The timing of this transition can be seen in the SST records at MD97-2120 (figures 4.15a & 5.6), MD97-2121 (figure 4.15b) and MD06-2986 (figure 5.7). Although the preferred age for sample OBD 18 places it in MIS4, at 1δ the sample clearly could be from sediment deposited during MIS3.

5.8.6 Age of the lower inorganic silt at Okarito Pakihi

From figure 5.2 is can be seen that the transition from between a lower organic silt downward into a lower grey inorganic silt has been dated in two cores being cores 0004 and 0112b. In the interpretation of Vandergoes et al (2005) these two transitions are not of the same age.

In core 0004 samples BPB3 (57±12 ka by $IRSL_{blue}$ and 60±20 ka by TL_{UV}), BPB4 (48±6 by $IRSL_{blue}$ and by TL_{UV}) and BPB5 (75±10 $IRSL_{blue}$ and 75±10 TL_{UV}) are situated in the lowermost grey silt unit for that core. These samples are situated within 100 cm of the base of the overlying organic silt. The average of the IRSL ages for these samples is 60±9 ka which places a limit on the age of the upward transition into the organic silt. This age is clearly similar to that of the MIS3/4 transition which occurred at ~63-60 ka in the marine cores referred to above. So there is agreement with Vandergoes et al (2005) on the likely age for this silt, but not on the lateral correlation. The simple interpretation favoured in this (PhD) study is that these samples date the lower grey silt. There is a higher grey silt in core 0004 which appears to be an MIS2/3 deposit.

The Vandergoes et al (2005) age-depth model is effectively set or pinned by luminescence samples OKA1, OKA2, and OKA4 from core 0112b. They use the average of these ages to define the age of

the transition from an organic silt unit downward into a grey silt unit. In figure 5.2 above one can observe that this short core (and the luminescence samples) is at a substantial depth.

The following $IRSL_{blue}$ ages are from core 0112b and are in stratigraphic order:

OKA4: Has an age of 107 ± 30 ka and is situated a few cm above OKA3 and is just above the lower inorganic silt.
OKA3: Has an age of 177 ± 49 ka and is situated above OKA1 at the organic/inorganic silt transition.
OKA2: Is at saturation and is situated in the lower grey inorganic silt
OKA1: Has an age of 133 ± 64 ka and is situated in the lower grey inorganic silt below OKA2 & OKA3.

Samples from the lower grey silt in two of the Okarito cores (cores 0004 & 0112b) were approaching saturation and that this is admitted by Vandergoes et al (2005). Note that OKA1, OKA3 and OKA4, despite their clearly problematic nature, are part of the age model by virtue of a "pooled weighted mean age" of 127 ± 29 kyr. The arithmetic average is 139 ± 48 kyr. So how was the age and error weighting achieved? This was not discussed by Vandergoes et al (2005) but the procedure is discussed below. In the supplementary information Vandergoes et al (2005) state that "the large uncertainties for the samples from the lower silt layer (OKA 1-4) are due to the fact that the luminescence signal reaches saturation." Given that these samples are "approaching saturation" it is not clear how much emphasis can be placed on them. As discussed in relation to figure 5.5a below these samples are very deep compare to those from the other luminescence dated cores from Okarito.

The potential age spread for samples OKA1, OKA3 and OKA4 at 1σ is 69 ka to 236 ka. At 2 σ there is a significant probability that the age is younger than about 69 ka and similarly a significant probability that the age is greater than 236 ka . The samples are from separate horizons at different levels in the core, rather than 3 repeats on the same sample or horizon. The level of precision is rather underwhelming. The claim by Vandergoes et al (2005) that this transition in sedimentology and pollen content occurred at the MIS6/5e transition is not strongly supported by the age of these three samples. Assuming that the same unit is being dated this conclusion is reinforced by the distinct possibility that luminescence samples BPB2, BPB3, BPB4, and BPB5 were taken from below the lower organic silt. These samples indicate the lower inorganic silt may date from MIS4. On the other hand the grey silt dated by OKA1, OKA3, and OK4 could be a separate, deeper unit separated from the lower grey silt in core 0004 by another organic silt. There certainly is a wide depth separation.

5.8.7 Age-Depth Model at Okarito

In total Vandergoes et al (2005) report the ages of 119 samples, most of which yielded numerical ages, either by IRSL, post-IR-OSL, TL or ^{14}C. The ages for the Okarito cores are presented in the supplementary information for that paper. The chronology established for the site by Vandergoes et al (2005) is debatable. Only 19 of the 119 dated samples were used in the final age model, the usage being rather selective. Only 4 of 13 cores were used in constructing the age model. The final pollen record comes exclusively from two cores being core 913 and core OKA1.

The age-depth model adopted implies that there must be a large variation in sediment accumulation rate at the Okarito Pakihi. The composite core is dated using the radiocarbon ages down to about 3.5 m by Vandergoes et al (2005). Here the age is 17.3 ka, which is reasonable given the depth of the Kawakawa Tephra (c. 27 ka) at about 5.0 metres. Below the Tephra the next 4 to 5 metres supposedly contains all of MIS3, 4, 5a, 5b, 5c, 5d, 5e and part of MIS6. That is 110 to 120 kyr of sedimentation

(or at least of preservation). Vandergoes et al (2005) make no mention of significant unconformities in the profile so it is assumed here that they consider the record to be continuous.

Only one specific ^{14}C age older than 18.1 ka is used in the age model. This sample which is illustrated in a position below the Kawakawa Tephra in figure 2 of Newnham et al (2007b) and figure 2 of the supplementary information for Vandergoes et al (2005) has a calibrated age of 23.2 ka. It is not recorded in the equivalent figure 1 of Vandergoes et al (2005). It is not entirely clear which sample this age relates to but the most likely candidates are NZA11077, NZA11106 and NZA11108 or an average of these samples. From table 1 in the supplementary information for Vandergoes et al (2005) it is appears that these three samples are not considered to be part of the age model. Samples that are part of the age model are clearly defined as they are marked with the symbol Ψ. Although these ^{14}C ages are not part of the age model nevertheless Newnham et al (2007b) seem to imply in a visual manner in their figure 2 that they are. This is essentially a reproduction of figure 2 in the supplementary information to Vandergoes et al (2005). The strategy is applied to the listing of luminescence ages in the same figures by Newnham et al (2007b) and Vandergoes et al (2005). In figure 2 of the Vandergoes et al (2005) supplementary information (a graphic log of the stratigraphy) they list 28 luminescence ages. But in tables 2 and 3 of the supplementary information only 10 of the ages are marked with the Ψ symbol indicating inclusion in the age model. This gives the visual impression that the age model is backed by a huge number of numerical ages, whereas in reality many of the ages actually contradict the model, and a number of the ages could be miss-located.

There are 17 ^{14}C ages older than 25 ka that were not used in the age model. Perhaps some of the ^{14}C ages that are younger than the Tephra are redundant, given that there are at least 45 of them. The ^{14}C results presented in the supplementary information by Vandergoes et al (2005) include samples that are treated for possible contamination by younger carbon. Treated and non-treated samples differ in age but it is debatable that the differences are sufficient to warrant outright rejection or non-usage of all ^{14}C ages greater than 18 ka.

Only 10 IRSL/TL ages are incorporated in the age-depth model for the composite core from Okarito so from the total of 34 IRSL/TL there are 24 that are not used in the age-depth model. The youngest IRSL/TL age used in the age model is c. 42.4 ± 3.6 ka. There are 20 luminescence ages that are younger than 42 ka, 13 being younger 25 ka. So 26 dated samples (luminescence and ^{14}C) from middle MIS3 to early MIS2 are excluded from the age model. Two other inconvenient IRSL/TL dated samples with slightly older MIS3/4 ages are not used in the age model.

If one plots the luminescence age v depth for the adjacent cores that produced these samples (particularly cores 212, 0212b, and 0112b) then a reasonably smooth sedimentation rate is achieved from about 13 ka to 140 ka (figure 5.5a below). This rate is greater than would be anticipated on the basis of age-depth model adopted by Vandergoes et al (2005). As discussed above the implication is that 3 of the critical luminescence samples from core 4 could have been mislocated from below to above the lower organic.

In the supplementary information to Preusser et al (2005) it is indicated that there could be equilibrium problems with OBD-17 and OBD-18. So they were not included in the age model. But in terms of the age v depth chart (figure 5.5a) they fit nicely on the trend defined by the samples higher up the same core, giving support for a relatively young age for the peat.

As can be seen clearly from figures 5.2 and 5.5a the oldest samples collected from the Okarito Pakihi (OKA1, OKA3, and OKA4 from core 0112b) are very deep when compared with the other samples.

The samples could be dating a genuine MIS6 deposit but it requires a leap of faith that the stratigraphic correlation by Vandergoes et al (2005) is correct. It is not clear from figure 5.2 that the organic silt dated in core 0112b (OKA1, OKA3, and OKA4) is the same as the organic silt unit dated by luminescence methods at much shallower depths in several of the other cores.

When potted out on an age-depth chart (figures 5.5b, 5.5c) the ^{14}C ages also imply a reasonably steady sedimentation rate through MIS2 and well into MIS3. The mix of infinite and borderline ^{14}C dates in the buried organic silt in no way invalidates the possibility that this silt could be an early MIS3 deposit. There are two very distinct ^{14}C age outliers. These are "wood" samples that could have ages that are genuinely different to that of the enclosing sediment (washed into a shallow lake or swamp after erosion from a nearby area and showing a true age of growth?).

Figure 5.5a: $IRSL_{(blue)}$ age vs sample depth in cores from Okarito Pakihi, South Westland. Data from Vandergoes et al (2005)

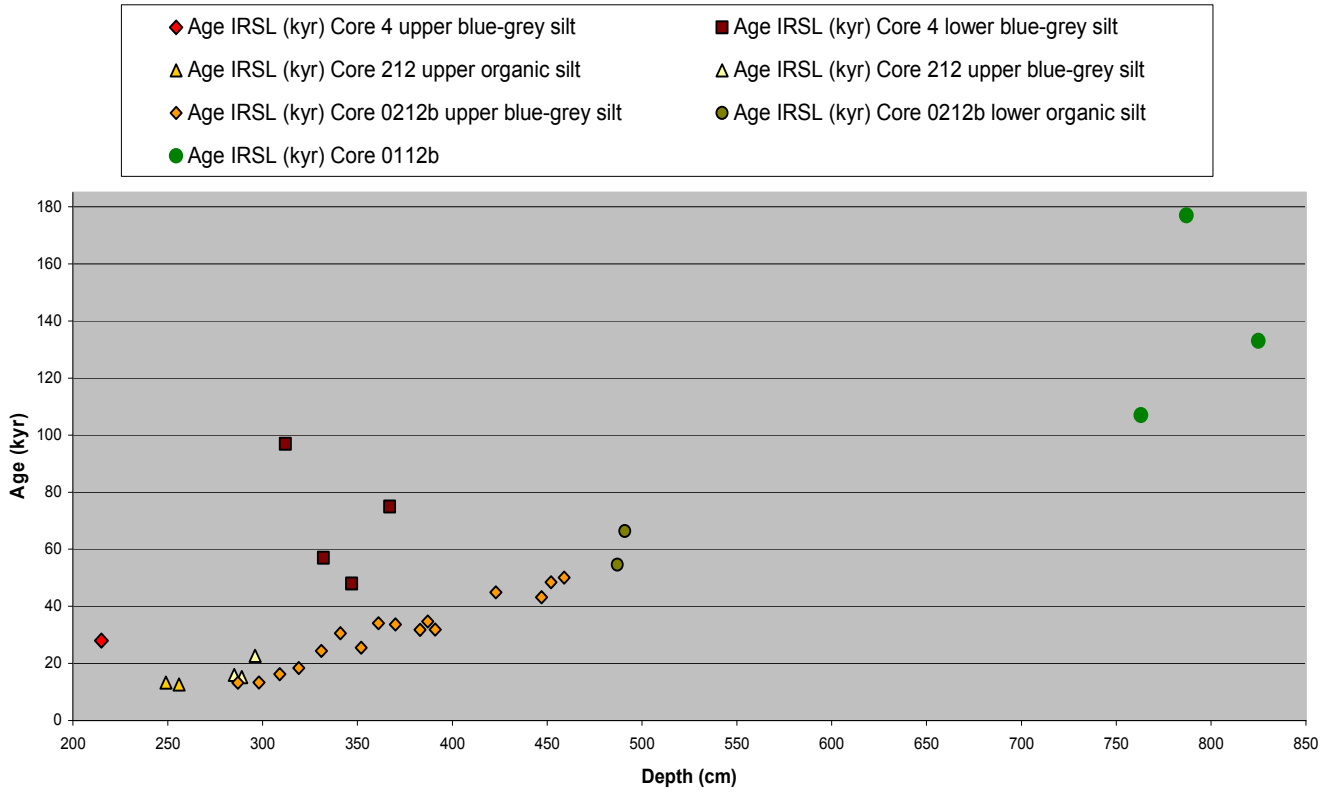

Figure 5.5b: ^{14}C Age vs sample depth, core OKA1, Okarito Pakahi, South Westland. Data from Vandergoes et al (2005)

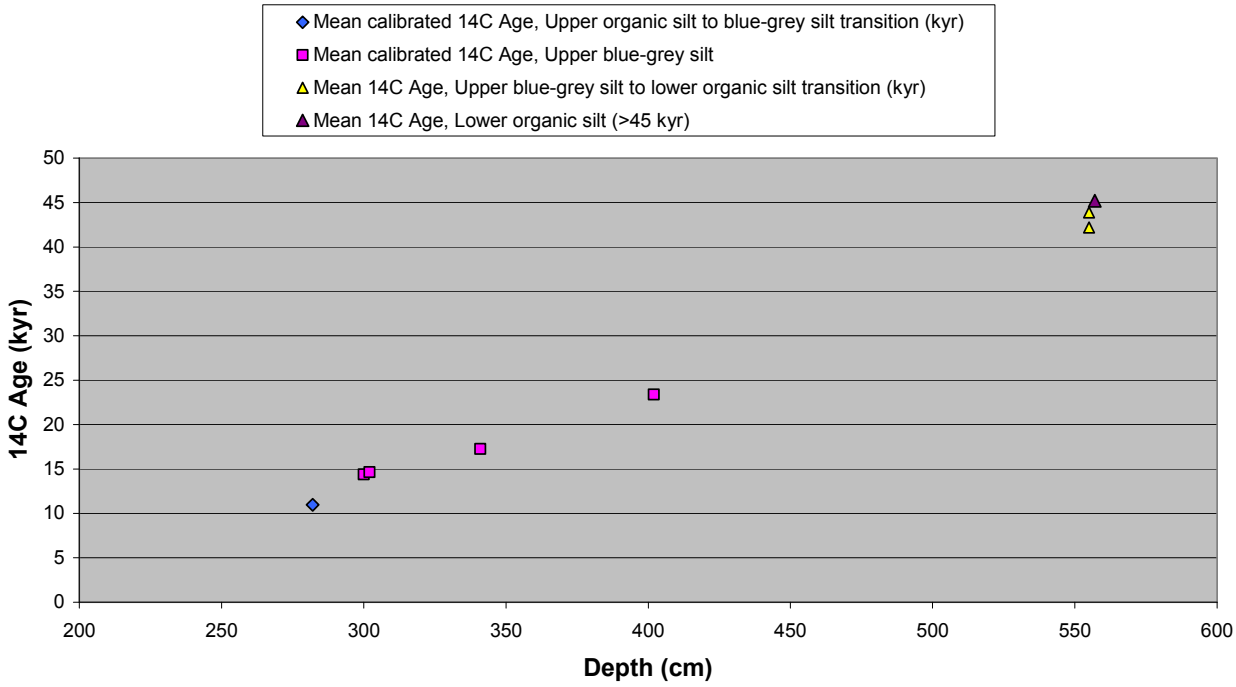

Figure 5.5c: ^{14}C Ages vs sample depth, core 860, Okarito Pakihi, South Westland. Data from Vandergoes et al (2005)

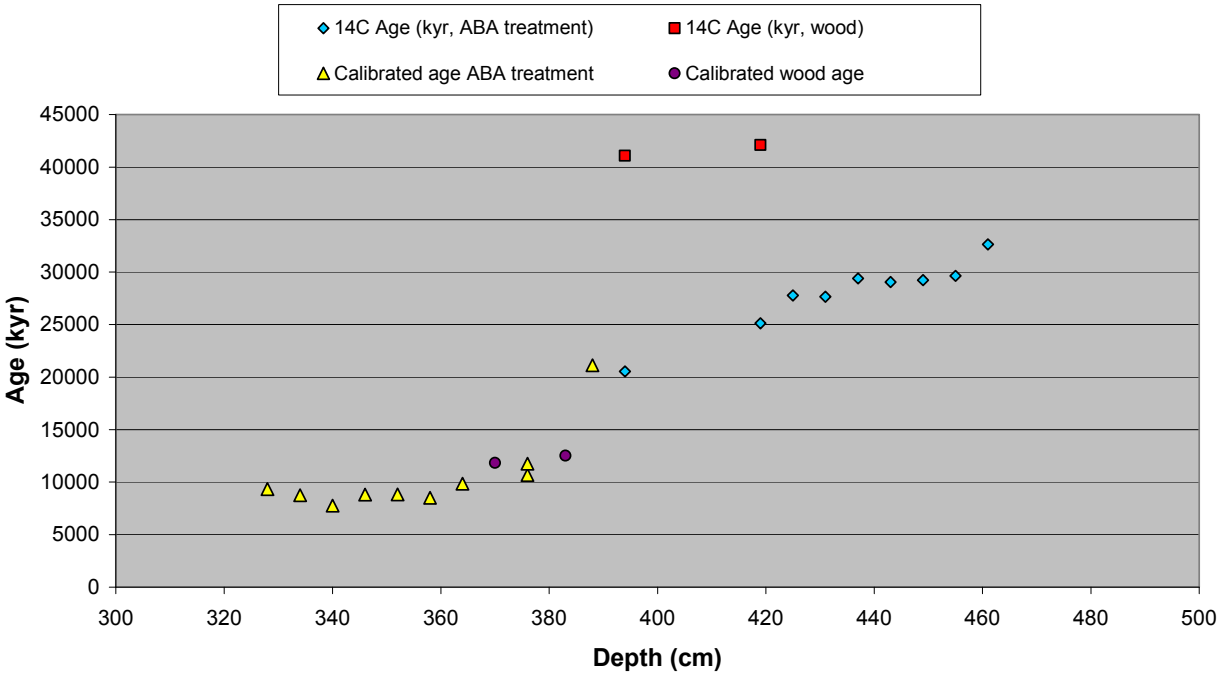

In relation to the age-depth model for the Okarito cores by Vandergoes et al 2005 the main points taken from this discussion are as follows:

- All numerical ages between 18 ka and 42 ka were disregarded in assembling the age model.
- Two cores were sampled for pollen. The pollen record is a (spliced) composite from these two cores. Radiocarbon ages were obtained from these cores but all of the samples that made it into age model are dated at less than 16 ka.
- The age model does not contain IRSL or TL ages from these two "pollen" cores.
- All the numerical ages older than 16 ka that they actually used are correlated from the other cores so the samples that are used are all older than 42 ka.
- There are a number of inconsistencies in the use of ages from the Okarito Pakihi.
- Luminescence samples from core 0212b clearly define the age of the upper portion of the lower organic unit indicate that the upward transition from this unit into the overlying grey silt occurred at around 50 ka. This timing is well into MIS3. These sample ages do not make it into the Vandergoes et al (2005) age-depth model.
- The age of the transition from the lower organic silt down into the lower grey silt is more problematic. If one takes the simplest view of the stratigraphy and luminescence samples from core 0004 then this transition probably falls at the MIS3/4 boundary.
- The weight of evidence from the ^{14}C and luminescence dating carried out at Okarito favours an interpretation in which the lower organic silt was most likely deposited during the early portion of MIS3. Alternatively the stratigraphy may be more complex than previously recognized, with more than one buried organic silt and a lack of stratigraphic continuity across the locality.

The hypothesis advanced here in relation to the composite core and pollen record from Okarito is that:

- The 0.0 to 3.0 m deep portion of pollen record (the upper organic silt/peat) from the Okarito composite core dates from the Holocene period.
- The 3.0 to 5.5 m deep portion (upper grey inorganic silt) of the Okarito composite core dates mainly from the MIS2/1 transition back to the middle of MIS3.
- The 5.5 to 8.6 m deep portion (lower organic silt) of the Okarito composite core derives from early to middle MIS3. This is an interpretation that is (more or less) in accord with the numerical dating by Vandergoes et al (2005).
- The 8.6 to 9.7 m deep portion (lower grey inorganic silt) of the composite core derives from MIS4, an interpretation that is also in accord with the numerical dating by Vandergoes et al (2005).

This hypothesis fits with the simplest interpretation of the numerous luminescence and radiocarbon ages obtained from the 13 individual cores at the Okarito Pakihi site. It fits with the simplest core to core correlation of the Late Quaternary stratigraphy at this locality. It fits with the results of a considerable number of detailed palaeoclimatic studies in the New Zealand region, both onshore and offshore.

5.9 CORRELATION OF PEAKS IN TREE POLLEN WITH MARINE ISOTOPE STAGES

5.9.1 Comparison of the Okarito pollen record with climate proxy records from other sites

In section 5.8 it is shown that the ^{14}C and luminescence dating at Okarito can provide support for interpretation of the lower organic silt at the Okarito Pakihi Bog as an early MIS3 deposit. The climate probably varies in a similar and more-or-less synchronous manner along the entire length of the West Coast region. In this scenario one would expect that evidence for similar climatic conditions would be available for the same period in other parts of the region. In fact there is evidence in favour of near interglacial conditions elsewhere in the region at that time. Justification of this interpretation requires a major overhaul of the marine isotope stage correlation for the Late Quaternary period in North Westland. This is undertaken in Chapter 6. In section 5.9 of Chapter five the sequence of Late Quaternary strata at the Okarito Pakihi Bog are placed into a wider context extending across the New Zealand region and beyond. The same general context applies to the Late Quaternary sequence from North Westland.

As demonstrated above, if an approximately constant sedimentation rate is applied at Okarito below the onset of the Holocene, and if most of the ^{14}C and IRSL ages are accepted, then the base of the lower organic silt may have an age as recent as c. 62 to 65 ka. In this scenario the inorganic/organic boundary is assigned to the MIS3/MIS4 transition rather than the MIS5e/6 transition. The view presented here is that this would cause the Okarito pollen diagram to make much more sense as it would align this record with-

i) The tree pollen record at DSDP 594 situated immediately east of the South Island by Heusser & van der Geer (1994) which has a substantial peak early in MIS 3.
ii) The high resolution pollen record from marine core TAN0513-14 situated in the south Tasman Sea adjacent to Westland by Ryan et al (2009) which shows dryland tree pollen (podocarp/ hardwood + beech) pollen at a consistent level between 30% and 55% of the total flora through early to middle MIS3.
iii) The high resolution SST record from marine core SO136-GC3 situated in the south Tasman Sea adjacent to Westland (Pelejero et al 2006, Barrows et al 2007) which demonstrates strong warming during MIS3 reaching or approaching the modern level.
iv) The high resolution SST record from marine core MD06-2986 in the south Tasman Sea adjacent to Westland (Kolodzeij 2010) which demonstrates strong warming during MIS3 reaching or approaching the modern level.
v) The climate in the Westland area determined from beetle remains (Burge 2007, Burge & Shulmeister 2007a, 2007b).
vi) The pollen record from coverbeds on the Rutherglen Formation at Candle Light near Camerons in North Westland reported by Moar & Suggate (1996). Luminescence dating carried out for this PhD indicates that these cover beds which contain an interglacial and/or interstadial flora that is likely to extend into it MIS3.
vii) The interstadial to interglacial pollen and plant macrofossil record from Schulz Creek in North Westland described by Moar et al (2008) which has been dated by luminescence methods (this PhD) to MIS3.
viii) The interstadial pollen record from Sunday Creek in North Westland by Dickson (1972) which has been dated by luminescence methods (this PhD) to MIS3.

iv) The high resolution carbonate record at marine core DSDP 594 (Nelson et al 1993) at 45°31.41'S, 174°56.88'E in the Bounty Trough off the east coast of the South Island which demonstrates strong MIS3 warming.

v) The winter and summer SST curves for MIS3 from core DSDP 594. The temperature record is based on dinoflagellate cyst assemblages by Marret et al (2001) with 4 prominent upward spikes during MIS3, mimicking the Byrd ice-core $\delta^{18}O$ curve from Antarctica. A similar SST record was produced for this core by Wells & Okada (1997) using the modern analogue technique on planktonic foraminifera.

vi) The high resolution Mg/Ca SST record from MD97-2120 by Pahnke et al (2003) at 45°32'S 174°56'E, on the Chatham Rise. This record demonstrates repeated warm spikes reaching or approaching the modern level during MIS3.

vii) The high resolution alkenone based SST records for cores MD97-2120 and MD97-2121 (at 40°22.8'S 171°29.9'E) summarised in fig 3 of Pahnke & Sachs (2006). Both sites exhibit pronounced SST maxima during the early portion of MIS3.

viii) The SST records of marine cores ODP 1119 at 44°45.33'S 172°23.6'E (fig 2 of Hayward et al 2008, Hayward et al 2004) and ODP 1123 at 41°47.2'S 171°29.9'E (fig 8 & fig 11 of Crundwell et al 2008, Hall 2001) situated to the east of the South Island. Both sites exhibit multiple near modern SST peaks during MIS3.

ix) The distinct MIS4 cooling and early MIS3 recovery revealed by $\sigma^{18}O$ from a Tasmanian speleothem (Geode et al 1994).

x) The MIS3 record of clastic sediment content for core MD88-770 at 46°01'S, 96°28'E by Bareille et al (1994).

xi) The phytolith records from the lower portion of the North Island (Carter 2007, Carter 2002, Carter & Lian 2001).

xii) The MIS3 record of pollen from woody taxa at Lake Selina and Tullabardine Dam in Tasmania by Colhoun (2000). The Okarito record also bears a striking resemblance to the non-dated pollen record from marine core E55-6 at 38°51.2'S, 141°03.8'E just off the Victorian margin of SE Australia by Harle (1997).

xiii) The Mg/Ca SST records from ODP 1168A from the west Tasmanian margin (42°36.6'S 144°24.8'E) by Nurnberg et al (2004) and ODP 1172A from the East Tasman Plateau (43°57.6'S 149°55.7'E) by Nurnberg & Groeneveld (2006).

xiv) The well-dated high resolution SST record between 24 ka and 64 ka at core MD01-2378 in the Timor Sea off the Western Australian margin (13°04.950′S, 121°47.270′E) by Durkop et al (2008).

xv) The high resolution SST records at ODP 1233 off the Chilean Pacific margin at 41°S by Kaiser et al (2007), ODP 1089 in the southern South Atlantic at 43°57'S 9°53'E by Cortese et al (2002, 2007) and RC11-120 at 43°31'S 79°52'E by Martinson et al (1987).

xv) The pollen and temperature-index record between 55 ka and 10 ka from core HE94-2B at Taiquemo, Chile (Heusser et al 1999, 2006) which also exhibits a remarkable similarity to the SST record from core MD 97-2120.

xvi) The pollen records from Lake Omapere in Northland (Newnham et al 2004), Lake Poukawa in Hawkes Bay (Shulmeister et al 2001, Okuda et al 2002, and Shane et al 2002) and Onepoto basin in Auckland (Shane & Sandiford 2003).

This list contains a number of high resolution sea surface temperature records from mid latitude marine cores being: MD06-2986, SO136-GC3, DSDP 594, MD97-2120, MD97-2121, RC11-120, MD88-770, ODP 1168A, ODP 1172A, ODP 1119, ODP 1123, ODP 1089, and ODP 1233, and the low latitude core MD01-2378. These cores essentially ring the Southern Ocean and demonstrate significant episodic sea surface warming during MIS3. Pahnke et al (2003, 2008) demonstrate that the timing of MIS3 warm events at MD 97-2120 on the Chatham Rise is likely to be synchronous with that from several

Antarctic ice core sites, notably the Byrd ice core. This is particularly interesting given the uncanny resemblance between the *Dacrydium cupressinum* peaks in the Okarito pollen record (figures 3 & 5 of Newnham et al 2007a) and the MIS3 isotopic temperature record from the Byrd and Vostok ice cores. Other cores from the Southern Ocean that display substantial millennial scale SST variability during MIS3 include MD84-527 at 43°49.3'S, 51°19.1'E (from diatoms, Pichon et al 1992); MD88-770 at 46°01'S, 96°28'E (from diatoms, Waelbroeck et al 1995); and MD94-103 at 43°32'S, 86°32'E (from planktonic foraminifera, Sicre et al 2005). Southern South Atlantic cores PS1768-8 at 43°13.2'S, 11°44.3'E; PS1756-5 at 48°53.9'S, 6°42.8'E; PS1768 at 52°36.5'S, 4°28.5' E by Esper and Zonneveld (2007) each demonstrate MIS3 summer sea surface temperatures (based on dinoflagellate cysts) that were from time to time greater than the present.

Marine cores MD97-2120, DSDP594, TAN0513-14, MD06-2986 and SO136-GC3 situated either side of the South Island are particularly interesting in terms of comparison between pollen spectra and SST with the pollen spectra from Okarito. The Alkenone based SST record at MD97-2120 is displayed in figure 4.15a from chapter 4. The SST record from this core based on Mg/Ca ratios in planktonic foraminifera is displayed in figure 5.4. These figures can be compared directly with the Okarito pollen record in figure 5.3 above.

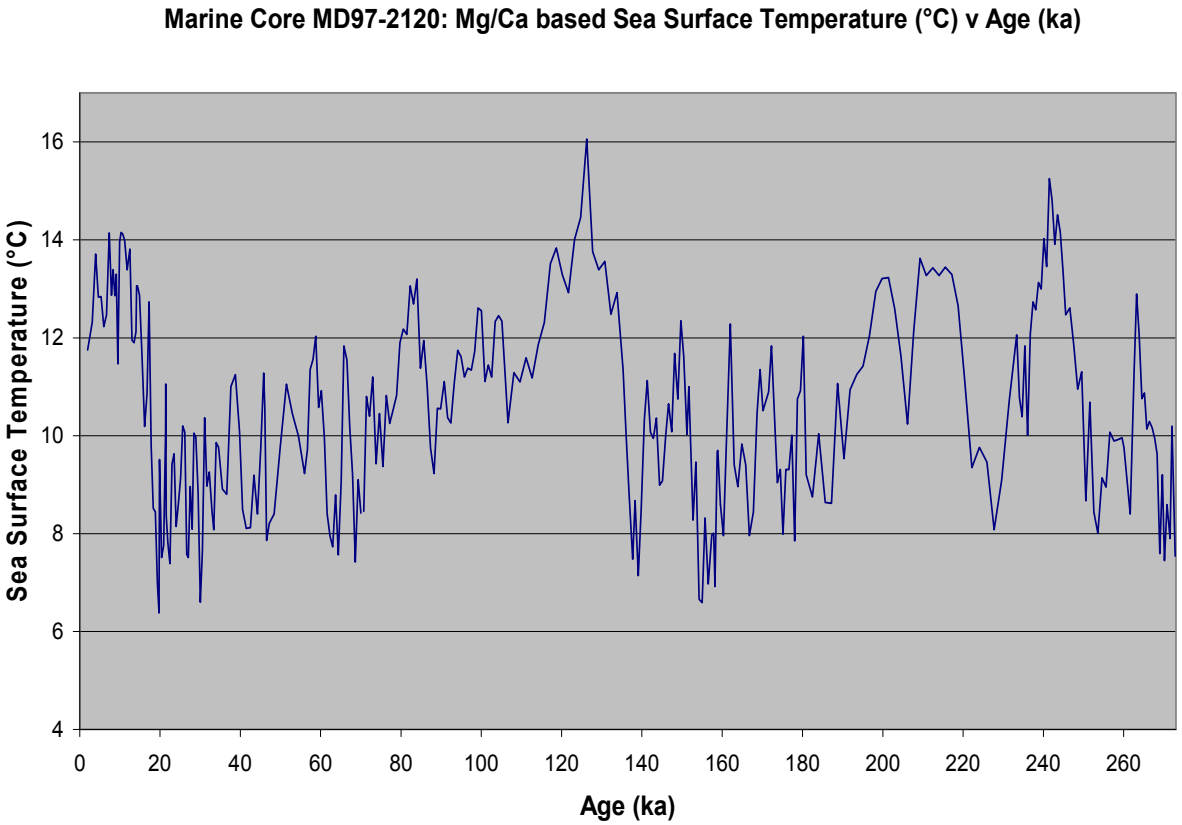

Figure 5.6: Mean annual sea surface temperature at marine core MD97-2120 from Pahnke et al (2003). The temperature is based on Mg/Ca ratios from planktonic foraminifera. Note the interstadial peaks at c. 60-50 ka which approach the SST for the late Holocene. This record is confirmed by the high-resolution alkenone-based SST for the same core by Pahnke & Sachs (2006) displayed in figure 4.15a (chapter 4).

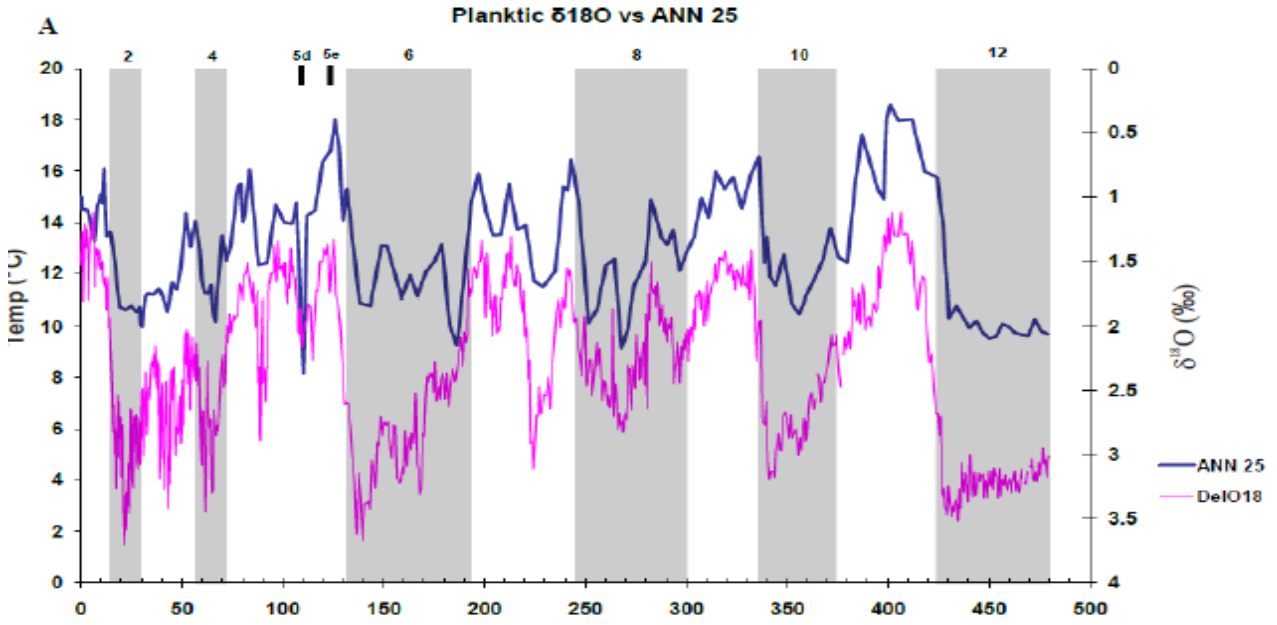

Figure 5.7: Planktic $\delta^{18}O$ and SST (ANN 25 model) for marine core MD06-2986, Tasman Sea immediately offshore from Hokitika (figure 4.13a from Kolodzeij 2010).

The strong MIS3 SST spike recorded from 60 ka to 50 ka at marine core SO136-GC3 in the Tasman Sea immediately offshore from Westland (Barrows et al 2007; Pelejero et al 2006) reached around 14 to 15˚C. This is similar to the modern mean SST. This high resolution record is presented in figure 5.8. SST was measured independently by alkenone unsaturation and MAT on foraminiferal abundance.

In addition a very detailed SST record by Kolodziej (2010) is available from marine core MD06-2986, situated even closer to Okarito. This record is presented in figure 5.7. Here there was a strong and sustained SST spike to about 14˚C from 60 ka to 50 ka. In terms of duration the MIS3 SST spike (approx 10 kyr) is almost as long as the Holocene. The sustained local SST maxima during early MIS3 is higher than the modern mean annual sea-level air temperature for Westland. The modern land–based mean annual temperature record is produced in figure 1.4. It includes every long-lived sea-level climate station along the entire West Coast, from Karamea (Arapito) to Puysegur Point). Generally the modern annual surface air temperature varies between about 11˚C and 12 ˚C.

Interestingly the pollen diagram from Vandergoes et al (2005) (their figure 1) shows a pattern of last glacial forest cover that is almost identical to figure 6 of Colhoun et al (1999) for Lake Selina in Tasmania. The transition from tree to shrub/herb dominance in the pollen spectra is dated by ^{14}C at Lake Selina at less than 52.1 ± 5.8 kyr and more than 33.8 ± 1.1 ka. Previously this transition has been assumed to have occurred at the MIS5a/4 transition, a conclusion that warrants reinvestigation in light of the close spaced luminescence dating at Okarito.

In the supplementary information of Vandergoes et al (2005) they make the following statement:

> "Pollen concentrates and organic residues from the base of core OKA1 between 554 and 600 cm (Supplementary Table 1) provide age estimates that are close to or beyond the limit of radiocarbon dating and indicate that the organic unit is older than 45,000 ^{14}C BP."

This statement is perfectly reasonable and is supported by the luminescence dating. But they finally assign the top of the lower organic unit to the MIS5a/4 transition (c.70 ka). The conclusion reached here is that this is an intra-MIS3 transition. The alkenone and faunal based sea surface temperature at marine core SO136-GC3 (fig 2 in Barrows et al 2007) and core MD06-2986 (Kolodzeij 2010, figure 5.7) is quite mild prior to 45 ka and shows a sharp decline from about 45 ka onward. In the alternative stratigraphy proposed in this thesis the SST records from SO136-GC3 and MD06-2986 supply part of the reason for the abrupt change in the nature of sedimentation and vegetation at the transition from the lower organic unit to the upper silt in the Okarito cores. Similar Mg/Ca based SST reductions are also noted around 45 ka for marine cores RC11-120 and E11-2 (56° S 115°W) by Mashiotta et al (1999) and marine core MD97-2120 by Pahnke et al (2003). Other SST records that exhibit strong cooling post 45 ka include ODP 1089 (Cortese et al 2002, 2007) southwest of Capetown and ODP 1233 (Kaiser et al 2007) off the Chilean Pacific margin and MD97-2121 (Pahnke & Sachs 2006) of the eat coast of the North Island (NZ). The SST record for core MD97-2121 is displayed in figure 4.15b (chapter 4).

In addition to the temperature records from individual marine cores in the Southern Ocean there are long continuous temperature records from Antarctic ice cores. Stenni et al (2003) analyse the temperature variation for the both the drill-collar location and oceanic moisture source of the EPICA Dome C ice core. They demonstrate a marked cooling event from about 45 to 40 ka both at the ice core site and in adjacent areas of the Southern Ocean. This is the interval between Antarctic interstadials A2 and A1. Cooling of the sea surface seems to be even more dramatic at that time than during the LGM. It is suggested here that this 2°C to 3°C intra-MIS3 event is likely to have left an imprint in Westland both onshore and in the nearby sea surface temperature record from core SO136-GC3 situated about 100 km NW of Hokitika.

One surprising characteristic of the Vandergoes et al (2005) interpretation of the Okarito record is the total absence of any hint of significant climatic amelioration revealed by pollen for the entire period encompassing MIS3 and MIS4. In fact stronger warming seems to be recorded during the middle of MIS2 than during MIS3 on the basis of podocarp/hardwood pollen. This finding deserves special attention by Vandergoes et al (2005) but receives none, other than a cursory mention of the "glacial geomorphic record of the last (Otira) glaciation from north Westland" and a reference to Suggate & Waight (1999), which they appear to take as the authority for that statement. It should be noted that there actually is no implication of a near-continuous tree-less vegetation in north Westland during MIS3 by Suggate and Waight (1999), only a lack of full interglacial vegetation. Careful reading of Suggate & Waight (1999), Moar & Suggate (1996) and Moar et al (2008) clearly demonstrates that pre LGM soil situated in exposed locations (e.g. Schulz Creek) contains podocarp and beech pollen and macrofossil remains that predate the c. 27 ka Kawakawa tephra. Therefore the Vandergoes et al (2005) interpretation of the Okarito pollen record is anomalous in terms of comparison with north Westland.

Vandergoes et al (2005) claim that (their interpretation of) the Okarito tree pollen record is similar to that of the tree pollen and carbonate records for DSDP (Deep Sea Drilling Project site) 594 by Heusser and van der Geer (1994) and Nelson et al (1993). But both records from DSDP 594 contain major MIS3 spikes indicating pronounced warmth. Based strictly on the pollen diagram and setting aside the luminescence dating the more obvious correlation is that the Okarito composite core from about 6 to 8.3 m matches nicely with the abrupt changes in the MIS3 portion of the DSDP 594 carbonate and pollen records. It is demonstrated above that there are viable alternative interpretations of the ^{14}C and luminescence dating at Okarito so there is potential for an alternative isotope stage correlation.

Vandergoes et al (2005) also refer to the Mg/Ca sea surface temperature (SST) record from core MD97-2120 (see figure 5.2 above) on the Chatham Rise by Pahnke et al (2003) in connection with an early onset of MIS2. But they fail to mention that the MIS3 Mg/Ca SST record for marine core MD97-2120 is one characterised by several prominent spikes that reach or approach the late Holocene SST level. Relatively high MIS3 SST is also displayed in the alkenone based record from the same (MD97-2120) core by Pahnke

& Sachs (2006). The alkenone-based record is displayed in figure 4.15a. Here the MIS3 temperature is in accord with relative warmth demonstrated for the same period by onshore (NZ) climate sensitive proxy records. These include phytoliths by Carter (2007) and Carter & Lian (2000), beetles by Burge (2007) and Marra et al (2008), and pollen by Okuda et al (2002), Shane & Sandiford (2003), and Wright et al (1995). It is also consistent with the pollen, carbonate and SST records from DSDP 594. For MIS3 the temperature record of Pahnke et al (2003) is not consistent with that implied for Okarito by Vandergoes et al (2005).

Figure 5.8 Faunal-based SST at marine core SO136-GC3 situated on the continental shelf off North Westland: from Barrows et al (2007)

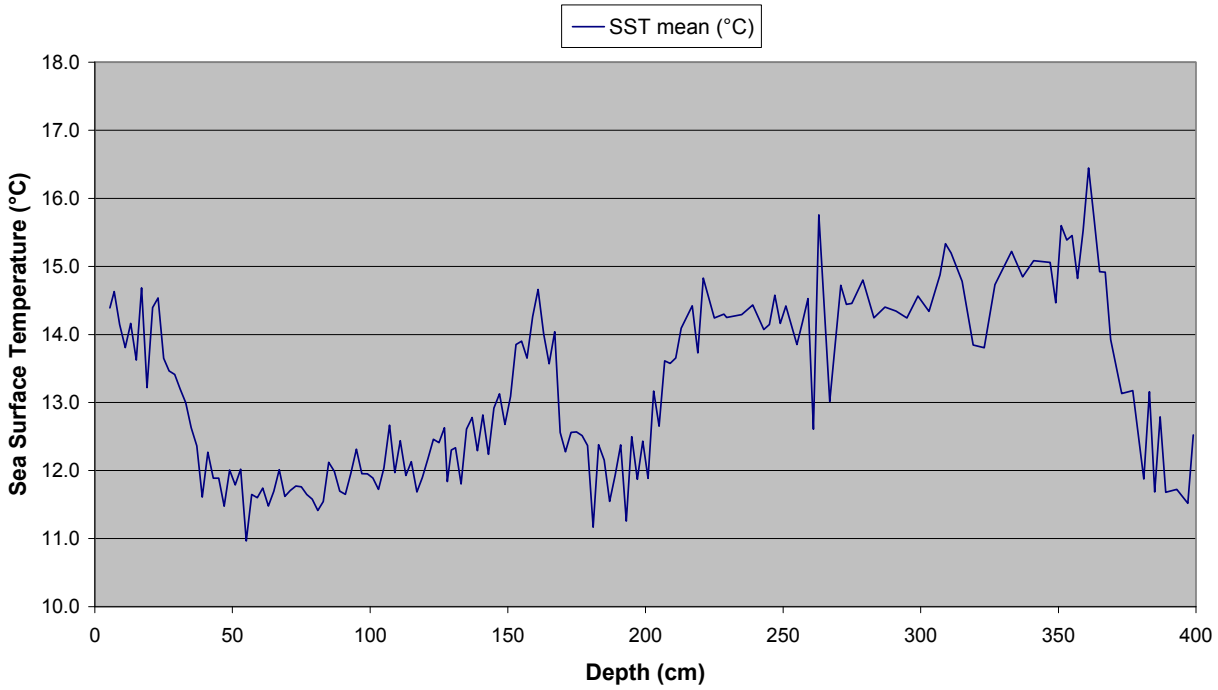

For Westland the closest high resolution sea surface temperature records are situated in the south-eastern Tasman Sea. These are from cores SO136-GC3 (figure 5.8) situated at 42°18'S; 169°53'E, about 100 km NW of Hokitika and MD06-2986 situated on southernmost margin of the Challenger Plateau at 43˚ 26, 91"S, 167˚ 54, 00"E. Pelejero et al (2006) and Barrows et al (2007) discuss alkenone palaeothermometry for SO136-GC3. The raw SST data for SO136-GC3 do not appear to have been placed in any publically accessible archive. SST versus depth data were supplied by email by Dr T Barrows on request. From figure 2a of Barrows et al (2007) the strong temperature from about 140 to 170 cm spike falls into the early portion of MIS3, while the temperature depression from about 170 to 210 cm falls into MIS4. The curve is a consensus view of SST based on a combination of results from the modern analog technique (MAT) and the revised analog method (RAM). It is matched in figure 5.2b of Barrows et al (2007) by a very similar alkenone based SST record from this core.

Kolodziej (2010) details the faunal based SST for MD06-2986. The early MIS3 temperature record at both of this site and at SO136-GC3 is characterized by strong warming that bears a striking resemblance to the DSDP 594 records of SST, carbonate, and pollen. The top (MIS1 to MIS4) portion of the SST record for both SO136-GC3 and MD06-2986 resemble the Okarito pollen record, but only if one assumes that the Vandergoes et al assignation for the MIS4 to MIS6 period is incorrect. MIS4 to MIS6 are prominently represented in SO136-GC3 and MD06-2986. In both cases the SST from about 132 to 78 ka is broadly comparable to that of the Holocene. The age model for the uppermost part of core SO136-GC3 was established using a basic spline fit with no smoothing through 14 ^{14}C-

Accelerator Mass Spectrometry (AMS) ages. Barrows et al (2007) demonstrate convincingly that the alkenone SST record for core SO136-GC3 is realistic by providing similar results from high resolution MAT (modern analogue technique) and RAM (revised analogue method) faunal based temperature estimates.

The SST record from cores SO136-GC3 and MD06-2986 illustrated in figures 5.7 and 5.8 is particularly important. The strong temperature spike during the early portion of MIS3 is present in both cores. For MD06-2986 the SST is based on three methods that use planktonic foraminifera (being MAT; RAM & ANN methods). Lowermost tropospheric air temperatures in North Westland are strongly influenced by the temperature of the sea surface in the south Tasman Sea. The surface air temperature of North Westland is intimately connected with nearby maritime conditions due to the prevailing westerly wind that comes directly off the south Tasman Sea. Changes in climate along the length of the Westland region are almost certainly similar in magnitude. For instance it is unlikely that relative difference in coastal climates at Westport (Buller area) and Okarito (South Westland) has ever changed greatly. It should be expected intuitively that changes in vegetation close to the coast will occur more or less simultaneously along the length of the region. Any proposal that this pattern has broken down should be accompanied by a plausible justification. This consideration has implications for the Okarito pollen profile given the pronounced late MIS3 warmth demonstrated from beetle fossils near Westport by Burge (2007).

Pollen zones 2 to 6 of Vandergoes et al (2005) bear an uncanny resemblance to phytolith zones H to D of Carter (2007) and phytolith zones A to E of Carter & Lian (2000) from deep loess profiles in the lower North Island. Both are dated by optically stimulated luminescence. A literal interpretation of the ages in both cases indicates several major spikes in tree pollen during MIS3. In the study by Carter (2007) the core has a length of 7.4 metres with a steady accumulation rate. In Carter & Lian (2000) the core has a length of 6.4 metres with an inferred steady accumulation rate. The Carter (2007) and the Carter & Lian (2000) phytolith records give strong support for substantial MIS3 climatic amelioration following MIS4.

The vegetation record described by Burge (2007) and Burge and Shulmeister (2007a, 2007b) for the Westport area demonstrates closed canopy forest during MIS3 and possibly MIS4. This work is discussed briefly in Chapter 6. The Westport record is quite different to that of Vandergoes et al (2005) but it is in good accord with that of Nelson et al (1993) and Heusser & van der Geer (1994) for DSDP594, Barrows et al (2007) and Pelejero (2006) for SST at SO136-GC3, Pahnke et al (2003) for SST at MD97-2120, Kolodzeij (2010) for SST at MD06-2986 and with various vegetation records from the North Island.

Vandergoes et al (2005) conclude that in the post-MIS4 period Southern Hemisphere insolation forcing has an impact on local climate at an orbital timescale. This is perfectly reasonable. However their conclusions with regard to the position of MIS3 and MIS4 in the composite core have as much to do with expectations coloured by the imprint of preconceived theory as they do with the actual data presented. This is a common theme in terms of published palaeoclimatic studies for Westland, where potentially viable alternative hypotheses are typically not discussed or even proposed for testing.

5.9.2 MIS5 at Okarito

Vandergoes et al (2005) and Newnham et al (2007b) assert that the pollen record from their composite core reveals the vegetation history from MIS5a to MIS5e and the later part of MIS6 (figs 1 & 2 in Vandergoes et al). However, it is readily apparent from figures 3 & 5 of Newham et al (2007) (see figure 5.2 above) that there is no clear analogue for the Holocene (the top 3.3 m is Holocene)

vegetation and climate of south Westland anywhere in the lower portion of the composite record. It is assumed here that the Holocene vegetation at the Okarito site is reasonable representative of full interglacial conditions. In figure 2 of Newnham et al (2007b) the most striking feature of the Holocene (upper organic layer) pollen record at this site is the dominance of podocarp/hardwood species (primarily by Dacrydium cupressinum), generally constituting > 90% and never significantly < 85% of the total. In contrast the podocarp/hardwood component of the pollen in the lower organic silt dips below 30% at four separate depths. The maximum podocarp/hardwood pollen content of the lower organic silt touches 75% briefly once, and 65% briefly on 3 additional occasions. Other key differences include the abundance of tree fern spores in the upper organic layer but near absence in the lower organic layer. In terms of small trees and shrubs Myrsine is nearly absent during the Holocene but persistently present in the lower organic layer. Phylocladus ,Caprosma, Halocarpus and Quintinia are nearly absent through the latest Holocene but abundant through the lower organic layer. These features of the pollen record appear to indicate a persistent difference in either the climate or the immediate physical environment between the two organic layers.

There is no solid evidence in the pollen record from Okarito for a substantial period of stable climate in the basal portion the lower organic silt. This is the position that according to Vandergoes et al (2005) correlates with MIS5e. At this position in the record there is only a short lived transition into and out of what would ordinarily be considered interstadial conditions. One solution to the issue is that the grey inorganic silt below the lower organic silt is much more likely to be situated in MIS4 than in MIS6. That immediately aligns the entire pollen record with almost every other modern high-resolution record covering this period in the New Zealand region. The counter-argument is that the highly selective choice of "reliable" ages by Vandergoes et al (2005) is the correct approach.

A comprehensive review of climatic conditions in New Zealand during MIS5e has not been carried out for this PhD project. However, note that Okuda et al (2002) concluded MIS5e was significantly warmer and moister than the Holocene in Hawkes Bay from the pollen record in a long drill core at Lake Poukawa. Further they note that the period including MIS5d to 5a was from 3.5 to 5 °C colder than the Holocene at Lake Poukawa. MIS5e is particularly prominent in the SST records from marine core SO163-GC3 located about 100 km NW of Hokitika (Pelejero et al 2006, Barrows et al 2007), marine core MD97-2120 located on the Chatham Rise (Pahnke et al 2003) and marine core DSDP 594 located on the southern flank of the Chatham Rise (Wells & Okada 1997).

A brief digression is in order at this point because the timing of the MIS6/5e transition and the duration of MIS5e are is also relevant to the discussion (in Chapter 6) of the marine terraces defined as Candlelight and Whisky Formations in North Westland. It is also pertinent in terms of the presence or absence of a sustained MIS5e interval at about 8.3 m depth in the Okarito composite core. This episode is supposedly represented by a brief peak in the podocarp/hardwood fraction of the pollen. The peak is coupled with the sustained presence of substantial montane vegetation which, by comparison is greatly diminished during the Holocene.

In terms of this PhD project it is suggested that full interglacial conditions during MIS5e were likely to have been as prolonged as that of the Holocene in New Zealand. If this was the case it would be expected that the podocarp/hardwood component of the Okarito flora would show a sustained plateau during MIS5e, and the montane component would show a sustained minimum. This is the general pattern demonstrated in the tree pollen component of marine core DSDP594 from the Chatham Rise by Heusser & van der Geer (1994), supported by the oxygen isotope and carbonate records from the same core and similarly at core TAN0513-14 immediately offshore from Westland by Ryan et al (2009).

Note that global eustatic sea level had recovered to the full interglacial level at or before 132 ka (e.g. Esat et al 1999) at a number of well dated localities around the globe. This timing is discussed in more detail below. Rising sealevel was accompanied by a full recovery of the atmospheric climate. There is no particular reason to suspect that Westland was any different in this regard. If this "early" recovery from MIS6 is correct it presents a minor problem for Vandergoes et al (2005) in respect of the timing they adopt for the MIS6/5e transition. It means that it is unlikely that the weighted average age from samples OKA1, OKA3, and OKA4 can be used to infer the precise age of the grey "glacial" silt that was sampled (weighted mean age supposedly 127 ka). The three samples each had an attached error as would the averaged age, but the averaged age and error is essentially statistically meaningless. This implies that they have not securely dated either the base of the organic silt or the MIS6/5e transition. If this assertion is accepted then one of the major findings of the study is cast into doubt. They imply that climatic trends at Okarito are broadly consistent with the northern driver model (orbital forcing at high northern latitudes controlling growth and collapse of continental scale ices sheets) for West Coast climate from MIS6 through MIS4. Upon careful consideration of their dating and age model for the Okarito cores it is concluded here that the results do not strongly support or contradict any model of orbital forcing for glaciation or deglaciation prior to MIS3. The Vandergoes et al (2005) position is also contradicted by that of Sutherland et al (2007) who carried out a programme of cosmogenic isotope dating on moraine boulders in South Westland. Sutherland et al (2007) suggest that local (Southern Hemisphere) summer insolation was a primary driver for glaciation in South Westland during MIS5.

Vandergoes et al (2005) also imply that from about MIS4 onward the regional summer insolation pattern may provide an alternative to the "bipolar seesaw" in explaining differences in hemispheric climate trends. However, if the age model is altered as proposed in this thesis, then the data (the Okarito pollen record) can just as easily be interpreted as evidence supporting the bipolar climate seesaw.

In terms of the relative warmth of MIS5e in North Westland and comparison with modern conditions it is worth noting figure 5 in Pelejero et al (2006). They record a mean SST at marine core SO136-GC3 for the period 131 to126 ka of 18.4°C compared with a modern mean of 15.4 °C and an LGM figure of 10.8°C. So coming back to the Okarito record once more why is it that the claimed MIS5e pollen record seems to indicate relatively cool climate, when just offshore the sea surface temperature was probably substantially greater than in the recent past?

A further curiosity in the Okarito pollen record as interpreted by Vandergoes et al (2005) is the lack of any real distinction in the percentage of podocarp pollen between the peaks of MIS5a, 5c, and 5e. Further, the pollen diagram shows the presence of podocarp forest continuously though MIS5d and 5b. This pattern has not previously been proposed for any other locality in Westland. In the Suggate model as expressed in Suggate & Waight (1999) and Moar & Suggate (1996) there are significant vegetative differences between the interstadial and interglacial peaks. This includes variations in the ratio of beech to rimu in a number of pollen diagrams. This ratio appears to increase as the climate cools from interstadial to stadial conditions. Vandergoes et al (2005) illustrate beech as overwhelmingly dominant in the canopy tree pollen at Okarito during MIS6 but barely making an impression in the record during stadial periods from MIS5d to 4. There is little evidence that MIS4 climatic conditions at Okarito were less amenable to the proliferation of beech than during MIS6. The problem disappears if the lower inorganic grey silt dates from MIS4 rather than MIS6.

In the interpretation of Vandergoes et al (2005) and Newnham et al (2007b) the Okarito core does not contain loessic silt from a major glacial event claimed by Preusser et al (2005) to have occurred during

MIS5d in North Westland. Ice-cover during this event would need to have been of similar extent to the LGM to have produced the widespread moraine and fluvioglacial outwash that Preusser et al (2005) assign to it. At Nelson Creek/Bell Hill the outwash terrace is linked directly to a classical glacial moraine that is situated down valley from what has previously been though to be the LGM terminus. So for at least one locality this supposed MIS5 advance had greater ice extent than during MIS2. This general point has been recognised by others, notably Newnham et al (2007b) who state the following:

> "The Okarito pollen record should also provide a test of the recent suggestion that the Loopline Formation in North Westland involved glacial advances in MIS5d and 5b, as well as during MIS4 (Preusser et al., 2005). This contention is not consistent with the model proposed here whereby grass pollen peaks indicating lowering of treeline should be correlative with major glacial advance in the Westland region. Nevertheless, the expansion of subalpine shrub communities during the reduced forest phases of MIS5 indicate cool, humid phases which could have triggered the comparatively minor advances suggested by Preusser et al. (2005)."

This statement is reasonable except that Preusser et al (2005) do not comment on the magnitude of MIS5 glaciations in Westland. Nor does the Okarito composite core contain loessic silt that might be correlated with a potential major MIS5a glacial event identified further south in the Cascade Valley by Sutherland et al (2007). These conflicts simply disappear if the base of the Okarito pollen record is in MIS4. In that scenario the Okarito composite core is not deep enough to record events that occurred during MIS5.

5.9.3 Nestegis Pollen in Quaternary deposits from Westland/Buller: Implications for climate and stratigraphy

In New Zealand there are 4 species of Nestegis which are currently distributed through the North Island and the northern part of the South Island. The four species are:

N. apelata (restricted to the area from the Bay of Islands to South of Great Barrier Island)
N. cunninghamii}
N. lanceolata} (all three currently distributed as far south as coastal areas of the
N. montana} northern South Island, Moar 1984.)

None of these species has colonised the Westland/Buller region during the Aranui Interglacial (Holocene). Nor were they present at the LGM or through MIS2. Established practice has seen the presence or absence of Nestegis pollen being used to infer that past climate in Westland was either interglacial or glacial. The rational for this practice dates back at least to Moar (1984) where it is formalised. In the abstract from this paper Moar states:

> "Pollen grains of the tree genus Nestegis (Oleaceae) have been identified in interglacial sites along the west coast of the South Island from Westport to Hari Hari, but they are not recorded in any post-glacial site in the South Island. The pollen records provide a means of recognising interglacial sites along the west coast of northern South Island."

In practice this assumption means that the presence of Nestegis pollen in any particular Quaternary deposit from Westland and Buller is taken to indicate that the deposit dates either from MIS5 or MIS7. In the initial conception by Moar (1984, 1988) then Moar & Suggate (1996) Nestegis identified in MIS5 soil/peat/silt meant a deposit could be assigned either to MIS5e (deposits on the Waimea and

Rutherglen Formations) or MIS5c (deposits on the Awatuna Formation). Such an assignation normally includes reference to accompanying Rimu and/or Kahikatea and/or Rata pollen.

Restriction of soil containing Nestegis pollen to fully interglacial climates is a major portion of the justification of the "Suggate model" of Late Quaternary stratigraphy for North Westland. Recently Moar et al (2008) have used the presence of Nestegis to infer that initial deposition of soil on a wave cut platform at Schulz Creek occurred during MIS5e. Further, they have used the disappearance of Nestegis upward through the profile to infer transition into MIS5d, which implies that they now consider Nestegis to be restricted to a single substage within MIS5. As discussed above in relation to Okarito, Nestegis is clearly not restricted to MIS5e at that locality. If the Vandergoes et al (2005) dating and correlation is accepted then Nestegis was present at Okarito during MIS5a, which contradicts but might not be fatal to the Suggate model.

Known occurrences of Nestigis pollen from Westland and Buller are summarised in table 5.6 below. Several points can be summarised from this table and references therein:

1. Nestegis pollen is present in the basal organic soil on most pre-LGM raised marine terrace where that soil rests directly on the marine deposits (or at least all those terraces sampled so far) including the Karoro, Rutherglen, Awatuna and Waites Formations. Nestegis appears to be an almost ubiquitous component of the coastal pollen flora for soils deposited during the "Kaihinu Interglacial".

2. Nestegis pollen is present in organic soil resting on the Waimea Formation at each site where a detailed study has been carried out. So Nestegis colonised Westland immediately following the Waimea Glaciation. Presumably the presence of Nestegis indicates that part of the soil was deposited during the Kaihinu Interglacial.

3. Nestegis pollen declines in abundance in company with Rimu, Kahikatea, and Rata during the transition from the Kaihinu Interglacial to the Otira Glaciation.

The presence or absence of Nestegis pollen is not of itself a dating tool for Quaternary deposits in Westland. The main implication of its presence is that climate is likely to have been relatively warm. The absence of Nestegis from Westland during the Holocene is probably either simply an accident in biogeography relating to rates of colonization or perhaps the extreme severity of the MIS2 period pushing this species sufficiently far to the north as to prevent expansion back into its former range at a later date. It may have little to do with the climatic tolerance of this group of species. Kauri is an example of a species that grows happily when introduced to the modern coastal climate of Westland and Nelson, both areas being well outside the current natural reproductive range. It is likely that the modern climate in coastal Westland is suitable for both the growth and reproduction of Nestegis. There is no reason to assume conditions are presently less suitable than during the Nestegis bearing interval in the Okarito cores of Vandergoes et al (2005).

Table 5.6: *Nestegis* pollen in Quaternary deposits of North Westland			
Site	**Formation**	**Position of *Nestegis* pollen in soil/peat/loess**	**Reference**
Kumara Cemetery J32/60403815	Waimea	Base	Fig 8a, Moar & Suggate (1996)
Chesterfield Road J32/56503970	Waimea(1)	Base-mid portion of profile M81/7	Fig 7a, Moar & Suggate (1996)
Chesterfield Road J32/56204010	Waimea(2)	Base-mid portion of profile M81/8	Fig 7b, Moar & Suggate (1996)
Grahams Terrace K30/92955970	Waimea	Basal portion of profile M83/16	Fig 8,b, 8c Moar & Suggate (1996)
Blue Spur Road J33/47002970	Waimea		Moar & Suggate (1973); Moar (1984)
Okarito	Not defined	Throughout Pre MIS2 peat	Fig 1, Vandergoes et al (2005); Newnham et al (2007b)
Greens Beach I34/114973 I34/103969	Not defined	Pre MIS2	Moar & McKellar (2001)
Hatters Creek J32/53953310	Not defined (Under Loopline Fm)	Profile M83/20	Fig 6b, Moar & Suggate (1996)
BA Road, Nth of Kapitea Ck. J32/56154140	No defined, Clay lens underlying Loopline Fm	Lower sample	Moar & Suggate (1996)
Martins Quarry	Waites?	Consistent in the bottom 1/3, Intermittent above	Fig 6, Moar & Suggate (1979; Moar & Suggate (1996)
Sand Quarry, Cape Foulwind area NZMS 1 S32/007686	Waites		Moar & Suggate (1979, 1996)
Waimea Creek gravel quarry (Westport) NZMS 1 S32/082656	Virgin Flat (Karoro Interglacial)		Fig 4, Moar & Suggate (1979); Moar & Suggate (1996)
Bullock Creek, Punakaiki K30/72909955	Awatuna	Throughout, up to 4.5 %	Fig 4c, Moar & Suggate (1996)
Schulz Creek, near 12 Mile, Coast Road	Not defined (likely Awatuna)	Base to middle, rare at top in profile B	Fig 3, Moar et al (2008)
Sunday Creek Tributary J32/54904040	Awatuna (type section)	Throughout except the very top.	Fig 4b, Moar & Suggate (1996)
Candle Light J32/59454690	Rutherglen	Throughout	Fig 4a, Moar & Suggate (1996)
"Fergusons Pond", South Beach J32/61055450	Karoro	Up to 11 %	Moar & Suggate (1996), Soons & Lee (1984)

Moar & Suggate (1996) and Neall et al (2001) discuss gaps in the history of soil deposition in Westland. There is a prominent gap in deposition noted for sites like Chesterfield Road on the Loopline Formation and Kumara Cemetery (Waimea Formation) where most of MIS3 is thought by them to be missing. In their conclusions Neall et al (2001) infer that "OIS3 is not represented at Kumara". Some of these gaps disappear when the isotope stage correlation changes. For instance in the new correlation (proposed in this thesis) the MIS3 gap is minimised because the fluvioglacial gravel of the Loopline Formation becomes an intra-MIS3 (rather than MIS4) deposit. Neall et al (2001) also imply that there is no MIS 3 marine terrace preserved in the Kumara area in North Westland, a conclusion that is reexamined in chapters 4 and 6 of this thesis. If the Loopline Formation dates from MIS3 then marine deposits beneath this Formation, notably the Awatuna Formation near Chesterfield Road, could derive from MIS3 as well.

In the alternative stratigraphy and correlation advanced here for North Westland the same implication is drawn, i.e. that the where Nestegis pollen is present the climate during deposition was generally relatively warm, and potentially close to the warmth of the modern climate, at least for short periods of up to a few thousands of years. With regard to Nestegis the primary difference is that its presence would be extended from MIS5e through MIS5c, MIS5a, and on to early MIS3.

5.9.4 *Nestegis* Pollen at Okarito and Implications for the Definition of MIS5e in Westland

The Okarito Pakihi composite core sets a benchmark in terms of climate and vegetation for Westland. The dating of the record is important not just to the interpretation of climatic events at Okarito but also the Late Quaternary climate of the whole region. Pollen from the genus Nestegis is present continuously and in significant quantity through the lower organic silt at Okarito. The presence of Nestegis through the lower organic silt can be seen clearly in figures 3 & 5 of Newnham et al (2007b). The Newnham et al (2007b) model indicates Nestegis is present continuously from MIS5e to MIS5a, which is contrary to the assumptions underpinning the Suggate model.

If the hypothesis that the lower organic silt at Okarito dates from MIS3 is accepted then it follows that Nestegis was present in the Okarito flora during that period. This would make Okarito the sole locality in Westland where this is recognized. It is a significant departure from and is basically incompatible with the Suggate model. The reason for significance is not in the possible presence of the genus at one locality in South Westland, but in the potential implications for the age of soils

. This alternative age model advanced here implies this genus was probably present in South Westland for c. 10 to 15 ka during early MIS3. In the new hypothesis (this thesis) Nestegis is indicative of relatively mild climatic conditions, but it is not a defining characteristic of full interglacial conditions. If this new interpretation is correct then the Okarito record tends to contradict (if not invalidate) a substantial proportion of most previously published MIS5e to MIS3 climate histories for this region, notably that by Moar & Suggate (1996) and more recently by Moar et al (2008). The solution advanced here is that most of the Nestegis bearing soils formed in North Westland and Buller during the "Kaihinu interglacial" age from MIS5a to MIS3 rather than MIS5e to MIS5c. It also implies that the Kaihinu interglacial was much more recent than previously supposed.

During the Holocene Nestegis has not been present in Westland, the closest occurrence being in Northwest Nelson. Nestegis is traditionally presumed to be indicative of mild conditions with temperatures similar to or exceeding Holocene conditions.

5.9.5 Penultimate Interglacial at Greens Beach, South Westland

A number of ramifications arise from a new age-depth model for the Okarito composite core of Vandergoes et al (2005). The potential repositioning of Nestegis pollen into MIS3 calls into question the conclusions from several previous published studies of climate and vegetation in Westland. One such study is that by Moar and McKellar (2001) which relates to Greens Beach, a locality near Lake Ianthe in South Westland.

Pollen recovered from buried soil at two sites at Greens Beach has yielded an important climate record. Two ^{14}C ages are reported from organic deposits that are overlain by fluvioglacial gravel at Greens Beach. They are NZ3379A at 29.6 ± 0.85 ka and NZ 4378A at 38.0 ± 2.85 ka. An assumption has been made that soil at the two sites, being Pukutuaro Cliff (grid ref I34/103969) and Opuku Cliff (grid ref I34/114973), is from the "Kaihinu (or last) interglacial". In other words soil deposition was

confidently assigned to the MIS5e to MIS5c period. The key data supporting the isotope stage correlation is the presence Nestegis pollen in the organic soil. This is also the primary data supporting rejection of the ^{14}C ages. Nestegis pollen is assumed by Moar & McKellar (2001) to be indicative of interglacial climatic conditions. Rejection of the two ^{14}C ages occurs because the Suggate model does not support interglacial climatic conditions during MIS3. The possibility that a younger "interstadial flora" might not differ greatly from an interglacial flora is not discussed.

Vandergoes et al (2005) demonstrate that a significant quantity of Dacrydium cupressinium (Rimu) pollen was deposited during a minor interstadial in South Westland between the two periods of most extreme glaciation associated with the LGM (after 26 ka), so a flora with "interstadial affinities" can clearly become established very quickly in South Westland. Detailed analysis of the pollen record from Okarito indicates that significant interstadial events postdating MIS5c almost certainly occurred in South Westland. Even without adjustment to the age-depth model for the Okarito composite core of Vandergoes et al (2005) one can argue on the basis of figures 2 & 3 of Newnham et al (2007b) that Nestegis was present in South Westland during MIS5a. If a new age-depth model is accepted for the Okarito composite core then Nestegis was present in South Westland during MIS3. It is suggested here that the complete absence of significant interstadial events in South Westland between the LGM and MIS5c is rather unlikely and that there are several other potential correlations that could be made for the soils from Greens Beach.

Irrespective of the interpretation of pollen in the Okarito composite core the Late Quaternary climate history advanced in this thesis identifies Nestegis pollen in post MIS5c soils from the Waimea, Rutherglen and Awatuna Formations in North Westland. In this context the use of Nestegis as indicator that a soil belongs to MIS5e becomes circular logic. This same general line of argument is advanced in Chapter 6 in relation to a Nestegis bearing soil at Schulz Creek in North Westland that is described in detail by Moar et al (2008).

One of the problems with the existing interpretation of the climatic and stratigraphic interpretation of occurrences of Nestegis pollen is the supposed climate sensitivity of this genus, a sensitivity that is assumed from its modern geographical range but not tested against potential modern reproductive viability outside of its this range. In relation to the Suggate model and MIS correlation, how is it that Nestegis colonized Westland at the very beginning of MIS5e but failed to do so during the Early Holocene? The MIS5e colonization supposedly occurred after a long absence during MIS6. This glacial stage is likely to have been at least as severe and prolonged as MIS2. So what is responsible for the difference in vegetative response? The published record does not contain a clear answer to this question.

In the new stratigraphy and isotope stage correlation proposed here the Nestegis pollen bearing deposits at Okarito and Greens Beach that are discussed above shift from MIS5 to MIS3. In North Westland the Karoro Formation shifts from MIS7 to MIS5a, the Rutherglen Formation to MIS5a/4 and the Awatuna Formation to Early MIS3. Each formation is overlain by Nestegis bearing soil (see table 5.6). In this scenario Nestegis is probably not totally absent during MIS4 and MIS3 stadial periods, most likely being confined to localised coastal refugia from time to time. Complete elimination of Nestegis from the local flora occurred during late MIS3 or MIS2.

As discussed above in relation to the pollen record from the Okarito composite core of Vandergoes et al (2005) there was probably a prolonged period of warm climate more or less right through MIS5 (substages 5e to 5a) in the Westland region. This conclusion is drawn from the SST record at marine core SO136-GC3 (Pelejero et al 2006, Barrows et al 2007) situated in the south Tasman Sea about 100

km NW of Hokitika. This period had a duration of c. 50 kyr which would be ample for recolonisation of the region by this genus following MIS6.

5.9.6 Late MIS3 Climate near Westport

Burge (2007) compiled an exceptionally detailed climatic record from a site at Wilsons Lead Road near Westport. The locality was previously referred to as "The Hill" by Moar & Suggate (1979). The grid reference is NZMS E2385410, N5935067. At this site there is a deep profile though soil, peat and aeolian sand which has been dated using the radiocarbon method. The palaeoclimate and palaeovegetation for this site have been synthesized by Burge (2007) largely from analysis of assemblages of beetle remains. The key results of relevance to this project are the findings that at c. 36 ka the mean summer temperature was equivalent to the modern mean; the mean winter minimum temperature was ~ 2°C colder than the modern mean (but within 1σ error) and the mean precipitation was close to the mean modern precipitation. So, at least for a short time around 36 ka, the climate in the Westport area was probably close to interglacial in nature but with somewhat enhanced seasonality. It is also noted that Burge (2007) analysed samples from unit KR-A3 at another site near Westport (Keoghans Road), which reveals a similar climate. This site is dated to a similar period but with less certainty. The sites sampled by Burge (2007) are situated on marine platforms of the Waites Formation. Radiocarbon dating on the Waites Formation is discussed briefly in the main body of Chapter 6. The palaeoclimate interpreted from beetle remains at these localities is difficult to reconcile with the pollen record by Vandergoes et al (2005) from Okarito, unless the Okarito record has been incorrectly dated.

5.9.7 Growth Rate Limitations

It has almost universally been assumed that temperature and precipitation are the primary controls on species composition/diversity in Westland forests during the Late Quaternary period. Vandergoes et al (2005) and Newnham et al (2007) follow the standard line in this regard. Another limiting factor that potentially exerts control over species diversity in Westland is the response of vegetation to variations in atmospheric CO_2 concentration. This factor is addressed briefly by Burge (2007) for sites near Westport. The discussion relates to the relative frequency of sexual reproduction and the life cycle of grasses and canopy trees. If a low atmospheric CO_2 concentration constrains sexual reproduction more in trees than in grasses then pollen spectra from a soil at a site where there is no change in vegetative cover may nevertheless exhibit a relative decline in tree pollen abundance that is not related to temperature, precipitation or wind patterns. This hypothesis could be extended to the relative frequency of pollen from different species of trees whereby for an individual site a stable mix of species might not be reflected in the pollen diagram.

The rise and fall of atmospheric CO_2 concentration closely follows the stadial/interstadial rise and fall of temperature in Antarctic ice cores, notably in the Byrd, Vostok and Taylor Dome cores. More particularly Indermuhle et al (2000) show that during MIS3 atmospheric CO_2 concentration varied cyclically approximately in synchronisation with temperature over a range of c. 30 ppm (220 to 190 ppm) from c. 62 ka to c. 33 ka, before declining further into MIS2. CO_2 is essentially plant food. The atmospheric CO_2 concentration potentially affects plant growth rates, length of the growing season, plant reproduction, species migration rates, timing of colonisation, and interspecies competition. As the limits of tolerance are approached the effects of variation in an already low atmospheric CO_2 concentration may increase in importance and could begin to dominate over temperature and precipitation. For many species plant growth slows dramatically at an atmospheric CO_2 concentration below 200 ppm, equivalent to that of the LGM. Although worthy of mention this subject is beyond the

scope of this project. An extensive database of published growth rate variability under controlled CO_2 concentrations that can be found at http://www.co2science.org (Go to Data on the top menu, then Plant Growth). This website categorises plant growth research in terms of dry weight (biomass) and photosynthesis (Net CO_2 exchange rate).

There is minimal published research on the response to CO_2 concentration variation by species endemic to Westland. The following table is sourced from the co2science website:

Journal References	Experimental Conditions	300 ppm
Hogan *et al.* (1996)	open-top chamber	37%
Hogan *et al.* (1997)	open-top chamber	39%
Hollinger (1987)	pots (4 liter)	44%

Table 5.7: Enhanced growth of *Nothofagus fusca* (Hook.f.) Oerst. [Red Beech] under conditions of elevated atmospheric CO_2 concentration.

In the last column the CO_2-induced growth (increase) response, expressed as the percent increase in photosynthesis for a 300 ppm increase in the air's CO_2 concentration above ambient conditions. Across most tested species the opposite response is generally observed when the CO_2 concentration is decreased (i.e. photosynthesis decreases). It appears that atmospheric CO_2 concentration does influence the rate of photosynthesis in *Nothofagus fusca*, a species that is presently common in North Westland north of the Taramakau River.

5.10 AN EXAMINATION OF PREVIOUS LUMINESCENCE DATING IN NORTH WESTLAND

5.10.1 Background

Detailed discussion of the dating of various Late Quaternary Formations is undertaken in Chapter 6. In this part of Chapter 5 discussion focuses on the estimation of the radioactivity of Quaternary sediments from Westland. In terms of the validation of past luminescence dating programmes from North Westland there are two key questions addressed here.

- Have the methods been cross validated
- Has the measurement of radionuclide related dose rates been validated

The first question is at least partially answered above in the discussion on luminescence dating at the Okarito Pakihi. The sediments dated at Okarito were able to provide internally consistent ages by two luminescence methods both giving ages that are not inconsistent with ^{14}C dating from the same locality. But this is a single site and might not be representative of the region as a whole. This method-to-method comparison is continued here for dating undertaken on samples from North Westland.

Consistency with the results of ^{14}C dating does not mean that the luminescence dating at that locality is free from potentially systematic errors. So the second bullet point is discussed in terms of the potential

for systematic errors that may affect the outcome of dating on all samples dated by similar methods. The potential error in question relates to measurement of radionuclide dose rates.

Note that in the following discussion all dating on all the samples has been carried out either on the silt fraction of the samples (polymineral fine grains at a grainsize of 4-11 μm) or K-feldspar from the fine sand fraction. Whereas optical dating on quartz does not appear to be particularly reliable in North Westland (Preusser et al 2006) the dating of K-feldspar does appear to have been more successful. This view of IRSL dating on K-feldspar is held by Newnham et al (2007b) who state:

> "Although optical dating of feldspar from some regions seems to systematically underestimate the known age of a sample due to fading of the luminescence signal, previous experience with luminescence dating in Westland indicated that feldspars from there apparently were not affected by this phenomenon (Almond et al., 2001; Hormes et al., 2003; Preusser et al., 2005)."

Table A4.1 (in Appendix 4) lists the majority of luminescence ages that are available from previously published studies from the West Coast region. These ages form the basis for a series of method-to-method linear regressions illustrated in figures 5.9a to 5.9g.

5.10.2 Method to Method Linear Regression of Luminescence Dating Results

At this point it is informative to examine inter-method linear regressions for luminescence dating in Westland. One such comparison is presented in figure 5.3 above. At Okarito two methods being $IRSL_{(blue)}$ and $TL_{(UV)}$ compare favourably from 0 to about 75 ka. But can this be replicated at other sites? A further seven linear regressions are supplied in figure 5.9. The underlying age data for figure 5.9 is derived from table A4.2. All the data points graphed here represent samples that were dated by more than one luminescence method. The "best fit" trend lines and R2 values are as per automatic calculation in Microsoft Excel. The red diagonal lines represent a 1:1 relationship. Generally the trend line is not equivalent to a 1:1 relationship. Where the trendline is offset and steeper it may be recording a relationship that deteriorates as time accumulates.

With regard to figures 5.9a to 5.9g it is clear that there are no particularly tight relationships between the results of the different dating methods adopted by Preusser et al (2005) for samples taken in North Westland.

The following general comments are made in relation to this graphical display of luminescence ages:

- $IRSL_{(blue)}$ dating generally gave similar ages to $OSL_{(UV)}$ dating (see figure 5.9a),
- $IRSL_{(blue)}$ dating generally gave younger ages than $TL_{(blue)}$ dating (see figure 5.9b),
- $IRSL_{(blue)}$ dating generally gave younger ages than $TL_{(UV)}$ dating beyond about 60 kyr but similar at <50 kyr (see figure 5.9c),
- $IRSL_{(UV)}$ dating generally gave younger ages than Post-IR-OSL dating (see figure 5.9d),
- $OSL_{(UV)}$ dating generally gave slightly younger ages than $TL_{(UV)}$ dating (see figure 5.9e),
- $TL_{(UV)}$ dating seems to have given slightly younger ages than $TL_{(blue)}$ dating (see figure 5.9f).

From the ages produced by Preusser et al (2005) three groups of ages give comparatively younger ages when compared with the other methods. These are $IRSL_{(blue)}$, $IRSL_{(UV)}$, and $OSL_{(UV)}$. Dating by $IRSL_{(blue)}$, appears to have been successful, or at least internally consistent at Okarito. This is discussed above in relation to dating by Vandergoes et al (2005).

As discussed in sections 5.3 to 5.6 for many of the samples there does appear to be an issue with incomplete bleaching during deposition. In North Westland the $IRSL_{(blue)}$, $IRSL_{(UV)}$, and $OSL_{(UV)}$ methods seem to be least affected by partial bleaching. This issue is discussed by Preusser et al (2005) in relation to samples from Kamaka and is discussed further in Chapter 6 of this thesis. As a general comment the absence of a tight relationship between IRSL dating and any other form of luminescence dating in the study by Preusser et al (2005) leads to a suggestion here that all six methodological variants have suffered to some extent from incomplete bleaching.

Figure 5.9a: Linear regression of $IRSL_{(blue)}$ vs $OSL_{(UV)}$ ages from dating by Preusser et al (2005) on samples from North Westland

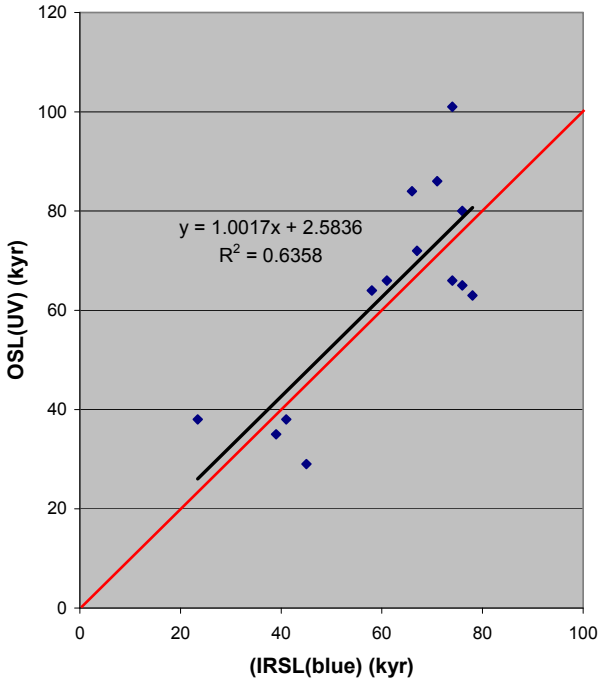

Figure 5.9b: Linear regression of $TL_{(blue)}$ vs $IRSL_{(blue)}$ ages from dating by Preusser et al (2005) on samples from North Westland

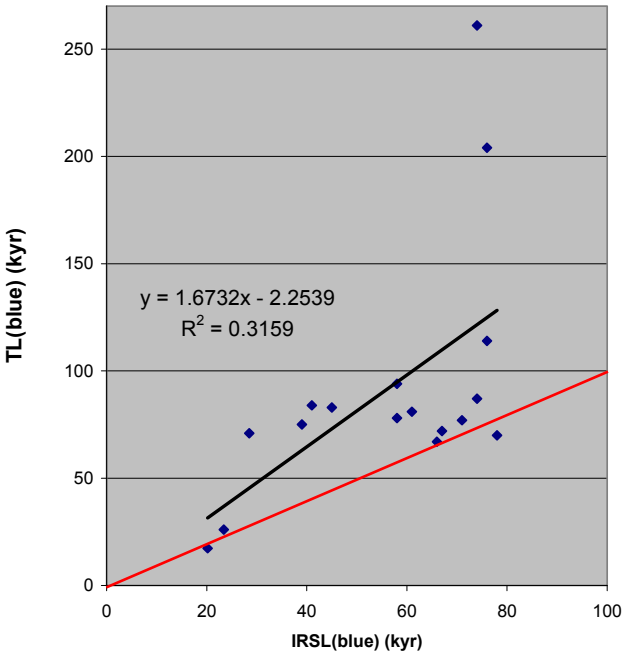

Figure 5.9c: Linear regression of $IRSL_{(blue)}$ vs $TL_{(UV)}$ age from dating by Preusser et al (2005) on samples from North Westland

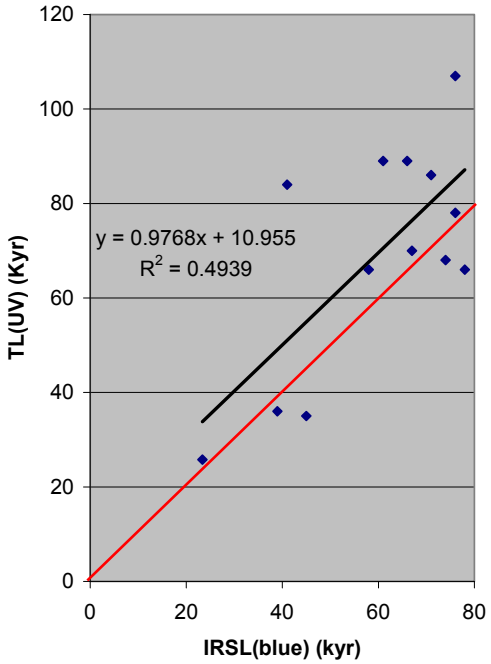

Figure 5.9d: Linear regression of $TL_{(UV)}$ vs $OSL_{(UV)}$ age from dating by Preusser et al (2005) on samples from North Westland

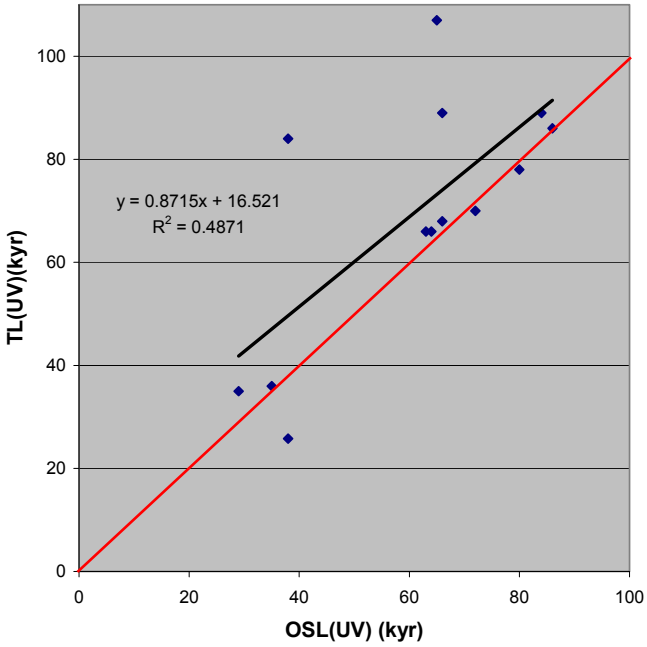

Figure 5.9e: Linear regression of post-IR-OSL vs IRSL(UV) age from dating by Preusser et al (2005) on samples from North Westland

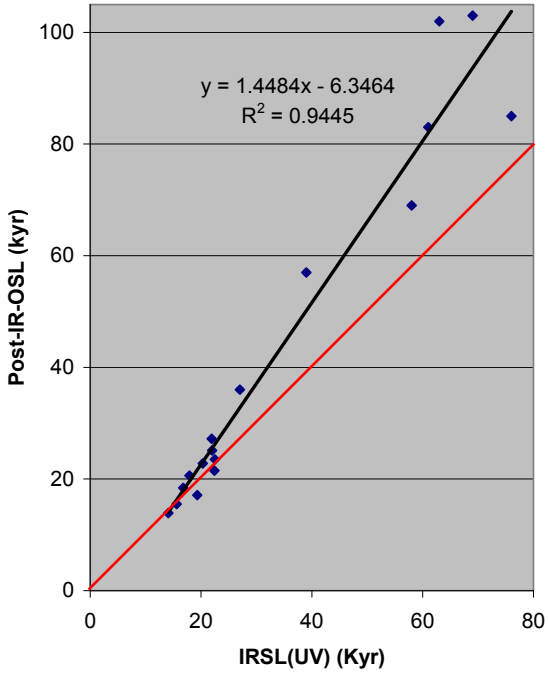

Figure 5.9f: Linear regression of $TL_{(UV)}$ vs $TL_{(blue)}$ ages from dating by Preusser et al (2005) on samples from North Westland

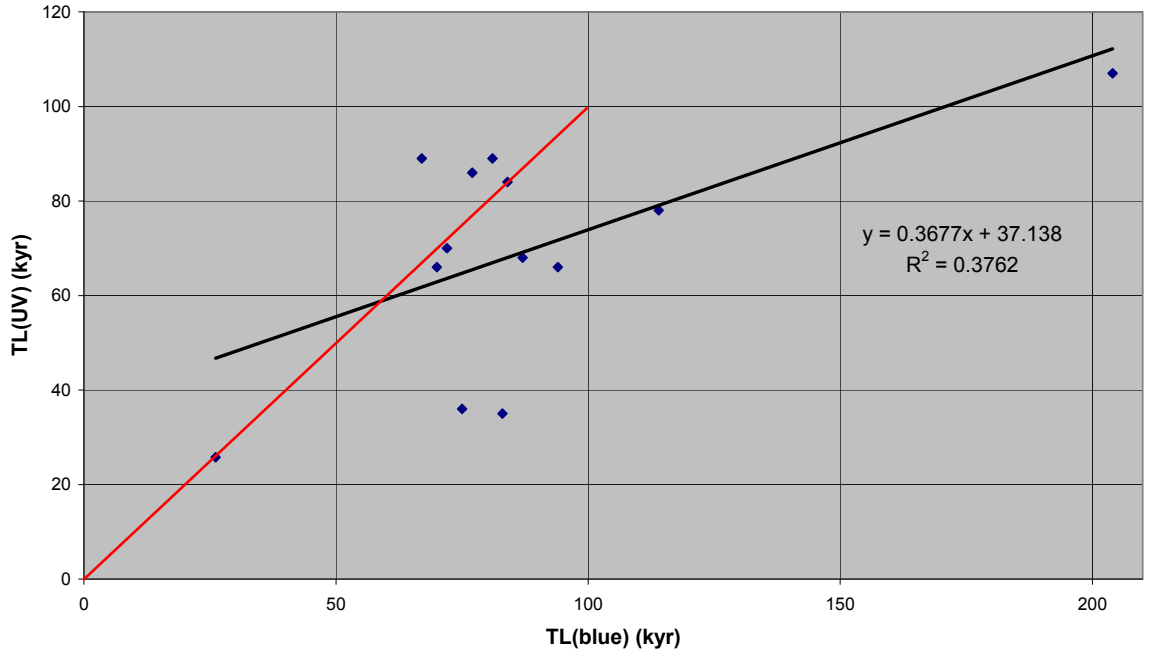

Figure 5.9g: All $IRSL_{(blue)}$ and $IRSL_{(UV)}$ ages vs all other luminescence ages from dating Preusser et al (2005)

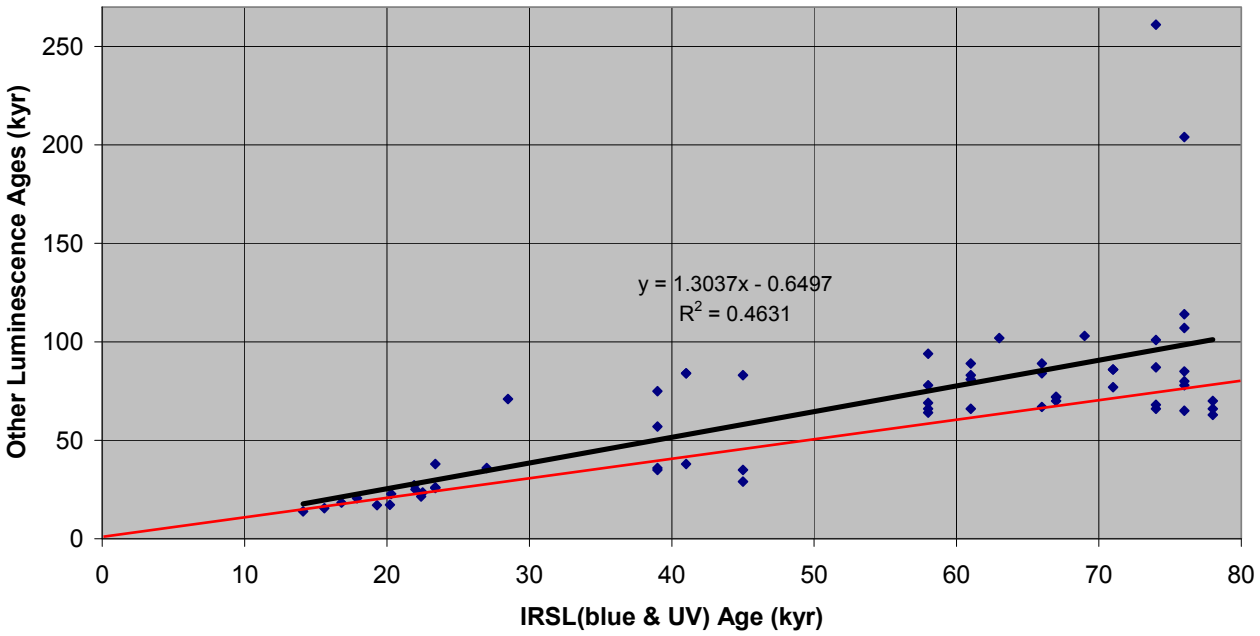

It is also suggested here that post-IR-OSL dating and $TL_{(blue)}$ dating were relatively unsuccessful in the dating campaign by Preusser et al (2005), though post-IR-OSL dating appeared to fare better at Okarito (see figure 5.4a, 5.4b) in dating by Vandergoes et al (2005).

Overall it is suggested that:

- The Post-IR-OSL ages > 25 ka from North Westland should be rejected,
- The $OSL_{(UV)}$ ages > 65 ka should be rejected,
- The $TL_{(blue)}$ ages > 80 ka should be rejected,
- The $TL_{(UV)}$ ages > 80 ka should be rejected.
- The $IRSL_{(blue)}$ or $IRSL_{(UV)}$ age should generally be preferred where more than one method has been used on a sample, though $OSL_{(UV)}$ ages may be acceptable as well.
- As discussed in sections 5.3 to 5.6 partial bleaching can not be ruled out for most of the $IRSL_{(blue)}$ and $IRSL_{(UV)}$ ages.

In terms of polymineral finegrained samples that were dated and accepted by Preusser et al (2005) using multiple methods there are none that have an $IRSL_{(blue)}$ or $IRSL_{(UV)}$ age that is greater than 80 ka. One feature common to the older (>80 ka) $IRSL_{(blue)}$ ages by Preusser et al (2005) is that the material dated was all K-feldspar from the 100 to 300 micron size range. These samples from Nelson Creek and from the Hokitika Gravel Quarry gave IRSL ages between 80 ka and 115 ka. But there was no cross-check on these via other dating methods. At both of these localities Preusser et al (2005) have proposed a change in the marine isotope stage correlation for fluvioglacial deposits that were sampled. As discussed in section 5.6 the evidence favouring this reassignment change is tenuous and in relation to Nelson creek there is good reason to suggest the $IRSL_{(blue)}$ ages may be up to 3 times that of the depositional age. The reassignment that they propose is barely plausible and by no means proven. In other words the dated material was sand rather than silt. This can be seen in table 5.6.f above. In addition many of these samples were from fluvial gravel or marine sand rather than from silt.

In relation to the dating programme under discussion Preusser et al (2005) state:

> "The only luminescence component that is obviously affected by (anomalous) fading is IRSL-UV, which is measured during the double-SAR protocol of Banerjee et al. (2001). This trend of underestimation is clearly seen when plotting IRSL-UV versus post-IR-OSL (Fig. 13) and by the systematic underestimation of IRSL-UV ages in comparison to calibrated radiocarbon ages at Raupo."

So is this difference in sample ages between $IRSL_{(UV),}$ and post-IR-OSL really indicative of fading of the IRSL signal as claimed by Preusser et al (2005) or is it a result of incomplete bleaching of the post-IR-OSL signal at deposition. Comparison between these two methods is possible for a total of 17 samples from the Preusser et al (2005) programme. A few of the younger samples (from Raupo in the Grey Valley) are backed by ^{14}C ages. At this locality the paired luminescence ages all agree or at least overlap within 1σ error. The number of samples from this locality is probably not large enough to be definitive because it is entirely possible that the differences measured here occurred by chance rather than by a systematic fading problem. Close examination of the text from Preusser et al (2005) disclosed the following comments in relation to samples from Raupo:

> "Storage tests over a period of at least 12 months did not produce any evidence of anomalous fading for the samples investigated (Hormes et al., 2003). However, the fading ratio might be too low to be detected during a relatively short period of time."

And,

> "In addition, there is no systematic difference between the IRSL-MAA and OSL-MAA ages (Fig. 12) but this would be expected in the presence of anomalous fading as IRSL and GLSL result from different recombination processes."

So from actual measurements there is no solid evidence for anomalous fading of the $IRSL_{(UV)}$ signal in samples by Hormes et al (2003). Nevertheless Preusser et al (2005) rely on anomalous fading of the $IRSL_{(UV)}$ signal to explain why this method gave consistently younger ages than post-IR-OSL. Preusser et al (2005) conclude:

> "that IRSL and OSL ages reported here are, with the exception of most of the IRSL-UV ages, not affected by (anomalous) fading and, as a consequence, do not systematically underestimate but most likely give the real age of sediment deposition, providing that the samples were completely bleached prior to deposition."

As reported in section 5.7 in relation to luminescence dating for this PhD project Dr Rieser found no evidence for anomalous fading. No other investigation in this region has shown this to be a significant issue. On a number of samples three of the methods agree within error, being $IRSL_{(UV)}$, $IRSL_{(blue)}$, and $OSL_{(UV)}$. If there is a problem it may lie in the measurements for post-IR-OSL . This method produced significantly older ages at the Phelps goldmine. One potential solution is that post-IR-OSL might be affected by incomplete bleaching, rather than $IRSL_{(UV)}$ being subject to anomalous fading. The relevant samples from the Phelps mine are discussed further in relation to the "Craig Formation" in section 5.6 above.

5.10.3 Comparison of Dose Rates Reported from Various Luminescence Dating Programmes

The following is a brief comparison and discussion of mean dose rates reported from a number of luminescence dating campaigns in the Westland region. The conclusion reached here is that IRSL dating by these authors has tended to overestimate the depositional age, not as a result of dose rate measurement but as a result of partial bleaching during deposition.

The Preusser et al (2005), Hormes et al (2003), Vandergoes et al (2005) and Berger et al (2001) data are assembled in tables A4.1a to A4.1g (Appendix four). Many of the samples were dated by more than one method. The luminescence dating methods used in these studies are:

$IRSL_{(blue)}$	Preusser et al; Vandergoes et al; Hormes; Berger et al
$IRSL_{(UV)}$	Preusser et al (2005)
Post-IR-OSL	Preusser et al (2005) & Vandergoes et al (2005)
$TL_{(blue)}$	Preusser et al (2005)
$TL_{(UV)}$	Preusser et al; Vandergoes et al; Hormes; Berger et al
$OSL_{(UV)}$	Preusser et al (2005)
$OSL_{(green)}$	Hormes et al (2003)

At the Phelps mine a substantial number of OSL, IRSL and TL ages fail to make an acceptable distinction in age between two silt units that are claimed to be separated by c. 20 kyr. In other words they fail to distinguish the age of silt layers that Preusser et al (2005) assign to MIS4 and MIS5a (or MIS5c). In sections 5.3 to 5.6 and 5.8 (above) the usefulness of IRSL, OSL and TL dating is examined in relation to deposits in North Westland. In some cases these samples begin to suffer from saturation at around 60 to 70 ka, particularly when dated by $TL_{(blue)}$ or post-IR-OSL. Another study which seems to encounter a similar issue is that by Shane et al (2002), who dated lake sediments from Hawkes Bay by OSL, with results that appear to substantially overestimate the depositional age beyond about 60 ka.

In relation to the $IRSL_{(blue)}$ dating carried out for this PhD the measured dose rates are on average about 30% higher that those measured by Preusser et al (2005) Vandergoes et al (2005), Hormes et al (2003) and Berger et al (2001). The relevant measurements are summarised in table A4.1. The Rieser/Rose/Shulmeister measurements for U and Th are consistently higher, as are the measurements for K-feldspar in the silt fraction. There may be no need for reconciliation between these datasets if the differences are governed largely by the process of sample selection.

5.10.4 Discussion

The Rieser/Rose/Shulmeister (1^{st} & 2^{nd} rounds) programme covers sites from North Westland. In the first round a mixture of sand and silt samples were taken. In the second round all the samples were silt/soil samples. Sandy materials were avoided in the second sampling campaign in order to target polymineralic fine-grained material for dating by $IRSL_{blue}$. The Preusser et al (2005) samples are from the same general area within North Westland. The Vandergoes et al (2005) samples (Preusser is a co-author) are from Okarito in South Westland. The Berger et al (2001) samples are from Blue Spur in North Westland, and Saltwater Forest in South Westland. The full results from all the available luminescence dating samples are presented in tables A4.1a to A4.1g (Appendix 4).

The Preusser et al (2005) samples SDC1, 2, 3 & 6 from Sunday Creek are excluded from 5^{th} row of table 5.10. This was done to highlight the impact on the mean U and Th content. These samples are marine sand with a very high radionuclide-bearing heavy-mineral content and relatively low K-feldspar content. The higher U & Th content seems to balance the low K-feldspar content so the overall dose rate is similar to the other samples. The same coupled low K-feldspar and high Th & U pattern is apparent in RR9 and RR19. Both samples had a high heavy mineral content, particularly RR19.

Some samples taken during this project contain very high but real quantities of minerals that contain U and Th. These several of these minerals have a very high SG and are concentrated preferentially in comparison to low SG minerals in some environments. Fluvial and littoral (sea beach) environments produce the right depositional and sorting mechanisms to concentrate U and Th bearing minerals. At the same time the same environments can act to reject low SG K-rich minerals, particularly in some littoral settings. In North Westland very heavy ilmenite/garnet rich beach-sand is typically relatively fine-grained and almost always contains elevated concentrations of Monazite, Xenotime, and Uranothorite. Sphene is another thorium/uranium bearing mineral of moderate SG that is also common in North Westland fluvial and littoral sediments. In beachsands at Barrytown sphene can constitute from 1 to 3% of the sand, and it is common in the silt fraction.

Study	No. of samples	*a*-value	Grain-size (µm)	Mean U (ppm)		Mean Th (ppm)	Mean K (%)	Mean dD/dt (Gy/ka) Optical methods	Mean dD/dt (Gy/ka) TL methods
				Total	From Ra, Pb, Bi				
Rieser, Rose, Shulmeister. 1st Round	Silt: 6 Sand: 11 All: 17	0.0635 0.048(2) 0.0595	4 to 11		3.76 3.79 3.78±0.19	12.16 17.65 15.72	1.90 1.56 1.78	3.52 3.54 3.53	
Rieser, Rose, Shulmeister. 2nd Round	Silt: 13	0.088±0.14	4 to 11		3.29±0.18	14.04±0.17	1.88±0.04	4.097±0.37	
Preusser et al 2005	Silt: 33	0.07±0.02	4 to 11	2.87±		11.61±0.43	1.32±0.04	3.145±0.3	3.16±0.3
Preusser et al 2005	Sand: 17	0.07±0.02	100-300	2.82±0.15		14.14±0.53	1.56±0.03	3.46±0.18	
Preusser et al 2005 excl. SDC1,2,3&6	Sand: 13	0.07±0.02	100-300	2.44±0.08		10.84 ± 0.47	1.76±0.04	3.45±0.15	
Vandergoes et al 2005	Silt: 34	0.07±0.02	?	2.23±0.09		9.16±0.19	1.32±0.10	2.51±0.2	1.54±0.16
Berger et al 2001	Mixed: 14		4 to 11	3.25±0.41		10.64±1.31	1.45±0.05	3.17±0.18	

Table 5.8: Summary of the radionuclide and dose rate data produced from luminescence sampling programmes in the West Coast region from this (PhD) project as well as those of Preusser et al (2005), Vandergoes et al (2005); and Berger et al (2001).

The mean dose rate from 19 silt samples taken during this (PhD) project is 3.91 Gy/ka. That by Preusser et al (2005) for 33 silt samples is 3.145 Gy/ka. So the mean dose rate reported for silt from North Westland by this study is ~24% greater than that by Preusser et al (2005). It is also ~55% greater than that by Vandergoes et al (2005) for samples from South Westland.

5.10.5 Potassium, Uranium and Thorium Content of Westland Silt Samples

Nineteen silt samples taken for luminescence dating during this (PhD) project had a mean K content of 1.89%. This compares with a mean of 1.32% from 33 samples by Preusser et al (2005), a mean of 1.32% from 34 samples by Vandergoes et al (2005) and 1.45% by Berger et al (2001). So the mean K content in silt from North Westland by this study is ~43% greater than that by Preusser et al (2005) from the same general area and some of the same horizons.

The thorium content of 19 silt samples from this (PhD) project is 13.45 ppm. That from 33 silt samples by Preusser et al (2005) is 11.61 ppm. So the mean thorium content of silt in North Westland by this study is ~ 16% greater than that by Preusser et al (2005).

The uranium content of 19 silt samples from this project is 3.44 ppm. That from 22 silt samples by Preusser et al (2005) is 2.87 ppm. So the mean uranium content of silt in North Westland by this study is ~20% greater than that by Preusser et al (2005)

Potassium bearing minerals

A general assumption made by Preusser et al (2005) Vandergoes et al (2005), Newnham et al (2007) and Berger et al (2001) is that the potassium content of the sand and silt is situated primarily in K-Feldspar. This has not been demonstrated in any study of Westland sand to date. The sand and silt in most of the Late Quaternary deposits is relatively fresh and texturally immature. In terms of

provenance it has been derived recently by erosion from nearby mountain ranges. A large proportion of the marine, littoral and fluvioglacial sediment is of a "first cycle" origin. There is a substantial content of non-weathered or to moderately weathered sand and silt. The sediments contain abundant phylosilicates dominated by biotite and muscovite, both of which have substantial potassium content. The parent terrane contains sources of phlogopite and stilpnomelane which are also potassium-bearing. Collectively these minerals can constitute a significant portion of the total mass the sediment.

In terms of polymineral finegrain IRSL dating it does not matter whether the potassium is within the feldspars or some other mineral. But this is not the case when dating sand sized materials.

Preusser et al (2005) make the following statement:

> "Average K-contents of K-rich feldspars of 12.57 ± 0.5% were assumed following Huntley and Baril (1997)."

When dating sand-sized feldspars one has to know the K-content, as K deposits an internal radiation dose in the large grains. This can be measured, for example using a beta counter. 100% pure K-feldspars have a maximum of around 16% potassium, but one rarely deals with 100% pure fractions. Because few OS laboratories have beta counters the K-content is typically 'assumed' and relevant literature is cited. For the external doserate in the sediment, the gammaspectrometric measurement is used and includes all non-feldspar K-bearing minerals. As internal potassium accounts for about 1/3 of the total doserate the purity estimate can impact on IRSL ages. Potentially these ages could be up to about 10% too old (for pure K-feldspar) or 30% too young (pure Na-feldspar). [pers com U Rieser]

5.10.6 Uranium and Thorium content of Westland beach sand

Eleven sand samples taken for OSL dating during this study returned a mean uranium content of 3.79 ppm. This compares with 17 sand samples taken by Preusser et al (2005) which yielded a mean uranium content of 2.82 ppm. So the mean uranium content in sand from North Westland by this study is ~34% greater than that by Preusser et al (2005). The thorium content of the sand from this study is 17.65 ppm. That from sand sampled by Preusser et al (2005) is 14.14 ppm. The result from this study is ~25% greater than that by Preusser et al (2005). The potassium content of the sand samples in these two studies is similar.

As a brief digression it is worth noting that Holocene beach sand underlying the coastal plain at Barrytown has been examined in detail in connection with the commercial extraction of heavy minerals including gold, ilmenite, zircon, monazite, rutile, thorite, uranothorite, and xenotime. In terms of environmental effects of possible mining of the deposits one of the primary concerns raised was the potential for concentration of radioactive elements by mining and beneficiation processes. Reports were compiled on the radiological implications by Roberts & Whitehead (1991) and Whitehead & Roberts (1991). These authors summarise the Uranium and Thorium content of typical heavy mineral sands from this extensive and relatively high-grade deposit. In the Barrytown deposits raw sand samples had thorium contents ranging from 0.06 gm/kg to 0.16 gm/kg or 60 to 160 ppm. This was assessed both by chemical methods (Readings of Lismore) and gamma spectroscopy (National Radiation Laboratory, Christchurch). The U^{238} content of the sand was estimated at 0.03 gm/kg or 30 ppm. It was also suggested that the U^{238} content is about 1/5 of the thorium content.

In terms of the location of U and Th in the sand at Barrytown the heavy minerals identified as likely primary hosts were monazite, xenotime, and uranothorite. Interestingly, the low-density stream in the mineral beneficiation process reported a "surprisingly high" thorium content during wet separation. It was surmised that this thorium was most likely a minor component of the medium density minerals sphene and cerium epidote. Sphene is present at a concentration of around 1 – 3% in the raw sand.

By comparison the Thorium and Uranium content of beachsand samples from the various luminescence dating programmes appears to be substantially lower (~10 - 45 ppm) than that at Barrytown. With respect to Thorium it is lower by an order of magnitude (9 – 15 ppm) on average across all samples.

The total uranium content of sand samples taken in the first luminescence sampling round for this PhD project was ~ 10-11 ppm. The maximum total measurement was 19.7 ppm for RR19 from heavy mineral rich Holocene beachsand at Rapahoe.

5.10.7 Comparison of Luminescence Dating Results

Comparison of the results of the dating programmes listed in table 5.10 is difficult because the samples are generally from different sites and different materials. So the following discussion is a somewhat qualitative analysis rather than a strictly quantitative one.

The most striking differences between these dating projects are the relatively higher mean dose rates, higher uranium, higher thorium and higher K-Feldspar content measured from the samples for this (PhD) project when compared with the measurements by Preusser et al (2005), Berger et al (2001) and Vandergoes et al (2005). The difference could have occurred by chance through the choice of genuinely more radioactive samples during this PhD project. It is unlikely to be due to overestimation of radionuclide contents during the laboratory analysis of the samples taken during this project as the calibration of instruments used in this study is carried out to the highest possible standard. It could be due to underestimation of the radionuclide content of samples taken during the other dating programmes considered here but this cannot be determined at present. If this is a systematic difference due primarily to the last of these possibilities then it is likely that the majority of ages produced during these other dating projects have been overestimated. In that case there will be a significant impact on the conclusions drawn from those studies, and an impact on conclusions drawn in Chapter 6 with respect to detailed discussion of some of the key sites in North Westland.

One interesting outcome of a systematic reduction in the age of samples taken for luminescence dating by Vandergoes et al (2005) is that it would bring the luminescence and ^{14}C ages from Okarito into much closer alignment. This would strengthen the case for the utility of luminescence dating in Westland. It would also decrease the need to assume significant remnant contamination by younger carbon in the pre-treated/cleaned ^{14}C samples at Okarito.

Study	Uranium Content	Thorium Content	K Feldspar content	Dose Rate
Preusser et al (2005)- silt	Higher	Slightly higher	Higher	Higher
Preusser et al (2005)- sand	Higher	Similar	Higher	Similar
Vandergoes et al (2005)- silt	Much higher	Higher	Higher	Much higher
Berger et al (2001)- mixed	Similar	Slightly higher	Higher	Higher

Table 5.9: Comparison of luminescence dating programmes in the Westland region with the mean results from this PhD project (higher means that the mean result from this PhD project is higher)

In table 5.9 the mean values obtained for this PhD project are compared with those obtained from the other three published studies. The assessment of whether or not the mean result from this project is "higher" or lower is generalised and does not refer to individual sites or samples. The results for number of individual stratigraphic horizons sampled for this PhD project and by Preusser et al (2005) are summarised in table 5.10 below. The doserate depends on additional factors like water content, which depends entirely on the a-value. This value was measured directly for each sample taken during this project but is assumed by Preusser et al (2005). So the a-value is not directly comparable.

Sample	U (ppm)	Th (ppm)	K %	A	Dose (Gy)	Dose Rate (Gy/kyr)	Age (ka)
Silt samples from State Highway 7, Kamaka, Grey Valley							
RR21	***3.63±0.17***	***14.18±0.07***	***2.09±0.04***	***0.09±0.007***	***152.9±5.3***	***4.34±0.37***	***35.3±3.2***
KMK4	3.03±	13.12±0.39	1.69±0.04	0.07±0.02	130±13	3.4±0.3	39±5
KMK3	3.09±	12.51±0.38	1.72±0.05	0.07	151±5	3.5±0.3	45±4
KMK2	3.38±	12.5±0.37	1.69±0.05	0.07	142±12	3.6±0.3	41±5
Silt samples from the Type-Section of the Awatuna Formation, Chesterfield							
RR8	***3.3±0.29***	***8.2±0.4***	***1.27±0.05***	***0.084±0.007***	***93.6±2.0***	***2.69±0.27***	***34.8±3.5***
SDC4	1.96±0.06	7.97±0.24	0.72±0.02	0.07	150±14	2.0±0.2	71±10
SDC5	2.44±0.08	10.03±0.3	0.98±0.03	0.07	167±14	1.9±0.02	58±8
SDC7	2.7±0.08	9.09±0.27	1.24±0.3	0.07	226±16	2.8±0.02	61±8
SDC8	3.1±0.09	11.27±0.34	1.27±0.04	0.07	230±19	3.0±0.3	58±7
Samples from marine sand at the Type-Section of the Awatuna Formation, Chesterfield							
RR9	***6.97±0.15***	***28.4±0.8***	***0.86±0.04***	**N/A**	***229±13.8***	***3.84±0.28***	***47.8±6.6***
SDC3	4.00±0.12	24.76±0.74	0.71±0.03	0.07	209±14	3.3±0.3	65±5
SDC2	4.16±0.12	25.14±0.75	0.89±0.03	0.07	282±52	3.6±0.2	81±11
Silt samples from the lower silt at the Phelps Goldmine, Southside, Hokitika							
RR2	***4.1±0.34***	***16.2±0.07***	***1.25±0.05***	***0.052±0.011***	***116.6±5.8***	***3.47±0.32***	***33.6±3.6***
PGM4	2.57±0.09	12.5±0.37	1.72±0.05	0.07	272±15	3.6±0.3	74±8
PGM3	3.38±0.09	13.18±0.4	1.69±0.05	0.07	252±21	3.8±0.3	66±8
PGM2	2.94±0.09	12.72±0.38	1.48±0.05	0.07	259±57	3.4±0.3	76±18
PGM1	2.4±0.07	9.76±0.29	0.79±0.02	0.07	169±11	2.4±0.2	67±8
Silt samples from the upper silt at the Phelps Goldmine, Southside, Hokitika							
RR3	***3.21±0.14***	***11.6±0.5***	***1.89±0.11***	***0.061±0.005***	***196.3±10.3***	***3.46±0.31***	***56.8±5.9***
PGM9	2.9±0.10	11.56±0.53	1.39±0.03	0.07	247±14	3.3±0.3	76±8
PGM8	3.01±0.10	12.49±0.57	1.48±0.03	0.07	213±10	3.5±0.3	61±6
PGM7	1.89±0.06	7.94±0.33	0.97±0.02	0.07	156±5	2.2±0.2	69±5
PGM6	2.95±0.10	11.57±0.53	1.35±0.03	0.07	189±4	3.3±0.3	58±5

Table 5.10: Comparison of luminescence dating results for individual horizons/localities. Samples taken for this PhD project have the prefix RR, all others being from Preusser et al (2005).

Locality	Uranium	Thorium	K Feldspar	Dose	Dose Rate	Age
Kamaka	Higher	Higher	Higher	Lower	Higher	Lower
Awatuna Fm, Chesterfield (silt unit)	Higher	Similar	Slightly Higher	Lower	Similar	Lower
Awatuna Fm, Chesterfield (Marine Sand)	Higher	Higher	Similar	Lower	Similar	Lower
Phelps Mine (lower silt)	Higher	Similar	Higher	Similar	Similar	Slightly Lower
Phelps Mine (upper silt)	Higher	Higher	Similar	Similar	Slightly Higher	Lower

Table 5.11: Comparison of luminescence ages for individual horizons. "Higher" means that the concentration from sampling for this PhD project is potentially greater than that from the Preusser et al (2005) sampling program.

The following comments are qualitative rather than quantitative. In terms of whether or not one or more of these luminescence dating projects has systematically overestimated or underestimated the age of the dated materials it is not presently possible to say for certain. The measurements for uranium, thorium, and K-feldspar are consistently higher when one contrasts this study against the other three studies. This is the case when all samples from each study are averaged and compared as in tables 5.8 and 5.10. It is possible, that even had exactly the same methodologies had been adopted in all four studies, a similar divergence could be produced via differences in the radionuclide contents of various randomly collected samples. There are not enough samples taken from the same sites in the different studies to enable a definitive assessment of this issue.

In table 5.10 samples taken from the same horizon are compared. Overall the radionuclides measured for this project have greater concentrations than those measured by Preusser et al (2005). The differences could have arisen by chance. However, there is some consistency in that the Uranium, Thorium and K feldspar concentrations all tend to be higher in the samples taken for this thesis. This tends to make the dose rate higher. In addition the measured "equivalent dose" tends to be lower. Collectively this causes the ages measured in this study to be less than those by Preusser et al (2005).

Unfortunately budgetary constraints relating to this PhD project prevented the indulgence of multiple sampling for each locality. The decision to sample many localities rather than a few was taken before some of the issues discussed here had become apparent.

There is one clear-cut difference between the methods adopted for luminescence dating for this project and the other projects discussed here. This is the a-value which was measured directly for each individual sample in this project. In contrast the alpha value was given a global average of 0.07±0.02 in each of the other three projects discussed here (being Preusser et al 2005, Vandergoes et al 2005, and Berger et al 2001). This may have a small impact on the final ages but if the global value is approximately in the middle of the locally expected range the effect on sample ages may be somewhat random and could average out in groups of samples taken from the same sedimentary unit.

One conclusion reached from consideration of the luminescence dating carried out by others in the Westland region is that the various dating methods each tend to provide a limit on the depositional age. There is no evidence for consistent underestimation of ages for samples taken during this project or the other projects discussed here in relation to laboratory procedures. As discussed in section 5.2 to 5.6

above there is evidence for incomplete bleaching, which has almost certainly caused some ages to be overestimated. In general in chapter 6 when discussing ages from Preusser et al (2005); Vandergoes et al (2005) and Berger et al (2001) the sampled horizons will be considered to be no older than the sample ages imply. So for some samples the depositional age may be younger than the numerical age. In relation to these three studies the scatter in sample ages appears to be worse in materials that are older than about 50-60 ka. In terms of the size of the 1σ error as a percentage of the sample age this also appears to increase in materials that are older than about 50 ka.

There is evidence of North to South variation in the average dose rate from luminescence samples taken to date in Westland. The average dose rates from seven studies are as follows:

5.36 Gy/ka	2 samples	Westport	Burge & Shulmeister (2007)
3.90 Gy/ka	30 samples	North Westland	Rose (2010)
3.82 Gy/ka	6 samples	Grey Valley	Hormes et al (2003)
3.15 Gy/ka	50 samples	North Westland	Preusser et al (2005)
3.17 Gy/ka	8 samples	Blue Spur & Saltwater Forest	Berger et al (2001)
2.51 Gy/ka	34 samples	Okarito	Vandergoes et al (2005)
0.78 Gy/ka	2 samples	Knights Point, South Westland	Cooper & Kostro (2006)

This south to north increase may be a consequence of changing sediment provenance. There appears to be sufficient natural variation along the West Coast such that it would be unwise to read too much into the differences between the average dose rates form the various studies. Preusser et al (2005) note that K-feldspar is more abundant in North Westland than in South Westland and the schists that contribute much of the sediment in South Westland are K-feldspar poor in comparison to granite. Granitic basement is more extensive in North Wetland so the fine sediment in North Westland carries more K-feldspar than that in South Wetland, contributing to higher dose dates in North Westland.

One additional study (Herman 2009) probed the OSL age of quartz from in-situ bedrock schist samples in the Southern Alps. A geothermal gradient was established for determination of the exhumation rate in the Whataroa-Perth catchment assuming an OSL closure temperature of around 30 to 35 deg C. They obtained an average dose rate of 3.27 Gy/ka from 13 samples. The range was 2.44 to 5.18 Gy/ka. Much of the sediment in the foreland (Westland lowlands) is derived from the schist belt. One would anticipate that sediments shed off the schists should, on average, have a similar dose rate. In this context there is nothing remarkable about the dose rates measured in the studies listed above, particularly given the potential for selective deposition of radiogenic minerals in littoral and fluvial environments.

CHAPTER SIX: QUATERNARY STRATIGRAPHY AND CLIMATE HISTORY, NORTH WESTLAND, SOUTH ISLAND, NEW ZEALAND

6.1 INTRODUCTION

6.1.1 Focus and Structure for Chapter Six

In chapter six the mid Quaternary to Holocene stratigraphy and climate history of North Westland is described. In this region the particular combinations of climate and sedimentary processes that produce glacial, fluvioglacial, fluvial and marine strandline deposits have occurred repeatedly through time. The essential characteristics of these deposits are much the same regardless of age. Similarly the combination of climate and sedimentary processes operative during interglacial and interstadial periods has occurred repeatedly, producing deposits that are similar in nature on each occasion. Type sections and sedimentology for most of the Late Quaternary formations are defined and described by Suggate and Waight (1999). The reader is referred to that publication for detailed descriptions. The same strategy is adopted for pollen diagrams from soil profiles from this region. These are presented in the published literature and will not be reproduced in detail here.

As is typical of Late Quaternary deposits in regions undergoing steady tectonic uplift, in North Westland there tends to be better preservation of younger deposits and poorer preservation of older deposits. In terms of the structure of the description of the Quaternary in North Westland there is some logic in describing the younger deposits first and the older deposits last. After all, much of the evidence for the age of the deposits, and therefore the correlation with climate events, sea level maxima and minima, and the estimation of uplift rates is therefore associated with the younger part of the sequence.

In arguing the merits of a newly proposed chronostratigraphy for North Westland the most compelling evidence relating to age control is associated with the younger part of the sequence, and it would be convenient to deal with this part of the sequence first. However, in terms of standard chronostratigraphic practice generally, and in terms of established practice in defining Quaternary sequences in New Zealand, the older deposits are almost always described first and the younger last. This is the format adopted here. It is also the format adopted for other publications that systematically describe Quaternary deposits in this region, particularly mapping projects. These include Nathan (1975, 76, 78a, 78b), Laird (1988), Johnston (1983), Roder & Suggate (1990); Suggate (1984), and Suggate & Waight (1999).

In the following discussion the older formations have ages assigned on the basis of correlation with "marine oxygen isotope stages" as defined by Martinson et al (1987) and Imbrie et al (1984). This has been standard practice in the decade's long process of creation of the Suggate model. However, a correlation does not imply that numerical ages are available in support of the interpretation. "Numerical ages" are defined here as ages that are produced via methods that include radiometric dating (particularly ^{14}C dating), luminescence dating, and cosmogenic isotope dating. By contrast correlations are "educated guesses" are often based largely on the nature of the sediment, transitions in pollen diagrams for the associated soils, assumed uplift rates, the assumed palaeo sea level and the elevation above present mean sea level. Correlation with a marine isotope stage (MIS) is not of itself a form of numerical dating, it merely implies an numerical age. Isotope stage correlations that are backed by numerical ages are more likely to be secure than those that are not.

In this chapter a wide range of data is presented in the context of a new marine isotope stage correlation. Contrasts between the new correlation and the Suggate model are discussed.

Aspects of the stratigraphy and geology of the deposits that are of interest here include:

i) The relative ages of the climate events, geomorphic surfaces, lithological units, and transitions between such units,
ii) Correlation between these events,
iii) The relative timing of erosional and aggradational events,
iv) The timing of sea level maxima and minima,
v) The extent of glacial ice.

Interpretation of climate changes in climate based on pollen recovered from peat, organic soil and loess is one of the foundations of the Suggate model. There are no published records of pollen deposition in North Westland that are known to be continuous for the last 100 kyr. This fragmented record has been assembled into a composite in table 6 of Moar & Suggate (1996).

It has previously been assumed (Moar & Suggate 1996; Suggate & Waight 1999, Moar et al 2008) that for North Westland, the last occurrence of full interglacial conditions coincided with MIS5e (~130 ka to ~120 ka) and the deposition of the Rutherglen Formation. Soils on terrace surfaces that contain one "full interglacial" flora (other than the Holocene) have been assumed to date from MIS5e. There are potentially viable alternative interpretations. In North Westland there are no soil profiles that contain two separate zones that each have a full interglacial flora (as defined by Moar & Suggate 1996). This raises the question of how one defines a full interglacial flora for North Westland? This has been discussed briefly in chapter 5 in relation to the pollen record from the Okarito Pakihi reported by Vandergoes et al (2005) and Newnham et al (2006). The issue is also raised in Chapter 5 in relation to the use of *Nestegis* in the definition of MIS5 deposits in Westland by Moar et al (2008) and Moar & Suggate (1996).

One of the aims of this project is to refine the climate history and marine isotope stage correlation for North Westland. Achieving this requires secure dating of at least one of the raised marine terraces. For this reason the primary targets for dating have been the Rutherglen and Awatuna Formations, both of which are potentially within the range of IRSL dating. The strategy is not to attempt to confirm the prior isotope stage correlation but to consider the previously available dating and the new ages in terms of the simplest model consistent with the evidence.

If the Awatuna Formation strandline is correlated with MIS5c or MIS5a then the implication is that finite ^{14}C ages from the organic soil resting on its surface are unlikely to be depositional ages. In the Suggate model the Awatuna Formation is assigned to MIS5c so finite ^{14}C ages from the base of the overlying soil are discarded, irrespective of whether or not contamination by younger carbon can be proven. There is cause for concern because each locality where the soil on this formation has been dated by ^{14}C yields a mixture of finite and infinite ages, generally older towards the base.

If the main strandline of the Awatuna Formation is correlated with MIS3 the option of accepting relatively old ^{14}C ages is open, and the implication is that there was a significant sea level high stand in North Westland during MIS3. The nature of the climate during MIS3 in North Westland is largely unknown. There have not previously been any detailed studies specifically targeting this period for North Westland, probably partly due to a perceived lack of MIS3 deposits in this region. The most relevant publications include:

- Burge (2007) – A study of MIS4/3 climate for the Westport area.
- Burrows et al (2008) – A study of post MIS6 climate at a coastal site north of Greymouth.
- Vandergoes et al (2005) – A study of post MIS6 climate at Okarito in South Westland.

- Pelejero et al (2006) and Barrows et al (2007) – Studies that produced a high resolution record of sea surface temperatures at core SO136-GC3 in the Tasman Sea about 100 km off the coast of North Westland.

In the new marine isotope stage correlation proposed here there are a number of fluvioglacial and marine deposits assigned to MIS3. This is a significant departure from the Suggate model and requires a detailed justification. In order for a new correlation to be accepted it needs to be in accord with the available evidence and to fit the evidence better than the prior model.

6.1.2 Climate, Vegetation and Pollen in Westland during MIS3

Chapters 4 and 5 contain an extended discussion of regional climate during MIS3. It is concluded that there is a very good record of MIS3 climate and sedimentation at Okarito. This is a new interpretation of luminescence dating and palynology reported by Vandergoes et al (2005). The Okarito composite profile contains a pollen assemblage with a number of interglacial/interstadial affinities including the continuous presence of the genus *Nestegis* (Oleaceae). The dating is not sufficiently precise to determine the duration of this period, which could be interpreted as containing as many as 4 upward temperature spikes.

MIS3 is not likely to have been a period of continuous glacial climatic conditions in Westland. There is growing evidence from different parts of New Zealand that the early part of MIS3 was in fact quite warm. For instance the Auckland area supported a rimu (*Dacrydium cupressinum*) dominated forest between 60.5 and 50.5 ka (Shane & Sandiford 2003). Shulmeister et al (2001) reached a similar conclusion on the timing of a period of warm climate (c. 55-50 ka) on the basis of a pollen assemblage of "near-interglacial affinity" from Lake Poukawa (Hawkes Bay). Based on analysis phytoliths in a dated loess core Carter (2007) found evidence for remarkably warm early to middle MIS3 climate for the Wairapapa region. Carter & Lian (2000) demonstrate periods of warm MIS3 climate in a well dated loess core from the south eastern North Island. Burge (2007) demonstrates near-modern mean summer temperature, at least for a short time, around 36 ka in the Westport area. How likely is it that this was the only MIS3 warm-period in Westland? How likely is it that this was the warmest or most stable climatic episode during MIS3 in Westland?

Evidence for relative climatic warmth during MIS3 is reiterated here because it is important in relation to marine isotope stage correlations for the Rutherglen and Awatuna Formations in particular. The likely occurrence of this period of relatively mild climate in South Westland opens the palynology and stratigraphy in North Westland to discussion and reinterpretation. This is carried out on a formation by formation basis in Chapter 6.

The occurrence of relatively warm conditions in North Westland during the early part of MIS3 would allow the deposition of organic soils that yield a combination of *Nestegis* and *Dacrydium cupressinum* pollen and both finite and infinite ^{14}C ages. In this scenario a mix of finite and infinite ages does not automatically imply that the finite ages are caused by samples being contaminated with significantly younger carbon. Further, any claim that contamination was the cause of the production of a finite age would require specific justification.

In the Suggate model *Dacrydium cupressinum* is presumed to prefer warm(ish) and wet(ish) conditions in Westland. This species has a wide distribution in New Zealand, being a major component of modern lowland forests as far south as southern Stewart Island. So at present lowland podocarp forest dominated by *Dacrydium cupressinum* survives well at a latitude of about 47° to 47.3°S where the modern climate is significantly colder than that of Westland. By comparison Okarito is at latitude 43.2°S. So the presence of *Dacrydium cupressinum* pollen in a

Late Quaternary soil from Westland cannot realistically be taken to indicate that local climate at that time was similar to the present as this species clearly has a reasonably wide climatic tolerance.

Given the findings of Chapter 5 my approach here is that local evidence for interstadial to interglacial climatic conditions during MIS3 should not be unexpected, and should be accepted if the balance of evidence favours that interpretation.

6.1.3 The "Suggate Model"

In the main part of this chapter the middle to late Quaternary stratigraphy of North Westland is discussed in detail. For easy reference the marine isotope stage correlation from Suggate & Waight (1999) is presented in Table 6.1.

Table 6.1: Existing Quaternary Stratigraphy and Marine Isotope Stage correlation for Westland as proposed by Suggate and Waight (1999) with the addition of the 3 highest marine benches which are situated outside the area covered in that study. The column listing supporting ages does not include IRSL dating carried out during this (PhD) project. Nor does it include luminescence dating by Hormes et al (2003), Berger et al (2001), Preusser et al (2005) or Vandergoes et al (2005).

Isotope Stage	Formation Glacial / Interglacial	Glacial Stage	Glacial Advance	Supporting Ages
1	Nine Mile 2 Nine Mile 1	Aranui Interglacial		
2	Moana (minor interval) Larrikins 2_2 Larrikins 2_1	Otira Glaciation	Kumara 3 Kumara 2_2	^{14}C, IRSL, OSL ^{14}C, IRSL, OSL
3/2	Larrikins 1			
3	None (important interval)		Kumara 2_1	^{14}C, IRSL, OSL
4	Loopline			
5a	Craig?	Kaihinu Interglacial		^{14}C, IRSL, OSL
5b	None			Nil
5c	Awatuna			^{14}C, IRSL, OSL
5d	None			Nil
5e	Rutherglen			AAR
6	Waimea	Waimea Glaciation	Kumara 1	IRSL
7	Karoro Scandinavia	Karoro Interglacial		Nil Nil
8	Tansey	Waimaunga Glaciation	Tansey 2 Re-advance Tansey 1	Nil Nil
9	Caledonian			Nil
10	Cockeye	Nemona Glaciation		Nil
11	Whisky Candlelight			Nil Nil
12	Mudgie Ridge	Kawhaka Glaciation		Nil

In order to provide a further point of reference two illustrations are provided at this point. These are figures 6.1 and 6.2 prepared specifically for this PhD thesis. Figure 6.1 is a representation of the Quaternary stratigraphy of North Westland with some changes and additions to that given in table 6.1. Figure 6.2 shows the marine terrace sequence with elevations as measured between North Beach and Point Elizabeth.

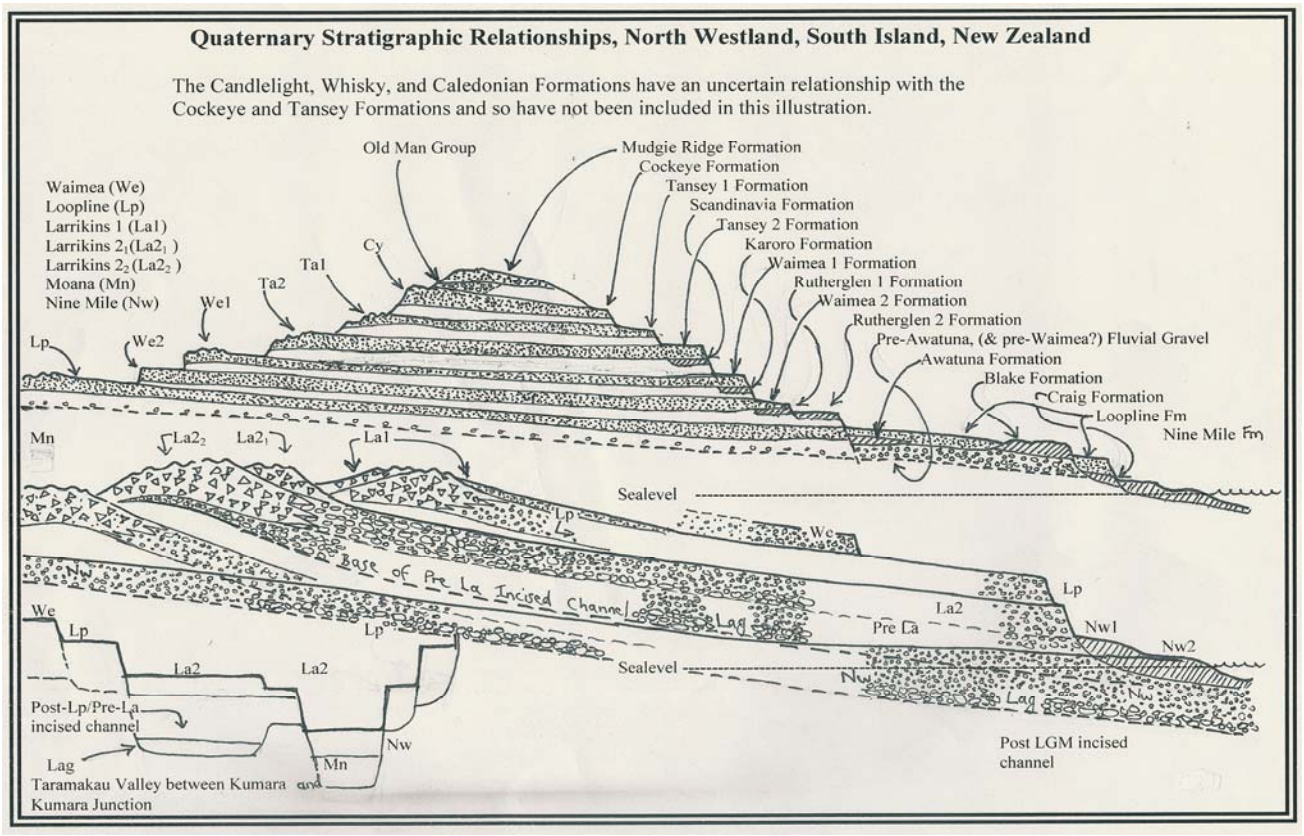

Figure 6.1 Quaternary Stratigraphic Relationships, North Westland, South Island, New Zealand

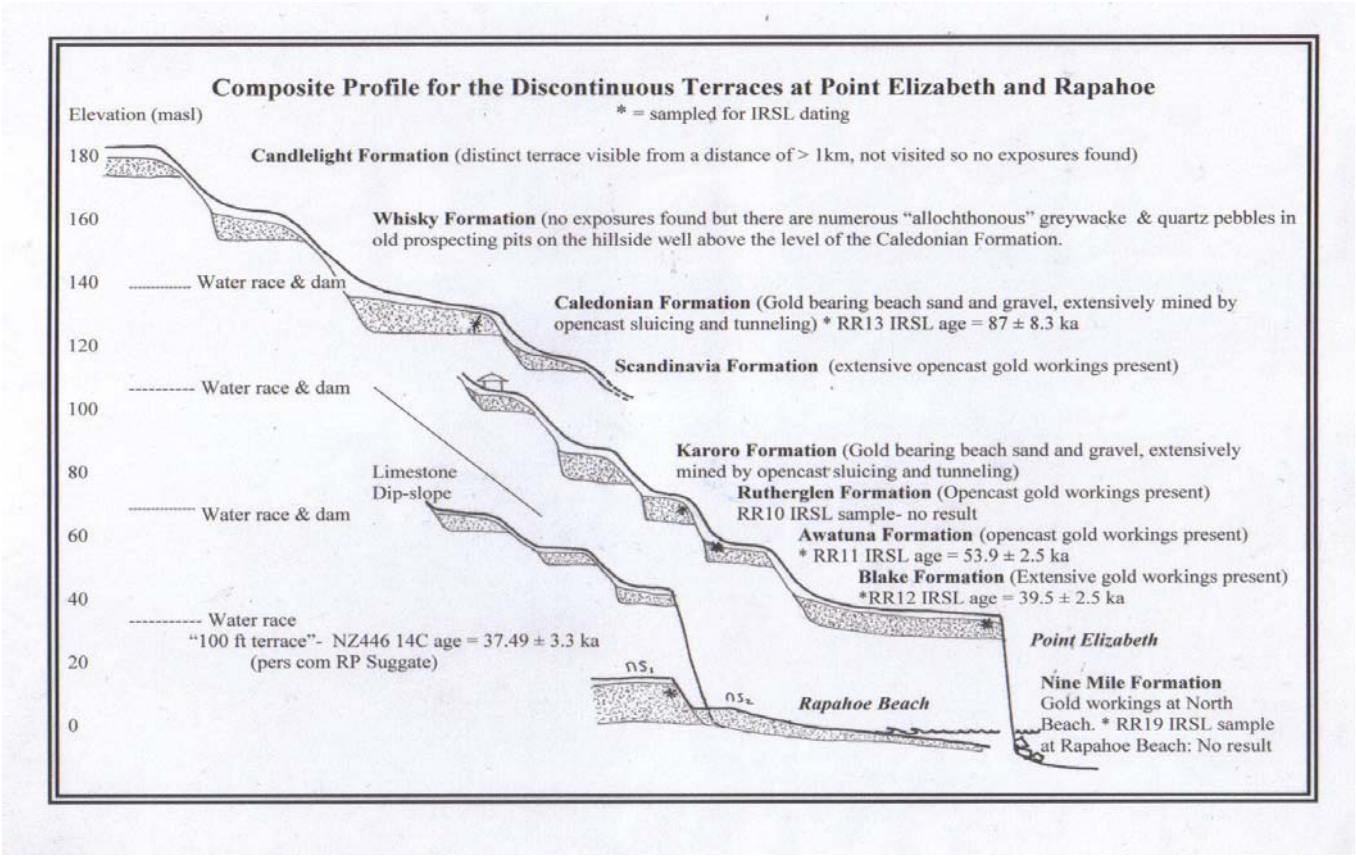

Figure 6.2 Composite Profile for the Discontinuous Terraces at point Elizabeth

6.2 REVISED QUATERNARY STRATIGRAPHY, DATING AND CLIMATE HISTORY

6.2.1 Mudgie Ridge Formation (Kawhaka Glaciation)

The Mudgie Ridge Formation is defined by Suggate and Waight (1999) who assign it to MIS12. The type section is Mudgie Ridge Road. The only change proposed here is the marine isotope stage correlation. There are no numerical ages available for the Mudgie Ridge Formation. Nor are there numerical ages for the next younger (Cockeye) formation. At present any marine isotope stage correlation (including that by Suggate and Waight 1999) is purely speculative. Therefore no firm isotope stage correlation is made here for the Mudgie Ridge Formation.

The Mudgie Ridge Formation contains the only confirmed deposits from the Kawhaka Glaciation. There are no complete/continuous sections currently exposed through the formation. The Kawhaka Glaciation was described by Suggate & Waight (1999) as follows:

> "The Mudgie Ridge deposits represent the Kawhaka Glaciation (new glaciation name)."

During the Kawhaka Glaciation there was a substantial glacial advance. The nature of the sediments deposited during the advance is the only evidence cited by Suggate & Waight (1999) in support of a relatively cold climate during this glaciation. Sediments deposited at Mudgie Ridge during this glaciation include glacial till, lake beds and aggradational fluvioglacial gravel. In the limited area over which this formation outcrops glacial ice extended approximately as far seaward from the Southern Alps as it did during the Waimean and Otiran Glaciations.

Known outcrops of the Mudgie Ridge Formation are currently restricted to the Mudgie Ridge area (grid ref J32 3200N 5900E) in the Waimea Forest between Stafford Loop Road and the "Old Christchurch Road" in the Arahura Valley. Similar deposits are present at Stony Creek about 7 km SE of Hokitika (Suggate & Waight, 1999). These are assumed but not proven to be of the same age as the Mudgie Ridge Formation. The glacial nature of the deposits is determined by sedimentology rather than geomorphic expression. The Mudgie Ridge Formation is situated on a ridge line. The Formation is highly dissected and the original geomorphic expression has been more-or-less totally destroyed.

6.2.2 Pre Cockeye Fluvial Incision

Given the very restricted distribution of the Mudgie Ridge Formation is assumed that deposition of the Cockeye Formation was preceded and accompanied by widespread fluvial incision and strath cutting. This resulted in the destruction of much of the older Mudgie Ridge Formation. Destruction of the Mudgie Ridge Formation continued during subsequent glacial and fluvial erosional episodes.

6.2.3 Cockeye Formation (MIS6, Nemona Glaciation)

The most complete description of the Cockeye Formation is that by Suggate and Waight (1999) who assign it to the Nemona Glaciation. This formation was originally defined by Suggate (1965) and redefined by Suggate (1985). The Manuka Formation in the Buller River catchment area is thought by Suggate (1988) and Roder & Suggate (1990) to be the equivalent to the Cockeye Formation and was assigned by Suggate (1988) to the Nemona Glaciation. There are no numerical ages available for the Cockeye Formation or for the Manuka Formation. Therefore any marine isotope stage correlation is

purely speculative (including that by Suggate & Waight 1999). Therefore no firm isotope stage correlation is made here for the Mudgie Ridge Formation.

The Nemona Glaciation was described by Suggate & Waight (1999) as follows:

> "The Cockeye Formation represents the Nemona Glaciation (Suggate 1985)".

As a formal definition this might be considered to be rather succinct or "brief but effective". The formal definitions of the Waimaunga and Waimea Glaciations are similar in nature. When it was defined by Suggate (1965) the Cockeye Formation represented the deposits of the Waimaunga Glaciation. Subsequently Suggate (1985) separated these glacial and fluvial deposits were into two parts being the (older) Cockeye and (younger) Tansey Formations. The Tansey Formation was assigned to the Waimaunga Glaciation and the Cockeye Formation to the (new) Nemona Glaciation.

Suggate (1965) defined the Waimaungan Stage as:

> "embracing all those deposits laid down after the beginning of the cooling that led to the Waimaungan Glaciation and before the warming that led to the Terangi Interglacial".

This economical definition implies that the older part of the Cockeye Formation (excluding the Tansey Formation) predates the "Terangi Interglacial". The "Terangi Interglacial" was not identified in North Westland by Suggate and Waight (1999).

Other than the sedimentology of the glacial and fluvioglacial deposits of the Cockeye Formation no supporting data are supplied or cited by Suggate (1965), Suggate (1985), or Suggate & Waight (1999) in relation to the nature of the climate immediately prior to, during, or immediately following the deposition of the Cockeye Formation. No data are available on the palynology of the first soils deposited on the Cockeye Formation. Therefore the definition of the Nemona Glaciation relies almost entirely on sedimentology.

It is suggested here that the Cockeye Formation is more likely to correlate with MIS6 than MIS10. The basis for this suggestion is a revised tectonic uplift rate (as summarised in chapter 7) and the proposed younger correlations for each successively lower and/or younger formation in the North Westland sequence. Any such correlation for the Cockeye Formation will would be based on assumption relating to the continuity of the tectonic uplift rate determined for the period prior to the deposition of the Scandinavia Formation (the oldest firm indictor of local base level in any area where the Cockeye Formation is present).

The type section for the Cockeye Formation was defined by Suggate (1965) as an area of outcrop on a forestry road in the Nemona Forest at NZMS260 map grid K32/706457 in the upper portion of the New River catchment area. The glacial and fluvioglacial nature of the Cockeye deposits is determined by sedimentology and geomorphic expression. In the Cockeye Creek area there are reasonably well preserved moraines and fluvioglacial outwash terraces. Glacial till and outwash gravel is (or has been) exposed in numerous forestry road cuttings. Gravel of the Cockeye Formation is variably weathered both within and between outcrops.

As mapped out in detail by Suggate & Waight (1999) the terminal moraines formed during the Nemona Glaciation are located mainly seaward of the LGM terminal moraines. This implies that glacial ice was at least as extensive during this period as during the LGM. So it is likely that the local ice volume was comparable to that of the LGM.

An area of formerly "unnamed gravels" mapped and labeled as "xp" by Nathan (1978b) at the head of Red Jacks and the Ongionui River (12 Mile Creek) in the Grey Valley has since been re-defined as

Cockeye Formation by Suggate & Waight (1999). Nathan (1978b) has this terrace being older than the coastal Whisky and Caledonian Formations. This is an assumption as there are no known contact relationships. Areas mapped as "xp" (Nathan 1978b) or Cockeye Formation (Suggate & Waight 1999) in the Grey Valley are on the inland side of the Brunner-Mt Davy Anticline at the Southern tip of the Paparoa Range. The Caledonian and Whisky Formations are on the opposite (seaward) of this actively developing regional-scale anticlinal structure. So little can be read into the relative elevations of the respective surfaces across this structure. However, the established relative age assumption is carried though to this PhD thesis. Given the projected elevation of the Cockeye Formation in the Greymouth-New River area it is plausible that the Cockeye Formation is older than both the Caledonian and Whisky Formations, not withstanding the potential for tectonic deformation of these surfaces.

In the Suggate stratigraphy as expressed by Suggate & Waight (1999) there are no marine shoreline deposits between the Nemona and Waimaunga Glaciations in the Kumara-Moana map area. Nathan (1978b) [1:63360 scale map and associated notes , Sheet S44, for the Greymouth area just to the north of the Kumara-Moana map sheet by Suggate & Waight 1999] illustrates two high strandlines (Whisky and Caledonian) that are younger then the "xp" unit. So it is likely that Nemona fluvioglacial deposition was followed by a marine transgression and probably by a dramatic reduction in ice extent. There is no record of an associated climate change via analysis of pollen. By analogy with the MIS2/1 transition the following assumptions are made:

i) That there was a substantial period of fluvial incision and strath cutting in the major valleys during the post Nemona deglacial period.

ii) That rising sea level and marine transgression during the later part of the deglaciation probably caused a period of fluvial aggradation in the main valleys.

iii) That the transgression culminated in the deposition of the Candlelight Formation on a wave-cut cut platform just east of Rapahoe and probably at Point Elizabeth. These sediments are better preserved between Charleston and the Tiropahi River, with a mapped area of about 1 km^2.

6.2.4 Candlelight Formation (MIS5e)

The Candlelight Formation is defined by Nathan (1975) in relation to cemented brown ilmenite-rich marine sand and gravel deposits at an elevation of 180- 190 metres near Charleston.

There is a topographic feature that is assumed to be a marine bench at 180 to 190 metres above sealevel at Point Elizabeth. This has not been confirmed in outcrop as the locality is inaccessible, clad in very thick rainforest, and underlain by rugged limestone karst topography. This level is assumed to correlate with the Candlelight Formation. Suggate (1992) identified a 180 m marine terrace a few kilometres to the east at Rapahoe. Assignment of the 180-190 m terrace to the Candlelight Formation is dependent on coast parallel correlation from the Charleston area.

Nathan (1975) implies that the Candlelight Formation was deposited during an interglacial that was "older than the Terangi Interglacial". Other than the sedimentology of the marine sand/gravel deposits of the Candlelight Formation no supporting data are supplied or cited by Nathan (1975) in relation to the climate immediately prior to, during, or immediately following the deposition of the Candlelight Formation. No data are available on the palynology of the first soils deposited on the Candlelight Formation.

There are no numerical ages available for the Candlelight Formation. Therefore any marine isotope stage correlation is speculative. Two terraces that are present at Point Elizabeth are assigned here to MIS5e being the Candlelight and Whisky Formations. The Candlelight Formation is assigned to

the early part of MIS5e. The age-estimate for the Candlelight Formation is 135 to 130 ka based on the dating of marine terraces that are at lower elevations in the sequence described here. These include the Scandinavia, Caledonian, Karoro, Rutherglen and Awatuna Formations, the dating of which seems to imply a more or less continuous tectonic uplift rate. The age estimate for the Candlelight Formation assumes a "near present" local sealevel during deposition and an uplift rate of ~ 1.35 to 1.4 mm/yr. The uplift rate (calculation summarised in chapter 4) is based on the assumption that the (lower) Whisky, Caledonian and Karoro Formations correlate with Early-MIS5e, MIS5c and MIS5a respectively. Numerical dates that provide support for the age of these formations are discussed below.

The relative ages of the Candlelight and Cockeye Formations are unclear as there are no observed contact relationships. The elevation of the Cockeye fluvioglacial surface the New River area, projected down-slope to the northwest, is sufficiently high that it could have been truncated by a lower Candlelight strandline. On the other hand a higher elevation for the Cockeye surface would also be consistent with aggradation of fluvioglacial gravel across an older Candlelight surface.

The strandline elevations for both the Candlelight and Whisky Formations at Point Elizabeth are substantially higher than the nearest outcrops of the Tansey Formation (about 115 to 120 m at South Beach, Suggate & Waight 1999). There are no known contact relationships between the Tansey Formation and either marine Formation. There is no evidence that these marine Formations were overwhelmed by Tansey deposits. If buried marine strandline deposits did exist it is likely that they would have been discovered by the gold prospectors during the mid to late 1800's and early 1900's. If this had occurred the deposits would have been noted by the local Mines Wardens in annual reports compiled for the comprehensive "Mines Statement" assembled annually by the Mines Department for the Minister of Mines. This document was reported each year to the House of Representatives and subsequently published by the Government. Deeply buried deposits of this type were prospected by the miners then reported by the Mines Wardens. These include strandlines at Craigs Freehold (Craig Formation- see below), Scandinavia Hill (Scandinavia Formation), Candle Light (Rutherglen Formation), Blue Spur and Big Paddock (Karoro Formation) and Chesterfield (Lamplough Lead/Awatuna Formation). Marine deposits are not preserved at the surface at an elevation south of Greymouth that is appropriate for correlation with the Candlelight or Whisky Formations. The erosional base of the Tansey Formation (about 100 m) at Mill Creek, South Beach is substantially lower than the expected base for the Candlelight and Whisky Formations. It is likely that fluvial activity during and prior to the deposition of the Tansey Formation would have resulted in the destruction of the Whisky and Candlelight Formations if they were present.

Nathan (1978b) provides a prior justification for the reasonable assumption that the Whisky and Candlelight Formations are older than the Tansey Formation. In his stratigraphy these two marine units are older than his mapped Cockeye Formation. However, Suggate & Waight (1999) have re-defined Nathan's "Cockeye" Terrace level as Tansey Formation. So logically following Suggate & Waight (1999) the Candlelight and Whisky Formations are older than the Tansey Formation.

The marine terrace sequence is well developed in the Charleston area, where the Candlelight Formation as defined by Nathan (1975) is assigned to MIS13 by Suggate (1992). The assignation is displayed in figure 2(2) and figure 3A of Suggate (1992), but it is purely speculative as there are no numerical ages.

Correlation of the Candlelight Formation with MIS5e (this thesis) has the unavoidable effect of altering the MIS correlation for the younger Karoro Interglacial. Logically Karoro Interglacial, which is named after the Karoro Formation and represents the state of the climate during the deposition of the Karoro Formation, cannot correlate with MIS7 if an older deposit (the Candlelight

Formation) is assigned to MIS5e. The proposed isotope stage correlation the Karoro Formation in this study is MIS5a so the Karoro Interglacial should encompass MIS5a. This correlation does not rely on that proposed here for the Candlelight Formation. In the new isotope stage correlation there are no longer any confirmed MIS7 raised marine deposits in Westland, unless terraces situated east of the Alpine Fault (as described by Bull & Cooper 1986 and Ward 1988) are considered. These terraces have not been examined as part of this project.

A warm climatic episode encompassing MIS5e could be termed the "Charleston Interglacial". If a stratotype was to be selected it would come from the Candlelight and Whisky Formations in the Charleston area. This is beyond the scope of this project though.

6.2.5 Whisky Formation (Late MIS5e)

The Whisky Formation is defined by Nathan (1975) in relation to cemented brown ilmenite-rich marine sand and gravel deposits at an elevation of 165- 170 metres near Charleston. At Point Elizabeth deposits that are assumed to correlate with Whisky Formation (from Charleston) are situated at an elevation around 155 to 160 metres above sealevel.

The Whisky Formation as defined by Nathan (1975) is assigned to MIS11 by Suggate (1992). The assignation is displayed in figure 2(2) and figure 3A of Suggate (1992). There are no numerical ages available for the Candlelight Formation. Therefore any marine isotope stage correlation is speculative including that by Suggate (1992).

Nathan (1975) implies that the Whisky Formation was deposited during an unnamed interglacial that was "older than the Terangi Interglacial". Other than the sedimentology of the marine sand/gravel deposits of the Whisky Formation no supporting data are supplied or cited by Nathan (1975) in relation to the climate immediately prior to, during, or immediately following the deposition of the Whisky Formation. No data are available on the palynology of the first soils deposited on the Whisky Formation.

The Whisky Formation was not dated by IRSL during this project. The Whisky Formation is assigned to MIS5e here largely on the basis of the long-term uplift rate (the same strategy is employed in the Suggate model) and the assumptions that the Caledonian Formation correlates with MIS5c, the Karoro Formation with MIS5a and the Rutherglen(1) Formation with the MIS5a/4 transition. The estimated age for the Whisky Formation is c. 115-120 ka which coincides with the end of MIS5e. The timing of the MIS5e/5d transition is discussed below.

The proposed timing of terrace formation requires some discussion. There is a substantial (up to 20 to 30 m) difference in elevation between the Candlelight and Whisky Formations at Point Elizabeth. It is assumed that the Candlelight Formation was deposited at a sea level equivalent to or slightly higher than the modern level at or before 130 ka and that the Whisky Formation was deposited at a sea level equivalent to or slightly lower than the modern level. In that case a substantial part of the difference in terrace elevation is due to tectonic uplift. This implies that there is potentially around 12 to15 kyr in which to accumulate tectonic uplift. There is some flexibility in terms of the sealevel and uplift rate. Using the mean uplift rate of 1.35 to 1.4 mm/yr suggested in Chapter 7 around 16 to 20 m of uplift would be a reasonable expectation which matches reasonably well with the separation between the two terraces, given that they might not have formed at the same sealevel and that the isostatic effects of local sea level and ice volume changes have not been considered.

It is assumed here that the Whisky Formation was deposited or isolated at or near the end of the MIS5e sealevel highstand (i.e. at the MIS5e/5d transition). This transition is defined by the timing

of the change in oceanic bottom-water $\delta^{18}O$ and global ice volume rather than the transition in surface climate at the end of the Eemian period. Kukla et al (1999), Klotz et al (2003) and Shackleton et al (2003) present a strong case for extension of the Eemian period in Continental Europe well past the MIS5e/5d transition. The interglacial/glacial (surface climate) transition occurred at c. 114 ka according to Klotz et al (2003) and 110 ka according to Shackleton et al (2003). Kukla et al (1999) suggest the Eemian period had a duration of at least 13 kyr and recognise that this period partially overlaps MIS5e. They also find that MIS5e commenced prior to the beginning the Eemian period. In terms of marine oxygen isotopes it was found by Jouzel et al (2002) and Martinson et al (1987) that the MIS5e/5d transition occurred after 120 ka. Waelbroeck et al (2002) illustrate in their figures 2 & 4 that this transition occurred at c. 116 ka. This is supported by Shackleton et al (2003) who defined the MIS5e/5d transition at c.115 ka. From a compilation of radiometrically dated corals McCulloch et al (1999, 2000) illustrate sealevel at or above the modern level until c. 117 ka. Muhs et al (2002) assembled a large database of U/Th ages on corals from Bermuda and Hawaii that indicates high sea level until c. 115 ka. From a study of oceanic bottom-water temperature change Martin et al (2002) indicate that the MIS5e/5d transition occurred post 120 ka. Finally in a review of Last Interglacial climates Kukla et al (2002) state:

> "Between ca. 130,000 and 116,000 yr ago, the climate over much of the globe was at first warmer than, and later not very different from, that of the last 10 millennia."

Taken as a group these various studies indicate that eustatic sea level was probably close to the modern level as late as 115 ka. So it is not unreasonable to suggest that the marine terrace represented by the Whisky Formation could have been occupied until about this time (i.e. as late as c. 115 to 116 ka). But does this then overlap with the MIS5d sea level minimum?

The first sea level minimum in MIS5d was achieved at c. 107-109 ka in studies by Shackleton et al (2003) and Martin et al (2002), at c. 107-112 ka by Martinson et al (1987), 110-112 ka by Waelbroeck et al (2002) and 108-110 ka by Jouzel et al (2002). It is also worth noting from Petit et al (1999) that at the Vostok ice core site in Antarctica the isotopic temperature, CH_4 concentration, and $\delta^{18}O$ of atmospheric O_2 (a proxy sealevel indicator) reach minimum at c. 107-112 ka. Winograd et al (2006) place the temperature minimum for MIS5d at c. 108-112 ka on the basis of $\delta^{18}O$ in calcite from the Devils Hole cave system in Nevada. So on balance it is not unreasonable to suggest that the relatively short-lived MIS5d sea-level minimum occurred at c 107-112 ka and does not overlap the proposed minimum age for the Whisky Formation.

At Point Elizabeth the base of the thick soil-like cover (4 m+) on the Whisky Formation has not been observed in outcrop. Nathan (1978) noted that just east of Rapahoe the Whisky Formation consists of cemented brown gravel, which is almost certainly of marine origin. This deposit was first mapped by Gage (1952) who illustrated a high marine terrace at Trig Point CB (elevation of 532 ft or 162 m).

During the early 1990's an area of Whisky Formation was mined for gold inland (east) of Rapahoe using earthmoving machinery including a hydraulic excavator. Clean heavy-mineral bearing sand containing discoidal pebbles and cobbles was exposed. The gravel component is dominated by granite, Haast Schist and Torlesse Greywacke and so could not have had an immediately local source. At Point Elizabeth and Rapahoe there are no nearby in-situ outcrops of these rocks. The source for the Haast Schist and Torlesse Greywacke component of the gravel is situated many 10's of kilometres away in the Southern Alps to the east of the Alpine Fault. Non-local provenance is a feature common to strandline deposits of each of the raised marine terraces in this region.

In each of the raised marine strandline deposits the high heavy mineral content of the clean sand, including gold, garnet and ilmenite (Suggate & Waight 1999), the very low silt content, and the

mainly discoidal nature of the pebbles and cobbles is indicative of transport in a marine shoreline and near-shore environment. Much of the transport is likely to have occurred in the swash zone, the general direction of transport being from southwest to northeast. This sedimentary environment has been established for strandline deposits of the Scandinavia, Karoro, Rutherglen, Awatuna and Nine Mile Formations by Suggate & Waight (1999). It is extended in this thesis to include the clastic sediments of the Whisky, Caledonian, Blake and Craig Formations and probably the Candlelight Formation.

The Whisky strandline has not been identified south of Greymouth but there are remnants to the north, particularly near Point Elizabeth and Charleston. At Point Elizabeth the elevation of the Whisky Fm is slightly higher than the 130 to 140 m level expected for the Tansey(1) Formation when projected to the position of the Rutherglen Formation strandline at Candle Light near Camerons. So fluvial erosion both during and subsequent to the Waimaunga Glaciation and marine erosion during and subsequent to the deposition of the Caledonian Formation could have destroyed most of the Whisky Formation south of Greymouth.

6.2.6 Pre Tansey Fluvial Incision

Between Greymouth and Hokitika the Cockeye Formation outwash terraces are significantly higher than those of the Tansey(1) Formation. From the distribution of remnant Mudgie Ridge and Cockeye surfaces it is assumed that large parts of these Formations had been destroyed prior to the deposition of the Tansey(1) Formation. By analogy with destruction of the parts of the Larrikins and Loopline Formations during the MIS2/1 transition and during the Holocene, a substantial part of this destruction is likely to have preceded and accompanied the marine erosion events (Candlelight & Whisky) defined above. Pre-Tansey strath cutting is also likely to have occurred at the onset of the Waimaunga Glaciation when bed load matched or exceeded the transport capacity of the main rivers. This would promote lateral erosion at the expense of incision.

6.2.7 Tansey(1) Formation (MIS5d, Waimaunga Glaciation)

The Tansey Formation was first defined by Suggate (1985a). It was redefined by Suggate & Mildenhall (1991) and again by Suggate & Waight (1999) who separated the formation into two sub-units of differing age and correlated both these with MIS8 (c. 270 - 250 ka). They do not present a specific justification for assigning both the Tansey(1) and Tansey(2) Formations to MIS8. The Tansey Formation contains the deposits of Waimaunga Glaciation. There are two sets of terminal moraines (Tansey(1) & Tansey(2)) corresponding to the two outwash surfaces. The timing of the each glacial advance and fluvial aggradation that followed is similarly poorly constrained. Suggate & Waight (1999) do not comment on any alternative explanations for the glacial retreat and readvance that resulted in the Tansey(2) Formation. The Tansey(1) Formation contains till and aggradational fluvioglacial gravel. The type locality is defined by Suggate (1985a) and is situated in the area between grid references J32/615445 and J32/617444. Suggate & Waight (1999) correlate the Tansey Formation with the Harry Formation of the Upper Buller Gorge that is described by Suggate (1988).

The exact stratigraphic relationship between the Tansey(1) and Whisky Formations is uncertain as there are no known outcrops in close proximity.

There is no direct numerical age control for deposits of the Tansey(1) Formation. There are no numerical ages on any of the older fluvioglacial deposits. There are no direct contact relationships with the Scandinavia Formation. But based on the gradient of the upper surface of the Tansey(1)

Formation in the Waimea Forest area and the elevation of the Scandinavia strandline Suggate & Mildenhall (1991) suggest this formation is older than the Scandinavia Formation.

In terms of this thesis the Tansey(1) Formation is correlated MIS5d rather than MIS8 (Suggate model). This correlation is based on assumptions as follows:

- That the Tansey(1) formation is younger than the Whisky Formation(late MIS5e).
- That the Tansey(1) Formation is older than the Caledonian Formation.
- That the Tansey(1) Formation is older than the Scandinavia Formation.
- That the tectonic uplift rate for the period prior to the deposition of the Scandinavia Formation (the first firm indictor of local base level in an area where the Tansey Formation is present) also applies to the period between the deposition of the Tansey(1) and Scandinavia Formations.

The new assignation speculative but is supported by luminescence dating undertaken during this project on the Scandinavia, Caledonian, Karoro, Waimea and Rutherglen Formations, all of which are stratigraphically younger than the Tansey(1) Formation. The new MIS correlation is a large change from that of the Suggate model. However, beyond MIS2 that model has not been confirmed by numerical dating. Note that for each Late Quaternary Formation discussed here the "Suggate-age"/"Rose-age" ratio is similar.

In the absence of numerical dating the proposed timing for the Waimaunga Glaciation and the deposition of the Tansey(1) Formation is provisionally c. 107-112 ka coinciding with the MIS5c eustatic sea level minimum, assuming a northern Hemispheric driver for this glaciation. This age and forcing mode are both speculative, particularly given recent proposals for southern Hemispheric forcing of glaciation in South Westland at c. 79ka by Sutherland et al (2007) and at 34-28 ka by Suggate & Almond (2005), and southern Hemispheric forcing of zonal westerly winds by Rother & Shulmeister (2006) and Shulmeister et al (2004).

Given the younger than expected $IRSL_{(blue)}$ ages on the Scandinavia, Caledonian, Karoro and Rutherglen Formations it is possible that the basal cover beds on the Tansey(1) Formation might fall within the age range datable by $IRSL_{(blue)}$.

Other than the sedimentology of the glacial and fluvioglacial deposits of the Tansey Formation no supporting data are supplied or cited by Suggate (1965), Suggate (1985), or Suggate & Waight (1999) in relation to the climate immediately prior to, during, or immediately following the deposition of the Tansey Formation. No data are available on the palynology of the first soils deposited on the Tansey Formation. Therefore the definition of the Waimaunga Glaciation relies almost entirely on sedimentology. The Waimaunga Glaciation was described by Suggate & Waight (1999) as follows:

"The Tansey Formation represents the Waimaunga Glaciation, following the revision of the sequence by Suggate 1985".

In the Suggate model it is assumed that the Waimaunga Glaciation was preceded by a significant climatic deterioration from an un-named interglacial. This assumption is based on comparison with the transition from the Karoro Interglacial to the Waimea Glaciation (Karoro Formation to Waimea Formation). The suggested climate change culminated in the deposition of the Tansey Formation. There is no hard evidence for such climate change via analysis of pollen.

The Tansey(1) deposits are the result of accumulation during a glacial advance, thick fluvioglacial deposits mapped by Suggate & Waight (1999) linking with glacial till in adjacent moraines notably at the head of Fushia Creek (Grid ref J32 44700N 6600E). As mapped by Suggate & Waight

(1999) the terminal moraines formed during Tansey(1) deposition are located mainly seaward of the LGM terminal moraines. This implies that glacial ice was at least as extensive during this period as during the LGM and further that the local ice volume was probably comparable to that of the LGM.

There is no recorded evidence of a coarse degradational lag deposit capping the Tansey(1) aggradational gravel and no evidence of elevated alluvial gold grades near the surface (absence of gold workings and no indication of high grades from prospecting activities). If the thick Tansey(1) deposits resulted mainly from aggradation then the implication is that aggradation was preceded by more than 50 metres of fluvial incision/strath cutting (into the older Cockeye Formation). The timing and duration of the incision event is poorly constrained. The Tansey(1) surface is ~ up to 40 to 50 m lower than the Cockeye surface in the upper reaches of Eight Mile Creek in the New River catchment. The base of the pre-Tansey incision is up to 100 m below the surface of the Cockeye formation here. Construction of the Tansey(1) Formation required up to 50 metres of fluvial aggradation. The deposition of the Cockeye Formation was likely complete by c.140 ka being the approximate commencement warming at the Vostok ice core site in Antarctica (Petit et al 1999). Rapid aggradation resulting in the accumulation of the Tansey Formation probably commenced no earlier than 112 ka, based on cooling into MIS5d at Vostok. In this scenario there is likely to have been a period of up to 32 kyr during which the "pre-Tansey" incision could have occurred. As shown in figure 4.17 Antarctic climate proxies indicate the mid-point of the MIS6/5e transition probably occurred no later than 135 ka. So if the isotope stage correlation is correct then the minimum duration between Cockeye is likely around 23 kyr. An interval of 32 to 23 ka is certainly enough time to achieve the difference in elevation between the Cockeye and Tansey Formations given the proposed coastal uplift rate of c. 1.35 mm/yr (see table 4.5 in Chapter 4).

Suggate and Waight (1999) mapped the Tansey Formation as two separate fluvioglacial outwash terraces grading up to separate moraines. One terrace is incised below the other. This implies substantial erosion rather than a simple depositional hiatus. The duration of the incision event is unknown. It is assumed that deposition of the Tansey(1) Formation during the Waimaunga Glaciation was followed by a transition to significantly warmer climate, glacial recession, reduction in ice volume, potential isostatic rebound and fluvial incision in the major valleys.

6.2.8 Caledonian Formation (MIS5c, Scandinavia Interglacial)

The Caledonian Formation was defined McPherson (1967) and includes marine deposits on high-level terraces in the Westport area. Deposits on these terraces where subdivided by Nathan (1975, 1976, 1978a), the Caledonian Formation being retained for strandline sediments at ~ 102-120 m elevation.

Near-shore erosion occurred during and immediately following the sea level maximum. Strandline sediments of the Caledonian Formation were deposited permanently at this time. The southernmost locality known to contain deposits of the Caledonian Formation is Point Elizabeth. Here the Caledonian Formation is at an elevation of 125 to 135 m above S.L. (from GPS measurements [see table 7.3]). It is suggested here that this formation was deposited during a marine transgression following the Waimaunga Glaciation. At Point Elizabeth these remnants of the Caledonian Formation are backed by a 10 to 15 m marine cliff cut into indurated Cobden Limestone.

Nathan (1978b) identified the ~120 m (Caledonian) level at Rapahoe, a few kilometres to the east of Point Elizabeth. This is the basis for the naming of the terrace at Point Elizabeth. Laird (1988) also adopted the name "Caledonian Formation" for 105-120 m terrace remnants situated between Canoe Creek (Barrytown) and the Punakaiki River. The Caledonian Formation at Caroline Terrace near

Westport is assigned to the Waiwhero Interglacial by McPherson (1967) but is not assigned to a named interglacial by Nathan (1975, 1978a, b).

Nathan (1975) implies that the Caledonian Formation was deposited during an (unnamed) interglacial that was "older than the Terangi Interglacial". Other than the sedimentology of the marine sand/gravel deposits of the Caledonian Formation no supporting data are supplied or cited by Nathan (1975) in relation to the climate immediately prior to, during, or immediately following the deposition of the Caledonian Formation. No data are available on the palynology of the first soils deposited on the Caledonian Formation.

The best exposures of the Caledonian Formation in the Greymouth area are situated in the extensive gold workings (sluice faces, tunnels and water races) at Darkies Terrace (grid ref J32 6700N 6350E) which is situated between North Beach (Cobden) and Point Elizabeth. Here it is composed largely of clean heavy mineral bearing sandy gravel containing discoidal pebbles and cobbles deposited in a strandline and near-shore environment. These deposits are present over a shore parallel distance of at least 400 metres. The gravel component includes granite, Haast Schist and Torlesse Greywacke which cannot have a local source. The underlying bedrock at Point Elizabeth is the Cobden Limestone.

Silt-bearing sand from a short gold exploration tunnel into the Caledonian Formation near Point Elizabeth was dated during this project. Sample RR13 (Grid Ref NZMS260 J31 N 6690 E 6345) gave an age of 87.1 ± 8.3 ka (by multiple aliquot $IRSL_{blue}$) which potentially places the deposition into MIS5c (at 2σ error) or 5a. This is the preferred age. The same sample also returned a less precise age of 98.6 ± 24.4 ka (by single aliquot $IRSL_{blue}$). There are two ages because the dose rate for this sample was determined twice at the National Radiation Laboratory. Sample RR13 was deposited in an energetic littoral environment as indicated in table 5.4. The main sediment sources are distant from the sample site and the potential for complete bleaching of the luminescence signal prior to burial are good. So the sample should be completely bleached. There is no indication of anomalous fading. So the IRSL(blue) ages should reflect the true depositional age and there is no reason to suspect that these ages are an underestimate. The Caledonian Formation is assigned here to MIS5c, though an MIS5a correlation is not ruled out on the basis of the sample age.

Although sample RR6 from the (lower) Scandinavia Formation at Scandinavia Hill returned an older age at 123.3 ± 12.7 ka this sample is considered to be a maximum age. Sample RR6 was approaching luminescence saturation and was taken from a sediment that is much more likely to suffer from partial bleaching (resulting in potential age overestimation) than RR13 at Point Elizabeth.

Given the elevation of the sample site at ~ 125 m (basal contact) to ~135 m (upper surface) one would anticipate an MIS5e terrace at around 160 m. A substantial marine terrace (Whisky Formation) does exist at ~ 150 to 160 m at Point Elizabeth. At Point Elizabeth the Scandinavia Formation is at a lower elevation than the Caledonian Formation. It is proposed here that the Caledonian and Scandinavia Formations represent a pair of shorelines within the same substage.

However, this would tend to indicate the Scandinavia Fm is no older than ~ 100 ka, whereas an age of 123.3 ± 12.7 ka was obtained from sample RR6 at Scandinavia Hill (see below).

There are no known outcrops in positions that allow an assessment of the stratigraphic relationships between the Caledonian and Tansey(1&2) Formations. Known outcrops of the Caledonian Formation are restricted to the area north of the Grey River and west of the Paparoa Range. The elevation of the Caledonian Strandline at Point Elizabeth is ~ 120 to 125 metres. This is slightly

lower than the Tansey(1) surface at Candle Light near Camerons, but a little higher than the Tansey surface just inland from Paroa and South Beach.

There is at least partial preservation of the Candlelight, Whisky and Caledonian Formations to the north of Greymouth. So why are these formations not preserved south of Greymouth? If we consider all rock strata older than the Quaternary period to be "basement" then the basement rock south of Greymouth and situated between the modern coastline and the Southern Alps is relatively soft compared with the basement rocks north of Greymouth. South of Greymouth marine erosion has occurred on a combination of Quaternary (non-basement) fluvioglacial gravel and Tertiary (basement) marine mudstone, siltstone and fine sandstone of the Blue Bottom Group. The Blue Bottom Group is easily eroded by fluvial processes even by small streams. On this soft bedrock medium sized streams and rivers are capable of widespread strath cutting in relatively brief periods of time. So the Scandinavia, Karoro, Rutherglen and Awatuna Formations are only partially preserved between Hokitika and Greymouth. In addition is possible that the position of the coastline during deposition of the Candlelight, Whisky, and Caledonian Formations may simply have been seaward of the Scandinavia, Karoro and Rutherglen marine cliffs. So the elimination could have been due to a combination of marine and fluvial erosion. There is no particular need to invoke differential uplift as an explanation.

In Suggate (1992) the position of the Caledonian Formation at Caroline Terrace near Westport has been misidentified (fig 2(1) & fig 3A). The order of terraces from higher to lower as defined by Nathan (1975) is Candlelight, Whisky, Caledonian, Addison, Virgin Flat, and Waites. Without explanation Suggate flips this to Caledonian, Candlelight, Whisky, Addison, Virgin Flat, and Waites. One crucial error in Suggate (1992) is failure to recognise the presence of the Caledonian Formation at the surface of the northwest end of Caroline Terrace. Here marine sand outcrops over a large area at an elevation of ~ 130-135 m (grid ref K29 3070N 9300E). Deposits include cemented heavy mineral rich sand that has in the past been prospected and mined for gold. The marine terrace sequence is well developed in the Charleston area, where the Caledonian Formation as defined by Nathan (1975) is assigned to MIS9 by Suggate (1992).

6.2.9 Scandinavia Formation (MIS5c, Scandinavia Interglacial)

The Scandinavia Formation was first defined by Suggate (1985) who placed the depositional event in the Scandinavia Interglacial. This definition was amended by Suggate & Mildenhall (1991) who placed this formation in the Karoro Interglacial. The type section for the Scandinavia Formation is located at Scandinavia Hill, Stafford (grid reference NZMS 260 J32 N 583640 E 235340). The upper surface of the exposed marine strandline sediments is situated at an elevation 110 m. The elevation of the Scandinavian Formation was measured by GPS (see table 7.3) at Darkies Terrace, Point Elizabeth (grid ref J32 6700N 6350E) at approximately 112-118 m. At Point Elizabeth the marine terrace representing the Scandinavia Formation is present as small discontinuous remnants exposed by historic gold mining. These remnants are backed by a 10 to 15 m marine cliff cut in indurated Cobden Limestone (formerly higher but the cover of Caledonian Formation beachsand has been stripped by historic mining on the upper side of the Scandinavian marine cliff).

Suggate (1992) and Suggate & Waight (1999) correlate the Scandinavia Formation with the Virgin Flat Formation from the Westport-Charleston area. In the Suggate model the Scandinavia Formation is correlated with MIS7e and given an age of c. 238-240 kyr (fig 3 & table 4, Suggate 1992). The Virgin Flat Formation was defined by McPherson (1978). Prior to this PhD project there were no numerical ages for the Scandinavia Formation, or any other MIS7 marine or fluvioglacial terrace in Westland or Buller. So the assignment of the Scandinavia Formation to MIS7 has always been rather speculative.

For the purposes of this PhD thesis the definition of Suggate (1985) is preferred for the Scandinavia Interglacial and Scandinavia Formation. This means removal of the Scandinavia Formation from the Karoro Interglacial and reinstatement of the Scandinavia Interglacial. In this thesis the Scandinavia Formation is correlated with MIS5c. Separation of the Scandinavian and Karoro Formation into separate interglacial periods is discussed in relation to the Karoro Formation below.

As discussed by Suggate (1985) the Scandinavia Formation is composed of rusty coloured marine sand and gravel deposited in a strandline and near-shore environment. At the type section the heavy mineral content of sand in the strandline deposit is quite high and the deposit has been mined for alluvial gold by sluicing. At Darkies Terrace between Point Elizabeth and North Beach the Scandinavia Formation is composed largely of clean heavy mineral bearing sand containing discoidal pebbles and cobbles. Here a large proportion of the formerly in-situ deposit has been mined for alluvial gold by opencast sluicing. The gravel component includes granite, Haast Schist and Torlesse Greywacke. As discussed in relation to the Whisky and Caledonian Formations these lithologies do not have an immediately local source and have reached the point of deposition/preservation through a combination of glacial, fluvial and marine transport processes.

At the type section the strandline deposits are overlain by a silt horizon which is in turn buried by fluvial gravel. A single sample (RR6, Grid ref NZMS260 J32 N 3640 E 5340, photo in Appendix one) from this soil at Scandinavia Hill gave an $IRSL_{(blue)}$ age of 123.3 ± 12.7 ka. This is the first ever attempt to directly date the Scandinavia Formation at the type locality. RR6 was taken at the type locality at ~ 115 m (GPS measurement) amsl. The 1σ error is wide enough for a plausible correlation either with MIS5e or MIS5c.

Sample RR6 was taken from a relatively inorganic grey silt of fluvial origin. So it dates the commencement of fluvial accumulation above the littoral deposits. As discussed in chapter 5 (sections 5.3 to 5.7) there are incomplete bleaching issues for a number of luminescence samples taken from fluvial sediments in North Westland. Incomplete bleaching appears to be more prominent in inorganic samples deposited relatively quickly from turbid water and particularly when there is an immediate association with fluvial gravel. This is how the sample has been classified in table 5.4. Consequently the sample age is considered to be a maximum age. The depositional age is more likely to be younger, rather than older than the IRSL age. For this reason, and because there is a younger IRSL age (87.1 ± 8.3 ka) on the older Caledonian Formation a correlation with MIS5c is preferred over a correlation with MIS5e. This choice is supported by the correlation of the younger Karoro Formation with MIS5a.

RR6 is approximately half the age implied by the Suggate model (early MIS7e = ~ 235 to 240 ka). If the age really is around 123 ± 12.7 ka and the eustatic sea level around +4 to +6 metres then the long-term average uplift rate is around 0.9 to 1.0 mm / year for the Awatuna to Stafford area. This rate is slightly less than calculated on the basis of ages for the Awatuna and Rutherglen Formations. If the correlation was with MIS5c and a eustatic sea level no higher than -10 to -20 m then the uplift rate would be higher (~1.1 to 1.3 mm/yr) and in line with that expected for the Awatuna Formation.

The interpretation favoured here is that there is minimal coast parallel tilting between Point Elizabeth and Scandinavia Hill. This would imply that the Caledonian Formation was destroyed at Scandinavia Hill during the deposition of the Scandinavia Formation. If the Scandinavia Formation was instead correlated with the 125-135 m terrace at Point Elizabeth this would still imply at most a minor coast parallel tilting and retention of the MIS5c correlation given ages of 87.1 ± 8.3 and 98.6 ± 24.4 ka derived by $IRSL_{blue}$ on sample RR13 near Point Elizabeth.

At Sawyers Creek near Awatuna the surface of the Scandinavia strandline is at least 60 metres below the projected level of upper surface of the Cockeye Formation and according to Suggate and Waight (1999) it is c. 50 m lower than the Tansey surface. If the coast parallel correlation presented here is correct then the Caledonian Formation (were it present at Scandinavia Hill) would also be lower than the Tansey surface and would likely truncate that surface.

6.2.10 Tansey(2) Formation (MIS5b, Unnamed Stadial Event)

The Tansey(2) Formation was defined by Suggate and Waight (1999). The primary change proposed here is the marine isotope stage correlation, which is with MIS8 in the Suggate model. Potentially the formation name from Tansey(2) as a significant interstadial separating Tansey(1) and (2) is proposed. The usage is continued in order to maintain consistency with the Suggate terminology. In this thesis the Tansey(2) Formation is correlated with MIS5b. Both correlations are speculative. There are no numerical ages available for the Tansey(2) Formation. The MIS5b correlation is supported by $IRSL_{(blue)}$ dating undertaken during this project on the Scandinavia, Caledonian, Karoro, Waimea, Rutherglen and Awatuna Formations. In this context note the identification of a major glaciation for MIS5b or MIS5a in the Cascade Valley in South Westland by Sutherland et al (2007).

The Tansey(2) deposits are the result of fluvioglacial accumulation during a glacial advance that is allocated to a younger stadial event than that responsible for the Tansey(1) surface. The implication is that an interstadial event occurred between the two Tansey depositional events. According to Suggate & Waight (1999) there is a cross-cutting relationship between the Tansey(2) and Tansey(1) moraines at Big Fushia Creek (Grid ref J32 4400N 6600E). In the same area within the New River catchment the Tansey(2) outwash surface is 20 metres lower than the Tansey(1) outwash surface. The elevation difference requires an episode of fluvial incision and strath cutting (into the older Tansey(1) and Cockeye Formations). The timing and duration of the incision event is poorly constrained. Suggate and Waight (1999) illustrate fluvial incision prior to the deposition of Tansey(2) to a depth well below the base of the Tansey(1) deposits. The incision as depicted is at least 40 to 50 metres, followed by 20 to 30 metres of aggradation to form the Tansey(2) surface.

As mapped by Suggate & Waight (1999) the terminal moraines formed during Tansey(2) deposition are located mainly seaward of the LGM terminal moraines. This implies that glacial ice was of similar extent to that of the LGM during this period and further that the local ice volume was likely to have been comparable to that of the LGM. Fluvioglacial deposition was followed by marine transgression. Palynological studies have not been carried out on the Tansey(2) coverbeds. So there is no evidence from pollen to confirm an associated change in climate or vegetation. It is assumed that deglaciation occurred during the marine transgression associated with the Karoro Interglacial.

The assumed transition from the Waimaunga Glaciation to the Karoro Interglacial by Suggate & Waight (1999) is an analogy with the Waimea-Kaihinu glacial to interglacial climate transition. The Waimea/Kaihinu transition is supported by changes in pollen within the overlying soils, notably at Chesterfield Road (profiles in figure 7 of Moar & Suggate 1996). The Waimaunga-Karoro transition is not supported directly by palynological evidence in North Westland.

There are no contact relationships between the Tansey Formation and the Scandinavia or Caledonian Formations. Near Mill Creek (South Beach, Greymouth) Suggate and Waight (1999) have mapped a sea-cliff against the western margin of the Tansey Formation. Here the Karoro wave cut platform and the upper surface of the beach deposit are at an elevation well below the base of the Tansey Formation. At the strandline against the sea-cliff (grid ref J32 5450N 6140E) the

Karoro Formation contains large blocks of slumped marine siltstone of the Mio-Pliocene Eight Mile Formation which is the local bedrock here. The base of the Tansey Formation is perched above the exposed Eight Mile Formation at the sea cliff. So the Tansey Formation at this locality is older than the Karoro Formation.

At present there is no particular reason to suppose that the Tansey(2) surface is older than the Caledonian or Scandinavia surfaces. At Point Elizabeth where it has been dated the Caledonian surface is at higher than the nearest locality where exposures of the Tansey Formation contain fluvial gravel (near Mill Creek, South Beach).

There is no recorded evidence of a coarse degradational lag deposit capping the aggradational Tansey(2) gravel. Surficial bouldery lag deposits are common on the Waimea, Loopline, and Larrikins Formations. The base of each lag deposit commonly has an elevated alluvial gold grade, and sometimes evidence of past gold mining and exploration. There is no evidence for elevated alluvial gold grades near the surface of the Tansey Formation.

6.2.11 Karoro Formation (MIS5a, Karoro Interglacial, Antarctic Interstadial Event A7)

The most recent definition of the Karoro Formation is by Suggate and Waight (1999). This follows the previous description by Suggate (1985) where the deposition of this formation is placed in the Karoro Interglacial. Suggate & Waight (1999) correlate the Karoro Formation with MIS7a and by reference to Suggate (1992) give it an age of c. 198 kyr. The primary change proposed here is the isotope stage correlation which changes from MIS7a to MIS5a, the rationale for which is discussed in detail below and includes discussion of the three $IRSL_{blue}$ samples taken form coverbeds on the Karoro Formation.

In the literature search for this project no explicit definition for the Karoro interglacial was found. The earliest reference found relating to the Karoro Formation is Suggate (1965) (figures 22 and 24) where it is placed in the Terangi Interglacial, making it potentially equivalent to the Addison Formation (Westport - Cape Foulwind - Charleston area) of Nathan (1975) and McPherson(1967). The Karoro Formation was also placed in the Terangi interglacial by Moar & Suggate (1973).

Following the Tansey(2) glacial advance a transition to warmer climate (pollen in soil on the Karoro Formation at “Ferguson’s Pond”, South Beach) accompanied a marine transgression. Near-shore erosion/planation occurred during the sea level maximum. Erosion was accompanied by the deposition of strandline sediments directly onto the wave cut platform. These sediments are defined as Karoro Formation. The type locality is at Karoro in Greymouth (Grid ref 5820N 5600E). The Formation outcrops discontinuously from Point Elizabeth north of Greymouth to Blue Spur inland from Hokitika.

The Karoro Formation is composed of rusty coloured (oxide stained) marine sand and gravel deposited in a strandline and near-shore environment. At the type section the heavy mineral content of sand in the strandline deposit is quite high and the deposit has been mined for alluvial gold by tunneling. At Darkies Terrace between Point Elizabeth and North Beach the Karoro Formation is composed largely of clean heavy mineral bearing sand containing discoidal pebbles and cobbles. The gravel component includes granite, Haast Schist and Torlesse Greywacke and as discussed in relation to the Whisky Formation this gravel does not have an immediately local source.

In view of the IRSL ages from the Awatuna and Rutherglen Formations and the implied uplift rate an age of ~80 ka (MIS5a) might be anticipated for the Karoro Fm. That would fit with an MIS5c correlation for the Caledonian and Scandinavia Formations.

6.2.11a Luminescence Dating

During this project three $IRSL_{blue}$ samples were taken from coverbeds on the Karoro Formation. Two, being RR22 (84.3±8.7 ka) and RR23 (65.7±5.7 ka), were taken from one profile at the "Ferguson's Pond" locality (grid ref NZMS260 J32 N 5450 E 6610) near Mill Creek, South Beach. This 4 m thick soil sequence rests on thick (10 m) marine sand and gravel about 200 m west of the Karoro strandline. The elevation is approximately 75 m, less than 10 metres lower than the strandline at the marine cliff situated about 200 m to the SE. At 1σ the samples imply an age inversion, but at 2σ the ages overlap.

Sample RR23 comes from the middle of a 0.5 m thick light brown sandy silt situated below the uppermost clean marine/aeolian sand at this site. This upper sand has a thickness of 0.45 m. The sample is situated 0.2 m above the top of the main marine sand at this site. RR22 is situated 1.2 m above RR23 and comes from the middle of a dark brownish-grey silt that contains abundant wood.

Sample RR34 was taken from a 2.2 m thick exposure of the Karoro coverbeds at a site situated about 300 m north of Fergusons Pond (grid ref NZMS 260 J32 5480N 6095 E). This sample was 0.15 m above the contact with the underlying marine sand. It has an $IRSL_{(blue)}$ age of 92.5 ± 9.4 ka.

The numerical average or the three IRSL ages is 80.8 ka. At the RR34 sample locality there is no strong evidence for fluvial deposition and no particular reason to suspect the sample suffers from partial bleaching. The coverbed sequence is substantially thicker at Fergusons Pond, the sample locality for RR22 and RR23. But there is no strong evidence for fluvial deposition here. So there is no particular reason to suspect that either of these samples suffer from partial bleaching. Therefore the samples are interpreted as giving solid evidence for the age of the coverbeds at this site.

Table 6.2 Luminescence ages from the Karoro Formation, this PhD project.

Lab Code	Field Code	$IRSL_{(blue)}$ Age (kyr)	Elevation	Locality	Grid reference (NZMS260)
WLL527	RR22	84.3 ± 8.7	75 m	South Beach (Kr)	J32 N 5450 E 6610
WLL528	RR23	65.7 ± 5.7	73 m	South Beach (Kr)	J32 N 5450 E 6610
WLL537	RR34	92.5 ± 9.4	72-75 m	South Beach (Kr)	J32 N 5480 E 6095

From previous mapping it is not entirely clear whether the Ferguson's Pond profile belongs to the Karoro Formation or the Rutherglen Formation. The site was mapped as Rutherglen Formation by Suggate and Waight (1999). Soons and Lee (1984) and Nathan (1978) mapped it the site as Karoro Formation. But at that time the Rutherglen Formation had not been defined. The locality is virtually right on the Rutherglen strandline as mapped by Suggate and Waight (1999). Inspection of the immediate area as part of this project reveals a previously unidentified strandline (Grid ref J32 5480N 6075E) that may be the eastern limit of the Rutherglen Formation. This is situated several hundred metres to the west of the strandline mapped by Suggate & Waight (1999) at Ferguson's Pond. The new position proposed for the innermost Rutherglen strandline is slightly lower than that mapped by Suggate & Waight, reducing the apparent coast-parallel tilting between this locality and the type area at Rutherglen. This strandline is also present on terrace fragment to the south (Grid ref J32 5420N 6065E) and just north of Power Road, Karoro (Grid ref J32 5400N 4450E).

There is no evidence of a break in slope on the Karoro surface between the Ferguson's Pond sample site and the potential Rutherglen strandline. This is best seen on a long narrow terrace fragment situated slightly further to the south (Grid ref 5400N 6100E). Here there is no there evidence for a step in the contact between the marine sand and the underlying Stillwater Mudstone. There is no

visible evidence for a change in the thickness of the soil across an otherwise obscured Rutherglen Strandline. It should be noted that the Fergusons Pond site is at the western end of a narrow ridgeline, the tip of which had been bulldozed flat to create a logging skid-site prior to IRSL sampling. This occurred subsequent to mapping by Suggate & Waight (1999) and AAR sampling by Soons & Lee (1984). So the face sampled in this (thesis) project is an exposure that did not exist in 1984.

Regardless of whether the three IRSL samples are from the base of soil on the Karoro Formation or the Rutherglen Formation the implication is that the deposit is likely younger than 100 ka and therefore would correlate with MIS5c to MIS4 rather than MIS5e or MIS7.

AAR ages

Two wood samples (one Pittosporum and one Libocedrus) taken from the Fergusons Pond locality (grid ref J32/610555450) have been dated by amino acid racemisation (Brad Pillans on behalf of Soons and Lee). The results are reported in Pillans (1990). The wood that was dated gave ages of 120 ka ± 30% for BJP153A & 140 ka ±30% for BJP153B. These are the only AAR results anywhere within this region. At the lower end of the wide 1φ spread the AAR ages are entirely consistent with an age of 80-100 ka. The AAR results do not permit the formation to be reliably be assigned to a substage. They do suggest that the samples are more likely to date from MIS5 than MIS7 which is the previous assignation for the Karoro Formation. Note that the 1δ errors are given as a percentage. This is not standard modern practice but it is how they were reported by Pillans (1990). No attempt is made to reinterpret the precise meaning of the error range here.

At the time of writing the degree of precision that is possible with amino acid dating on samples from North Westland is debatable. Amino acid dating requires reasonably well preserved organic materials and some knowledge of the long-term climate history of the sample site. The rate of racemisation is temperature dependant, being relatively faster under warmer conditions. The rate is potentially site and/or region specific and has not been determined specifically for North Westland either with reference to other AAR samples or to other dating techniques that produce numerical ages. The temperature correlation used to calculate the two AAR ages is based on the current temperature difference between the southern North Island (where the method is marginally better established) and the West Coast. Unfortunately, there are no continuous climate records for the local area so the temperature history is rather bare. Rates of racemisation are uncertain so confidence in the precision of the dating is modest at best. Pollen from soil overlying the beach sand was described by Soons and Lee (1984). It indicates an interglacial climate and a temperate rain forest flora.

These AAR ages were originally discussed by Moar & Suggate (1996) under the assumption that they were taken from soil on the Rutherglen Formation. This is a substantial part of the justification for assignment of the Rutherglen Formation to MIS5e in the Suggate model. Similarly this forms much of the justification for correlation of the Karoro Formation with MIS7.

If the Ferguson's Pond site is Karoro Formation then IRSL ages potentially put this Formation into MIS5a. Three IRSL samples were taken from genuine Rutherglen Formation sites from 300 to 600 metres NW of Ferguson's Pond. These are discussed below in relation to the age of the Rutherglen Formation. The conclusion reached is that the older part of the Rutherglen Formation should be correlated with latest MIS5a or early MIS4, in which case the Karoro Formation would likely correlate with peak MIS5a.

6.2.11b Relationship between the Karoro and Scandinavian Formations

The relationship between the Karoro and Scandinavia Formations was defined at Scandinavia Hill (Stafford) by Suggate and Mildenhall (1991). The Scandinavia strandline and sea-cliff were first identified here by Suggate (1985). This was an amendment to the stratigraphy illustrated in figure 24 of Suggate (1965) where the Karoro Formation is shown at the foot of this marine cliff.

A subsidiary (Karoro) strandline was proposed by Suggate & Mildenhall (1991), its location being defined by old opencast gold workings (at K32 3670N 5350E) situated about 300 m to the northwest of similar workings at the Scandinavia strandline near Scandinavian Hill. In this interpretation two strandlines were deposited in separate marine isotope substages. The substages are MIS7a at 240 ka and MIS7e at 198 ka so the interval between events is of the order of 40 kyr. There is a question mark over the existence of two distinct marine formations at the type locality for the Scandinavia Formation because the simple presence of a double strandline does not necessarily imply separate sealevel high-stands. The position adopted here is that the subsidiary strandline, if present, is part of the Scandinavia Formation, and that the Karoro Formation does not outcrop at Scandinavia Hill.

The Karoro strandline was not actually observed by Suggate & Mildenhall (1991) as it was obscured by fluvial gravel debris and thick forest regrowth. There is no surficial terrace riser at the presumed strandline. Both fossil beaches are covered by what is mapped by Suggate & Waight (1999) as sheet of fluvial gravel that is continuous and unbroken over a shore normal distance of about 1 km. It is assumed by Suggate & Mildenhall (1991) and Suggate & Waight (1999) that deposition of the fluvial gravel post-dates both the Karoro and Scandinavian strandlines and is therefore likely to have buried a terrace riser if one was present.

The claim by Suggate & Mildenhall includes an assumption that two wave cut platforms are separated by a "step" in the bedrock (see their figure 1). Separation of the Scandinavia and Karoro Formations across such a step was not demonstrated unequivocally by Suggate & Mildenhall (1991) or by Suggate & Waight (1999). Nor did they demonstrate that such a step could not have formed within a single sealevel maximum (as has happened from Greymouth to Gladstone during the shorter Holocene sealevel maximum).

In the Suggate model the fluvial gravel is at least 40 kyr younger than the Scandinavia Formation. It rests almost immediately on the Scandinavia Formation and is separated from it at the types section by < 50 cm of grey fluvial silt. The uplift rate estimated by Suggate (1992) for Scandinavian Hill is 0.48 mm/yr. Over 40^{+} kyr this implies uplift of around 20 metres the eustatic sea level for the second event being 5 m higher than for the first. So there should be a difference in strandline elevation of around 15 m.

Elsewhere in this region, deposits of a single sealevel maximum can contain multiple gold-rich strandlines. Examples include the Nine Mile Formation at Ruatapu, Awatuna, Greymouth, Rapahoe, Barrytown, North Nine Mile Beach, and Carters Beach. Similarly in the Karoro Formation in the "Big Paddock" area near Blue Spur there is a wide scatter of old shafts and tunnels which indicates gold is not always confined to a single narrow zone within a marine placer deposit. Some of these areas have been drilled intensively for heavy minerals. The Barrytown, North Nine Mile Beach and Carters Beach areas are prime examples. At Barrytown the geomorphology and heavy mineral distribution for the coastal plain here is summarised by Suggate (1989). Suggate demonstrates multiple enrichment zones associated with an upper beach face depositional environment within individual sea level maxima. In one shore-normal transect north of Canoe Creek there are 7 individual Holocene strandlines. At Canoe Creek Suggate (1989) demonstrated

the presence of as many as five of the strandlines buried by a Holocene fluvial gravel fan in excess of 10 metres thick sourced from Canoe Creek.

The buried strandline deposits at Canoe Creek are potentially analogous to the buried strandlines at Scandinavian Hill. Here fluvial gravel (probably sourced mainly from Waimea Creek and German Gully) was deposited on the marine Scandinavia Formation during and/or following a significant regression of the shoreline. This regression must have been over a distance of at least 1 km as the gravel is preserved over a coast-normal distance of 1 km on the high terrace at Scandinavian Hill. If that comparison holds then there is no particular reason to assume that the gravel deposition was delayed significantly. An alluvial fan could easily have commenced its building phase here prior to creation of the "Karoro" strandline situated 300 m northwest of the Scandinavia strandline. In fact construction of an alluvial fan could have contributed to local progradation of the coastline, so the second strandline might not have been caused entirely by a significant change in sea level or tectonic uplift. The final thickness of this gravel is 10 to 15 metres (surface at ~ 120 –125 m) at Scandinavian Hill.

Suggate and Mildenhall (1991) describe pollen (J32f135) from a carbonaceous silt layer within the fluvial gravel. The soil contains abundant pollen from Nothofagus fusca (Red Beech), Coprosma, Dacrydium cupressinium (Rimu), Phylocladus (Toa Toa), Ascarina lucida (Hutu) and Tupeia Antarctica. The latter two species are noted by them as indicative of temperate interglacial conditions. Note that they did not identify Nestegis pollen in this sample. They state specifically that lack of Nestegis does not negate the interglacial aspect of the pollen spectrum, which is relevant to comments made in respect of this genus in chapter 5 of this thesis. This is the oldest site from North Westland to have yielded a flora of this nature. The flora extracted from the gravel unit could potentially be indicative of the climate current soon after the deposition of the Scandinavia Formation. Given that the gravel has an interglacial character there could be a number of potential isotope stage correlations for it. These include MIS7e, 7c and 7a, all of which are potentially viable within the constraints of the Suggate model. There are presently no criteria available to make a distinction between these options. The choice of MIS7a has not been justified. In terms of the correlation proposed in this thesis the "interglacial" flora from the fluvial unit on the Scandinavia Formation probably relates to MIS5c.

The two lines of gold workings at Scandinavia Hill could easily be in alluvium from the same isotope substage. But it shouldn't be assumed that the old workings necessarily relate strictly to zones of enrichment, particularly the slightly lower area. The presence of the second area of sluicing could just as easily be a consequence of long forgotten issues around gold-claim boundaries and availability of water for sluicing purposes. Suggate & Mildenhall (1991) were unable to provide a precise elevation for the "Karoro" Strandline at Scandinavia Hill as the "gold lead" is no longer exposed. The evidence that the second or seaward strandline at Scandinavian Hill is the Karoro Formation is not strong. There is no particular reason to assume that the Karoro Formation was any higher near Scandinavia Hill here than it is at Blue Spur or South Beach, Greymouth. At Scandinavian Hill the terrace surface is high enough that it could have survived inundation by the Karoro sea level maximum. If so then the Karoro strandline would be situated slightly to the west of this terrace.

With the above discussion in mind the writer determined to investigate the altitudes of these surfaces more closely. Suggate & Mildenhall (1991) claim that the Karoro Formation at Hou Hou Creek (to the SW of the Arahura Valley and 9 km SW of Scandinavia Hill) has a "top altitude" of 82±3 m. This area was examined during this PhD project. Road development for new residential subdivisions here (in the Blue Spur area) during the 2008 to 2011 period has exposed the Karoro Formation at the easternmost strandline. The top altitude was measured by GPS (see table 7.3) and it is 76 to 77 m. Similarly the top altitude for this formation was measure at a new road cutting for

a new residential subdivision at Paroa (near Greymouth). The top altitude here is 82 to 83 m. Under the assumption that any coast parallel tilting is distributed approximately evenly from Greymouth to Hokitika the expected altitude of the Karoro Formation at Scandinavia Hill should be approximately 78 to 80 m. But the Karoro strandline proposed for this location by Suggate & Mildenhall (1991) is shown in their figure 1 to have an elevation of approximately 100 m.

In order to clarify the situation further the Scandinavia Hill area was also revisited. The top altitude on the Scandinavia Formation at the type section was measured by GPS at 115 m. Another new exposure was discovered in a road cutting at "Ballarat Rise" (another new residential subdivision) adjacent to Gillams Gully Road about 2 km SW of Scandinavia Hill. The road climbs up the NW end of the terrace mapped by Suggate and Waight (1999) as Karoro Formation. The NW end of the terrace is about 100 m seaward of the Karoro strandline as illustrated in figure 1 of Suggate and Mildenhall (1991). Clean sandy gravel and pebbly sand of the Scandinavia Formation outcrops here and has a top altitude of 99 metres. This site is approximately 20 m too high for correlation with the Karoro Formation.

One could argue that the alternative suggestions advanced here in respect to the Karoro Formation and the fluvial unit at Scandinavian Hill are speculative. These suggestions are backed by more direct observation than those of Suggate & Mildenhall (1991) and Suggate and Waight (1999) and by IRSL dating. It is concluded that the fluvial gravel is likely to be approximately the same age as Scandinavia Formation at Scandinavia Hill. The same sheet of gravel is also situated on Scandinavia Formation German Gully and Sawyers Creek about 1 km NE of Scandinavia Hill. Here (grid ref J32 3800N 5470E) the surface elevation is ~ 135-140 m above sealevel so the fluvial gravel is likely to be thicker there. This surface is too high to be correlated with the older part of the Waimea Formation situated (grid ref J32 3880N 5500E) just to the NE of Sunday Creek.

The geomorphic evidence from South Beach, Karoro and Point Elizabeth is for a modest difference in elevation between the Karoro and Rutherglen(1) Formations. In other parts of the world MIS5a has been found to have produced multiple strandlines, often with two prominent sub-equal sea level maxima separated by a minor marine regression and transgression. Examples include coral terraces at Huon Peninsula and Barbados and clastic deposits on wave cut platforms at the Calabrian coast of Italy. It is generally assumed that the maxima occurred at ~ 85-83 ka and ~ 80-77 ka. It is possible that the Karoro and Rutherglen(1) Formations represent local maxima at about this time.

6.2.12 Waimea Formation (MIS5a/4 Transition, Waimea Glaciation, Kumara-1 Advance)

6.2.12a Introduction

The Waimea Formation was first defined by Suggate (1965), a definition continued by Suggate (1985). The description has been updated by Suggate and Waight (1999) who correlate the Waimea Formation with the maximum cold phase of MIS6 and give it an age of c. 150 kyr. However, there are no numerical ages that give direct support to an MIS6 correlation. The most notable change made by Suggate & Waight (1999) was recognition of a "degradational" fluvial terrace level at an elevation slightly lower than the main outwash terrace at Chesterfield Road, Chesterfield. The aggradational level is termed Waimea(1) and the degradational level Waimea(2). Suggate & Waight (1999) and Suggate (1990) make a local correlation with the Tophouse Formation from the Buller Valley The primary alteration proposed in this thesis is the marine isotope stage correlation for the Waimea(1) Formation. This proposal places the formation into the MIS5a/4 transition and/or MIS4 proper. Dating that supports a correlation with climate events more recent than MIS6 is discussed below, and is summarised in section 6.2.12d.

Following the Karoro Interglacial a major increase in ice volume in the Southern Alps produced a widespread glacial advance with widespread deposition of till and fluvioglacial gravel. These deposits constitute the Waimea Formation. The glacial portion of the Waimea Formation, which has not been subdivided, is represented by a well defined moraine belt that is particularly well preserved in the Blackwater Creek / Foleys Creek area between Kumara and Moana. The type locality defined by Suggate (1965) is: "at grid reference S51/693584, 2 miles east of Goldsborough where outcrops on old tracks show poorly exposed till containing angular blocks up to 4 ft across."

At Callaghans (grid ref J32 3500N 6000E) the Waimea(1) Formation includes near-surface degradational fluvial gravel (lag deposit) overlying thick aggradational fluvioglacial outwash gravel which in turn overlies a deeper basal degradational fluvial gravel situated on local Neogene bedrock. Both degradational levels contain elevated alluvial gold grades. By the peak of the glacial advance a bouldery lag deposit had accumulated above a "false bottom" consisting of relatively fine grained outwash gravel. This shallow lag (base at 6 to 8 m below the surface) was explored by cable-tool drilling and mined for gold by Bucketline Dredging and hydraulic excavator/floating-screen methods at Callaghans.

In the Callaghans area the basal degradational gravel, which is situated below the Waimea Formation, was formed in buried gullies that grade down to a widespread ancient floodplain of the ancestral Kapitea Creek. These gullies were part of the drainage system off Italians Hill and associated ridgelines to the west of Callaghans. The buried landscape was explored between 1865 and 1900 by tunneling. Deep gold bearing channels were mined by hydraulic sluicing. This floodplain and tributary gully system was buried by 30 to 40 metres of fluvioglacial aggradation during the Waimea Glaciation. The evolution of this Sub-Waimean landscape predates the Waimea Glaciation. The relative timing of the creation of this landscape and the deposition of the Karoro and Scandinavian Formations is unknown. It is clear that at that time the sub-Waimean lag materials were being deposited in a fluvial system for which the base-level was below the sea level that applied here during the deposition of the Karoro and Scandinavian Formations. The sub-Waimean lag deposits have not been observed in contact with either the Karoro of the Scandinavian Formation. They could potentially correlate with the pre-Awatuna fluvial deposits at the type section of the Awatuna Formation (which are discussed below) and/or the pre-Loopline fluvial deposits at Blakes Terrace (which are discussed below).

The terminal moraines formed during the Waimea Glaciation (Kumara 1 Advance, Waimea(1) Formation as mapped by Suggate & Waight 1999) are located mainly seaward of the LGM terminal moraines. This implies that glacial ice was at least as extensive during this period as during the LGM and further that the ice volume was comparable to or greater than that of the LGM.

6.2.12b Pollen in Soil on the Waimea(1) Formation

Chesterfield Road

Moar and Suggate (1996) present a pollen diagram for profile M81/7 which is situated in a 0.8 metre deep soil on the Waimea(1) Formation adjacent to Chesterfield Road. One ^{14}C age is reported from this profile being NZ6240 at 24.00 ± 0.65 ka. The sample is from organic rich soil at a depth of 0.7 to 0.8 m and does not date the underlying fluvial gravel.

At M81/7 (see table 6.3) on the Waimea(1) Formation the basal zone contains a relatively cool climate assemblage, followed upward by a dramatic increase in Dacrydium cupressinum, an upwards decline then a second rise in Dacrydium cupressinum (rimu). The intervening decline in rimu pollen is accompanied by a sharp increase in Nothofagus fusca. This pattern is almost identical to that in M81/8 from nearby on the Waimea(2) Formation. The presence of Nestegis is

significant at these two profiles. Moar and Suggate (1996) appear to have assumed there is little difference between the ages of the lowermost portion of the soil at these two sites.

Table 6.3 Pollen zones in soil profiles M81/7 and M81/8 on the Waimea Formation at Chesterfield Road. Depths are from profile M81/8.

Zone	Depth	Pollen
	---------- 0.2 m	
CRW4		*Dacrydium cupressinum* (Rimu) increases upward and is dominant at the top. Myrsine and Poaceae decrease upward
	---------- 0.45 m	
CRW3		*Nothofagus fusca* important at base, Nothofagus Menzeisii present, *Dacrydium cupressinum* (10%+ throughout). *Nestegis* disappears before the top. Metrosiderous declines upward.
	---------- 0.75 m	
CRW2		Dominated by tree pollen, *Weinmannia* predominant at base. *Dacrydium cupressinum* (up to 50%) & *Phyllocladus* predominant in middle, *Nothofagus fusca* (type) rare at base but dominant at the top (up to 40%). *Nestegis* and *Metrosiderous* present.
	---------- 1.15 m	
CRW1		Dominated by herbs and shrubs. Poaceae , Asteraceae, *Coprosma, Myrsine* frequent at base but declining upward. Tree pollen consistently low throughout.
	---------- 1.6 m	
		Fluvioglacial Gravel

Grahams Terrace

Grahams Terrace is one of the "classic" Late Quaternary sites from the Westland Region (situated at grid ref. NZMS 260 K32 9295N 5970E in the Grey Valley). It is discussed by Mew et al (1986); Hammond et al (1991); Berger et al (1994); Moar & Suggate (1996) and Suggate & Almond (2005).

The first report of the soil stratigraphy on Grahams Terrace is by Mew et al (1986). They describe 10 profiles from a loess cover of variable thickness ranging from about 0.5 to 1.7 metres. The sites were situated at 100 metre intervals adjacent to a forestry road. These profiles were sampled to check for the presence of the Kawakawa tephra which is present here with a maximum thickness of 8 cm. In one profile the tephra was present under loess at a depth of ~95 cm in a profile about 160 cm thick. The tephra has an age of ~26 ka based on ^{14}C dating at other sites (Wilson et al 1988). The area sampled is at an elevation of ~270 m.

Two similar profiles (M83/16, M83/17) are reported by Moar & Suggate (1996) from this locality. Both are in cuttings adjacent to a forestry road about 8 km SSE of Nelson Creek settlement. The Kawakawa Tephra was reported by Moar & Suggate (1996) to be approximately in the centre of pollen zone GT3 in both profiles. It is assumed by Moar & Suggate (1996) that pollen zone GT3 represents the last glacial period and that pollen zone GT1 represents MIS5a (their table 6), largely on the basis of rare *Nestegis* pollen at that level. This correlation is entirely speculative as there are no numerical dates to back it up.

Tables 6.4 & 6.5 briefly summarise the pollen zones in profile M83/16 from figure 8 of Moar & Suggate (1996) and anther site discussed by Suggate and Almond (2005).

Table 6.4 Pollen zones in a soil profile on the Waimea Formation at Grahams Terrace, Grey Valley.

Zone	Depth	Pollen
	---------- 0.3 m	
GT4		*Dacrydium cupressinum* (Rimu) dominant (up to 60%), *Weinmannia* (Kamahi), *Metrociderous* (Rata) (Holocene)
	---------- 0.4 m	
GT3		*Poaceae* dominant, *Asteracae*, *Coprosma*, *Myrsine*. Minor *Halocarpus* & *Nothofagus fusca*
	---------- 1.0 m	
GT2		*Poaceae* dominant, *Halocarpus* up to 20%, *Nothofagus fusca* up to 15% *Phylocladus* up to 10%, *Coprosma* up to 10%, *Myrsine*
	---------- 1.3 m	
GT1		*Nothofagus fusca* up to 40%, *Nothofagus Menziesii* up to 15%, *Dacrydium cupressinum* up to 20% (all decline upwards), *Phylocladus*, rare *Nestegis*
	---------- 1.6 m	
		Fluvioglacial Gravel

Table 6.5 Soil sequence at Grahams Terrace

0.0 m	----------	Surface at Grahams Terrace	
		Peat/Forest litter with tree roots	Holocene?

0.5 m		Grey? massive silt/ silt loam	

		Peat	

		Sand	

1.1 m	xxxxxxxx	Silty peat/ peaty silt, Kawakawa Tephra in centre	

		Grey? massive silt/ silt loam	Loopline?

1.5 m		Silty peat to peaty silt	

		Peat	
2.0 m	----------		
		Grey? massive silt/ silt loam	Waimean?
2.4 m	----------		
		Fluvial gravel	Waimea Fm

In their figure 5A Suggate and Almond (2005) juxtapose a condensed version of the pollen diagram from profile M83/17 (of Moar & Suggate 1996) against a profile of the coverbeds from Grahams Terrace. They note that at Grahams Terrace the soil thickness varies over short distances. It is clear from their figure 5A that the lower most peat and lowermost massive silt in the above profile are not present at pollen profiles M83/16 and M83/17. It is proposed here that the lower peat and massive silt are preserved in a hollow/channel. This would imply non-accumulation or erosion of the lower part of the sequence at some points on this terrace. If we hypothesized a constant sedimentation rate for the above profile and assign an age of 27 ka to the Kawakawa Tephra then the age of the base of the coverbeds here would be about 65 ka. That would imply that the fluvioglacial gravel of the Waimea Formation could comfortably be correlated with MIS4 or with MIS5a or older isotope stages depending on the presence or absence of stratigraphic breaks and phases of non-deposition.

Moar & Suggate (1996) suggest that the MIS3 portion of the record is only rudimentary at Grahams Terrace. This seems to be based on an assumption of very slow deposition or erosion which is in turn based on the assumption that the base of the profile dates from MIS5. As shown in Chapter 5 (this thesis) the presence of *Nestegis* at the base of pollen profile (zone GT1) can not be taken as confirmation that MIS5 deposits are present here, because this genus is arguably present to c. 50 ka (MIS3) in organic silt at Okarito. The lower peat in the Grahams Terrace profile (see Suggate & Almond (2005) could date from the early portion of MIS3 and could rest on MIS5a/4 loess.

Blue Spur Road

This locality is at the edge of the Waimean Terrace overlooking the Hokitika Valley. These samples are not from precisely the same section as the Berger et al (2001) TL ages. However the ^{14}C ages by Moar & Suggate (1973) seem to be compatible with the TL ages by Berger et al (2001).

Table 6.6 Soil stratigraphy on the Waimea Formation at Blue Spur (from Moar & Suggate 1973)

Depth (cm)	Description
0-30	Surface soil
30-60	Grey silty clay, slightly-organic band in middle
60-75	Grey-brown silty clay with minor organic material
75-180	Brown silty clay, progressively more organic downwards
180-220	Clayey silt, grading down to
220-230^{+}	Gravel, up to 4 cm diameter
	12 m poorly sorted gravel } Northeastward along Blue Spur Road
	12 m^{+} marine gravel } towards Clarke Creek

Further detail is presented in figure 2 of Moar & Suggate (1973).

The pollen diagram (fig 3) of Moar and Suggate (1973) has Dacrydium cupressinum (Rimu) dominating in "pollen zone d" at about 65% to 90% of the total pollen to a depth of 0.8 metres then a decline in this species to a "background" level from 0.9 to 1.6 metres in pollen zones "c & b". Podocarpus (Kahikatea, Matai), Phyllocladus (Toatoa), Metrosideros (Southern Rata) and Ascarina pollen are also at a maximum in the upper 0.9 metres. The interval 0.8 to 0.9 metres presumably corresponds to the MIS2/1 transition. From 0.95m to 1.55 m Nothofagus menziesii (Silver Beech) and Nothofagus fusca (Red Beech) dominate the tree pollen. Total pollen from trees and shrubs reaches a minimum at 0.9 to 1.05 m, but does not drop below 60%, while tree pollen alone reaches a minima of about 40% at this depth. So the most likely position for the LGM in this profile is at 0.9 to 1.05 m. The pollen diagram implies that during the LGM there were substantial areas of full canopy forest in the vicinity of this site. At this time the forest was dominated by Nothofagus menziesii. This species gradually gives way downward to Nothofagus fusca from about 1.25 m to 1.6 m. From 1.55 m to 1.7 m (pollen zone A) Dacrydium cupressinum becomes increasingly important, dominating the tree pollen at 1.7 m and constituting about 45% of the total here. Nothofagus is only a small part of the pollen spectrum at 1.7 m.

The base of the Blue Spur Road profile is considered by Moar & Suggate (1973) to be representative of an interstadial period between the $K2_1$ (Loopline Fm) and $K2_2$ (Larrikins Fm) glacial advances and that it can't be inferred that the temperature was as mild as it is today. This is important because they subsequently changed their opinion after finding Nestegis pollen in the lower part of the soil profile here. In Chapter 5 Nestegis pollen is discussed in detail, particularly in

respect of the Okarito composite core by Vandergoes et al (2005). It is concluded in Chapter 5 on the basis of intensive ^{14}C and luminescence dating at Okarito that Nestegis was potentially a significant element within the flora at Okarito during the early portion of MIS3. The following is from Moar and Suggate (1996):

> "At Blue Spur near Hokitika (Moar & Suggate, 1973), the base of the coverbeds was at first thought to be no older than mid-Otiran, because of finite radiocarbon ages. Revision of the age interpretation (Moar, 1988) followed acceptance that some radiocarbon ages from older sites were too young because of contamination by modern carbon (c.f. Grant-Taylor & Rafter, 1971; Moar & Suggate, 1979) followed by confirmation of this at Blue Spur Road and by the identification of interglacial Nestegis pollen (Moar, 1984) in the lower part of the pollen sequence." and

> " Moar and Suggate (1973) accepted ages of 30,300 BP in zone BS1, and of 23,800 and 21,200 in zone BS 2, but Moar (1988) later rejected them because of probable contamination by modern carbon."

But the extent of contamination by "modern carbon" has never been demonstrated at this site. Contamination is an inference based largely on the preference of Moar (and Suggate) for an interglacial correlation which essentially means MIS5 or >80 ka for the base of the soil at this site. In light of the pollen diagram and dating for the Okarito composite core by Vandergoes et al (2005), as discussed in chapter 5 this preference is rather speculative. Moar and Suggate (1973) had the following to say about contamination:

> "The ages come in stratigraphic order and are sufficiently different to suggest that the samples are not roots extending downwards from any particular higher horizon. There is a slight danger of contamination of individual samples from carbon in other parts of the organic layer, but the degree of such contamination would have to be exceptionally great to significantly alter the ages. Modern contamination from above the top grey silt is considered unlikely. Accordingly the ages are thought to be substantially correct and the base of the organic layer to be rather more than 30,000 years old."

6.2.12c Radiocarbon and Luminescence Dating of the Waimea Formation and Coverbeds

Grahams Terrace

The Kawakawa tephra was described by Mew et al (1986) from a depth of about 0.95 in a 1.5 m deep profile at Grahams Terrace (grid ref NZMS 260 K32 928588). The thickness of the macroscopic Tephra is variable with a maximum of 8 cm. Samples were taken from 3 cm above and 3 cm below the Tephra for thermoluminescence dating by Berger et al (1994). These returned ages of 15.8 ± 1.6 ka and 17.2 ± 2.4 ka which appear to underestimate the "known" age of the tephra (c. 27.1 kyr cal).

Hammond et al (1991) trialed a number of chemical pretreatments on samples taken from immediately adjacent to the Kawakawa tephra at Grahams terrace. The oldest ^{14}C age obtained in this study was NZA329 with a non-calibrated age of 19.65 ± 0.35 ka. NZA329 was a residue from NZA328 after treatment in hot 70% HNO_3. The untreated organic silt from NZA328 yielded an age of 11.85 ± 0.1 ka. The non-calibrated age for the tephra was quoted as 22.58 ± 0.23 ka (Wilson et al 1988). In terms of ^{14}C contamination in Westland this site essentially represents a "worst case scenario". Although the "soil" is relatively deep here it is not protected in any way from infiltration by carbon-bearing groundwater or penetration by fine rootlets. This issue is discussed at length in chapter 5. There is no reason to assume that contamination is this severe at all West Coast sites.

The findings of Hammond et al (1991) and Berger et al (1994) for loess on Grahams Terrace, where contamination of organic matter by younger carbon has been demonstrated, have been used as part of the justification for rejecting much older ^{14}C ages from other sites. This practice has been adopted by Vandergoes et al (2005) for ^{14}C ages from Okarito (discussed in the introduction to Chapter 5), Moar (1988) for soil at Blue Spur Road, Moar & McKellar (2001) for soil at Greens Beach, selectively by Moar et al (2008) for soils at Schulz Creek, and Moar & Suggate (1996) for a number of localities. But the practice extends back to Moar & Suggate (1979) at Cape Foulwind and Dickson (1972) for the Lamplough Lead at Chesterfield.

For some of the Grahams Terrace samples there is no question that contamination has occurred. As the limit of ^{14}C dating is approached a tiny trace of contamination by "young" ^{14}C is enough to produce an erroneous age. Nevertheless, there are a number of localities that have produced ages that are essentially infinite, or in other words where the ^{14}C content is at or beyond the detection limit. What this proves is that post c. 50 ka contamination by younger carbon is not ubiquitous, otherwise it would not be possible to generate an infinite age. It also means that at some sites the mobility of carbon in groundwater is proven to be very limited. Given this limited ^{14}C mobility at some "older" sites clearly one should be wary of dismissing relatively old finite ages from a soil that has produced an infinite age. One can't automatically assume contamination on the basis of an a priori conviction that the soil is considerably older than the ^{14}C detection limit.

At Okarito (Vandergoes et al 2005, supplementary information) and Cape Foulwind (Moar & Suggate 1979) treatments designed to strip assumed ^{14}C contamination from relatively old samples has failed to convincingly demonstrate a significant change in sample age.

Berger et al (1994) [Quat. Sci. Rev. 13: 309-333] also sampled the loess on Grahams Terrace for dating purposes. They used thermoluminescence and reported ages of 23.6 ± 0.6 from loess 3 cm above the Kawakawa Tephra, and 24.5 ± 0.6 ka 3 cm below the tephra. If the ^{14}C age of Wilson et al (1988) is correct then Berger et al (1994) have demonstrated that TL is a method that may be applicable to loess deposits in North Westland.

The dating work at Grahams Terrace raises questions about accumulation rates. The loess that overlies the tephra correlates with MIS2. For the existing isotope stage correlation for the Waimea Formation to be correct the underlying 70cm of silty sediment must encompass loess and soil accumulation during MIS3, 4, 5a, 5b, 5d 5e and probably at least part of MIS6, a potential depositional period is at least 110,000 years. This is certainly possible but also unproven. Does the underlying glacial outwash gravel really correlate with MIS6? Have there been periods of soil erosion between about 26 ka and 140 ka? Has the loess volume been reduced by post depositional leaching? If the loess collected at an approximately uniform rate then the base of the profile could easily correlate with MIS4, MIS5b or MIS5d depending on the accumulation rate.

Blue Spur Road

Soil / loess profiles on the Waimea Formation at Blue Spur near Hokitika have been described by Berger et al (2001), Moar & Suggate (1973) and Moar & Suggate (1996). Several non-calibrated ^{14}C ages reported by Moar & Suggate (1973) from loess/soil exposed in a road cutting (Blue Spur Road) on the Waimea Formation near Hokitika are listed in table 6.7. The three samples were cleaned to remove potential contamination by younger carbon, the comment by Moar & Suggate being: samples were "treated with boiling 40% HF, after washing in 7% HCl, the residue was acetolysed in the usual way."

Table 6.7 ^{14}C ages from cover beds on the Waimea Formation at Blue Spur

Sample	Sample Depth	^{14}C Age (yr B.P.)
NZ705	150 cm	21,200 ± 350
NZ744	155 cm	23,800 ± 300
NZ1058	175 cm	30,300 ± 3300

All three dated samples are situated stratigraphically below the LGM which is here interpreted to occur at the tree pollen minimum (discussed above). This minimum is at a depth of 0.95 to 1.05 m. NZ705 and NZ744 have non-calibrated ages of 21,200 ± 350 and 23,800 ± 300 years respectively. These are similar to the age commonly quoted for the Kawakawa Tephra (~22.6 ^{14}C ka, Wilson et al (1988)). In a recent review by Lowe et al (2008) the proposed age for the Kawakawa Tephra is 27.097 ± 0.957 ka (cal). In terms of the pollen spectra and physical depth these two samples are in a position where one would expect to find this tephra. So there is no particular reason to make an *a-priori* assumption that non-treatable contamination by younger carbon has occurred at this depth. Sample NZ1058, at a depth of 175 cm has a non-calibrated age of 30.3 ± 3.3 ka. The calibrated age would be expected to be c. 32.5 ka. The potential existence of a substantial *Dacrydium cupressinum* dominated forest cover at this site some time between say 33 ka and 40 ka bears comparison with pollen spectra from Okarito and from Schulz Creek (discussed below in relation to the Awatuna Formation). It also bears comparison with the climate and vegetation described from by Burge & Shulmeister (2007) from "The Hill", and with that from Martins Quarry described by Suggate & Moar (1979) both of which are sites near Westport. "The Hill" and Martins Quarry are discussed below in relation to the "Waites Formation".

Berger et al (2001a) used thermoluminescence ($TL_{(UV)}$) and infrared stimulated luminescence ($IRSL_{(blue)}$) as dating methods at Blue Spur near Hokitika. Here they sampled soil/loess situated on fluvioglacial gravel of the Waimea Formation, and sand from the underlying Karoro Formation. The details of the sample analyses are listed Appendix four and are summarised as follows:

Table 6.8 Luminescence ages from Blue Spur by Berger et al (2001)

Sample	**Depth (cm)**	**Material**		**Age (ka)**	**Comment by Berger et al**
	~35	Tephra		c. 27 ka	(Kawakawa Tephra)
BSR 91-5	~90	Loess	TL	46.9 ± 7.3	Stratigraphically reasonable
BSR 91-9	~ 190	Loess	TL	53 ± 16	Probably Underestimated
BSR 91-1		Marine sand	IRSL	44 ± 17	Incorrect (underestimated)

Berger et al (2001) express the view that the BSR-91-1 age is underestimated, based largely on the expected age. The sample is from marine sand that has been mapped as Karoro Formation which in the Suggate model dates from MIS7. At 1σ there is no age reversal between BSR 91-9 and BSR 91-1.

As discussed in Chapter 5 (sections 5.3 to 5.6) thermoluminescence dating has been somewhat problematic in North Westland. In dating at Kamaka, Sunday Creek and at the Phelps Mine Preusser et al (2005) [tables 5.1, 5.2 and 5.3 of this thesis] have shown that this method was prone to substantial overestimation sample ages in silts from those sites. This is one of the most emphatic

findings from that study. So unless there is specific evidence to the contrary there is no need to suggest that the thermoluminescence ages from Blue Spur underestimate the depositional age of the sediment. The simplest interpretation is that the ages are correct. The same point can be made in relation to the IRSL age (BSR 91-1). In this case it is not the ages that are being reinterpreted. They are what they are. It is the subsequent interpretation of Berger et al (2001) that is being questioned and this is simply science in action.

The upper two TL ages (samples BSR 91-5 and BSR 91-9) are from loess situated on the Waimea Formation. The stratigraphic position is similar to that for a group of three ^{14}C ages by Moar & Suggate (1973) from a nearby locality. The ^{14}C ages are discussed above. They have been dismissed as contaminated by younger carbon (Moar 1988, Moar & Suggate 1996).

Even if the fluvial gravel situated between BSR 91-9 and BSR91-1 is part of the Waimea(1) Formation it would be expected that the first loess situated on this unit would have begun to accumulate rapidly during Waimea(2) deposition. It should be younger than Waimea(1). In this thesis it is suggested that the Waimea(2) event dates from about 65 to 60 ka. The deeper of the two TL samples gives an age that is in fair agreement with that expectation and a new marine isotope stage correlation (MIS4) proposed in this thesis.

The Kawakawa tephra (c. 27 ka) has been identified at about 35 cm below the surface. The overlying loess (L1a) is clearly from MIS2. Could most of the next 70 cm of loess/soil below the tephra be derived from glacial activity during MIS3/4? At a depth of ~ 90 cm (below the surface) a $TL_{(UV)}$ age of 46 ± 7.3 ka was considered to be stratigraphically reasonable by Berger et al (2001) implying that material at a depth between 35 and 90 cm could be from MIS3.

The $TL_{(UV)}$ age of 53 ± 16 ka from a depth of ~190 cm was considered to be an underestimate by Berger et al (2001). Given the size of the 1σ the age is consistent with loess deposition during MIS3 and/or MIS4, even if the preferred age is an underestimate. In that case the underlying fluvioglacial outwash gravel could potentially have been deposited during MIS4, MIS5a or MIS5b. If this is the case then the marine sand (Karoro Formation) situated below the outwash gravel (Waimea Formation) could have been deposited during MIS5a or MIS5c. If the marine sand dated by Berger et al (2001) at Blue Spur is the Karoro Formation and if it was deposited during MIS5a then the $IRSL_{(blue)}$ age of 44 ± 17 ka (i.e. up to 61 ka at 1δ and 78 ka at 2δ) is not unreasonable.

Upper Chesterfield Road

There are no ^{14}C ages for the Waimea(1) Formation or it's coverbeds at Upper Chesterfield Road. Preusser et al (2005) dated loess and sand from a gravel Quarry at "Upper Chesterfield Road" (grid ref: J32 568397). The ages are given in table 6.9.

Table 6.9 Luminescence ages from the Upper Chesterfield Road gravel quarry by Preusser et al(2005)

Upper sample of loess cover (sample UCS3)
{$IRSL_{(UV)}$ age 27 ± 3 kyr
{post-IR-OSL age 36 ± 3 kyr
Lower sample of loess cover (sample UCS2)
{$IRSL_{(UV)}$ age 39 ± 4 kyr
{post-IR-OSL age 57 ± 6 kyr
Sand from the uppermost part of the gravel (sample UCS1)
$IRSL_{(blue)}$ age 81 ± 7 kyr

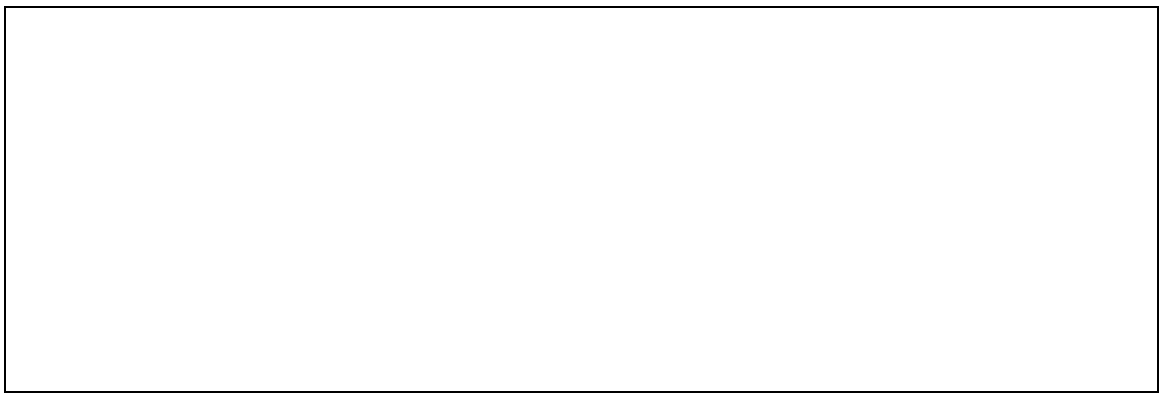

Preusser et al (2005) consider that post-IR-OSL dating is probably more reliable than $IRSL_{(UV)}$ dating for West Coast samples. This issue is discussed in detail in Chapter 5 where it is concluded that this claim by Preusser et al (2005) is difficult to sustain from the data presented in their paper. Sample UCS1 at 81 ± 7 ka is described in their *section 4.6*. The sampled material is a sand horizon within gravel at a small relatively shallow quarry in the older part of the Waimea Formation. At 1σ this age is compatible with fluvial aggradation as recently as 74 ka. At 2σ it is compatible with deposition in the early portion of MIS4. It should be noted that the dating of sand from fluvioglacial is discussed at length in Chapter 5 (section 5.6). It is concluded that $IRSL_{(blue)}$ samples similar to UCS1 but taken from a quarry at the Nelson Creek Farm Settlement almost certainly suffer badly from incomplete bleaching and therefore overestimate the depositional age.

Preusser et al (2005) correlate sample UCS1 with MIS5b or MIS5a but suggest that this represents reworking of material situated in the Waimean Terrace during a degradational event (Waimea(2)). The "degradational" event resulted in the creation of an adjacent and slightly lower terrace. Although the dated material is clearly from the older terrace they decided that it does not represent the original depositional age of that fluvial gravel. However, no evidence is supplied in support of this interpretation. An examination of the site during this PhD project failed to provide any evidence in support of the re-working hypothesis. So if the sample age is acceptable then it is more likely to date the Waimea(1) Formation and the culmination of aggradation during the first phase of the Waimea Glaciation.

Sunday Creek (this project)

A single IRSL sample (RR25, Grid ref NZMS260 J32 N 3890 E 5555) was taken from the coverbeds on the Waimea(1) Formation during this project. The site is in gravel quarry adjacent to a forestry road located immediately above Sunday Creek near Awatuna. The sample, which returned an age of 75.9 ±7.6 ka comes from the base of a 3.8m thick soil sequence on the Waimea(1) Formation.

As discussed in Chapter 5 (sections 5.6 and 5.7) there are significant issues relating to the dating of fluvioglacial sediments by luminescence methods. In table 5.4 the IRSL samples taken during this PhD project are classified in terms of the likelyhood of complete bleaching at deposition and sample RR25 is classed as having a poor to moderate chance of complete bleacing. Given that there was nothing particularly abnormal about the sample during the dating process, with no sign of anomalous fading, the sample is considered here to represent the maximum likely age of deposition.

There are a total of two IRSL ages that can be considered to directly date the deposition of the Waimea Formation in North Westland. These are RR25 and UCS1. The sample ages are 75.9 ±7.6 ka and 81 ± 7 ka respectively. Both are considered here to be maximum ages. In this light they are in accord with the IRSL dating on the older Karoro, Scandinavia and Caledonian Formations discussed above.

6.2.12d Relative ages of the Rutherglen and Waimea Formations

The relative ages of the Waimea and Rutherglen Formations have been defined at Candle Light near Camerons. Here it has been confirmed that a Rutherglen Formation strand line that is no higher than 62 metres amsl truncates outwash gravel of the Waimea Formation (upper surface at about 80 metres amsl). So the Waimea Formation is older than the Rutherglen Formation. What if the 70 to 75 m Rutherglen Strandline (present at South Beach) had been destroyed at Candle Light by a more recent marine incursion? In that case the relationship between the Waimea(1) Formation and the older part of the Rutherglen Formation would have been destroyed as well. In Suggate & Waight (1999) the relatively low elevation of the Rutherglen Fm here is explained as the result of active folding of the surface. It is likely that the Rutherglen(1) event would have truncated the Waimea(2) surface if this terrace represents the younger Waimean event. There are a number of forestry road cuttings at Candle Light that expose the Waimea Formation. There is no evidence that the Waimean fluvioglacial outwash as mapped by Suggate & Waight (1999) has overtopped Rutherglen strandline deposits here.

At Candle Light the Rutherglen Formation is overlain by fluvial gravel, which has been assumed to be Loopline Formation. There is no data available on the age of this gravel so correlation with a "pre Loopline" event can't be ruled out.

The evidence at South Beach is that there is only a minor terrace riser at the inner edge of the Rutherglen Formation. If this relationship held constant as far south as Blue Spur then the Waimea Formation could easily overlie the Rutherglen Formation at Blue Spur.

Near Chesterfield Road and Sunday Creek the Rutherglen strandline is not present, having been destroyed during deposition of the Awatuna Formation. At the type section of the Awatuna Formation in a tributary of Sunday Creek (a few hundred metres south from Chesterfield Road) the inner Awatuna strandline clearly truncates the Waimea Formation. Had the Rutherglen Formation been present here it appears from the mapping by Suggate and Waight (1999) that it would probably have truncated the older (higher) part of the Waimea Fm.

6.2.12e Summary of Numerical Dating of the Waimea Formation

In the Suggate model the Waimea Formation is correlated with MIS6. However, $IRSL_{blue}$ samples taken during this project on or from the Karoro, Scandinavia and Caledonia Formations (which are clearly older than the Waimea Fm) produced ages that are younger than MIS6. In order for the Waimea Formation to have been deposited during MIS6 the results for samples RR22, RR23, RR13, and RR6 must all be incorrect and must all vastly underestimate the ages for these older formations. Similarly the ages for RR25 and USC1 need to be approximately half of the depositional age in order for the MIS6 correlation to be correct. On balance the writer considers both cases to be very unlikely. On the basis of the available numerical dating the simplest interpretation is that the Waimea Formation is no older than MIS5a. A correlation with MIS5b is possible but less likely than a correlation with MIS4. There is an unavoidable element of speculation as to the true depositional age. The literature search conducted for this project has failed to find any non-contestable numerical dating that gives direct support to an MIS6 correlation. So given the weight of numerical dating evidence, speculation that this formation dates from MIS6 is probably unwarranted.

There are no other numerical ages by any method that directly date the Waimea Formation. All other numerical ages from coverbeds resting on the Waimea Formation centre on ages less than 60 ka. Given the summary above it is in fact no surprise that such ages (e.g. around 53 ± 16 ka by TL_{UV} at Blue Spur) have been obtained from the base of loess situated on Waimean surfaces.

In the Suggate model the lower Waimean terrace at Chesterfield, about 10 to 12 metres below the higher surface, has previously been assumed to be a minor degradational feature but this has not been justified in detail. It is likely to date from MIS4 but could also have been deposited during MIS5a.

The timing proposed here for the Waimea Glaciation is similar to that of potentially similar events from a number of regions within the South Island:

- Almond et al (2001) describe two glacial moraines (M3 and M4) from South Westland that may be correlatives of the Waimea Formation. They report limiting ages of 80 ka and 50 ka. These moraines are overlain by the L3 and L4 loess sheets.
- Northern Fiordland (CA3 at 83 to 75 ka based on cosmogenic isotope dating, Cascade Valley, Sutherland et al 2007)
- Eastern Fiordland (A6, Lake Te Anau, Williams et al 1996). Williams (1996) defined the Aurora 6 glacial advance in Fiordland. This event was given limiting ages of 91 to 67 ka based on U/Th dating of speleothems.
- In the Canterbury region a peak in the rate of loess deposition was reported at 73 ± 13 ka by Berger et al (2001b) particularly with reference to sites at Cust, north of Christchurch, at Barry's Bay, and at the Timaru Brickworks.
- Cosmogenic isotope ages of 76 ± 8 ka and 83 ± 7 ka have been obtained from roche moutonnee at Cradle Mountain in Tasmania by Fink et al (2000).
- A notable cooling event is recorded in isotopic and trace element analysis of a Tasmanian speleothem by Geode (1994) during the period from about 79 to 73 ka. This speleothem record displays rapid, deep, simultaneous changes in Mg content, Sr content, $\delta^{18}O$ and $d^{13}C$.

So a correlation with late MIS5a would be is consistent with a range of other evidence for significant cooling in the South Island and Tasmania at this time. In addition

The numerical ages discussed above (RR25, UCS1) above place limits on the termination of the Waimea Glaciation which could be as recent as 68 ka at the 2σ limit even with overestimation due to partial bleaching. Given that the samples could be overestimates as a result of partial bleaching the Waimea Formation could have been deposited in MIS4. If that was the case it would place a constraint on the age of the Rutherglen Formation, which is discussed below. Conversely the ages of the Rutherglen and Awatuna Formations places a constraint on the minimum age for the Waimea Formation. The fluvioglacial aggradation that produced the Waimea Formation was succeeded by fluvial incision and deposition of the marine strandline deposits of the Rutherglen Formation.

With climatic warming following the Waimea Glaciation an organic soil was deposited on the Waimea(1) and older surfaces. This is the lowermost organic soil/peat on the Waimea outwash surfaces. It may also correspond to the lowermost organic soil/peat on the Rutherglen(1) Formation.

6.2.12f Glacioisostasy and Fluvial Incision in Relation to Changes in Ice Volume

During the Waimea Glaciation there was an ice sheet of regional extent in the Southern Alps with an accompanying piedmont skirt encroaching onto the West Coast lowlands. The margin of the

glacial ice is defined in the mapping of Suggate and Waight (1999). The Waimean moraines are generally situated well to the seaward side of the LGM moraines. Ice was at least as extensive at this time as during the LGM.

The large Waimean ice mass almost certainly caused significant regional-scale isostatic downwarping of the crust. This process has been studied and described in relation to the Southern Alps for the LGM by Matthews (1965) who modeled the impact of the Pleistocene ice mass on the warping of the crust and the impact of the release of the ice load during deglaciation. It was calculated that:

> "Isostatic uplift along the West Coast since the last glaciation is likely to be about 50 ft."

In relation to fluvial processes and the gradient of rivers in this region the impact of warping of this magnitude is likely to be significant. It is assumed that analogous isostatic processes operated during each of the preceding glaciations of the scale of the LGM. The "wavelength" of the warping is on a scale of at least many tens of kilometres (figure 6, Matthews 1965). As for the LGM the magnitude of the down-warping during the more widespread Waimean Glaciation is assumed to have been in the order of 10 to 20 metres, which is potentially a significant faction of the eustatic sea level depression at that time. Given that the Southern Alps ice volume is extremely sensitive to modest changes in climate, down-warping and post-glacial relaxation have probably occurred repeatedly in this region during the Quaternary period. This is likely to have had an impact on the timing an extent of fluvioglacial aggradation during ice sheet growth, on fluvial incision during ice sheet ablation, and on local sea level. In terms of incision a general scenario is as follows:

> With the onset of warming leading to interglacial/interstadial conditions the Southern Alps ice sheet is reduced in volume. Crustal rebound would initially be fairly rapid. The phase relationship with changes in eustatic sea level is unknown and may be different for different glacial events. The result of rapid rebound is likely to be an abrupt change in local base level and an increase in gradients within the local fluvial system. When the base level is low this encourages fluvial incision and strath cutting in all the major valleys. Incision is aided by reduced sediment supply during the glacial retreat phase. Incision is likely to be more focused and more rapid during deglaciation than at other times in the climatic cycle.

Alluvial gold bearing lag deposits formed during periods of rapid incision are sufficiently different in character from aggradational fluvioglacial deposits that it is tempting to assign distinct formation names to them, even though they are generally buried by fluvial aggradation associated either with renewed glaciation or episodes of rising sea level.

At present there is insufficient numerical dating of Late Quaternary deposits in Westland to constrain the timing of events associated with deep post-glacial incision in this region. This was one of the original goals of the thesis project. Preliminary reporting was carried out by Rose (2000a, b) but this research thread has not been investigated further.

6.2.13 Rutherglen(1) Formation (MIS5a to MIS4)

6.2.13a Introduction

The Rutherglen(1) Formation was first defined by Suggate (1985). The definition was updated by Suggate and Waight (1999). They correlate the Rutherglen Formation with MIS5e and give it an age of 125-115 kyr. The primary change proposed here is the marine isotope stage correlation. This correlation is constrained by that for the Karoro Formation (MIS5a) which is older and the Awatuna Formation (early MIS3) which is younger than the Rutherglen Formation. In the new

stratigraphy proposed here the Rutherglen Formation is assigned to the MIS5a to MIS4 period. Dating that supports a correlation with climate events more recent than MIS5e is discussed below, and is summarised in section 6.2.13b.

Following the Waimea Glaciation there was a transition to warmer climate. This can be seen in pollen diagrams for soil profiles at Grahams Terrace (Grid K30/92955970, Fig 8b, 8c Moar & Suggate 1996), Kumara Cemetery (Grid J32/60403815, Fig 8a Moar & Suggate 1996), and Chesterfield Road (Grid J32/56204010, Fig 7a, Moar & Suggate 1996). The climate transition is likely to have been accompanied by a marine transgression. Near-shore erosion/planation occurred during the transgression and during the sea level maximum. Beach sediment was deposited directly onto local bedrock. The Rutherglen(1) Formation was largely deposited during and following the peak of the transgression. The magnitude and duration of local sea level change that caused the deposition of the Rutherglen(1) Formation is unknown.

Rutherglen(1) Formation strand-lines have previously been identified at ~68-72 metres above mean sea level at Karoro and South Beach, 62-65 m at Rutherglen and Candle Light, and 65-70 m Point Elizabeth. Rutherglen(2), strandlines are present at ~58-59 metres at Gladstone just north of New River, at South Beach and at Point Elizabeth.

It is not known whether the Rutherglen(2) formation is distinct from the 56m strandline at Houhou Creek, the 53 m strandline at Sunday Creek, the 58 m strandline at Gladstone, the 55 m deposits at Stanton Crescent, Karoro, and the 55-60 m strandline at Point Elizabeth. In the model favoured here (minimal coast parallel tectonic tilting) these deposits could all represent the same event, a possibility that has not previously been raised in relation to the Suggate model.

At Karoro and South Beach the strandline that separates the Karoro and Rutherglen(1) Formations is a rather subtle feature. It is a gentle riser on the terrace separating two surfaces that both slope gently towards the sea. The elevation difference at the strand line is only a few metres. The Karoro surface slopes up to a higher elevation at its strandline.

In the Suggate model the Rutherglen(1) Formation is assigned to the Kaihinu Interglacial period. The alternative timeline proposed here implies a climate that was less stable than envisaged in the Suggate model, varying sharply at the millennial scale through Late MIS5a, MIS4 and 3. The individual warm phases are of insufficient duration to be classed as full interglacial, in the manner envisaged in the Suggate model. If temperatures reached the modern level this could have been occurred over a few hundreds to a few thousands of years. In this timeline proposed for this thesis the Kaihinu Interglacial transfers from MIS5e/5c to a combination of the MIS5a/MIS4 transition and early to middle MIS 3.

6.2.13b Summary of Numerical Dating of the Rutherglen Formation

According to Moar and Suggate (1996) the Rutherglen Formation was deposited during MIS 5e. This is based primarily on the amino acid racemisation (AAR) dating discussed previously in relation to the Karoro Formation. The position adopted here is that the AAR samples were taken from the Karoro Formation rather than the Rutherglen Formation. When coupled with consideration of the nine IRSL samples dated for this PhD project this contributes to a rejection of the MIS5e correlation for the Rutherglen Formation. Five of these returned $IRSL_{(blue)}$ ages and are the only numerical ages currently available for the Rutherglen formation. Four contained insufficient polymineral finegrained material and so could not be dated. The sample ages are listed in table 6.10. There are no $IRSL_{blue}$ sample ages that support correlation of the Rutherglen(1) Formation with MIS5e.

Table 6.10 Luminescence ages from the Rutherglen Formation, this PhD project.

Lab Code	Field Code	$IRSL_{(blue)}$ Age (kyr)	Elevation	Locality	Grid reference (NZMS260)
WLL149	RR10	No result	65-70 m	North Beach (Ru1)	J31 N 6620 E6330
WLL277	RR14	No result	56-60 m	South Beach (Ru1)	J32 N 5530 E 6060
WLL297	RR15	65.9 ± 5.4 ka	52-55 m	South Beach (Ru1)	J32 N 5530 E 6060
WLL278	RR16	No result	52-56 m	South Beach (Ru1)	J32 N 5530 E 6060
WLL172	RR17	63.6 ± 10.5 ka	69 m	Power Road (Ru1)	J32 N 5700 E 6130
WLL151	RR18	No Result	68 m	Power Road (Ru1)	J32 N 5700 E 6130
WLL531	RR26	71.7 ± 8.8 ka	62 m	Candle Light (Ru1)	J32 N 4700 E 5950
WLL532	RR27	96.5 ± 10.2 ka	63-64 m	Candle Light (Ru1)	J32 N 4700 E 5950
WLL536	RR33	56.3 ± 7.1 ka	65-68 m	South Beach (Ru1)	J32 N 5490 E 6065

The sampled localities are:

- RR14, RR15, RR16 (Grid ref NZMS260 J32 N 5530 E 6060) from sand in Road cuttings at the Tasman View Subdivision, South Beach, Greymouth;
- RR 33, (Grid ref NZMS260 J32 N 5490 E 6065), in soil exposed in the bank of a drain next to a culvert adjacent to a road leading to a ravel Quarry at the Tasman View Subdivision;
- RR 26 and RR 27 (Grid refs NZMS260 J32 N 4700 E 5950) in soil an old sluice face at Candle Light inland from Camerons.
- RR17, RR18 (Grid ref NZMS260 J32 N 5700 E 6130) from the terrace immediately north of Power Road, Karoro. The exposure is in a cutting on north side of Mac Ferguson's driveway.
- RR 10 (Grid ref NZMS 260 J31 N 6620 E 6330) at North Beach, Cobden.

Samples RR 10, 14, 16, and 18 failed to give results as the quartz was too dim for OSL dating and the silt content was too low for polymineral finegrain IRSL dating to be applied.

The elevations of these samples are systematically higher than for the Awatuna Formation samples. All of these ages are less than 100 ka, though one (RR27 @ 96.5 ± 10.2 ka) could make it over 100 ka within the 1φ bound. Sample RR27 is stratigraphically above RR26 which is from the same locality (71.7 ± 8.8 ka) so at 1φ there is an apparent age inversion in that profile. In terms of the meaning of these sample ages it should be noted that RR15 was from fine silty marine sand and RR17 came from the laminated marine silt at their respective profiles. RR26 comes from grey laminated silt situated below the uppermost 1 metre of interlayered clean marine sand and silt at Candle Light. So these three samples directly date the Rutherglen Formation and are probably the best results from the group for that reason.

As discussed in Chapter 5 (sections 5.6 and 5.7) there are potential issues relating to IRSL dating, in particular the possibility tat samples could be affected by partial bleaching of pre-existing D_e during deposition. In table 5.4 all the IRSL samples taken during this PhD are classified in terms of the likelihood of complete bleaching at deposition. The aeolian and littoral environments are much less likely to be adversely impacted than colluvial, fluvial or glacial environments. The further the sampled material has travelled away from fluvioglacial environments and the longer the time since the sampled material was subject to fluvioglacial process the more the greater the likelihood of complete bleaching. With regard to IRSL samples taken from the Rutherglen(1) Formation at South Beach and Karoro, RR15, RR17, and RR26 are from shallow marine and littoral sediments. RR33 is likely to have a substantial aeolian component being an organic rich soil taken from

beneath a loessic cover with the profile being free of any evidence of fluvial activity. Of the five samples these ones have the best chance of complete bleaching. Of four RR15, RR17 and RR33 are furthest from potential fluvioglacial influences.

In light of the above the IRSL samples that best define the age of the Rutherglen Formation are RR15 (65.9±5.4 ka) and RR17 (63.6±10.5 ka) which give an arithmetic average age of 64.7±8 ka. Sample RR33 is from the organic-rich basal 0.2 m of the soil profile at the Rutherglen strandline close to RR15. The thickness of the coverbeds is 1.3 m at this site. This sample was dated at 56.3 ± 7.1 ka, which is in excellent agreement with the ages of RR15 and RR16, given that it should be slightly younger and dates the abandonment of the strandline rather than its creation.

Sample RR26 dated at 71.7 ± 8.8 ka was taken from a grey inorganic laminated silt bed at the Rutherglen strandlie at Candle Light. The silt bed is both underlain and overlain by littoral sand and could potentially have a fluvial origin as it may represent ponding behind a beach ridge during progradation of the beach. There was nothing particularly abnormal about the sample during the dating process, with no sign of anomalous fading. Given a potential fluvial influence the sample age is considered here to represent the maximum likely age of deposition. At 1δ it overlaps the ages of RR15 and RR16.

Sample RR27 dated at 96.5 ± 10.2 ka is from a 1 m thick laminated grey silt unit that rests above the marine sand at Candle Light. It is situated immediately below a thick cover sequence containing 4 wood bearing organic soil horizons each separated by fluvial gravel. This sample is either fluvial or lacustrine. It was deposited after the seaward progradation of the coastline away from this site. In the context of the discussion in chapter 5 (sections 5.6 and 5.7) this sample is viewed as having a poor to moderate chance of complete bleaching during deposition. Therefore little weight is placed on this sample in the assessment of the depositional age of the Rutherglen Formation. Nevertheless, at 1δ the sample age is well short of a convincing correlation with MIS5e.

As a group the samples point to a likely depositional age of ~ 65 ± 8 ka. The simplest interpretation is that during the deposition of the Rutherglen Formation the coastline was in a position similar to that occupied when the Karoro Formation was being deposited. It is not clear whether deposition of the Rutherglen Formation occurred during a eustatic sea level maximum and it is not clear the degree to which the innermost strandline represents deposition following a marine transgression.

The timing of Late Quaternary sea level maxima is discussed in chapter 4 where it is concluded that during MIS3/4 eustatic maxima coincide with peak warmth during Antarctic interstadial events. In terms of the preferred IRSL age there is potential to correlate the Rutherglen(1) Formation with a number events including Antarctic warm events A4, A5, and A6. Note that Cutler et al (2003) and Thompson & Goldstein (2003) illustrate a -20 m sea level maximum around 73 ka at the close of MIS5a. This maximum is separated from the main MIS5a maximum by an intervening eustatic minimum that was at least 10 m lower. A sea level maximum with similar timing is identified by Lambeck & Chappell (2001), Potter et al (2003), Linsley (1996), Dumas et al (2005), and Chappell et al (1996).

In addition to numerical ages from samples taken directly from the Rutherglen Formation there are a number of "limiting $IRSL_{blue}$ ages" that have been shown on stratigraphic grounds by Suggate & Waight (1999) to be in formations/materials that are older than the Rutherglen Formation. These are listed in table 6.11 below. Samples that are omitted from the list include those that have not been convincingly demonstrated to be older than the Rutherglen Formation via stratigraphic relationships and samples that have probably been affected either by partial bleaching during deposition or by anomalous fading.

Table 6.11 Luminescence ages that help define the maximum possible age of the Rutherglen Formation

Field Code	$IRSL_{(blue)}$ Age (kyr)	Locality	Formation	Grid reference (NZMS260)	Study
UCS1	81 ± 7	Chesterfield Rd Quarry	Waimea 1	J32 568397	Preusser et al (2005)
RR25	75.9 ± 7.6	Sunday Creek	Waimea 1	J32 N 3890 E 5555	This study
RR22	84.3 ± 8.7	South Beach	Karoro	J32 N 5450 E 6610	This study
RR23	65.7 ± 5.7	South Beach	Karoro	J32 N 5450 E 6610	This study
RR34	92.5 ± 9.4	South Beach	Karoro	J32 N 5480 E 6095	This study
RR6	123.3 ± 12.7	Scandinavian Hill	Scandinavia	J32 N 3640 E 5340	This study
RR13	87.1 ± 8.3	Point Elizabeth	Caledonian	J31 N 6690 E 6345	This study
RR13	98.6 ± 24.4	Point Elizabeth	Caledonian	J31 N 6690 E 6345	This study

Individually and as a group the luminescence ages in table 6.11 are consistent with the proposed depositional age of the Rutherglen Formation (65±8 ka). These ages are classified individually in table 5.4 and discussed individually in the context of the formations from which they were derived and none are accepted here in a non-critical manner. In order for the Rutherglen Formation to be correlated with MIS5e as per the Suggate model not only would the ages for RR15, RR17, RR33, RR26, and RR27 need to be incorrect, but all of the ages listed in table 6.11 would also have to be incorrect (as they are derived from formations that are older than the Rutherglen Formation). In terms of this PhD project the likelihood that the Rutherglen Formation was deposited during MIS5e is seen as being remote and does not warrant further discussion. The isotope stage correlation established by Moar & Suggate (1996) for the Rutherglen Formation has no direct or bounding numerical age control. The correlation proposed in this thesis is supported by direct luminescence dating at four localities and by bounding ages on the Waimea, Karoro, Scandinavian and Caledonian Formations which are all older than the Rutherglen Formation. It is supported by bounding ages on the younger Awatuna Formation at two localities.

Given the maximum elevation of the marine deposits of the Rutherglen Formation at approximately 74 to75 m a minimum uplift rate of 1.1 mm/yr is implied if the local and eustatic sealevels were no higher than the modern level. If the eustatic sealevel was lower than the modern level then the uplift rate would be greater than this, depending to some extent on the local isostatic effects of changes in the position of the coastline and the extent of glacial ice in nearby Alpine regions.

6.2.13c Pollen in Soil on the Rutherglen Formation

At Candle Light near Camerons a thick soil and gravel sequence overlies beach sediments of the Rutherglen(1) Formation. The site has been described by Moar and Suggate (1996). A detailed profile through the soil sequence resting on the Rutherglen Formation at Candle Light is presented in relation to IRSL samples RR26 and RR27 in Appendix 1. The geological context is given in figure 6.3 above.

The notion that species composition, as revealed by the pollen content of a soil, can be used as a method of dating a soil without sub substantial support from a numerical dating method is not applied in this thesis. Nor are changes in climate that are interpreted from pollen assigned to particular marine isotope stages (e.g. presence of *Nestegis* implying correlation with MIS5e) without the support of numerical dating. This position is unlike Moar & Suggate (1996), Moar & McKellar (2001) and Moar et al (2008). The rational is discussed in relation to the pollen diagram from Vandergoes et al (2005) in Chapter 5. Consequently, although the pollen diagram for the Candle Light locality indicates that for CL2 climate was likely to have been mild and moist, it is not used to infer much more than that.

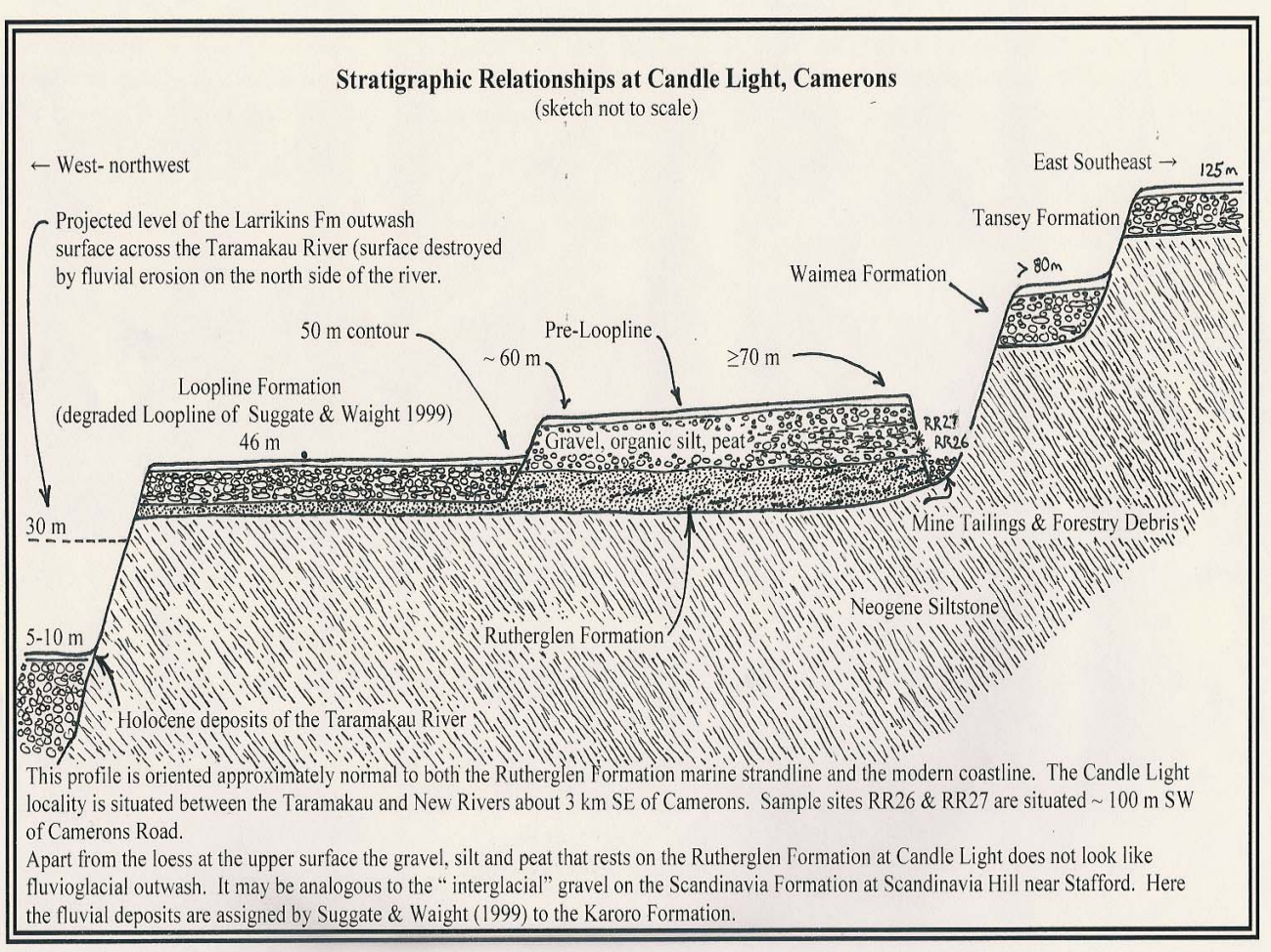

Figure 6.3 Stratigraphic relationships at Candle Light, Camerons

Table 6.12 Key features of the pollen zones identified by Moar & Suggate (1996) for the Candle Light site.

Zone	Pollen
---------- 1.6 m	
CL5 (MIS5b)	*Nothofagus fusca* dominates (90%$^{+}$)
---------- 1.8 m	
CL4 (MIS5c)	*Nothogagus fusca* dominates, up to 20% *Dacrydium cupressinum*, *Nestegis* present
---------- 2.2 m	
CL3(MIS5d)	*Nothofagus fusca* dominates, *Nothofagus menziesii* abundant, *Nestegis* present, minor *Dacrydium cupressinum*
---------- 3.4 m	
CL2 (MIS5e)	*Dacrydium cupressinum up to 20%, Nestegis* common, *Nothofagus fusca* minor at base but dominant at top, *Nothofagus menziesii* minor at base but important at top
---------- 4.7 m	
CL1 (MIS5e)	Common- *Metrosideros*, *Weinmannia*, *Quintinia*, *Coprosma*, *Myrsine*, Present- *Nestegis, Freycintia, Phyllocladus*. Podocarps not well represented with the exception of *Dacrocarpus*
---------- 4.8 m	Sample from a lower inorganic level: *Nothofagus* & *Podocarpus totara* or *P. hallii* and scattered wood present

6.2.14 Waimea(2) Formation

The Waimea(2) is defined by Suggate and Waight (1999). They considered this fluvial deposit to be a degradational feature and did not differentiate Waimea(2) from Waimea(1) in terms of their marine isotope correlation. The Waimea(2) Formation was not sampled for IRSL dating during this project. There are no numerical ages available for the base of the cover beds on the Waimea(2) Formation. The lower TL age in loess on the Waimea(1) Formation at Blue Spur Road (discussed above) may coincide with the deposition of the Waimea(2) Formation.

The Rutherglen(1) formation is potentially older than Waimea(2) but there are no known contact relationships. On stratigraphic grounds Awatuna Formation is clearly younger than the Waimea(2)Formation.

The general nature of the fluvial sediments contained in the Waimea(2) formation is the similar to that within the Waimea(1) Formation. The Waimea(2) Formation has not been traced inland to glacial moraines despite being found by the writer at Callaghans in a position previously mapped as Waimea(1) moraine by Suggate & Waight (1999).

Deposition of the upper gravel under this surface was preceded or accompanied by fluvial incision of unknown depth. There is potential for a glacial event or a re-advance producing fluvioglacial aggradation. The "degraded surface" is about 10 to 12 m lower than the initial Waimea surface.

In relation to the new stratigraphy proposed in this thesis the term "Waimea(2)" is not ideal given the implication that there may be a significant interstadial separating Waimea(1) and (2). The original names are retained here to maintain consistency with the terminology of the Suggate model. Kapitea Formation is a potential alternative but formal definition of a new formation is not warranted at this time.

As there are no numerical ages providing a distinction between Waimea(1) and Waimea(2) no isotope correlation is made for this unit. However, is it clearly younger than the Waimea(1) Formation and possibly younger than the Rutherglen Formation.

6.2.14a Pollen and Radiocarbon Ages from the Cover Beds on the Waimea (2) Formation at Chesterfield Road

Moar & Suggate (1996) report ^{14}C ages from profile M81/8 on the lower Waimea terrace at Chesterfield Road. These are 31.0 ± 1.4 ka for NZ5426 and 34 ± 1.9 ka for NZ5425. Both are from a peat layer at a depth of 0.85 to 0.95 m. The total soil depth on the Waimea Formation here is about 1.6 metres. These sample ages have previously been considered to be minimum ages in view of the potential for contamination by younger carbon. In relation to ^{14}C dating at Chesterfield Road Moar and Suggate (1996) suggest:

> "In view of the known translocation of organic matter (cf. Mew et al., 1988) in the cover deposits, all of these ages are unacceptable."

This claim by Moar & Suggate (1996) is unsubstantiated with regard to these samples. Both ^{14}C ages from profile M81/8 are equivalent to a calendar ages that are several thousands of years older. The ^{14}C ages are consistent with luminescence ages from a nearby site on Chesterfield Road by Preusser et al (2005). The luminescence ages are discussed below.

At soil profile M81/8 the lowest depth of c.27 kyr Kawakawa tephra shards is reported by Moar and Suggate (1996) to be 44cm. This is on the lower (Waimea(2)) terrace.

Moar and Suggate (1996) present a pollen diagram (M81/8) for a 1.6 metre deep soil profile on the Waimea(2) Formation. The basal zone contains a relatively cool climate assemblage, followed upward by a dramatic increase in *Dacrydium cupressinium* (Rimu), then an upwards decline then a second rise in *Dacrydium cupressinium* (rimu). The intervening decline in rimu pollen is accompanied by a sharp increase in *Nothofagus fusca* (Red Beech). This is a pattern similar to that from the profile on the Rutherglen Formation at Candlelight (described below).

Mew et al (1988) discuss loess in profiles on the Waimea(2) and Loopline terraces near Chesterfield Road. The Kawakawa tephra is generally found in the top 35 cm (found in 6 of the cores). They suggest that the base of the loess on the Waimea(2) Formation (higher terrace) could potentially be as young as 60 kyr or as old as 90 kyr. According to Mew et al this depends on whether carbon-bearing horizons are soils that represent periods of reduced deposition. But this presupposes that accumulation of organic soil is significantly slower than that of loess. Potentially the underlying gravel could correlate with MIS4 (~60-70 ka), MIS5a (~70-85 ka), MIS5b (~85-95 ka), MIS5c or MIS5c (~ 95-107 ka).

There are no published accounts of direct contact relationships between the Waimea(2) Awatuna Formations or between the Waimea(2) and Rutherglen(2) two formations. No such contact was observed during fieldwork for this project.

6.2.15 Rutherglen(2) Formation

The Rutherglen(2) Formation is defined by Suggate and Waight (1999). The primary change proposed here is the marine isotope stage correlation.

As discussed above Suggate and Waight (1999) identified two depositional levels within the marine Rutherglen Formation. At Gladstone and South Beach the lower (~58-60 metres above mean sea level) level has an identifiable strandline. They assumed this feature represents a regressive still-stand following the MIS5e transgression. No evidence is presented in support of this speculative claim.

It is not known whether the Rutherglen(2) formation is distinct from the 56 m strandline at Houhou Creek, the 53 m strandline at Sunday Creek, the 55 m deposits at Stanton Crescent (Karoro), and the 55-60 m strandline at Point Elizabeth. In the model favoured here (minimal coast parallel tectonic tilting) these deposits could all represent the same event. This possibility is not discussed by Suggate & Waight (1999).

At Point Elizabeth the sea level was stable for long enough at the now uplifted 55-60 metre level to form a distinct terrace in the relatively hard Cobden Limestone. The 45 m level at Point Elizabeth is more prominent though and certainly contains more extensive alluvial gold workings. This level is correlated with the Awatuna Formation in this thesis.

There are no numerical ages for the Rutherglen(2) Formation. So it is difficult to provide a clear distinction between the ages of the Rutherglen(1) and Rutherglen(2) Formations. The Rutherglen(2) Formation is assigned here by correlation to Antarctic interstadial event A5 from the early MIS3 with a possible age of about 69-68 ka. It is assumed that the age of the Rutherglen(2) Formation is bracketed by that preferred for the Rutherglen(1) Formation (A6 @ 73-71 ka) and that preferred for the Awatuna Formation (A4 @ 62-58.5 ka). If Antarctic interstadial events A6 (proposed Rutherglen(1) correlation) and A4 (proposed Awatuna Formation correlation) are

recognised then there is almost an expectation that the intervening A5 event will be represented. One implication is that the Rutherglen(2) Formation might not have been formed during a simple regressional still-stand following the Rutherglen(1) high-stand (the Suggate and Waight interpretation).

In this thesis use of the name "Rutherglen(2)" Formation maintains consistency with the terminology of the Suggate model.

Climate may have deteriorated further as indicated by changes in the flora (pollen) at Candle Light. Deposition of the Rutherglen(2) Formation may have been followed by a modest marine regression (and/or abrupt tectonic uplift). This could have been accompanied by renewed glacial activity.

At South Beach the Rutherglen(2) strandline contains old gold workings situated against the marine cliff (cut into the Rutherglen Formation proper) since destroyed by a residential development.

6.2.16 Pre Awatuna Formation Fluvial Deposits

In the Suggate model there are no recognised fluvioglacial deposits within the interval separating the Rutherglen and Awatuna marine events. At its type locality in a small tributary of Sunday Creek the Awatuna Formation rests on fluvial gravel of unknown age. The gravel is unlikely to be degraded Waimea Formation fluvioglacial gravel (older than the Rutherglen Formation) as the base of the Waimea is above the Awatuna Formation in the marine cliff here.

The Awatuna Formation also rests on fluvial gravel in gold exploration drill holes by Minerals Ltd (Stewart, 1988) near EA Road, just to the north of Kapitea Creek. The origin of the gravel is unknown. It could be either glacial or interglacial. This gravel is recognized by Suggate & Moar (1996) to predate the Loopline Formation. But they do not comment on its relationship with any of the older Quaternary Formations because the Awatuna Formation is was not exposed at the road cutting which is the site of their pollen sample (J32/56154140).

At Viaduct Creek (intersection of Stafford Loop Road and Gillams Gully Road) in the lower Arahura Valley there was a pre-Loopline fluvial incision event of substantial magnitude. At that time Waimea Creek entered the Arahura Valley along an incised channel (defined by gold exploration drill holes) that takes in the deep "Wheel of Fortune" hydraulic elevating claim (an old gold mine). The old claim is situated at grid ref J32 3600N 5200E. Gold-rich bouldery lag deposits were formed during the incision event. These were subsequently buried by fluvioglacial outwash. The Wheel of Fortune claim is situated on the projected line of the Awatuna and Rutherglen marine strandlines. The base of the Awatuna Fm marine deposits would have an elevation of about 40 to 45 metres here. Whereas gold exploration drill-holes by the Rimu Gold Dredging Company show that the base of the fluvial channel is at an elevation of ~ 15 to 18 m. It is possible that the channel postdates the Rutherglen Formation. Given that the Awatuna Formations rests on fluvial gravel at its type section near Chesterfield Road it is likely that the Wheel of Fortune Channel pre-dates the Awatuna Formation.

Locality	Sample Number	Conventional ^{14}C Age (ka)	1δ error (ka)	Calibrated ^{14}C Age	1δ error (ka)
Sunday Creek	NZ574	39		41.2	
	NZ704	40.4		42.4	
	NZ742	38	2.15	41.62	2.23
	NZ703	32.9	1.05	35.95	1.3
	NZ743	>51		>49	
	NZ702	>50		>48	
Bullock Creek	NZ734	>50.9		>48.95	
	NZ735	>48.6		>46.65	
Schulz Creek	NZ2724	42.7	1.3	44.888	1.23
	?	22.28	0.13	24.97	0.35
Point Elizabeth	NZ446	37.4	2.15	38.95	1.13
Grahams Terrace	NZ329	19.65	0.35	21.47	0.45
Hatters Creek	NZ6497	>32.5		>35	
Stafford Loop Road	NZ4407	18.95	0.3	20.72	0.41
	NZ4408	17.75	0.25	19.17	0.37
Chesterfield Road	NZ5426	31	1.4	34.47	1.76
	NZ5425	34	1.9	37.25	2.02
	NZ6240	24	0.65	27.05	0.69
	NZ5633	17.5	0.3	18.89	0.37
Kamaka	?	22.3	0.35	24.99	0.48
Cape Foulwind	NZ732	42.4	3.4	44.91	2.89
	NZ733	>46.8		>44.85	
	NZ1086	34.1	1.2	37.19	1.25
	NZ1087	>49.0		>47.05	
	NZ1088	32.6	1.45	36	1.57
	NZ1089	38.6	1	41.27	0.75
	NZ1090	35	1.35	37.89	1.39
	NZ1091	37.4	2.45	41.73	2.57
	NZ1092	39.7	1.3	42.12	1.02
The Hill	NZ4409	12.2	0.2	12.416	0.332
	NZ3169	15.95	0.35	17.277	0.337
	NZ4047	17.95	0.25	19.404	0.404
	NZ4046	18.65	0.25	20.411	0.426
	NZ3168	31.6	1.7	35.29	2.01
	NZ1618	38.3	3.3	42.56	2.7
	NZ1617	30.7	1.3	33.85	1.65
Martins Quarry	NZ2708	33	1.9	36.69	2.01
	NZ2709	37.1	2.3, -1.8	41.45	2.33

Table 6.13 Radiocarbon ages, Intcal 09 calibration

6.2.17 Awatuna Formation (MIS3, Kaihinu Interglacial)

6.2.16a Introduction

The Awatuna Formation was first defined by Suggate (1965). The definition was updated by Suggate (1985) when the original formation was split into two parts, the older being the Rutherglen Formation and the younger the Awatuna Formation. The description was further refined by Suggate and Waight (1999) who correlate this formation with MIS5c. The Awatuna Formation is largely composed of strandline and near-shore marine sand, silt and gravel Suggate (1992) suggests

the Awatuna Formation has an age of c. 100 kyr by Suggate (1992). The primary change proposed here is the marine isotope stage correlation which becomes early MIS3.

In their table 6 Moar & Suggate (1996) align the pollen zones at Candle Light (described above in relation to the Rutherglen(1) Formation) with those at the type section of Awatuna Formation section. The correlation indicates the marine transgression that produced the Awatuna strandline coincides with pollen zone CL4 at Candle Light. So in the Suggate model the deposition of the Awatuna Formation is preceded by a eustatic sea level minimum during MIS5d. In this model there is no major MIS5d glacial advance in North Westland.

6.2.16b Geology and Sedimentology

The type locality (Grid ref NZMS 260 J32 4030N 5490E) is situated in a small incised gully (a tributary of Sunday Creek) just to the south of Chesterfield Road. Here beach sand and gravel of the Awatuna Formation is at an elevation of 45 to 53 metres and directly overlies fluvial gravel of uncertain affinity. The marine sediments are overlain by fluvioglacial gravel of the Loopline Formation. The stratigraphic relationships at this site are illustrated in figure 6.4 below. In reporting on gold exploration drilling Stewart (1988) has shown that the Awatuna Formation extends from the Sunday Creek area to EA Road on the north side of Kapitea Creek. Here (Grid ref J32 4220N 5600E) the upper surface of the Awatuna Formation is at an elevation of 52 m.

The stratigraphy at the type section has been described previously by Dickson (1972), Moar & Suggate (1996), and Preusser et al (2005). It is broadly as follows:

The stratigraphy at this locality is as follows:

1. Surface soil Loess Overbank silt	(RR24)	c. 1m
2. Fluvioglacial gravel of the Loopline Formation		c. 15m
3. Moderately organic silt grading upward into gravel		0.2 m
4. Wood-bearing highly-organic silt	(RR8)	0.2 m
5. Grey non-organic silt		0.05 to 0.1 m
6. Interlayered fluvial gravel and silt		c. 1m
7. Marine strandline deposits of the Awatuna Formation	(RR9)	4-5 m^{+}
Fluvial gravel of unknown affinity		Thickness unknown (base not exposed).
Local bedrock composed of Neogene siltstone (exposed in the adjacent marine cliff).		

Two sketches of site stratigraphy at the type section of the Awatuna Formation are provide in Appendix One as part of the general site description for IRSL samples RR8 and RR9, along with two photographs of the exposure at sample site RR9. The illustration above provides additional detail on the stratigraphy and the thickness of various units at the site. The broader stratigraphic relationships for the site are shown in figure 6.4.

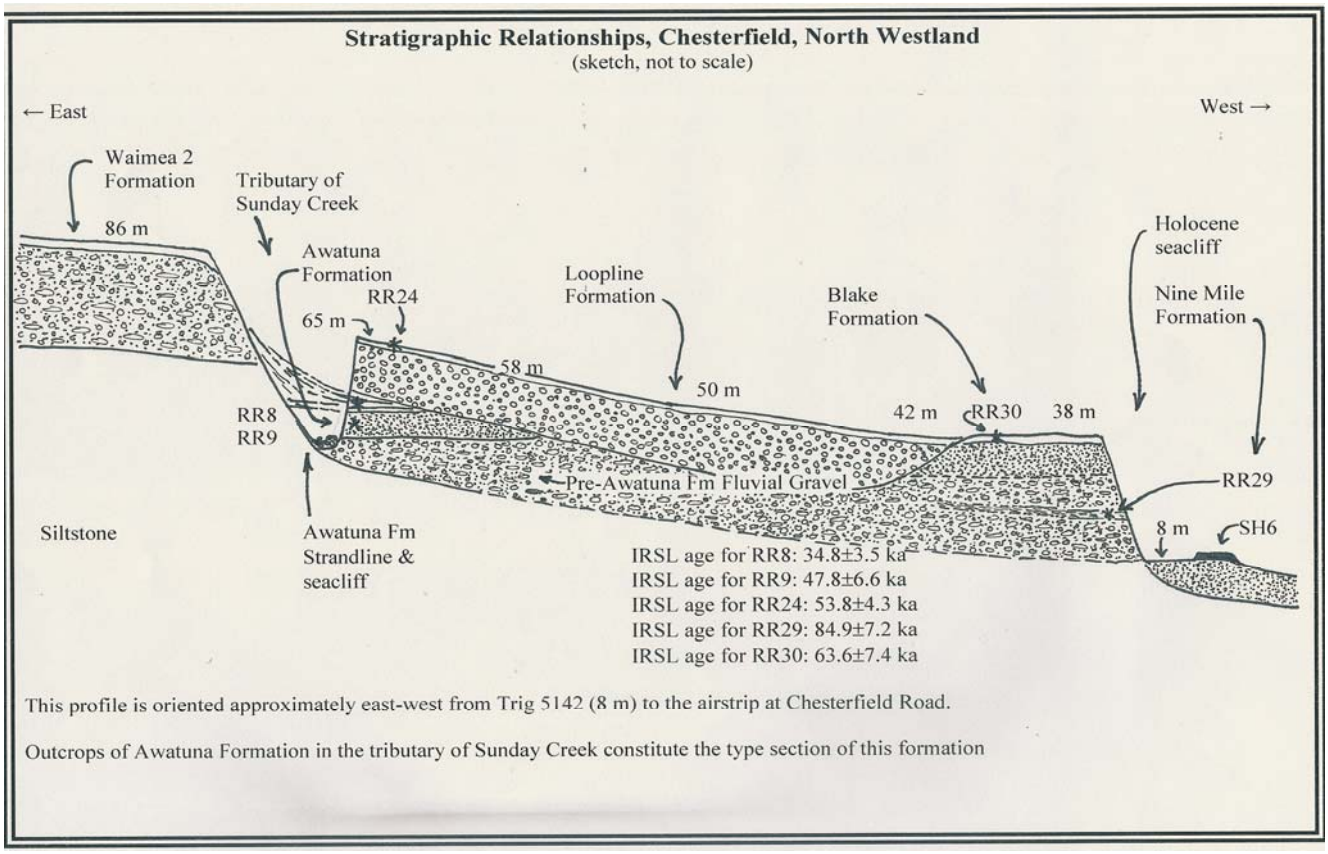

Figure 6.4 Stratigraphic Relationships at Chesterfield, North Westland

As can be seen in figure 6.4 the type section for the Awatuna Formation is situated at the foot of an old sea cliff. The cliff was being formed at the same time as the deposition of the Awatuna Formation. The nature of the coverbeds on the Awatuna Formation suggest initial and probably immediate deposition of material derived by continued erosion of the sea cliff. This was followed by burial under a large fluvioglacial outwash fan built by the activity of Kapitea Creek. The incision through the sequence by a tributary of Sunday Creek occurred some time later.

The Awatuna type section is known in the geological literature primarily as a result of sampling for pollen and ^{14}C dating by Dickson (1972). It is well known on the West Coast as the site of an alluvial "gold rush" during the 19th Century. Although not illustrated in figure 6.4 the buried strandline sediments are honeycombed by mine tunnels because the sand was very rich in gold. These tunnels were accessed from the Sunday Creek tributary, and from deep vertical shafts over a distance of several hundred metres along strike. The sand is exceedingly rich in heavy minerals. The dominant heavy minerals by mass are garnet and ilmenite. Zircon and sphene are abundant. Monazite, uranothorite, rutile and scheelite are present in trace amounts. A number of these minerals contain unusually high concentrations of radioactive elements and this is significant in terms of luminescence dating. The dating method selected needs to be suitable for the type of sediment being dated.

The Awatuna strandline was formed in a littoral environment. But the sandy gravel and pebbly sand has a thickness of 4 to 5 metres. The upper 2 to 3 m of the deposit was formed in the swash zone and sediments within this zone should have been reasonably well bleached due to repeated exposure on the beach surface. The lowermost 1 to 2 m portion of the deposit is likely to have formed below mean sea level in a subaqueous environment. So complete bleaching is not completely assured, particularly given the potential for local erosion of older material from the sea cliff and the older fluvial gravel situated beneath the Awatuna Formation.

Several luminescence samples from this site have given anomalously old IRSL ages. The mineral dated is sand-sized K-feldspar and the samples come directly from what should be considered (even in a West Coast context where heavy mineral deposits are common) to be outrageously heavy mineral rich. As discussed in Chapter 5 (section 5.6.4) this is a clear-cut red flag in terms of the IRSL dating on sand-sized K-feldspar.

6.2.17c Luminescence Dating at the Type Section (this project)

For this project a number of samples were taken from the Awatuna Formation for IRSL dating. The results are presented in table 6.14.

Table 6.14 IRSL dating, Awatuna Formation, this study

Lab Code	Field Code	$IRSL_{(blue)}$ Age (ka)	Elevation (approx)	Locality	Grid Reference (NZMS 260)
WLL219	RR8	34.8 ± 3.5	50 m	Chesterfield	J32 N 4030 E 5490
WLL220	RR9	47.8 ± 6.6; 54.0±7.3	48 m	Chesterfield	J32 N 4025 E 5480
WLL171	RR11	53.9 ± 7.6	44-45 m	North Beach	J31 N 6625 E 6320
WLL524	RR20	42.5 ± 6.8	45 m	Schulz Creek	J31 N 7425 E 6730

The type section of the Awatuna Formation, which is situated at Chesterfield, is one of the "classic" West Coast Quaternary sites. Samples RR8 and RR9 were taken from this locality during this project. RR9 from within the marine beach sand gave a multiple aliquot $IRSL_{(blue)}$ age of 47.8 ± 6.6 ka (being the preferred age), and a single aliquot $IRSL_{(blue)}$.age of 54.0 ±7.3 ka. RR8 from the middle to lower portion of the organic soil overlying the marine sand here gave an $IRSL_{(blue)}$ age of 34.8 ± 3.5 ka. These ages differ significantly from those reported by Preusser et al (2005) for the same locality. The Preusser et al ages are discussed below.

There are strandlines at ~ 50-55 m, 47-51 m (probably the same but about 2 km apart), and 35-38 m, in the North Beach (Cobden) to Point Elizabeth area. The 47 to 55 m strandline from North Beach is correlated here with the Awatuna Formation.

In terms of the dating process none of these samples performed in a manner that was in any way out of the ordinary. None showed evidence of anomalous fading so there is no need to assume the ages are underestimated.

Sample RR9 is taken from a littoral deposit that would normally be assumed to have been very well bleached prior to deposition.

Sample RR8 comes from the centre of a wood-bearing organic silt that probably accumulated relatively slowly and would normally be assumed to be well bleached. This silt overlies 1 m of fluvial gravel and silt that rests on Awatuna Formation strandline deposits. This material was deposited after the initial retreat of the Awatuna strandline. Sample RR8 should be younger than sample RR9. It places a limit on the age of the Awatuna Formation but does not date it directly. Samples RR9 and RR8 also places a limit on the age of the overlying Loopline Formation but do not date it directly.

Sample RR20 is taken from a wood-bearing organic silt that rests directly on sandy littoral gravel of the Awatuna Formation. The sample site is within 50 metres of the innermost position of the strandline. In the profile from this site the sampled horizon is overlain by about 4 metres of interbedded fluvial gravel and silt. The sampled material would normally be assumed to have accumulated relatively slowly. It does not appear to be either a fluvial or a colluvial sediment. There is no particular reason to assume that the sample suffers from incomplete bleaching so the

sample should reflect the depositional age. This sample places a limit on the age of the Awatuna Formation but does not date it directly.

Strictly on the basis of samples taken during this PhD project the preferred age for the deposition of the Awatuna Formation is given by the MAA $IRSL_{(blue)}$ age of 47.8 ± 6.6 ka for sample RR9 (though there is a second slightly older age SAR $IRSL_{(blue)}$ age of 54.0 ±7.3 ka). This is in accord with the younger ages for RR8 and RR20. It is also in accord with the age from RR11, which overlaps RR8 even though there is a possibility of incomplete bleaching at deposition.

The preferred age of ~ 48 ka for the innermost strandline of the Awatuna Formation is in accord with the preferred age of the older Rutherglen Formation (~ 65 ka, this thesis).

Given the elevation of the Awatuna Formation strandline an uplift rate of > 1.0 mm per year is implied as the sea level was probably substantially lower than the modern level at that time.

6.2.17d Radiocarbon Dating at the Type Section

Grant-Taylor & Rafter (1971) and Dickson (1972) reported conventional ^{14}C ages ranging from about 32 ka to 51^{+} ka for this site. These have recently been revised and the amended ages (RP Suggate pers com) are:

Table 6.15 Radiocarbon ages, Awatuna Formation type section.

Sample	Original age	Revised age	Material
NZ574	>39 ka	45.447 ± 9.368 ka	Carb. silt ~1ft below the Loopline gravel
NZ704	>40.4 ka		Peat, 16-19" above the marine gravel;
NZ742	38 ± 2.15 ka	37.405 ± 2.608 ka	Wood, duplicate of NZ703;
NZ703	32.9 ± 1.05 ka.	32.874 ± 1.332 ka	Peat, 6-8" above the marine gravel;
NZ743	>51 ka	>50 ka	Wood, a few cm below NZ742:
NZ702	>50 ka	>50 ka	Peat, 1 ft 4" above the beach gravel.

The Intcal-09 calibrated age for original ages of the samples listed in table 6.15 is shown in table 6.13 which is a compilation of the individual ^{14}C sample ages quoted in this thesis.

The ^{14}C ages from the Awatuna Formation type section do not rule out soil deposition between 62 ka and 35 ka. Therefore, the underlying Awatuna Formation beach deposit could have been formed during an early to middle MIS3 "interstadial" sea level maximum that was associated with or followed by interstadial climatic conditions.

The $IRSL_{(blue)}$ sample taken (RR9, this study) from the marine sand at this locality gave ages of 47.8 ± 6.6 ka and 54.0 ± 7.3 ka. At 1σ these IRSL ages are compatible with the ^{14}C ages from the overlying soil. $IRSL_{(blue)}$ sample RR8 at 34.8 ± 3.5 ka was taken from the middle of the same organic soil that was dated by the radiocarbon method. At 1σ this sample is compatible with the finite radiocarbon ages listed above.

Should several of these ^{14}C ages be discarded as being contaminated simply because they do not fit the expected 100 ka age (Suggate model) of the underlying marine gravel? Even if some of the ^{14}C ages are rejected on the basis of possible contamination, the soils concerned may still be no older than c. 50 ka at the base. So for the Awatuna Formation an early MIS3 correlation is viable regardless of whether or not there has been some degree of contamination of the ^{14}C samples.

As demonstrated in chapter 5 with respect to the composite core from Okarito by Vandergoes et al (2005) there seems to have been a strong temptation for the rejection of ^{14}C ages in spite of contrary evidence. The fragility of the contamination argument has also been demonstrated above in relation to ^{14}C dating of soil on the Waimea Formation at Blue Spur. Rejection relies to a significant extent on an assumption that the presence of *Nestegis* in a Westland pollen profile definitely implies a deposit has an interglacial character and so must date from MIS5 or MIS7. It is submitted here that this assumption has not been proven in relation to the dated sequence at Okarito, and that this probably applies elsewhere in Westland. *Nestegis* is present in the pollen spectrum in the buried soil profile at the type section of the Awatuna Formation. This was sufficient reason for Moar & Suggate (1996) and Suggate & Waight (1999) to reject the finite ages.

The second powerful reason for rejecting finite radiocarbon ages at the type section of the Awatuna Formation is that the Loopline Formation rests on the Awatuna Formation here. Previously there has been no doubt that the Loopline Formation was deposited during MIS4 despite the potential for finite ages in the underlying soil here. The age of the base of the Loopline Formation at this site is discussed in the next section of chapter 6.

The available ^{14}C ages for the soil on the Awatuna Formation do not rule out subdivision of this formation into an older higher elevation part and a younger lower elevation and possibly regressive part (Blake) both of which can be correlated with early MIS3.

6.2.17e Luminescence Dating by Preusser et al (2005) at the Awatuna Type Section

Preusser et al (2005) conducted a dating programme on two stratigraphic units at the type section of the Awatuna Formation (their Section 4.2 and figure 6). These are a buried marine sand/gravel and the overlying buried organic-rich silt. Samples were taken from sections at J32 537398 and J32 544398. They have interpreted their luminescence dating results in a manner that provides some support for the Suggate model. The luminescence ages by Preusser et al (2005) are given in table 6.16.

The Marine Sand

In the Suggate model the anticipated age for the marine sand of the Awatuna Formation is ~100 ka (MIS5c). Preusser et al (2005) correlate the marine sand/gravel with MIS5, without specifying a substage, largely on the basis of the age returned for sample SDC1 at 118 ± 28 ka and SDC2 at 81 ± 11 ka. At this site SDC1, taken from the base of the marine unit, is the odd one out. It has by far the largest 1σ error, larger than any other sample in their entire 50 sample dating programme. The MIS5 attribution is justified by Preusser et al (2005) through the claim that the upper part of the marine sand may have suffered post depositional reworking and exposure to light. This means they can reject the sample SDC3 (64 ± 5 ka) in particular. They comment that:

> "The original depositional age of the sediment is thus most likely given by the age of the basal sample (118,000 ± 28,000 yr)."

Note that the discussion of method to method regression of luminescence ages from Chapter 5 of this thesis raises questions as to the validity of several luminescence dating methods as applied by Pruesser et al (2005). There is a dramatic scatter in luminescence ages for samples from that study and that by Vandergoes et al (2005) that are older than about 60 ka. This does not inspire much confidence in the quoted age for sample SDC1.

Table 6.16 Dating of the Awatuna Formation marine sand at Chesterfield by Preusser et al (2005)

Sample	Age (ka)	1σ Error (ka)	Method	Location in profile
SDC1	118 ± 18	24%	$IRSL_{(blue)}$ MAA/FS	Base of marine sand
SDC2	81 ± 11	13.5%	$IRSL_{(blue)}$ MAA/FS	Middle of sand
SDC3	64 ± 5	7.8%	$IRSL_{(blue)}$ MAA/FS	Top of sand
SDC4	71 ± 10	14.1%	$IRSL_{(blue)}$ MAA/FG	Base of silt
	86 ± 9		$OSL_{(UV)}$	
SDC5	58 ± 8	13.8%	$IRSL_{(blue)}$ MAA/FG	Top of silt
	64 ± 10		$OSL_{(UV)}$	
SDC6	71 ± 8	11.3%	$IRSL_{(blue)}$ MAA/FS	Base of marine sand
SDC7	61 ± 8	13%	$IRSL_{(blue)}$ MAA/FG	Base of silt
SDC8	58 ± 7	12%	$IRSL_{(blue)}$ MAA/FG	Top of silt
	77 ± 11		$OSL_{(UV)}$	

FG = polymineral fine grains; FS = k-rich feldspar from fine sand

As noted above in relation to the site geology the only method used by Preusser et al (2005) in the dating of the strandline sediment is IRSL on sand-sized K-feldspar. The method is completely inappropriate for this sediment. In sediment of this nature the largest proportion of the luminescence signal from the K-feldspar grains is derived from those grains situated close to heavy mineral grains that contain a very high concentration of radioactive elements. In this case the sand contains extreme concentrations of zircon (potentially in the 0.1 to 1.0% range by mass) and uranothorite in particular and relatively low concentrations of K-feldspar. The low-K / high-U+Th nature of samples SDC1, SDC2, SDC3 and SDC6 can be seen in table A4.2e (Appendix 4). Note that the K content given for these samples in that table is not solely from feldspar and may create in incorrect impression of the feldspar content of the sand. Minerals of low specific gravity, including K-feldspar, make up a smaller than normal proportion of the sand in the strandline sediments at this locality. Due to the large number of radiometric point sources it is inevitable that the D_e measured on the K-feldspar will be too high and will cause age overestimation. Even though a considerable number of sand samples were collected (for OSL on quartz) one of the primary reasons why sand-sized K-feldspar was not dated during this PhD project is that this effect was predicted in advance by Dr Rieser.

Two of the luminescence samples taken by Preusser et al (2005) from the strandline sediment at this locality are (from their figure 6) derived from the basal 10 to 20 cm of the deposit and is situated very close to the older underlying fluvial gravel. This is an erosional contact formed in a subaqueous environment. It is reasonably likely that these samples contain poorly bleached sand derived directly by basal erosion.

As a consequence of the above the IRSL sample ages for SDC1, SDC2, SDC3, and SDC6 are not relevant to the age of the Awatuna Formation, except that:

- they collectively provide an extreme bounding upper age limit
- the youngest of the four sand samples (at 64±5 ka) almost certainly overestimates the age of the deposit.

The spread of ages across these four samples should have alerted Preusser et al (2005) that the results are problematic. It is clear that marine strandlines of this nature are not occupied

continuously for long periods of time given the changeability of eustatic sea level and the fact that the landscape is undergoing tectonic uplift. Ages of 118±28 ka and 64±5 ka are incompatible in a sediment that was potentially deposited over a few hundred to a few thousands of years.

The "reworking" hypothesis proposed by Preusser et al (2005) makes little sense. They fail to present any evidence for exposure by reworking or for the nature of reworking. Was it fluvial, aeolian or marine? Why is the sediment exclusively composed of clean sand/gravel transported by marine processes with essentially little completely foreign material introduced by aeolian of fluvial processes? Why is the sand/gravel not intercalated or intimately mixed with horizons containing cobbles and pebbles of more-or-less spherical shape rather than the discoidal pebbles/cobbles that are actually present? Why have heavy-mineral rich laminae identical with other marine strandline deposits not been destroyed? How is it that the sandy unit maintained its elevated alluvial gold content to the extent that the grades were still high enough to sustain non-mechanised underground mining? The high gold grades in the upper half of the marine unit rules out both aeolian deposition and aeolian reworking. In an examination of the site carried out in during luminescence sample collection for this project it was ascertained that there is:

i) No evidence for a significant break in deposition within the marine unit.
ii) No evidence for post depositional reworking within the marine unit.
iii) No evidence that sand within the marine unit was exposed to light prior to the deposition of the overlying silt.
iv) No evidence that the overlying organic-rich silt is substantially (i.e. 10's of thousands of years) younger than the marine sand.

In terms of the analysis carried out for this PhD project these sample ages are rejected and not considered further in the determination of the age of the Awatuna Formation. The only sample of the littoral sand from this locality that has been dated by an appropriate method is RR9 (MAA $IRSL_{(blue)}$ age = 47.8 ± 6.6 ka; SAR $IRSL_{(blue)}$ age 54.0 ± 7.3 ka).

The Organic Rich Silt

Samples from the "organic-silt" at the Awatuna Formation type section were also dated by the OSL_{UV}, TL_{blue} and TL_{UV} methods by Preusser et al (2005). This dating is discussed in Chapter 5 (section 5.6.4). The sample ages are listed in table 6.17.

Table 6.17 Luminescence ages for the organic silt at the Awatuna Formation type section. SDC3 to SDC8 are by Preusser et al (2005). RR8 & RR9 are from this (PhD) study.

Sample	$IRSL_{blue}$ age (ka)	OSL_{UV} age (ka)	TL_{blue} age (ka)	TL_{UV} age (ka)	Material
RR8	34.8 ± 3.5				Organic-rich silt
SDC8	58 ± 7	78 ± 9			Organic-rich silt
SDC7	61 ± 8	81 ± 9	77 ± 11	86 ± 17	Organic-rich silt
SDC5	58 ± 8	94 ± 14	64 ± 10	66 ± 10	Organic-rich silt
SDC4	71 ± 10	77 ± 10	86 ± 9	89 ± 14	Organic-rich silt
SDC3	64 ± 5				Marine Sand
RR9	47.8 ± 6.6; 54.0 ±7.3				Marine Sand

Preusser et al (2005) suggest with respect to SDC5 (58 ± 8 ka by $IRSL_{blue}$), SDC7 (61 ± 8 ka by $IRSL_{blue}$), and SDC8 (58 ± 7 ka by $IRSL_{blue}$) that overestimation of the each age is very unlikely so these samples should represent a maximum age for the deposition of the silt. On the basis of these

ages the simplest conclusion that is that the silt unit was deposited at c. 58 ± 8 ka. In addition SDC4 from the base of the silt has an $IRSL_{blue}$ age of 71 ± 10 ka.

The silt unit is part of the coverbed sequence for the Awatuna Formation. Samples taken from the silt provide limiting ages for the deposition of the Awatuna Formation but they do not date this formation directly. The profiles represented in figure 6 of Preusser et al (2005) are through a sequence that is exposed intermittently over a distance of 30 to 50 metres. Internally the silt unit is quite variable. At the site from which RR8 was taken, which must be very close to the Preusser et al (2005) sample profiles, the bottom 1 m of the silty section is clearly a fluvial sediment. In addition the top portion of the silty unit grades up into the overlying gravel. So at least at the site sampled during this PhD project the silt unit is dominantly of fluvial origin. RR8 was selected from that part of the silt unit that was the most highly organic and contained the greatest concentration of macroscopic wood remains. The intention was to sample from the portion of the unit that was likely to have been deposited at the slowest rate. All up as much as 75% of the unit has a largely fluvial origin. From the information supplied by Preusser et al (2005) it is not possible to tell the precise nature of samples SDC4, SDC5, SDC7, and SDC8. If the profiles displayed by Preusser et al (2005) have a similar sedimentology to that sampled for this thesis then it is possible that each of these four samples has a fluvial origin.

Given that it appears to be much lower in the unit than RR8, SDC4 is particularly suspect because there was 1 m of fluvial material below RR8. The $OSL_{(UV)}$ ages on SDC4, 5, 7 & 8 is indicative of the problem. The OSL signal should bleach much more readily than the IRSL signal (minutes compared to hours). Yet despite the various issues apparent in the OSL performance of quartz in Westland, these quartz samples contain a higher D_e than the feldspar in the polymineral finegrained component. This is a very clear red flag indicating that extreme caution should be used in the interpretation of the ages. In terms of this PhD thesis these samples the IRSL ages provide the only useful age information. Further the IRSL ages place a bounding limit on the possible age of the silt at this site. The mean of the sample ages is not firm indication of the depositional age. SDC4 is particularly suspect because it is probably fluvial in nature and so should not be used in forming a mean age. The other three samples average at ~ 58.5±8 ka which is the upper age limit accepted here. This limit is older than the only acceptable age on the underlying littoral sand (RR9). It is older than the only other IRSL age on the silt (RR8). As noted above and in table 5.4 both RR8 and RR9 have been deposited in environments that should ensure thorough bleaching. Incomplete bleaching would cause age overestimation for the deposit.

A hiatus is implied by Preusser et al (2005) after the deposition of the Awatuna Formation via the reworking hypothesis. But, according to Suggate & Waight (1999) there is no evidence of a break in deposition between the marine sand and the organic silt. No evidence was observed for a significant depositional break at the sand/soil transition during sampling for this (PhD) project. So it is assumed that silt deposition commenced soon after deposition of the marine sand, probably as soon as the sea retreated off the Awatuna strandline. The dated section is in close proximity to (i.e. within a few 10's of metres) a substantial marine cliff, which is clearly a potential source of fluvial sediment. So there is no particular reason to assume the silt unit was deposited particularly slowly. In other words the physical location provides an opportunity the local deposition of small alluvial fans and for the deposition of thick silt. There is no reason to expect this would require more than a few thousands of years. So the silt unit may be no more than a few thousands of years younger than the underlying marine sand. The silt ages (luminescence and ^{14}C) are consistent with this suggestion.

The useful information that can be extracted from the three dating programmes carried out at this locality is in accord with an early to early-middle MIS3 age for the deposition of the Awatuna Formation. This is the simplest interpretation of the age and sample data and is in accord with the

best data available for the age of the older Rutherglen Formation. The pollen spectra for the silt unit is not indicative of cold climate and that is about as far as the interpretation of the pollen should be taken.

The Overlying Fluvial Gravel

In relation to the fluvial gravel of the Loopline Formation Preusser et al (2005) state in the abstract to their paper:

> "Luminescence ages determined from two key sites of the Loopline Formation confirm the previous correlation of this unit with MIS4. This indicates the Late Pleistocene glaciers reached their maximum extent in North Westland during the early part of the Otira Glaciation."

And in the main text:

> "The majority of luminescence ages from the Sunday Creek site support the correlation the upper gravel unit with MIS4, as postulated by Suggate (1965, 1990)."

No other formation is mentioned by name in the abstract to the Preusser et al (2005) paper. The conclusion that the Loopline Formation dates from MIS4 is one of their major findings. They do not date the Loopline Formation directly at the type section of the Awatuna Formation (one of their two key sites). Their suggestion that this formation was deposited during MIS4 is speculative. On close examination the support for their conclusion from their own dating on the underlying silt is weak at best. Preusser et al (2005) suggest overestimation of the ages for samples SDC5, 7 & 8 (58 ± 8 ka, 61 ± 8 ka and 58 ± 7 ka) is unlikely on the basis of zeroing of the signals prior to burial. These dated samples are from deposits stratigraphically below the gravel. An MIS4 correlation is not supported by several finite ^{14}C ages from this silt. Nor is that correlation supported by 14C ages that are beyond the detection limit. Nor is an MIS4 correlation for the Loopline Formation supported by luminescence dating undertaken for this thesis project as RR8 from the silt at this locality gave an $IRSL_{blue}$ age of 34.8 ± 3.5 ka, and RR9 from the underlying sand gave $IRSL_{blue}$ ages of 47.8 ± 6.6 ka (multiple aliquot) and 54.0 ± 7.3 ka (single aliquot). If we ignore prior preconceptions about the age of the Loopline Formation then most obvious correlation is with MIS3 because on balance the gravel would be presumed to be younger than the various acceptable or semi-acceptable ages at the Awatuna Formation type section.

Relationship with the (older) Waimea Formation

The marine strandline at the Awatuna Formation type section is stratigraphically younger than the Waimea Formation. IRSL-SAR sample UCS1 by Preusser et al (2005) was dated at 81 ± 7 ka and taken from a quarry in fluvial gravel (J32 568397) of the Waimea Formation at Upper Chesterfield Road. It is described in their *section 4.6*. The sampled material is a sand horizon within gravel at a small relatively shallow quarry in the older part of the Waimea Formation.

Preusser et al (2005) correlate sample UCS1 with MIS5b or MIS5a but suggest that the gravel here was reworked following initial deposition during the Waimea(1) event, though the sample site is still part of the Waimea(1) terrace. Reworking is claimed by Preusser et al (2005) to have occurred during erosion that led to creation of the slightly lower and immediately adjacent Waimea(2) terrace. Although the dated material is clearly from the older terrace they have decided that it does not represent the original depositional age of that fluvial gravel. The implication is that the older Waimean terrace is older than the supposedly reworked sample and so older than 81 ± 7 ka. However, no evidence is supplied in support of this interpretation. On examination of the site no

evidence was observed in support of the re-working hypothesis. So if this is correct the sample directly dates the original deposition of the gravel of the higher Waimean terrace and the age for the culmination of or at least the highest level of aggradation during the Waimean Glaciation.

Regardless of whether the age for UCS1 represents the culmination of fluvioglacial aggradation or subsequent degradation it is clear that both Waimean surfaces were truncated during the creation of the Awatuna strandline and the adjacent marine cliff. So if the age (81 ± 7 ka) is correct then it provides a clear-cut maximum age for the Awatuna Formation which could not be older than MIS5a. Further it should be noted that during this PhD project the base of the 4 m deep soil on the Waimea(1) outwash terrace was sampled (RR25) and dated using the $IRSL_{(blue)}$ method. The sample locality (Grid ref J32 N 3890 E 5555) is adjacent to Sunday Creek about 1.5 km southeast of the Awatuna Formation type section. The sample age is 75.9 ± 7.6 ka which also places an MIS5a limit on the age of the Awatuna Formation. Deposition of the Awatuna Formation required the prior removal of a minimum of 40 metres thickness of Waimean outwash and underlying Pliocene Eight Mile Formation siltstone. The marine cliff formed at Chesterfield at this time was similar in scale and nature to the Holocene marine cliff situated about 2 km to the northwest.

Both of these samples (UCS1 and RR25) are from material that either is, or could be fluvial. As discussed above in relation to the age of the Wamea Formation both samples may overestimate the depositional age of the Waimea Formation.

6.2.17f Pollen in Soil on the Awatuna Formation at the Type Section

A detailed study of the palynology of the soil was carried out by Dickson (1972). In the basal half of the soil the pollen flora is dominated by *Nothofagus fusca* (red beech) but includes significant *Dacrydium cupressinum* (rimu). *Nothofagus fusca* is not by itself a strong indicator of climate given that it has a wide tolerance from fully interglacial to near stadial conditions at a number of sites in North Westland. *Nestegis* pollen is present throughout the sampled profile except at the very top (summarised in fig 4b, Moar & Suggate 1996). The flora has previously been assumed to be indicative of relative warmth, probably requiring at least interstadial climatic conditions. Change in the species composition of pollen occurs toward top of the soil sequence, rimu pollen declining in abundance first followed by a simultaneous decline of *Nothofagus fusca* and *Nestegis* and expansion of *Poaceae* towards the top. In the interpretation of Moar & Suggate (1996) this implies the onset of stadial conditions near the top. Silt deposition was then interrupted by deposition of fluvial gravel. This gravel has previously been assumed to be a fluvioglacial deposit but apart from pollen in the underlying silt there is little evidence that the basal part of the gravel has a glacial affinity. The gravel has been assigned by Suggate & Waight (1999) to the Loopline Formation.

6.2.17g New Locality

At Stanton Crescent, Karoro (Greymouth) strandline deposits are found underlying a terrace with a surface elevation of about 50 to 55 metres. This locality is assign here to the Awatuna Formation. Remnants may also be present at several other points above SH7 at Karoro. The Stanton Crescent deposit is mapped by Suggate & Waight (1999) as a landslide, making the sand slumped Rutherglen Formation. The Rutherglen Formation is present further up slope at Stanton Crescent with the Karoro Formation further inland so mass movement by slumping is a possibility. The terrace surface does not appear to be deformed though. Where it can be seen the sand is flat lying and undisturbed. It is at the elevation that would be expected for the Awatuna Formation given its position relative to the Karoro Formation at Awatuna and Blue Spur. The occurrence of the Awatuna Formation at Stanton Crescent provides a linkage between the type section near Chesterfield and Point Elizabeth to the north.

6.2.17h Dating at Point Elizabeth

Sample RR11 is derived from the Awatuna Formation at a site between North Beach (Cobden) and Point Elizabeth. The sample elevation is 51-52 m by GPS. The $IRSL_{(blue)}$ age is 53.9 ± 7.6 ka. This age overlaps that of RR20 (42.5 ± 6.8 ka) from a similar elevation at Schulz Creek (see below) to the north of Rapahoe and is compatible with ^{14}C ages from Schulz Creek.

RR11 was obtained from the base of the cover beds on the Awatuna Formation exposed in a road cutting at the innermost margin of this terrace and comes from a clayey silt that contains angular limestone rubble. This unit may have been deposited by colluvial processes. The silt rests directly on littoral gravel. The sample site is very close (within 20 metres) to the landward limit of the strandline sediment and is backed by a low marine cliff. Consequently it is possible that, owing to a relatively short transport distance and potentially rapid depositional mechanisms, RR11 may have been incompletely bleached at deposition implying the potential for age overestimation, the extent of which is uncertain.

6.2.17i Dating at Schulz Creek

The Schulz Creek locality is situated at SH6, near 12 Mile Bluff, north of Rapahoe. The stratigraphy and climate history for the raised marine platform at Schulz Creek is outlined by Burrows (1997) and Moar et al (2008). Here a peaty soil situated within a few 10's of metres of the ancient marine cliff rests on beach gravel about 45 to 48 metres above sea level. Based on plant macro-remains and comparison with other sites in north Westland Moar et al (2008) assign the strandline deposits to MIS5e. The plant remains, including *Dacrydium cupressinum* (rimu) and *Nestegis* pollen led them to correlate the peaty soil with MIS5e and 5d.

Sample RR20 (Grid ref NZMS260 J32 N 7425 E 6730), was collected during this project from the base of the soil just above the beach deposits at a road cutting (SH6) adjacent to Schulz Creek. It produced an $IRSL_{(blue)}$ age of 42.5 ± 6.8 ka. This overlaps the ^{14}C ages nicely and provides support for the view that this terrace could be correlated with an early MIS3 sea level maximum. The sample age is not accepted uncritically here. An effort was made to select the sample from that part of the base of the coverbeds has the highest organic content including macroscopic wood remains. This should ensure relatively slow deposition, the greatest aeolian input and the least possible fluvial input. Nevertheless the base of the coverbed sequence is overlain by around 4 metres of interbedded silt, silty sand and fine silty gravel that has a fluvial origin. So sample RR20 is assessed here as providing a maximum age as there is a modest chance that the sediment is affected by partial bleaching.

Moar et al (2008) report that a conventional ^{14}C age of $> 51^{+}$ ka or 48.13 ± 7.05 ka (on reanalysis) has been obtained for NZ736 collected by Young (1966). The sample comes from profile B2 on the this terrace. They also report that three ages of 50^{+} ka have been obtained from the soil two from samples collected during 1955 and 2005.

Road cuttings on the landward side of the highway expose up to 12 metres of interbedded alluvial slope deposits. This includes gravel derived from the nearby "bedrock" sandstone/conglomerate bluffs of the old sea-cliff. The slope deposits are situated at the base of the steep sea cliff, fanning out and thinning to the west across the relatively flat raised marine strandline deposits. The alluvial deposits contain 7 organic silt layers labeled A to G by Moar et al (2008). The basal layer (G) of the slope deposits produced a non-calibrated ^{14}C age of 42.7 ± 1.3 ka (NZA2724). Upwards in the sequence layer E produced a non-calibrated ^{14}C age of 22.28 ka ± 0.15 ka. Moar et al (2008) also discuss a ^{14}C age of 48.13 ± 7.05 ka. Moar et al (2008) appear to have had no problem accepting

these ages. So these steeply dipping fan-like deposits seem to span MIS3 and MIS2. Plant macrofossils in the silt layers include the leaves of *Nothofagus menziesii* at layer G. Moar et al (2008) recognise that there is an implication the site contained closed canopy forest during MIS3 and compare the result with that of Burge & Shulmeister (2007a, b) from a site near to Westport.

If up to 12 metres of MIS3 and MIS2 alluvium collected against the old sea cliff from around 42 ka onward, where are the deposits that should have collected during MIS5c to MIS4? The simplest answer is that such deposits do not exist, the reason being that the strandline dates from early MIS3 as indicated by the $IRSL_{(blue)}$ age for RR20. In this case (as at the type section of the Awatuna Formation) much of the discussion of climate by Moar et al (2008) based on the pollen diagrams in soil immediately overlying the marine deposit needs to be reassessed, as the soil would no longer correlate with MIS5.

The primary reason for an MIS5e correlation for the marine sediments on this terrace is the presence of *Nestegis* pollen near the base of the soil. As discussed in detail in chapter 5 in relation to the pollen record at Okarito and in chapter 6 in relation to both the type section of the Awatuna Formation and the soil sequence at Candle Light (on the Rutherglen Formation) there is good evidence for the presence of the genus during the early portion of MIS3 in North Westland. The luminescence and radiocarbon dating at Schulz Creek can be interpreted as providing strong evidence in favour of this position. This conclusion supports the stance taken here with regard to the presence of *Nestegis* at Okarito during MIS3 (see discussion in chapter 5).

6.2.18j Dating at Bullock Creek

The dating from Chesterfield, Point Elizabeth and Schulz Creek compares favourably with ages from a gravel quarry adjacent to SH6 about 200 yards north of Bullock Creek at Punakaiki. The numerical ages from this site are NZ 734 @ 45.899 ± 5.404 ^{14}C ka and NZ 735 @ 49.222 ± 11.108 ^{14}C ka. These are revised ages supplied by Dr RP Suggate. The original ages listed in Grant-Taylor & Rafter (1971) are: NZ 734 >50.9 ka from wood in the gravel pit; and NZ 735 >48.6 ka from peat on beach gravel.

In figure 4a of Moar & Suggate (1996) a pollen diagram is presented for the Bullock Creek quarry. This shows *Nestegis* to be a ubiquitous component of the flora over the basal 3 m. *Nestegis* persists at the site even when *Dacrydium cupressinum* declines to virtual absence and while *Nothofagus fusca* and *Nothofagus menziesii* dominate the pollen spectrum. The presence of *Nestegis* here enabled Moar & Suggate to correlate the basal pollen zone with MIS5c. Presumably this is the favoured age for the underlying marine sand as well, making the raised marine deposit at Bullock Creek equivalent to the Awatuna Formation.

6.2.17k Discussion and Correlation

Collectively the luminescence ages from the Awatuna Formation have implications for the interpretation of past ^{14}C dating. The depositional age at the base of the soil on the Awatuna Formation seems to be either at or beyond the useful limit of ^{14}C dating in this region. So there have always been several ways in which the sample results could be interpreted. Taken at face value the luminescence ages from this project indicate that the Awatuna Formation has a depositional age that is almost certainly less than 60 ka. The simplest conclusion is correlation with an early MIS3 sea level maximum. As noted above in relation to dating at the type section of the Awatuna Formation the best available numerical age for the Awatuna Formation is that for RR9 (multiple aliquot $IRSL_{(blue)}$ age of 47.8 ± 6.6 ka (being the preferred age), and a single aliquot $IRSL_{(blue)}$.age of 54.0 ±7.3 ka). There may be deposits from more than one MIS3 sea level maximum recorded in North Westland and there is some physical evidence for this at Point

Elizabeth. But it does not seem to make much sense worrying greatly about differences in elevation of just a few metres between localities when these can easily be accommodated by small coast parallel variations in the uplift rate. The MIS3 global sea level history is problematical and controversial and there are few local (NZ) records of high quality for this period.

The Awatuna Formation is probably the result of a marine transgression that peaked no earlier than 60 ka. The correlation adopted here is with Antarctic warm event A4 at about 62 to 58.5 ka (early MIS3).

In the Suggate model the Awatuna Formation has been assigned to MIS5c (c.100 ka), a correlation that is unlikely in light of the IRSL dating carried out during this PhD project. The preferred IRSL based correlations for the Karoro (MIS5a) and Rutherglen (MIS4) Formations support a younger age assignment for the Awatuna Formation. There are no good-quality numerical ages taken from this formation that support its assignment to MIS5c or to MIS5a. The ^{14}C ages from the base of the soil at Schulz Creek, Bullock Creek and at the type section suggest the underlying beach deposits could have formed as late as c. 50 ka. Suggate and Moar (1996) and Dickson (1972) conclude that the whole of the overlying soil at the type section is likely to be > 50 ka, having rejected the finite ages that were produced from this soil. But Moar et al (2008) correlate the basal soil at Schulz Creek with MIS5e. So effectively in the "Suggate model" the marine sand must be Rutherglen Formation rather than Awatuna Formation. This does not fit comfortably with the coast parallel correlation of Suggate (1992) or the proposed uplift rate therein. The primary reasons for making an MIS5e correlation at this locality are the presence of macroscopic remains of *Dacrydium cupressinum* (Rimu) and Northern Rata in the basal soil, and the presence of *Nestegis* pollen near the base of the soil. They make an *a priori* assumption that MIS5e was the last episode during which *Nestegis* was widespread in North Westland. Rimu has been noted in pollen studies from the LGM in South Westland. This demonstrates clearly that this species is tolerant of relatively cool conditions. So by itself the presence of Rimu is insufficient to diagnose interglacial conditions at Schulz Creek, and might not even properly diagnose interstadial conditions. Therefore an MIS5e correlation for the base of the soil at Schulz Creek is rather tenuous.

It is argued in this thesis that there could be up to five MIS4 to MIS3 raised marine terraces in North Westland (Rutherglen(1); Rutherglen(2); Awatuna; Blake and Craig) and that the associated strandlines are likely to coincide with eustatic sea level maxima. If this is the case then each depositional event is likely to be relatively brief, perhaps no longer than a few thousands of years. In this scenario the first organic silt/soil developed on the upper surface of the marine deposit probably correlates with the next younger interstadial.

In chapter 5 a detailed examination is conducted on the dating and correlation of various parts of the Okarito composite core (of Vandergoes et al 2005) and its associated pollen spectra. One question that arises from that discussion is whether or not it is actually possible to distinguish a warm interstadial pollen sample from an interglacial pollen sample. In the past one of the unspoken criteria for ruling out an MIS3 correlation for a *Dacrydium cupressinum* or *Nestegis* pollen bearing soil has been the assumption that the local climate during MIS3 was not warm enough to sustain widespread mature forest dominated by an interglacial-like flora. The justification for such a claim has all but disappeared with the publication by Barrows et al (2007) and Pelejero (2005) of sea surface temperature records for marine core SO136-GC3 and the completion of SST studies at marine core MD06-2986 by Kolodziej et al (2010). The sea surface temperature was relatively warm here during the early portion of MIS3.

6.2.18 Waites Formation (Early MIS3?)

6.2.18a Introduction

The Waites(1) Formation is defined by Nathan (1975, 1976, 1978a) and McPherson (1967, 1978). The primary change proposed here is to the marine isotope stage correlation of Suggate (1992) which changes from MIS5e to early MIS3.

The Waites Formation is the lowest pre-Holocene raised marine platform in the Westport to Charleston area. This formation is likely to be the equivalent of the Awatuna Formation. It has been dated by the radiocarbon method. Radiocarbon ages are available from three sites in the Cape Foulwind-Addisons Flat area.

6.2.18b Radiocarbon Dating in the Cape Foulwind Area

The ^{14}C ages listed below are derived from Grant-Taylor and Rafter (1971). They have more recently been revised at GNS (pers. com. RP Suggate). The original conventional and revised ages, as supplied by Dr Suggate, are given in table 6.18. The precise nature of the revision is unclear but the changes are relatively small and it is assumed here that the revised ages are still conventional ages. These ages are also compiled in table 6.13 where the original conventional ages are accompanied by equivalent calibrated ages calculated using the Incal-09 programme. The samples come from an exposure (grid ref K29 3870N 8350E) in the marine cliff at Cape Foulwind. The site is reached via a track from the car park / lookout to the modern beach. At the car park the surface is Waites Formation. The dated material comes from a thin peat horizon (within the Waites Formation) situated just above a raised marine platform. There is a thin (< 30 cm) basal marine conglomerate overlying the local bedrock (Tertiary siltstone). The conglomerate is overlain by a thin (< 30 cm) band of peat which is overlain by a thick sequence of beach sand and dune sand.

The pollen spectrum (fig 5 Moar & Suggate, 1979) from a 20 cm thick profile through the peat at this site is not conspicuously *Dacrydium cupressinum* bearing, though this species, along with *Metrociderous* is present at the top of the profile. *Nestegis* and *Nothofagus Menziesii* are absent. *Nothofagus fusca* is a minor component. Tree/shrub pollen totals less than 20% at the base and increases steadily to 95% of the total at the top of the profile. Leptospermum (Kanuka) dominates towards the top. *Halocarpus bidwillii* is prominent in the middle of the profile. The mix of species appears to indicate cool climate at the base, with slight warming upwards, but not to a level that would normally be considered interglacial. Moar & Suggate (1979) proposed that the stratigraphy of the site represents marine regression rather than transgression.

The ages listed above are significant in the context of this PhD project because they represent another example of total rejection of data in the Suggate model. In this case Moar & Suggate (1979) suggest that the samples are contaminated by younger carbon and assign the marine deposits to MIS5. Subsequently Suggate (1992) assigned the Waites Formation to MIS5e without presenting any justification for this classification. There could be contamination of these samples by young carbon. However, repeated dating of material from NZ1089 after treatment to clean the sample gives results that still overlap at 1 SD.

Table 6.18 Radiocarbon ages from the Waites Formation at Cape Foulwind

NZ ^{14}C Sample No	Original ^{14}C Age	±	Revised ^{14}C Age	±	Description
732	42400	3400	42724	4503	Wood from 10 inch peat and on thin sandy marine gravel
733	>46800		>50000		Peat
1086	34100	1200	34064	1458	Peat

1087	>49400		57283	27203	Peat 6 inches above gravel
1088	32600	1450	32637	1749	Wood 6 inches above gravel
1089	38600	1000	38587	3693	Wood 6 inches above gravel
1090	35000	1350	35073	1662	Wood pretreated from 1089
1091	37400	2450	37405	3159	Wood as per 1090
1092	39700	1300	39859	1624	Wood as per 1090

The assumption that the marine episode necessarily dates from MIS5 has not been proven. The ^{14}C ages fit just as well with a marine transgression during latest MIS4 to early MIS3. In this alternative hypothesis an early MIS3 sea level maxima is the cause of rapid formation of a marine wave cut platform on soft Neogene siltstone / fine sandstone bedrock. Marine planation could be followed by early MIS3 peat accumulation at Cape Foulwind marine cliff site thence by a second marine transgression that over-rides the site without destroying the peat. Deposition of marine sand is then followed and/or accompanied by mid MIS3 dune sand deposition and marine regression. As discussed below there are at least five fossil strandlines on this terrace in the area between Cape Foulwind and "Wilson's Lead" (line of old gold workings), a marine strandline) that crosses Wilson's Lead Road near the eastern margin of the Waites Formation.

Moar and Suggate (1979) and Suggate (1992) had (the usual) reason to make an assumption that the Waites terrace dates from MIS5. A "sand quarry" just north of the Junction between Wilson's Lead Road and the Cement Works pipeline Track near Cape Foulwind (Grid ref approx NZMS 260 K29 3460N 8600 E) was sampled for pollen. The sample point in "lagoonal beds" is thought to be stratigraphically above the ^{14}C dated "beach track" sample site described above. Two samples from the sand quarry site have pollen spectra that contain *Dacrydium cupressinum* and the genus *Nestegis*. So the familiar argument implying an interglacial climate applies for this site and for the Waites Formation in general. There are no ^{14}C ages available for this site. Another similar site referred to by Moar & Suggate (1979) as being located "c. 1 km along the track to the cement works" (i.e. to the north of the sand quarry) was also sampled and was also *Nestegis* bearing as is the Cape Foulwind cliff site and a profile at Martins Quarry (discussed below). It is assumed that the samples adjacent to the pipeline track are situated stratigraphically below the ^{14}C dated profile from "The Hill" which is described below.

In Burge (2007) a suggestion is made that the Waites Formation dates from MIS5a. This appears to be based on consideration of the correlation presented in Nathan et al (2002). Close examination shows that Nathan et al do not assign the Waites Formation to any particular substage within MIS5 and it should be noted that RP Suggate was one of the co-authors (the lowest terrace is simply separated into 5a being the marine component and 5b being the fluvial component). This is significant in terms of the climatic correlation made by Burge. The two main sites sampled for fossil beetle remains may both be situated on an MIS4/3 transition or early MIS3 wave-cut platform. There is no numerical dating in the Westport area confirming the Nathan et al (2002) or Suggate (1992) isotope stage correlation for the Waites Formation. Nor is there any numerical dating directly on older Quaternary deposits in the Westport area except a for group of speleothems from Metro Cave. So the existing isotope stage correlation for the sequence here is rather tenuous.

The elevations of the lowest marine strandlines in the vicinity of "The Hill", have been revealed by heavy mineral (ilmenite) exploration and mapping conducted by Austpac Titanium and Buller Minerals Limited. This unpublished work summarises the results of dozens of exploratory drillholes onto maps and cross-sections and demonstrates the presence of heavy mineral rich strandlines beneath the more surficial and low-grade aeolian dunes. The strandline elevations are as follows:

Strandline under the "Bradshaws (West)" dune system: 16-17 m Waites Formation

Strandline under the "Pipeline" dune system: Formation	16-17 m	Waites
Strandline under the "Larsons" dune system: Formation	20 m	Waites
Strandline at "Wilsons Lead" (old gold workings): Formation	24 m	Waites
Strandline under the "Lower Magazine" dune system: Formation	27 m	Waites
Strandline under the "Upper Magazine" dune system	30-35 m	Virgin Flat Fm

The naming of the dune systems is informal. It comes from maps and cross sections by Austpac Titanium. These elevations are particularly interesting given that Suggate (1992) illustrates the lowest strandline at c. 30-35 m, which he correlates with MIS5e (despite an error in his figure 3).

Strandline	Formation	Approx. elevation of strand line (m)	Suggate (1992) MIS Correlation
Nine Mile	Nine Mile	3	1
Bradshaw's (West)	Waites	16-17	5
Pipeline	Waites	16-17	5
Larson's	Waites	20	5
Wilsons Lead	Waites	24	5
Lower Magazine	Waites	27	5
Upper Magazine	Virgin Flat	~30 –35	5
Gallagher's Lead	Virgin Flat	40-43	5/7
O'Toole's Lead	Addison	56 (lower) 60 (upper)	7
Addisons Lead	Addison	67	9
Shamrock Lead	Addison	85-90?	-
Browns Terrace	Addison?	95	-
Caroline Terrace	Caledonian	133-135	15/13
Whisky Candlelight	Whisky Candlelight	Higher than Caledonian	

Table 6.19: Suggate (1992) correlation for raised marine strandlines near Westport (altitude estimates from this study).

6.2.18c Radiocarbon Dating at "The Hill", Wilson's Lead Road

The group of ages listed here were reported by Moar and Suggate (1979). The site is on Wilson's Lead road between Addisons Flat and Cape Foulwind (41°47'S, 171°30'E NZMS E2385410, 5935067) and is illustrated in figures 6.2 and 6.3 of Burge (2007).

Table 6.20 Radiocarbon dating at "The Hill". Wilson's Lead Road

Sample (cm)	Depth	Location & Description	^{14}C Age	Calibrated Age (Burge)	This study
NZ4409	35-42	Organic/sand, profile 74/4	12,200 ± 200		
NZ3169	72-82	Organic/sand, profile 74/4	15,950 ± 350		
NZ4047	137-147	Organic/sand, profile 74/4	17,950 ± 250	21,300 ± 200	21,500 ± 250
NZ4046	157-167	Organic/sand, profile 74/4	18,650 ± 250	22,000 ± 750	22,600 ± 250
Kawakawa Tephra		Organic silt, profile 74/4	22,590 ± 230	27,097 ± 957	27,500±1000
NZ 3168	212-222	Organic clay, profile 74/4	31,600 ± 1700	$37{,}040\pm^{1960/}_{1720}$	$35{,}400\pm^{2000/}_{1800}$
NZ1618	Position not well recorded		38,300 ± 3300 (basal layers, same site)		40,600 ± 3300
NZ1617	Position not well recorded		30,700 ± 1300 (basal layers, same site)		32,800 ± 1300

These conventional ^{14}C sample ages listed in table 6.20 are also compiled in table 6.13 where the original ages are accompanied by equivalent calibrated ages calculated using the Incal-09 programme. The samples came from deposits exposed in a road cutting. Samples NZ4047, NZ4046 and NZ3168 are from an organic sand and clay unit situated in profile 74/4 on the NE side of the Wilson's Lead Road. This unit is situated beneath re-deposited dune sand and rests on older dune sand (likely >36 ka given the above ages from the organic clay). This site has been discussed in detail by Burge (2007) and Burge & Shulmeister (2007a, b). Age calibration by Burge (2007) was carried out per Weninger et al (2006).

In terms of the issues that are argued repeatedly in this thesis "The Hill" is of interest because it is one of a small number of pre MIS2 sites in this region where the radiocarbon ages have not previously been dismissed out of hand. This is possibly because the results are seen to represent the age of the cover beds rather than the timing of formation of the terrace. The presence of the Kawakawa Tephra at this locality was noted by Burge (2007) and does not appear to have been known to Moar & Suggate (1979). There is a clear contrast with the handling of the older ages from the base of the Waites Formation at Cape Foulwind and Martins Quarry. The pollen diagram from "The Hill" bears a striking resemblance to another recorded by Moar & Suggate (1979) at "Junction Crossing" (approx grid ref K29 3430 N 8600E), which is a site on the Waites Formation near Wilsons Lead Road close to its junction with the "Cement Works (pipeline) Track". There are no ^{14}C ages from the Junction Crossing site.

It appears that Moar & Suggate (1979) have assumed there has been extensive modification of the geomorphology of most of the Waites Formation in the Cape-Foulwind – Cement Works – Wilson's Lead Road area. This has not been demonstrated by them. The dunes situated on the Waites terrace in the vicinity of "The Hill" mantle marine sand deposits (not exposed) that were drilled intensively during ilmenite mineral exploration by Buller Minerals/Austpac Titanium. This part of the Waites Formation shore platform contains several marine strandlines that have not been completely obscured by subsequent remobilization of dune sand and can be recognised in the geomorphology of the Waites terrace. So at "The Hill" the lower part of the dune sand is likely to have been deposited soon after the underlying marine sand. This conclusion is in harmony with an early MIS3 age for the cutting of the shore platform and a literal interpretation of the ^{14}C ages from Cape Foulwind.

Further, there are a striking series of paired beach/dune systems preserved in the geomorphology of the (older) Virgin Flat Formation at Addisons Flat about 5 km SE of "The Hill" adjacent to Wilson's Lead Road. Several of these SSW-NNE trending features have shore parallel lengths of up to 4 km. Remobilisation of dune sand in the Wilson Lead Road-Addisons Flat area is not a ubiquitous feature of the landscape.

6.2.18d Radiocarbon Dating and Pollen from Martins Quarry

Martins Quarry is situated at grid ref NZMS 260 K30 7290N 9955E. A familiar issue arises in connection with ^{14}C dating at this locality. The quarry is in a fluvial terrace deposited by the Buller River and is mapped as Waites Formation by Moar & Suggate (1979) and Nathan (1976). The surface at the site is at an elevation of c. 24-28 m above sea level. Silt and peat with a thickness of 2.2 metres and rests on about 0.8 m of blue-grey sand that sits on Buller River gravel. The pollen spectra from this profile bears a striking resemblance to the lower 2/3 of that from the Okarito composite core of Vandergoes et al (2005). The similarity includes the curves for *Nestegis* and *Dacrydium cupressinum.* Both are particularly abundant in the lower part but decline sharply mid-way up the profile.

The elevation of the Waites surface at Martins Quarry (24-28 m) is slightly higher than the elevation of marine sand on the widespread Waites marine terrace situated between Cape Foulwind and Addisons Flat. On the basis of geomorphology and mapping by Nathan (1976) there appears to be physical connection between the fluvial terrace at Martins Quarry and marine member sand of the Waites Formation, so the ages of the marine and fluvial terraces are likely to be similar.

Moar and Suggate (1996) assign the base of the cover beds to MIS5e (their table 6). This is the portion of the profile in which from 25% to 50% of the pollen is from *Dacrydium cupressinum.* The top of the profile (at a depth of 50 cm) is assigned to MIS5c, probably on the basis that very small amounts of *Nestegis* pollen are present to a depth of 60 cm. It is particularly notable that the profile contained radiocarbon samples at depths of 167-177 cm (peat- NZ2708) and 220 cm (*Dacrydium cupressinum* wood- NZ2709). The upper sample returned a non-calibrated age of 33.0 ± 1.9 ka. The lower sample returned a non-calibrated 37.1 $^{+2.3}_{-1.8}$ ka (age as originally quoted). These ages are listed in table 6.13. The following quote relating to these two radiocarbon ages is by Moar & Suggate (1979):

> "Radiocarbon ages suggest Martins Quarry is an Otiran site" ---- "on stratigraphic grounds this is improbable. It is therefore considered that these samples too have been contaminated by younger carbon and a late Oturi Interglacial age is the most probable."

It appears that the only evidence required for the dismissal of radiocarbon ages is an assumption that the site is too old to produce finite ages, based on similar dismissals of similar radiocarbon ages at other sites within the region. Even if the conclusions reached are correct the unproven assumption is frustrating. To be fair there was minimal solid evidence for warm early MIS3 climate in the 1970's and 1980's when much of the sampling and analysis was originally carried out. So the tendency to opt for much older ages is easily understandable.

Comparison with the dating of the Okarito composite core is pertinent here. If the contamination argument is set aside in relation to the Martins Quarry site, then the pollen and ^{14}C samples could be recording an MIS3 interstadial period of substantial duration. This would have relevance to the published climatic record by Burge and Shulmeister (2007a,b) for the Westport area even if there is contamination of the Martins Quarry radiocarbon samples by younger carbon. It also has relevance to the region as a whole. A pattern of early to middle MIS3 *Nestegis* bearing cover beds could begin to emerge and would potentially include profiles from Okarito, Greens Beach, Blue Spur Road, Chesterfield Road, Grahams Terrace, Candle Light, Hatters Creek, Sunday Creek, Bullock Creek, Cape Foulwind, (Westport) Cement Works pipeline track, and Martins Quarry.

The various ^{14}C ages from the Westport/Addisons Flat area that are discussed here are not used in this thesis as support for an MIS3 correlation for the Waites Formation. These ages give no more and no less support to that correlation than they do to a correlation with any MIS5 substage. As discussed in relation to the Awatuna Formation the key point is that these ages do not rule out a correlation with the early portion on MIS3. Whether some of the ages are at or near the limit of the ^{14}C method and whether some of the ages may effectively be "infinite ages" has effectively no bearing on choice between the correlations under discussion.

6.2.18e $^{230}Th/^{234}U$ Dating of Speleothems from Metro Cave, Charleston

Radiometric dating has been undertaken by Williams (1982) on speleothems from Metro Cave in the Nile (or Waitakere) River Valley near Charleston. The ages produced are relevant to the Quaternary history of Buller and North Westland though not crucial to this PhD. The study is discussed here in the interests of completeness. The question asked is: do the speleothem ages rule out the stratigraphic model proposed in this thesis?

Metro Cave is cave is part of the Aranui Cave system which acts as the active subterranean path for Aranui Creek. The cave system joins the upper open-air portion of the Creek with the Nile River. Williams based a tectonic uplift calculation on an inference that the long-term rate of fluvial down-cutting in the cave system is equivalent to the long-term rate of uplift and concluded that the tectonic uplift rate for the Westport area is c. 0.27 mm/yr. This is broadly in agreement with the estimate of Suggate (1992) at c. 0.35 mm/yr. Suggate (1992) noted that the uplift rate estimate by Williams (1982) is "not well constrained" but is similar to his own estimate. The estimate by Williams is based on a single sample (No. 24) from an elevation of 27 m above local base level (i.e. the level of the Nile River adjacent to the cave) and dated by the U/Th method at 120 ± 45 ka. The 1σ error is rather large so the age could easily fit a correlation anywhere from MIS6 to MIS5a, and might relate to a sea-level minimum rather than a maximum (Williams assumes a sealevel maximum).

Metro Cave site is situated inland from the Candlelight, Whisky, Caledonian, Addisons, Virgin Flat, and Waites Formation strandlines and so presumably has not been overwhelmed directly by the sea during the last 120 ± 45 ka. Base level here is not sea level. It is the level of the modern Metro resurgence adjacent to the Nile River at c. 28-30 m above modern sea level. So sample No. 24 is approximately 55-57 m above modern sea level. The cave is approximately 5.5 km from the modern coastline so the average river gradient is around 5.0 to 5.5 m/km, less in the lower 3 km and greater from 3 to 6 km inland.

Table 6.21: $^{230}Th/^{234}U$ ages for speleothems from Metro Cave by Williams (1982)

Sample No.	Site	Height above base level (m)	Height above modern sea level (m)	Age (ka)
24	Derf section	27	55-57	120 ± 45 (75 to 165 ka at 1σ)
25	Biclops	30	58-60	50 ± 30 (20 to 80 ka at 1σ)
26	Sticky Trap	18	46-48	31 ± 6
27	Hall of Refuges	11	39-41	44 ± 5
28	Conference Walk	14	42-44	50 ± 3
29	Paddy Fields	9	37-39	42 ± 2
30	Pigalle Corner	2	30-32	18 ± 4
31b	Cave Pearls	2	30-32	23 ± 3
31c	Cave Pearls	2	30-32	26 ± 1

If sample 24 was deposited at the time of formation of the Waites Formation the Metro Cave site would have been about 3.5 km from the Waites (34-36 m), Virgin Flat (40-45 m) and Addison Formation (65-72 m) marine strandlines. If the Nile River at that time maintained a gradient 5.0 to 5.5 m/km during each sea level maximum then one might expect that at the cave the floodplain of the Nile River would have been about 12 to 18 m higher than the Waites strandline. The floodplain adjacent to the cave during Waites deposition might be expected to have been at a modern elevation of (34-36 plus 15-20) 46-52 metres and during Virgin Flat deposition at (40-45 plus 12-18) 52-63 m. Consequently speleothem formation during the Waites and/or Virgin Flat marine episodes is a tenable hypothesis. The assumption would be that the long-term rate of downcutting is approximately equivalent to the rate of tectonic uplift. So it would be feasible for the abandoned flow levels in the Aranui Cave system to correlate with the sea level present during deposition of the Waites Formation.

Samples 30, 31b, 31c and 26 are from a period that is normally assumed to be fully glacial in this region. So speleothem formation appears to occur at this site under the coldest possible climatic conditions (confirmed at the Hollywood cave near Charleston by Whittaker et al (2011). This is during a time of low sea level and probably substantial coastal retreat. Samples dating from 31 ± 6

ka to 18 ± 4 ka and correlating with a very low sea level were not subsequently overwhelmed by either post-glacial sea level rise or post-glacial fluvial aggradation.

If one assumes that the Waites Formation is equivalent to the Awatuna Formation and further that it dates from c. 48 ka then is it possible that U/Th samples 25 and 28 (50 ± 30 ka, 50 ± 3 ka) may relate to this event. The sample elevations (58-60 m, 46-48 m) are certainly high enough, given an expected Nile River floodplain elevation of about 46-52 m at that time. All that can really be said from this is that these speleothem ages do not rule out an MIS4 or MIS3 correlation for the Waites and Virgin Flat Formations.

The critical question is how sample 24 (120 ± 45 or 75 to 165 ka at 1σ) at an elevation of 58-60 m should be interpreted. In terms of its age this sample is an outlier in comparison with the others from the site. Using the 1σ bound sample 24 could be as young as 75 ka. At 2σ the sample could be as young as 30 ka which is well within the age span covered by the other samples from the Metro Cave system. While this discussion on speleothems is somewhat speculative it does indicate that the conclusion by Williams (1982) of uplift at ~ 0.27 mm/yr at Charleston is not the only viable rate that is in accord with the ages of dated speleothems at Metro cave.

The surface topography of the area suggests that there has been at least 60 m of fluvial incision in the Nile River/Aranui Creek area since these two streams were last connected as purely surface features. Nearby there are fluvial terraces at c. 160 m (Aranui Creek/Awakiri River) and 200^{+} m (Awakiri River/Totara River), and a terrace to the seaward side of the cave at 232 m ("*Sub e"* trig point). Therefore it is likely that there has been at least 200 m of uplift at the Metro cave since the area was last inundated by the sea, but the real figure could easily be greater than 230 m.

The conclusion reached here is that the speleothem ages from Metro Cave do not rule out an MIS3 correlation for the Waites Formation. The ages do not provide convincing support for such a correlation.

6.2.19 Pre-Blake Fluvial Incision (MIS4?)

6.2.19a The Chesterfield Channel

At Blake's Terrace near Awatuna a buried incised fluvial channel referred to here as the Chesterfield Cannel, predates both the Loopline and Blake Formations. At the Holocene Sea Cliff between Awatuna and Chesterfield the base of the channel is no higher than 6 m above mean sea level. The stratigraphy here is illustrated in figure 6.5 below.

The deeper portion of the gravel in the Holocene marine cliff between Chesterfield and Awatuna is almost certainly not Loopline Formation. It is more likely to correlate with the fluvial gravel that is situated below the Awatuna Formation at its type section and below the Awatuna Formation in alluvial gold drill holes (by Waitangi Minerals Ltd) at EA Road.

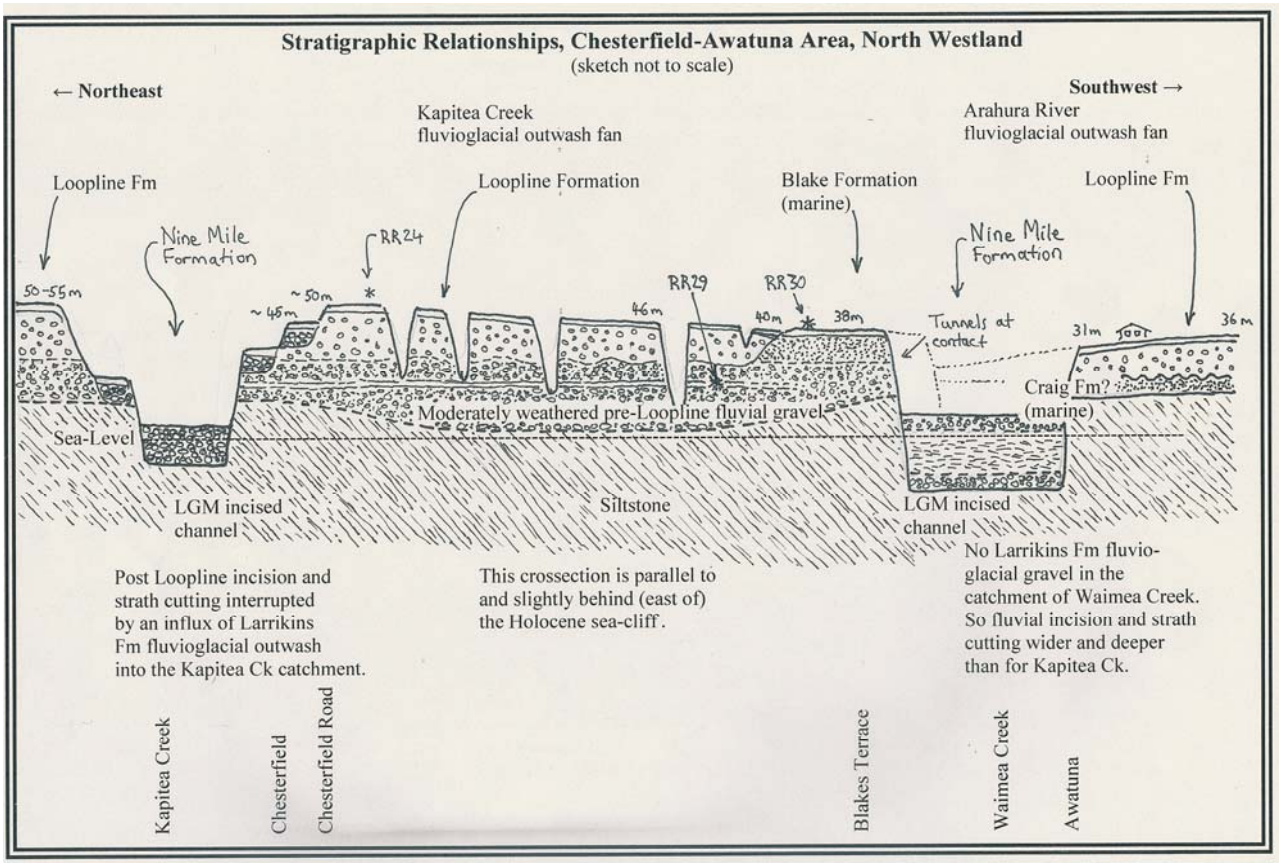

Figure 6.5: Stratigraphic Relationships, Chesterfield-Awatuna Area, North Westland

Towards the top of the stratigraphic sequence within the channel there is an apparently continuous, laterally extensive, grey-coloured silt and fine sand band which is exposed intermittently along the Holocene marine cliff between Awatuna and Chesterfield over a distance of more than 1 km. The silt and fine sand horizon is up to 4 m thick. During this PhD project a single luminescence sample was taken from this silt horizon. The sample (RR29 Grid ref J32 N 4005 E 5220) returned an $IRSL_{(blue)}$ age of 84.9±7.2 ka. Note that RR29 gave a result that to Dr Rieser looked "quite excellent". The sampled material is situated about 15-18 m below the terrace surface or about 19-22 m AMSL. This is lower than the base of the Blake Formation (29 m nearby in the same Holocene seacliff). The silt overlies aggradational fluvial gravel so the luminescence age presumably relates to filling of the underlying channel than incision of a new channel. The silt unit has an unconformable/channelised and iron cemented upper surface. At sample site RR29 the silt is directly overlain by slightly too moderately weathered/oxidised fluvial gravel that is probably older than the relatively non-weathered gravel of the Loopline Formation. The transition upward into Loopline Formation gravel occurs about 10 to 12 m below the terrace surface. This transition can be observed in several road cuttings at the Holocene seacliff between Awatuna and Chesterfield.

The gravel situated below the thick silt band is slightly more oxidised than that situated above the silt band. This does not imply a substantially older age thought that is possible. The degree of weathering displayed here is similar to that typically seen in exposures of Waimea Formation fluvial gravel. So it is perhaps not surprising that RR29 returned an $IRSL_{(blue)}$ age similar the $IRSL_{(blue)}$ ages for RR25 (75.9±7.6 ka) and UCS1 (81 ± 7 ka), both from the Waimea1 Formation. Unfortunately, it appears that fluvial silt is a deceptive material for IRSL dating in Westland. While the laboratory performance of the samples tends to be excellent this obscures a tendency for fluvial silt to be poorly bleached at deposition. The very nature of the sediment (clay, silt and very fine sand and the widespread nature of the deposit in a setting where the gradient of the river is relatively high) is indicative of probable deposition in turbid water. The potential "source to sink"

distance is relatively short and probably no more than 10 to 15 km. Sediment transport duration could be measured in hours, much of the transport occurring during zero light conditions (night). As discussed in chapter 5 (sections 5.6 and 5.7) the extent of partial bleaching is extremely difficult to diagnose without solid support from an independent dating method. This is demonstrated clearly with IRSL, OSL, TL and ^{14}C dating at Kamaka (section 5.6.2). The fluvial silt from which RR29 was taken is similar to that from which RR21 was taken at Kamaka. Sample RR29 is classified in table 5.4 in terms of the likelihood of complete bleaching at deposition. This is considered to be poor to very poor. The likelihood that the sample age is a good representation of the depositional age for this silt bed is relatively low. RR29 provides a maximum age for deposition of this silt.

The RR29 sample site is close (within 50 m) to the margin of the marine Blake Formation (see below). At Blakes Terrace the Blake Formation has an upper surface at about 36 to 42 m (spot elevations taken from the 1:25,000 scale compilation sheet J32D for NZMS 260 J32). At RR29 the Blake Formation has been cut away by fluvial erosion that preceded the deposition of aggradational gravel of the Loopline Formation. Prior to this erosional event the Blake Formation probably extended across and above the fluvial silt at the RR29 sample site. So RR29 probably provides a maximum age for Blake Formation and a minimum age for deeper part of the underlying gravels within the Chesterfield Channel.

The relationship between the fluvial silt unit at 18-22 m AMSL and the Blake Formation is unclear due to erosional fluvial activity postdating the deposition of the silt unit. This erosion preceded the deposition of the Loopline Formation and caused the destruction of the Blake Formation immediately above RR29.

At the type section of the Awatuna Formation the marine gravel/sand rests on a fluvial unit, so the apparent stratigraphic relationship at Blakes Terrace (marine over fluvial) is not unprecedented. A similar relationship also exists with regard to the older of two marine deposits at the Phelps goldmine south of Hokitika (see below), and at EA Road on the North side of Kapitea Creek.

6.2.19b Buried Fluvial Deposits at the Phelps Mine

At the Phelps Goldmine at Southside near Hokitika (Grid Ref NZMS260 J33 N 2805 E 4280) rusty stained marine sand and gravel assigned here to the "Blake Formation" unconformably overlies fluvial gravel. From drilling and trenching here by L&M Mining Ltd is estimated (this thesis) that the fluvial gravel beneath Blake Formation is approximately 3 to 4 m thick. The marine sand has an unconformable upper surface with an elevation of 19-21 m above MSL. It is unconformably overlain by fluvial gravel. The same situation (fluvial beneath marine) is present at a similar elevation in now largely overgrown exposures at the same elevation at J33 N 2750 E 4230; J33 N 2625 E 4000 and J33 N 2700 E 4170 either side of the "Rimu Channel". So there is no strong evidence of downward tilting in a south-westerly direction. At the first three locations a strandline is evident at the point where the sand pinches out in an inland direction. At each site the marine sand also terminates in a seawards direction but the nature of the termination is uncertain. At site J33 N 2750 E 4230 the sand has been tunneled by gold miners and gold can be panned easily from the sand taken from these tunnels.

6.2.19c The Houhou Channel

As shown in figure 6.4e of Suggate & Waight (1999) and as discussed by Cotton & Stewart (1989) a deeply incised fluvial channel of unknown age is present beneath a raised marine beach under the modern floodplain of at Houhou Creek. The beach deposits overlie lacustrine silt and deeper fluvial gravel. On the basis of elevation the marine strandline deposit that overlies this channel is likely to

be the Blake Formation though it is mapped as Awatuna Formation by Suggate & Waight (1999). The channel is incised well below the base of the Waimea, Karoro and Awatuna Formations.

6.2.20 Blake Formation (MIS3)

The Blake Formation is an informal name for marine sand deposits at Blake's Terrace, Awatuna. The only known exposure of most of the thickness of this unit at Blakes Terrace is in an old mine shaft in the yard of a house at the western edge of the terrace. This shaft has been used for various purposes and was not entered as part of this project. It could potentially be used as a "stratotype for this Formation. According to the landowner there are also tunnels into the beachsand that were once accessible mid-way down the overgrown terrace face (the Holocene sea cliff). These were not investigated. Blake Formation deposits have been observed to extend from grid ref J32 N 4005 E 5275 to J32 3970N 5200E (a distance of about 750 m). Surficial deposits of the Blake Formation at Blake's Terrace are at an elevation of about 36m to 42m AMSL (spot elevations from the 1:25,000 scale compilation sheet J32D for NZMS 260 J32). This Formation has been observed during this project in exposures at what had previously (1:50,000 scale mapping by Suggate & Waight 1999) been assumed to be the surface of the Loopline Formation. It has also been exposed more recently (2011) in a new surficial slip face on the Holocene marine cliff at Awatuna and has a basal elevation here at 29 m (by GPS measurement). The exposures on the terrace are in cuttings in private access roads and bulldozed tracks on the terrace surface. The shallow part of the Formation consists of pebble bearing marine sand that may have accumulated at least partly by aeolian processes adjacent to an active strandline. The old mine shaft at the terrace surface serviced mine tunnels at an unknown depth. The presence of historic gold-mining tunnels indicates that there is a buried marine strandline at Blake's Terrace. Discussions with a land-owner at the site indicated that the tunnels are probably at least 10 metres below the surface and that they "daylight" at the nearby Holocene marine cliff. The elevation of the tunnel entrances was not assessed directly during this project. The tunnels are likely to be near the base of the marine unit which is probably at an elevation of around 25 to 30 m at the sea cliff, an elevation that is likely to increase inland up the tunnels.

Exposures in the private access track that leads up onto Blake's Terrace at luminescence sample site RR29 (Grid ref J32 N 4005 E 5220) indicate there is a sharp transition between deep fluvial deposits (full thickness of the Quaternary sequence at that point) and the sequence at RR30 (Grid ref J32 N 4005 E 5275) where the sediments immediately underlying the surface soil are of marine and/or aeolian origin.

At grid ref J32 N 4005 E 5275 the rather oxidised marine sand of the Blake Formation is overlain by approximately 0.8 to 1.2 m of grey largely inorganic silt and brown organic rich silt. Luminescence dating sample RR30 was taken from the margin of an access track at this locality and returned an age of 63.6 ±7.4 ka. The sample point was 0.95 to 1.00 m below the modern terrace surface. The top of the Blake terrace has a relatively low surficial gradient. Therefore one would expect the depositional enviroment to relatively non-energetic. This may be slightly illusory because laterally only a few 10's to perhaps 100 m away the Blake Formation was destroyed by fluvial erosion. It was replaced here after fluvialioglacial aggradation by a younger deposit that is coincidentally at the same altitude along the splice. This younger outwash is probably part of the Loopline Formation. The contact is wedge shaped with the Loopline gravel thinning onto the Blake Formation in a southerly direction. At sample site RR30 the sampled organic silt rests on thin grey sandy silt that could easily be fluvial. The transition is illustrated in sketches in Appendix one. Therefore a fluvial content cannot be ruled out in sample RR30 (especially due to mixing by bioturbation). The sample potentially contains organic, aeolian and fluvial components. As a consequence there is a moderate likelihood that the sample suffers from incomplete bleaching via

an overbank silt component. Therefore the IRSL age for this sample is regarded as a maximum age for the sample and might not be a reliable indicator of the depositional age.

There are two buried pre-Holocene strandlines in the "Phelps Gold-mine" at Southside, Hokitika. The older of these strandlines is correlated here with the Blake Formation and is separated from the younger "Craig Formation" by a buried sea-cliff. The sea-cliff was cut in fluvial and marine gravel during the deposition of the Craig's Formation. There is excellent exposure of the Blake Formation in an old gold prospecting tunnel here. The older deposit is significantly more cemented than the younger deposit. It rests unconformably on alluvial gravel rather than the local sandstone basement and has an eroded upper surface. The overlying bouldery fluvial gravel contains rip-up clasts of cemented Blake Formation. The upper surface has a maximum elevation of around 20 metres at its inner margin, which could be up to 5 metres lower than its original but now truncated surface. So the proposed maximum strandline elevation of ~ 20 to 25 m is similar to that of the Blake Formation at Blakes Terrace and favours direct correlation of these deposits.

The inner strandline elevations for potential Blake Formation localities are:

Locality	**Maximum Elevation Above modern** MSL	**Initial Elevation Above palaeo** MSL	**Probable Tectonic Uplift**
Southside (Phelps Goldmine):	20-25 m	3-5	15-22
Houhou Creek:	35-38 m	3-5	31-35
Blake's Terrace:	36-41 m	3-5	31-37
Point Elizabeth:	35-38 m	3-5	30-35

The altitude of the upper surface of the "Blake" Formation at Southside is estimated from an unpublished report on alluvial gold drilling and trenching by L&M Mining Ltd (Anon 1988) at the Phelps mine and from observations of outcrops (this project). Drill hole number 6 of that programme struck the Blake Formation 19.6 m below the surface. The collar elevation was approximately 38 m, giving an elevation at the Loopline/Blake contact of 19-20 m several tens of metres west of the inner margin of the strandline. Exposures in a long tunnel at the Phelps mine indicate that the upper surface of the Blake Formation is an unconformable (erosional/channelised) contact with the overlying fluvial Loopline Formation at this locality. The maximum thickness of the marine unit in the tunnel is 2 m. It is unlikely that the pre-erosional thickness of the marine unit was less than 5 metres (by comparison with other Quaternary and Holocene marine beach deposits in this area, including the buried Craig Formation on the same property which has an intact soil cover and a thickness of 5 to 6 m from the same drilling programme). The original upper surface of the Blake Formation could have been as high as 25 metres. This estimate is slightly lower than for several other potential correlative deposits. While the gold bearing marine sand and gravel does pinch out the upper contact is an angular unconformity. So the easternmost observation of this unit might not represent its full former distribution. It could be argued that the presence of the younger Craig Formation (not observed unequivocally anywhere to the north (where the uplift rate should be greater and preservation should be more likely) is suggestive of a relatively rapid uplift rate at Southside.

It is not clear that the Blake strandline at Southside is the innermost strandline here. It is simply the most landward strandline identified in the area to date. So correlation with deposits in the Blue Spur- Houhou Creek and Awatuna areas to the northeast is somewhat conjectural.

Table 6.22 Luminescence ages from the Blake Formation

Lab	Field	Age	Elevation	Location	Grid Ref

Code		Code (ka)	AMSL (m)		(NZMS260)
WLL535	RR30	63.6 ±7.4	35 m	Blake's Terrace	J32 N 4005 E 5275
WLL296	RR12	39.5 ± 2.4	30-33 m	Point Elizabeth	J31 N 6780 E 6350
WLL217	RR4	No result	15-20 m	Southside	J33 N 2795 E 4260
WLL147	RR5	No result	20 m	Southside	J33 N 2805 E 4260

Several samples were taken from the Blake Formation for IRSL dating during this project. Two returned polymineral finegrain $IRSL_{blue}$ ages from silt. These are RR12 and RR30. RR30 is discussed in detail above. The two failed IRSL samples (RR4 & RR5) are from iron-stained but otherwise clean sand taken from the older of the two buried strandlines at Southside, Hokitika. The quartz in these samples was unsuitable for OSL dating and there was insufficient polymineralic silt for IRSL dating.

At Point Elizabeth $IRSL_{blue}$ sample RR12 (Grid ref J31 N 6780 E 6350) was taken from a face in a small opencast gold mine at an elevation of 30-32 m. The sample age is 39.5 ± 2.4 ka and is derived from the silt content of a marine sand layer about 1.5 to 2 m below the terrace surface. The sample consists of slightly silty littoral sand. The site is distant from sources of fluvial, colluvial or lacustrine sediment. Given that the sample site is an old goldmine, which points to deposition in a marine strandline situation. The nature of the sediment makes it clear that deposition was not in an offshore marine environment. So the polymineral finegrained IRSL signal should have been completely bleached at deposition. The elevation of the marine sand at this locality is too low for correlation with the Awatuna strandline at RR11. The low terrace contains the most extensive raised marine deposit at Point Elizabeth. The maximum elevation of this surface is 38 metres. A conventional ^{14}C age of 37.4 ± 2.15 ka for NZ 446 was reported by Grant-Taylor and Rafter (1971) for wood in soil on the "100 ft terrace" situated between Rapahoe & Point Elizabeth. This has been revised to 37.48 ± 3.319 ka (RP Suggate pers com).

Given that the IRSL sample least likely to have been incompletely bleached at deposition is RR12 and given that there is a similar 14C date from the same general locality the age for RR12 at 39.5 ± 2.4 ka is the preferred IRSL age for the Blake Formation. This is a rather young age but it fits nicely between the IRSL ages obtained during this project on older Awatuna Formation and the younger Craigs Formation. On the basis of the information available the Blake Formation is likely to have been deposited during MIS3.

6.2.21 Craig Formation (MIS3)

6.2.21a Introduction

The Craig Formation is an informal name for buried marine and littoral sand, sandy gravel and associated estuarine/overbank silt situated beneath the Loopline Formation either side of Pine Creek, Southside, Hokitika. The Formation has been exposed in mine faces dating from the early 1990's and in old tunnels leading under the terrace from the Holocene seacliff. Silt has been sampled for luminescence dating from three stratigraphic levels at two localities being the Phelps mine (J33 418276) and Pine Creek quarry (J33 426281). Both sites are alluvial gold mines. They are situated just south of the Hokitika River and just east of Holocene sea cliff near Hokitika. The marine strandline portion of the Craig Formation was discovered by alluvial goldminers around the year 1900. Strandline deposits here were mined by tunneling for many years in the early 1900's. For several years in the early 1990's an opencast goldmine was operated here by the landowner. This provided large new exposures through the Quaternary sequence and excellent access for sampling. These sediments have not previously been assigned to any formation, mainly because the primary exposures lie outside of the Kumara-Moana 1:50,000 map area (Suggate & Waight 1999).

The Phelps mine was prospected by an L&M Mining/McConnell Dowell Joint Venture in the late 1980's. A report (Anon 1988) summarizing the work is on file at Crown Minerals (Ministry of Economic Development). The Pine Creek Quarry was also prospected by L&M Mining at about the same time. The report is titled: Final Report, Prospecting Operations, Mining Permit 41-354, MG Davidson, Pine Creek, Hokitika.

The provisional name adopted this marine deposit is derived from that of the owner of the property at the time of gold discovery. At that time the site was known as "Craig's Freehold", a name that found its way into the official mining records of that era. The uppermost portion of the Craig Formation was dated by Preusser et al (2005) who did not assign the unit to a particular formation. The upper surface of the innermost strandline of the Craig Formation is situated at a maximum elevation of around 10-12 metres above sea level. This elevation is calculated from the collar elevation of L&M Mining exploratory drill holes and the depth at which the upper surface of the marine unit was encountered. The strandline deposit rests directly on weathered Pliocene sandstone and pebble conglomerate of the Eight Mile Formation which is defined by Suggate & Waight (1999). This is demonstrated in drill logs (Anon 1988) and has been observed directly by the writer while gold mining was occurring at this site.

The Craig Formation includes a marine strandline situated against a fossil (buried) sea-cliff. At the sea-cliff there is an unconformable relationship between this formation and:

- The underlying Plio-Pleistocene Eight Mile Formation fluvial sandstone and fine conglomerate, which is also present in the footing of the sea-cliff.
- The Late Quaternary fluvioglacial gravel exposed near the base in the face of the sea-cliff and situated beneath the Blake Formation.
- The Blake Formation which is also behind the sea-cliff.
- The fluvioglacial gravel that immediately overlies the Blake Formation.

Prior to the deposition of the Craig Formation Late Quaternary fluvioglacial gravel clearly extended well to the NW of the sea-cliff. The seacliff was created during a landward advance of the coastline prior to the deposition of the Craig Formation. The base of the Craig Formation is cut into local bedrock to a level below the base of the older Quaternary fluvioglacial gravel. Coastal advance was accompanied by widespread marine planation. The marine cliff is similar to the Holocene equivalent (a few hundred metres to the west). Prior to the mine being partially backfilled by mine tailings the "Craigs" marine cliff was clearly exposed within the southeast wall of the pit.

At the Phelps mine the gold-bearing beach sand and gravel of the Craig Formation is overlain by a thick wood-bearing silt unit. The wood-bearing brown silt is presumably only slightly younger than the underlying marine sand. Here is no evidence for a depositional hiatus or erosional break at the contact. This soil/silt is referred to as an estuarine unit by Preusser et al (2005) but they provide no evidence that the environment of deposition was in the tidal zone. By analogy with modern beach environments in this region the exceptionally high gold grades (which generally develop in the swash zone) in the underlying sand indicate that the upper surface of the marine sand was almost certainly significantly above mean sea level at the time of deposition, perhaps by as much as 2 to 4 metres. The preferred environment for heavy mineral concentration is in the swash zone. So it is likely that the wood bearing silt was deposited on a surface that was higher than the mean high sea level (springs). Therefore it is unlikely the soil/silt is estuarine and more likely that it has fluvial overbank origin. This silt is overlain directly by fluvioglacial gravel.

Table 6.23 Luminescence ages from the Craig Formation, this project

Lab Code	Field Code	$IRSL_{blue}$ Age (ka)	Elevation AMSL (m)	Location	Grid Reference (NZMS 260)
WLL535	RR3	56.8 ±5.9	25 m	Southside	J33 N 2780 E 4230
WLL296	RR2	33.6 ± 3.6	9-11 m	Southside	J33 N 2780 E 4230
WLL217	RR1	No result	8-10 m	Southside	J33 N 2780 E 4230

At the Phelps Goldmine the stratigraphy is as follows:

Sediment	**MIS correlation by Preusser et al (2005)**
Loess c. 1m	MIS2
Outwash Gravel $7m^{+}$	MIS2 (Larrikins Fm)
Grey Overbank silt c. 0.3 to 1m	MIS4 (Loopline Fm)
Outwash Gravel $9m^{+}$	MIS4 (Loopline Fm)
Brown Soil/silt (wood bearing)	MIS5
Marine Sand 5 to 6 m	MIS5
Eight Mile Formation	Pliocene

Additional detail is given on the stratigraphy in relation to luminescence samples RR1, RR2 and RR3 can be found in Appendix 1.
N.B. In figure 6.6a the geomorphological context for the Phelps mine is displayed. This is relevant to the age of the Loopline Formation at the Hokitika Quarry which is situated immediately to the north across the Hokitika River from moraines mapped on the terrace above Arthurstown.

6.2.21b Luminescence dating at the Phelps Goldmine

Wood bearing organic soil accumulated directly on beach sand/gravel of the Craig Formation at the Phelps opencast goldmine. The soil contains logs/stumps up to 20 cm thick. A single luminescence sample (RR2) was taken from this soil (see figure 6.8 for the general geological context). This yielded an $IRSL_{blue}$ age of 33.6 ± 3.6 ka. No pollen analyses are available for this unit. A second sample, RR1 was taken from clean beachsand below RR2. It failed to return an age as the quartz in the sand proved unsuitable for OSL dating and the silt content was insufficient for poly-mineral dating by IRSL. A single sample (RR3) taken from a silt/loess horizon within the overlying Loopline Formation yielded an $IRSL_{blue}$ age of 56.8 ±5.9 ka. The ages of these samples are discussed in Chapter 5 (section 5.6.3) along with samples dated by Preusser et al (2005) from the same locality.

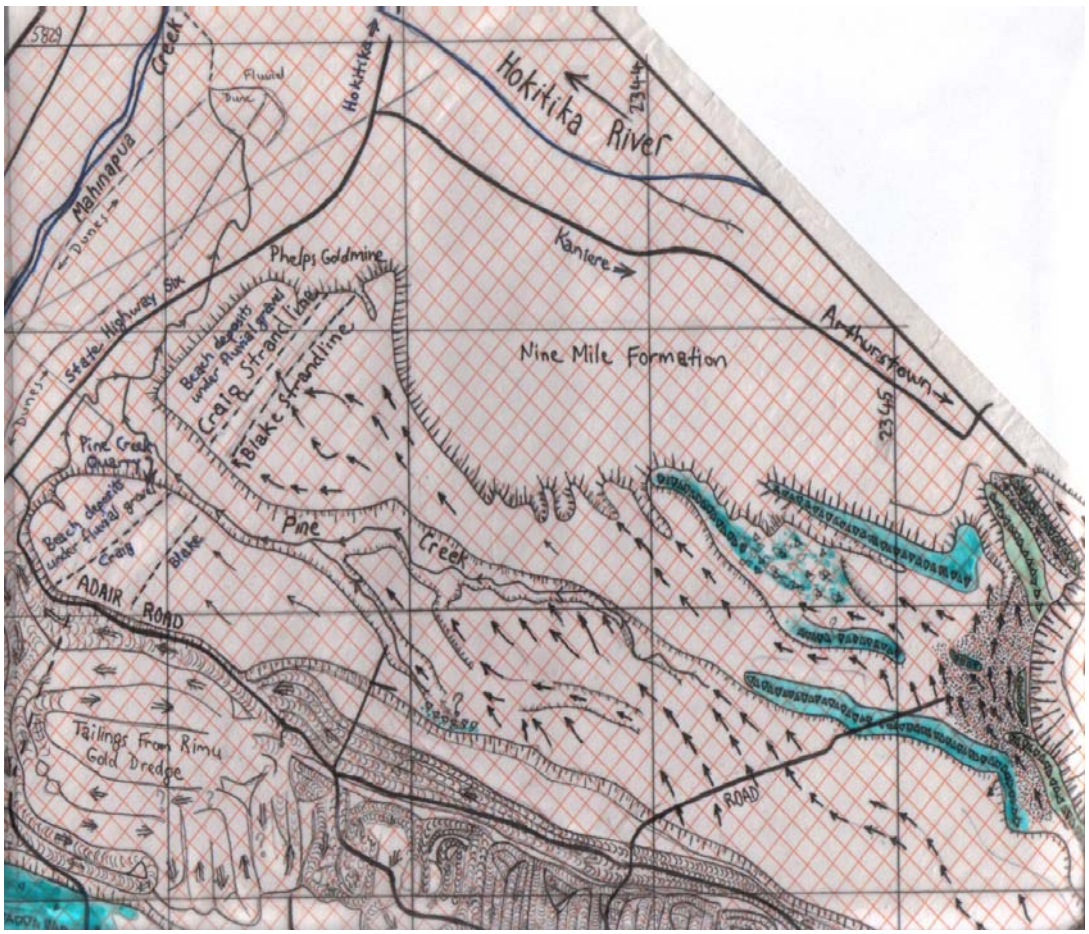

Figure 6.6a (above): General geomorphological context for the Phelps Mine

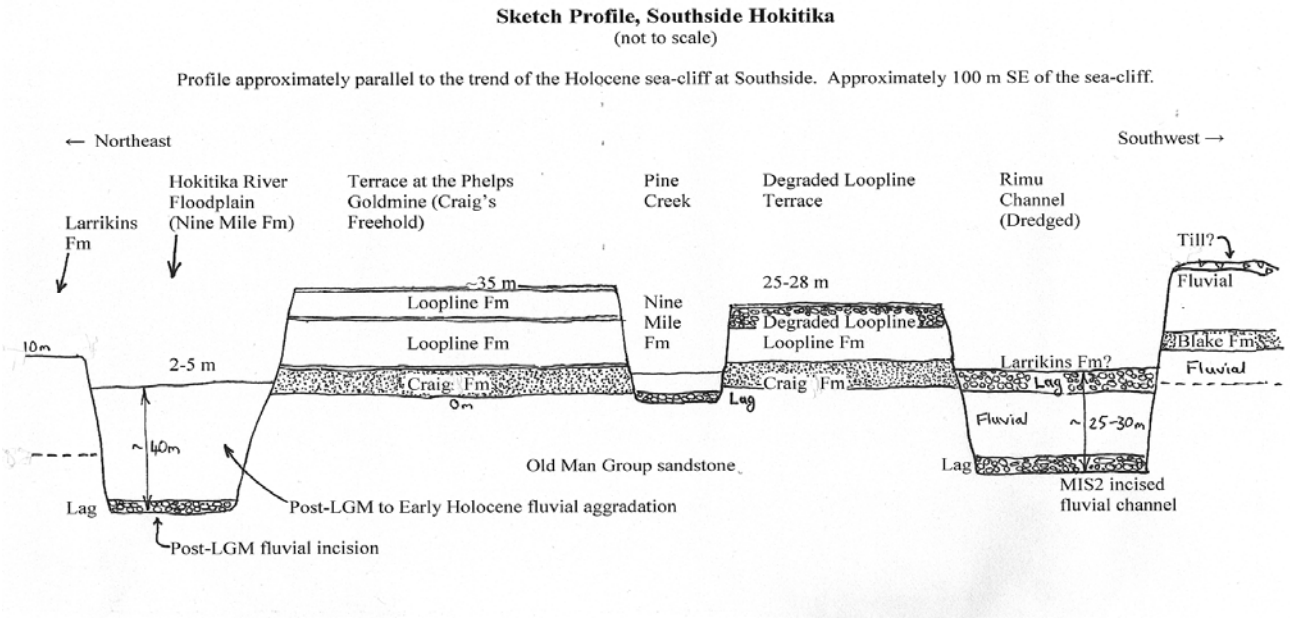

Figure 6.6b: Sketch Profile, Stratigraphic Relationships, Southside Hokitika

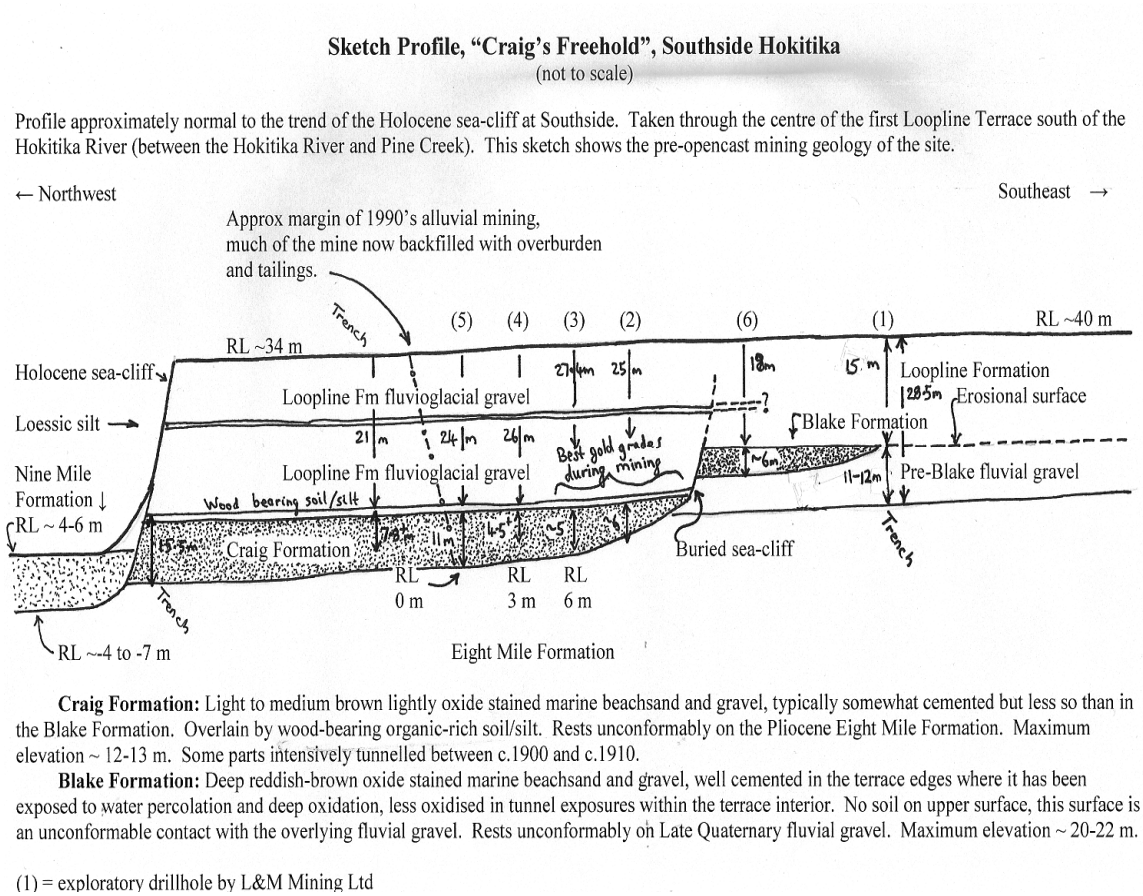

Craig Formation: Light to medium brown lightly oxide stained marine beachsand and gravel, typically somewhat cemented but less so than in the Blake Formation. Overlain by wood-bearing organic-rich soil/silt. Rests unconformably on the Pliocene Eight Mile Formation. Maximum elevation ~ 12-13 m. Some parts intensively tunnelled between c.1900 and c.1910.

Blake Formation: Deep reddish-brown oxide stained marine beachsand and gravel, well cemented in the terrace edges where it has been exposed to water percolation and deep oxidation, less oxidised in tunnel exposures within the terrace interior. No soil on upper surface, this surface is an unconformable contact with the overlying fluvial gravel. Rests unconformably on Late Quaternary fluvial gravel. Maximum elevation ~ 20-22 m.

(1) = exploratory drillhole by L&M Mining Ltd

Figure 6.7 Sketch Profile, Stratigraphic Relationships, Craig's Freehold, Southside, Hokitika

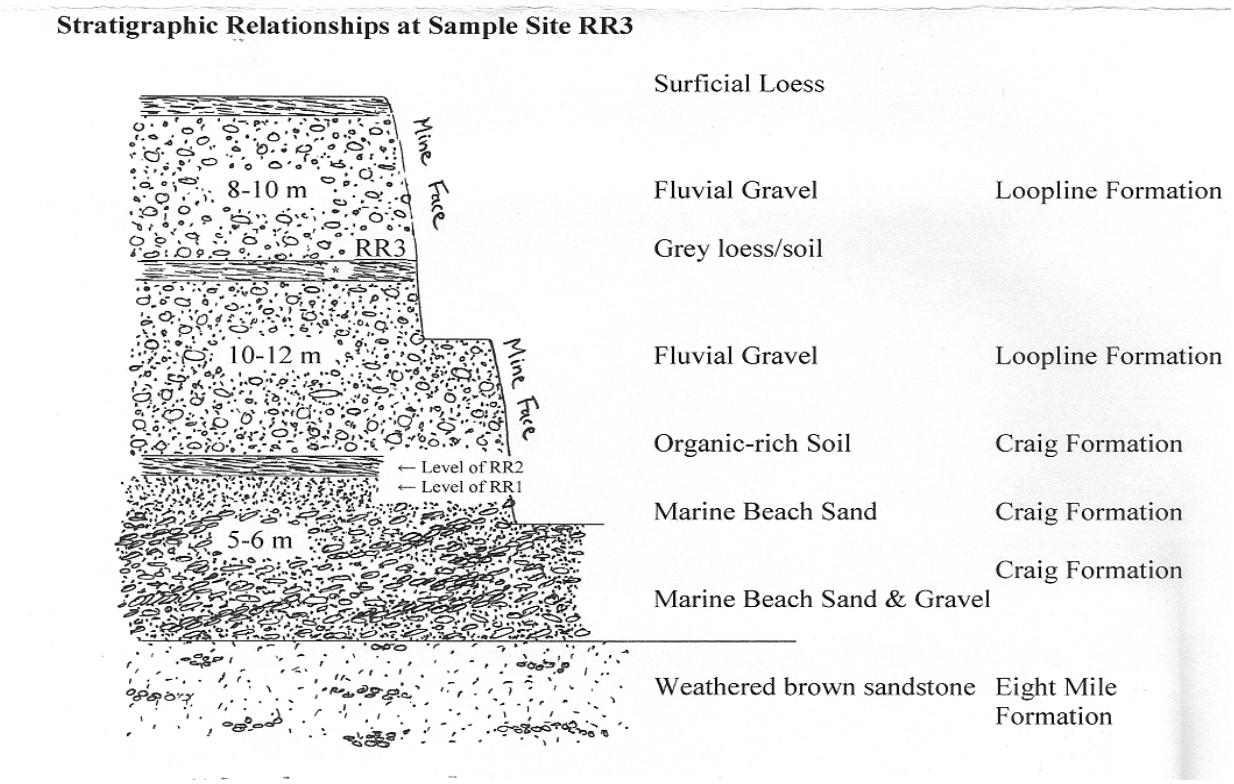

Figure 6.8 Stratigraphic relationships at sample sites RR1, RR2 and RR3

The grey overbank silt

Samples RR2 and RR3 are classified in table 5.4 in terms of the likelihood that the sediment was completely bleached prior to deposition. As discussed in section 5.6.3 and shown in figure 6.8, sample RR3 was taken from a silt unit that is immediately underlain and overlain by fluvioglacial gravel. Preusser et al (2005) have suggested that this unit is an overbank silt and this interpretation is accepted here. Therefore there is a continuous sequence of fluvial sediment at least 20 metres thick resting above the strandline deposits of the Craig Formation. As discussed at length in Chapter 5 (section 5.6) fluvioglacial sediments, including overbank silt, are not good targets for luminescence dating and this includes polymineral finegrain IRSL dating. This realisation has largely occurred in the literature after RR3 was sampled and after the sampling undertaken by Preusser et al (2005). For reasons discussed in section 5.6.3 all the samples taken from this silt bed (listed in table 6.24) are very likely to have been pervasively affected by poor bleaching at deposition. So all of these samples are likely to significantly overestimate the age of deposition, even the youngest of them and that sample is RR3. The most generous assessment is that the youngest polymineral finegrain $IRSL_{blue}$ ages provide a maximum bounding age for the deposition of the silt. Incomplete bleaching is likely to be a major reason why the IRSL ages (and the OSL and TL ages) fail to make a distinction between the depositional age of this silt and that of the silt situated below the lower fluvioglacial gravel unit.

Preusser et al (2005) to assign the uppermost fluvial gravel at the Phelps Mine to the Larrikins Formation. There is no evidence for this apart from the IRSL and OSL age at the base of the overlying loess. This terrace has not been mapped as Larrikins Formation in the past. The site is outside the coverage of published 1:50,000 and 1:63,360 scale geological mapping so a reinterpretation by Preusser et al (2005) was warranted. Previously it has been assumed that the Larrikins Formation is situated at an elevation of about 10 m at the level of the Hokitika Primary School (Grid ref J32 3000N 4460E) within the urban Hokitika on the north side of the Hokitika River. The school site is within the area mapped at 1:50,000 scale by Suggate & Waight (1999). This terrace is about 25 to 30 m lower than the adjacent Loopline (Hokitika airport) terrace just to the north. It can be traced to extensive moraines at an elevation of c. 40-50 m at Kaniere township about 4 km up-valley from Hokitika. As for Kumara the ice-proximal portion of the Larrikins Formation at Kaniere is the location of a very large placer gold deposit that was explored and mined extensively by tunneling and dredging during the 19th and 20th centuries.

There may be Larrikins Formation terraces and meltwater channels south of the Hokitika River (potentially including the upper surface at the Phelps Mine) that are older than the one mapped at the Hokitika Primary School. The upper outwash unit at the Phelps mine underlies a surface that can be traced inland to moraines near Rimu and Woodstock, previously assumed to be Loopline Formation. However this outwash gravel could represent an early phase of the Larrikins event during early MIS2 or the MIS3/2 transition. The terrace surface at the Phelps mine at Southside is at essentially the same elevation at the terrace beneath the Hokitika Airport. The Airport Terrace is mapped as Loopline Formation by Suggate & Waight (1999). There is no particular reason why the two terraces, flanking the north and south sides of the Hokitika River, should be of precisely the same age.

The wood-bearing organic rich silt

This silt unit is situated below the lower fluvioglacial gravel unit and above the littoral sand of the Craig Formation. Preusser et al (2005) have interpreted this unit to be an estuarine deposit. No evidence is cited in support of this interpretation and no such evidence was observed by the writer during (or before) this PhD project. At the base the unit is composed of sandy silt with a gradational contact down into the Craig Formation. Slightly higher the silt is highly organic with

abundant macroscopic wood fragments. This layer is around 30 cm thick. It grades up into sandy moderately organic silt then up into pebbly silty sand and finally into fluvioglacial gravel. The wood-bearing organic silt is the only portion of this unit for which there is any prospect of slow deposition. Other portions of the silt could have potentially accumulated over a period from weeks to a few 10's of years. A single sample was taken from the wood-bearing organic rich silt for polymineral finegrain IRSL dating during this project. This is sample RR2. Despite the presence of fluvial silt immediately above RR2 contains silt that should have been well bleached at deposition. This sample returned an $IRSL_{blue}$ age of 33.6 ± 3.6 ka, being the youngest of all the samples taken at the Phelps Mine and the adjacent Pine Creek Quarry. On the basis of dating carried out during this project this is the preferred depositional age for the organic silt situated above the Craig Formation strandline deposits. The sample does not date the deposition of the strandline sediment. It indicates the strandline formed prior to 33.6 ± 3.6 ka. So it is compatible with the next youngest sample age from this project being that for RR12 on the Blake Formation at Point Elizabeth.

A number of luminescence samples were taken by Preusser et al (2005) from the silt overlying the Craig Formation. These are discussed in chapter 5, section 5.6.3. There the following comment is made:

> "The upward transition into aggradational fluvial gravel is from a moderate-energy fluvial environment into a high energy fluvioglacial environment. Partial bleaching of quartz OSL and TL have been demonstrated. So the potential for partial IRSL bleaching through this transition is very high. Even a modest degree of partial bleaching would potentially put the Preusser et al (2005) late MIS5-MIS4 assignment for the lower silt in doubt. For the "younger samples" an inherited D_e corresponding to 30 to 40 kyr would bring the Preusser et al (2005) results into line with RR2 (33.6±3.6 ka). But this would be difficult to reconcile with the ^{14}C ages reported in figure 7 of Preusser et al (2005) which are reported to be on wood remains found in the overbank deposits."

At the current time this difference can't be easily resolved. The IRSL dating by Preusser et al (2005) tends to indicate an older age than RR2. But at the same time it does not rule out an early to middle MIS3 age for the Craig Formation. Nor do the Preusser et al ages support that correlation. As discussed in section 5.6.3 the OSL and TL dating carried out at this site is regarded as having little value, except that it provides an alert that partial bleaching is a potential issue in the silt that rests on the Craig Formation. It should be recalled that this site is situated close to a number of glacial moraines. Thick older fluvioglacial gravel deposits are present within 10's of metres of the face that was sampled. These deposits were exposed to erosion in the seacliff while the silt unit was being deposited. The silt accumulated in subaqueous conditions. Given the sandy and pebbly nature of much of the silt the water flow was frequently relatively energetic. The nature of modern rivers and streams in Westland is such that under these types of conditions the water is very turbid. This is likely to have been the case at the Phelps Mine and the situation bears comparison with Kamaka (see section 6.6.2) where precisely the same issues are in play.
At the Phelps Pit Preusser et al (2005) report a number of ^{14}C results from wood in the grey "overbank" silt deposits (situated between the two fluvial gravel units) as follows:

B-6885 > 56 kyr	B-6889 > 52 kyr
B-6887 > 53 kyr	B-6891 > 53 kyr
B-6886 > 54 kyr	B-6890 > 52 kyr
B-6888 > 56 kyr	

The ages are essentially infinite. This seems to indicate that the gravel unit situated below the silt is probably older than 50 kyr. The only primary issue with this finding is that, from the writers examination of the site over many visits, the upper silt unit (in the middle of the fluvioglacial gravel) is not conspicuously wood-bearing. Dr RP Suggate suggested (pers com) that samples, taken from the grey silt/loess during a visit to this site with myself during the late 1990's, don't

contain much pollen. The lower "estuarine" unit contains abundant wood, including logs up to 20 cm in diameter. If one were intending to collect samples for ^{14}C dating then the lower silt, which is highly organic (peaty) is the more obvious target. The upper silt has the visual appearance of a grey loess or gley-podzol.

Table 6.24 Luminescence ages from Southside, Hokitika by Preusser et al (2005)

Phelps Gold Mine			Pine Creek Quarry		
Sample	IRSL ages (ka)	OSL	Sample	IRSL ages (ka)	OSL
Loess					
PGM11	#19.3 ± 2.5	**17.1 ± 1.5			
PGM10	#22.4 ± 2.3	**21.5 ± 2.1			
Outwash Gravel 7m+	Larrikins Formation (Preusser et al 2005))				
Grey Overbank Silt					
PGM9	#76 ± 8	**85 ± 8	PIC1	†74 ± 15	*66 ± 15
PGM8	#61 ± 6	**83 ± 8	PIC2	†78 ± 14	*63 ± 9
PGM7	#69 ± 6	**103 ± 10			
PGM6	#58 ± 5	**69 ± 7			
RR3	†56 ±5.9 (this PhD project)				
Outwash Gravel 9m+	Loopline Formation (Preusser et al 2005)				
Brown "Estuarine" Deposits / Soil					
PGM5	#63 ± 6	**102 ± 10	PIC3	†76 ± 11	*80 ± 13
PGM4	†74 ± 8	**101 ± 25			
PGM3	†66 ± 8	*84 ± 9			
PGM2	†76 ± 18	*65 ± 17			
PGM1	†67 ± 8	*72 ± 12			
Marine Sand	Craig Formation (This study)				
Eight Mile Formation (Pliocene)	(† = $IRSL_{(blue)}$; # = $IRSL_{(UV)}$; ** = post-IR-OSL; *=$OSL_{(UV)}$)				

Table 6.25 Comparison of luminescence ages from the "estuarine unit" at the Phelps Mine. Note that several methods were also dated four methods including TL_{blue} and TL_{UV} methods. The comparison is as follows:

Sample	**IRSL age (ka)**	**OSL age (ka)**	**TL_{blue} age (ka)**	**TL_{UV} age (ka)**
PGM5	#63 ± 6	**102 ± 10		
PGM4	†74 ± 8	**101 ± 25	261 ± 48	
PGM3	†66 ± 8	*84 ± 9	67 ± 10	89 ±17
PGM2	†76 ± 18	*65 ± 17	204 ± 40	107 ± 13
PGM1	†67 ± 8	*72 ± 12	75 ± 9	70 ± 12
PIC3	†76 ± 11	*80 ± 13	114 ± 17	78 ±12

† = $IRSL_{(blue)}$; # = $IRSL_{(UV)}$; ** = post-IR-OSL; *=$OSL_{(UV)}$

6.2.22 Hatters Creek Interstadial deposits (MIS3)

The Hatters Creek site (grid ref J32 5395N 3310E) is situated at the mouth of a steep gully draining off the hills on the north side of the Arahura Valley. The floodplain in the gully merges imperceptibly with the surface of a widespread fluvial terrace that was deposited by the Arahura River. The modern surface level at the Hatters Creek site is mapped as Loopline Formation by Suggate & Waight (1999). Here two buried silt/soil intervals and three fluvial gravel units (as

shown in figure 6.9) were exposed in a face created by alluvial gold mining beneath the surface of the Loopline Formation. Unfortunately the site has been buried due to restoration at the alluvial gold mine.

It is highly unlikely that fluvial activity was absent in the valley of Hatters Creek during the last glacial period (following completion of Loopline deposition), particularly during the LGM, so it makes sense to correlate the uppermost fluvial gravel unit with the Larrikins Formation. This gravel extends to a depth of about 3 m beneath the terrace surface.

The first buried silt at a depth of 3 to 3.8 m and an elevation of c.80 m is probably situated above gravel of the Loopline Formation. This silt was sampled (NZ6497) for ^{14}C dating. The result (Soons, JM pers. com. in Moar & Suggate 1996) was a conventional ^{14}C age of $>32.5^{+}$ ka (> 35 ka cal., Incal-09). The silt rests on fluvial gravel that is presumed to be part of the Loopline Formation. So the ^{14}C age implies the Loopline Formation is older than c. 35 ka and that the Larrikins Formation is younger than this.

Moar & Suggate (1996) report two pollen diagrams (their Figures 6a and 6b), one for each silt unit. At Hatters Creek the sequence is shown in figure 6.9.

Figure 6.9: Stratigraphy and pollen at Hatters Creek.

Depth	Material	Correlation	Organic Content
0	Surface Soil	Holocene	Abundant organic material
0 to 3 m	Gravel	Larrikins?	Minimal
3 to 3.8 m	Silt	Interstadial (Chesterfield)	Organic rich with wood fragments and *Nothofagus* leaves. Pollen dominated by *N. menziesii*, with *N. fusca* also present. Also *Asteraceae*, *Coprosma, Poaceae, Hebe, Myrsine & Elytranthe*
3.8 to 8 m	Gravel	Loopline?	Minimal
8 to 9 m	Silt	Interstadial (Hatters Creek)	Organic rich with wood and *Nothofagus* leaves. Pollen includes *Nestegis* and low frequency *Dacrydium cupressinum, Podocarpus, Coprosma* and *Psuedopanax.* The pollen is dominated by *Nothofagus*, mainly *N. menziesii*, but *N. fusca* is common as well.
9 to 10 m	Gravel	pre Loopline lag deposit	Minimal

The Hatters Creek site (grid ref J32 5395N 3310E) is situated at the mouth of a steep gully draining off the hills on the north side of the Arahura Valley. The floodplain in the gully merges imperceptibly with the surface of a widespread fluvial terrace that was deposited by the Arahura River. The modern surface level at the Hatters Creek site is mapped as Loopline Formation by Suggate & Waight (1999). Here two buried silt/soil intervals and three fluvial gravel units (as shown in figure 6.9) were exposed in a face created by alluvial gold mining beneath the surface of the Loopline Formation. Unfortunately the site has been buried due to restoration at the alluvial gold mine.

It is highly unlikely that fluvial activity was absent in the valley of Hatters Creek during the last glacial period (following completion of Loopline deposition), particularly during the LGM, so it makes sense to correlate the uppermost fluvial gravel unit with the Larrikins Formation. This gravel extends to a depth of about 3 m beneath the terrace surface.

The first buried silt at a depth of 3 to 3.8 m and an elevation of c.80 m is probably situated above gravel of the Loopline Formation. This silt was sampled (NZ6497) for ^{14}C dating. The result (Soons, JM pers. com. in Moar & Suggate 1996) was a conventional ^{14}C age of $>32.5^{+}$ ka (> 35 ka cal., Incal-09). The silt rests on fluvial gravel that is presumed to be part of the Loopline Formation. So the ^{14}C age implies the Loopline Formation is older than c. 35 ka and that the Larrikins Formation is younger than this.

Moar & Suggate (1996) report two pollen diagrams (their Figures 6a and 6b), one for each silt unit. At Hatters Creek the sequence is shown in figure 6.9.

Figure 6.9: Stratigraphy and pollen at Hatters Creek.

Depth	Material	Correlation	Organic Content
0	Surface Soil	Holocene	Abundant organic material
0 to 3 m	Gravel	Larrikins?	Minimal
3 to 3.8 m	Silt	Interstadial (Chesterfield)	Organic rich with wood fragments and *Nothofagus* leaves. Pollen dominated by *N. menziesii*, with *N. fusca* also present. Also *Asteraceae*, *Coprosma, Poaceae, Hebe, Myrsine & Elytranthe*
3.8 to 8 m	Gravel	Loopline?	Minimal
8 to 9 m	Silt	Interstadial (Hatters Creek)	Organic rich with wood and *Nothofagus* leaves. Pollen includes *Nestegis* and low frequency *Dacrydium cupressinum, Podocarpus, Coprosma* and *Psuedopanax.* The pollen is dominated by *Nothofagus*, mainly *N. menziesii*, but *N. fusca* is common as well.
9 to 10 m	Gravel	pre Loopline lag deposit	Minimal

The deeper of the silt horizons is at an RL of around 70 m. A correlation with soil on either the Awatuna (at Sunday Creek) or Blake (at Awatuna) Formations is likely. The mix of tree species is similar to that identified from pollen in the silt that overlies the marine sand at the type section of the Awatuna Formation. It is not possible to say for certain whether the pollen represents an interglacial or interstadial climate. Previously the presence of *Nestegis* would have pointed to a fully interglacial affinity. However, as discussed elsewhere in this thesis this assumption is questionable

6.2.23 Loopline Formation (MIS3, Otira Glaciation, Kumara 2_1 Advance)

6.2.23a Introduction

This formation was originally defined by Suggate (1965) and named from the Loopline Road about 8 km south of Kumara. Suggate (1985), Suggate & Waight (1999) and Nathan et al (2002) correlate the Loopline Formation with MIS4. Suggate (1965) defined the type locality for the Loopline Formation as a 20 ft high outcrop of outwash gravel below the aggradational surface derived from the "outer" Loopline Moraine. The exposure is situated at S51 714620 on the south bank of Kapitea Creek. In fieldwork for this PhD it has been determined that Kapitea Creek received a large influx of outwash gravel during the younger glacial advance that produced the Larrikins Formation. This younger gravel covers significant areas of older Loopline Formation at Loopline Road between the Stafford Loop Road and the Kapitea Reservoir (figure 6.10 below). It may also be present at the Loopline type section.

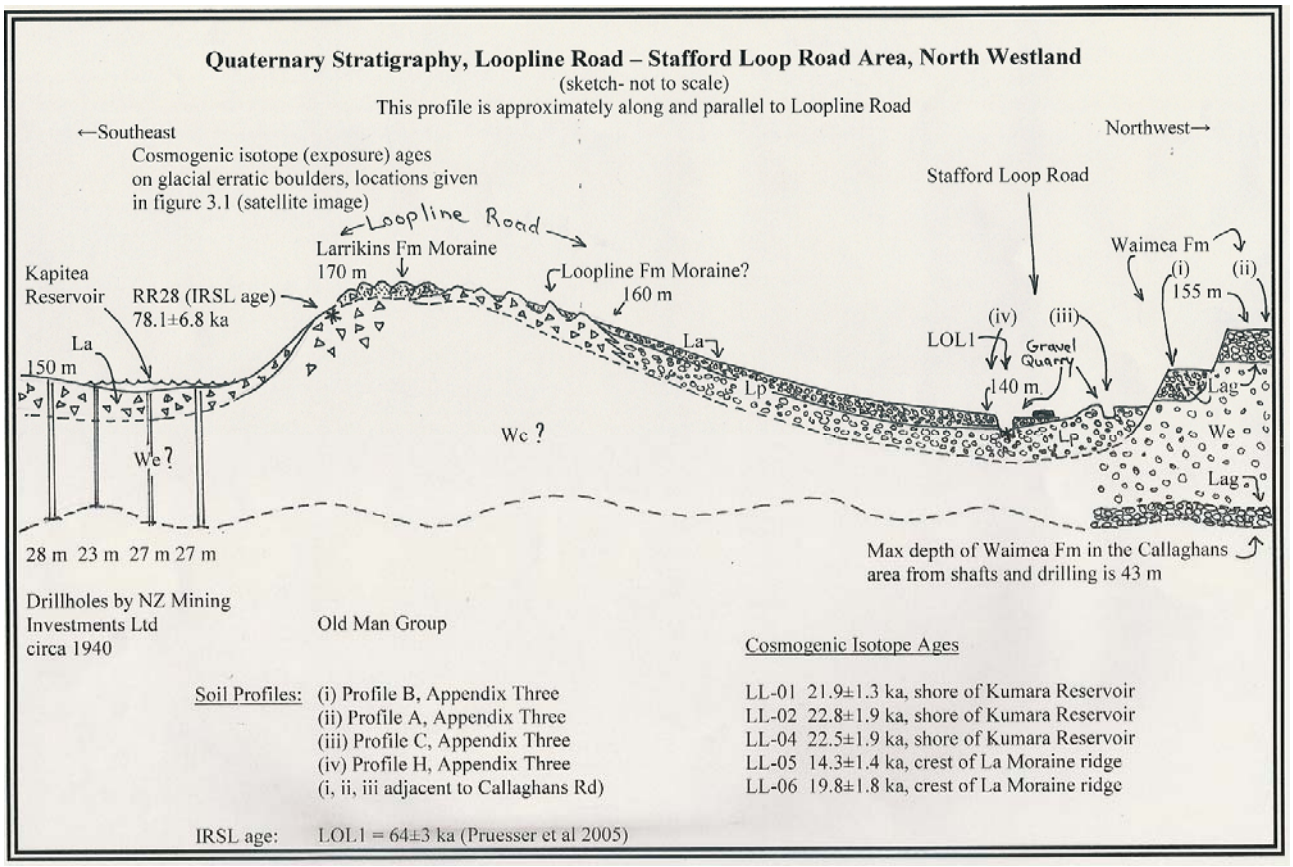

Figure 6.10 Quaternary Stratigraphy, Loopline Road-Stafford Road area, North Westland

According to Suggate (1965) the Loopline Formation contains two distinct moraine belts the older of these being linked to the outwash at the type section. Two separate outwash surfaces were also recognised. The similarity of the surface features of two sets of moraine and outwash was thought to imply these events were not separated by a full interglacial period. In addition there was no known marine cliffing of the older outwash terrace in the period between the two glacial advances. This lack of marine cliff formation still appears to hold as the Loopline Formation is younger than the Craig Formation. No post-Craig intra-MIS3 episodes of marine cliff formation have been identified in this PhD project.

The two main moraine belts that made up a substantial part of the Loopline Formation, as originally defined, are situated either side of the combined Kapitea and Kumara reservoirs. These man-made

lakes (hydroelectric scheme) occupy an area mapped as recessional Loopline Formation by Suggate & Waight (1999). Adjacent to both reservoirs older (seaward) moraine has a youthful appearance. There are large erratic boulders scattered across the surface of this moraine and on the recessional surface. In conjunction with Dr Tim Barrows six of these boulders have been sampled for dating by the cosmogenic isotope method. At the time of writing four of the samples have produced ages. None of these samples are older than 25 ka. So at least in terms of this part of the Loopline surface the most recent glacial activity is clearly associated with the last glacial maximum. These samples are discussed below in relation to the Larrikins Formation. The relevance to the Loopline Formation is that the similarity in the surface features of the two moraine belts referred to by Suggate (1965) is due to the fact that both moraines have been directly moulded by ice during the LGM, so the surface features are likely to be only a few thousand years different in age here. Just to the North of the Kapitea Reservoir spillway an older "Loopline" soil on the surface contains an identifiable layer of Kawakawa tephra near the base of the cover beds. The currently accepted age for this tephra is c. 27 ka. Therefore at least part of the Loopline Formation is older than this in this area.

The most recent definition of the Loopline Formation can be found in Suggate and Waight (1999). They propose that the Loopline Formation was deposited during a major MIS4 (c.70-60 ka) glacial advance. This correlation was loosely based on the selective use of the available radiocarbon ages from organic material in soils overlying and underlying the fluvioglacial gravel of this formation. Given the evidence available at that time, assignment to MIS4 was reasonable. The marine isotope stage correlation for the Loopline Formation is reexamined here in light of new numerical age data and it is proposed that the Loopline Formation was deposited during an early to middle MIS3 glacial advance.

The Loopline Formation is composed largely of glacial till and aggradational fluvioglacial gravel. It contains a relative paucity of gold-rich placer deposits. Gold is generally most abundant in bouldery lag deposits. Such lag deposits exist within the Loopline Formation but they are not as extensive or well developed as those of the Larrikins Formation or the Waimea Formation. This may indicate that there were differences in the environment of deposition between these events or that the duration of the events was not the same. It is tempting to speculate that relative to the Loopline event, the Larrikins event occurred at a time of lower sea level, deeper fluvial incision, more focused strath-cutting and steeper fluvial gradients in the main valley systems. It appears that meltwater discharge was focused along fewer and narrower flow paths during the Larrikins event, particularly the later stages of this event.

6.2.23b Kawakawa Tephra in Soil on the Loopline Formation

The Kawakawa tephra is present near the base of loess on Loopline Formation surfaces for instance at Chesterfield Road. This means that ^{14}C dating of materials situated on or within the Loopline Formation could return finite ages. Work on loess thickness, mineralogy and volcanic ash distribution by Mew et al (1988) and Neall et al (2001) is not in conflict with an MIS3 correlation for the Loopline surface. Mew et al (1988) suggest that there is no particular reason why the underlying glacial outwash gravel can't be as young as 40 ka, though it could also be older. So the potential for an MIS3 correlation for the Loopline Formation has been recognised for some time. This is not in conflict a single ^{14}C age of 17.5 ± 0.3 ka (NZ5633, pollen profile M81/9, Moar & Suggate 1996) obtained from soil overlying the Loopline Formation adjacent to Chesterfield Road on the same terrace at grid reference J32 N 4070 E 5520.
Neall et al (2001) confirmed that in the Kumara area the tephra occurs through the loess and organic soil (about 45 cm thick) that rests on the Loopline Formation, and in the upper half of the loess on the Waimea and Cockeye Formations. Trace amounts of redeposited tephra can be found in loess on the Larrikins Formation, and in the lower half of the loess on the Waimea and Cockeye

Formations. They correlate the Loopline Formation with MIS4, an assumption that is based largely on the Suggate model. Neall et al (2001) do not provide numerical age control so this conclusion is unproven. They infer that MIS3 was not severe here, that there are no loess deposits from this period, and no significant outwash deposits (at the surface at least) from this period.

6.2.23c Numerical dating relevant to the age of the Loopline Formation

This study

A single $IRSL_{blue}$ sample was taken during this PhD project from the base of the soil profile on the Loopline Formation at grid reference J32 N 4070 E 5525 adjacent to Chesterfield Road. The age is for RR24 is 53.8±4.3 ka. Given that the sample is from the cover beds it does not define the depositional age of the Loopline Formation. The profile at the sample site is shown in Appendix one. Sample RR24 is situated immediately below a 20-40 mm thick heavily iron-cemented layer that extends laterally for a distance of several metres and this could potentially have influenced the dose rate received by this sample. In terms of laboratory performance there was no evidence of disequilibrium. The material that was sampled is fluvial overbank silt with minor organic content rather than loess (which is present further up the profile (but did not require dating as it is above the tephra horizon). Fluvial deposits, including silt, have not proven to be particularly suitable targets for luminescence dating in Westland. This thesis provides several clear examples and this site is potentially another. Sample RR24 is classified in table 5.4 in terms of the likelihood of complete bleaching at deposition. The sample is considered to have a poor to moderate chance of complete bleaching. Therefore the sample age is viewed as a maximum age and therefore the upper surface of the Loopline gravel could be younger than the sample age.

In mapping by Suggate & Waight (1999) the Loopline Formation overlies the Rutherglen Formation just inland from the Hokitika Airport and at Candle Light near Camerons. So the Loopline Formation must be younger than the Rutherglen Formation, which has a proposed depositional age of c. 66 ka in this PhD thesis. The Loopline Formation overlies the Awatuna Formation at Chesterfield (Suggate 1985: Moar & Suggate 1996; Suggate & Waight 1999; Preusser et al 2005; this PhD thesis) and so must be younger than the Awatuna Formation. The type section of the Awatuna Formation has a proposed depositional age of c. 48 ka in this PhD thesis. Silt resting just above the strandline sediments has been dated by ^{14}C yielding a mix of finite ages and results beyond detection. Contamination by younger carbon has previously been proposed but not proven so the finite ages still stand. Sample RR8 from this silt yielded an IRSL age of 34.8 ± 3.5 ka. Even under the likely influence of partial bleaching, IRSL samples from this unit taken by Preusser et al (2005) returned ages of 58 ± 8 ka (SDC5), 61 ± 8 ka (SDC7), 58 ± 7 ka (SDC8) and 71 ± 10 ka (SDC4). Preusser et al (2005) stated that the samples ages are very unlikely to overestimate the depositional age. Collectively provide a maximum age for the base of the Loopline Formation at the Awatuna Formation type section. The dated silt horizon is in direct contact with the base of the Loopline Formation and in fact grades up into it. Given that the Loopline Formation is composed internally almost exclusively of fluvioglacial sediment it will be difficult to date directly via ^{14}C and luminescence methods. At the time of writing dating at the Awatuna type section provides the best available control on the age of the Loopline Formation.

The Loopline Formation has a channelised margin against the Blake Formation at Blake's Terrace near Awatuna so it must be younger than the Blake Formation, the preferred IRSL age for which is 39.5 ± 2.4 ka. The Loopline Formation overlies the Craig Formation at Southside so it must be younger than the Craig Formation. The preferred IRSL age for the Craig Formation (this PhD project) is sample RR2 at 33.6 ± 3.6 ka. As discussed in relation to the Craig Formation above and in Chapter 5 (section 5.6.3) the depositional age for this formation is rather problematic.

Logically if these IRSL ages are correct the Loopline Formation cannot be older than MIS3. This evidence is perhaps not absolutely ideal but in the case of the dated silt at the Awatuna type section it is more simply circumstantial. Previously correlation with MIS3 was not favoured because the Waimea Formation was assumed to correlate with MIS6. This made it almost imperative that the Loopline Formation should be slotted into MIS4. However, now there is solid numerical dating evidence that the Waimea Formation is very unlikely to have been deposited in MIS6. It is unlikely to be older than MIS5a. The Waimea(1) and Waimea(2) Formations could potentially both correlate with MIS4. On the basis of the available IRSL dating the Rutherglen Formation could also be correlated with MIS4 further reducing the freedom in terms of correlation for the Loopline Formation.

Numerical age data that help to provide a maximum likely age for the Loopline Formation include:

- A maximum age of 84.9 ± 7.2 (RR29 by $IRSL_{blue}$) from a fluvial silt/fine sand unit situated below the base of the Loopline Formation at Blakes Terrace near Awatuna provides a limiting (maximum) age.
- A maximum age of 75.9 ± 7.6 ka (RR25 by $IRSL_{blue}$) from the base of the coverbeds on the aggradational fluvioglacial gravel of the Waimea Formation at Sunday Creek provides a limiting age. The upper surface of the Loopline Formation is incised below that of the Waimea Formation nearby at Chesterfield Road and clearly postdates the age of the Waimea Formation.
- A maximum age of ~ 63.6 ±7.4 ka from the base of the soil cover on the Blake Formation (early MIS3/late MIS4 for RR30 by $IRSL_{blue}$ which is probably an overestimate) at Blakes Terrace. Commencement of soil deposition here probably predates the fluvial aggradation that produced the Loopline Formation at Blakes Terrace.
- The mean age obtained by Preusser et al (2005) for the organic soil/silt immediately overlying the Craig Formation via $IRSL_{blue}$ is c. 65 ± 7 ka. The Loopline Formation rests on this silt and logically should be younger than that age.
- Ages of 47.8 ± 6.6 ka and 54.0 ± 7.3 ka (Early MIS3 ages (RR8 by multiple aliquot and single aliquot $IRSL_{blue}$ dating) were obtained for the Awatuna Formation at its type section. These ages are from marine sand situated beneath the Loopline Formation.
- An age of 37.8 ± 3.8 ka (RR9 by $IRSL_{blue}$) was obtained from peaty soil underlying the Loopline Formation at the type section of the Awatuna Formation.
- ^{14}C ages (NZ574 @ 45.447 ± 9.368 ka, NZ742 @ 37.405 ± 2.608 ka, NZ703 @ 32.874 ± 1.332 ka, NZ743 @ >50 ka, & NZ 702 @ >50 ka from Grant-Taylor and Rafter 1971) have been obtained from peaty soil underlying the Loopline Formation at the type section of the Awatuna Formation.
- Ages of 58 ± 8 ka, 61 ± 8 ka, and 58 ± 7 ka (Early MIS3, SDC5, SDC7 and SDC8, each by $IRSL_{blue}$) were from the organic silt beneath the Loopline Formation at the type section of the Awatuna Formation by Preusser et al (2005). In addition SDC4 from the base of the silt has an $IRSL_{blue}$ age of 71 ± 10 ka that overlaps SDC5, 7 & 8 within 1σ. Preusser et al (2005) suggest that overestimation the ages of SDC5, 7, & 8 is very unlikely. Therefore presumably the Loopline Formation is younger than about 58 ± 8 ka here.
- An age of 64 ± 5 ka (early MIS3/late MIS4 for SDC3 by $IRSL_{blue}$) was obtained from the top of the marine sand at the type section of the Awatuna Formation by Preusser et al (2005). There are additional luminescence ages by Preusser et al (2005) from the marine sand here that are discussed above in relation to the Awatuna Formation.
- Given the stratigraphic relationships reported in this thesis, by Suggate & Waight (1999), Moar & Suggate (1996) and by Suggate (1992) the Loopline Formation is likely to be younger than a number of additional $IRSL_{blue}$ ages from the Rutherglen and Awatuna Formations (being RR11 @ 53.9 ± 7.6 ka and RR12 @ 39.5 ± 2.4 ka at Point Elizabeth; RR20 @ 42.5 ± 6.8 ka at Schulz Creek; RR33 @ 56.3 ± 7.1 ka, RR15 @ 65.9 ± 5.4 ka, RR17@ 63.6 ± 10.5 ka at South Beach and Karoro).

Some of this evidence could be viewed as circumstantial but the quantity of data is almost overwhelming. There are no numerical ages of any type taken directly from the Loopline Formation indicating unequivocally that the Loopline Formation dates from MIS4.

Numerical age data that could be used to define a minimum age for the Loopline Formation includes:

- An age of 53.8±4.3 ka (early MIS3 for RR24 by $IRSL_{blue}$) from the base of the soil immediately overlying the Loopline Formation at the intersection of Chesterfield Road and EA Road. As discussed above this sample was taken from fluvial silt in a fluvioglacial environment. Even though the site is several km from the glacial terminus it should be regarded as proximal in terms of transport time and the sample is likely to suffer from partial bleaching. So the age is likely to be an overestimate. The Loess higher up the profile at this locality also contains the Kawakawa Tephra (c. 27 ka). Sample RR24 is situated immediately below a 20-40 mm thick heavily iron-cemented layer that extends laterally for a distance of several metres and this could potentially have influenced the dose rate received by this sample.
- An age of 56.8±5.9 ka **(**early MIS3 for RR3 by $IRSL_{blue}$) from a buried grey silt/loess horizon resting on the Loopline Formation at Southside, Hokitika. This silt could represent either a (brief?) hiatus in gravel accumulation during Loopline deposition, or a longer hiatus prior to deposition of the Larrikins Formation. This sample has been discussed previously. It is likely to suffer from partial bleaching as are the other samples taken by Preusser et al (2005) from this unit.
- An $IRSL_{blue}$ age of 78.1 ± 6.1 ka (RR28, Grid Ref NZMS J32 N 3370 E 6125) was obtained from the base of a surface soil on an area mapped by Suggate & Waight (1999) as Loopline Formation Moraine adjacent to the Kapitea Reservoir. The till beneath the soil here is almost exclusively composed of fresh Torlesse Greywacke detritus. In this area gravel provenance that is near to exclusively Torlesse Greywacke is associated with the Larrikins Formation rather than the Loopline Formation (Neall et al 2001). This site is within a few hundred metres of glacial erratic boulders situated on the same terminal moraine landform that were sampled during this PhD project for cosmogenic isotope dating by Tim Barrows (ANU Canberra) and myself. It is strongly suspected that this age the sample age for RR28 reflects an extreme case of partial (near zero) bleaching prior to deposition. An alternative interpretation is that the sample is from a previously unrecognised unit exhumed by glacial erosion and not re-buried by younger till during the Loopline and Larrikins events.
- An MIS4/3 age (LOL1 @ 64 ± 5 ka by $IRSL_{blue}$) from a gravel quarry near the intersection of Loopline Road and Stafford Loop Road. The sample was taken by Preusser et al (2005). Details are somewhat sketchy but the sample is apparently from a sand layer in the upper portion of the section. As discussed at length in Chapter 5 IRSL dating of sand from fluvioglacial sediment in an ice proximal situation is unlikely to yield a quality depositional age. The position taken here is that this sample has yielded an age that is influenced by partial bleaching. Although this cannot be proven for LOL1 it has been demonstrated for samples in the same geological context approximately the same distance from the relevant terminal moraine at Nelson Creek (see section 5.6.1).
- Cosmogenic isotope ages 22.8 ± 1.9 ka (LL-02), 22.4 ± 1.9 ka (LL-04), 14.2 ± 1.4 ka (LL-05), 19.7 ± 1.8 ka (LL-06) have been obtained on glacial erratic boulders on Moraine previously mapped as Loopline Formation adjacent to the Kapitea and Kumara Reservoirs by Suggate & Waight (1999). These boulders are situated close to the RR28 and LOL1 luminescence sample sites.
- At the Hatters Creek locality it is seems that the Loopline Formation underlies the upper buried silt unit (dated at >32.5 ka by ^{14}C) here. The Loopline Formation is likely to be older than the silt.
- The Kawakawa tephra dated at c. 27 ka is present near the base of grey loessic silts that rests on the Loopline Formation at Chesterfield.

This assessment should be compared with the luminescence ages from Okarito by Vandergoes et al (2005) which are summarised in table 6.27. There are two units of particular relevance to the age of the Loopline Formation, being the lower organic silt and the upper grey silt. Pollen from the upper grey silt is thought to represent stadial climatic conditions.

Site	Sample	IRSL(blue)	Post IR-OSL	Unit
101	OBD-1	13.2 ± 1.1	13.1 ± 1.2	Upper grey silt
102	OBD-2	13.3 ± 1.2	12.4 ± 1.3	Upper grey silt

103	OBD-3	16.2 ± 1.4	15.8 ± 1.4	Upper grey silt
104	OBD-4	18.4 ± 1.6	16.8 ± 1.4	Upper grey silt
105	OBD-5	24.4 ± 2.1	24.3 ± 2.2	Upper grey silt
106	OBD-6	30.6 ± 2.5	32.3 ± 2.7	Upper grey silt
107	OBD-7	25.5 ± 2.1	25.6 ± 2.2	Upper grey silt
108	OBD-8	34.1 ± 2.8	34.5 ± 2.9	Upper grey silt
109	OBD-9	33.7 ± 2.9	34.3 ± 3.1	Upper grey silt
110	OBD-10	31.8 ± 2.8	34.3 ± 3.2	Upper grey silt
111	OBD-11	34.7 ± 2.9	37.0 ± 3.2	Upper grey silt
112	OBD-12	31.9 ± 2.6	32.6 ± 2.7	Upper grey silt
113	OBD-13	44.9 ± 3.8	46.3 ± 4.3	Upper grey silt
114	OBD-14	43.2 ± 3.7	42.4 ± 3.6	Upper grey silt
115	OBD-15	48.4 ± 4.2	51.8 ± 5.0	Upper grey silt
116	OBD-16	50.1 ± 4.3	53.0 ± 4.6	Upper grey silt
117	OBD-17	54.6 ± 4.6	59.3 ± 5.7	Lower Organic Silt
118	OBD-18	66.4 ± 5.4	68.5 ± 5.8	Lower Organic Silt

Table 6.27: The sequence of luminescence ages in stratigraphic order from Core 0212b, Okarito Pakihi, Vandergoes et al (2005).

At Okarito the $IRSL_{blue}$ age at the transition from the organic silt upward into the grey silt is c. 50.1 ± 4.3 ka. As discussed in Chapter 5, for the purposes of this PhD thesis, $IRSL_{blue}$ is considered to produce more consistent ages than Post-IR-OSL in Westland. At core 0212b this appears to be the case, with substantially less variance in sample ages and a more consistent progression of ages down the core. There is a rapid upward change in the percentage of tree pollen in the Okarito composite at the transition from organic-silt to grey-silt. This transition is from an interstadial assemblage to a stadial assemblage. At face-value the timing is consistent with the age of the ice maximum for the Aurora 5 glacial advance (48-46ka) in Fiordland from Williams (1996). It is also consistent with the timing of the glacial advance that produced the L2 loess and M4a moraine in the Saltwater Forest area of South Westland which has been assigned limiting ages of 45 to 50 ka by Almond et al (2001).

In summary the available numerical age data are suggestive of deposition of the fluvioglacial Loopline Formation commencing no earlier than c. 58 ± 8 ka. Completion of deposition occurred no later than c. 41 ± 5 ka. The most intensively dated sequence is situated at Okarito. Here the key climatic transition, probably leading into the $Kumara2_1$ glacial advance and the deposition of the Loopline Formation, occurred at c. 50 ka. This proposal is broadly consistent with the bulk of the available numerical ages that bracket the event. It is also consistent with the timing from Barrows (2007) and Kolodzeij (2010) of an abrupt cooling of the sea surface temperature at marine cores SO136-GC3 and MD06-2986 adjacent to Westland following the early MIS3 thermal maximum at these sites. Similar cooling is evident at the same time in the SST at marine core MD97-2120 on the Chatham Rise (Pahnke et al 2003). A Southern Ocean cooling event is also demonstrated from ice core (EPICA Dome C) isotopic evidence and is dated at 45 – 40 ka by Stenni et al (2003).

Comparison with the timing of climate events elsewhere in the middle latitudes of the Southern Hemisphere is relevant at this point. Some key findings are as follows:

- Denton et al (1999) discuss climate change at Isla Grande de Chilo, Southern Chile. Here Gramineae pollen peaks represent cooling at 47.11 ka to 44.52 (^{14}C) ka.
- Mackintosh et al (2006) carried out cosmogenic isotope dating on moraines near Mt Field in the Tasmanian highlands. This work revealed a substantial glacial advance at 44-41 ka coinciding with a potential atmospheric temperature reduction of 7-8° C and an ELA lowering of up to 1100 m.
- Nurnberg & Groeneveld (2006) provide a long SST record for marine core ODP1172A which is situated on the East Tasman Plateau at 43°57.6' S, 149°55.7' E. Here a deep SST minimum occurred at c. 40 ka. Temperature depression at this time was as great as at the LGM.
- A long record of sea surface temperature was reported by Pahnke et al (2003) for marine core MD97-2120 situated at 45°32'S 174°56'E on the Chatham rise. A period of cool surface temperature commenced at c. 50 ka and ended at c. 40 ka with one modest but brief warming at around 45 ka.
- Nelson et al (1993) described the sampling of marine core DSDP594 situated at 45°31.41' S, 174°56.88' E on the Chatham Rise. They illustrate a sharp reduction in $CaCO_3$ content between 7 m and 6.5 m dated at c.48 ka to c.42 ka. Then from about 39 ka onward the $CaCO_3$ content is consistently low. From the same marine core Heusser and van der Geer (1994) report a decline in tree pollen commencing at c. 50 ka.
- Shane & Sandiford (2003) discuss pollen from Onepoto basin in the Auckland area. Rimu pollen peaks at c. 70-67 ka, c. 60-50 ka, and c.37-34 ka and declines abruptly from c. 50 ka. *Nothofagus fuscapora* pollen is at a continuous peak from c. 48-26 ka, the transition from a low percentage occurring c. 51-48 ka. There appears to have been a major climate transition here at 51-48 ka.
- Wright et al (1995) discuss pollen in marine cores S794 and S803. The transition from pollen zone 1 to Pollen zone 2 occurs at c. 43 ka by ^{14}C (c. 44 ka cal) and indicates substantial cooling. There is also as harp change in $CaCO_3$ at c. 43 ka (14C). Relatively warm oceanic surface water was present at these sites from about 59 ka to 43 ka.
- Carter (2007) extracted phytoliths from a loess core taken at Otaraia in the Wairarapa Valley, Lower North Island, New Zealand. The transition from the (lower) phytolith zone G to the (upper) phytolith zone (H) occurred at c 40 ka from (Carters) fig 4.4. This transition consist of an abrupt decline in tree pollen. The timing is based on an OSL sample age of 44.7 ± 2.7 ka from slightly deeper in the profile.
- Shulmeister et al (2001) and Okuda et al (2002) discuss pollen from a sediment core at Lake Poukawa, Hawkes Bay. The PK6/PK5 pollen zone transition at c. 50 ka represents a change from relatively mild moist conditions to cool dry conditions. The timing of the transition is based on OSL dating and Tephrochronology.
- Ice core isotopic evidence indicates substantial cooling from c. 48-42 ka at the Vostok core site in Antarctica (Petit et al 1999). This cooling occurred between Antarctic interstadials A3 and A2. Similar cooling occurred at Siple Dome in Antarctica. There ice core isotopic evidence from Brook et al (2005) indicates substantial cooling events at c. 52-47 ka (btw A3 and A2) and c. 45-40 ka (btw A2 and A1).
- The well-dated high-resolution SST record at core MD01-2378 in the Timor Sea off the Western Australian margin (13°04.950′S, 121°47.270′E) by Durkop et al (2008) demonstrates a period of substantial cooling from c. 46 ka to c. 39 ka.
- Heusser et al (2006) showed that the *Nothofagus dombeyi* pollen (Southern Beech) spectra at Tagua Tagua, Southern Chile indicates a period of severe cold climatic conditions commencing at c. 53 ka. A partial recovery occurred from around 50 - 48 ka. This was followed by a further decline from about 48 ka to 42 ka. A substantial recovery peaked at about 39 ka, lasting to 33 ka, followed by a long sustained period of cold climate through to 16 ka.
- Figure 28 of Heusser et al (1999) establishes the relative prevalence of evergreen forest and Subantarctic parkland at Taiquemo for the past 60,000 years. Evergreen forest peaked at c. 57-47 ka, with a minimum at c.46-43 ka followed by a modest peak in evergreen forest from about 43-42 ka.
- Kaiser et al (2007) describe a rapid and sustained drop in alkenone SST at ODP202-1233 (41°00'S, 74°27'W) off the southern Chilean Pacific margin at c. 52 ka.
- Zech et al (2008) reviewed the evidence for the timing of glaciation in Chile between 30°S and 40°S. They find that the maximum extent of glacial ice during the last glaciation occurred between 40 ka and 35 ka. This was attributed to a northward shift and/or intensification of the westerly air stream over this latitude band.

The timing of these independently dated events within and outside of North Westland indicates that there was a regional scale cool episode from c. 50 ka (cal) to 40 ka (cal) with at least one modest but brief interstadial episode. The purpose of assembling this information is to show that glaciation in Westland at this time would be consistent with a variety of contemporaneous features of the climate in the mid to high southern latitudes.

From around 40 ka onward it is assumed that eustatic sea level was in a generally falling trend. Partial to glacial retreat coinciding with declining sea level and continuing tectonic uplift would tend to encourage widespread fluvial incision and strath cutting in the major river systems of North Westland. If this was the case then a significant part of the middle to late MIS3 period (between about 45 ka and 34 ka) might not be represented by widespread surficial fluvial deposits or by visible terrace features in the main valleys. The onset of widespread glaciation at c. 34 ka culminating at c.28 ka, as proposed by Suggate & Almond (2005), would have led to widespread fluvial aggradation in the main valley systems of North Westland. This is likely to have resulted in burial of middle MIS3 fluvial terraces and fluvial deposits beneath MIS3/2 transition fluvioglacial outwash. Another glacial advance dated at c. 24.5- 21.5 ka by Suggate & Almond (2005) continued this burial process.

A fan shaped body of MIS2 till and outwash has been identified (this study) to the west of the Kapitea Reservoir and Kumara Reservoir areas. This relatively young outwash is quite distinctive lithologically, being composed almost exclusively of greywacke with only minor granite. Similar greywacke dominated gravel is not present on the Loopline terrace surface at Chesterfield Road, which indicates that Kapitea Creek had probably commenced fluvial incision in the Chesterfield area when the youngest part of the "Loopline" Moraine was being constructed adjacent to the Kapitea and Kumara Reservoirs. This Moraine belt is discussed further in the context of the Larrikins Formation below. On the basis of cosmogenic isotope dating on glacial erratic boulders it appears that parts of the type section for Loopline Formation moraine, thought previously to date from MIS4, may in fact be MIS2 Larrikins(1) Formation dating from around 22 ka. If this is the case then there might not be any numerical dates that give a tightly constrained minimum age for Loopline moraine anywhere in North Westland.

There is a prominent Holocene sea-cliff adjacent to State Highway 6 from Blake's Terrace at Awatuna northward to Kapitea Creek. In the cliff face there are a number of exposures of parts of the Quaternary sequence below the Loopline surface. Several sub-units are exposed. About midway up the cliff face a thick (several metres) fluvial silt/fine sand horizon is present. This unit is laterally continuous over a distance of about 2 km along the marine cliff. The gravel immediately above the silt is moderately weathered in some exposures. The surface 5 to 10 metres of gravel has a comparatively fresh appearance. This uppermost gravel is granite rich and almost certainly not a correlative of the greywacke dominated (probable Larrikins Formation) till and surficial outwash at Loopline Road adjacent to Kapitea reservoir that is mapped by Suggate & Waight (1999) as Loopline Formation. The sequence adjacent to Kapitea Reservoir is exposed in a gravel quarry near the intersection of Loopline Road and Stafford Loop Road and is as follows:

----------	0 m	
Thin dominantly organic soil with minimal loess		On probable Larrikins Formation
----------	~0.3 m	
Relatively fresh greywacke dominated gravel		Probable Larrikins Formation c.22 ka?

----------	~2.5 m		Probable unconformity
Peat		}	
Grey silt		}	Discontinuous unit
Brown silt		}	
----------	~3.0 m		
Somewhat weathered granite-rich fluvioglacial gravel (base not exposed)			64 ± 5 ka (LOL1, Preusser et al 2005) Depth of sample LOL1 uncertain

The lower gravel unit at the Stafford Loop Road Quarry is similar in appearance to the uppermost gravel in exposures at the Holocene Sea Cliff between Chesterfield and Awatuna. The greywacke dominated gravel is not present at the sea cliff in this area, but similar gravel is present at the sea cliff in the Larrikins outwash terrace further north at Kumara Junction.

Clearly there was an influx of greywacke dominated gravel into the upper portion of Kapitea Creek coincident with the deposition of the older portion of the Larrikins Formation. This does not appear to have accumulated across the Loopline outwash surface further down-valley in the vicinity Chesterfield. Either the young outwash gravel is not recognised due to mixing with older gravel in the lower portion of Kapitea Creek, or this creek has previously incised a channel below the aggradational Loopline surface that was not subsequently overtopped during the Larrikins event in the Chesterfield area. The second option is likely because the Kawakawa tephra is widespread in the loess on the Loopline terrace at Chesterfield (Mew et al 1988). Note that generally Larrikins Formation outwash is not overlain by a substantial thickness of grey loess, which distinguishes this formation from the Loopline Formation. Kapitea Creek is recognised by Suggate & Waight (1999) as a meltwater channel active during Larrikins deposition, the meltwater being sourced from terminal positions situated east of the Kapitea and Kumara Reservoirs (but not relating to ice overtopping the Loopline terminal position as proposed here).

6.2.23d Luminescence Dating at the Nelson Creek Farm Settlement Gravel Quarry

Preusser et al (2005) (their section 4.7 and table 6.28 in this thesis) report the results of luminescence dating for samples from a gravel quarry at the Nelson Creek Farm Settlement near Souters Creek, Bell Hill (K32 934534). The site is mapped as Loopline Formation by Nathan et al (2002) and is assigned to MIS4 by them. The luminescence ages are as follows:

Table 6.28: Luminescence ages from the Nelson Creek farm settlement gravel quarry by Preusser et al (2005)

Soil Sequence	(upper)	NCL 4	13.9 ± 1.5 kyr	post IR-OSL
			14.1 ± 1.5 kyr	$IRSL_{UV}$
	(lower)	NCL 3	15.5 ± 1.5 kyr	post IR-OSL
			15.6 ±1.7 kyr	$IRSL_{UV}$

Gravel Sequence		NCL 1	109 ± 8 kyr	$IRSL_{(blue)}$-SAR/FS
		NCL 2	113 ± 8 kyr	$IRSL_{(blue)}$-SAR/FS

At face value the dating from this quarry implies there is:

MIS2/1 transition loess/soil
No LGM loess/soil
No MIS3 loess/soil
No MIS4 loess/soil
No MIS5b loess/soil
No MIS5c loess/soil
No MIS5d loess/soil

MIS5 coarse fluvioglacial gravel

Inspection of much of the terrace carried out (on foot) for this project indicates that the soil/loess cover is relatively thin, i.e. generally no more than 0.5 m, across the entire terrace surface, including at the sampled quarry. The terrace surface has a relatively "youthful" appearance. At the quarry site the gravel is fluvioglacial in character. The surface rises in an uninterrupted manner to the south at a moderate to steep grade and merges with a well defined moraine loop topped by large glacial erratic boulders. This moraine is situated within 1.5 km of the quarry so the "Loopline" terrace in question is an immediately ice-proximal outwash surface. In association with Tim Barrows (ANU, Canberra) 4 large glacial erratic boulders have been sampled from this moraine for cosmogenic isotope dating. The results of this work that are relevant to the Nelson Creek Farm Settlement quarry are discussed in Chapter 5 (section5.6.1). The geomorphology of the area and the location of the sample sites are shown in figures 3.6 and 5.1. At the time of writing two of the large erratic boulders have confirmed ages. The exposure ages for samples LPL-08 and LPL-11 are 35.3 ± 3.0 ka and 25.0 ± 2.1 ka. It is clear in the field (and from figure 5.1) that the moraine and outwash surfaces are genetically linked. The implications of these ages are discussed in section 5.6.1 in terms of the likelihood of partial bleaching in luminescence samples NCL1 and NCL2. It is concluded that the sample ages for NCL1 and NCL2 are not likely to be true depositional ages. Erratic boulders from two additional "Loopline" terraces have been dated as part of this project in conjunction with Dr Barrows. Both terraces fall within the area mapped by Suggate and Waight (1999). One terrace is situated at the top end of Twelve Mile Valley. The other is situated at the Blair Farm Settlement. The sample locations for both terraces are shown in figure 3.5. These two sites are discussed further below.

The next prominent belt of moraines up valley from the gravel quarry site (towards Lake Brunner) are mapped by Suggate & Waight (1999) as Larrikins Formation (MIS2). These moraines have been mapped as Larrikins Formation by Suggate and Waight (1999). The relationship with the Nelson Creek Farm Settlement terrace is shown in figures 3.4 and 3.6. In terms of geomorphic character, and the state of preservation the Nelson Creek moraine loop is similar to the "type section" for Loopline moraine at Loopline Road near the Kumara/Kapitea reservoir and to the "Loopline" moraine/outwash at the "Blair's Farm Settlement" between Kokiri and Molloy's Lookout in the Arnold Valley.

Preusser et al (2005) suggest the cover beds are up to 1 m thick in the Nelson Creek quarry. Previously it has been assumed that the till and outwash gravel that forms the terrace dates from MIS4 (Suggate model). The site is just outside the area mapped by Suggate & Waight (1999) for the Kumara-Moana 1:50,000 geological map sheet. Preusser et al (2005) suggest the options for correlation are the Loopline and Waimea Formations, and then opt in favour of the Waimea Formation without indicating the divergence from mapping by Nathan et al (2002). Just to the west, (grid ref K32 5450N 8850E) Suggate and Waight (1999) map the Waimea Formation as an older and much higher terrace level, which is the interpretation favoured here and means the much lower Nelson Creek terrace is probably not part of the Waimea Formation. That does not automatically imply it is part of the Loopline Formation though.

Soils on the higher level terrace have been described by Hammond et al (1991), Mew et al (1986) and Moar & Suggate (1996) and Suggate & Almond (2005) from profiles at a forestry road situated on Grahams Terrace (grid ref NZMS 260 K32 928588). Pollen diagrams, ^{14}C dating, and the Kawakawa Tephra from the Grahams Terrace site are discussed above in relation the age of the Waimea Formation.

At the Nelson Creek gravel quarry samples loess samples NCL3 and NCL4 by Preusser et al (2005) yielded very young OSL and IRSL ages implying that deposition may have occurred during the last

deglaciation between about 16 ka and 13 ka. The thin loess rests on fluvial gravel. Samples NCL1 and NCL2 imply the gravel was deposited around 100 - 120 ka. The dated material consists of sand rather than silt and the fraction dated was fine sand. Preusser et al (2005) correlate the gravel with MIS5d. There is no sign of the development of a significant organic soil/silt beneath the loess at this site. So Preusser et al (2005) are implying either a very long depositional hiatus, or basal soil dissolution, or soil erosion. These options were not discussed. These ages would be more plausible if the outwash dates from early MIS2 or late MIS3. However, if the outwash dates from about 110 kyr as suggested by the IRSL ages then there is clearly a problem. Most other Late Quaternary surfaces previously thought to be older than MIS4 exhibit organic horizons of significant thickness situated below the MIS2 loess.

Thick loess dating from MIS2 was deposited within about 2 km to the northwest at Grahams Terrace. The Kawakawa tephra is present at Grahams Terrace and is described by Hammond et al (1991). Some thermoluminescence work was done at Grahams Terrace (Berger et al 1994) confirming the age of the tephra. Radiocarbon dating carried out at Grahams Terrace by Hammond et al (1991) confirms an MIS2 origin for a major part of the loess at the site. In addition the c. 27 ka Kawakawa tephra is present as a macroscopic layer at Grahams terrace, as discussed above in relation to the coverbeds on the Waimea Formation. So thick loess from the LGM is present nearby on older surfaces (not just loess from the more recent period of deglaciation). There has been no sampling for the Kawakawa tephra at the Nelson Creek / Souters Creek quarry site. As discussed by Neall et al (2001) traces of this tephra are found at most older sites where a detailed examination has been carried out. Sampling for the tephra would be an interesting exercise for the Nelson Creek Quarry site particularly if it is actually an MIS5 feature.

6.2.23e Luminescence dating at a Gravel Quarry near Hokitika

The Hokitika Gravel quarry is situated in fluvioglacial gravel at grid reference J33 456295. This terrace has been mapped as Loopline Formation by Nathan et al (2002). They assign the terrace to MIS4. Preusser et al (2005) state clearly in their abstract that the Loopline Formation dates from MIS4 and that the terrace at this site has previously been mapped as Loopline Formation. They are correct in suggesting that the terrace has not been traced directly back to a moraine ridge. The implication by Preusser et al (2005) is that the terrace might not actually be Loopline Formation. Luminescence dating of the cover beds for the Hokitika Quarry by Preusser et al (2005) gave results as follows:

Soil at the Hokitika Gravel Quarry

BSG 4	21.9 ± 2.1 ka by $IRSL_{UV}$, SAR/FG	27.2 ± 2.2 kyr by post-IR OSL from base of soil
BSG 5	22.0 ± 2.8 ka by $IRSL_{UV}$, SAR/FG	25.1 ± 2.8 kyr by post-IR OSL from base of soil

This compares with samples taken from the surficial cover at the Phelps mine which gave the following results:

Soil at the Phelps Mine

PGM 11	19.3 ± 2.5 ka $IRSL_{UV}$	17.1 ± 2.1 kyr	post-IR OSL upper sample
PGM 10	22.4 ± 2.3 ka $IRSL_{UV}$	21.5 ± 1.5 kyr	post-IR OSL lower sample

Samples were also taken for luminescence dating from sand layers about 1.2 m below the top of the gravel at the Hokitika Gravel Quarry by Preusser et al (2005). The sample ages are as follows:

Luminescence Dating of Gravel at the Hokitika Quarry

BSG 1	82 ± 6 ka $IRSL_{blue}$ SAR/FS from gravel below the soil
BSG 2	85 ± 6 ka $IRSL_{blue}$ SAR/FS from gravel below the soil

BSG 3 88 ± 8 ka $IRSL_{blue}$ SAR/FS from gravel below the soil

Preusser et al (2005) suggest that several small aliquots of one sample gave a non-skewed distribution of equivalent doses, implying complete bleaching of the IRSL signal prior to deposition. They also say that all other samples from similar sediments collected for their study indicate complete bleaching. They then state: "Age overestimation due to partial bleaching of the IRSL signal thus seems rather unlikely." This conclusion is not supported by their linear regression of IRSL and TL ages (their figure 8). Their conclusion is examined in detail in Chapter 5 (sections 5.6, and in particular section 5.6.5). In the discussion of potential partial bleaching issues and the implications various North Westland localities and sediment types it is concluded that IRSL dating on sand-sized feldspar is not an acceptable method. This conclusion applies to the Hokitika gravel quarry. The likelihood that sand sampled from this quarry was fully bleached prior to deposition is remote. As noted in section 5.6.5 the site is simply too close to the terminal glacial position for a claim of full bleaching to be sustainable. Any such claim would need to be backed with strong evidence specific to the samples concerned and this was not provided by Preusser et al (2005). As noted in Chapter 5, sites proximal to glacial moraines provide a near perfect opportunity for deposition of partially bleached sediment. Unfortunately, short of intensive single grain dating on individual samples there is no way to properly assess the extent of partial bleaching. The most secure strategy is to avoid proximal fluvioglacial materials in favour of materials that are more likely to be well bleached. Such materials include loess and slowly deposited organic soil, but even these materials can be problematic in ice proximal situations. Partial bleaching has impacted on samples taken by Preusser et al (2005) and on samples taken during this PhD project. Many of these samples probably would not have been collected if the potential for partial bleaching had been better recognised in the early 2000's. Sampling efforts would have been concentrated at other sites.

Prior to the study by Preusser et al (2005) the gravel at the Hokitika Pit was defined as Loopline Formation. The Hokitika Airport is less than 1 km NW from the Hokitika Gravel Quarry. The surface at the airport was mapped as Loopline Formation by Suggate & Waight (1999) and is situated on the same terrace as the Hokitika Gravel Quarry. No more than 1 km inland (east) from the Hokitika Airport the Loopline Formation (same terrace) overlies the Awatuna Formation and the Rutherglen Formation (as also mapped by Suggate & Waight 1999). So these formations provide a limiting age for the Loopline Formation on the north side of the Hokitika River. Logically the Loopline Formation at the Hokitika gravel quarry must be younger than the Awatuna and Rutherglen Formations, both of which have preferred ages less than 85 ka in this study.

In terms of local cross-cutting stratigraphic relationships the Loopline Formation at the Hokitika gravel quarry must also be substantially younger than the physically higher Karoro Formation and Waimea Formations mapped by Suggate & Waight (1999) close by in the Blue Spur area. These Formations have been dated during this PhD project. The preferred correlation for the Karoro Formation is MIS5a and for the Waimea Formation either MIS5a or MIS4. If these correlations are accepted it leaves a very short interval for all of the events required for marine planation and deposition of the Rutherglen and Awatuna Formations prior to fluvial incision and commencement of the aggradation which resulted in the accumulation of the Loopline Formation all completed by about 85 ka. This is circumstantial evidence that IRSL samples BSG1, BSG2, and BSG3 have been influenced by partial bleaching. Many of the IRSL samples used in the dating of these older formations are from materials and sites that are less likely to have been influenced by partial bleaching than the samples at the Hokitika gravel quarry.

At the Hokitika Gravel Quarry it would appear there is a substantial depositional break between the gravel and the base of the coverbeds. As discussed above a rather similar pattern holds at the Nelson Creek Farm Settlement. This "erosional" or "non-depositional" event is not recorded at the radiocarbon and luminescence dated profiles (see Moar & Suggate 1973, Berger et al 2001) from

the Waimea Formation on the immediately adjacent (higher) terrace. These samples are discussed above in relation to the Waimea Formation. Here soil deposition occurred over an extended period prior to the LGM. In addition the soil stratigraphy on the higher terrace shows alternation between loess and peat accumulation. Nor is the "erosional" event recorded on the Waimea Formation at Sunday Creek (this study), Chesterfield road (Preusser et al 2005, Mew et al 1988), Blake's Terrace (this study), Kumara Cemetery or Grahams Terrace (Moar & Suggate 1996), or at Tasman View (Karoro and Rutherglen Formations, this study). The large hiatus or erosional break beneath the soil at the Hokitika Pit (~ 60 kyr) and at Nelson Creek (~ 95 kyr) is unexplained.

6.2.23f The Loopline Formation in the Arnold Valley between Kokiri and Moana

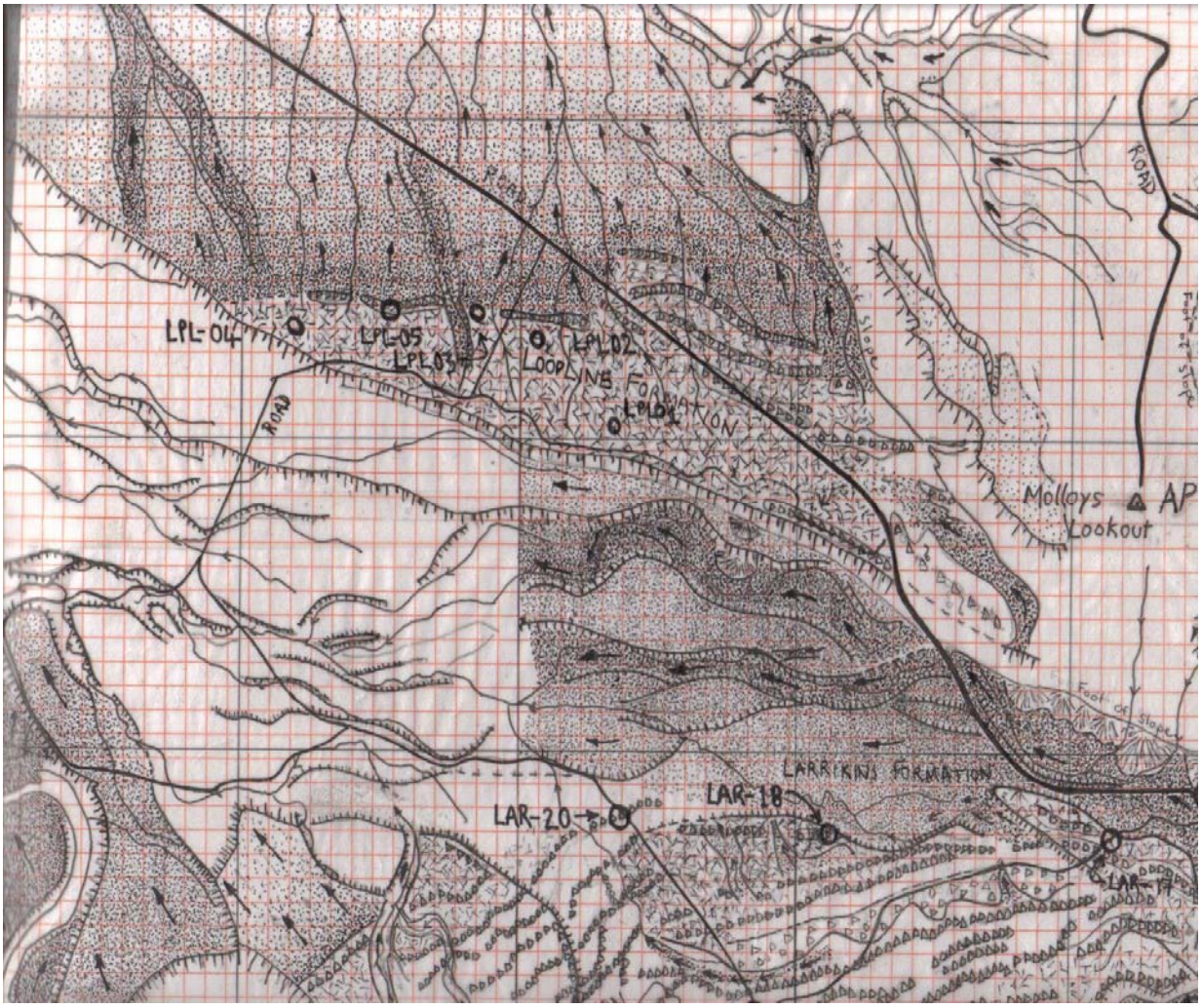

Figure 6.11 Loopline and Larrikins Formations in the Blair Farm Settlement area, Arnold Valley.

A number of cosmogenic isotope samples were taken large glacial erratic boulders from the Blair Farm Settlement area (see figure 6.11) in collaboration with Dr Tim Barrows. At the time of writing results are available for 3 samples taken from the Loopline Formation at the Blair Farm Settlement. These are LPL-02, LPL-04 and LPL05 with ages of 20.7±2 ka, 13.0± 1.3 ka and 19.2±1.6 ka respectively. The ages are listed in table 6.29 below. It is reasonably clear that these ages probably place the upper end of this Loopline terrace, including the moraine and adjacent fluvioglacial outwash firmly within the LGM. The result is similar to that using the same dating method at Loopline Road. The Loopline terrace at the Blair State farm has previously been mapped as Loopline Formation by Suggate & Waight (1999) and by Nathan (1978). These deposits at the

Blair Farm Settlement have previously been assumed to have an MIS4 age. At least at the surface it now appears that this is not the case.

Two very large glacial erratic boulders were sampled from the head of 12 Mile Valley just to the east of Molloys Lookout for cosmogenic isotope dating (see figure 6.12). Samples LPL-06 and LPL-07 yielded ages of 29.4±2.5 and 20.1±1.9 ka respectively. These samples are from an area mapped by Suggate & Waight (1999) as Loopline Formation and by Nathan (1978) as Waimea Formation. The samples tend to indicate that this moraine at this locality should be correlated with MIS2. The moraine at the head of 12 Mile Valley is significantly higher than that at the Blair Farm Settlement to the west of Molloys Lookout. The disparity is just sufficient for a suspicion that the higher surface might be slightly older than the lower surface. The surface features at both sites share a similar state of preservation with the moraine at the Nelson Creek Farm settlement (section 6.2.23d). The ages for LPL-06 and LPL-07 are similar to those for LPL-08 and LPL-11. The surfaces are at similar elevations and share a similar relationship to the younger Larrikins Formation. So it is tempting to conclude that these surfaces may have been formed during the same glacial advance within the early portion of the LGM.

Sample	Lab code	$[^{10}Be]_c$ ($x10^4$ g^{-1})	Σ Production rate (atoms $g^{-1}.yr^{-1}$)	Exposure age (ka)
Loopline Formation (Arnold River valley)				
LPL-02	ANU-M392-22	11.3 ± 0.75	5.507 ± 0.384	20.7 ± 2.0
LPL-04	ANU-M392-10	6.92 ± 0.48	5.357 ± 0.374	13.0 ± 1.3
LPL-05	ANU-M392-24	10.1 ± 0.43	5.297 ± 0.369	19.2 ± 1.6
Loopline Formation (Molloys Lookout)				
LPL-06	ANU-M392-25	17.1 ± 0.80	5.836 ± 0.407	29.4 ± 2.5
LPL-07	ANU-M430-27	11.6 ± 0.75	5.799 ± 0.404	20.1 ± 1.9

Data are normalised to NIST SRM 4325 assuming $^{10}Be/^{9}Be = 3.00 \times 10^{-11}$ Carrier $^{10}Be/^{9}Be = <1 \times 10^{-15}$.

^{10}Be decay constant = 4.62×10^{-7} yr^{-1}.

Table 6.29: Cosmogenic isotope ages from the Arnold Valley – Moana area.

Given the ages for samples LPL-06 (29.4 ± 2.5 ka), LPL-08 (35.3 ± 3.0 ka from Nelson Creek) and LPL-11 (25.0 ± 2.1 ka from Nelson Creek) it is tempting to conclude that a substantial portion of the Loopline Formation may have been deposited towards the end of MIS3 and/or during the MIS3/2 transition. Glaciation has been proposed for this period previously by Suggate & Almond (2005).

6.2.24 Chesterfield Interstadial (Late MIS3/Early MIS2)

Fluvial silt and soil was deposited on the Loopline outwash surface following Kumara2_1 glacial advance. This was followed by widespread soil erosion (Neall et al 2001) particularly on older surfaces. An iron pan was formed at the base of the soil at some localities. Peat then accumulated on the eroded surface.

A soil / loess sequence on the upper surface of the Loopline Formation at the junction of EA Road and Chesterfield Road contains a zone with substantial wood fragments close to its base. The

pollen in the profile is discussed by Moar & Suggate (1996). The peat zone contains substantial *Nothofagus* (beech) pollen, indicating a period of modest climatic amelioration subsequent to the deposition of the underlying glacial outwash gravel. As reported by Suggate & Moar (1996) a ^{14}C age of 17.5 ± 0.3 ka was obtained from highly organic material at the base of the loess/soil this site. This age has been rejected on the basis of assumed contamination by young carbon, at least partly because the 27 ka Kawakawa tephra has been recovered from loess on the same terrace, presumably at a similar or shallower depth. Luminescence sample RR24 comes from brown silt situated below the peat at this locality (grid ref J32 N 4070 E 5525) and returned an $IRSL_{(blue)}$ age of 53.8±4.3 ka. If the age is correct then the clear implication is that a forest containing *Nothofagus* was present at the site for at least part of MIS3. This could perhaps be correlated with the near-interglacial conditions at around 37-34 ka at "The Hill" on Wilson's Lead Road near Westport (Burge 2007).

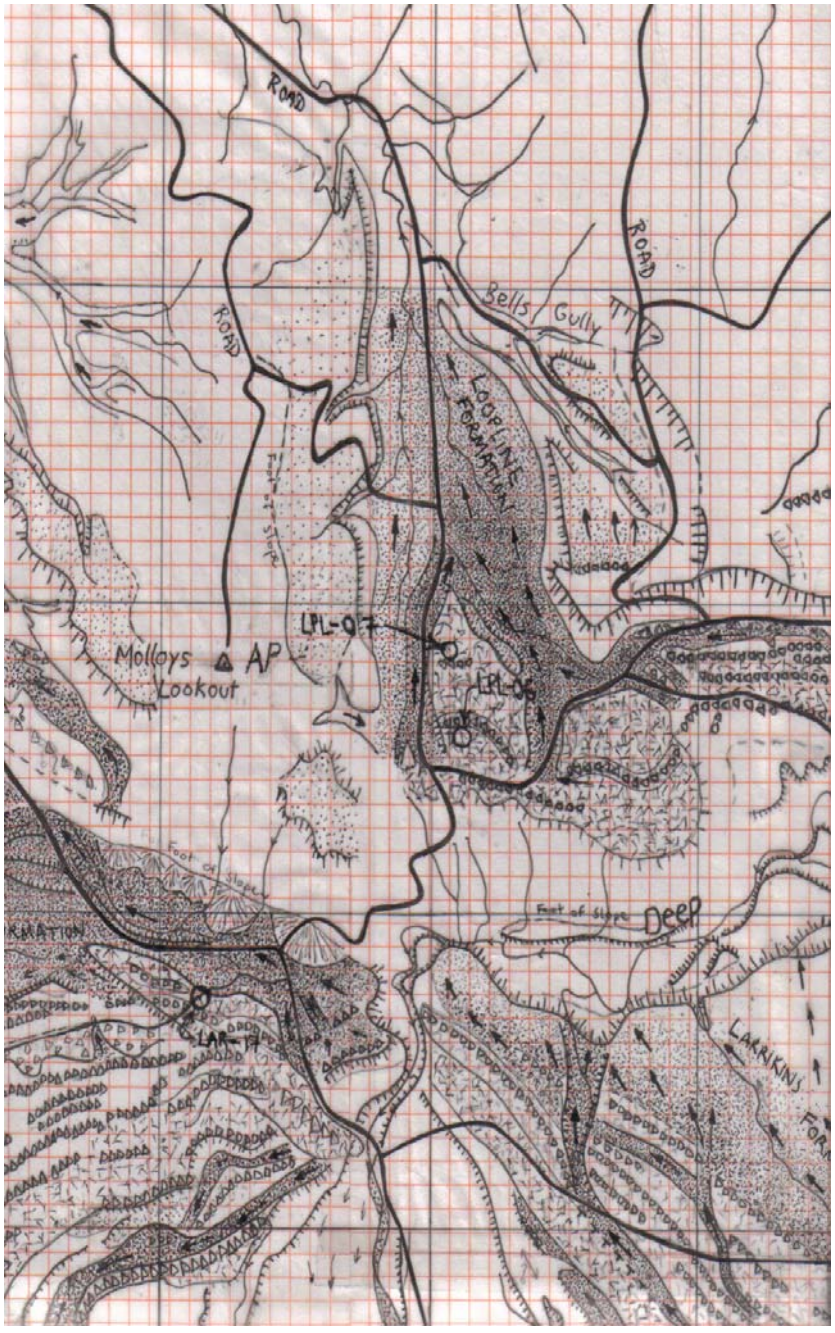

Figure 6.12 Loopline Formation in the Molloys Lookout area, Arnold Valley near Kotuku

6.2.25 Larrikins(1) Formation (MIS2 Stadial, Otira Glaciation, Kumara 2_{2a} Advance)

6.2.25a Introduction

This is an informal re-definition of parts of the Loopline Formation. The previously description for these deposits can be found in Suggate and Waight (1999). Another relevant paper is that by Suggate and Almond (2005) which extends the LGM is South Westland back to c.34 ka.

For North Westland the Larrikins Formation is generally held to correlate with the Last Glacial Maximum. Deposits consist largely of glacial till, lake beds, and fluvioglacial outwash gravel. Landforms include fluvioglacial floodplains and belts of moraine. In addition the surface expression hides buried channels that are probably of strictly fluvial rather than fluvioglacial origin. The Larrikins(1) Formation postdates deposition of the Kawakawa Tephra (circa 27 ka).

One of the key localities defining the relationship between the Loopline Formation and the Larrikins Formation is situated in a cutting beside Stafford-Loop Road close to the Dillmanstown dam adjacent to the Kapitea Reservoir. Here Larrikins till rests above older till that may be Loopline Formation. At this site there is an intervening soil that includes a peat layer and the Kawakawa Tephra. A radiocarbon age has been reported from the peaty layer by Burrows (1988).

Given the relatively young ages obtained off four "Loopline" surfaces the question arises as to what actually constitutes the Loopline Formation. It certainly appears that glacial advance and retreat was a rather dynamic process right though the LGM and that in some areas potential "Larrikins age" deposits obscure an older landscape of uncertain antiquity.

6.2.25b Radiocarbon Dating, Dillmanstown Dam, Stafford Loop Road

There are some question marks over the timing and significance of events during the LGM. The type locality for the Larrikins Formation is situated in the vicinity of Larrikins Flat. Close by and just north of the Kapitea Reservoir spillway at grid ref J32 3680 N 6215 E near Dillmanstown a well-defined moraine complex has been separated into two parts of different age. The site is a road cutting adjacent to Stafford Loop Road. The samples are from a thin peaty silt horizon situated beneath about 3 m of surficial till. Two radiocarbon ages from this site were discussed by Burrows (1988). The conventional ^{14}C ages for NZ 4408 and NZ 4407 are 18.95 ± 0.3 ka & 17.75 ± 0.25 ka respectively using a half life of 5730 years. Calibrated ages (Intcal-09) for these samples are given in table 6.13 above. The silty peat may represent a modest warming / interstadial prior to an ice advance around 22 ka (cal). Suggate & Almond (2005) propose that the till above the peat is Larrikins(2) Formation from a glacial advance at 24.5 to 21 ka. It is suggested the till below the peat is Larrikins(1) Formation from a glacial advance around 34 ka to 28 ka glacial. The age of the till beneath the peat is assumed as there are no numerical ages. However, the 27 ka Kawakawa Tephra has been found at the base of the peat at this site. As discussed below four cosmogenic isotope ages have been obtained from glacial erratic boulders on the surface of similar moraine adjacent to the Kumara Reservoir. This locality is mapped as Loopline Formation by Suggate & Waight (1999). It is situated 3.5 to 4 km to the south of the ^{14}C dated Kapitea spillway site. The maximum surface exposure age is 22.8 ± 1.9 ka (LL-02, see section 6.2.25c below).

It is not entirely clear whether the till overlying the peaty horizon at grid ref J32 3680 N 6215 E should be classified as Larrikins(1) or Larrikins(2). It is mapped by Suggate & Waight (1999) as Larrikins(1). But they have not recognized the substantially greater extent of Larrikins ice that is implied by the new cosmogenic isotope ages at Loopline Road. For the purposes of this thesis the

position of the Larrikins till in this area is redefined to coincide with the crest of the Loopline moraine to the west of the Kumara and Kapitea reservoirs as shown in figure 6.14.

6.2.25c Cosmogenic Isotope Dating, Kumara Reservoir

In the upper Kapitea area just west of the Kapitea and Kumara reservoirs there is a broad north-south oriented belt of moraine and ice-proximal meltwater channels. The meltwater channels run down slope to the west and northwest. This complex was mapped as Loopline Formation by Suggate & Waight (1999), and presumably represents the source area for gravels in the type section of the Loopline Formation. Part of this complex was examined during this project and samples were taken for cosmogenic isotope dating.

Six samples were collected for cosmogenic isotope (exposure) dating on glacial erratic boulders in the vicinity of the Loopline Road and the Kumara and Kapitea Reservoirs (locations in figure 6.13). The samples were collected by the writer and Dr Tim Barrows of ANU Canberra. Sample processing and age calculations were carried out by Tim Barrows. The boulders are situated in an area mapped as terminal and recessional moraine by Suggate & Waight (1999). The area has been assigned to the Loopline Formation, and is in fact part of the type section for Loopline Moraine.

The Loopline Formation is correlated with MIS4 in the Suggate model, so it should produce exposure ages of around 65 ka. The new exposure ages (received from Tim Barrows 9/10/08) are much younger and as they stand at present they are:

Sample	Age	Grid Ref		
LL-02	22.8 ± 1.9 ka	J32	N327	E819
LL-04	22.4 ± 1.9 ka	J32	N334	E814
LL-05	14.2 ± 1.4 ka	J32	N335	E814
LL-06	19.7 ± 1.8 ka	J32 N338 E816		

These ages indicate a probable cessation of deposition around 22 Ka with a single outlier at around 14 ka. So it seems that at least one of the exceedingly prominent moraine ridges adjacent and just west of the Kumara and Kapitea Reservoirs is, at least in part and at the surface, a feature that formed during MIS2. The same can be said for the recessional moraine under the Kumara Reservoir and to the east of the reservoir.

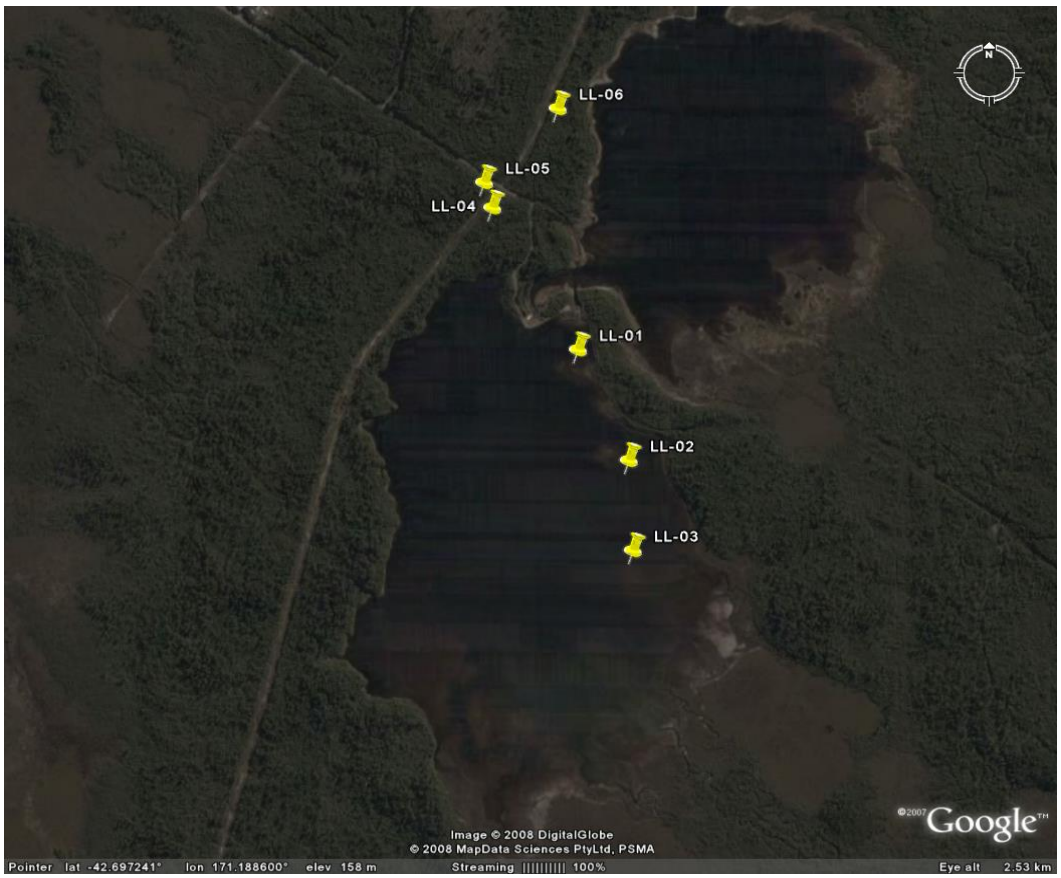

Figure 6.13 Location of cosmogenic isotope sample sites adjacent to the Kumara Reservoir. In this image the lake at the bottom (south) is the Kapitea Reservoir. The lake at the top is the Kapitea Reservoir.

It is worth noting that most of the erratic boulders on these moraines are composed of Torlesse greywacke and low rank semi-schist. Exposures in road cuttings and cuttings associated with the Kumara Reservoir dam indicate that the shallow alluvium is almost exclusively composed of greywacke and schist. The granitic component is moderate to minor. The predominant characteristic of the outwash gravel comprising the Loopline Formation is its substantial granitic component.

The original photographs taken of the boulders by the writer have not survived. Several of the boulders are covered by root-mat and shrubs and situated beneath a higher canopy so the photographs were not particularly informative. The boulders situated on the lake floor have been submerged each time the site has been revisited and so could not be re-photographed. Each of the boulders was of substantial size being both longer and wider than 2.0 m and higher than 1.5 metres from base to top.

6.2.25d Stafford Loop Road Quarry

There is a road-metal quarry near the intersection of Stafford Loop Road and Loopline Road (J32 602342). The provenance of the fluvioglacial gravel has not been studied in detail, but there appears to be a significant difference between the Loopline and the Larrikins gravel visible in the quarry face. The Loopline gravel contains substantially more granitic detritus than the overlying Larrikins detritus. Similar differences are also apparent between the mineralogy of soils on the different terrace levels in the Kumara area (Neall et al 2001).

Surficial loess and Peat

Upper gravel, 2 to 4 m thick. Abundant greywacke and relative paucity of granitic detritus.

Discontinuous but locally thick (~1m) buried organic soil.

Lower gravel, 3 m^{+} thickness, base not exposed. Rich in granitic detritus.
Somewhat more weathered than the upper gravel.

Preusser et al (2005) sampled material from the Stafford Loop Road Quarry. Sample LOL1 returned an IRSL-SAR age of 64 ± 5 kyr. Presumably the sample came from a sandy horizon in the lower, older gravel unit. While this is speculation it is backed to some extent by the shallow coverbed stratigraphy at other sites in this general area (including a number of soil profiles, see Appendix 3), by the presence of a macroscopic (c.27 ka) Kawakawa tephra bed in coverbeds on the Loopline Formation nearby at the Kapitea Reservoir, by 14C dating of peat overlying the Loopline Fm at Stafford Loop Road adjacent to the Kapitea Reservoir and finally by cosmogenic isotope dating (see above) of erratic boulders of the Larrikins Formation on nearby moraine surfaces. If LOL1 was derived from the upper gravel at this site then there is clear evidence for extreme partial bleaching at deposition. The upper gravel is Larrikins Formation, is almost exclusively composed of very fresh greywacke detritus and was deposited during the LGM. One noteworthy feature of the quarry is that the east face contains a discontinuous but locally thick (~1m) dark organic soil layer that separates the upper greywacke gravel from the lower granitic dominated gravel. Unfortunately this part of the quarry face was buried by bouldery backfill before it could be recorded in detail. The buried soil probably represents both a substantial depositional hiatus and possibly a period of interstadial climate.

The fluvioglacial material from which LOL1 was derived is presumed (this study) to be part of the underlying gravel being either the Waimea(2) formation or the Loopline Formation. As discussed at length in Chapter 5, IRSL dating of sand from fluvioglacial sediment in an ice proximal situation is unlikely to yield a quality depositional age. The position taken here is that LOL1 is very likely to have yielded an age that is influenced by partial bleaching. Although this cannot be proven it has been demonstrated for samples in the same geological context approximately the same distance from the relevant terminal moraine at Nelson Creek (see section 5.6.1).

In the Stafford Loop Road – Loopline Road area referred to here the surficial features are dominated by deposits of the Larrikins(1) Formation. The surface soil is thin and loess is relatively poorly developed, as opposed to the normal expectation for Loopline Formation surfaces. This interpretation is substantially different to that presented by Suggate & Waight (1999), in which the surface features are defined as Loopline Formation.

A similar sequence is preserved in a shallow cutting adjacent to an exotic forestry track at Grid ref J32 3600 N 6050 E the profile (profile D from Appendix 3) which is summarised immediately below. This site is about 700 m down the track from the starting point at Stafford Loop Road. Here the track widens out to into logging skid site. The sequence is:

	Spoil
---	
25 cm	Brown organic soil with abundant roots and stumps
---	
20 cm	Reddish-brown greywacke pebble conglomerate
10 cm	Light brown greywacke pebble conglomerate

30-35 cm	Grey laminated sandy silt and silty sand

5-10 cm	Light brown silt
---	
30 cm	Medium to dark brown organic silt

0-10 cm	Grey silt
---	
50 cm plus	Light brown sandy granite rich gravel

In terms of pebble provenance the shallow gravel at the Stafford Loop Road quarry is more like the gravel of the Larrikins Formation in the Dillmanstown-Kumara area than that in more distal exposures of the Loopline Formation. Cosmogenic isotope dating of erratic boulders on moraine about 1 km east of the quarry indicates a surface age of around 22 ka. This is the main belt of Loopline Moraine and is essentially the type section for that moraine. The moraine should be MIS4 but appears likely that a substantial part of the more surficial glacial till dates from MIS2. It is proposed here that the shallow gravel at the Stafford Loop Road quarry is part of the Larrikins(1) Formation and that the surface here dates from the LGM as indicated by cosmogenic isotope ages on glacial erratic boulders on the highest moraine ridges west of the Kumara reservoir and from the recessional surface to the east.

Further complicating the picture in this area is an outcrop (grid NZMS260 J32 N3660 E6075) adjacent to the Kumara Cemetery Road. The site stratigraphy is illustrated in soil profile F (Appendix 3). At this site and at soil profile E1 and E2 (Appendix 3) there is an upper Holocene organic soil overlying LGM loess which in turn overlies organic rich soil situated above gravel of the Loopline Formation. Further to the south at soil profile D (see above) the sequence is similar but with the addition of pebbly gravel above the lower organic soil. Further south again one reaches the Stafford Loop Road Quarry site where the pebbly gravel thickens into a bouldery greywacke conglomerate. The greywacke conglomerate is clearly of variable thickness and the thickness appears to increase towards the east in the direction of the moraine ridges adjacent to the Kapitea Reservoir and the Kumara reservoir.

The lower fluvial gravel unit at the Stafford Loop Road quarry could be older than the marine Awatuna Formation. The available ages certainly don't rule this out. At the type section near Chesterfield Road the Awatuna Formation rests on older fluvial gravel. This is likely to be the case at Blakes Terrace adjacent to SH6 at Awatuna, though it has not been observed in outcrop. It is the case in gold exploration drill holes that penetrate beneath the Loopline surface at EA road (see Stewart 1988).

This leaves two very prominent Larrikins moraine ridges here. The older moraine is situated to the west of the Kapitea and Kumara Reservoirs and is classified here as Larrikins(1) Formation. The younger moraine is situated to the east of the Kapitea/Kumara Reservoirs and west of State Highway 73. The younger moraine is further subdivided (as per Suggate & Waight 1999) into the Larrikins(2_1) and Larrikins(2_2) Formations.

In the new interpretation advanced here the Stafford Loop Road radiocarbon site close to the northernmost extremity of the Kapitea Reservoir has Larrikins(1) till resting on peaty silt that in turn overlies Loopline Moraine. Here the potential for significant contamination by younger ^{14}C was not raised by Burrows (1988). The ages don't contradict the established model. The key similarity between this site and the Raupo/Kamaka sites, where ^{14}C dating has been seen to produce acceptable ages, is rapid burial by fluvioglacial sediment (till) immediately following soil development.

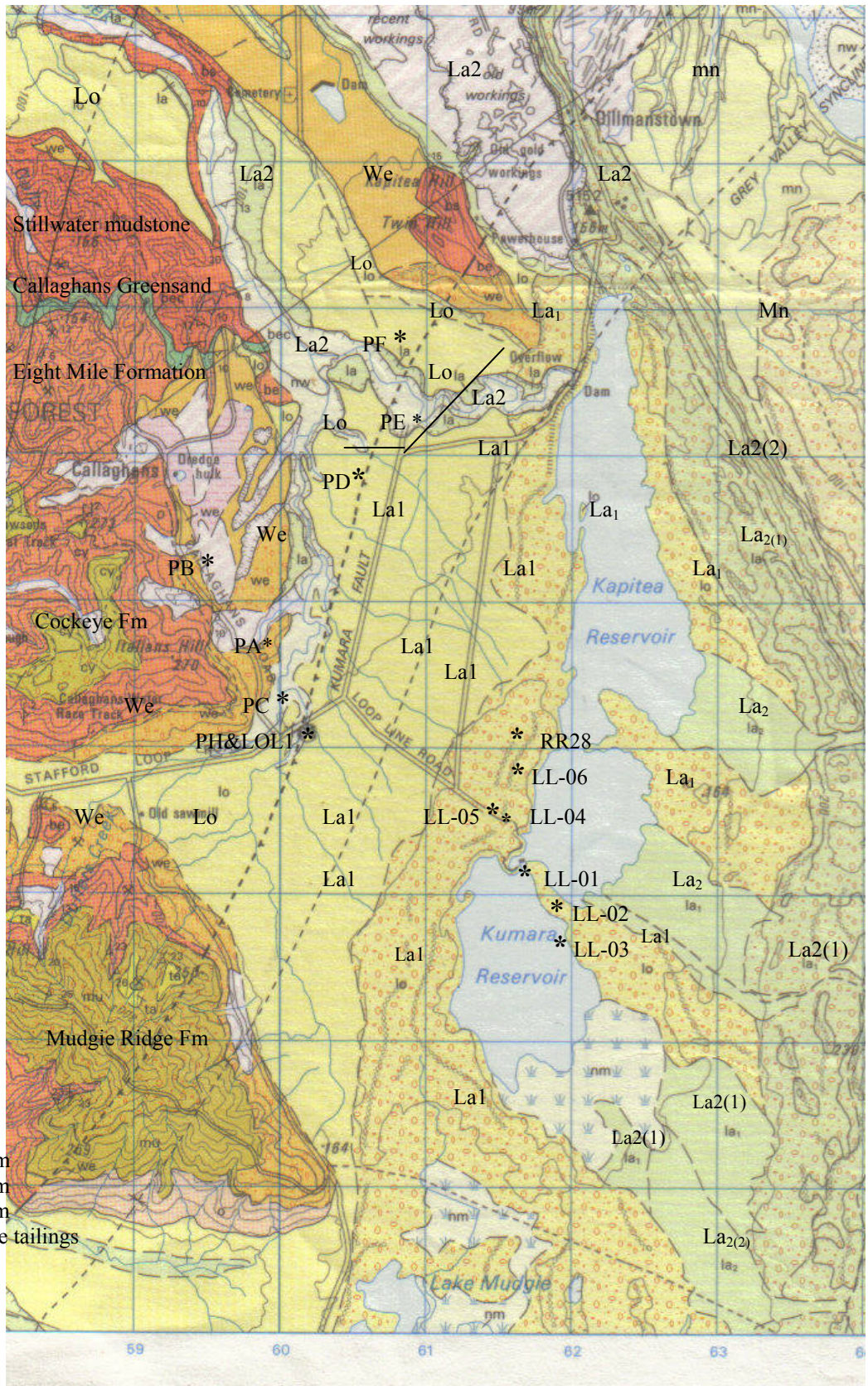

Figure 6.14 Geology of the Kumara Reservoir-Kapitea Reservoir area (base map from Suggate & Waight 1999) showing the locations of IRSL samples RR28 & LOL1, & cosmogenic isotope dating samples LL-01 to LL06 & the location of soil profiles PB to PH (from Appendix 3).

Burrows (1988) interpreted the radiocarbon ages from the Stafford Loop Road site, along with pollen from the peat, to imply a c. 1000 year hiatus representing "only a brief episode of freedom from ice coverage along the fluctuating ice margin, rather than a full interstadial".

The radiocarbon ages from the Stafford Loop Road site overlap those from a site at Raupo as reported by Hormes (2000) and Hormes et al (2003).

6.2.25e Numerical Dating at Kamaka

During this project one sample (RR21) was taken for $IRSL_{blue}$ dating from a well-known exposure of interbedded silt and gravel from a Larrikins Formation terrace. The sample site is situated in a road cutting adjacent to State Highway 7 at Kamaka in the Grey Valley. The sample returned an age of 35.3 ± 2.9 ka.

The Kamaka site contains a sequence that has several metres of fluvial gravel overlying fine-grained deposits are presumed to have formed during a modest interstadial event. The silty sediment has previously been dated by ^{14}C by Denton et al (1999) and Gage & Suggate (1958). The sequence at this locality has also been dated by luminescence methods by Preusser et al (2005).

The section was described by Suggate (1965) and more recently by Suggate and Almond (2005). Suggate (1965) comments on the pollen flora from the silt at this locality which includes 2% tree pollen, 10% herb and shrub pollen and 82% grass pollen. Denton et al (1999) reported fourteen non calibrated ^{14}C ages from the silt. These are, from top to bottom:

> 22.42 ± 0.23 ka; 22.46 ± 0.24; 22.36 ± 0.19; 22.62 ± 0.20; 22.16 ± 0.31; 22.49 ± 0.33; 22.10 ± 0.79; 22.57 ± 0.20; 22.86 ± 0.20; 22.73 ± 0.20; 22.68 ± 0.22; 22.65 ± 0.24; 21.99 ± 0.22; 22.38 ± 0.19 ka.

The non calibrated ^{14}C age from Gage and Suggate (1958) is 22.3 ± 0.35 ka. The ^{14}C ages correspond to a calendar age of around 27 ka. At this site the precise nature of the ^{14}C ages makes it difficult to accept the luminescence age for RR21 (this study) at 35.3 ± 2.9 ka. This appears to overestimate the age of this silt unit.

The silt appears to postdate the Kawakawa Tephra (which has a calendar age of around 27 ka). At the 1φ error there is little prospect of an overlap with RR21. So the single IRSL sample taken for this PhD project from Kamaka appears to overestimate the depositional age. Suggate and Almond describe the locality as follows:

The site (Fig. 6E) shows 3m of lacustrine sand, silt and clay, with a thin clay band with plant fragments at the base, separating coarse gravels above and below; the upper gravel has a markedly irregular base (Suggate, 1965). An age of 22,300 ± 350 ^{14}Cyr BP (ca 26,200 cal. yr BP) was obtained, and pollen, dominated by grass, indicated a bleak climate. Denton et al. (1999a, Fig. 3, caption) obtained 14 more ages ranging from 21,990 ± 220 to 22,860 ± 200 ^{14}Cyr BP (ca 25,900 to 26,800 cal. yr BP and averaging ca 26,300 cal. yr BP), so that the age of this site is firmly established. The lacustrine beds were attributed (Suggate, 1965) to temporary damming of the Grey valley by outwash from the much closer moraines in the Arnold valley. The upper gravel at Kamaka, >5m thick, is la2 outwash. The underlying gravel is thought to be la1 outwash, with the lacustrine beds formed in a short interval following the la1 culmination, when the Grey valley was temporarily dammed.

Table 6.31 Luminescence ages in stratigraphic order from Kamaka by Preusser et al (2005)

Sample	$IRSL_{blue}$ (ka)	TL_{blue} (ka)	OSL_{UV} (ka)	TL_{UV} (ka)	Method
KMK 8a	25.8 ± 2.4				MAA/FS
KMK 8b	24.4 ± 1.5				SAR/FS
KMK 7	28.5 ± 2.4	71 ± 21			MAA/FG
KMK 5a	21.8 ± 2.1				MAA/FS
KMK 5b	24.3 ± 1.5				SAR/FS
KMK 4	39 ± 5	75 ± 13	35 ± 6	36 ± 10	MAA/FG
KMK 3	45 ± 4	83 ± 16	29 ± 4	35 ± 4	MAA/FG
KMK 2	41 ± 5	84 ± 35	38 ± 5	84 ± 8	MAA/FG
KMK 6	23.4 ± 3.6	26.1 ± 2.9	38 ± 4	25.8 ±	MAA/FG
KMK 1	20.2 ± 2.1	17.3 ± 4.0			MAA/FG

FS = polymineral fine grains; FG = k-rich feldspar

Preusser et al (2005) report $IRSL_{blue}$ ages for 8 samples from the silt exposed in the road cutting at Kamaka. These are discussed in their section 4.1 and figure 5 and are provided in table 6.29 above. Five of these ages appear to be reasonably close to the ^{14}C age. At 1σ KMK7, 6, 8a and 8b have $IRSL_{blue}$ ages that are consistent with the ^{14}C ages. At 2σ KMK5a is also consistent with the ^{14}C ages.

KMK 1 is from the base of the fine-grained unit. At 2σ it does no overlap the ^{14}C age for the overlying organic layer and there is an apparent age inversion. It is tempting to reject KMK 1 on the basis that it underestimates the age.

The $IRSL_{blue}$ ages for KMK 2, 3 and 4 (41 ± 5 ka, 45 ± 4 ka, & 39 ± 5 ka) appear to be too old. These are the only $IRSL_{blue}$ ages from Westland that were rejected outright by Preusser et al (2005). These ages were rejected on the basis of incomplete bleaching. In figure 5 of Preusser et al (2005) these three samples are Stratigraphically above KMK1 and KMK 6 which are both much younger. The fact that Preusser et al (2005) do not mention failed IRSL results for other localities could be because most of the other localities do not have good ^{14}C control. The dating by Preusser et al (2005) for the Kamaka locality produced a mixture of accepted and rejected results. The likelihood that this is the only locality sampled during that programme that has incomplete bleaching issues is not high. It is also notable that $IRSL_{blue}$ was by far the most successful luminescence method tested at this locality. The other methods trialed here (TL_{blue}, OSL_{UV}, & TL_{UV}) performed poorly as can be seen in table 6.29.

The fine grained unit dated by ^{14}C and luminescence at this site is at an elevation well below the upper surface of the Loopline Formation in this part of the Grey Valley. So it is probable that the Grey River is responsible for a substantial fluvial incision and strath cutting event here subsequent to the deposition of the Loopline Formation.

So a number of $IRSL_{blue}$ samples (4 by Preusser et al 2005, and 1 from this project) have been unable to match the ^{14}C dating at Kamaka. Dr Rieser, who preformed the analysis for RR21, stated that the sample behaviour was neither excellent nor problematic. The sample is clearly affected by partial bleaching as are a number of other samples from Kamaka. As discussed in detail in Chapter 5 (sections 5.5 to 5.7) and in particular in section 5.6.2 partial bleaching is very difficult to detect. It cannot be corrected for in MAA polymineral finegrain IRSL dating. This is the primary technique used on this silt bed during this study and that by Preusser et al (2005). Sample RR21

produced an age that is closer to that expected from 14C dating than did samples KMK2, KMK3, and KMK4. This could have occurred purely by chance.

6.2.26 Raupo Interstadial Deposits (MIS2)

The following discussion relates to a site at Raupo in the Grey valley. The site is situated between the settlements of Totara Flat and Ahaura. It consists of an old gravel quarry in which the faces provide deep exposures into a sequence composed of gravel, sand, silt and clay. The sequence is:

Surface soil and loess

Fluvioglacial gravel (Larrikins Formation/Kumara2_1 outwash gravel) ~8 m thick
---
Interlayered silt, organic silt, sand, organic clay and sandy gravel ~ 1 m thick
---
Fluvioglacial gravel (Larrikins Formation/Kumara 1 outwash gravel) ~ 9m thick
---
Sand unit
--- Base of exposure

Accumulation of outwash gravel presumably resumed soon after this. Hormes (2000) attributed the upper outwash unit to the Moana Formation (Kumara3 advance, which did not begin until at least 18 ka (cal). Preusser et al (2005) have renamed the upper gravel unit as Larrikins Formation (Section 4.1 & fig 4). They report IRSL/post-IR OSL ages (RUG 1 & 2) of 18.9 ± 1.6 and 16.1 ± 1.1 ka from one horizon. These ages don't quite overlap at 1σ.

From the main silt unit RPO 2/1 & RPO 2/2 barely overlap at 1σ. Otherwise the luminescence ages are in fair agreement with ^{14}C from the same site.

Hormes (2000) produced a total of 55 ^{14}C ages ranging from 18.3 ± 0.2 ka to 19.8 ± 0.13 ka (^{14}C years) or 21.35 to 23.89 ka (cal) from the fine grained overbank deposits containing alternating silt and organic layers. The mean age for the uppermost layer is 22.35 ka (cal) implying deposition was probably complete by about 22 ka (cal).

Hormes et al (2003) split the fine grained section into 4 units for ^{4}C dating. The results, calibrated to calendar years are:

Organic Layer A (Top)	mean age of 22.35 ka
Organic Layer B	mean age of 22.47 ka
Organic Layer C	mean age of 22.93 ka
Organic Layer D (Bottom)	mean age of 22.96 ka

The IRSL ages coincide reasonably well with calibrated ^{14}C ages from the same locality. Together the two methods confirm an LGM correlation for the Larrikins Formation at Raupo. The nature of the fine grained unit accompanied by ^{14}C and luminescence ages was interpreted by Hormes et al (2003) as evidence that aggradation represented by the lower gravel unit came to an end before

23.25 to 23.89 ka. Originally this gravel was correlated with the Larrikins(2_2) Formation. This was changed to the Larrikins (2_1) Formation by Preusser et al (2005). Glacial advance associated with Larrikins (2_1) was probably followed a brief glacial retreat commencing no later than 23 ka (cal) then renewed glacial advance probably by ~22 ka resulting in the accumulation of the Larrikins (2_2) outwash.

Preusser et al (2005) provide two IRSL/post-IR OSL ages for the sand unit beneath the lower gravel unit. These are RLG1 and RLG2 at 31 ± 2 and 33 ± 4 ka respectively. It is not clear whether the sand unit defines the base of the aggradational gravel. The interpretation placed on these dates here is that the lower gravel probably correlates with Larrikins(1), and that aggradation resulting from a cooling climate is likely to have commenced by about 31 ± 2 ka. These two samples are at an elevation well below the upper surface of the Loopline Formation in this part of the Grey Valley. So it is probable that the Grey River is responsible for a substantial fluvial incision and strath cutting event here subsequent to the deposition of the Loopline Formation.

The Raupo ^{14}C ages are similar to those from the peat horizon at Stafford Loop Road, Dillmanstown (see below). The nature of the sediment at both sites implies a potentially significant warming at ~ 23 to 22 ka (cal) in the Grey Valley. The warming is likely to have been associated with a modest glacial recession. A significant warming is also recorded by Hellstrom et al (1998, 2000) at ~ 21 to 23 ka in a speleothem $\delta^{18}O$ record from a cave in the Nelson area.

Hormes et al (2003) discuss the potential for contamination of the ^{14}C dating samples by younger carbon. They conclude that only 3 of the 55 samples showed evidence of possible low level contamination. So there is little no evidence for significant contamination by younger ^{14}C in the organic bearing soil at the Raupo site. A similar conclusion holds for the radiocarbon dating by Denton et al (1999) at Kamaka. The key similarity between the two sites is rapid burial by fluvioglacial sediment following soil development. So why are ^{14}C ages from similar (but older) sites elsewhere in north Westland, and also subject to rapid burial, almost automatically assumed to suffer from contamination by younger carbon? A number of sites discussed above, including Bullock Creek, Cape Foulwind and Sunday Creek gave a mix of finite ages and ages that were beyond detection. For samples from Cape Foulwind (see discussion of the Waites Formation above and table 6.18) sample cleaning failed to shift the sample age substantially. This implies at worst a low level of contamination post ~ 50 ka for some samples at these sites. Naturally each sample and each site should be taken on its own merits.

6.2.27 Pre Larrikins(2) Fluvial Incision (MIS3/2)

6.2.27a Introduction

The accumulation of Larrikins(2) fluvioglacial outwash is preceded by the development of deeply incised fluvial channels at Adair Road between Rimu and Takutai, and at Kumara. It is inferred that rapid fluvial incision occurred during an interstadial event that was accompanied by a reduced input of glacial sediment into the fluvial system. Incision was probably aided by a very low MIS3/2 sea level which almost certainly increases gradients in the fluvial system. The precise timing of this deep incision event is uncertain but must fall into this general interval.

6.2.27b The Rimu Channel

A substantial abandoned fluvial valley is situated between the settlements of Rimu (J33 2450N 4600E, upstream end) and Takutai (J33 2700N 4100E, downstream end) just south of Hokitika. This is known as the Rimu Channel. It has a bold geomorphic expression. It is flanked by slightly older degradational terraces that post-date the Loopline fluvioglacial outwash sheet. The channel was a meltwater path for at least part of the Hokitika River during the early to middle portion of the LGM. It is incised below the base of the fluvioglacial gravel on the adjacent terraces. It is also incised below the base of the marine Blake and Craig Formations. The channel has been drilled intensively for alluvial gold and was extensively mined by bucketline gold-dredging. At the Holocene sea cliff the channel has a depth about 30 metres below the surface of the Nine Mile Formation (at least 25 metres below sea level). This is around 60 metres below the surface of the adjacent Loopline Formation. Contact relationships at Rimu (the head of the channel) demonstrate that incision predates the latest Larrikins Moraines and the Moana moraines. At Takutai the channel truncates the Blake and Craig marine strandlines and the Loopline Formations.

The Rimu Channel was drilled intensively for alluvial gold and extensively mined by bucketline dredging from the 1920's to the 1950's. The alluvial gold won from the Rimu Channel was mainly derived from an extremely bouldery lag deposit situated at the bedrock contact. This lag deposit was overlain by around 12 to 15 metres of aggradational outwash gravel and a surficial 5 to 8 metre deep lag deposit. The surface gradient is essentially the same as the gradient at the base of the channel. The gradient appears to be too steep for the aggradational gravel to have accumulated during a sea level maximum (by comparison with the gradient below the floodplains of the modern Grey, Taramakau and Hokitika Rivers). So it is assumed that this incised channel formed when sea level was low. Incision is likely to have been simultaneous with that in the channel buried beneath the Larrikins Formation at Kumara Junction (the Kumara Channel).

6.2.27c The Kumara Channel

In the Taramakau Valley the Larrikins terrace contains a buried deeply incised fluvial channel that runs approximately along the line of State Highway 73 between Kumara and Kumara Junction. The channel runs approximately parallel to the modern incised channel of the Taramakau River and has been identified from alluvial gold exploration drill holes. The upper end of the channel between Kumara and Dillmanstown was mined extensively by tunneling and hydraulic sluicing from the 1870's to the 1930's. The bedrock contact at the base of the channel is at an elevation of approximately zero metres at the Holocene sea cliff. At Kumara Junction the depth of the bedrock contact is 50+ metres below the surface of the adjacent Loopline terrace surface.

The timing of the deepest stage of channel incision is uncertain. Unfortunately the stratigraphic relationships between the channel gravel and the nearby Loopline gravel can not be observed due to a lack of outcrop. It is assumed that the channel post-dates the deposition of the Loopline

Formation. This judgement is made on the basis that the Taramakau River was large, capable of very rapid fluvial incision, and needed somewhere to flow subsequent to the deposition of the Loopline Formation. It is clear the main portion of the Taramakau did not flow via the valley of Kapitea Creek at that time. Unavoidably it must have discharged within the general path adopted by meltwater from the Taramakau Glacier during the more recent Larrikins event.

6.2.28 Cosmogenic isotope dating in the Aratika- Deep Creek-Moana area.

A large number of samples were taken for cosmogenic isotope dating from glacial erratic boulders in the Aritika-Deep Creek-Moana area in collaboration with Dr Tim Barrows. The samples are listed in table 6.30 and the sample locations are shown on figures 3.3, 3.4, 3.6, and 3.7. These samples were taken for the purpose of dating the Larrikins(2) and Moana Formations. The ages have been provided by Dr Barrows.

Sample	Lab code	$[^{10}Be]_c$ ($x10^4$ g^{-1})	Σ Production rate (atoms $g^{-1}.yr^{-1}$)	Exposure age (ka)
Moana Formation (Lake Brunner)				
MNA-03	ANU-M422-03	3.78 ± 0.35	5.152 ± 0.359	7.3 ± 0.8
MNA-04	ANU-M421-19	4.97 ± 0.24	5.247 ± 0.366	9.5 ± 0.8
MNA-05	Not run			
MNA-06	ANU-M422-04	7.64 ± 0.41	5.414 ± 0.377	14.1 ± 1.2
MNA-07	ANU-M421-20	7.63 ± 0.37	5.442 ± 0.379	14.1 ± 1.2
MNA-08	ANU-M422-05	7.68 ± 0.41	5.403 ± 0.377	14.3 ± 1.3
MNA-09	Not finalised			
MNA-10	ANU-M430-21	4.97 ± 0.36	5.377 ± 0.375	9.3 ± 0.9
LAR-09	ANU-M392-21	7.95 ± 0.59	5.554 ± 0.387	14.4 ± 1.5
Larrikins Formation (Lake Brunner)				
LAR-01B	ANU-M422-06	9.45 ± 0.47	5.844 ± 0.407	16.2 ± 1.4
LAR-02	ANU-M392-19	9.33 ± 0.97	5.774 ± 0.403	16.2 ± 2.0
LAR-03	ANU-M392-20	11.7 ± 0.68	5.805 ± 0.405	20.3 ± 1.8
LAR-04	ANU-M422-07	9.51 ± 0.42	5.778 ± 0.403	16.5 ± 1.4
LAR-05	ANU-M422-08	9.93 ± 0.75	5.777 ± 0.403	17.2 ± 1.8
LAR-06	ANU-M430-22	9.54 ± 0.55	5.852 ± 0.408	16.4 ± 1.5
LAR-07	ANU-M422-10	11.6 ± 0.55	5.577 ± 0.389	20.9 ± 1.8
LAR-08	ANU-M422-11	9.38 ± 0.40	5.579 ± 0.389	16.9 ± 1.4
LAR-10	ANU-M422-12	9.20 ± 0.37	5.774 ± 0.403	16.0 ± 1.3
LAR-11	ANU-M392-22	11.2 ± 0.61	5.585 ± 0.389	20.1 ± 1.8
LAR-12	ANU-M422-13	10.3 ± 0.69	5.758 ± 0.401	18.0 ± 1.7
LAR-14	ANU-M430-23	8.99 ± 0.56	5.664 ± 0.395	15.9 ± 1.5
LAR-15	Not precipitated			
LAR-16	Not finalised			
LAR-17	ANU-M422-14	9.48 ± 0.48	5.396 ± 0.376	17.6 ± 1.5
LAR-18	Not finalised			
LAR-19	ANU-M422-15	8.67 ± 0.52	5.412 ± 0.377	16.1 ± 1.5
LAR-20	ANU-M430-26	9.35 ± 0.60	5.420 ± 0.378	17.3 ± 1.6

Data are normalised to NIST SRM 4325 assuming $^{10}Be/^{9}Be = 3.00 \times 10^{-11}$
Carrier 10Be/9Be = <1 x 10-15. 10Be decay constant = 4.62 x 10-7 yr-1.

Table 6.31: Cosmogenic isotope ages from the Aratika-Deep Creek-Moana area

As can be seen in figure 3.7 and from Maps 3, 4 and 5 (map pocket) the samples from the Larrikins Formation were derived from a broad area occupied by Larrikins Formation moraine and outwash surfaces. The sample ages span the period from 15.9±1.5 ka to 20.9±1.8 ka. There is no particularly convincing age clustering across the moraine belt.

6.2.29 Larrikins(2_1) Formation (MIS2, Otira Glaciation, Kumara(2_{2b}) advance)

The Larrikins(2_1) Formation contains deposits from a glacial re-advance that followed a modest retreat during the LGM. At Kumara the outwash deposits are situated mainly in a post Larrikins(1) incised valleys. Just east of the Kumara and Kapitea reservoirs outwash from the Larrikins(2_1) event spreads out onto the recessional Larrikins(1) surface. This was mapped in detail by Suggate & Waight (1999) but they had defined the recessional surface as Loopline Formation. Larrikins(2_1) deposits include glacial till and outwash gravel. Landforms include outwash terraces and moraines. The moraines are situated in belts located mainly inside (up-valley of) the Larrikins(1) moraines. Fluvioglacial deposition occurred mainly in recently incised river valleys. Subsequently the shallow portion of the outwash deposits were either destroyed or overwhelmed at Kumara.

The Kumara(2_1) event included the deposition of a large complex ice proximal gold placer deposit in what is known as the Rimu Channel near Hokitika and in similar deposits between Dillmanstown and Kumara. At Dillmanstown gold was concentrated in several stratigraphic levels at Larrikins Flat, Dillmanstown. Loess deposition continued on older surfaces during the Larrikins (2_1) event.

Following the glacial advance there was a brief interstadial event (Raupo event, see below) probably accompanied by glacial recession. Recession is likely to have caused a reduction in fluvioglacial bedload.

6.2.30 Larrikins(2_2) Formation (MIS2, Otira Glaciation, Kumara(2_{2c}) re-advance)

The Larrikins (2_2) Formation contains deposits from a glacial re-advance and reinvigorated proximal fluvioglacial deposition that followed a modest and likely brief retreat during the LGM. The outwash deposits are situated mainly in post Larrikins(2_1) incised valleys. Deposits also include till beneath moraine situated in belts located mainly just inside (up-valley of) the Larrikins(2_1) moraines. Landforms include outwash terraces and moraines. The event included the deposition of a large ice proximal gold placer deposits at Kumara and Kaniere. Loess deposition continued on older surfaces.

The timing of the Larrikins (2_2) aggradational event is assumed to be ~21 to 19 ka (cal). Following the Kumara(2_2) glacial advance there was a significant glacial retreat accompanied by abrupt fluvial incision. At Kumara this incision defines the maximum extents of the Moana and Nine Mile Formations. This incision event is caused by a reduction in sediment throughput within the fluvial system, the very low sea level at this time and possibly by isostatic uplift due to reduced ice loading in the Southern Alps. The glacial retreat coincides with a modest climatic warming.

6.2.31 Moana Formation (MIS2, Otira Glaciation, Kumara(3) advance)

No changes have been proposed to the definition, age, or isotope stage correlation for the Moana Formation. This Formation contains deposits from a glacial re-advance and reinvigorated proximal fluvioglacial deposition that followed a modest and likely brief retreat during the LGM. It was deposited during a substantial glacial re-advance circa 19 to 18 ka (cal). The outwash deposits are situated mainly in post Larrikins(2_2) incised valleys. Deposits also include till situated in moraine belts located mainly just inside (up-valley of) the Larrikins(2_2) moraines. Landforms include outwash terraces which can be traced down valley several kilometres from the terminal moraines in the main valleys. The gradients on these surfaces are steeper than that of the post-glacial Nine Mile Formation. So eventually the Nine Mile Formation overwhelms the Moana Formation, either by overtopping it or by destruction during lateral erosion.

The readvance fell short of the Kumara (2_2) position and was probably relatively short lived (no significant gold in ice proximal placer deposits). The advance concluded with an abrupt shift to warmer climate and catastrophic region-wide collapse of all glaciers. Spectacular fluvial incision occurred immediately after the Moana event in all the major valleys. Incision was aided by very low eustatic sea level and potentially by rapid local isostatic uplift.

In South Westland moraine correlated with the Moana Formation overlies organic material dated at 16.45 ± 0.2 ka (Whataroa area, Moar 1980) and 15.3 ± 0.12 ka (Waiho area, S. Nathan as reported by Suggate 1990) by ^{14}C. It is suggested here that this corresponds to a calendar age of around 19 to 18 ka. The conclusion of Suggate (1990) and Suggate & Waight (1999) is that the Kumara 3 advance occurred between 16 ka and 14 ka.

A number of glacial erratic boulders from the Moana Formation in the Moana area were sampled for cosmogenic isotope dating during this PhD project. The sampling was done in conjunction with Dr Tim Barrows. The sample ages produced to date are listed in table 6.30. The sample locations are specified in figures 3.4 and 3.7. They are also specified in map 5 (map pocket). The spread of sample ages is from 7.3±0.8 ka to 14.4±1.5 ka. The ages cluster around 14.3±1.3 ka.

This advance was followed by climatic warming and rapid deglaciation during the MIS2/1 transition leading to the Aranui Interglacial (which commenced at c. 14 ka). There are no IRSL ages for the Moana Formation in North Westland at present.

6.2.32 Nine Mile Formation (MIS1/Holocene, Aranui Interglacial)

A single sample (RR19) was taken from slightly raised beachsand deposits of the Nine Mile Formation at Rapahoe beach. The quartz sand in the sample proved unsuitable for OSL and the sample contained insufficient polymineralic silt for IRSL dating.

The Nine Mile Formation contains deposits that accumulated as the result of rising eustatic sea level after the LGM. This includes fluvial and marine backfill in deeply incised fluvial channels on the continental shelf and on-land. It includes coastal marine high-stand deposits that have accumulated during the period of high MIS1 sea level. It includes fluvial deposits that are associated with modest downcutting following achievement of the MIS1 sea level maximum. Downcutting is associated with post 7 ka tectonic/isostatic uplift. The marine strandline deposits range in elevation from about 0 to 12 metres, depending on the location. The Nine Mile Formation includes widespread organic soil situated on these surfaces.

At Awatuna the maximum elevation of Holocene beach deposits is ~6 m above present mean sea level. So uplift and/or isostatic recovery (from glaciation) is implied for the Holocene. If it is

assumed that the strandline materials formed at some time between 6.0 ka and 3.0 ka and that local sea level was no higher than +2 metres during that period then uplift of around 3 to 5 metres is likely (given that these are swash zone deposits that can be found 0 to 3 metres above sea level at modern West Coast beaches. So the modern uplift rate is in the range 0.4 to 1.7 mm/yr, which does not help in distinguishing between the different stratigraphic scenarios outlined above.

There are two ^{14}C ages that are relevant to the age of the older (raised) portion of the marine strandline deposits. The first is a age of 4720 ± 70 years BP by Suggate (1968) is from a log in estuarine deposits 2 m below the top of the Nine Mile Fm terrace at Rapahoe Beach. The terrace surface is about 8 m above mean sea level. The second is an age of 6330 ± 80 years BP by Nathan (1976). The sample is wood from a "one-boulder-thick" layer on a 3-m shore platform close to post-glacial cliff about 3 km east of Cape Foulwind. [details derived from Suggate (1992)]

At Barrytown, Rapahoe, North Beach, Karoro, South Beach, Gladstone and Camerons (along about 40 km of coastline) the older part of the Nine Mile Formation is significantly higher than at Awatuna. It is at an elevation of up to 12 metres at South Beach (Suggate & Waight, 1999). It is reasonable to suggest there has been 7 to 10 metres of uplift since ~6 ka. The average rate could be as high as 1.7 mm/year and is unlikely to be much less than 1.0 mm/yr. It might exceed this range if the older part of the Nine Mile Formation is younger than 6 ka at Gladstone.

In the existing (Suggate) model the long term uplift rate is much slower than the short term rate. An assumption has been made in the existing model that the Holocene rate is an aberration. But there is no particular reason to assume that the Holocene uplift rate here is anomalous unless one is wedded to the idea that the Awatuna formation has to correlate with MIS5. In the context of uplift during the Holocene my long term rate of around 1.15 to 1.4 mm/yr does not appear to be unreasonable.

CHAPTER SEVEN: TERRACE AND MARINE STRANDLINE CORRELATION AND A PROPSED STRATIGRAPHIC MODEL

7.1 INTRODUCTION

Previously the only "complete" sequence of marine terraces described from the West Coast region was that from the Charleston-Addisons-Cape Foulwind area near Westport (Nathan 1975, 1976). Suggate (1992) attempted a coast parallel correlation from Westport to Hokitika. This analysis relies on matching a series of incomplete terrace sequences and requires an uncomfortable number of assumptions, particularly with respect to long distance correlation across the major river valleys. In order to minimise the number of assumptions and to provide a better baseline for correlation an examination of the marine strandline sequence at Point Elizabeth has been undertaken. This sequence constitutes the basis for the revised late Quaternary North Westland stratigraphy proposed in this thesis, and underpins the associated marine isotope stage correlation.

The survey at Point Elizabeth involved clambering though the thick undergrowth looking at the remains of old alluvial gold workings situated in undisturbed marine beachsand/gravel. The marine strandline elevations were assessed (approximately) with compass and abney level by short line-of-site measurements and later by hand-held GPS measurements. Abney measurements started from sea level at the South end of the Point Elizabeth track and from the Trig Point at Point Elizabeth at the North end. The two abney survey lines met in the middle. The terrace elevations calculated from this work are given in table 7.1 below. This survey was augmented by spot heights, taken using a handheld GPS unit, from terraces situated between Twelve Mile Bluff (north of Greymouth and Hokitika (table 7.3).

7.2 RAISED MARINE STRANDLINES AT POINT ELIZABETH

In the Greymouth to Hokitika area the most complete sequence of raised terraces is located at Point Elizabeth just north of Greymouth. There are at least 9 separate pre-Holocene strandlines here as illustrated in figure 7.1. They are situated on the seaward side of the Twelve Apostles Range both above and below the Point Elizabeth walking track. The sequence is unusually condensed in coast-normal width at Point Elizabeth because the underlying Cobden Limestone is hard and resistant to physical erosion by marine processes. There are few permanent watercourses because cave systems within the limestone tend to drain most of the ground water and a substantial part of the surface flow (via sinkholes and near surface cracks). At Point Elizabeth there are no glacial or fluvial systems that would tend to destroy the evidence for marine benches. Consequently, subaerial erosion is minimised.

The Point Elizabeth terraces constitute a benchmark against which terrace elevations from other localities in North Westland can be compared. The terraces were formed during local sea level high-stands. Each highstand was of sufficient duration for shoreline and near shore erosion to cut a low gradient marine bench in the limestone, without completely destroying older, higher benches. The marine benches are all cut obliquely across the seaward dipping limestone. They are less well preserved in the calcareous mudstone that both overlies and underlies the limestone.

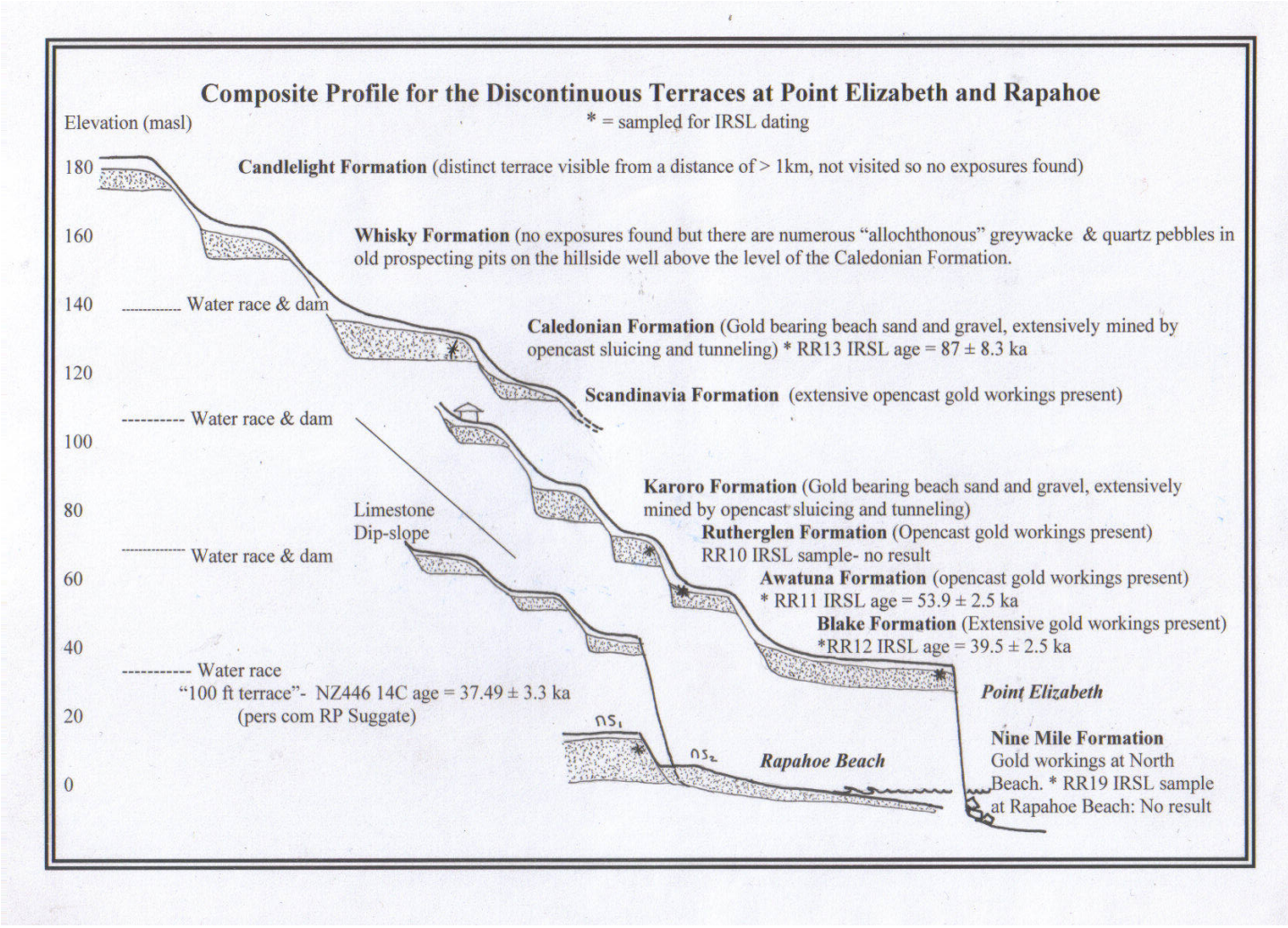

Figure 7.1 Composite profile for the discontinuous marine terraces at Point Elizabeth

Formation	**Greymouth area Surface Elevation** (metres amsl)	**Hokitika area Surface Elevation** (metres amsl)
Nine Mile 2 (Holocene)	3-6.	3-6.
Nine Mile 1 (Holocene)	8-12.	6-8.
Craig	15-17	10-12.
Blake	35-38	<38
Awatuna	48-52	<56
Rutherglen 2	55-60	?
Rutherglen 1	65-70	?
Karoro	80-84	75-76
Scandinavia	112-118	115-118
Caledonian	125-135	?
Whisky	~155-165	?
Candlelight	~180	?

Table 7.1a Marine terrace elevations in the Greymouth-Point Elizabeth area

Strandline	Formation	Approx. elevation of strand line (m)	Suggate (1992) MIS Correlation
Nine Mile	Nine Mile	3	1
Bradshaw's (West)	Waites	16-17	5
Pipeline	Waites	16-17	5
Larson's	Waites	20	5
Wilsons Lead	Waites	24	5
Lower Magazine	Waites	27	5
Upper Magazine	Virgin Flat	~30 –35	5
Gallagher's Lead	Virgin Flat	40-43	5/7
O'Toole's Lead	Addison	56 (lower) 60 (upper)	7
Addisons Lead	Addison	69 (upper surface by GPS)	9
Shamrock Lead	Addison	<88 (by GPS on top of overlying fluvial gravel)	-
Browns Terrace	Addison?	95	-
Caroline Terrace	Caledonian	133-135	15/13
Whisky	Whisky	Higher than Caledonian	
Candlelight	Candlelight		

Table 7.1b Marine terraces in the Westport-Charleston area

7.2.1 Terrace Nomenclature

The three oldest raised marine terraces are not recorded and not commented on by Suggate & Waight (1999) as they do not outcrop on the Kumara-Moana (1:50,000) geological map sheet. The Point Elizabeth locality where these terraces are present is just outside the mapped area. The terraces are noted by Suggate (1992) and by Nathan (1978) from the Rapahoe to Point Elizabeth area. However, Suggate and Nathan make different correlations with the Westport-Charleston sequence. Suggate has the Whisky Formation at Rapahoe at an elevation of ~180 m at Rapahoe, several kilometres to the east of Point Elizabeth. Nathan has cemented brown gravel defined as the Whisky Formation at 150 to 165 m at Rapahoe. In addition Suggate (1992) (fig 3) has transposed the naming of the Candlelight and Caledonian Formations. Nathan identifies the 120 m (Caledonian) level at Rapahoe but Suggate does not. The marine terrace nomenclature for these higher terraces was established by Nathan (1975) for the Charleston area near Westport. These definitions have priority. Nathan (1978) produced a 1:63,360 scale map of the Greymouth area. The Quaternary sequence mapped for the Greymouth area by Nathan (1978) is fully consistent with Nathan (1975), whereas Suggate (1992) is not. The nomenclature of Nathan (1978) is adopted here for the high marine terraces at Point Elizabeth.

For the purposes of this thesis the three highest terraces are defined using the terminology of Nathan (1978) rather than that of Suggate (1992). This requires that the next terrace in the sequence above the Whisky Formation must be the Candlelight Formation. In the Charleston area Nathan (1975) has the Caledonian Formation as the terrace immediately below the Whisky Formation. Lower in the sequence the terminology of Suggate & Waight (1999) applies with respect to the Scandinavia, Karoro, Rutherglen and Awatuna Formations. The lowest marine bench at Point Elizabeth has been given the informal name "Blake Formation". This formation includes marine deposits at an elevation of ~ 29 m (base) to 40 m at Blakes Terrace, Awatuna. A potential alternative name for this terrace is "Raleigh Formation", taken from the small township that was once situated at Point Elizabeth during the 19th Century on the 35 metre terrace.

At Point Elizabeth a number of the ancient strandlines were mined intensively for gold between about 1865 and 1900. The historic gold workings help to define the position of strandlines up to an elevation of approximately 125-135 metres. The highest workings identified at Point Elizabeth during this project (Caledonian Formation) are higher than all the marine strandline outcrops situated between Greymouth and Hokitika. To date the highest level at Point Elizabeth proven to contain marine beach deposits is the Whisky Formation (~155 to 165 metres). At this level there are a number of gold prospecting shafts that contain abundant redeposited beach pebbles. At Point Elizabeth there is at least one terrace that is higher still, at about 180-190 metres. It is almost certainly of marine origin.

At Point Elizabeth the Caledonian Formation is higher than outcrops of the Scandinavia Formation at Stafford. The Caledonian terrace is reasonably continuous here whereas the Scandinavia Formation consists of discontinuous terrace remnants. The Caledonian Formation is too high for an acceptable correlation with the Karoro Formation at Karoro unless there has been significant differential uplift over the short distance between Karoro and Point Elizabeth. At Point Elizabeth there are discontinuous strandline deposits at around 80-90 metres that are good candidates for the Karoro Formation.

The abney and GPS survey reached the elevation of the Caledonian Formation at 125 to 135 m (amsl). The height at that point matches that estimated from the 1:50,000 topographic map (Sheet J31). Two additional higher terraces are present, the lower of which was visited on foot. Both can be identified on the 1:50,000 scale topographic map (NZMS260 J31) and that is the source of the elevation estimate at those levels.

At Point Elizabeth each level up to that of the Caledonian Formation contains old (pre 1900) alluvial gold workings. The Whisky Formation contains marine gravel under a thick soil cover. This gravel was identified in shallow gold prospecting shafts sunk by the miners rather than from actual gold mines. The Whisky Formation was not mined in the area examined, probably due to lack of water rather than a lack of gold.

The Craig Formation (new informal name) is the lowest of the pre LGM raised marine deposits in North Westland. The writers' interpretation is that this formation is probably not present at Point Elizabeth. The "Craig Formation" is the lower of a pair of buried strandlines situated in an opencast alluvial goldmine at Southside, Hokitika. Previously it has been assumed this strandline is part of the Awatuna Formation but at Southside the elevation is too low. Pre-1910 the locality was known as "Craigs Freehold", named after a former owner of the property.

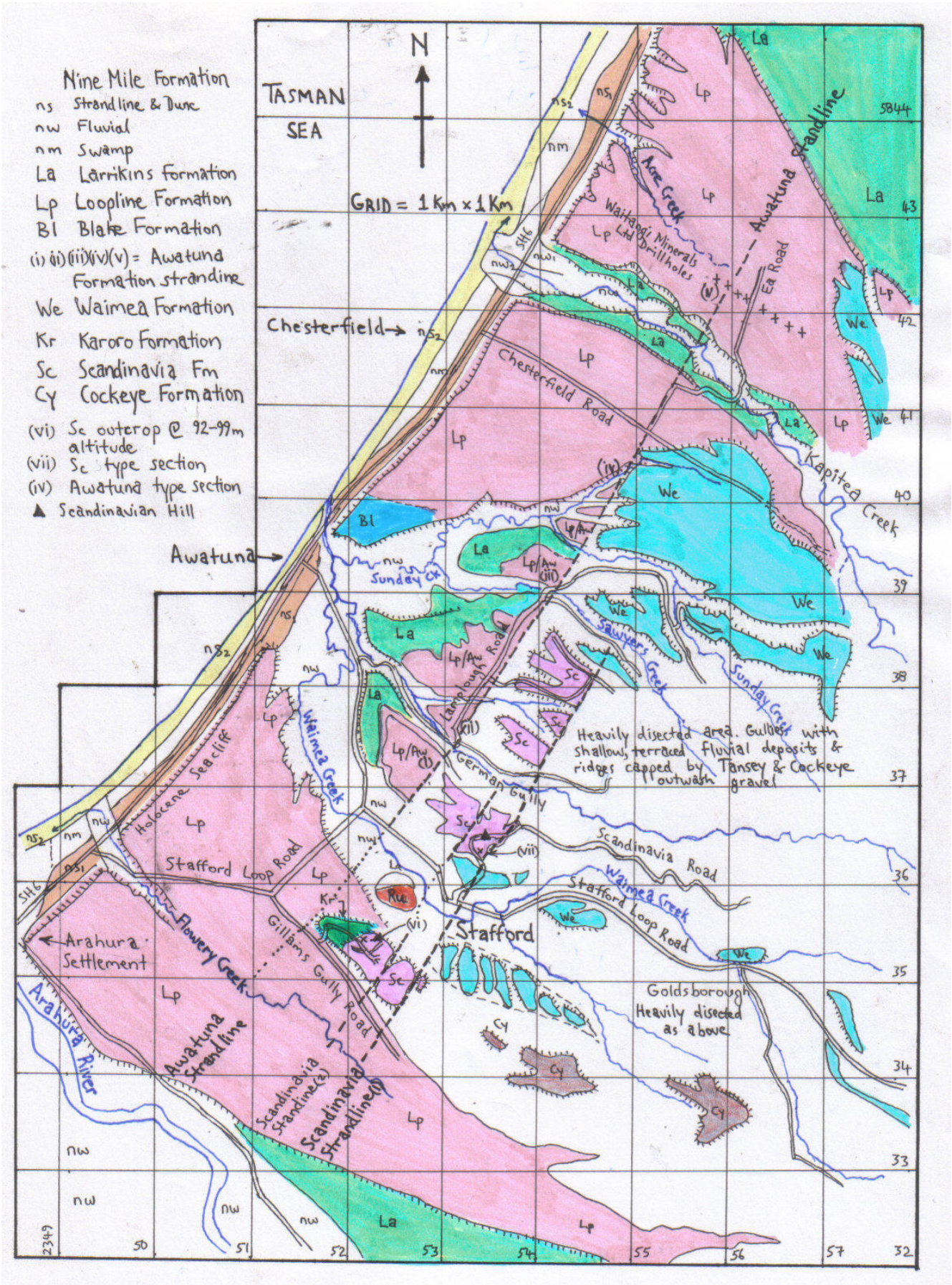

Figure 7.2 Map of significant Late Quaternary features in the Chesterfield-Awatuna-Stafford area.

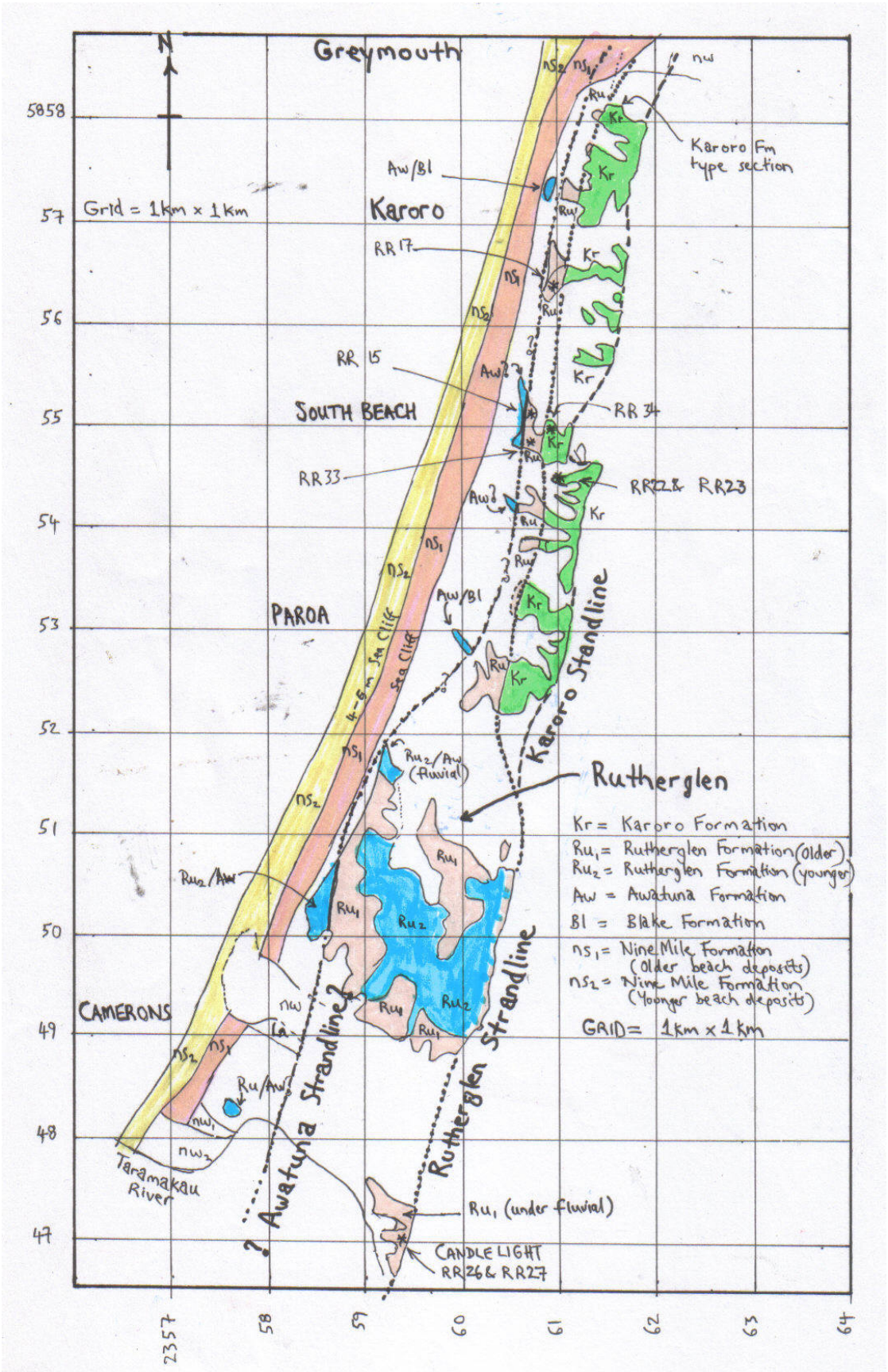

Figure 7.3 Map of significant Late Quaternary features in the area between Greymouth and Camerons.

7.2.2 The Westport-Charleston Terrace Sequence

In table 7.1b the equivalent marine sequence form the Westport-Charleston area is listed. The sequence from this area is described by Nathan (1975) and MacPherson (1978). The later is a detailed examination of the heavy mineral content of West Coast beach sand. For the lower part of the sequence the naming of marine terrace levels can be traced back to MacPherson (1967).

For the Westport-Charleston area the estimated elevations from Nathan (1975) are somewhat problematical because there is significant coast parallel tilting (up to the south, down to the north). The elevations for the Waites, Virgin Flat and Addison Formations are taken primarily from the Westport end where the uplift rate is not as great. For instance the elevation of the inner margin of the Addison Formation rises to around 90 metres towards Charleston. Downward tilting of Caroline Terrace (down to the north) was recognized by Nathan (1978). On Caroline Terrace (inland from Addisons Flat and SW of the Buller River the Caledonian Formation was mapped at the surface by Nathan (1978). Gold bearing strandline deposits are present here at an elevation of about 130-140 m. This is at the northern end where downward tilting has had the greatest effect. Interestingly Nathan (1975) maps the Caledonian marine bench at Charleston (where it should be higher) at 105-120 m.

It should also be noted that at Addisons Flat the inner Addison Fm strandline is at an elevation of about 75 metres, which is as much as 55-65 metres below the level of the Caledonian Formation at Caroline Terrace only a few hundred metres to the east. So it appears likely that the marine unit on the north end of Caroline Terrace might actually be the Whisky Formation.

On geomorphic grounds it is likely that there is a high marine strandline at around 200-230 metres running along the foot of the Paparoa Range at the inner (SE) margin of Caroline terrace. This might be too high to be correlated with the Candlelight Formation.

Unpublished work by the writer not associated with preparation of this thesis includes air photo interpretation in the Westport-Charleston area and analysis of old gold mining and ilmenite exploration data. This work has led to the conclusion that several of the marine terraces in this area contain multiple well-defined strandlines. These levels include the Nine Mile, Waites, Virgin Flat and Addison Formations. Some of these well-defined geomorphic features are separated by no more than 1 to 2 metres of elevation. Depositional ages might perhaps be separated by as little as a few decades to a few thousands of years. This observation is relevant in terms of discussion of the significance of what may be multiple strandlines much further south at Scandinavian Hill near Stafford.

7.3 AGES EXPECTED FROM THE SUGGATE MODEL

One point worth noting from table 7.1a is the regular spacing of terrace elevations. It is clear that, in the absence of a full set of terraces at any other locality in North Westland, great care needs to be taken in assigning formation names. Slight variations in uplift rates between localities could cause a mismatch to occur.

One of the problems with marine isotope stage correlation for terrace sequences like those at Point Elizabeth and Charleston is, as pointed out by Ward (1988), that there are multiple potential correlations. In the absence of good quality numerical dating each correlation can potentially be justified and there may be little basis for choosing one over another. This is a fundamental issue and a primary focus of this PhD project. The nature of the problem is apparent in figure 7.4 below. The ages that would be anticipated from the prior marine isotope stage correlation by Suggate & Waight (1999) have not been validated in the dating programme carried out for this thesis.

In the following table IRSL ages from this project are categorized in terms of the Geological Formation from which the samples were derived. Broadly speaking the ages are younger for the younger formations and older for the older formations.

Table 7.2: Terrace Ages and Marine Isotope Stage correlations expected from the Suggate model contrasted with numerical ages from this PhD project

Formation	Expected Age (Suggate model)		IRSL and cosmogenic isotope ages (this study) (ka)
	Isotope Stage	Age (ka)	
Nine Mile	MIS1	Holocene	Not dated
Moana	MIS2	16-34	~14-15 (cosmogenic isotope ages)
Larrikins(2)	MIS2		~16-22 (cosmogenic isotope ages)
Larrikins(1)	MIS2		~28-36 (cosmogenic isotope ages)
Loopline	MIS4	~60-70	Not dated directly
Craigs (informal)	MIS 5a	~80	33.6
Blake (informal)			39.5
Awatuna & Blake	MIS5c	~100	47.8 ± 6.6
Pre-Awatuna (fluvial (a), glacial (b)			(a) <84.9 (b) <78.1
Rutherglen	MIS5e	~125	65.9, 63.6
Waimea	MIS6	~140-160	<75.9
Karoro	MIS7a	~198	<92.5, <84.3, 65.7
Scandinavian	MIS7e	~235-240	<123.3
Tansey	MIS8		Not dated
Cockeye	MIS10		Not dated
Caledonian	MIS15		87.1
Whisky	MIS11		Not dated
Candlelight	MIS13		Not dated
The MIS correlation for the Caledonian, Whisky and Candlelight Formations is from Suggate (1992).			

7.4 STRANDLINE ELEVATIONS AND SHORE PARALLEL CORRELATION, HOKITIKA TO POINT ELIZABETH

7.4.1 The Younger Fluvioglacial Terraces

Much of the dating relevant to the age of the younger part of the marine terrace sequence has been carried out on the fluvioglacial Larrikins and Loopline Formations. In North Westland correlation with the marine isotope stages is unambiguous only as far back as the Larrikins(2) Formation (MIS2). That is to about 22 ka. Given that cosmogenic isotope ages from glacial erratic boulders on four different "Loopline" surfaces have yielded LGM ages the age of the Loopline Formation is certainly open to debate. The interpretation proposed here is that the ice limit during the deposition of the Larrikins(1) glacial till in these areas may have been more extended (in a seawards/northwesterly direction) than it was during the deposition of the Loopline Formation. Consequently, significant portions of the Loopline Formation are mantled with Larrikins(1) till and outwash gravel.

Cosmogenic isotope ages on glacial erratic boulders in the Nelson Creek Farm Settlement area and at the head of Twelve Mile Valley raise the possibility that parts of the Loopline Formation date from Late MIS3 to early MIS2. This is particularly interesting given that the Kawakawa tephra has been found close to the base of the loessic soil on the Loopline Formation in the general vicinity of the Chesterfield Road – Ea Road intersection. It has previously been assumed (Neale et al 2001) that there was a depositional hiatus or erosional period following MIS4 during which soil was

deflated from or not deposited on the Loopline Formation. No compelling evidence was presented for that view. Nor is the cosmogenic isotope dating compelling as it relates to another site. It does invite reconsideration of the implications of finite radiocarbon ages and MIS3 luminescence ages from the base of the Loopline Formation at the type section of the Awatuna Formation.

It is assumed that the existing physical correlation by Suggate & Waight (1999) of the distal portions of the "Loopline terrace" from the Grey Valley to the Hokitika Valley can be accepted. This means the formation can be correlated from Stillwater to Camerons to Kapitea Creek to the Arahura Valley to the Hokitika airport and across the Hokitika River to Southside. Radiocarbon ages do not rule out an MIS3 or MIS4 correlation for this formation at present. The IRSL ages produced during this project can be interpreted as evidence against correlation with MIS4. Dating is compounded by the finding that the Loopline Formation is a composite of several fluvioglacial events.

7.4.2 Correlation between Marine and Fluvioglacial Terraces

The Loopline Formation is particularly important with respect to the age of the youngest pre-Holocene marine terraces because it rests on those strandlines. There are marine strandline deposits beneath the Loopline Formation at EA Road on the north side of Kapitea Creek, at Sunday Creek near Chesterfield, on the north side of Waimea Creek, on both sides of Houhou Creek at Blue Spur, at Southside on the southern margin of the Hokitika Valley, and on both sides at the seaward end of the Rimu Channel. There are a number of strandlines buried under the Loopline Formation. These represent the inner margins of the Craig, Blake, Awatuna and Rutherglen Formations. If an age limit is established for the base of the Loopline Formation then this also acts as an age limit on the top of the marine deposits. On balance the IRSL ages from this project suggest an early to middle MIS3 age for the basal deposits of the Loopline Formation. This makes it possible for the Craig's, Awatuna and Rutherglen Formations to be correlated with MIS3 and/or MIS4.

The marine Karoro Formation is mapped as being overlain by the fluvioglacial Waimea Formation at Blue Spur. So the age of the Karoro Formation is constrained by the lower limit of ages on the Waimea Formation.

The shore parallel correlation proposed as a result of this PhD project is illustrated in figure 7.4 below**.**

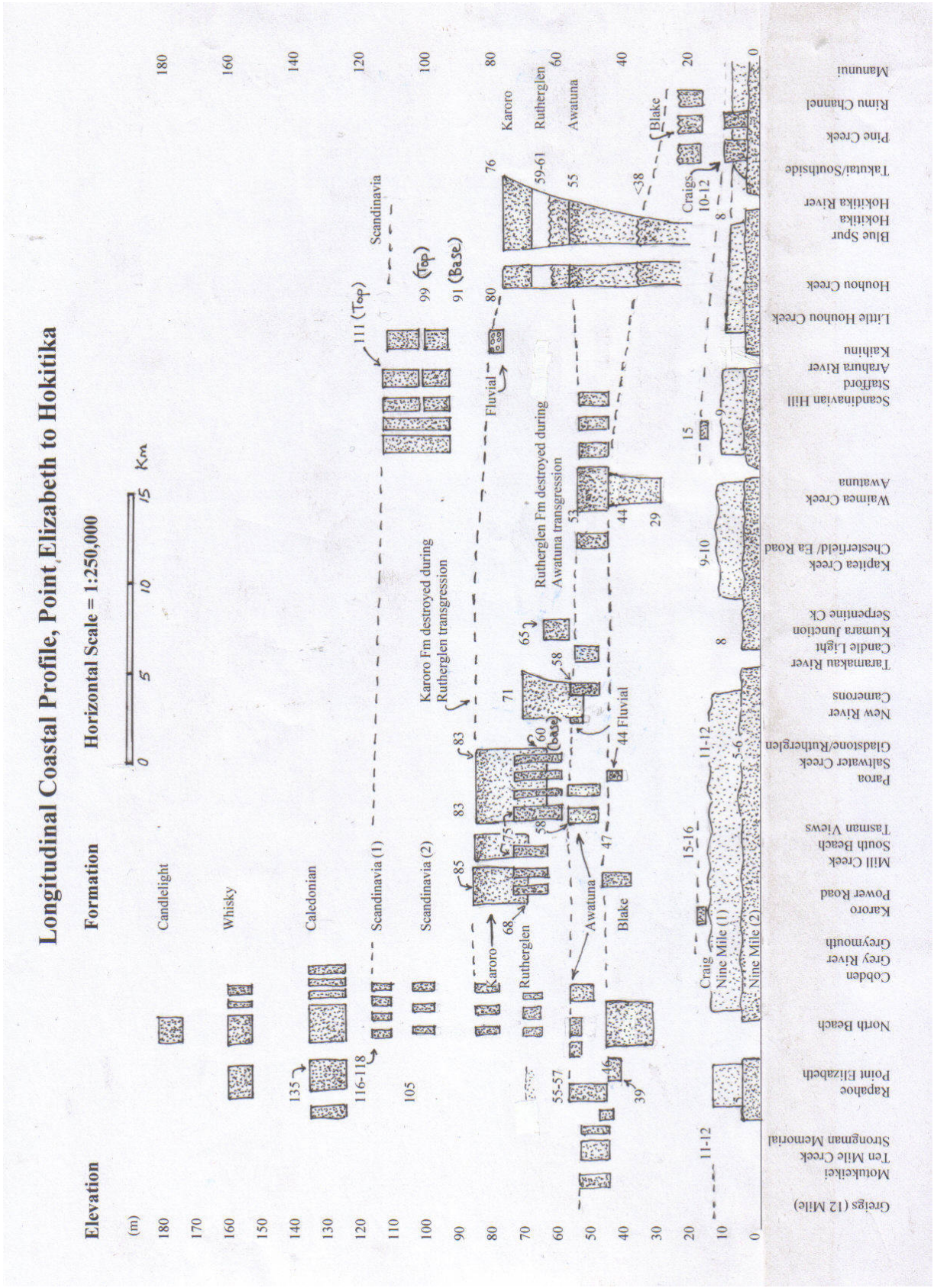

Figure 7.4 Longitudinal Coastal Profile, Point Elizabeth to Hokitika

Table 7.3 (below) Elevations of Quaternary surfaces in North Westland

Nine Mile Formation

General Location	Formation	Elevation amsl (m)	Latitude (S)	Longitude	Comments
Rapahoe Beach	Nine Mile 1	11 to 12	42° 22.687'	171° 14.236'	Near east end of Point Elizabeth Track. Sample site RR19
Cobden	Nine Mile 1	11 to 12	42° 25.882'	171° 12.437'	Monroe Street, east of dunes. This terrace extends to the stat of the Point Elizabeth Track at North Beach
Grey District Council Office	Nine Mile 1	11 to 12	42° 27.177'	171° 12.672'	Rose garden adjacent to Alexander Street
Greymouth Aquatic Centre/ Croquet Club	Nine Mile 1	11 to 12	42° 27.670'	171° 12.052'	Adjacent to Car Park
Karoro Bowling Club	Nine Mile 1	11 to 12	42° 27.962'	171° 11.431'	Footpath
Greymouth Cemetery, Karoro	Nine Mile 1	13 to 15	42° 28.089'	171° 11.277'	Harriet Herbertson Memorial
Loris Place, Paroa	Nine Mile 1	13 to 14	42° 29.080'	171° 11.012'	Outside Paroa Kindergarten
South Beach Overbridge (SH6)	Nine Mile 1	15 to 17	42° 29.451'	171° 10.715'	Adjacent to SH6 and the Greymouth-Hokitika Rail Line. 2 to 3 m of dunesand on beachsand.
Coulson Road/ Gadd Road	Nine Mile 1	11 to 12	42° 30.293'	171° 10.495'	20 m west of intersection and low marine cliff.
Paroa Tennis Club	Nine Mile 1	11 to 12	42° 30.855'	171° 10.189'	Adjacent to Rutherglen Road (North Side)
Gladstone	Nine Mile 1	10 to 11	42° 31.752'	171° 09.634'	Osmond Road- Hammer Drive intersection, Graveled yard outside IPL Plywood factory
Paroa-Gladstone	Nine Mile 1	9	42° 31.024'	171° 09.917'	About half way between the two. Outer edge immediately above younger strandline and above SH6.
Camerons	Nine Mile 1	7 to 8	42° 33.037'	171° 08.700'	Driveway to Kotuku Saddlery
Chesterfeld	Nine Mile 1	9 to 10	42° 37.339'	171° 05.130'	Inner (east) margin adjacent to SH6
Awatuna	Nine Mile 1	6 to 7	42° 38.197'	171° 04.142'	Inner (east) margin adjacent to SH6, east of railway.
Awatuna-Arahura	Nine Mile 1	9	42° 38.838'	171° 03.545'	Halfway between Awatuna and Arahura. Inner margin adjacent to SH6 and the Hokitika Railway.
Kaihinu	Nine Mile 1	10 to 11	42° 40.769'	171°00.535'	Intersection of One Mile Line Road and SH6. Probable dune sand.
Hokitika	Nine Mile 1	7 to 8	42° 42.791'	170° 58.125'	Corner of Sewell and Park Streets
Hokitika	Nine Mile 1	13 to 14	42° 41.722'	170° 59.402'	Adjacent to SH7 at opening to Houhou Valley. Bouldery heavy mineral rich beachsand.

Craig Formation (below)

General Location	Formation	Elevation amsl (m)	Grid Reference/ Lat-Long	Comments
Phelps Mine	Craig	10 to 12	NZMS260 N2770 E4230	Top of beach/base of soil. Opencast goldmine.
Paroa Driveway	Craig or Nine Mile 1	14 to 15	42° 31.110' S 171° 10.065'	Driveway, Bernie and Cath Monk, South of the Paroa Tennis Club and Saltwater Creek
SH6, Cobden Bridge	Craig?	16 to 17	42° 26.734' S 171° 13.086'	15 m long horizontal solution features in limestone indicative of an ancient water table. Observed on upright joint planes in a long road cutting.
Smith St, Greymouth	Craig	15 to17	42° 26.963' S 171° 12.890'	Marine beach sand, foundations of the Sundowner Motel (office) near the Grey River (Cobden) road bridge

Blake Formation

General Location	Formation	Elevation amsl (m)	Latitude	Longitude	Comments
Phelps Mine	Blake	25+	NZMS 260 J33	N 2780	Old mine tunnels, unconformable upper surface (truncated by fluvial gravel
Hou Hou Creek	Blake/Awatuna	<38	Grid J32 583135	234690	Suggate
Blakes Terrace, Awatuna	Blake	45 Top	NZMS 260 J32	N 4005 E 5275	Ilmenite-rich beachsand under <1m of soil
Blakes Terrace, Awatuna	Blake	29 Base	42° 37.905'	171° 04.397'	Fine to medium sand resting on fluvial gravel
Stanton Crescent, Karoro	Blake/Awatuna	45-47 Top	42° 28.629'	171° 11.288'	Top of marine, turning circle at the top of the street
Private section, Paroa	Blake/Awatuna	45 Top	42° 30.990'	171° 10.479'	Fluvial gravel under Stean May's lawn
Private section, Paroa	Blake/Awatuna	41 Base	42° 30.975'	171° 10.475'	Base of gravel on hard siltstone under Stean May's Water Tank.
Private Road, Rapahoe	Blake	45-46 Top, 43 Base	42° 22.777'	171° 14.158'	Thin marine gravel
Point Elizabeth	Blake	42-44 Top of marine	42° 23.074'	171° 13.124'	Back margin of the terrace against the inner limestone cliff
Point Elizabeth	Blake	34-35 Top	42° 22.836'	171° 13.151'	Top of marine gravel and sand within 100 m of the Point. Close to RR12
Nine Mile	Blake	39 Base	42° 21.608'	171° 14.960'	Marine gravel outcropping on east side of SH6 at the old James Mine road turnoff
Strongman Mine Memorial	Blake	44 Base	42° 20.990'	171° 15.389'	Base of thin (~3 m) marine gravel at strandline
Punakaiki	Blake	25-26Top	42° 06.986'	171° 19.778'	Car park, Punakaiki Visitor Centre

Awatuna Formation

General Location	Formation	Elevation amsl (m)	Latitude	Longitude	Comments
Schulz Creek, Motukiekie	Awatuna	52 by GPS	42° 19.586'	171° 16.057'	Sample site RR20. Top of beach gravel, base of soil. Adjacent to SH6
Picnic Table, Motukiekie	Awatuna	52	42° 19.779'	171° 15.895'	Top of beach gravel, base of soil. Adjacent to SH6
Ten Mile Lookout	Awatuna	52	42° 20.142'	171° 15.653'	Top of beach gravel. South side of Ten Mile Creek, adjacent to SH6
Nine Mile, D&S Bell Driveway	Awatuna	~54-55	42° 42.070'	171° 15.248'	Est. for base of soil on beach. Adjacent to SH6
Private road, Rapahoe	Awatuna	54-55	42° 22.813'	171° 14.129'	Terrace overlooking Rapahoe, on lawn next to caravan.
Miners Dam, Point Elizabeth	Awatuna	57	42° 23.139'	171° 13.158'+E98	Immediately inland (east) of Point Elizabeth track
Gold workings, north end of North Beach	Awatuna	45-47	42° 23.602'	171° 13.004'	Base of gravel. Limestone boulders and mine tailings on strandline, Point Elizabeth track.
Road cutting, private road, North Beach	Awatuna	51-52	42° 23.803'	171° 18.002'	Sample site RR11. Top of beach gravel, base of soil. Overgrown slip adjacent to road
Tasman View, South Beach	Awatuna?	58	42° 29.699'	171° 11.014'	Base of soil- top of beach gravel at strandline.
Goldtown Road, Rutherglen	Awatuna?	50.5 top of fluvial, 49 at base	42° 31.661	171° 09.934'	Cutting in side of farm track. 1.5 m fluvial gravel under 2 m soil about 75 m east of the Holocene seacliff.
Hammer Terrace, Gladstone	Awatuna/ Rutherglen?	57-58 Surface 56-57 marine	Grid K32 585220 42° 32.352'	235840 171° 09.386'	Rear of narrow terrace btw Rutherglen Fm and the Holocene seacliff.

Hammer Terrace, Gladstone	Awatuna/ Rutherglen?	53-54 Surface 53 marine	Grid K32 585220 42° 32.358'	235840 171° 09.335'	Front of narrow terrace btw Rutherglen Fm and the Holocene seacliff.
Sunday Creek	Awatuna	53	Grid NZMS260 K32	N 4030 E 5475	Base of soil- top of beach gravel at strandline. Type section.
Sawyers Creek	Awatuna	53 Top of sand 46 Base of marine	42° 38.561	171° 05.672'	At the strandline just south of Sawyers Creek
Sebastapol Creek	Awatuna	46-49 Base of marine gravel	42° 39.097'	171° 05.200'	Coarse gravel on hard siltstone. In road cutting on Lamplough Lead Road just north of German Gully
Hou Hou Creek	Awatuna/ Rutherglen?	56	Grid K32 583080	234680	Top of beach (Suggate)

Rutherglen Formation

General Location	Formation	Elevation above mean sea level (m)	Latitude	Longitude	Comments
Rapahoe	Rutherglen	66-67 surface	42° 22.935'	171° 14.002'	Extensive terrace at Point Elizabeth Track, no marine outcrops observed, under forest
North Beach	Rutherglen	75 surface	42° 23.844'	171° 13.038'	Terrace fragments at this level, some with alluvial gold workings. Sample site RR10 71-73 m
Karoro	Rutherglen	73-75	42° 28.777'	171° 11.436'	Sand-soil contact, Adjacent to Mackley Fergusons driveway North of Power Road. Sample site for RR17/18. Within 25 m of strandline.
Tasman View, South Beach	Rutherglen	71-73	42° 29.961'	171° 11.075'	Sand-soil contact, adjacent to main water reservoir tank and access track to east of current subdivision. Sample site for RR33
Tasman View, South Beach	Rutherglen	65-66	42° 29.799'	171° 11.012'	Sand-soil contact, road cutting (since landscaped) adjacent to subdivision road on east side. Sample site for RR15/16
Forestry track off Marsden Road	Rutherglen	78	42° 30.51'	171° 11.090'	Top of soil at a forestry skidsite just west of the Rutherglen strandline.
Farm Paddock, Goldtown Road, Rutherglen	Rutherglen	67-68	42° 31.793'	171° 09.352'	On surface (erosional) 2 to 3 m lower than the Rutherglen highpoint about 100 m to the SSW. Terrace overlooks the Holocene seacliff.
Hammer Terrace, Gladstone	Rutherglen	65-67 Top <50 base	42° 32.011'	171° 09.611'	Gravel and heavy mineral rich nature of the sand indicates this is at or very close to a significant strandline
Rutherglen-New River Road	Rutherglen	70-73	42° 32.606	171° 10.378'	Not well exposed but pebbly sand evident close by. Upper surface of paddock just west of road. Sand relatively fine grained and poor in heavy minerals
Rutheglen-New River Road	Rutherglen	67-68	42° 33.043'	171° 10.122'	Not well exposed but pebbly sand evident close by. Upper surface of paddock just west of road. Sand relatively fine grained and poor in heavy minerals. Overlooking New River.
"Big Paddock" area, Cement Lead Road, Blue Spur	Rutherglen?	59 to 61	42° 43.105'	171° 00.724'	Madman's Tunnel, Top of beachsand/gravel, base of fluvial gravel. Tunnel located in the base of a gully incised into Waimea Formation outwash.

Karoro Formation

General Location	Formation	Elevation above mean sea level (m)	Latitude	Longitude	Comments
Milton Road, Karoro	Karoro	67-68 Base	42° 28.140	171° 11.677	Base of marine gravel on hard siltstone at Rotary Club viewing platform. Type section.

Arnotts Heights, Karoro, Greymouth	Karoro?	77-80	42° 28.191	171° 11.576	Turning circle, west end of Arnotts Heights,
Arnotts Heights, Karoro, Greymouth	Karoro	84-85	42° 28.269	171° 11.747	SE end of Arnotts Heights at end of road. Upper surface of sand
Cummings subdivision, Arnotts Heights, Karoro	Karoro	85-86	42° 28.300	171° 11.810	Maximum elevation of marine strandline deposits
Cummings subdivision, Arnotts Heights, Karoro	Karoro?	83	42° 28.335	171° 11.885	Upper surface. Lagoonal/lacustrine fine sand and silt with pebbly gravel at base
Cummings subdivision, Arnotts Heights, Karoro	Karoro?	87-88	42° 28.330'	171° 11.911'+E56	Uppermost surface overlying lacustrine sand. 4 to 5 m thick silt and peaty soil overburden.
Terrace north of Power Road	Karoro	77-80	42° 28.700	171° 11.470	Adjacent to Rutherglen strandline at Mackley Fergusons House, rises higher to the east of the house.
Terrace at east end of Power Road	Karoro	80-81	42° 29.089'	171° 11.798'	Surface of soil. Approximate mid-point on terrace at east end of Power Road, Karoro.
Terrace at east end of Power Road	Karoro	86-88	42° 29.060'	171° 11.624'	Surface of soil close to inner (east) edge of the terrace at the east end of Power Road, Karoro.
Rear of Tasman View Subdivision	Karoro	76	42° 29.933'	171° 11.244'	Upper surface of sand on track to small gravel quarry
Rear of Tasman View Subdivision	Karoro	81-82	42° 30.033'	171° 11.552'	Upper surface at main access track
Forestry track off Marsden Road	Karoro	79-81 Top, 76-78 Base	42° 30.124'	171° 11.541'	Innermost (eastern) limit at strandline and marine cliff.
Forestry track off Marsden Road	Karoro	79-82 Top	42° 30.561'	171° 11.380'	Innermost (eastern) limit at strandline and marine cliff.
Rutherglen north of Saltwater Creek	Karoro	60	42° 31.350'	171° 10.690'	Base of fine to medium grained marine sand on hard siltstone
Rutherglen north of Saltwater Creek	Karoro	71	42° 31.331'	171° 10.732'	Top of fine to medium sand, base of sandy beach gravel
Rutherglen north of Saltwater Creek	Karoro	81-82	42° 31.287'	171° 10.816'	Top of beach deposit close to Karoro strandline
Blue Spur Road	Karoro	72-73 Top	42° 43.620'	171° 00.809'	Karoro beachsand/gravel in road cutting at bottom end of driveway. Under remnant soil that is below an unconformable upper contact with fluvial gravel. Grid J33 N2930 E4730
Blue Spur Road	Karoro	68 Base	42° 43.620'	171° 00.809'	Karoro beachsand/gravel in road cutting at bottom end of driveway. Base on weathered fluvial pebble conglomerate.
Ballarat Terrace Subdivision, Blue Spur	Karoro	75-76 Top	42° 43.647'	171° 00.955'	Top of marine under wood bearing soil, both under thick fluvial fan deposits derived from the adjacent marine cliff.
Blue Spur	Karoro	<80	grid K33 583005	234885	Base of soil- top of beach. Between McIntyres Creek and Hou Hou Creek (Suggate 82m)

Scandinavia Formation

General Location	Formation	Elevation amsl (m)	Latitude	Longitude	Comments
Ballarat Terrace, Stafford	Scandinavia	99 Top 90 Base	42° 40.346	171° 04.425'	Road cutting in new subdivision. Beach sand and gravel overlain by thin (2 to 3 m) fluvial gravel and soil. Approx 500 m west of eastern strandline.
Ballarat Terrace, Stafford	Scandinavia	103-104	42° 40.383'	171° 04.488'	Surface of soil at midpoint (thin neck) of terrace.
Scandinavian Hill, Stafford	Scandinavia	115-118 Top	42° 38.811'	171° 05.596'	Road cutting at eastern-most strandline, Scandinavia Hill. Type Section

Gold Workings above Point Elizabeth track	Scandinavia	116-118 Top, 112 base	42° 23.298'	171° 13.208'	Flat area stripped of sandy gravel by gold miners, backed by marine cliff in hard limestone
Gold Workings above Point Elizabeth track	Scandinavia?	99-104 base	42°	171°	Flat area stripped of sandy gravel by gold miners, backed by marine cliff in hard limestone

Caledonian Formation

General Location	Formation	Elevation amsl (m)	Latitude	Longitude	Comments
Old TV repeater site, Nine Mile	Caledonian	123	42° 21.252'	171° 15.293'	Site overlooking SH6 at Nine Mile, marine gravel exposed in access track
Gold Workings above Point Elizabeth track	Caledonian	130-132	42° 23.480'	171° 13.229'	Sample site RR13, tunnel in marine sand close to strandline
Gold Workings above Point Elizabeth track	Caledonian	135-137	42° 23.448	171° 13.232'	Pre mining surface- sand-soil contact
Gold Workings above Point Elizabeth track	Caledonian	128	42° 23.333'	171° 13.233'	Flat area stripped of sandy gravel by gold miners, backed by marine cliff in hard limestone

Other Sites

General Location	Formation	Elevation amsl (m)	Latitude	Longitude	Comments
Lamplough Road	Karoro?	77-81	42° 38.365'	171° 06.277'	Mapped as marine Rutherglen by Suggate. No evidence of marine sand/gravel in this terrace (RVR), it is actually fluvial.
Stafford	Loopline?	~60	Grid 583600	345250	Mapped as marine Rutherglen by Suggate. No evidence seen in favour. Probably fluvial.
Ballarat Rise, Stafford	Karoro?	79-82	42° 40.277'	171° 04.360'	Subdivision off Gillams Gully Road. Shallow fluvial gravel on the terrace next to a terrace with an outcrop of the Scandinavian Fm. Terrace mined for gold.

7.4.3 The Lowest Pre-Holocene Marine Strandline

The lowest strandlines in the sequence preserved on land are located at Southside (Hokitika), at and at Point Elizabeth. The strandline elevations are ~10-12 m at Southside and 15-17 m in Greymouth. If these represent the same event then there has been more tectonic uplift at Greymouth than at Southside. This would then also apply to the older strandlines, perhaps to an even greater extent. The next lowest strandline has an elevation of about 20-25 m at Southside, 35 to 40m at Blakes Terrace (maybe lower if the top is dunesand) , and 35 to 38 m at Point Elizabeth.

The Karoro strandline is situated at around 85 m at Point Elizabeth, 84 m at Karoro, 81 to 83 m at South Beach and Paroa, and 75 to 76 m at Blue Spur (almost as far as Kaniere near Hokitika). So from Greymouth to Hokitika there is evidence for net tilting. Suggate (1991) mapped the Karoro Fm at Scandinavia Hill, Stafford at around 90-100 m. As discussed in chapter 6 the evidence for this interpretation is not strong. If these differences in elevation are the result of tilting then much of the tilting has probably occurred during the Holocene, because the inner margin of the Holocene in the Greymouth area is about 6 m higher than it is in the Hokitika area. There is little room for substantial pre-Holocene downward tilting to the south (short of invoking faulting, for which there is no evidence, reversal of tilting over time, or migration of fold axes). As long as this coast-parallel correlation is correct then there is a benchmark to hang the other strandline elevations off.

The correlation given here for the Karoro Formation is the same as that given by Suggate & Waight (1999). The differences between the coast parallel correlation advanced here and that of Suggate & Waight (1999) relate primarily to the younger strandlines.

7.4.4 Southside to Blue Spur

At Southside the lowest pre-Holocene strandline (Craig's Formation) is situated at an elevation of ~12 m with an overlying soil. An older strandline here has an elevation of about 20-25 metres and has an erosional upper surface. Both are buried by the Loopline Formation. Both strandlines contain old gold workings. They are exposed in and about the modern Phelps goldmine (north of Pine Creek) and the Birchfield goldmine (south of Pine Creek). In both cases it is assumed that the strandlines represent sea level maxima. This is reasonably clear-cut for the lower strandline, the inner margin of which is a marine cliff. The higher strandline is truncated by an unconformable upper surface and could potentially be a regressive or still-stand deposit.

SW of Pine Creek between Hokitika and Mahinapua the crests of the Holocene progradational beach ridges that form the coastal plain reach elevations of at least 8 metres above mean sea level. So the upper surface of the Holocene deposits is at a similar elevation here to that at Hokitika, at Awatuna, at Camerons, at Gladstone, and at Rapahoe. The Holocene may be slightly higher from Greymouth to South Beach, but otherwise there is little evidence for substantial coast parallel tilting at the coastline during the Holocene. It is possible that the slightly higher elevation from Greymouth to South Beach (max of 12 m) might simply reflect earlier deposition or earlier stabilization of the position of the coastline rather than more rapid uplift.

There is no published correlation between the marine strandlines at Southside and those about 5 km northeast at Blue Spur. The proposal advanced here is based on the observation that there is only modest coast parallel tilting of the much older inner strandline of the Karoro Formation over a distance of about 4 km at Blue Spur. So unless there has been a fault offset across the Hokitika River then the younger strandlines should be at comparable elevations on the North side of the Hokitika River. In that case it is rather unlikely that the c.56 m strandline at Blue Spur would correlate with the 20-25 m strandline at Southside. It is more likely that the <35-38 m strandline from Blue Spur correlates with a regressive phase of the same event at Southside. This implies there is no known correlative for the 12 m strandline (Craig Formation) at Blue Spur. In support of this view point it should be noted that there is presently no evidence for coast parallel tilting of the 56 m or 38 m strandlines at Blue Spur. In addition it should be noted that there are marine deposits at about 53 and 35-40 m further north near Awatuna, which can also be interpreted as evidence for minimal coast parallel tilting.

In further support of the interpretation advanced here there is no evidence for tilting over a shore parallel distance of about 2 km along the two buried (Blake & Craig) strandlines at Southside. Nor is there any direct evidence of fault displacement on any pre Holocene surface in the Hokitika area. Nor is there published evidence for coast-normal warping of Quaternary surfaces near Hokitika.

The conclusion reached here is that the lower strandline at Southside (Craig Formation at 10-12 m) has not been identified at Blue Spur and that it is likely, but not proven that the higher of the two strandlines at Southside (20-25 m) correlates with the lower strandline at Blue Spur.

7.4.5 Blue Spur to Chesterfield

At Blue Spur there are marine strandline deposits at ~35 m, 56 m and 75 to 76 metres. The 1:50,000 scale mapping by Suggate & Waight (1999) defines these as Awatuna Formation, Rutherglen Formation and Karoro Formation respectively. But which strandline is the real Awatuna Formation? Suggate and Waight (1999) mapped the ~35 m strandline at Blue Spur as a continuation of the 53 m strandline (Awatuna type section) at Chesterfield. The argument is that the 56 m strandline at Blue Spur is the Rutherglen Formation.

This could be the case if there has been coast parallel tilting between Chesterfield and Blue Spur. Suggate (1992) uses the Karoro Formation as the benchmark in evaluating the tilting. His interpretation is that the Karoro strandline has an elevation of c.100 m at Scandinavia Hill and c.82 m at Blue Spur, a fall of ~ 18 m. As shown in Chapter 6 the Karoro strandline is almost certainly not present at Scandinavia Hill. There are fragments of fluvial terraces at around 80 to 85 m near Scandinavia Hill (table 7.3) that could be equivalent to the Karoro Formation. In addition there is effectively no discernable tilting on the inner Holocene strandline from Awatuna to Hokitika. There is no evidence for coast normal fault displacement in the missing section (Arahura Valley). It would be expected that the same tilting process applied to the Rutherglen and Karoro Formations. Mapping by Suggate & Waight (1999) identifies the Rutherglen Formation at Stafford. However, there are no proven outcrops of Rutherglen strandline deposits in the Chesterfield-Scandinavia Hill area. So the tilting hypothesis is difficult to test in terms of elevations on the supposed Rutherglen strandline.

Intuitively if there was coast parallel tilting from Chesterfield to Blue Spur one would expect proportionately less tilting of the Awatuna Formation than the Karoro Formation (given that it is supposedly about half the age, i.e. MIS5c versus MIS7 in the Suggate model). But Suggate & Waight are suggesting up to 18 m of tilting on the Awatuna Formation. If tilting had occurred throughout the time since the deposition of the Karoro Formation one would expect a greater differential for the Karoro Formation, yet this does not appear to exist. Field investigations for this project indicate a maximum coast parallel tilting of 10 m between Point Elizabeth and Blue Spur.

The tilting anomaly disappears if the 56 m strandline at Blue Spur is redefined as Awatuna Formation. Then there is minimal tilting on the Karoro Formation, minimal tilting on the Awatuna Formation, and minimal tilting on the lower strandline, which becomes the Blake Formation. The Blake Formation is then close to 35 m at Blakes Terrace (Awatuna) and at Blue Spur.

The reassignment of the 56 m strandline at Blue Spur is not contradicted by any existing numerical dating or by any climate related data (for instance pollen). But how likely is it that the 56 m strandline really could be Rutherglen Formation (Suggate model). At the Tasman View subdivision (South Beach, Greymouth) there is less than 10 metres difference between the elevations of the Rutherglen and Karoro strandlines. The same relative difference holds in the Power Road area at Karoro and at Arnotts Heights (Karoro). But at Blue Spur the difference is no less than 20 metres (about double that at South Beach). There is only about a 6 m difference in elevation between the strandline elevation of the Karoro Formation between South Beach and Blue Spur. This means the difference in average long-term uplift rate between these localities is minor. If the 56 metre terrace at Blue Spur really is Rutherglen Formation, then it is unlikely to be Rutherglen(1). It could possibly be Rutherglen(2). However, as discussed in chapter five there is no available outcrop or other information that clearly distinguishes the Rutherglen(2) and Awatuna Formations. Between Greymouth and Hokitika the two formations have not been recorded at the same locality to date. The elevations are similar. In the Suggate model both are supposedly from the same "interglacial period" (MIS5e (regressive) and 5c respectively). Even at Point Elizabeth the evidence for separation of these fragmentary strandlines could be interpreted differently.

So the evidence that the Rutherglen Formation is present as a 56 m strandline at Blue Spur is actually rather weak. The evidence that the 56 m terrace is the Awatuna Formation is slightly better but not compelling.

It should be noted that the Karoro Formation at Blue Spur, as mapped by Suggate and Waight (1999) has a shore normal width of 1.5 km north of Houhou Creek, and 2 km in the vicinity of Cement Lead Road. The evidence from the location of gold workings (shafts and tunnels) in the Cement Lead Road area (formerly Known as "Big Paddock" in the gold rush period of the late 1800's) is there are one or more buried strandlines 1 to 1.5 km NW of the innermost (most easterly) Karoro strandline. The elevation of the upper surface of the marine deposits has been established at Madman's Tunnel (name of this extensive gold mining tunnel supplied by the current land owner) near the northern end of Cement Lead Road. The site is in the bottom of a steep sided gully incised into the Waimea Formation and is classified as Rutherglen Formation in table 7.3. Here the contact between the marine and overlying fluvial gravel has an altitude of 59 to 61 m (GPS measurement). This is substantially lower than the main Karoro strandline. This deposit could easily be correlated with the Rutherglen Formation on elevation and stratigraphic grounds. In this scenario the Rutherglen Formation has does not have a substantial sea cliff against the Karoro Formation (but then it doesn't at Karoro or South Beach either). At Blue Spur the contact relationship would be buried beneath the Waimea Formation and not readily observed. This scenario restores the relative elevations between each of the primary strandlines and means the pattern of tectonic uplift makes sense.

On the north side of the Arahura Valley an area of old gold workings was mapped by Suggate and Waight (1999) at the end of the spur situated at grid ref J32 N 3550 E 5180 between Gillams Gully Road and Liverpool Bills Gully. The terrace contains a thin (~5m) fluvial gravel deposit. The upper surface is at an elevation of around 80 m which is too high for the Rutherglen and Awatuna Formations. Although Suggate and Waight (1999) map Rutherglen Fm deposits at N 3600 E 5250 examination of the area has so far failed to produce any evidence for marine alluvium at this locality. Given that the site is in an embayment into the valley of Waimea Creek it is more likely that this terrace is fully fluvial.

Note there is no evidence for coast parallel tilting at the Awatuna strandline between grid ref J32 N 4200 E 5630 (where it occurs in gold exploration drill holes) and German Gully where it can be observed exposed in a terrace margin at J32 N 3740 E 5290. The Awatuna strandline can be traced from north of Kapitea Creek to outcrops at its type section near Chesterfield Road, then Sawyers Creek, then Sebastopol Creek, then German Creek, then along a clearly defined marine cliff to Waimea Creek. Gold workings are present in the strandline at the Lamplough Lead (Awatuna type section near Chesterfield Rd), Sawyers Creek, and Sebastopol Creek. Regardless of this interpretation, at Sebastapol Creek the basal contact of the Awatuna Formation on the Eight Mile Formation has an elevation of 46 to 49 m (GPS measurement). The upper surface is visible some 5 m higher at German Gully. So the Awatuna Formation could easily correlate with the 56 m strandline further south at Blue Spur.

The small area of Rutherglen Formation mapped by Suggate & Waight (1999) near Sawyers Creek at grid ref J32 N 3915 E 5440 was examined as part of this project. This is a fluvial deposit rather than a marine deposit. There is no Rutherglen strandline at this locality but the Awatuna strandline is present here. There are no confirmed outcrops of marine Rutherglen Formation between the Arahura and Kapitea Valleys this is the most logical correlation.

An alternative but probably less likely proposition is that the Rutherglen Formation is the highest marine strandline at Blue Spur, the Karoro Formation having been destroyed (as at Rutherglen north

of New River and Candle Light north of the Taramakau River). This would mean a faster long-term uplift rate at Hokitika than further north in the Greymouth area. One interesting consequence would the increased potential for preservation of additional discrete marine strandlines near Hokitika, which might include the buried 12 m and 20-25 m strandlines at Southside. This interpretation is not favoured here, largely because the Holocene uplift rate is less near Hokitika than at Greymouth. The evidence is not compelling for either option though. One could argue that the oldest strandline at Blue Spur can't be the Rutherglen Formation because it is overlain by the Waimea Formation (which is younger than the Rutherglen Formation). But the Waimean outwash cannot be traced back to Waimean moraines here so can it not be claimed with certainty that the fluvial deposits are Waimea Formation. Luminescence dating has been carried out by Berger et al (2001) on the soil overlying the fluvial gavel that is supposedly Waimea Formation at Blue Spur. The ages are discussed in relation to the (assumed) underlying Karoro Formation in Chapter 6 and are substantially younger than would be expected if the Suggate model is correct. A similar situation holds for the Rutherglen Formation at Candle Light further north. Here the elevation of fluvial gravel on the Rutherglen Formation is difficult to reconcile with the expected elevation of the Loopline Formation.

In this scenario there is minimal tilt across the Arahura valley. At Blue Spur the Scandinavia Formation has been destroyed by erosion during the deposition of the Karoro Formation while the Karoro has been preserved, the opposite being the case north of the Arahura Valley. Is this special pleading? The answer is no. Similar scenarios are acceptable at Candle Light (grid ref J32 N 4700 E 5940) where the Karoro and Scandinavia Formations have been entirely destroyed due to erosion that preceded the deposition of the Rutherglen Formation. This is also the case at the Awatuna Formation type-section where the Rutherglen Formation was destroyed by erosion preceding deposition of the Awatuna Formation, and from Gladstone to Karoro where most of the Awatuna Formation was destroyed during erosion preceding the deposition of the Nine Mile Formation.

One test of the various options is the presence or absence a lower strandline in the Chesterfield area. During fieldwork for this project new marine sand exposures of the Blake Formation have been located at Blakes Terrace, about 100-400 m east of SH6 at Awatuna (grid ref J32 N 4005 E 5275). The upper surface of the marine deposit is no probably higher than 38 metres. This is a good match for the 35 to 38 metre strandline at Blue Spur, the 33-35 m level at Point Elizabeth and possibly the 18-25 m strandline at Southside. In this scenario the implication is that there has been minimal tilting across the Arahura Valley and in fact minimal tilting from Point Elizabeth to Blue Spur.

The marine at Blakes Terrace was not identified by Suggate & Waight (1999), but RP Suggate (pers com) was aware via historic records relating to underground gold mining, that such deposits could be present here.

7.4.6 Chesterfield to Camerons

At its type section near Sunday Creek at Chesterfield the Awatuna Formation is situated at an elevation of about 53 m. A little further north (just east of EA road and north of Kapitea Creek) the Awatuna Formation is found at about 53 m in gold exploration drill holes. At this stage it is assumed that the Awatuna strandline bends seaward from Chesterfield to Camerons then parallels the Coastline up to Point Elizabeth. It is present at Point Elizabeth and at Stanton Crescent (Karoro) but has not been mapped between Karoro and EA Road.

The Rutherglen and Karoro Formations are not present at Chesterfield. They were truncated/destroyed by erosion during the deposition of the Waimea and Awatuna Formations.

The Rutherglen strandline at Candle Light (Grid ref J32 N 4700 E 5950) inland from Camerons is at an elevation of ~ 62 metres. It is assumed by Suggate & Waight (1999) to be too high to be correlated with the Awatuna Formation. Here the Karoro Formation is missing. It was truncated/destroyed during the erosion that accompanied deposition of the Rutherglen Formation.

7.4.7 Camerons to Karoro

At Karoro (Greymouth) the Karoro Formation has been reported at an elevation of ~ 95 metres. This is based on geomorphic rather than outcrop information. The highest known Quaternary marine outcrop at Karoro is lower than 90 metres and this elevation includes the overlying soil that is about 3 metres thick. Just south of Mill Creek (inland from Paroa) the strandline is also almost certainly below 90 metres.

In the Suggate model the Awatuna Formation would have to be lower than 60 m near Gladstone since it has not been mapped here. At Gladstone and South Beach the lower strandline of the Rutherglen Formation is at an elevation of no more than ~58 - 60 m. The main part of the Rutherglen Formation at Rutherglen is supposed to be at around 67 m (Suggate & Waight 1999), The Rutherglen(1) strandline at Karoro is at ~68 - 70 m. The Rutherglen(1) strandline elevation is similar (about 65-70 m) in the vicinity of the Tasman View subdivision just south of Mill Creek. At Candle Light (on the Bundi Road inland from Camerons) the rather conspicuous Rutherglen strandline is no higher than 62 metres (own estimate and estimate by Moar &Suggate 1996[fig3]). This is about 6-8 m lower than at Karoro. It is tempting to speculate that the Rutherglen Formation strandline at Candle Light might be slightly younger than the one at Karoro. Other factors may come into play including tectonic tilting.

There is a step in the "Loopline" terrace at Grid ref N4770 E 5900. It is possible that the step is a marine cliff. On the seaward side of the step exposures in a road cutting reveal the slightly lower (seaward) terrace surface is underlain by fluvial gravel that in turn sits on marine sand and gravel. This terrace riser could potentially define either the Rutherglen(2) or the Awatuna strandline. Alternatively it could simply be a degradational feature in the Loopline gravel. The marine sand is no higher than 50 m here, substantially lower than the maximum level at the innermost Rutherglen strandline a few hundred metres away at Candle Light.

There is (to my eye) an apparently undisturbed and probably in-situ beach sand and gravel deposit at approximately 55m at Karoro (Stanton Crescent) in Greymouth. This has been mapped as slumped Karoro Formation by Suggate and Waight (1999), an unlikely match as the deposits on the terrace immediately above are almost certainly Rutherglen(1) Formation. The Stanton Crescent deposit could be either Rutherglen(2) or Awatuna Formation.

7.4.8 Karoro to Point Elizabeth

At Point Elizabeth near Greymouth there are strandlines at 33 to 38 metres (offset by a north-south trending reverse fault), 48-52 m, and 55-57 metres. Any of these could be correlated with the Awatuna Formation.

The lower marine deposits at Point Elizabeth are at an elevation that is similar to the Blake Formation at Blakes Terrace (~ 35 m) and the lower marine deposit at Blue Spur (~ 35 m). So there is no particular reason to assume coast parallel tilting for deposits at the 35 metre level. Given the difference in IRSL ages between samples RR12 and RR9 there is no particular reason to assume the 35 metre level correlates with the Awatuna Formation.

If the assumption of no net tilting from Greymouth to Blue Spur holds then there may be either one or two low raised terraces (equivalent to the 12 m and 20-25 m levels from Southside, Hokitika) that are not represented at Point Elizabeth.

There is also a possibility that the type locality for the Awatuna Formation correlates with Rutherglen 2 at Gladstone and South Beach. The elevation (<60 m) is about right.

So there are strandline deposits situated between 45 and 60 metres elevation at Houhou Creek, Awatuna, EA Road, Candle Light, Gladstone, South Beach (Tasman View Subdivision), Karoro (Power Road), and Point Elizabeth. Are these all Awatuna Formation? There are also strandline deposits at ~ 45 m elevation on a prominent terrace north of Rapahoe between 10 Mile Creek and 12 Mile Bluff. Deposits on this terrace are discussed by Moar et al (2008) and Burrows (1997).

There are strandline deposits at 65 to 76 metres at Blue Spur, Rutherglen, South Beach, Karoro, and Point Elizabeth. Are these all Rutherglen Formation?

At Point Elizabeth the Caledonian Formation is at ~ 125 to 135 m amsl. The terrace is much too high to correlate with the Karoro Fm at Karoro (which is probably < 90 m). There is no way we can tell at present whether or not there is a direct relationship between the Caledonian and Scandinavia Formations. It is assumed that the Scandinavia Formation is younger as there is a strandline at 112 to 118 m between the Caledonian and Karoro Formations at Point Elizabeth. The Caledonian Fm (at Pt Elizabeth) gave an $IRSL_{blue}$ age of 87.1 ± 8.3 ka and the Scandinavia Fm (at Scandinavian Hill) gave an IRSL age of 123 ka. However, the Caledonian sample is much more likely to have been fully bleached at deposition so the older age on the Scandinavia formation might not have a significant bearing on the correlation.

7.4.9 Simplest Coast Parallel Correlation

The simplest solution to the strandline elevation conundrum is:

1. That the 35-38 metre terraces at Point Elizabeth, Blakes Terrace, and Blue Spur represent the same sea level event.
2. That the 56 m terrace at Blue Spur represents the same sea level event as the 53 m terrace at Chesterfield, the 48-52 m level and/or the 55 to 57 m level at Point Elizabeth.
3. That the Rutherglen Formation is not present at Blue Spur unless it is present beneath the fluvioglacial Waimea Formation and simply has not been recognised as yet.
4. That strandline deposits of the Karoro Formation are at a maximum elevation of about 85 to 86 at Point Elizabeth and 75 to 76 m at Blue Spur near Hokitika.

This solution involves the smallest number of assumptions with regard to coast parallel tilting and correlation. It differs markedly from the Suggate model, but the evidence for the new alternative is more compelling than for its predecessor. The justification for the new coast parallel correlation is outlined in detail in chapter 5 where the stratigraphy and dating issues are described in more detail.

7.4.10 Inter-regional correlation of marine terraces

The Suggate (1992) and Suggate and Waight (1999) correlation utilizes the assumption that the marine terrace sequence from North Westland can be correlated with similar sequences from other parts of the globe, for instance the well dated Huon Peninsula sequence from Papua New Guinea. Terraces from a poorly dated sequence are assigned assumed ages. By taking the measured local elevations and comparing these with a global sea level curve one can derive an average uplift rate. This is essentially what has been done for North Westland. So far nobody has attempted to define a correlation coefficient between the North Westland terrace sequence and any other raised terrace sequence. However, this has been carried out for a supposed marine terrace sequence from the western slope of the Southern Alps in South Westland by Bull and Cooper (1986). As pointed out by Ward (1988) this approach can be problematic. Ward made the following observation with respect to this correlation:

"High apparent rates of uplift of 5 to 8 mm/yr, with permissible errors of 30 m or more, lead one to suspect that almost any semi-regular sequence of altitudes could be matched "successfully" to the New Guinea sea-level curve".

The corollary is that a single marine terrace sequence, even with accurate elevation measurements, can be matched to a late Quaternary sea level curve in a number of ways, each giving a high correlation coefficient. Given the cyclical nature of climate change, sea level fluctuation, and global and local ice volume fluctuation, a secure correlation requires firm independent evidence for the age of at least two of the marine terraces. The correlation method of Bull and Cooper (1986) was also examined in detail by Pillans (1990) who made some criticisms but reserved final judgment.

Numerical ages were not available to Bull & Cooper (1986) so that correlation is not secure. Until this study such evidence has been rather thin in North Westland. The model of Bull & Cooper is not directly supported by this PhD project. One of the primary arguments against the interpretation of the Bull & Cooper terraces (situated on the flanks of the Southern Alps) being marine in origin was the supposed age of the landscape between the Southern Alps and the Tasman Sea, which relates back to the fundamental basis of the Suggate model. If the age of the Quaternary deposits of "lowlands" is significantly younger than previously thought then the terrace correlations of Bull & Cooper (1986) might begin to look slightly more plausible.

7.4.11 Holocene uplift rates

The standard reference on Quaternary uplift in North Westland is Suggate (1992). In the Suggate model the long-term Late Quaternary uplift rate near the modern coastline is much slower than Holocene rate. It is assumed that the Holocene rate is an aberration that will be smoothed out over the longer term.

At Awatuna the maximum elevation of Holocene swash-zone deposits is ~6 to 8 m above present mean sea level. Uplift is implied for the Holocene. If it is assumed that these materials formed at some time between 6.0 ka and 3.0 ka and that local sea level was no higher than +2 metres during that period then uplift of around 2 to 5 metres is likely (given that swash zone deposits that can be found 0 to 4 metres above sea level at modern West Coast beaches. The current uplift rate could be anywhere in the range 0.33 to 1.7 mm/yr. Clearly this is not very precise.

At Barrytown, Rapahoe, North Beach, Greymouth Karoro, South Beach, Gladstone and Camerons (along about 40 km of coastline) the older part of the Nine Mile Formation is significantly higher

than at Awatuna. It is at an elevation of up to 12 metres at South Beach. So it is reasonable to suggest there has been 7 to 10 metres of uplift since ~6 ka. The average rate could be as high as 1.7 mm/year. It might be greater if the older part of the Nine Mile Formation is younger than 6 ka. There is no particular reason to assume that the Holocene uplift rate is anomalous.

Naturally any revision of the isotope stage correlation for the various Late Quaternary deposits would have an impact on the calculation of local uplift rates.

7.4.12 MIS3 in North Westland

In the Suggate model the area between Greymouth and Hokitika doesn't contain surficial or mappable fluvial, glacial or marine deposits from MIS5d, MIS5b, MIS5a or MIS3. So apart from soil/loess there is an implication that the climatic conditions favoured destruction and/or burial of these deposits during much of the last glacial period. The burial option works best for a relatively slow tectonic uplift rate. The other options are that the surface area occupied by deposits from these isotope stages is too small to map effectively, or that they are represented as an inconsequential thin veneer over the main (older) deposits. Neall et al (2001) go so far as to suggest that that there was an episode of widespread soil erosion during or following MIS3 resulting in the loss of MIS3 from these deposits.

In the Suggate model there are no widespread surficial deposits from the period between about 60 ka and 35 ka, a duration of ~ 25 kyr. The lack of MIS 3 deposits is surprising given the near certainty of substantial glacial events in the Southern Alps during the period. One assumption inherent in the Suggate model is that the deposits dating from MIS 3 were destroyed or overwhelmed during MIS 2. MIS 3 glacial outwash deposits are present in parts of Canterbury, Fiordland (Williams 1996) and South Westland (Almond et al 2001, Berger et al 2001). So what special feature of North Westland geology prevents deposits from this isotope stage being exposed at the surface here? Rivers kept flowing during this interval and it is likely that there were several significant glacial advances (c.f. findings relating to Fiordland by Williams 1996). Tectonic uplift was continuous in onshore areas and probably occurred at the long-term average rate. But no MIS3 fluvioglacial terraces were uplifted sufficiently to enable them to be preserved as surface features. So what has happened to the sediments that must have been produced and transported during this period? The standard answer would be that the most significant MIS3 fluvial and glacial deposits are mainly situated at depth in areas now occupied by the (younger) Larrikins (MIS2) or Nine Mile (post-glacial) Formations in channels incised as a response to generally low to moderate sea level. All other surfaces are MIS4 or older so they can't hide MIS3 deposits unless MIS3 deposits are present as a thin surficial veneer.

Sutherland et al (2007) present cosmogenic isotope dating evidence from erratic boulders on glacial moraine for major glacial events during MIS5a/5b and MIS3 in South Westland. At least locally these events produced greater ice extent than that during MIS2. In North Westland deposits from ice advances within the MIS5 stadial events could have been destroyed or overwhelmed by ice advances during MIS4 or MIS2. However, given the paucity of numerical ages such an assumption has to be regarded here as unproven.

There is an indication that late MIS3 fluvial deposits may be present beneath MIS2 in the Grey Valley at Kamaka and Raupo (Hormes et al 2003; Preusser et al 2005). The Larrikins Formation (MIS2) is extensive and could potentially obscure middle to early MIS3 deposits. So using the Suggate model as a guide one would be looking for incised channels that were subsequently "backfilled" and floodplain deposits that have been over-topped by massive sediment deposition during MIS2.

Cosmogenic isotope dating on glacial erratic boulders by the writer, in conjunction with Dr Tim Barrows, has demonstrated the likely presence of late MIS3 glacial till and outwash in the 12 Mile Valley and at the Nelson Creek Farm Settlement. These areas were previously thought to be MIS4 Loopline Formation. As discussed previously this finding raises the possibility that late MIS3 deposits could be present in other parts of North Westland.

In the Suggate model there are no MIS3 marine strandlines now situated on land. The presumed argument is that all evidence of strandline and near-shore deposition dating from MIS3 was destroyed or buried during the post-glacial marine transgression.

These are assumptions though. The deposits that have been thought to represent MIS4 have not been securely assigned to that stage by any numerical dating methods. Some of the ^{14}C ages from the base of the Loopline formation are finite ages. These have been disregarded in the past. The reasoning relies on a set of assumptions as follows:

- That glaciation during the MIS5a/4 transition and during MIS4, the deposits from which are contained in the Loopline Formation, was significantly more extensive than glaciation during MIS3.
- That glaciation during MIS2 was significantly mote extensive than during MIS3.
- That problematic ^{14}C ages can be dismissed as being contaminated by younger carbon.
- That the Awatuna Fm (lowest marine terrace) dates from MIS5c and that MIS5a strandline deposits either missing or contained in the Blake and Craig Formations.

One solution to the MIS3 problem is simply to change the rules. If we accept the simplest shore parallel strandline correlation, accept the simplest interpretation of the radiocarbon ages for the buried soils on the marine terraces, accept the simplest interpretation of the IRSL ages that are least likely to be affected by partial bleaching, avoid attempting a precise match with the global eustatic sea level curve, and allow substantial glacial events in MIS3 then an alternative model can be constructed for the depositional/erosional history for North Westland.

7.5 NEW QUATERNARY STRATIGRAPHY AND ISOTOPE STAGE CORRELATION FOR NORTH WESTLAND

7.5.1 The New Model

Based on IRSL dating carried out during this project the ages of some Quaternary deposits appear to be much younger than previously supposed. A new shore parallel correlation has been proposed for the marine strandline sequence and this requires a new marine isotope stage correlation. It implies a change of general context whereby some climatic events are of sub-orbital scale, whereas before the same events were thought to of orbital scale.

Isotope Stage	Event Name	Climate Type	Glacial Advance	Formation
1	Aranui Interglacial			Nine Mile
2	Otira	(ACR) Stadial	Kumara 3	Moana
	Interstadial			
	Otira	Stadial	Kumara2_{2c}	Larrikins 2_2
	Raupo	Interstadial		
	Otira	Stadial	Kumara2_{2b}	Larrikins 2_1
	Kamaka	Interstadial		
	Otira	Stadial	Kumara2_{2a}	Larrikins 1
3	Chesterfield	Interstadial		
	Otira	Stadial	Kumara 2_1	Loopline
	Kaihinu	Interstadial		Craig (Informal)
	Kaihinu	Interstadial		Blake (Informal)
		Stadial	--	Older Loopline?
	Kaihinu	Interstadial		Awatuna
	t	Stadial	--	
	Kaihinu	Interstadial		Rutherglen 2
4	Waimea2	Stadial	Kumara 1?	Waimea 2
	Kaihinu	Interstadial		Rutherglen 1
5a/4	Waimea1	Stadial	Kumara 1	Waimea 1
5a	Karoro	Interglacial		Karoro
5b	Waimaunga	Stadial	--	Tansey 2
5c	Scandinavia	Interglacial		Scandinavia Caledonian
5d	Waimaunga	Stadial	--	Tansey 1
5e		Interglacial		Whiskey Candlelight
6	Nemona	stadial	--	Cockeye
6/8?	Kawhaka	stadial	--	Mudgie Ridge

Table 7.4 Proposed climate history for North Westland

In table 7.4 a new stratigraphy and marine isotope stage correlation is defined for North Westland. The correlation and numerical ages are discussed in detail in Chapter 6. In normal usage such a correlation would carry substantial climatic implications. For North Westland such an implication is not clear-cut. It is not entirely clear that sea-level highstands necessarily correspond to local interglacial climatic conditions. The sedimentological evidence primarily relates to high sea level

rather than warm climate and local sea level could have a glacio-isostatic component. In this correlation all formations that pre-date the LGM are substantially younger than previously thought. The evidence for this new correlation is detail later in the chapter.

Note that there are older Plio-Pleistocene fluvioglacial gravels of the Old Man Group preserved in North Westland. These gravels include the dominantly fluvial Humphries and Donnelly Conglomerates and ice-proximal fluvioglacial deposits (including bouldery till) of the Jones Formation. These older deposits have not been studied during this PhD project. The terminology for these early Quaternary deposits is derived from Bowen (1965). These units are subdivisions within the Old Man Group. These are thought to be much older than the Late Quaternary formations that begin with the Mudgie Ridge Formation.

Table 7.5: Proposed Quaternary stratigraphic correlation between North Westland and Fiordland							
Quaternary Stratigraphy, North Westland (This study)			**Loess Unit (Almond et al 2001)**	**Hollywood Cave (Whittaker et al 2011)**	**Quaternary Stratigraphy, Fiordland (Williams, PW. 1996)**		
Formation Name	**Oxygen Isotope Stage**			**Negative Isotopic Excursions**		**Climatic Episode**	**Age (Fiordland**
Nine Mile	1 > 8 ka						
Waiho Loop	2			11.8-12.2			
Moana		14 ka		13.0-14.4 (ACR)	Aurora 1	Glacial	11-14 ka
						Interstadial 1	14-15 ka
Larrikins 2b		16-17 ka	M6, T6, 14-16.5 ka	15.0- 16.1	Aurora 2	Glacial	15-17 ka
(Raupo Interstadial						Interstadial 2	17-18 ka
Larrikins 2a		18-22 ka	M5, T5, 18-24 ka	21.4-22.6 ka	Aurora 3	Glacial	18-20 ka
(Kamaka Interstadial)						Interstadial 3	21-39 ka
Larrikins 1		???		24.2-25.5 ka			
(Chesterfield Interstadial)				29-30.5 ka			
Loopline 2		29-35 ka	M4b, T4b, >26,<36 ka	32-33.5 ka			
Craig	3	33-35 ka??		39-40 ka	Aurora 4	Glacial	40-41 ka
Blake	3	38-40 ka		42-43 ka		Interstadial 4	41-45 ka
Loopline 1			M4a ,T4a, >45, <50 ka	47.5-50.5 ka			
Awatuna		48-50 ka			Aurora 5	Glacial	46-48 ka
(Pre Awatuna Fluvial)				55-56 ka		Interstadial 5	49-66 ka
Waimea 2	4			61-63 ka	Aurora 6	Glacial	66-91 ka
Rutherglen	4	65-73 ka					
Waimea 1	4/5a		M3 <80 ka				
Karoro	5a	77-87 ka				Interstadial 6	92 ka

Tansey 2	5b		M2 ?		Aurora 7?	Glacial	
Caledonian/Scandinavian	5c	90-105 ka					
Tansey 1	5d		M2 ?		Whitestone?	Glacial	
Whisky/Candle Light	5e	115-130 ka					
Cockeye	6???		M1 >130 ka				
Mudgie Ridge	8/10???						
Porika					Moat Creek?	Glacial	
Humphries Conglomerate	Pliocene 2.1 Ma						
Jones Formation	Pliocene 2.4-2.5 Ma						
Donnelly Conglomerate							
Eight Mile Formation	Pliocene & older						

Column five lists prominent negative excursions in carbon and oxygen isotopic curves from a speleothem (HW3) from Hollywood Cave at an elevation of ~130 m near Charleston. The chronology is based on 18 Uranium series ages

7.5.2 Implications for the Tectonic Uplift Rate in North Westland

As a comparison for the strandline sequence in North Westland there is a sequence of raised marine terraces along the Marlborough coastline on the eastern coast of the South Island. This sequence is defined and discussed by Ota et al (1996) and is summarised in table 7.6 below.

Table 7.6 Proposed correlation (this thesis) between the Marlborough and North Westland raised marine sequences.

Terrace age (Ota et al 1996)	Sequence at Kaikoura Peninsula (Ota et al 1996)	Sequence along the Marlborough coast line (Ota et al 1996)	Sequence from North Westland (this study)
100 ± 5	I (105 ± 2 m)	Tarapuhi (165 ± 2 m)	Caledonian
96 ± 5	II (80 ± 2 m)	--	Scandinavian
84 ± 5	III (60 ± 2 m)	Kemps(Upper) (110± 2 m)	Karoro
73 ± 5	IV (50 ± 2 m)	Kemps (Lower) (90 ± 2 m)	Rutherglen
60 ± 5	V (40 ± 2 m)	Amuri Bluff (37 ± 2 m)	Awatuna/Blake

For the Marlborough coastline Ota et al (1996) estimate long-term uplift rates of 1.1 mm/yr at the Kaikoura Peninsula and 1.7 mm/yr at Amuri Bluff. So the coastal uplift rate of c. 1.15 to 1.4 mm/yr calculated for North Westland (table 8.1) is not unprecedented within the South Island.

The marine isotope stage correlation proposed here has implications for the tectonic uplift rate in North Westland. The correlation proposed here can not work if the uplift rate is in the range 0.3 to 0.5 mm/yr (as proposed by Suggate 1992). It does work at an uplift rate of approximately 1.1 to 1.4 mm/yr. There is nothing particularly unusual about uplift at such rates in areas that are situated within a plate tectonic boundary zone. This is not the first time that a high uplift rate has been suggested for coastal parts of Westland. Cooper & Kostro (2006) discuss the uplifted marine strandline at Knights Point in South Westland. They estimate an uplift rate of 0.86 mm/yr at this locality based on an IRSL age of 123 ± 7 ka from deposits at an elevation of 113 m.

CHAPTER EIGHT: SUMMARY OF IMPLICATIONS

8.1 SUMMARY OF IMPLICATIONS

In Chapter 7 the proposed stratigraphic framework and marine isotope stage correlation is presented for the mid to late Quaternary period in North Westland. The proposal differs significantly from that of the Suggate and Waight (1999) in that it maximises the direct use of the best available numerical dating. It specific explanation of the reasons why little weight is placed on some numerical ages produced in this and other studies.

It is concluded that the best available age data indicates there may be multiple MIS4/3 sealevel high-stands recorded on-land in North Westland. Eustatic sea level is generally thought to have been intermediate between full glacial and interglacial levels during MIS3. As discussed above local sea level doesn't always track the global eustatic curve. So it can't be assumed that a global eustatic sea level and a local uplift rate curve can be used to calculate the ages of sequence of raised terraces.

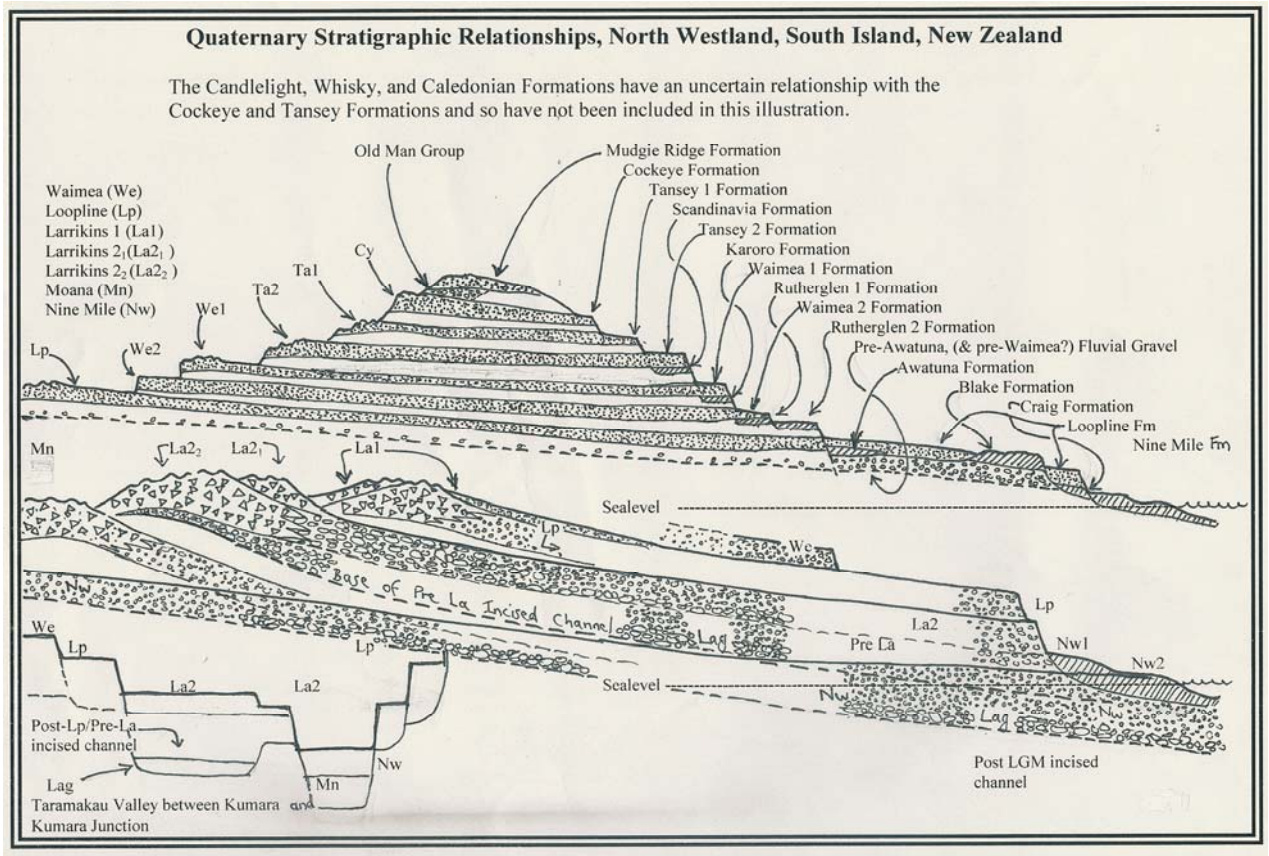

Figure 8.1: A new Quaternary stratigraphy for North Westland prepared for this PhD thesis

Assuming that the best correlation has been made between local and global/hemispheric scale climate events then there are a number of implications as follows:

1. The IRSL and cosmogenic isotope dating programmes produced relatively young ages for raised marine deposits and fluvioglacial deposits. These ages are not consistent with the previously established correlation between local deposits and hemispheric scale climatic events.

2. In Westland there is a terraced landscape containing Late Quaternary fluvioglacial and marine deposits that are mostly younger than MIS5e. Together the nature of the sediments and the pollen collected from ancient soils provide abundant evidence for variation of the climate here during the last 100 kyr.

Formation	**Marine Isotope Stage**	**Estimated calendar age (ka)**	**Greymouth-Point Elizabeth area**		
			Strandline elevation (m)	**Potential local sea level (m)**	**Uplift rate (mm / yr)**
Nine Mile	1	6	8-12	0 – 3	1.3-1.5
Moana Larrikins 2_2 Larrikins 2_1 Larrikins 1	2	14-15 { {16-21 22-24??			
Loopline	3	28-35			
Craig's	3	33-35	15-17	-30 to -35	1.25-1.6
Blake	3	38-40	35-38	-20 to -25	1.35-1.65
Awatuna	3	48-50	52	-20 to -25	1.4-1.60
Pre Awatuna fluvial gravel	(potentially pre Waimea 1)				
Rutherglen 2	3	??	55-60		
Waimea 2 degraded"	3	??			
Rutherglen 1	3	65-68	68-74	-20 to -30	1.3-1.5
Waimea 1	4/5a	68-77			
Karoro	5a	77-85	80-85	-10 to -20	1.2-1.35
Tansey 2	5b	90??			
Scandinavia Caledonian	5c	95-100 100-105	112-118 125-135	-10 to -15 -15	1.15-1.4 1.2-1.4
Tansey 1	5d	110			
Whisky	5e	116-118	155-165	0	1.3-1.4
Candlelight	5e	130	180-185	4	1.40
Cockeye	6???	140-150			
Mudgee Ridge	8 / 6???	250 / 180			
Important gap in the on-shore sedimentary record					
Humphreys Conglomerate		Hautawan-Marahauan at Findlay Creek (Suggate & Waight 1999)			
Jones Formation		~2.5 Ma, Suggate (1990)			
Donnelly Conglomerate		> 2.5 Ma			

Table 8.1 Proposed Quaternary stratigraphy and uplift rate for North Westland

3. Re-evaluation of the dating and palynology of silt deposits at the Okarito Pakihi bog (chapter 5) indicates that Nestegis bearing Dacrydium cupressinum dominated temperate rainforest could have been widespread in South Westland during early MIS3, probably from c. 62 ka to c. 50 ka.

4. Evaluation of Antarctic ice core isotopic records, marine SST records from the Southern Ocean and the New Zealand region (chapter 4) and various dated pollen based climate proxy records (chapter 5) is compatible with a substantial glacial episode in the Southern Alps commencing at c. 50 ka and lasting until c. 40 ka. This period of generally cold climate was followed by an interstadial even from about 40 ka to 35 ka consistent with the findings of Burge (2007).
5. In Westland the pollen record implies local climate responds rapidly to local and regional (Southern mid-latitude) forcing. This does not mean that a Northern Hemisphere influence is absent, but rather that it is not always dominant.
6. As discussed in chapter four, orbital-scale cycles in direct insolation and meridional insolation and temperature gradients may be an important factor in determining the timing, extent and volume of glacial ice-cover in the Southern Alps. Regional and Hemispheric-scale climate also responds to major millennial-scale fluctuations that are not entirely controlled by precession/obliquity cycles.
7. It is argued that, contrary to established practice, the presence in organic silt/peat of pollen from the genus *Nestegis* is not a fail-safe guide for attribution of these deposits to an interglacial climate. *Nestegis* has in the past survived interstadial climate conditions in Westland, and possibly stadial conditions in suitable refugia. It may have required the unusually harsh conditions of the long LGM period to fully eliminate this genus in this region.
8. A new coast parallel terrace correlation is presented in figure 7.4. The new stratigraphic proposal for North Westland is presented in figure 8.1 and tables 7.4, 7.5 and 8.1. The correlation is based on observed stratigraphic relationships, physical elevation, IRSL and cosmogenic isotope dating. This involves a simplifying assumption of minimal coast parallel tilting (or differential uplift).
9. At approximately 1.25 – 1.5 mm/yr the coastal uplift rate between Greymouth and Hokitika is around 2 to 3 times greater than the rate of ~0.45 mm/yr previously calculated by Suggate (1992). It is concluded that global eustatic sea levels should not be used unquestioningly in calculations of uplift rates in Westland without consideration of the potential isostatic overprint caused by ice-volume fluctuations in the Southern Alps.
10. On balance the available numerical dating indicates that the Waimea Glaciation reached its maximum extent in Westland during MIS5a or MIS4 probably after c.80 ka rather than during MIS6 as previously proposed. The shallower portions of the Waimea2 Formation were probably deposited during MIS4.
11. Based on a thorough evaluation of luminescence and radiocarbon dating it is likely that there are MIS4/3 raised marine terraces (Rutherglen, Awatuna, Blake and Craig Formations the later two being informal designations) preserved in North Westland. This implies a pattern of repeated MIS3 marine transgression and regression in North Westland. Further:
    i. Marine transgressions resulting in the deposition of (now raised) strandlines may have been synchronous with Antarctic interstadial episodes.
    ii. The repeated or cyclical development of peaty soil on the various marine terraces potentially indicates rapid climatic oscillations during MIS4 and MIS3. Interstadial warmth may approach interglacial conditions at least briefly while stadial cooling may approach full glacial conditions at least briefly.

12. The ages and elevations of the various MIS4 and MIS3 raised marine deposits lead to a suggestion that there may be local isostatic effects of rapid ice loading (stadial periods) and unloading (interstadial periods) in the South Island.
13. At the early MIS3 Awatuna Formation type section an organic-rich soil/peat separates the marine beds from the overlying Loopline Formation.
14. The internal sedimentology of the Loopline Formation above the Craig Formation at the Phelps Goldmine and in the Chesterfield area is suggestive of multiple fluvioglacial depositional events contributing to the accumulation of this formation.
15. The Loopline and Larrikins Formations are not probably not separated by the full duration of MIS3 as previously proposed by Suggate & Waight (1999) and are likely to be closer in age than previously thought. The "important interval" during the Otira Glaciation referred to in the stratigraphy of Suggate and Waight (1999) is likely to be shorter than they supposed. It is proposed here that deposition of the older portion of the Loopline Formation commenced around 50 ka and was probably complete by 40 ka. As sea level may have been relatively low during parts of this period substantial fluvial erosion and strath cutting may have occurred, isolating the major rivers within significantly incised channels. In the case of the Taramakau River the incised "Loopline" channel was overwhelmed by fluvioglacial outwash during the deposition of the Larrikins Formation.
16. In agreement with Suggate & Almond (2005) the local LGM commenced no later than ~34 ka. The furthest westward advance of ice during the LGM coincides with what have previously been mapped as MIS4 moraines of the Loopline Formation between Stafford Loop Road and Kapitea Reservoir, at the Blair Farm Settlement, in the Twelve Mile Valley and at the Nelson Creek Farm Settlement. Cosmogenic isotope dating of erratic boulders here demonstrates the surface deposits at Loopline Road are probably no older than c. 22 ka. A relatively thin apron of till and outwash buries older alluvium of contrasting provenance here.
17. In the Kumara to Kumara reservoir area the LGM is represented by at least 4 substantial ice advances each separated by a brief interstadial event the oldest probably post-dating 23 ka. Deposits associated with these advances are:
    i. The Larrikins 1 Formation
    ii. The Larrikins$2_{(1)}$ Formation
    iii. The Larrikins$2_{(2)}$ Formation
    iv. The Moana Formation

18. Deep fluvial incision has occurred repeatedly within North Westland. Rates and depths of incision are related to sediment supply, isostasy, tectonic uplift, and the position of the local base level (controlled to a substantial degree by rapid sea level fluctuation). Deep incision occurs rather abruptly and probably takes place during the early stages of a deglaciation or partial deglaciation. This is when the ice front is in full retreat. Glacial terminae are probably situated initially in sediment trapping proglacial lakes inland from the recently established moraine belt which acts as a dam. As discussed in Appendix five cessation of gravel delivery from the hinterland leads to canibalisation of fluvioglacial sediment by rivers seaward of the pro-glacial lakes. In North Westland rapid incision probably predates much of the rise in interglacial/interstadial sea level. Phases of incision are likely to have occurred at (but are not limited to) the following times:

    i. Following the deposition of the Mudgie Ridge Formation.
    ii. Following the deposition of the Cockeye Formation.
    iii. Following the deposition of the Tansey1 Formation.
    iv. Probably following the deposition of the Tansey2 Formation

v. Following the deposition of the Waimea1 Formation
vi. Following the deposition of the Waimea2 Formation (Prior to the deposition of the Awatuna and Blake Formations).
vii. Following the deposition of the Blake Formation. But prior to the deposition of the Loopline Formation.
viii. Post Loopline but pre Larrikins 2 deposition.
ix. Possibly intra Larrikins 2.
x. Post Larrikins 2 and pre Moana deposition (incision particularly deep at this time).
xi. Post Moana and pre Nine Mile deposition.

The following is a brief summary of North Westland soils containing an interglacial/interstadial pollen flora and the isotope stage correlation (this study) for the underlying Quaternary formation have:

i. An interglacial flora from fluvial gravel and silt overlying the MIS5c Scandinavia Formation at Scandinavia Hill (Suggate 1991).
ii. Probably an interglacial-like soil on the MIS5c Caledonian Formation but the pollen has not been assessed.
iii. At least 3 wood-bearing interglacial-like soils on MIS5a Karoro Formation marine sand at Ferguson's Pond (this study), at least one of which is fully interglacial (Soons & Lee 1984).
iv. At least 2 wood-bearing interglacial-like soils on the MIS5a/4 Waimea Formation fluvioglacial gravels (this study).
v. At least 2 wood-bearing interglacial-like soils on the MIS4/3 Rutherglen(1) Formation (Moar & Suggate 1996).
vi. A wood and *Nestegis* pollen bearing interglacial soil on the MIS3 Awatuna Formation.
vii. Wood-bearing organic soil on the "Craig and Blake Formations" (probably MIS3) which may correlate with the lower buried soil at Hatters Creek.
viii. A wood-bearing highly organic peaty soil intermittently preserved at the base of loess on Loopline Formation (probably MIS3) at Chesterfield Road and at several sites near Stafford Loop Road between the Kapitea Reservoir and Callaghans.
ix. A thin peaty layer between MIS2 till of the Larrikins Formation and till assumed to be Loopline Formation.

8.2 THE NULL HYPOTHESIS

In chapter two (section 2.1.2) a "null hypothesis" is proposed. The null hypothesis is the "Suggate model". The task undertaken in this thesis is to attempt to test this model to see whether it is likely to be incorrect. The Suggate model is based on a number of assumptions. If these can be shown to be incorrect then the null hypothesis is effectively shown to be incorrect. This does not mean that the alternative hypothesis is necessarily correct though.

The assumptions inherent in the Suggate model are listed in chapter 5, section 1.5 of this thesis. The analysis carried out during this project has shown a number of these assumptions to be either of doubtful validity or simply incorrect. The following comments on the null hypothesis are made in connection with the assumptions listed in section 1.5.

1. The practice of assuming older radiocarbon ages from a number of sites are incorrect and that the sampled material is contaminated by younger carbon is shown to be of suspect validity. While it may be true in specific instances the IRSL dating carried out during this project on samples from the type section of the Awatuna Formation demonstrates that the assumption cannot be sustained on the basis of existing data. This does not mean the assumption is false, but rather that it is presently not falsifiable, which is a fundamentally non-scientific position.

2. The practice of assuming that fluctuations in the extent of tall canopy forest dominated by podocarp species necessarily correlates with orbital-scale interglacial or strong interstadial climatic conditions is shown to be of doubtful validity based on the IRSL dating carried out during this thesis project.

3. The practice of assuming that marine strandline deposits necessarily correlate only with 1st order or orbital scale changes in eustatic sea level is shown to be of doubtful validity on the basis of the IRSL dating carried out during this PhD project. This assumption is a major component of the rationale for the marine isotope stage correlation inherent in the model.

4. The weight of evidence produced by the IRSL dating programme has demonstrated effectively that the Late Quaternary sequence in North Westland is almost certainly younger than is implied in the Suggate model.

5. Because the IRSL dating programme has provided numerical ages that places limits on the age of the various marine strandlines, this then provides a more secure baseline for the estimation of rates of tectonic uplift in the coastal zone between Twelve Mile Bluff and Hokitika. These uplift rates are greater than those implied by the Suggate model.

It is not concluded that the stratigraphic correlation proposed in this thesis is correct in all details. The new proposal is one alternative based on a range of available data. Future work is likely to alter aspects of this correlation. It is concluded that the null hypothesis as defined above, in other words the default model (the Suggate model), is unlikely to be correct.

8.3 DIRECTIONS FOR FUTURE WORK

The following are a number of suggestions for future on-shore investigation based on the newly proposed stratigraphic model:

1. It would be useful to target perhaps two or three of the raised marine formations for more intensive dating. Future sampling for IRSL dating should focus on silt beds rather than sand or gravel beds. Dating should be focused on areas were there has been little opportunity for substantial percolation of groundwater and where there is little evidence of transport of iron in solution.

2. Further collection of palynological samples from suitable profiles would be useful in terms of the understanding of climatic cycles and vegetative responses, particularly for sites with thick cover-bed sequences. This work should be extended to take in older formations including the Tansey, Whisky and Cockeye Formations, and would best be targeted at sites that have been accumulating surface sediment rather than those where past surface erosion is likely.

3. Further exposure age dating would be useful. This could focus on two issues:

    i. The age of glacial erratic boulders, and
    ii. Burial dating on coverbed sequences for both marine and fluvioglacial deposits.

Given the relative paucity of erratic boulders on moraines of the older glacial deposits (Waimea, Tansey and Cockeye Formations), burial dating on the coverbed sequences is likely to be a good option. This would help in giving realistic bounding ages for a number of formations that have not been dated directly before. In addition, given that the radionuclide content of Quaternary deposits in North Westland is relatively high, it should extend the maximum age for numerical dating.

4. It has become increasingly apparent that the Quaternary stratigraphy of North Westland is more complex than is readily apparent by examination of the surficial geomorphology. In the future the stratigraphy could be brought into better focus by additional observations of newly created exposures, particularly in deep alluvial goldmines. This type of observation tends to be rather fortuitous and requires such sites to be visited on a regular basis by experienced Earth Scientists.

5. U-series dating and stable isotopic studies on speleothems have not been widely attempted in North Westland. There is scope for identifying the age of former water tables in the Charleston, Fox River to Punakaiki and Point Elizabeth to Greymouth areas where limestone is abundant and known to contain cave complexes.

9.0 REFERENCES

Ahn, J.; Brook, E.J. 2008. Atmospheric CO_2 and climate on millennial time scales during the last glacial period. Science 322: 83-85.

Alexanderson, H.; Eskola, K.O.; Helmans, K.F. 2008: Optical dating of Late Quaternary sediment sequence from Solki, Northern Finland. Geochronometria 32: 51-59.

Almond, P.C.; Moar, N.T.; Lian, O.B. 2001. Reinterpretation of the glacial chronology of South Westland, New Zealand. New Zealand Journal of Geology and Geophysics 44: 1-15

Almond, P.C. 1996. Loess, soil stratigraphy and Aokautere ash on late Pleistocene surfaces in South Westland, New Zealand: interpretation and correlation with glacial stratigraphy. Quaternary International 34-36: 163-176

Anderson, B.; Lawson W.; Owens, I.; Goodsell, B. 2006 Past and future mass balance of 'Ka Roimata o Hine Hukatere' Franz Josef Glacier, New Zealand. Journal of Glaciology 52:597-607.

Anon, 1988. Report on prospecting mining licence 32-835, Pine Creek, Hokitika. L&M Mining Ltd Mineral Report Series M3017, Crown Minerals, Ministry of Economic Development.

Arz, H.W.; Lamy, F.; Ganopolski, A.; Nowaczyk, N.; Parzold, J. 2007. Dominant Northern Hemisphere climate control over millennial-scale glacial sea-level variability. Quaternary Science Reviews 26: 312-321.

Balescu, S. Dumas, B. Gueremy, P. Lamothe, M. Llenaff, R. Raffey, J. 1997. Thermoluminescence dating tests of Pleistocene sediments from uplifted marine shorelines along the southwest coastline of the Calabrian Peninsula (Southern Italy). Palaeogeography, Palaeoclimatology, Palaeoecology 130: 25-41

Banerjee, D. Murray, A.S.; Botter-Jensen, L.; Lang, A. 2001. Equivalent dose estimation using a single aliquot of polymineral finegrains. Radiation Measurement 33: 73-94.

Bar-Matthews, M.; Ayalon, A.; Kaufmann, A. 2000. Timing and hydrological conditions of sapropel events in the Eastern Mediterranean, as evidenced from speleothems, Soreq Cave. Chemical Geology 169: 145-156.

Barker, S.; Diz, P.; Vautravers, M.J.; Pike, J.; Knorr, G.; Hall, I.R.; Broecker, W.S. 2009. Interhemispheric Atlantic see-saw response during the last deglaciation. Nature 457: 1097-1102.

Bareille, G.; Grousset, F.E.; Labracherie, M. 1994. Origin of detrital fluxes in the southeast Indian Ocean during the last climatic cycles. Paleoceanography 9: 799-819.

Barrows, T.; Stone, J.O.; Fifield, L.K.; Creswell, R.G. 2001. Late Pleistocene Glaciation of the Kosciuszko Massif, Snowy Mountains, Australia. Quaternary Research 55(2): 179-189.

Barrows, T.T.; Juggins, S.; DeDeckker, P.; Calvo, E.; Pelejero, C. 2007. Long-term sea surface temperature and climate change in the Australian-New Zealand Region. Paleoceanography 22: PA2215,doi:10.1029/2006PA001328

Beavan, J.; Moore, M.; Pearson, C.; Henderson, M.; Parsons, B.; Bourne, S.; England, P.; Walcott, D.; Blick, G.; Darby, D.; Hodgkinson, K. 1999. Crustal deformation during 1994-1998 due to oblique continental collision in the central Southern Alps, New Zealand, and implications for seismic potential of the Alpine fault. Journal of Geophysical Research 104, B11: 25233-25255.

Bell, J.M. & Fraser, C. 1906. The Geology of the Hokitika Sheet, North Westland Quadrangle. New Zealand Geological Survey Bulletin, new series 1.

Berger, A.; Loutre, M.F. 1991. Insolation values for the climate of the last 10 million years. Quaternary Science Reviews 10: 297-317.

Berger, A. 1992. Orbital Variations and Insolation Database. IGBP PAGES/World Data Centre-A for Paleoclimatology Data Contribution Series #92-007. NOAA/NGDC Paleoclimatology Program, Boulder, Co, USA.

Berger, G.W.; Almond, P.C.; Pillans, B.J. 2001a. Luminescence dating and glacial stratigraphy in Westland, New Zealand. New Zealand Journal of Geology and Geophysics 44: 25-35.

Berger, G.W.; Ante, S.; Domack, E. 2010. Luminescence from glaciomarine sediment trap samples at the Antarctic Peninsula. Quaternary Geochronology 5: 244-249.

Berger, G.W.; Pillans, B.J.; Tonkin, P.J. 2001b. Luminescence chronology of loess-paleosol sequences from Canterbury, South Island, New Zealand. New Zealand Journal of Geology and Geophysics 44: 501-516.

Berger, G.W.; Pillans, B.J.; Palmer, A.S. 1994. Test of Thermoluminescence Dating of Loess from New Zealand and Alaska. Quaternary Science reviews 13: 309-333.

Berger, G.W.; Nielsen, E. 1991. Evidence from thermoluminescence dating for Middle Wisconsinan deglaciation in the Hudson Bay Lowland of Manitoba. Canadian Journal of Earth Science 28: 240-249.

Berryman, K. 1993. Distribution, age and deformation of late Pleistocene marine terraces at Mahia Peninsula, Hikurangi subduction margin, New Zealand. Tectonics 12: 1365-1379.

Berryman, K. 1980. Late Quaternary movement on White Creek Fault, South Island, New Zealand. New Zealand Journal of Geology and Geophysics 23: 93-101.

Bielefeld, B.1997. Investigation into albedo controlled energy loss during the last glaciation. GeoJournal 42: 329-336.

Blackwelder, B.W.; Pilkey, O.H; Howard, J.D. 1979. Late Wisconsin Sea Levels on the Southeast U.S. Atlantic Shelf based on In-Place Shoreline Indicators. Science 204:618-620.

Bloom, A.W.; Broecker, W.A.S.; Chappell, J.M.A.; Matthews, R.K.; Mesolella, K.J. 1974. Quaternary sea level fluctuations on a tectonic coast: new 230^{Th}/234U dates from the Huon Peninsula, New Guinea. Quaternary Research 4: 185-205

Blumberg, S.; Lamy, F.; Arz, H.W.; Echtler, H.; Wiedicke, M.; Haug, G.; Oncken, O. 2008. Turbiditic trench deposits at the South-Chilean active margin: A Pleistocene-Holocene record of climate and tectonics. Earth and Planetary Science Letters 268(3-4): 526-539.

Blunier, T.; Brook, E.J. 2001. Timing of millennial-scale climate change in Antarctica and Greenland during the last glacial period. Science 291: 109-112.

Bowen, F.E. 1965. Early Pleistocene glacial and associated deposits of the South Island, New Zealand. New Zealand Journal of Geology and Geophysics 10: 164-181.

Brook, E.J.; White, J.W.C.; Schilla, A.S.M.; Bender, M.; Barnett, B.; Severinghaus, J.P.; Taylor, K.C.; Alley, R.B.; Steig, E.J. 2005 Timing of millennial-scale climate change at Siple Dome, West Antarctica, during the last glacial period. Quaternary Science Reviews 24: 1333-1343.

Bryant, E.A.; Price, D.M. 1997. Late Pleistocene marine chronology of the Gippsland Lakes region, Australia. Physical Geography 18(4):318-334.

Budziak, D. 2004. Alkenones and sea surface temperature of sediment core GeoB 3007-1. doi: 10.1594/PANGAEA.227267.

Bull, W.B.; Cooper, A.F. 1986. Uplifted marine terraces along the Alpine Fault, New Zealand. Science 234: 1225-1228

Bull, W.B.; Cooper, A.F. 1988. New Zealand Marine Terraces: Uplift Rates (Reply). Science 240: 804-805.

Burge, P.I. 2007. A record of Environmental and Climate Change from the West Coast, South Island, New Zealand using Beetle Fossils. A thesis submitted in partial fulfillment of the requirements for the degree of Doctor of Philosophy in Geology in the University of Canterbury.

Burge, P.I.; Shulmeister, J. 2007a. Re-envisioning the structure of the last glacial vegetation in New Zealand using beetle fossils. Quaternary Research 68(1): 121-132.

Burge, P.I.; Shulmeister, J. 2007b. An MIS 5a to MIS 4 (or early MIS 3) environmental and climatic reconstruction from the northwest South Island, New Zealand, using beetle fossils. Journal of Quaternary Science 22(5): 501-516.

Burns, S.J. Fleitmann, D.; Matter, A.; Krammrs, J.; Al-Subbary, A.A. 2003. Indian Ocean Climate and an Absolute Chronology over Dansgaard/Oescher Events 9 to 13. Science 301: 1365-1367

Burrows, C.J. 1997. An interglacial macrofossil fauna from Schulz Creek, north Westland, New Zealand. New Zealand Journal of Botany 35: 187-194.

Burrows, C.J. 1988. Late Otiran and Aranuian radiocarbon dates from South Island localities. New Zealand Natural Sciences 15: 25-36.

Cabioch, G.; Ayliffe, L.K. 2001. Raised coral terraces at Malakula, Vanuatu, Southwest Pacific, indicate high sea level during Marine Isotope Stage 3. Quaternary Research 56(3): 357-365.

Cann, J.H.; Belperio, A.P.; Gostin, V.A.; Murray-Wallace, C.V. 1988. Sea level history, 45,000-30,000 years B.P. inferred from benthic foraminifera, Gulf of St Vincent, South Australia. Quaternary Research 29: 153-179.

Cann, J.H.; Belperio, A.P.; Gostin, V.A.; Rice, R.L. 1993. Contemporary benthic foraminifera in Gulf of St Vincent, South Australia, and a refined late Pleistocene sea-level history. Australian Journal of Earth Sciences 40: 197-211.

Carter, J.A. 2002. Phytolith analysis and paleoenvironmental reconstruction from Lake Poukawa core Hawkes Bay, New Zealand. Global and Planetary Change 33: 257-267.

Carter, J.A. 2007. Ancient Climate and Environmental History from Phytolith-occluded Carbon. Unpublished PhD Thesis, Victoria University of Wellington.

Carter, J.A.; Lian, O.B. 2000. Paleoenvironmental reconstruction from the last Interglacial using phytolith analysis, south eastern North Island, New Zealand. Journal of Quaternary Science 15(7): 733-743.

Carter, L.; Neil, H.L.; Northcote, L.2002. Late Quaternary ice-rafting events in the SW Pacific Ocean, off eastern New Zealand. Marine Geology 191: 19-35.

Carter, R.M.; Norris, R.J. 1976. Cainozoic history of southern New Zealand: An accord between geological observations and plate tectonic predictions. Earth and Planetary Science Letters 31: 85-94.

Cavaney, R.J. 1968. Glacial geology of the Kumara-Greenstone-Callaghans area, Westland, New Zealand. Unpublished report, Lime and Marble Ltd.

Cayre, O.; Lancelot, Y.; Vincent, E. 1999. Pale oceanographic reconstructions from planktonic foraminifera off the Iberian margin: temperature, salinity and Heinrich Events. Paleoceanography 14(3): 384-396.

Chappell, J. 1974. Geology of coral terraces, Huon Peninsula, New Guinea: A study of Quaternary tectonic movements and sea-level change. Geological Society of America Bulletin 85: 553-570.

Chappell, J. 1975. Geology of coral terraces, Huon Peninsula, New Guinea: A study of Quaternary tectonic movements and sea-level changes. Geol Soc Am Bull 86: 1484-1486.

Chappell, J. 1983. A revised sea level record for the last 300,000 years from Papua New Guinea. Search 14: 99-101.

Chappell, J. 2002. Sea level changes forced ice breakout in the last glacial cycle: new results from coral terraces. Quaternary Science Reviews 21(10): 1229-1240.

Chappell, J.; Omura, A.; Esat, T.; McCullock, M.; Pandolfi, J.; Ota, Y.; Pillans, B. 1996. Reconciliation of Late Quaternary sea levels derived from coral terraces at Huon Peninsula with deep sea oxygen isotope records. Earth & Planetary Science Letters 141: 227-236

Chappell, J.; Ota, Y.; Berryman, K. 1996. Late Quaternary coseismic uplift history of the Huon Peninsula, Papua New Guinea. Quaternary Science Reviews 15: 7-22.

Chappell, J; Shackleton, N.J. (1986). Oxygen isotopes and sea level. Nature 324: 137-140.

Chappell, J.; Veeh, H.H. 1978: ^{230} Th/^{234}U age support of an interstadial sea level of –40 m at 30,000 yr BP. Nature 276: 602-604.

Chen, JH; Curran, HA; White, B; Wasserburg, GJ; 1991. Precise chronology of the last interglacial period; ^{234}U-^{230}Th data from fossil coral reefs of the Bahamas. Geological Society of America Bulletin 103: 82-97.

Chinn, T.; Winkler, S.; Salinger, M.J.; Haakensen, N.; 2005. Recent glacier advances in Norway and New Zealand: a comparison of their glaciological and meteorological causes. Geografisker Annaler 87A(1): 141-157.

Choi, J.H.; Murray, A.S.; Cheong, C.S.; Chang, H.W. 2003. Luminescence dating of well-sorted marine terrace sediments on the southeastern coast of Korea. Quaternary Science Reviews 22: 407-421.

Choi, J.H.; Murray, A.S.; Cheong, C.S.; Hong, D.G.; Chang, H.W. 2003. The resolution of stratigraphic inconsistency in the luminescence ages of marine terrace sediments from Korea. Quaternary Science Reviews 22: 1201-1206.

Clark, P.U.; Hostetler, S.W.; Pisias, N.G.; Schmittner, A.; Meissner, K.J. 2007. Mechanisms for a ~7 kyr climate and sea-level oscillation during Marine Isotope Stage 3. In: Ocean Circulation Mechanisms and Impacts. Geophysical Monograph Series 173. American Geophysical Union. 10.1029/1736M15.

Clarke, M.L. 1996. IRSL dating of sands: bleaching characteristics at deposition inferred from the use of single aliquots. Radiation Measurements 24: 611-620.

Clarke, M.L.; Rendell, H.M. 1997. Stability of IRSL Spectra of Alkali Feldspars. Physica Status Solidi (b) 199, p. 597-604.

Clarke, M.L.; Rendell, H.M.; Wintle, A.G. 1999. Quality assurance in luminescence dating. Geomorphology 29: 173-185.

Clarke, G.K.C.; Marshall, S.J. 1999. A glaciological perspective on Heinrich events. Pp 243-262 in Clark, P.U., Webb, R.S., Keigwin, L.D. eds., Mechanisms of Global Climate Change at Millennial Time Scales; Geophysical monograph 112; American Geophysical Union; Washington DC.

Colhoun, E.A. 2000. Vegetation and climate change during the last Interglacial-Glacial cycle in western Tasmania, Australia. Palaeogeography, Palaeoclimatology, Palaeoecology 155: 195-209.

Colhoun, E.A.; Pola, J.S.; Barton, C.E.; Heijnis, H. 1999. Late Pleistocene vegetation and climate history of Lake Selina, western Tasmania. Quaternary International 57/58: 5-23.

Cooper, A.F.; Kostro, F. 2006. A tectonically uplifted marine shoreline deposit, Knights Point, Westland, New Zealand. New Zealand Journal of Geology and Geophysics 49: 203-216

Cortese, G.; Ablemann, A. 2002. Radiolarian-based paleotemperatures during the last 160 kyr at ODP site 1089 (Southern Ocean, Atlantic Sector). Palaeogeography, Palaeoclimatology, Palaeoecology 182: 259-286.

Cortese, G.; Ablemann, A.; Gersonde, R. 2007. The last five glacial-interglacial transitions: A high resolution 450,000-year record from the Subantarctic Atlantic. Paleoceanography 22; PA4203, doi:10.1029/2007PA001475.

Cotton, R.J.; Stewart, M. 1989. Alluvial gold resource evaluation, Houhou Creek, Hokitika. In Proceedings 23rd Annual Conference, NZ Branch, Australasian Institute of Mining and Metallurgy pp 13-35.

Cox, S.C.; Sutherland, R 2007. Regional geological framework of South Island, New Zealand and its significance for understanding the active plate boundary. In- A Continental Plate Boundary: Tectonics at South island, New Zealand. Geophysical Monograph Series 175, American Geophysical Union. 10.1029/175GM03.

Craw, D.; Youngson, J.H.; Koons, P.O. 1999. Gold dispersal and placer formation in an active oblique collisional mountain belt, Southern Alps, New Zealand. Economic Geology 94:605-614.

Crosta, X; Sturm, A.; Armand, L.; Pichon, J-J. 2004. Late Quaternary sea ice history in the Indian sector of the Southern Ocean as recorded by diatom assemblages. Marine Micropaleontology 50: 201-223.

Crowley, T.J.; Kim, K-Y. 1994. Milankovitch forcing of the last interglacial sea level. Science 265: 1566-1568.

Crundwell, M.; Scott, G.; Naish, T.; Carter, L. 2008. Glacial-interglacial ocean climate variability from planktonic foraminifera during the Mid-Pleistocene transition in the temperate Southwest Pacific. Palaeogeography, Palaeoclimatology, Palaeoecology 260: 208-229.

Cruz, F.W. Jnr.; Burns, S.J. Jercinovic, M.; Karmann, I.; Sharp, W.D.; Vuille, M. 2007. Evidence of rainfall variations in Southern Brazil from trace element ratios (Mg/Ca and Sr/Ca) in a late Pleistocene stalagmite. Geochimica et Cosmochimica Acta 71: 2250-2263.

Cutler, K.B.; Edwards, R.L.; Taylor, F.W.; Cheng, H.; Adkins, J. Gallup, C.D.; Cutler, P.M.; Burr, G.S.; Bloom, A.L. 2003. Rapid sea-level fall and deep-ocean temperature change since the last glacial period. Earth and Planetary Science Letters 206: 253-271.

Cutten, H.N.C. 1979. Rappahannock Group: Late Cenozoic sedimentation and tectonics contemporaneous with Alpine Fault movement. New Zealand Journal of Geology and Geophysics 22: 535-553.

Davis, B.A.S.; Brewer, S. 2009. Orbital forcing and role of the latitudinal insolation/temperature gradient. Climate Dynamics 32: 143-165.

Davis, B.A.S.; Brewer, S. 2011: A unified approach to orbital, solar, and lunar forcing based on Earths latitudinal insolation/temperature gradient. Quaternary Science Reviews 30: 1861-1874.

Denton, G.H.; Heusser, C.J.; Lowell, T.V.; Moreno, P.I.; Anderson, B.G.; Heusser, L.E.; Schluchter, C.; Marchant, D.R.; 1999. Interhemispheric linkage of paleoclimate during the last glaciation. Geografiska Annaler 81A: 107-153.

Delmonte, B.; Basile-Doelsch, I.; Petit J.-R.; Maggi, V.; Revel-Rolland, M.; Michard, A.; Jagoutz, E.; Grousset, F.; 2004. Comparing the EPICA and Vostok dust records during the last 220,000 years: stratigraphical correlation and provenance in glacial periods. Earth Science Reviews 66: 63-87.

Dickson, M. 1972. Palynology of a Late Oturi Interglacial and Early Otira glacial sequence from Sunday Creek (s51), Westland, New Zealand. New Zealand Journal of Geology and Geophysics 15: 590-598.

Ditlefsen, C. 1992. Bleaching of K-feldspars in turbid water suspensions: A comparison of photo – and Thermoluminescence signals. Quaternary Science Reviews 11: 33-38.

Doughty, A.M.; Denton, G.H.; Hall, B.L.; Putnam, A.E.; Schaefer, J.M.; Barrell, D.J.A.; Anderson, B.G. 2009. ^{10}Be cosmogenic exposure ages from Late Pleistocene moraines near Mary Burn, Lake Pukaki, Central South Island, New Zealand. pp 18 in Cortese, G.; Vandergoes, M.; Bostok, H. 2009 Past Climates Meeting 2009, 15-17 May 2009, Te Papa, Wellington, New Zealand, GNS Science Miscellaneous Series 23, 65 p.

Drysdale, R.N.; Hellstrom, J.G.; Zanchetti, G.; Fallick, A.E.; Sanchez Goni, M.F; Couchoud, J.; McDonald, J.; Maas, R.; Lohmann, G.; Isola, I.; 2009. Evidence for obliquity forcing of Glacial Termination II. Science 325: 1527-1531.

Duller, G.A.T. 1994. Luminescence dating of poorly bleached sediments from Scotland. Quaternary Science Reviews 13: 521-524

Duller, G.A.T. --- Single grain optical dating of glacigenic deposits. Quaternary Geochronology 1: 296-304.

Dumas, B.; Gueremy, P.; Raffy, J. 2005. Evidence for sea-level oscillations by the “characteristic thickness” of marine deposits from raised terraces of Southern Calabria (Italy). Quaternary Science Reviews 24: 2120-2136.

Dumas, B.; Huang, C.T.; Raffy, J. 2006. Record of MIS 5 sea-level highstands based on U/Th dated coral terraces of Haiti. Quaternary International 145-146: 106-118.

Durkop, A.; Holbourn, A.; Kuhnt, W.; Zuraida, R.; Andersen, N.; Grootes, P.M. 2008. Centennial-scale climate variability in the Timor Sea during Marine Isotope Stage 3. Marine Micropaleontology 66: 208-221.

Edwards, R.L.; Cheng, H.; Murrell, M.T.; Goldstein, S.J. 1997. Protactinium-231 dating of carbonates by Thermal Ionisation Mass Spectrometry: Implications for Quaternary climate change. Science 276: 782-786.

EPICA Community Members 2006. One-to-one coupling of glacial climate variability in Greenland and Antarctica. Nature 444(9): 195-198.

Esat, T.M.; McCullock, M.T.; Chappell, J.; Pillans, B.; Omura, A. 1999. Rapid fluctuations in sea level record at Huon Peninsula during the penultimate deglaciation. Science 283: 197-201.

Esat, TM; Yokoyama, Y. 2008. Issues in radiocarbon and U-series dating of corals from the last glacial period. Quaternary Geochronology 3: 244-252.

Esat, TM; Yokoyama, Y. 2006. Growth patterns of the last ice age coral terraces at Huon Peninsula. Global and Planetary Change 54(3-4): 216-224.

Esper, O.; Zonneveld, K.A.F. 2007. The potential of organic-walled dinoflagellate cysts for the reconstruction of past sea-surface conditions in the Southern Ocean. Marine Micropaleontology 65: 185-212.

Fink, D.; McKelvey, B.; Hannan, D.; Newsome, S. 2000. Cold rocks, hot sands: In situ cosmogenic applications in Australia at ANTARES. Nuclear Instruments and Methods in Physic Research B: 838-846.

Fink, D.; Williams, P.; Augustinus, P.; Shulmeister, J. 2009. Southern Hemisphere millennial glaciations during the past 30 ka driven by Antarctic Ice Sheet variability. pp21 in Cortese, G.; Vandergoes, M.; Bostok, H. 2009 Past Climates Meeting 2009, 15-17 May 2009, Te Papa, Wellington, New Zealand, GNS Science Miscellaneous Series 23, 65 p.

Fischer, H.; Fundel, F.; Ruth, U.; Twarloh, B.; Wegner, A.; Udisti, R.; Becagli, S.; Castellano, E.; Morganti, A.; Severi, M.; Wolff, E.; Littot, G.; Röthlisberger, R.; Mulvaney, R.; Hutterli, M.A.; Kaufmann, P.; Federer, U.; Lambert, F.; Bigler, M.; Hansson, M.; Jonsell, U.; de Angelis, M; Boutron, C.; Siggaard-Andersen, M-L.; Steffensen, J.P.; Barbante, C.; Gaspari, V.; Gabrielli, P.; Wagenbach, D. 2007. Reconstruction of millennial changes in dust emission, transport and regional sea ice coverage using the deep EPICA ice cores from the Atlantic and Indian Ocean sector of Antarctica. Earth and Planetary Science Letters 260: 340–354.

Fitzharris, B.B.; Hay, J.E.; Jones, P.D. 1992. Behaviour of New Zealand glaciers and atmospheric circulation changes over the past 130 years. The Holocene 2: 97-106.

Fitzsimons, S.J.; Pollington, M.; Colhoun, E. 1996. Palaeomagnetic constraints on the ages of glacial deposits in north-western South Island, New Zealand. Z. Geomorph. N.F. Suppl.-Bd. 105: 7-20.

Forman, S.L.; Ennis, G. 1992. Limitations of thermoluminescence to date waterlain sediments from glaciated fiord environments of western Spitzbergen, Svalbard. Quaternary Science Reviews 11: 61-70.

Fritz, S.C.; Baker, P.A.; Lowenstein, T.K.; Seltzer, G.O.; Rigsby, C.A.; Dwyer, G.S.; Taipa, P.M.; Arnold, K.K.; Ku, T-L, Lou, S. 2004. Hydrologic variation during the last 170,000 years in the Southern Hemisphere tropics of South America. Quaternary Research 61: 95-104.

Frumkin, A.; Ford, D.C.; Schwarcz, H.P. 1999. Continental oxygen isotopic record of the last 170,000 years in Jerusalem. Quaternary Research 51: 317-327.

Fuchs, M.; Straub, J.; Zoller, L.; 2005. Residual luminescence signals of recent river flood sediments: A comparison between quartz and feldspar of fine and coarse grain sediments. Ancient TL 23: 25-30.

Fuchs, M.; Wode, G.; Burkert, A. 2007. Chronostratigraphy of a sediment record from the Hajar mountain range in northern Oman: Implications for optical dating of insufficiently bleached sediments. Quaternary Geochronology2: 202-207.

Fuchs, M.; Owen, L.A. 2008. Luminescence dating of glacial and associated sediments: a review, recommendations and future directions. Boreas 37: 636-695.

Gage, M. & Suggate, R.P. 1958. Glacial Chronology of the New Zealand Pleistocene. Bulletin of the Geological Society of America 69: 589-598.

Gage, M. 1945. Tertiary and Quaternary Geology of Ross. Transactions of the Royal Society of New Zealand 75 (2): 138-159.

Gage, M. 1952. The Greymouth Coalfield. New Zealand Geological Survey Bulletin (n.s.) 45.

Gage, M. 1961a. New Zealand Glaciations and the duration of the Pleistocene. Journal of Glaciology 3: 940-943.

Gage, M. 1961b. On the definition, date, and character of the Ross Glaciation, Early Pleistocene, New Zealand. Transactions of the Royal Society of New Zealand 88: 631-638.

Gage, M. 1985. Glaciation in New Zealand – the first century of research. Quaternary Science Reviews 5: 189-214.

Gage, M; Suggate, R.P. 1958. Glacial chronology of the New Zealand Pleistocene. Geological Society of America Bulletin 69: 589-598.

Garver, J.I.; Kamp, P.J.J. 1999. Integration of zircon color and zircon fission-track zonation patterns in orogenic belts: application to the Southern Alps, New Zealand. Tectonophysics 349: 203-219.

Gemmell A.M.D. 1988. Thermoluminescence dating of glacially transported sediments: some considerations. Quaternary Science Reviews 7: 277-285.

Gemmell A.M.D. 1999. IRSL from fine-grained glaciofluvial sediment. Quaternary Geochronology 18: 207-215.

Genty, D.; Blamart, D.; Ouahdi, R.; Gilmour, M.; Baker, A.; Jouzel, J.; Ven-Exter, S. 2003. Precise dating of Dansgaard-Oeschger climate oscillations in Western Europe from stalagmite data. Nature 421: 833- 837

Gildor, H.; Tziperman, E. 2000. Sea ice as the glacial cycles climate switch: Rate of seasonal and orbital forcing. Paleoceanography 15: 605-615

Goede, A. 1994. Continuous early last glacial palaeoenvironmental record from a Tasmanian speleothem based on stable oxygen isotope and minor element variations. Quaternary Science Reviews 13: 283-291.

Geode, A.; McCulloch, M.; McDermott, F.; Hawkesworth, C. 1998. Aeolian contribution to strontium and strontium isotope variations in a Tasmanian Speleothem. Chemical Geology 149: 37-50.

Gonzales, M.A.; Weiler, N.E.; Guida, N.G. 1988. Transgessive deposits of the Mid-Wisconsin Interstadial from 33 to 40 South latitude, Argentine Republic: reliability of 14C ages. Journal of Coastal Research 4: 667-676.

Govin, A.; Michel, E.; Labeyrie, L.; Waelbroeck, C.; Dewilde, F.; Jansen, E. 2009 Evidence for northward expansion of Antarctic Bottom Water mass in the Southern Ocean during the last glacial inception. Paleoceanography 24, PA1202, doi:10.1029/2008PA001603, 2009

Gracia, F.J.; Rodriguez-Vidal, J.; Caceres, L.M.; Belluomini, G.; Benavente, J.; Alonso, C. 2008. Diapiric uplift of an MIS 3 marine deposit in SW Spain: Implications for Late Pleistocene sea level reconstruction and palaeogeography of the strait of Gibraltar. Quaternary Science Reviews 27: 2219-2231.

Grant-Taylor, T. L.; Rafter, T.A. 1971. New Zealand radio-carbon measurements-6. New Zealand Journal of Geology and Geophysics 14: 364-402.

Grapes, R.; Rieser, U.; Wang, N. 2010. Optical luminescence dating of a loess section containing a critical tephra marker horizon, SW North Island of New Zealand. Quaternary Geochronology 5: 164-169.

Hall, I.R.; McCave, I.N.; Shackleton, N.J.; Weedon, G.B.; Harris, S.E. 2001. Intensified Pacific inflow and ventilation in Pleistocene glacial times. Nature 412: 809-812.

Hammond, A.P.; Goh, K.M.; Tonkin, P.J.; Manning, M.R. 1991. Chemical pretreatments for improving the radiocarbon dates of peats and organic silts in a gley podsol environment: Grahams Terrace, North Westland. New Zealand Journal of Geology and Geophysics 34: 193-196.

Hancock, P.M. and Associates 1981. Alluvial gold potential of exploration licence 33-084, Ross. AMAX/Mineral Resources Limited. Unpublished open file mineral report MR1355 held by the Ministry of Economic Development.

Hanebuth, TJJ; Saito, Y.; Tanabe, S.; Vu, Q.L.; Ngo, Q.T. 2006. Sea levels during late marine isotope stage 3 (or older?) reported from the Red River delta (northern Vietnam) and adjacent regions. Quaternary International 145-146: 119-134.

Harle, K.J. 1997. Late Quaternary vegetation and climate change in southeastern Australia: palynological evidence from marine core E55-6. Palaeogeography, Palaeoclimatology, Palaeoecology 131: 465-483.

Hay, J.E.; Fitzharris, B.B. 1988. The synoptic climatology of ablation on a New Zealand glacier. International Journal of Climate 8: 201-205.

Hays, J.D.; Imbrie, J.; Shackleton, NJ. 1976. Variations in the earth's orbit: pacemaker of the ice ages. Science 194: 1121-1132.

Hayward, B.W.; Sabaa, A.; Grenfell, H.R. 2004. Benthic foraminifera and the Late Quaternary (last 150 ka) paleoceanographic and sedimentary history of the Bounty Trough, east of New Zealand. Palaeogeography, Palaeoclimatology, Palaeoecology 211: 59-93.

Hayward, B.W.; Scott, G.H.; Crundwell, M.P.; Kennett, J.P.; Carter, L.; Neil, H.L.; Sabaa, A.T.; Wilson, K.; Rodger, J.S.; Schaefer, G.; Grenfell, H.R.; Li, Q. 2008 The effect of submerged plateau on Pleistocene gyral circulation and sea-surface temperatures in the Southwest Pacific. Global and planetary Change 63: 309-316.

Hearty, P.J.; Hollin, J.T.; Neumann, A.C.; OLeary, M.J.; McCulloch, M. 2007. Global sea-level fluctuations during the last interglaciation (MIS 5e). Quaternary Science Reviews 26: 2090-2012.

Hellstrom, J.; Drysdale, R.; Couchoud, I.; Zanchetta, G.; Fallick, A.; Smith, T. 2009. A Southern Hemisphere lead at the last two glacial terminations, indicated by montane speleothems records from New Zealand and Italy. pp 29 in Cortese, G.; Vandergoes, M.; Bostok, H. 2009 Past Climates Meeting 2009, 15-17 May 2009, Te Papa, Wellington, New Zealand, GNS Science Miscellaneous Series 23, 65 p.

Hellstrom, J.C.; McCulloch, M.T. 2000. Multi-proxy constraints on the climatic significance of trace element records from a New Zealand speleothem. Earth and Planetary Science Letters 179: 287-297.

Hellstrom, J.; McCulloch, M.T.; Stone, J. 1998. A detailed 31,000-year record of climate and vegetation change, from the isotope geochemistry of two New Zealand speleothems. Quaternary Research 50: 167-178.

Henderson, G.M.; Slowey, N.C. 2000. Evidence from U-Th dating against Northern Hemisphere forcing of the penultimate deglaciation. Nature 404: 61-66.

Henley, R.W.; Adams, J. 1979. On the evolution of giant gold placers. Institution of Mining and Metallurgy. B41-B50.

Herman, F.; Rhodes, E.J.; Braun, J.; Heiniger, L. 2010. Uniform erosion rates and relief amplitude during glacial cycles in the Southern Alps of New Zealand, as revealed from OSL-thermochronology. Earth and Planetary Science Letters 297: 183-189.

Heusser, L.; Van de Geer, G. 1994. Direct correlation of terrestrial and marine paleoclimatic records from four glacial-interglacial cycles – DSDP 594, Southwest Pacific. Quaternary Science Reviews 13: 273-282.

Heusser, CJ; Heusser, LE; Lowell, TV. 1999. Paleoecology of the Southern Chilean Lake District – Isla Grande De Chiloe during middle-late Lianquihue glaciation and deglaciation. Geografiska Annaler 81A: 231-284.

Heusser, L.; Heusser, C.; Pisias, N. 2006. Vegetation and climate dynamics of Southern Chile during the past 60,000 years: results of ODP Site 1233 pollen analysis. Quaternary Science Reviews 16: 565-581.

Hippler, D.; Eisenhaur, A.; Nagler, T.F. 2006. Tropical Atlantic SST history inferred from Ca isotope thermometry over the last 140 ka. Geochimica et Cosmochimica Acta 70: 90-100.

Hogan, K.P., Whitehead, D., Kallarackal, J., Buwalda, J.G., Meekings, J. and Rogers, G.N.D. 1996. Photosynthetic activity of leaves of *Pinus radiata* and *Nothofagus fusca* after 1 year of growth at elevated CO_2. Australian Journal of Plant Physiology 23: 623-630.

Hogan, K.P., Fleck, I., Bungard, R., Cheeseman, J.M. and Whitehead, D. 1997. Effect of elevated CO_2 on the utilization of light energy in *Nothofagus fusca* and *Pinus radiata*. Journal of Experimental Botany 48: 1289-1297.

Hollinger, D.Y. 1987. Gas exchange and dry matter allocation responses to elevation of atmospheric CO_2 concentration in seedlings of three tree species. Tree Physiology 3: 193-202.

Hooker, B.L.; Fitzharris, B.B. 1999. The correlation between climatic parameters and the retreat and advance of Franz Josef glacier, New Zealand. Global and Planetary Change 22: 39-48.

Hormes, A. 2000. The 14C perspective of glacier recessions in the Swiss Alps and New Zealand. Inauguraldissertation der Philosophisch-naturwissenschaftlichen Fakultat der Universitat Bern.

Hormes, A.; Preusser, F.; Denton, G.; Hajdas, I.; Weiss, D.; Stocker, T.F.; Schlüchter, C. 2003. Radiocarbon and luminescence dating of overbank deposits in outwash sediments of the last Glacial Maximum in North Westland, New Zealand. New Zealand Journal of Geology and Geophysics 46: 95-106.

Houmark-Nielsen, M. 2008. Testing OSL failures against a regional Weichselian glaciation chronology from southern Scandinavia. Boreas 37: 660-667.

Hu, G.; Zhang, J.F.; Qui, W-L.; Zou, L.-P. 2010. Residual signals in modern fluvial sediments from the Yellow River (HwangHe) and the implications for dating young sediments. Quaternary Geochronology 5: 187-193.

Hughes, T. 2011. A simple hypothesis for the self destruction of ice sheets. Quaternary Science Reviews 30: 1829-1845.

Hutt, G.; Junger, H. 1992. Optical dating on glaciofluvial sediments. Quaternary Science Reviews 11: 161-163.

Huybers, P. 2006. Early Pleistocene glacial cycles and the integrated summer insolation forcing. Science 313: 508-511.

Huybers, P.; Wunsch, C. 2005. Obliquity pacing of the late Pleistocene glacial terminations. Nature 434: 491-494

Ijiri, A.; Wang, L.; Oba, T.; Kawahata, H.; Huanh, C-Y.; Huang, C-Y. 2005. Paleoenvironmental changes in the northern area of the East China Sea during the past 42,000 years. Palaeogeography, Palaeoclimatology, Palaeoecology 219:239-261.

Imbrie, J.; Hays, J.D.; Martinson, A.; Mix, A.C.; Morley, J.J.; Pisias, N.G.; Prell, W.L.; Shackleton, N.J. 1984. The orbital theory of Pleistocene climate: support from a revised chronology of the marine δ180 record. In Berger, A.L. et al. (eds): Milankovitch and Climate1: 269-305.

Imbrie, J; A. Berger, E.A. Boyle, S.C. Clemens, A. Duffy, W.R. Howard, G. Kukla, J. Kutzbach, D. G. Martinson, A. McIntyre, A.C. Mix, B. Molfino, J.J. Morley, L.C. Peterson, N.G. Pisias, W. L. Prell, M.E. Raymo, N.J. Shackleton , and J . R. Toggweiler. 1993. On the structure and origin of major glaciation cycles 2. The 100,000-year cycle. Paleoceanography 8(6): 699-735.

Imbrie, J.D.; McIntyre, A. 2006. SST vs time for core V30-40 (specmap.063), doi.10.1594/PANGAEA.441760.

Imbrie, J.D.; McIntyre, A. 2006. SST vs time for core V25-56 (specmap.060), doi:10.1594/PANGAEA.441758.

Imbrie, J.D.; McIntyre, A. 2006. SST vs time for core RC13-288 (specmap.063), dataset#441753.

Indermuhle, A.; Monnin, E.; Stauffer, B.; Stocker, T.F.; Whalen, M. 2000. Atmospheric CO2 concentration from 60 to 20 kyr BP from the Taylor Dome ice core, Antarctica. Geophysical Research Letters 27: 735-738.

Israelson, C.; Wohlfarth, B. 1999. Timing of the last interglacial high sea level on the Seychelles Islands, Indian Ocean. Quaternary Research 51: 306-316.

Itou, M.; Oba, T.; Kato, Y. Obliquity control on summer subtropical SST in the Kuroshio Extension region during the past 180,000-year. Frontier Research on Earth Evolution 2: 1-7.

Jaeschke, A.; Ruhlemann, C.; Arz, H.W.; Heilig, G.M.N.; Lohmann, G. 2007. Coupling of millennial-scale changes in sea surface temperature and precipitation off northeastern Brazil with high latitude climate shifts during the last glacial period. Paleoceanography 22. PA4206,doi:10.1029/2006PA0011391

Jouzel, J.; Hoffman, G; Parrenin, F.; Waelbroeck, C. 2002. Atmospheric oxygen 18 and sea-level changes. Quaternary Science Reviews 21: 307-314.

Jouzel, J.; Masson-Delmotte, V.; Cattani, O.; Dreyfus, G.; Falourd, S.; Hoffmann, G.; Minster, B.; Nouet, J.; Barnola, J.M.; Chappellaz, J.; Fischer, H.; Gallet, J.C.; Johnsen, S.; Leuenberger, M.; Loulergue, L.; Luethi, D.; Oerter, H.; Parrenin, F.; Raisbeck, G.; Raynaud, D.; Schilt, A.; Schwander, J.; Selmo, E.; Souchez, R.; Spahni, R.; Stauffer, B.; Steffensen, J.P.; B. Stenni, Stocker, T.F.; Tison, J.L.; Werner, M.; Wolff, E.W. 2007. Orbital and Millennial Antarctic Climate Variability over the Past 800,000 Years. Science, Vol. 317, No. 5839, pp.793-797.

Jury, A.P. and Hancock, P.M. 1989. Alluvial gold deposits and mining opportunities on the West Coast, South Island, New Zealand. Pp 147-153 in Kear, D (ed): Mineral Deposits of New Zealand. Australasian Institute of Mining and Metallurgy Monograph 13.

Kaiser, J.; Lamy, F.; Hebbeln, D. 2007. A 70-kyr sea surface temperature record off southern Chile (Ocean Drilling Program Site 1233). Paleoceanography 20: PA4009,doi:10.1029/2005PA001146.

Kamp, P.J.J. 1986. The mid Cenozoic Challenger Rift System of western New Zealand and its implications for the age of Alpine Fault inception. Geological Society of America Bulletin 97: 255-281.

Kamp, P.J.; Green, P.F; Tippett, J.M. 1992. Tectonic architecture of the mountain-foreland transition, South Island, New Zealand. Tectonics 11: 98-113.
Kanfoush, S.L,; Hodell, D.A.; Charles, C.D.; Guilderson, T.P.; Mortyn, P.G.; Ninnemann, U.S 2000. Millennial-scale instability of the Antarctic ice sheet during the last glaciation. Science 288: 1815-1818.

Kamp, P.J.J.; Whtehouse, I.W.S.; Newman, J. 1999. Constraints on the thermal evolution of Greymouth Coalfield. New Zealand Journal of Geology and Geophysics 42: 447-467.

Harle, K.J. 1997. Late Quaternary vegetation and climate change in southeastern Australia: palynological evidence from marine core E55-6. Palaeogeography, Palaeoclimatology, Palaeoecology 131: 465-483.

Kawamura, K.; Parrenin, F.; Lisiecke, L.; Uemura, R.; Vimeaux, F.; Severinghaus, J.P.; Hutterli, M.A.; Nakazawa, T.; Hoki, S.; Jouzel, J.; Raymo, M.E.; Matsumoto, K.; Nakata, H.; Motoyama, H. Fujita, S.; Goto-Azuma, K.; Fujii, Y.; Watanabe, O. 2007. Northern Hemisphere forcing of climatic cycles in Antarctica over the past 360,000 years. Nature 448: 912-916.

Keeling, R.F.; Stephens, B.B. 2001: Antarctic sea ice and the control of Pleistocene climate instability. Paleoceanography 16: 112-131.

Khodri, M.; Lecainche, Y.; Ramstein, G.; Braconnot, P.; Marti, O.; Cortijo, E.; 2001. Simulating the amplification of orbital forcing by ocean feedbacks in the last glaciation. Nature 410: 570-574.

Kiefer, T.; McCave, I.N.; Elderfield, H. 2006. Antarctic control on tropical Indian Ocean sea surface temperature and hydrography. Geophysical Research Letters 33. L24612,doi:10.1029/2006OL027097.

Kim, J-H.; Crosta, X.; Micel, E.; Schonten, S.; Duprat, J.; Damste, J.S.S. 2009. Impact of lateral transport of organic proxies in the Southern Ocean. Quaternary Research 71: 246-250.

Kindler, P.; Davaud, E; Strasser, A. 1997. Tyrrhenian coastal deposits from Sardinia (Italy): a petrographic record of high sea levels and shifting climate belts during the last interglacial (isotope substage 5e). Palaeogeography, Palaeoclimatology, Palaeoecology 133: 1-25.

Kirst, G.J.; Schneider, R.R.; Muller, P.J.; von Storch, I.; Wefer, G. 1999. Late Quaternary temperature variability in the Benguela current system derived from Alkenones. Quaternary Research 52(1): 92-103.

Klasen, N.; Fiebig, M.; Preusser, F.; Reitner, M.; Radtke, U. 2007. Luminescence dating of proglacial sediments from the Eastern Alps. Quaternary International 164-165: 21-32

Klemen, J.; Jansson, K.; De Anelis, H.; Stroeven, A. P.; Hattestrand, G. A.; Glasser, N. 2010. North American Ice Sheet build-up during the last glacial cycle, 115-21 kyr. Quaternary Science Reviews 29: 2036-2051.

Klotz, S.; Guiot, J.; Mosbrugger, V. 2003. Continental European Eemian and early-Wurmian climate evolution: comparing signals using different quantitative reconstruction approaches based on pollen. Global and Planetary Change 36: 277-294

Kohl, C.P.; Nishizumi, K. 1992. Chemical isolation of quartz for measurement of in-situ produced cosmogenic nuclides. Geochimica et Cosmochimica Acta 56(9): 3583-3587.

Kolodziej, A.P. 2011. Planktic foraminifera-based sea surface temperature estimates and Late Quaternary oceanography off New Zealand's West Coast. MSc Thesis, Victoria University of Wellington

Knuepfer, P.L.K. 1988. Estimating ages of Quaternary stream terraces from analysis of weathering rinds and soils. Geological Society of America Bulletin 100: 1224-1236.

Krbetschek, M.R.; Rieser, U.; and Stolz, W. 1996. Optical Dating: Some luminescence properties of natural feldspars. Radiation Protection Dosimetry 66, p.407-412

Kristen, I.; Fuhrmann, A.; Thorpe, J.; Rohl, U.; Wilkes, H.; Oberhänsli, H. 2007. Hydrological changes in Southern Africa over the last 200 ka as recorded in lake sediment from the Tswain impact crater. Southern African Journal of Geology 110: 311-326.

Kukla, G.; Gavin, J. 2005. Did glacials start with global warming? Quaternary Science Reviews 24 (14014): 1547-1557.

Kukla, G.; McManus, J.F.; Rousseau, D-D; Chuine, I. 1997. How long and stable was the last interglacial. Quaternary Science Reviews 16: 605-612.

Kukla, G.J.; Bender, M.L.; de Beauliue, J-L.; Bond, G.; Broecker, W.S.; Cleveringa, P.; Gavin, J.E.; Herbert, T.D.; Imbrie, J.; Jouzel, J.; Keigwin, L.D.; Knudsen, K-L.; McManus, J.F.; Merkt, J.; Muhs, D.R.; Muller, H.; Poore, R.Z.; Porter, S.C.; Seret, G.; Shackleton, N.J.; Turner, C.; Tzedakis, P.C.; Winograd, I.J. 2002. Last Interglacial climates. Quaternary Research 58(2): 2-13.

Labeyrie, LD; Duplessy, JC; Blanc, PL 1987: Variations in mode of formation of oceanic deep waters over the past 125,000 years. Nature 327: 477-482

Labeyrie, L.; Labracherie, M,; Gorfti, N.; Pichon, J.J.; Vautravers, M.; Arnold, M.; Duplessy, J-C.; Patern, M.; Michel, E.; Duprat, J.; Caralp, M.; Turon, J-L. 1996. Hydrographic changes of the Southern Ocean (Southeast Indian Sector) over the last 230 kyr. Paleoceanography 11(1): 57-76.

Laird, M.G. 1988. Sheet S37 – Punakaiki. Geological Map of New Zealand 1:63,360. Map (1 Sheet) with notes. Wellington, New Zealand. Department of Scientific and Industrial Research.

Lambeck, K.; Nakada, M. 1992. Constraints on the age and duration of the last interglacial period and on sea-level variations. Nature 357: 125-128.

Lambeck, K.; Chappell, J. 2001. Sea level change through the last glacial cycle. Nature 292: 679-686

Lambeck, K.; Yokoyama, Y.; Purcell, T. 2002. Into and out of the Last Glacial Maximum: sea-level change during Oxygen Isotope Stage 3 and 2. Quaternary Science Reviews 21(1-3): 343-360.

Lambert, F.; Delmotte, B.; Petit, J.R.; Bigler, M.; Kaufmann, P.R.; Hutterli, M.A.; Stocker, T.F.; Ruth, U,; Steffensen, J.P.; Maggi, V. 2008. Dust-climate couplings over the past 800,000 years from the EPICA Dome C ice cores. Nature 452: 616-619.

Lamothe, M.; Auclair, M. 1997. Assessing the datability of young sediments by IRSL using an intrinsic laboratory protocol. Radiation Measurements 27: 107-117.

Lanf, A. 1994. Infra-red stimulated luminescence of Holocene re-worked silty sediments. Quaternary Science Reviews 13: 525-528.

Laymon, C.A. 1991. Marine episodes in Hudson Strait and Hudson Bay, Canada, during the Wisconsin Glaciation. Quaternary Research 35: 53-62.

Lea, D.W.; Martin, P.A.; Pak, D.K.; Spero, H.J. 2002. Reconstructing a 350 kyr history of sea level using planktonic Mg/Ca and oxygen isotope records from a Cocos Ridge core. Quaternary Science Reviews 21: 283-293.

Lea, D.W.; Pak, D.K.; Belanger, C.L.; Spero, H.J.; Hall, M.A.; Shackleton, N.J. 2006. Paleoclimate history of Galapagos surface waters over the last 135,000 yr. Quaternary Science Reviews 25: 1152-1157.

Linsley, B.K. 1996. Oxygen-Isotope record of sea level and climate variations in the Sulu Sea over the past 300,000 years. Nature 380: 234-237.

Lisiecke, L.E.; Raymo, M.E. 2005. A Pliocene-Pleistocene stack of 57 globally distributed benthic $\delta^{18}O$ records. Paleoceanography 20(1): PA1003, doi:1029/2004 PA001071.

Longworth, H.R.; Bryden, H.L. 2007. Discovery and quantification of the Atlantic Meridional Overturning Circulation: the importance of 25N. pp 5-8 in Schmittner, A.; Chiang, J.C.H.; Hemming, S.R. (eds) Ocean Circulation: Mechanisms and impacts- past and future changes in meridional overturning. AGU Geophysical Monograph 173, American Geophysical Union, Washington DC.

Loulergue, L.; Parrenin, F.; Blunier, T.; Barnola, J-M.; Spahni, R.; Schilt, A.; Raisbeck, G.; Chappellaz, J. 2007. New constraints on the gas age-ice age difference along the EPICA ice cores 0-50 kyr. Climate of the Past 3: 527-540.

Lowe, D.J.; Shane, P.A.R.; Alloway, B.V.; Newnham, R.A.M. 2008. Fingerprints and age models for widespread New Zealand Tephra marker beds erupted since 30,000 years ago: a framework for NZ-INTIMATE. Quaternary Science Reviews 27: 95-126.

Lukas, S.; Spencer, J.Q.C.; Robinson, R.A. J.; Benn, D.I. 2007. Problems associated with luminescence dating of Late Quaternary glacial sediments in the NW Scottish Highlands. Quaternary Geochronology 2: 243-248.

MacAyeal, D.R. 1993. Binge/purge oscillations of the Laurentide Ice Sheet as a cause of the North Atlantic Heinrich Events. Paleoceanography 8(6): 775-784.

Mackintosh, A.; Anderson, B.; Hubbard, A.; Golledge, N.; Purdie, H.; Doughty, A.; Huybers, P.; Pierriehumbert, R.; Denton, G.; Barrell, D.; Chinn, T.J.H.; Andersen, B.; Finkel, M.; Kaplan, M.; Putnam, A.; Schaefer, J.; Schwartz, R. 2009. Drivers of Southern Hemisphere climate variability: a view from modeling of New Zealand glaciers. pp41 in Cortese, G.; Vandergoes, M.; Bostok, H. 2009 Past Climates Meeting 2009, 15-17 May 2009, Te Papa, Wellington, New Zealand, GNS Science Miscellaneous Series 23, 65 p.

Mackintosh, A.N.; Barrows, T.T.; Colhoun, E.A.; Fifield, L.K 2006. Exposure dating and glacial reconstruction at Mt Field, Tasmania, Australia, identifies MIS3 and MIS2 glacial advances and climate variability. Journal of Quaternary Science 21(4): 363-376.

MacPherson, R.I. 1978. Geology of Quaternary ilmenite-bearing coastal deposits at Westport, South Island, New Zealand. New Zealand Geological Survey Bulletin, 87.

Marra, M.J.; Crozier, M.; Goff, J. 2008. Palaeoenvironment and biogeography of late MIS 3 beetle fauna from South Taranaki, New Zealand. Journal of Quaternary Science ISSN 0267-8179.

Marshunova, M.S., 1961. The radiation and heat balance of the Arctic. Proceedings of the Arctic and Antarctic Scientific-Research Institute 229: 5–53.

Martin, P.A.; Lea, D.W.; Rosenthal, Y.; Shackleton, N.J.; Sarnthein, M.; Papenfuss, T. 2002. Quaternary deep water temperature variation derived from benthic foraminiferal Mg/Ca. Earth and Planetary Science Letters 198: 193-209.

Martinson, D.G.; Pisias, N.J.; Hays, J.D.; Imbrie, J.; Moore, T.C.; Shackleton, N.J. 1987: Age dating and the orbital theory of the ice ages: Development of a high resolution 0 to 300,000 year chronostratigraphy. Quaternary Research 27: 1-29.

Marret, F.; De Vernal, A.; Benderra, F.; Harland, R. 2001. Late Quaternary sea-surface conditions at DSDP Hole 594 in the southwest Pacific Ocean based on dinoflagellate cyst assemblages. Journal of Quaternary Science 16(7): 739-751.

Mashiotta, T.A.; Lea, D.W.; Spero, H.J. 1999. Glacial-interglacial changes in Subantarctic sea surface temperature and δ^{18}O-water using foraminiferal Mg. Earth and Planetary Science Letters 170: 417-432.

Mathews, W.H. 1965. Profiles of Late Pleistocene glaciers in New Zealand. New Zealand Journal of Geology and Geophysics 10: 146-163.

Mauz, B.; Hassler, U. 2000. Luminescence chronology of Late Pleistocene raised beaches in southern Italy: new data of relative sea-level changes. Marine Geology 170: 187-203.

Mauz, B.; Lang, A. 2004. Removal of the feldspar derived component from polymineral fine silt samples for optical dating applications: evaluation of chemical treatment protocols and quality control procedures. Ancient TL 22: 1-8.

Mazaud, A.; Vimeux, F; Jouzel, J. 2000. Short fluctuations in Antarctic isotope records: a link with cold events in the North Atlantic. Earth and Planetary Science Letters 177: 219-225.

McCulloch, MT; Tudhope, AW; Esat, TM; Mortimer, GE; Chappell, J; Pillans, B; Chivas, AR; Omura, A. 1999. Coral record of sea-surface temperatures during the penultimate deglaciation at Huon Peninsula. Science 283: 202-204.

McCulloch, MT; Esat, T. 2000. The coral record of last interglacial sea levels and sea surface temperatures. Chemical Geology 169: 107-129.

McGlone, M.S.; Turney, C.S.M.; Wilmshurst, J.M. 2004. Late-glacial and Holocene vegetation and climate history of the Cass Basin, central South Island, New Zealand. Quaternary Research 62(3): 267-279.

McKay, A. 1893. Geological Explorations of the Northern Part of Westland. P 132-200 in: Mines Statement to the NZ House of Representatives 1893 by the Hon. R.J. Seddon, Minister of Mines.

McKay, A. 1894. On the Geology of the Northern Parts of the South Island, and the Gold-bearing Drifts between the Teremakau and Mikonui Rivers. Ibid. 1892-93 22: 11-50.

McPherson, R.I. 1978. Geology of Quaternary ilmenite-bearing coastal deposits of Westport. NZ Geological Survey Bulletin (n.s.) 87. 95p

McPherson, R.I. 1967. Westport Ilmenite Deposits. N.Z. Geological Survey Report 21. Department of Scientific and Industrial Research, New Zealand.

Merritts, D.; Eby, R.; Harris, R.; Edwards, R.L.; Chang, H. 1998. Variable rates of Late Quaternary surface uplift along the Banda Arc – Australian plate collision zone, eastern Indonesia. pp 213-224 in Stewart and Vita-Finzi (eds) Coastal Tectonics (Geol Soc Spec Publ 146).

Mew, G. 1983. Application of the term Pakihi in New Zealand- A review. Journal of the Royal Society of New Zealand 13 (3): 175-198.

Mew, G.; Whitton, J.S.; Robertson, S.M.; Lee, R. 1983. Investigation of the properties and genesis of West Coast soils, South Island, New Zealand. 3. Soil Mineralogy. New Zealand Journal of Science 26: 85-97.

Mew, G.; Hunt, J.G.; Froggett, P.C.; Eden, D.N.; Jackson, R.J. 1986. An occurrence of Kawakawa Tephra from the Grey Valley, South Island, New Zealand. New Zealand Journal of Geology and Geophysics 29: 315-322.

Mew, G.; Thomas, R.F.; Eden, D.N. 1988. Stratigraphy of loessic cover beds at the Lamplough, West Coast, South Island, New Zealand. Journal of the Royal Society of New Zealand 18: 325-332.

Mew, G.; Lee, R. 1988. The genesis and classification of soils on wet terraces and moraines in New Zealand. Journal of Soil Science 39: 125-138.

Moar, N.T. 1984. Nestegis (Oleaceae) pollen in coastal sites in Westland. New Zealand Journal of Botany 22: 169-171.

Moar, N.T. 1988. Pollen analysis and the history of cover beds in North Westland, New Zealand. (Abstract) In: Eden, D.N. & Furkert, R.J. (eds), Loess: its distribution, Geology and Soils, p. 143. Balkema, Rotterdam.

Moar, N.T.; McKeller, I.C. 2001. Interglacial vegetation in South Westland, South Island, New Zealand. New Zealand Journal of Geology and Geophysics 44: 17-24.

Moar, N.T. & Suggate, R.P. 1973. Late Otiran and early Aranuian grassland in central New Zealand. NZ Journal of Ecology 3: 4-12.

Moar, N.T. & Suggate, R.P. 1973. Pollen analysis of late Otiran and Aranuian sediments at Blue Spur Road (S51), north Westland. New Zealand Journal of Geology and Geophysics 16: 333-344.

Moar, N.T.; Suggate, R.P. 1979. Interglacial and glacial vegetation in the Westport District, South Island. New Zealand Journal of Botany 17: 361-387.

Moar, N.T.; Suggate, R.P. 1996. Vegetation history from the Kaihinu (Last) interglacial to the present, West Coast, South Island, New Zealand. Quaternary Science Reviews 15: 521-547.

Moar, N.; Suggate, R.P.; Burrows, C.J. 2008. Environments during the Kaihinu Interglacial and Otira Glaciation, Coastal north Westland, New Zealand. New Zealand Journal of Botany 46: 49-63.

Morgan, P.G. 1911. The Geology of the Greymouth Subdivision, North Westland. New Zealand Geological Survey Bulletin, new series 13.

Muhs, D.R.; Simmons, K.R.; Steinke, B. 2002. Timing and warmth of the Last Interglacial period: new U-series evidence from Hawaii and Bermuda and a new fossil compilation for North America. Quaternary Science Reviews 21: 135-1383.

Nakada, M.; Kimura, R.; Okuno, J.; Moriwaki, K.; Miura, H.; Maemoku, H. 2000. Late Pleistocene and Holocene melting history of the Antarctic ice sheet derived from sea-level variations. Marine Geology 167: 85-103.

Nathan, S. 1975. Sheets S23/9 and S30 Foulwind and Charleston (1st ed.). "Geological Map of New Zealand 1:63360". Map (1 sheet) and notes (36 p.). NZ Department f Scientific and Industrial Research, Wellington.

Nathan, S. 1976. Sheets S23/9 & S24/7 Foulwind and Westport "Geological Map of New Zealand 1: 25,000" Department of Scientific and Industrial Research, Wellington New Zealand.

Nathan, S. 1978a. Sheets S31 and Part S32 – Buller-Lyell. Geological Map of New Zealand 1:63,360. Map (1 sheet) and notes (32 p). Wellington, Department of Scientific and Industrial Research.

Nathan, S. 1978b. Sheet S44 Greymouth (1st ed.). "Geological Map of New Zealand 1:63360". Map (1 sheet) and notes (36 p.). NZ Department of Scientific and Industrial Research, Wellington.

Nathan, S; Anderson, HJ; Cook, RA; Herzer, RH; Hoskins, RH; Raine, JI; Smale, D; 1986. Cretaceaous and Cenozoic sedimentary Basin of the West Coast region, South Island, New Zealand. New Zealand Geological Survey Basin Studies 1. 4 Sheets + 99p.

Nathan, S. Rattenbury, M.; Suggate, R.P. (compilers) 2002. Geology of the Greymouth area. Institute of Geological and Nuclear Sciences 1:250,000 geological map 12, 1 Sheet + 58p. Lower Hutt, New Zealand. Institute of Geological and Nuclear Sciences Limited.

Neall, V.E.; Stewart, R.B.; Wallace, R.C.; Williams, M.C.; Mew, G. 2001. Mineralogy, stratigraphy and provenance of soil coverbeds in the Kumara district, Westland. New Zealand Journal of Geology and Geophysics 44: 205-218.

Nelson, C.S.; Cook, P.J.; Hendy, C.H.; Cuthbertson, A.M. 1993. Oceanographic and climatic changes over the past 160,000 years at Deep Sea Drilling Project site 594 off Southeastern New Zealand, southwest Pacific. Paleoceanography 8: 435-458.

Newnham, R.M. Lowe, D.J. Green, J.D.; Turner, G.M.; Harper, M.A.; McGlone, M.S.; Stout, S.L.; Horie, S.; Froggett, P.C. 2004. A discontinuous ca. 80 ka record of Late Quaternary environmental change from Lake Omapere, Northland, New Zealand. Palaeogeography, Palaeoclimatology, Palaeoecology 207: 165-198.

Newnham, R.M.; Vandergoes, M.J.; Garnett, M.H.; Lowe, D.J.; Prior, C.; Almond, P.C. 2007a.
Test of AMS 14C dating of pollen concentrates using tephrochronology. Journal of Quaternary Science 22: 37-51.

Newnham, R.M.; Vandergoes, M.J.; Hendy, C.H.; Lowe, D.J.; Preusser, F 2007b. A terrestrial palynological record for the last two glacial cycles from southwestern New Zealand. Quaternary Science Reviews 26: 517-535.

Nicol, A.; Nathan, S. 2001. Folding and the formation of bedding-parallel faults on the western limb of Grey Valley Syncline near Blackball, New Zealand. New Zealand Journal of Geology and Geophysics 44: 127-135.

Nisancioglu, K.H. 2004. Modeling the impact of atmospheric moisture transport on global ice volume Thesis (Ph. D.), Massachusetts Institute of Technology, Dept. of Earth, Atmospheric, and Planetary Sciences

Norris, R.J.; Cooper, A.F. 2001. Late Quaternary slip rates and slip partitioning on the Alpine Fault, New Zealand. Journal of Structural Geology 23: 507-520.

Nunn, P.D.; Omura, A. 1999. Penultimate interglacial emerged reef around Kadavu Island, Southwest Pacific: implications for Quaternary island-arc tectonics and sea-level history. New Zealand Journal of Geology and Geophysics 42: 219-227.

Nurnberg, D.; Groeneveld, J. 2006. Pleistocene variability of the subtropical convergence at East Tasman Plateau- Evidence from planktonic foraminiferal Mg/Ca (ODP site 1172A). Geochemistry, Geophysics, Geosystems 7: Q04P11,doi:10.1029/2005GC000984.

Nurnberg, D.; Brughmans, N.; Schonfeld, J.; Ninnemann, U.; Dullo, C. 2004. Paleo-export, terrigenous flux and sea surface temperatures around Tasmania- Implications for glacial/interglacial changes in the subtropical convergence zone. American Geophysical Union Geophysical Monograph 151: 291-318.

Okuda, M.; Shulmeister, J.; Flenley, J.R. 2002. Vegetation changes and their climatic implication for the late Pleistocene at Lake Poukawa, Hawkes Bay, New Zealand. Global and Planetary Change 33: 269-282.

Oppo, D.W.; Linsley, B.K.; Rosenthal, Y.; Dannenmann, S.; Baufort, L. 2003. Orbital and suborbital climate variability in the Sulu Sea, western tropical Pacific. Geochemistry, Geophysics, Geosystems 4(1). 1003, doi:10.1029/2001GC000260.

Oppo, D.W.; Sun, Y. 2005. Amplitude and timing of sea-surface temperature change in the northern South China Sea: Dynamic link to the East Asian Monsoon. Geology 33(10): 785-788.

Ota, Y.; Chappell, J. 1996. Late Quaternary coseismic uplift events on the Huon Peninsula, Papua New Guinea, deduced from coral terrace data. Journal of Geophysical Research 101(B3): 6071-6082.

Ota, Y.; Machida, H. 1987. Quaternary sea-level changes in Japan. pg 182-224 In: Tooley, M.J. and Shennan, I. (eds) Sea-level Changes. The Institute of British Geographers special publication, ISSN 0073-9006; v 20.

Ota, Y.; Pillans, B.; Berryman, K.; Beu, A.; Fujimori, T.; Miyauchi, T.; Berger, G. 1996. Pleistocene coastal terraces of Kaikoura Peninsula and the Marlborough Coast, South Island, New Zealand. New Zealand Journal of Geology and Geophysics 39: 51-73.

Pahnke, K.; Zahn, R.; Elderfield, H.; Schulz, M. 2003. 340,000-year centennial-scale record of Southern Hemisphere climatic oscillation. Science 302: 948-952.

Pahnke, K.; Zahn, R. 2008. Southern Hemisphere water mass conversion linked with North Atlantic climate variability. Science 307: 1741-1746.

Pahnke, K.; Sachs, J.P. 2006. Sea surface temperatures of southern midlatitudes 0-160 kyr B.P. Paleoceanography 21, PA2003, doi:10.1029/2005PA001191.

Parrenin, F.; Barnola, J.M.; Beer, J.; Blunier, T.; Castellano, E.; Chappellaz, J.; Dreyfus, G.; Fischer, H.; Fujita, S.; Jouzel, J.; Kawamura, K.; Lemieux-Dudon, B.; Loulergue, L.; Masson-Delmotte, V.; Narcisi, B.; Petit, J-R.; Raisbeck, G.; Raynaud, D.; Ruth, U.; Schwander, J.; Severi, M.; Stephensen, J.P.; Svenson, A.; Udisti, R.; Waelbroeck, C.; Wolff, E. 2007. The EDC chronology for the EPICA Dome C ice core. Climate of the Past 3: 485-497.

Partridge, T.C.; Demenocal, P.B.; Lorentz, S.A.; Paiker, M.J.; Vogel, J.C. 1997. Orbital forcing of climate over South Africa: A 200,000 year rainfall record from the Pretoria saltpan. Quaternary Science Review 16: 1125-1133.

Pearson, C.F.; Beavan, J.; Darby, D.J.; Blick, G.H.; Walcott, R.I. 1995. Strain distribution across the Australian-Pacific plate boundary in the central South island, New Zealand, from 1992 GPS and earlier terrestrial observations. Journal of Geophysical Research 100 (B11): 22071-22081.

Peixoto, J.P.; Oort, A.H. 1992: Physics of climate. 520pp American Inst. Phys., New York

Pelejero, C.; Calvo, E.; Barrows, T.T.; Logan. G.A.; DeDecker, P 2006. South Tasman Sea alkenone palaeothermometry over the last 4 glacial cycles. Marine Geology 230: 73-86

Pelejero, C; Grimalt, J.O.; Heilig, S.; Kienast, M.; Wang, L. 1999. High resolution U^{k}_{37} sea-surface temperature reconstructions in the South China Sea over the past 220 kyr. Paleoceanography 14(2): 224-231.

Perg, L.A.; Anderson; R.S.; Finkel, R.C. 2001. Use of a new ^{10}Be and ^{26}Al inventory method to date marine terraces, Santa Cruz, California, USA. Geology 29: 879-882

Petit, J.R.; Jouzel, J.; Raynaud, D.; Barkov, N.I.; Barnola, J-M.; Basile, I.; Bender, M.; Chappellaz, J.; Davisk, M.; Delaygue, G.; Delmotte, M.; Kotlyakov, V.M.; Legrand, M.; Lipenkov, V.Y.; Lorius, C.; Le´pin, L.; Ritz, C.; Saltzman, E.; Stievenard, M. 1999. Climate and atmospheric history of the past 420,000 years from the Vostok ice core, Antarctica. Nature 399: 429-436.

Pichevin, L.; Cremer, M.; Giraudeau, J. Bertrand, P. 2005. A 190 kyr record of lithogenic grainsize on the Namibian slope: Forging a tight link between past wind strength and coastal upwelling dynamics. Marine Geology 24: 81-96.

Pichon, J-J.; Labeytir, L.D.; Bareille, G. Labracherie, M. Duprat, J.; Jouzel, J. 1992. Surface water temperature changes in the high latitudes of the Southern Ocean over the last glacial-interglacial cycle. Paleoceanography 7: 289-318.

Pillans, B. 1990a. Pleistocene marine terraces in New Zealand: a review. New Zealand Journal of Geology and geophysics 33: 219-231.

Pillans, B. 1990b. Late Quaternary marine terraces, South Taranaki-Wanganui. Miscellaneous Series Map 18, New Zealand Geological Survey.

Potter, E-K; Lambeck, K. 2003. Reconciliation of sea-level observations in the Western North Atlantic during the last glacial cycle. Earth and Planetary Science Letters 217: 171-181.

Potter, E-K.; Esat, T.M.; Schellmann, G.; Radtke, U.; Lambeck, K.; McCulloch, M.T. 2004. Suborbital-period sea-level oscillations during marine isotope substages 5a and 5c. Earth and Planetary Science Letters 225: 191-204.

Prescott, J.R.; Hutton, J.T. 1994. Cosmic ray contributions to dose rates for luminescence and ESR dating: large depths and longer-term time variations. Radiation Measurements 23: 497-500.

Preusser, F; Andersen, BG; Denton, GH; Schlüchter, C. 2005. Luminescence chronology of Late Pleistocene glacial deposits in North Westland, New Zealand. Quaternary Science Reviews 24: 2207-2227.

Preusser, F.; Ramseyer, K.; Schluchter, C. 2006. Characterisation of low intensity quartz from the New Zealand Southern Alps. Radiation Measurements 41: 871-877.

Putnam, A.E.; Denton, G.H.; Schaefer, J.M.; Barrell, D.J.A.; Andersen, B.G.; Kaplan, M.R.; Schwartz, R.; Finkel, R.C.; Doughty, A.M.; Travis, S. 2009. Timing and duration of the last glacial maximum inferred from a ^{10}Be surface-exposure chronology of the Lake Ohau terminal moraine complex, Southern Alps, New Zealand pp 45 in Cortese, G.; Vandergoes, M.; Bostok, H. 2009 Past Climates Meeting 2009, 15-17 May 2009, Te Papa, Wellington, New Zealand, GNS Science Miscellaneous Series 23, 65 p.

Randall, K.; Lamb, S.; Niocaill, M.C. 2011. Large tectonic rotations in a wide zone of Neogene distributed dextral shear, northeastern South Island, New Zealand. Tectonophysics 509:165-180.

Raymo, M.; Nisancioglu, K.H. (2003). The 41 kyr world: Milankovitch's other unsolved mystery Paleoceanography 18 (1): 10.1029/2002PA000791

Raynaud, D.; Barnola, J-M.; Chappellaz, J.; Blunier, T.; Indermuhle, A.; Stauffer, B. 2000. The ice record of greenhouse gases: a view in the context of future changes. Quaternary Science Reviews 19: 9-17.

Rendell, H.M.; Webster, S.E.; Sheffer, N.L. 1994. Underwater bleaching of signals from sediment grains: new experimental data. Quaternary Science Reviews 13: 433-435.

Rieser, U.; Bonnet, S.; Moulin, L.; Lacoste, A.; Lague, D.; Davey, P. 2009. Geomorphological implications of systematic age overestimations in the OLS dating of post-LGM fluvial terraces (Rangitikei River), New Zealand. Abstract # EP21C-0612. American Geophysical Union Fall Meeting.

Roberts, P.B.; Whitehead, N.E. 1001. Report to the Minister of Energy on the radiological implications of the Westland Ilmenite mining licence application for Barrytown, Westland. DSIR Physical Sciences DSIRPS-C-56, Nuclear Sciences Group, DSIR Physical Sciences, Lower Hutt, New Zealand.

Robertson, S.M.; Mew, G. 1982. The presence of volcanic glass in soils on the West Coast, South Island, New Zealand. New Zealand Journal of Geology and Geophysics 25: 503-507.

Roder, G.H.; Suggate, R.P. 1990. Sheet L29BD – Upper Buller Gorge. Geological map of New Zealand 1:50,000. Map (1 sheet) and notes (52 p.). Wellington. Department of Scientific and Industrial Research.

Rodriguez, AB; Anderson, J.B.; Banfield, L.A.; Taviani, M.; Abdulah, K.; Snow, J.N. 2000. Identification of a –15 m middle Wisconsin shoreline on the Texas inner continental shelf. Palaeogeography, Palaeoclimatology, Palaeoecology 158: 25-43.

Rhodes, E.J.; Pownall, L. 1994. Zeroing of the OSL signal in quartz from young glaciofluvial sediments. Radiation Measurements 23: 329-333.

Rohling, E.J.; Hemelben, C.; Kucera, M.; Roberts, A.P.; Schmeltzer, I.; Schulz, H.; Siccha, M.; Siddall, M.; Trommer, G. 2008. New constraints on the timing of sea level fluctuations during early to middle marine isotope stage 3. Paleoceanography 23: PA3219. doi:10.1029/2008PA001617

Rose, R.V. 1996. Summary of Miocene to Recent conglomerate provenance and gold content and Plate Boundary tectonics of the West Coast region. In The Changing face of West Coast Mining:

Proceedings of the 29th Annual Conference, Australasian Institute of Mining and Metallurgy New Zealand Branch pp 82-109.

Rose, R.V. 2000a. Factors influencing the formation of gold placer deposits in the West Coast Region, South Island, New Zealand: A preliminary model of the fluvioglacial environment. Unpublished Report, West Coast Commercial Gold Miners Association.

Rose, R. 2000b. Alluvial gold adjacent to glacial margins, West Coast, South Island, New Zealand. 2000 New Zealand Minerals & Mining Conference Proceedings, 29-31 October 2000. p 137-162.

Rother, H.; Shulmeister, J. 2006. Synoptic climate changes as a driver of late Quaternary glaciations in the mid-latitudes of the Southern Hemisphere. Climate of the Past Discussions 2: 11-19.

Rothlisberger, R.; Mudelsee, M.; Bigler, M.; de Angelis, M.; Fischer, H.; Hansson, M.; Lambert, F.; Masson-Delmotte, V.; Sime, L.; Udisti, R.; Wolf, E.W. 2008. The Southern Hemisphere at glacial terminations: insights from the Dome C ice core. Climate of the Past Discussions 4: 761-789.

Ryan, M.T.; Dunbar, G.B.; Vandergoes, M.J.; Hannah, M.J.; Neil, H.; Bostok, H. 2009. A preliminary 210 ka terrestrial palynomorph record from a marine sediment core, West Coast, South Island (abstract and poster). Past Climates Meeting 2009, Te Papa, Wellington. GNS Science Miscellaneous Series 23 p53.

Santoro, E.; Mazzella, M.E.; Ferranti, L; Randisi, , A.; Napolitano, E.; Rittner, S.; Radtke, U. (2009). Raised coastal terraces along the Ionian Sea coast of northern Calabria, Italy, suggest space and time variability of tectonic uplift rates. Quaternary International 206(1-2): 78-101.

Sasaki, K.; Omura, A.; Murakami, K.; Sagawa, N.; Nakamori, T. 2004. Interstadial coral reef terraces and relative sea-level changes during marine isotope stages 3-4, Kikai Island, central Ryukyus, Japan. Quaternary International 120(1): 51-64.

Schellmann, G.; Radtke, U.; Potter, E-K.; Esat, T.M.; McCulloch, M.T. 2004. Comparison of ESR and TIMS U/Th dating of marine isotope stage (MIS) 5e, 5c and 5a coral from Barbados – implications for palaeo sea-level changes in the Caribbean. Quaternary International 120(1): 41-50.

Schmittner, A.; Saenko, O.A.; Weaver, A.J. 2003. Coupling of the hemispheres in observations and simulations of glacial climate change. Quaternary Science Reviews 22: 659-671.

Schneider, R.; Muller, P.J.; Huhland, G. 1995. Late Quaternary surface circulations in the east-equatorial South Atlantic: evidence from alkenone sea surface temperatures. Paleoceanography 10(2): 197-220.

Seidov, D.; Maslin, M. 2001. Atlantic heat piracy and the bi-polar climate see-saw during Heinrich and Dansgaard-Oeschger events. Journal of Quaternary Science 16(4): 321-328.

Seward, D,; White P.J. 1992. Evolution and eversion of a Tertiary sedimentary basin, Paparoa Range, South Island, New Zealand: evidence from fission track dating. New Zealand Journal of Geology and Geophysics 35: 265-271.

Shane, P.; Sandiford, A. 2003. Paleovegetation of marine isotope stages 4 and 3 in Northern New Zealand and the age of the widespread Rotoehu Tephra. Quaternary Research 59(3): 420-429.

Shane, P.; Lian, O.B.; Augustinus, P.; Chisari, R.; Heijnis, H. 2002. Tephrostratigraphy and geochronology of c.a. 120 ka terrestrial record at Lake Poukawa, North Island, New Zealand. Global and Planetary Change 33: 221-242.

Shackleton, N.J. 2000. The 100,000 – year Ice Age cycle identified and found to lag temperature, carbon dioxide, and orbital eccentricity. Science 289: 1897-1902.

Shackleton, N.J.; Fairbanks, R.G.; Chiu, T.-C.; Parrenin, F. 2004. Absolute calibration of the Greenland time scale: implications for Antarctic time scales and for $d^{14}C$. Quaternary Science Reviews 23 (14-15): 1513-1522.

Shackleton, N.J.; Sanchez-Goni, M.F.; Pailler D.; Lancelot, Y. 2003. Marine Isotope Substage 5e and the Eemian Interglacial. Global and Planetary change 36: 151-155.

Shaefer, G.; Rodger, J.S.; Haywood, B.W.; Kennett, J.P.; Sabaa, A.T.; Scott, G.H. 2005. Planktic foraminiferal and sea surface temperature record during the last 1 Myr across the Subtropical Front, Southwest Pacific. Marine Micropaleontology 54: 191-212.

Shi, N.; Schneider, R.; Beng, H-J.; Dupont, L.M. 2001. Southeast trade wind variations during the last 135 kyr: evidence from pollen spectra in eastern South Atlantic sediments. Earth and Planetary Science Letters 187: 311-321.

Shulmeister, J.; Shane, P.; Lian, O.B.; Masaaki, O.; Carter, J.A.; Harper, M.; Dickinson, W.; Augustinus, P.; Heijnis, H. 2001. A long late-Quaternary record from Lake Poukawa, Hawkes Bay, New Zealand. Palaeoeography, Palaeoclimatology, Palaeoecology 176(1-4): 81-107.

Shulmeister, J.; Goodwin, I.; Renwick, J.; Harle, K.; Armand, L.; McGlone, M.S.; Cook, E.; Dodson, J.; Hesse, P.T.; Mayewski, P.; Curran, M. 204. The Southern Hemisphere westerlies in the Australasian sector over the last glacial cycle: a synthesis. Quaternary International 118-119: 23-53.

Sibson, R.H.; White, S.H.; Atkinson, B.K 1981. Structure and distribution of fault rocks in the Alpine Fault Zone, New Zealand. In: McClay, KR & Price, N.J. eds: Thrust and Nappe Tectonics pp 97-210.

Sicre, M.A.; Labeyrie, L; Ezat, U.; Duprat, J.; Turon, J.C.; Michel, E.; Mazaud, A. 2005. Mid-latitude Southern Indian Ocean response to Northern Hemisphere Heinrich events. Earth and Planetary Science Letters 240: 724-731.

Siddall, M.; Rohling, E.J.; Arz, H.W. 2008a. Convincing evidence for rapid ice sheet growth during the last glacial period. Pages News 16: 15-16.

Siddall, M. Rohling, E.J.; Thompson, G.W.; Waelbroeck, C. 2008b. MIS 3 sea level: data, synthesis and new outlook. Reviews of Geophysics: 46, RG4003, doi:10.1029/2007RG000226

Simms, A.R.; Kalchgruber, R.; Rodriguez, A.B.; Lambeck, K.; Anderson, J.B. In Press. Revisiting marine isotope stage 3 and 5a (MIS 3-5a) sea levels within the northwestern Gulf of Mexico. Global and Planetary Change 66: 100-111.

Sikes, E.L.; Howard, W.R.; Neil, H.L.; Volkman, J.K. 2002. Glacial-interglacial sea surface temperature changes across the subtropical front east of New Zealand based on alkenone unstaturation ratios and foraminiferal assemblages. Paleoceanography 17(2). 1012, 10.1029/2001PA000640.

Sikes, E.L.; Howard, W.R.; Samson, C.R.; Mahan, T.S.; Robertson, L.G.; Volkman, J.R. 2009. Southern Ocean seasonal temperature and Subtropical Front movement on the South Tasman Rise in the Late Quaternary. Paleoceanography 24 PA2201,doi:10,1029/2008PA001659.

Simms, A.R.; DeWitt, R.; Rodriguez, A.B.; Lambeck, K.; Anderson, J.B. 2009. Revisiting marine isotope stage 3 and 5a (MIS3 -5a) sea levels within the northwestern Gulf of Mexico. Global and Planetary Change 66(1-2): 100-111.

Soons, J.M. 2001. Evolution of the New River drainage system, Westland. New Zealand Journal of Geology and Geophysics 4: 137-143.

Soons, J.M. and Lee, P.A. 1984. An interglacial site on the West Coast, South Island. pp101-108 in Owens IF et al (1984) Geography for the 1980's, Proceedings of the Twelfth New Zealand Geography Conference, New Zealand Geographical Society, Christchurch, New Zealand.

Sowers, T.; Bender, M.; Labeyrie, L.; Martinson, D.; Jouzel, J.; Raynaud, D.; Pichon, J.J.; Korotkevich, Y.S. 1993. A 135,000-year Vostok-SPECMAP common temporal framework. Paleoceanography 8: 737-766.

Spencer, J.Q.; Bray, H.E.; Blum, M.D. 2001. Optically stimulated luminescence dating of Late Quaternary glaciogenic sediments in the upper Hunza valley: validating the timing of glaciation and assessing dating methods. Quaternary Science Reviews 23: 175-191.

Spotl, C. and Mangini, A. 2002. Stalagmite from the Austrian Alps reveals Dansgaard-Oeschger events during isotope stage 3: Implications for the absolute chronology of the Greenland Ice Cores. Earth and Planetary Science Letters 2003(1): 507-518.

Steig, E.J.; Morse, D.L.; Waddington, E.D.; Stuiver, M.; Grootes, P.M.; Mayewski, P.A.; Twickler, M.I.; Whitlow, S.I. 2000. Wisconsinian and Holocene climate history from an ice core at Taylor-Dome, Western Ross Embayment, Antarctica. Geografiska Annaller 82A: 213-235.

Steig, E.J. 2006. High resolution stable isotopes of ice core Taylor Dome to 230 kyr, doi:10.1594/PANGAEA.472831.

Stein, M.; Wasserburg, G.J.; Aharon, P.; Chen, J.H.; Zhu, Z.R.; Bloom, A.; Chappell, J. 1993. TIMS U-Series dating and stable isotopes of the last interglacial event in Papua New Guinea. Geochimica et Cosmochimica Acta 57: 2541-2554.

Stenni, B.; Jouzel, J.; Masson-Delmotte, V.; Rothlisberger, R.; Castellano, E.; Caltani, O.; Falourd, S.; Steffensen, J.P.; Johnsen, S.J.; Longinelli, A.; Sachs, J.P.; Selmo, E.; Souchez, R.; Steffensen, J.P..; Udisti, R. 2003. A late-glacial high-resolution site and source temperature record derived from the EPICA Dome C isotopic records (East Antarctica). Earth and Planetary Science Letters 217: 183-195.

Stewart, M. 1988. Report on drilling at Kapitea, Waimea, Westland County. Open File Report M1532, Crown Minerals, Ministry of Economic Development, Wellington

Stirling, C.H.; Esat, T.M; Lambeck, K.; McCullock, M.T. 1996. Timing and duration of the last interglacial: evidence for a restricted interval of widespread coral reef growth. Earth and Planetary Science Letters 160: 745-762

Stokes, S.; Bray, H.E.; Blum, M.D. 2001. Optical resetting in large drainage basins: tests of zeroing assumptions using single-aliquot procedures. Quaternary Science Reviews 23: 175-191.

Stuut, J-B.; Lamy, F. 2004. Climate variability at the southern boundaries of the Namib (southwestern Africa) and Atacama (Northern Chile) coastal deserts during the last 120,000 yr. Quaternary Research 62: 301-309.

Suggate, R.P. 1965. Late Pleistocene geology of the northern part of the South Island. New Zealand Geological Survey Bulletin 77. 91p.

Suggate, R.P. 1968. The thirty-foot raised beach at Rapahoe, north Westland. New Zealand Journal of Geology and Geophysics 11: 648-650.

Suggate, RP 1985a. The glacial/interglacial sequence of North Westland, New Zealand. New Zealand Geological Survey Record 7.

Suggate, R.P. 1985b. Where have all the glaciations gone? (Note). Proceedings of the Second CLIMANZ Conference held at Harihari, Westland, New Zealand, Feb 4-8 1985. p 47-48.

Suggate R.P. 1987. Active folding in north Westland, New Zealand. New Zealand Journal of Geology and Geophysics 30: 169-174.

Suggate, R.P. 1988. Quaternary deposition and deformation in the Buller and tributary valleys. New Zealand Geological Survey record 25: 51 p.

Suggate, RP. 1989. The postglacial shorelines and tectonic development of the Barrytown coastal lowland, North Westland, New Zealand. New Zealand Journal; of Geology and Geophysics 32: 443-450.

Suggate, RP, 1990. Late Pleistocene and Quaternary glaciations of New Zealand. Quaternary Science Reviews 9: 175-197.

Suggate, R.P. 1992. Differential uplift of middle and late Quaternary shorelines, northwest South Island, New Zealand. Quaternary International 15/16: 47-59.

Suggate, R.P. 1996. Detrital gold in North Westland. In Proceedings 29th Annual Conference, NZ Branch, Australasian Institute of Mining and Metallurgy pp 137-152.

Suggate, R.P.; Almond, P.C. 2005. The Last Glacial Maximum (LGM) in Western South Island, New Zealand: Implications for the Global LGM and MIS2. Quaternary Science Reviews 24 (16-17): 1923-1940.

Suggate, R.P.; Moar, N.T. 1970. Revision of the chronology of the Late Otira Glacial. New Zealand Journal of Geology and Geophysics 14: 742-746.

Suggate, R.P.; Mildenhall, D.C. 1991. Revision of the position of the Scandinavia Formation in the West Coast terrace sequence. New Zealand Geological Survey Record 43: 113-116.

Suggate, R.P. and Waight, T.E. 1999. Geology of the Kumara-Moana area. Sheets J32 and part K32. Institute of geological and Nuclear Sciences Geological Map 24. Institute of Geological and Nuclear Science Ltd, Lower Hutt, New Zealand.

Summerhayes, C.P.; Kroon, D. Rosell-Mela, A.; Jordan, R.W.; Schrader, H-J.; Hearn, R.; Villanueva, J.; Grima, H.J.O.; Eglinton, G. 1995. Variability in the Benguela Current upwelling system over the past 70,000 years. Progress in Oceanography 35: 207-251.

Sutherland, R.; Kim, K.; Zondervan, A.; McSaveney, M. 2007. Orbital forcing of mid-latitude Southern Hemisphere glaciation since 100 ka, inferred from cosmogenic nuclide ages of moraine boulders from the Cascade Plateau, Southwest New Zealand. Geological Society of America Bulletin 119: 443-451.

Suwa, M.; Bender, M.L. 2008. Chronology of the Vostok ice core constrained by O2/N2 ratios of occluded air; and its implication for the Vostok climate records. Quaternary Science Reviews 27: 1093-1106.

Svennson, A.; Andersen, K.K.; Bigler, M.; Clausen, H.B.; Dahl-Jensen, D.; Davies, S.M..; Johnsen, S.J.; Muscheler, R.; Parrenin, F.; Rasmussen, S.O.; Rothlisberger, R.; Seierstad, I.; Steffenson, J.P.; Vinther, B.M. 2008. A 60,000 year Greenland stratigraphic ice core chronology. Climate of the Past 4(1): 47-57.

Taylor, V.R.; Stowe, L.L. 1984. Reflectance characteristics of uniform earth and cloud surfaces derived from NIMBUS -7 ERB. Journal of Geophysical Research 89: 4987–4996.

Thompson, G.W.; Goldstein, S.L. 2005. Open-system coral ages reveal persistent sub-orbital sea-level cycles. Science 308: 401-404.

Thompson, G.W.; Goldstein, S.L. 2006. A radiometric calibration of the SPECMAP timescale. Quaternary Science Reviews 25: 3207-3215.

Tippett, M.J.; Kamp, P.J.J. 1993. Fission track analysis of the Late Cenozoic vertical kinematics of continental Pacific crust, South Island, New Zealand. Journal of Geophysical Research 98 (B9): 16119-16148.

Toggweiler, J.R.; Lea, D.W. 2010 Temperature differences between the hemispheres and ice age climate variability. Paleoceanography 25, PA2212, doi:10.1029/2009PA001758.

Trecker, M.A.; Gurrola, LO.D.; Keller, E.A. 1998. Oxygen-isotope correlation of marine terraces and uplift of the Mesa hills, Santa Barbara, California, USA. Pp57-69 in Stewart, I.S. & Vita-Finzi, C. (eds) Coastal Tectonics. Geological Society. London, Special Publications, 146.

Tyson, P.D.; Sturman, A.P.; Fitzharris, B.B.; Mason. S.J.; Owens, I.F. 1997. Circulation changes and teleconnections between glacial advances of the West Coast of New Zealand and extended periods of drought years in South Africa. International Journal of Climatology 17: 1499-1512.

Upuchi, E; Swift, S.A.; Ross, D.A. 1999. Late Quaternary stratigraphy, Paleoclimate and neotectonism of the Persian (Arabian) Gulf Region. Marine Geology 160: 1-23.

Vandenberghe, D.; Derese, C.; Houbrechts, G. 2007. Residual doses in recent alluvial sediments from the Ardenne (S. Belgium). Geochronometria 28: 1-8.

Vandergoes, M.J.; Newnham, R.M.; Preusser, F.; Hendy, C.H.; Lowell, T.V.; Fitzsimons, C.J.; Hogg, A.G.; Kasper, H.U.; Schluchter, C. 2005. Regional insolation forcing of Quaternary climate change in the Southern Hemisphere. Nature 436: 242-245.

Vermeersen, L.L.A.; Sabadini, R. 1999. Polar wander, sea-level variations and Ice-age cycles. Surveys in Geophysics 20: 415-440.

Vettoretti, G.; Peltier, W.R., 2003. Post-Eemian Glacial Inception. Part II: Elements of a Cryospheric Moisture Pump. Journal of Climate 16: 912–927.

Vimeaux, F.; Cuffey, K.M.; Jouzel, J. 2002. New insights into Southern Hemisphere temperature changes from Vostok ice cores using deuterium excess correlation. Earth and Planetary Science Reviews 203: 829-843.

Waelbroeck, C. 2004. Southern Ocean core MD89-101. PAGES Newsletter 99-3: 9.

Waelbroeck, C.; Labeyrie, L.; Michel, E.; Duplessy, J.C.; McManus, J.F.; Lambeck, K.; Balbon, E.; Labracherie, M. 2002. Sea level and deep water temperature changes derived from benthic foraminifera isotopic records. Quaternary Science reviews 21: 295-305.

Waelbroeck, C.; Jouzel, J.; Labeyrie, L.; Lorius, C.; Labracherie, M.; Stievenard, M.; Barkov, N.I. 1995. A comparison of the Vostok ice deuterium record and series from the Southern Ocean core MD88-770 over the last two glacial-interglacial cycles. Climate Dynamics 12: 113-123.

Waelbroeck, C.; Frank, N.; Jouzel, J.; Parrenin, F.; Masson-Delmotte, V.; Genty, D. 2008. Transferring radiometric dating of the last interglacial sea level high stand to marine and ice core records. Earth and Planetary Science Letters 265: 183-194.

Wang, Y.J.; Cheng, H.; Edwards, R.L.; An, Z.S.; Wu, J.Y.; Shen, C.-C.; Dorale, J.A. 2001. A high-resolution absolute dated late Pleistocene monsoon record from Hulu Cave, China. Science 294: 2345-2348.

Ward, C.M. 1988. New Zealand Marine Terraces: Uplift Rates. Science 240: 803-804.

Wallinga, J. 2002. Optically stimulated luminescence dating of fluvial deposits, a review. Boreas 31: 303-322.

Weninger, B.; Joris, O,; Danzeglocke, U. 2006. Calpal – Cologne Radiocarbon Calibration & Palaeoclimate Research Package. Universität zu Köln,Instutut für Ur-und Fruhgeschichte Radiocarbon laboratory.

Weninger, B.; Joris, O. 2008. A ^{14}C calibration curve for the last 60 ka: the Hulu U/Th timescale and its impact on understanding the middle to upper Paleolithic transition in Western Eurasia. Journal of Human Evolution 55: 772-781.

Wellman, H.W.; Willett, R.W. 1942. The geology of the West Coast from Abut Head to Milford Sound – Part 1. Transactions of the Royal Society of New Zealand 71: 282-306.

Wellman, H.W. 1979. An uplift map for the South Island of New Zealand, and model for the uplift of the Southern Alps. In: The Origin of the Southern Alps, edited by RI Walcott & MM Creswell. Bulletin of the Royal Society of New Zealand 18: 13-20.

Wells, P.; Okada, H. 1997. Response of nanoplankton to major changes in sea-surface temperature and movement of hydrological fronts over site DSDP 594 (South Chatham Rise, southeastern New Zealand) during the last 130 kyr. Marine Micropaleontology 32: 341-363.

Whitehead, N.E.; Roberts, P.B. 1991. Background to the DSIR review of radioactivity issues in the Westland Ilmenite Limited mining proposal at Barrytown. DSIR Physical Sciences Report-36. Nuclear Physics Group, DSIR Physical Sciences, Lower Hutt, New Zealand.

Williams, M.; Cook, E.; van der Kaari, S.; Barrows, T.; Shulmeister, J.; Kershaw, P. 2009. Glacial and deglacial patterns in Australia and surrounding regions from 35,000 to 10,000 years ago. Quaternary Science Reviews 28(23-24): 2398-2419.

Williams, P.W.; Neil, H.; Zhao, J-X. 2009. New Zealand cave records show distinctive Southern Hemisphere palaeoclimate signatures , LGM at Stage 4, no Younger Dryas, and a Polynesian Warm Period. pp 62 in Cortese, G.; Vandergoes, M.; Bostok, H. 2009 Past Climates Meeting 2009, 15-17 May 2009, Te Papa, Wellington, New Zealand, GNS Science Miscellaneous Series 23, 65 p.

Williams, P.F. 1996. A 230 ka record of glacial and interglacial events from Aurora Cave, Fiordland, New Zealand. New Zealand Journal of Geology and Geophysics 39: 225-241.

Williams, P.F. 1982. Speleothem dates, Quaternary terraces and uplift rates in New Zealand. Nature 292: 257-298.

Wilson, C.J.N.; Switsur, V.R.; Ward, A.P. 1988. A new 14C age for the Oruanui (Wairakei) eruption, New Zealand. Geological Magazine 125: 297-300.

Winograd, I.J.; Landwehr, J.M.; Ludwig, K.R.; Coplan, T.B.; Riggs, A.C. 1997. Duration and structure of the last four interglaciations. Quaternary Research 48: 141-154.

Winograd, I.J.; Landwher, J.M.; Coplen, T.B.; Sharp, W.D.; Riggs, A.C.; Ludwig, K.R.; Kolesar, P.T. 2006. Devils Hole, Nevada, $\delta^{18}O$ record extended to the mid-Holocene. Quaternary Research 66: 202-212.

Wohlfarth, B. 2009. Ice-free conditions in Fennoscandia during Marine Oxygen Isotope Stage 3? Technical Report SKB TR-09-12. Svensk Karnbranslehantering AB.

Wright, I.C.; McGlone, M.S.; Campbell, S.N.; Pillans, B.J. (1995). An integrated latest Quaternary (Stage 3 to Present) Paleoclimatic and Paleoceanographic record from offshore Northern New Zealand. Quaternary Research 44(2): 283-293.

Wright, JD; Sheridan, RE; Miller, K.G.; Uptegrove, J.; Cranmer, B.S.; Browning, J.V. 2009. Late Pleistocene Sea Level on the New Jersey Margin: Implications to Eustacy and Deep-Sea Temperature. Global and Planetary Change 66: 93-99.

Yamamoto, M.; Oba, T.; Shimamune, J.; Ueshima, T.; 2004. Orbital-scale anti-phase variation of sea surface temperature in mid-latitude North Pacific margins during the last 145,000 years. Geophysical Research Letters 31. L16311,doi:10,1029/2004GL020138.

Yokoyama, Y.; Esat, T.M.; Lambeck, K.; Fifield, L.K. 2000. Last ice age millennial scale climate changes recorded in Huon Peninsula corals. Radiocarbon 42: 383-401.

Yokoyama, Y.; Esat, T.M.; Lambeck, K. 2001a. Last-glacial sea-level change deduced from uplifted coral terraces of Huon Peninsula, Papua New Guinea. Quaternary International 83-85: 275-283.

Yokoyama, Y.; Esat, T.M.; Lambeck, K. 2001b. Coupled climate and sea-level changes deduced from Huon Peninsula coral terraces of the last ice age. Earth and Planetary Science Letters 193(3-4): 579-587.

Yokoyama, Y; Esat, TM. 2004. Long-term variations of uranium isotopes and radiocarbon in the surface seawater recorded in corals. In: Global Environmental Change in the Ocean and on Land, M. Shiyoni et al (eds) pp 279-309.

Yokoyama, Y; Esat, TM. 2006. Growth patterns of the last ice age coral terraces at Huon Peninsula. Global and Planetary Change 54(3-4): 216-224.

Yoshida, H; Brumby, S. 1999. Comparisons of ESR ages of corals using different signals at X- and Q-band: Re-examinations of corals from Huon Peninsula, Papua New Guinea. Quaternary Science Reviews 18: 1529-1536.

Youfeng, N.; Weiguo, L.; Zhisheng, A. 2008. A 130-ka reconstruction of precipitation in the Chinese loess Plateau from organic carbon isotopes. Palaeogeography, Palaeoclimatology, Palaeoecology 270: 59-63.

Young, D.J. 1963. A faulted and tilted Late Pleistocene terrace near Blackball. New Zealand Journal of Geology and Geophysics 6: 721-724.

Yu, P-S.; Chiu, T-C.; Wei, K-Y.; Chen, Y-Y. 2000. Planktonic foraminifera faunal assemblage and sea surface temperature variations in a warm-pool South China Sea record of the past 400,000 years: Images core MD97-2142. Journal of the Geological Society of China 43: 467-496.

Zhang, J.-F.; Li, S.; Tso, M.Y. W. 2001. Assessment of bleaching of k-feldspar grains. Radiation Measurements 33: 103-108.

Zhao, M.; Huang, C-Y.; Wang, C-C.; Wei, G. 2006. A millennial-scale U^{k}_{37} sea-surface temperature record from the South China Sea (8°N) over the last 150 kyr: Monsoon and sea-level influence. Palaeogeography, Palaeoclimatology, Palaeoecology 236: 39-55.

Zech, R.; May, J-H.; Kull, C.; Ilgner, J.; Kubik, P.W.; Veit, H. 2008. Timing of the late Quaternary glaciation of the Andes from ~15 to 40° S. Journal of Quaternary Science 23(6-7): 635-647.

Zhu, Z.; Marshall, J.F.; Chappell, J. 1994. Effects of differential uplift on Late Quaternary coral reef diagenesis, Huon Peninsula, Papua New Guinea. Australian Journal of Earth Science 41: 463-474.

Ziegler, M.; Nurnberg, D.; Caras, C.; Tiedemann, R.; Lourens, L.J. 2008. Persistent summer expansion of the Atlantic Warm Pool during glacial abrupt cold events. Nature Geoscience 1: 601-605.

Zuraida, R.; Holbourn, A.E.; Nurnberg, D.; Kuhnt, W.; Durkop, A.; Erichsen, A. 2009. Evidence for Indonesian throughflow slow-down during Heinrich Events 3-5. Paleoceanography 24: PA2205.doi:10.1029/2008PA00165

APPENDIX ONE: SUMMARY OF THE DETAILS OF INDIVIDUAL LUMINESCENCE SAMPLE SITES

The following is a summary of the information recorded on a site by site basis.

Samples RR1 & RR2, Lab Codes WLL216 & WLL169

Sampled by: RV Rose, J Shulmeister, U Rieser on 2/3 February 2002
Location: Phelps Mine Pit, Southside, Hokitika Elevation: ~ 9 to 12 metres a. m. s. l.
Map & Grid Ref: NZMS 260 J33 N 582780 E 234230
Formation: Craigs / Awatuna
Material: RR1 - Sand from the upper part of the "Craigs Formation" at the base of the main mine face, about 60 centimetres below the organic soil that sits on the ancient beachsand.
RR2 – From a 30 to 40 cm thick organic rich soil beneath the glacial Loopline Formation and overlying the beach sand of the "Craigs Formation".
Correlation: Previously OIS 5c or OIS 5a
Depth of Burial: RR1 ~20-25 m; RR2 ~20-25 m
Outcrop: Exposures in the mine faces in the bottom of the opencast gold mine.
IRSL Age: RR1: No IRSL age obtainable (quartz from marine sand)
RR2: IRSL age for RR2 is 33.6 ± 3.6 ka (4-11 micron feldspars from organic rich soil)

The sand of the Craigs Formation is situated between 20 and 25 metres below the surface of the overlying terrace. In the vicinity of the sample site the Craigs Formation has a thickness of about 10 to 12 metres. The soil that overlies the beachsand has an RL of 9 to 12 metres. The overlying Loopline Formation is composed of glacial gravel and has been correlated with OIS 4 by Preusser et al (2005). There is an IRSL age of 56.8 ± 5.9 ka (RR3) from a loess horizon within the Loopline Formation.

Stratigraphic Relationships at Sample Sites RR1a, RR1b & RR2

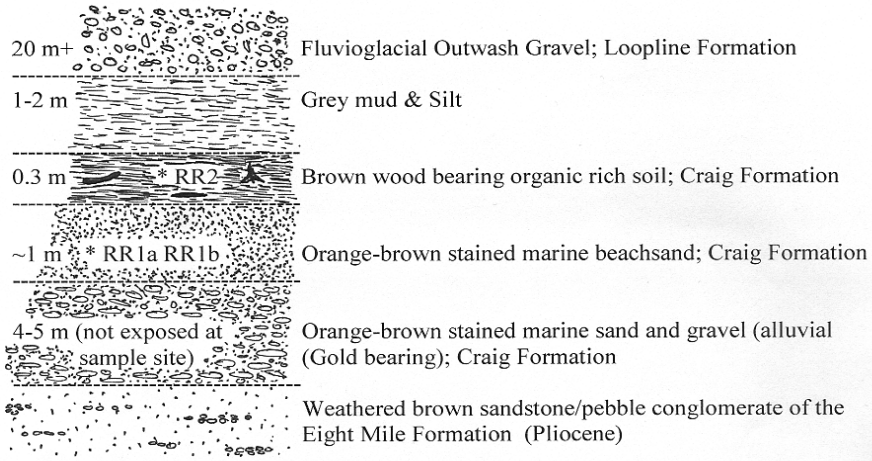

The full thickness of the Craig Formation has been established at the Phelps Mine by excavation in the (Hydraulic Excavator) and by exploratory drilling.

In the third of the photos above the sample point for RR1 & RR2 is just beyond the small pond in the far distance at the base of the mine-face. At the large pond in the foreground the two small "Islands" are Craig Formation, as is the lowermost portion of the mine face beyond the Islands. This is the portion hat has been undercut at the corner of the face. Above the undercut portion the face is composed of two units of fluvioglacial outwash separated by a thin grey silt layer. The silt layer is shown in the photos for RR3 below. On the left of this south facing view the tapering slope is composed of mine tailings and dumped overburden. In the mid 1990's the Craig Formation marine strandline was briefly exposed beneath the area of tailings in this view. This exposure was open over a length of about 100-150 m. At that time the site was inspected by the writer. The marine sand is underlain here by light brown weathered pebbly sandstone of the Eight Mile Formation. The Craig formation was extensively tunneled in the area of the pond in the foreground. Large quantities of mine timber (props etc) were excavated and processed though the mine plant when the mining was being conducted.

Sample RR3, Lab Code WLL170

Sampled by: RV Rose, J Shulmeister, U Rieser
Date: 2 / 3 February 2002
Location: Phelps Gold Mine, Southside, Hokitika
Elevation: ~ 25 metres a. m. s. l.
Map Ref: NZMS 260 J33
Grid: N 582805 E 234240
Formation: Loopline
Material: Buried podzolised soil/loess
Depth of Burial: 7-10 m
Outcrop: Exposure in the upper part of one of the mine faces at this property.
IRSL Age: RR3: 56.8 ± 5.9 ka (4-11 micron "feldspars" from organic rich soil)

Stratigraphic Relationships at Sample Site RR3

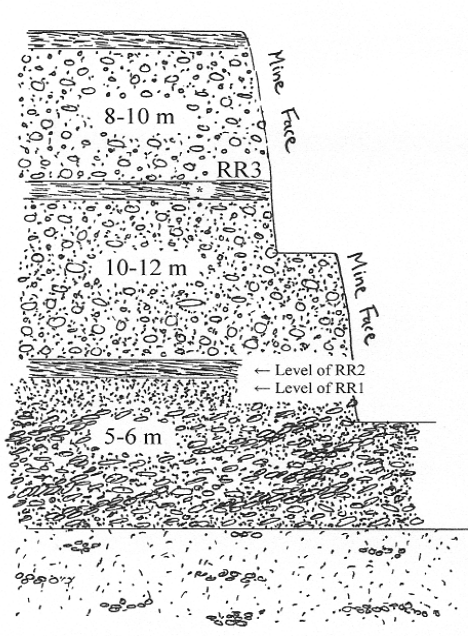

Surficial Loess	
Fluvial Gravel	Loopline Formation
Grey loess/soil	
Fluvial Gravel	Loopline Formation
Organic-rich Soil	Craig Formation
Marine Beach Sand	Craig Formation
Marine Beach Sand & Gravel	Craig Formation
Weathered brown sandstone	Eight Mile Formation

Photos:

Samples RR4 & RR5, Lab Codes WLL217 & WLL147

Sampled by: RV Rose, J Shulmeister, U Rieser on 2/3 February 2002
Location: Phelps Mine, Southside, Hokitika
Elevation: ~ 20 metres a. m. s. l.
Map & Grid Ref: NZMS 260 J33 N 582795 E 234260
Formation: Awatuna
Material: RR4 Clean but stained beachsand from the end of a long tunnel commencing at the base of the natural terrace face ct by the Hokitika River at the Phelps Mine.
RR5 Clean but stained beachsand from a short tunnel part way up the same terrace face but about 50 m SE of the portal of the RR4 tunnel.
Depth of Burial: RR4 ~15-20 m; RR5 originally ~20 m, but now much closer to the surface (3-4 m) due to the cutting of the terrace face.
Outcrop: Exposures in tunnels near to the opencast gold mine that was operational in the 1990's.
IRSL Age: None- insufficient silt in sample.

Stratigraphic Relationships at Sample Site RR4

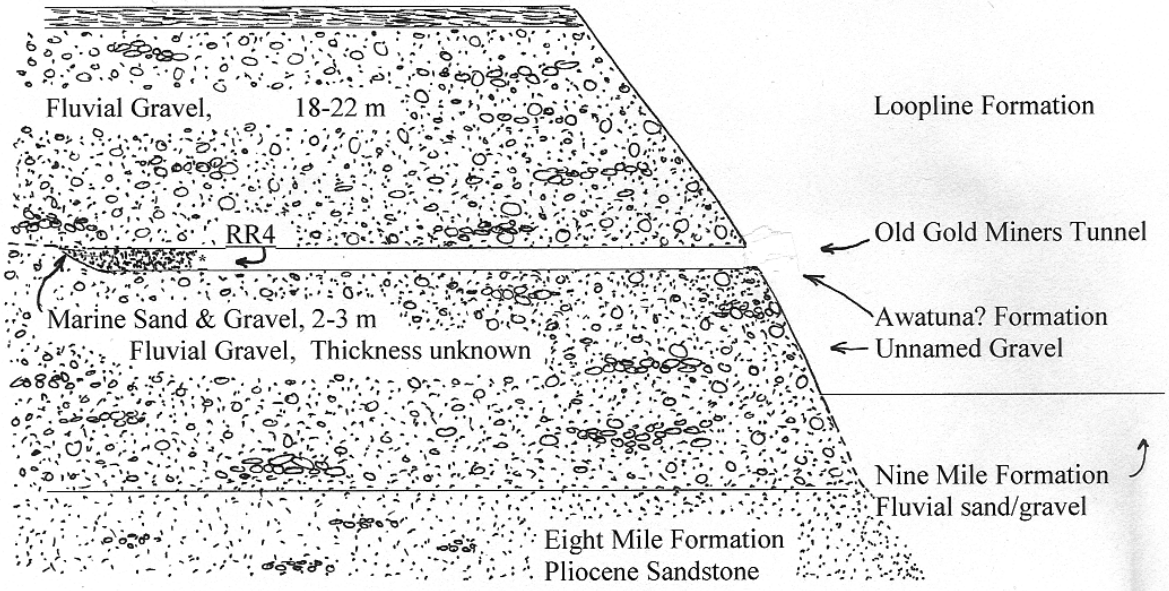

Stratigraphic Relationships at Sample Site RR5

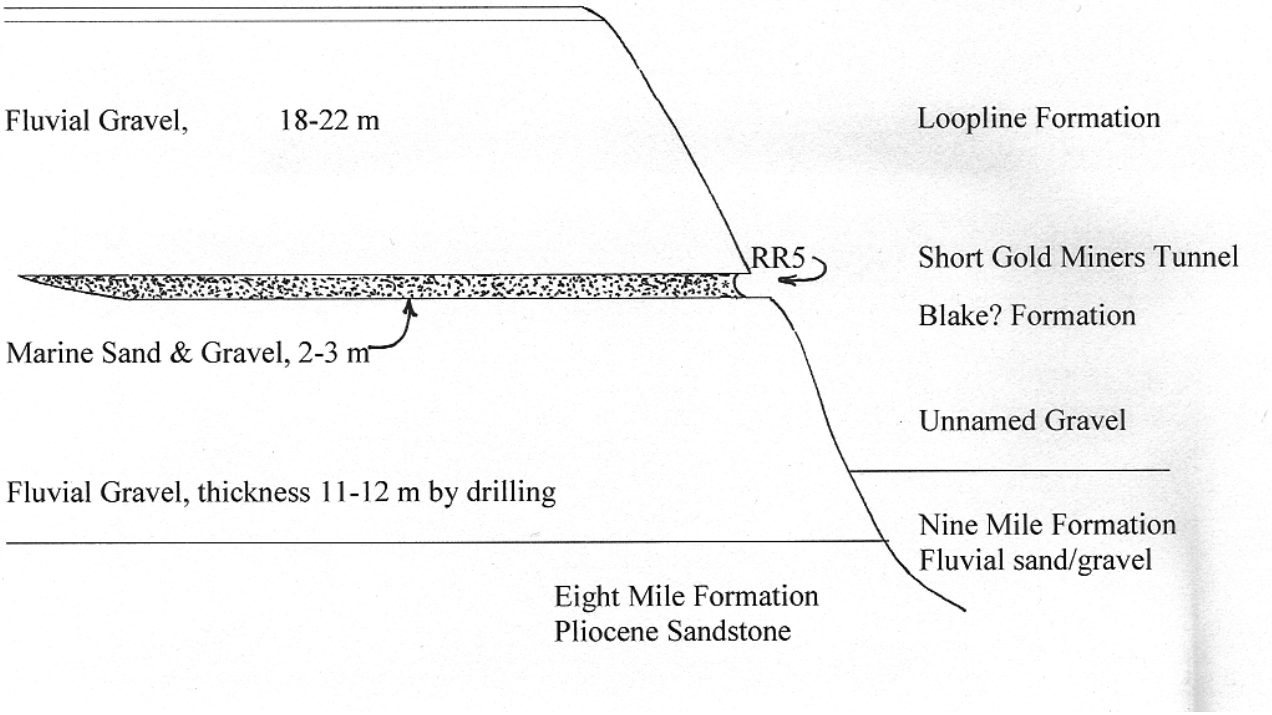

Samples RR6 & RR7, Lab Codes WLL218 & WLL148

Sampled by: RV Rose, J Shulmeister, U Rieser on 2 / 3 February 2002
Location: Scandinavia Hill, Stafford
Elevation: ~110-115 metres a. m. s. l.
Map & Grid Ref: NZMS 260 J32 N 583640 E 235340
Formation: Scandinavia
Material: RR6 – Soil that sits under a fluvial gravel deposit and on marine beach sand and gravel
RR7 – Sample from beach sand of the Scandinavia Formation about 1 m below RR6.
Depth of Burial: RR6 ~8 m
RR7 ~9 m
Outcrop: Exposures in a road cutting near Stafford (Scandinavia Road at Scandinavia Hill).
IRSL Age RR6: 123.3 ± 12.7 ka (4-11 micron feldspars from clay/soil)
RR7: No IRSL age obtainable on quartz from clean marine sand

Stratigraphic Relationships at Sample Sites RR6 & RR7

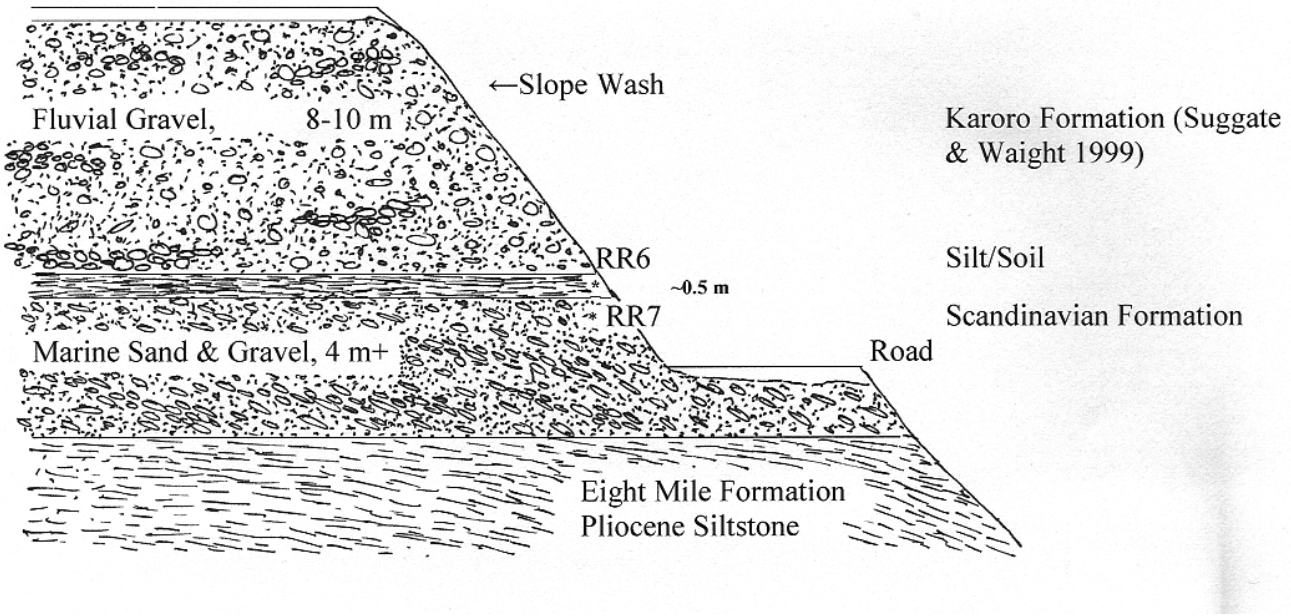

Photos: (below) Top: RR6 on the left, RR7 on the right

Bottom: The Scandinavia Formation in a road cutting at Ballarat Rise about 2 km SE of the RR6/RR7 sample site. Grid reference NZMS260 J32 N3540 E5220

Samples RR8 & RR9, Lab Codes WLL219 & WLL220

Sampled by: RV Rose, J Shulmeister, U Rieser on 2/3 February 2002
Location: Sunday Creek, Chesterfield
Elevation: ~ 50 to 55 metres a. m. s. l.
Map & Grid Ref: NZMS 260 J32; RR8: N 584030 E 235490; RR9: N 584025 E 235480
Formation: Awatuna ("Type Section)
Material RR8 - Organic soil underlying the (glacial) Loopline Formation and overlying about 1 metre of fluvial silts and gravel which rests on the beach sand of the Awatuna Formation.

RR9 – Sand from a sequence of interbedded sand and gravel horizons. Stratigraphically about 3 to 5 metres below RR8 and about 30 m to the SW.

Depth of Burial: RR8 ~15 m; RR9 ~18 m
IRSL Age RR8: 34.8 ± 3.5 ka (4-11 micron feldspars from organic rich soil)
RR9: 47.8 ± 6.6 ka (4-11 micron silt from marine sand, single aliquot)
RR9: 54.0 ± 7.3 Ka (4/11 micron silt, multiple aliquot)
Outcrop: Exposures in the steep west bank of a small tributary of Sunday Creek.

Stratigraphic Relationships at Sample Site RR9

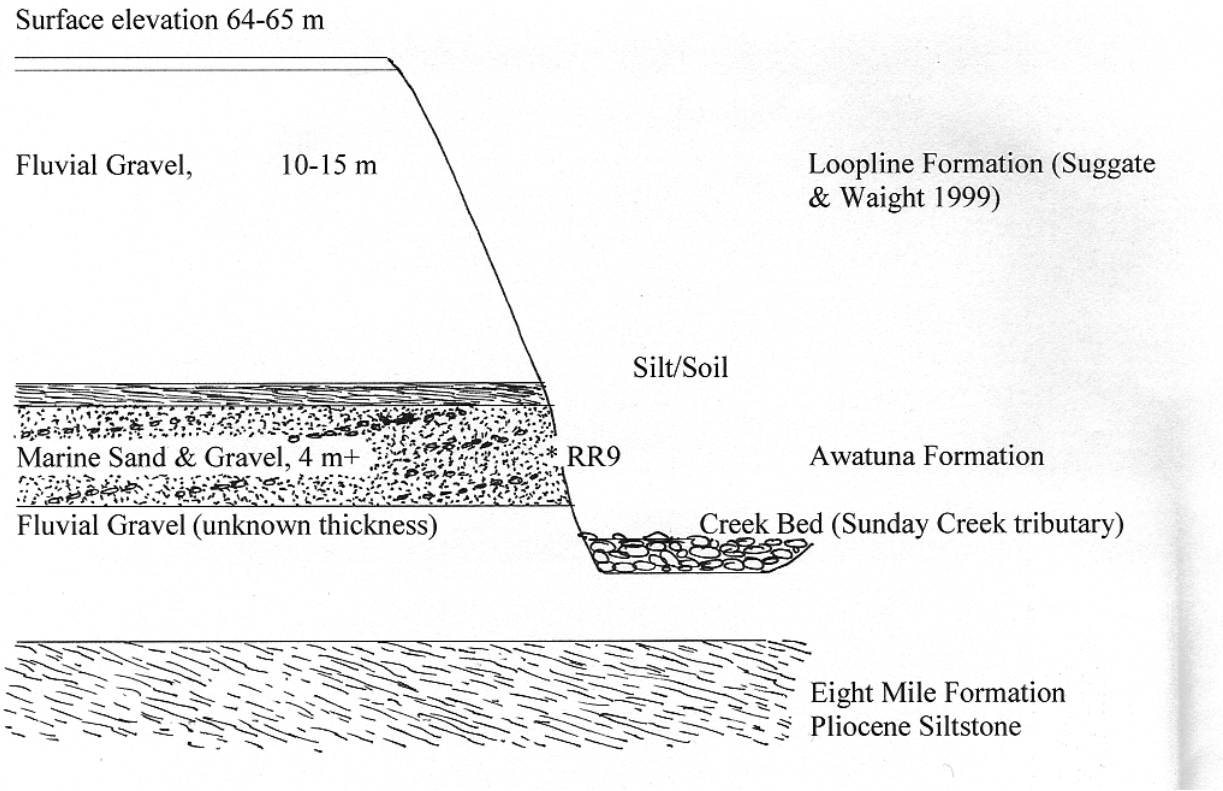

Stratigraphic Relationships at Sample Site RR8

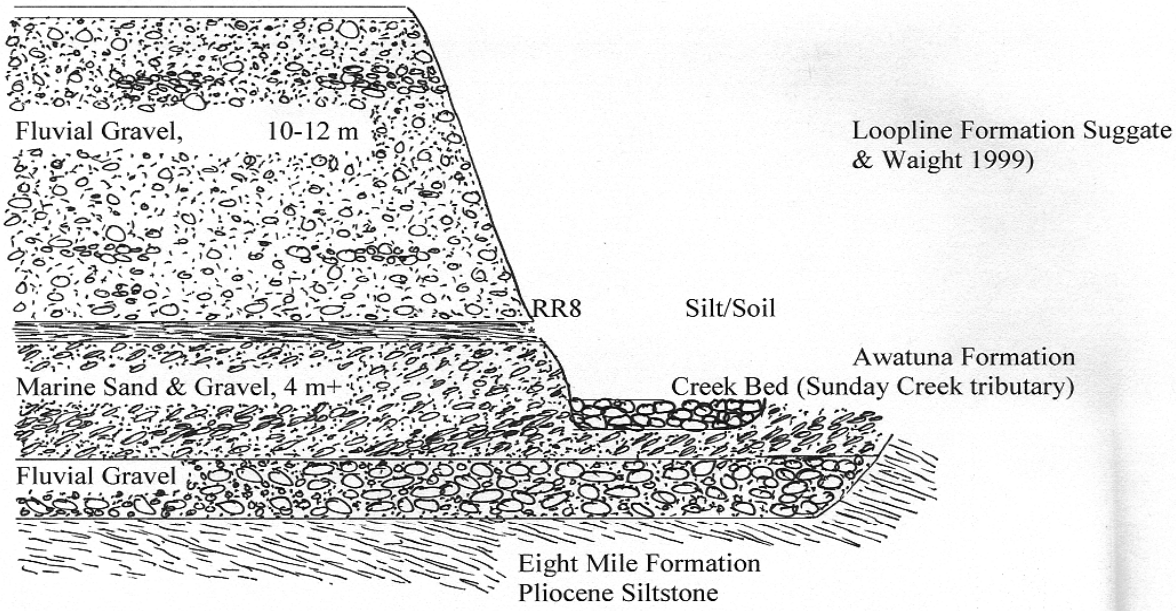

Detail

		10 m+ Fluvial Gravel
		0.2 m Moderately organic silt with some sand lenses
*	RR8	0.2 m Wood-bearing organic silt
		0.1 m Non-organic silt
		1.0 m Interlayered silt and fluvial gravel
		4 – 5m Marine sand and gravel (gold bearing, numerous tunnels)
		Fluvial gravel, thickness unknown

Photos: RR9 (below)

Sample RR10, Lab Code WLL149

Sampled by: RV Rose, J Shulmeister, U Rieser on 2/3 February 2002
Location: North Beach, Greymouth
Elevation: ~ 70 metres a. m. s. l. (the sandy unit that was sampled is overlain by brown weathered gravel at ~70 m measured by aneroid – Pat Suggate 9/2/03).
Map & Grid Ref: NZMS 260 J31 N 586620 E 236330
Formation: Rutherglen
Material: Clean friable marine beachsand
Depth of Burial: RR10 ~ 5 m
IRSL age: No age as the material did not prove to be suitable. The quartz was unsuitable and there was insufficient silt for the alternative method
Outcrop: The exposure is a cutting adjacent to a driveway near the Point Elizabeth reserve. The sample was taken from sand situated about 1 metre above the wave cut platform. R. Rose is in photograph of the sample site.

Stratigraphic Relationships at Sample Site RR10

Top of Exposure

Fine to medium Sand — Rutherglen Formation

Slightly Pebbly Sand — Rutherglen Formation

* RR10 — Rutherglen Formation

Fine to medium sand with some cross-bedding

3 cm of iron cemented sand at contact
Quartz & greywacke pebble & granule conglomerate

Tertiary Siltstone — Stillwater Mudstone

Exposed in a (private) road cutting at North Beach, Cobden

Photo: RR10

Sample RR11, Lab Code WLL171

Sampled by: RV Rose, J Shulmeister, U Rieser sampled on 2 /3 February 2002
Location: Access road to private property, North Beach, Cobden
Elevation: ~ 43 to 46 metres a.m.s.l. (48m at by aneroid at the top of the marine gravel, Pat Suggate 9/2/03).
Map & Grid Ref: NZMS 260 J31 N 58566250 E 2363200
Formation: Awatuna
Material: The sample is from a limestone boulder bearing silt/clay unit that rests on the storm tossed pebbles situated very close to the rear of the old strandline.
Depth of Burial: ~ 2 to 5 m
IRSL age: 53.9 ± 7.6 ka (4-11 micron feldspars from marine mud / silt)
Outcrop: Cutting / slip in the side of a driveway. The site is directly east and above / up-slope from the car park for the Point Elizabeth track. The photograph has Dr RP Suggate examining the sample site about 1 year after the sample was taken. The sample was taken from a point approximately at shoulder height just to the left of Dr Suggate.

Stratigraphic Relationships at Sample Site RR11

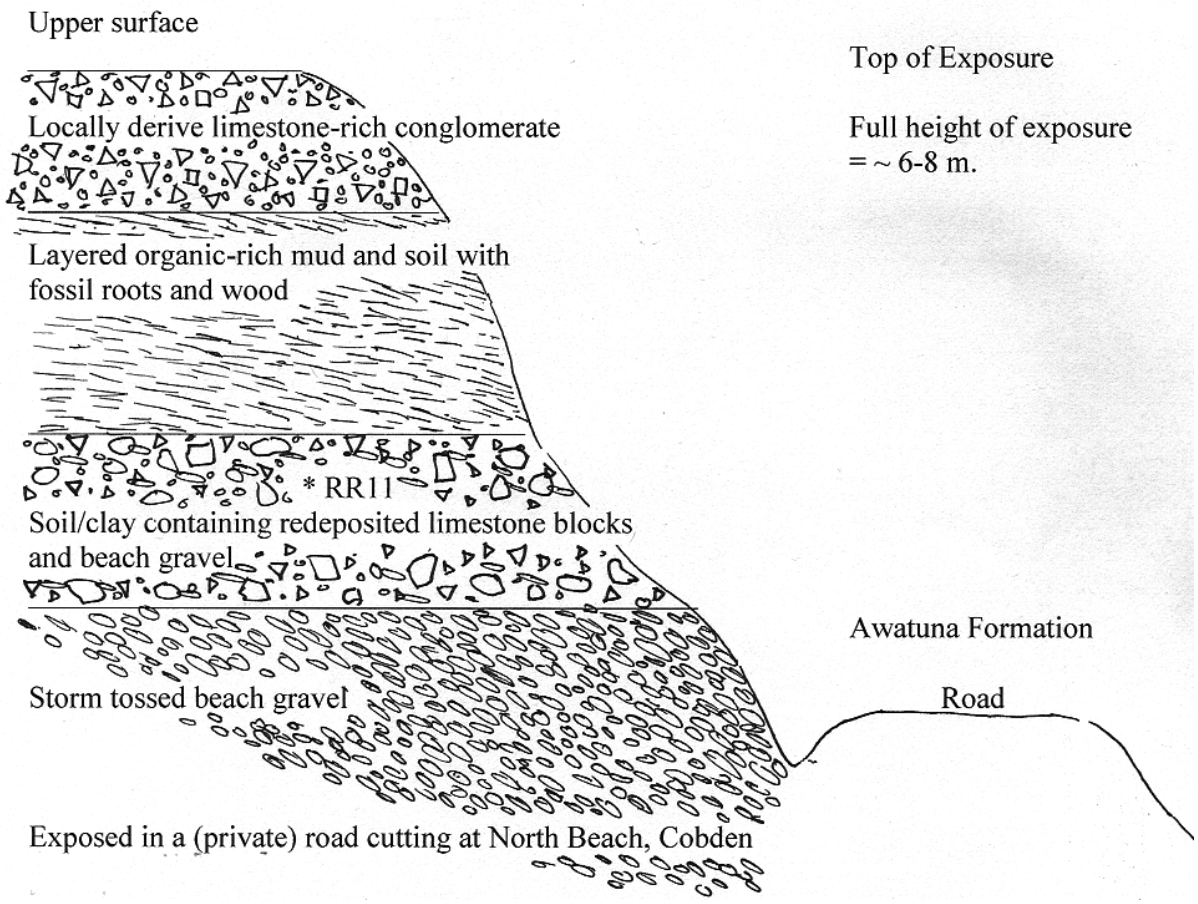

Photo: RR11. The photograph has Dr RP Suggate examining the sample site about 1 year after the sample was taken. The sample was taken from a point approximately at shoulder height just to the left of Dr Suggate.

Sample RR12, Lab Code WLL296

Sampled by: RV Rose, J Shulmeister, U Rieser on 3 February 2002
Location: Point Elizabeth
Elevation: ~ 30 to 33 metres a.m.s.l
Map and Map Ref: NZMS 260 J31 N 586780 E 236350
Formation: Awatuna / Raleigh
Material: Interlayered coarse sand and gravel. The sample was from a relatively thin sand bed about 1.5 to 2 metres below the modern ground surface.
Depth of Burial: 1 to 2 m
IRSL age: 39.5 ± 2.4 ka (silt from marine sand horizon)
Outcrop: Exposure in an old opencast mine face adjacent to the Point Elizabeth track.

Stratigraphic Relationships at Sample Sites RR12a and RR12b

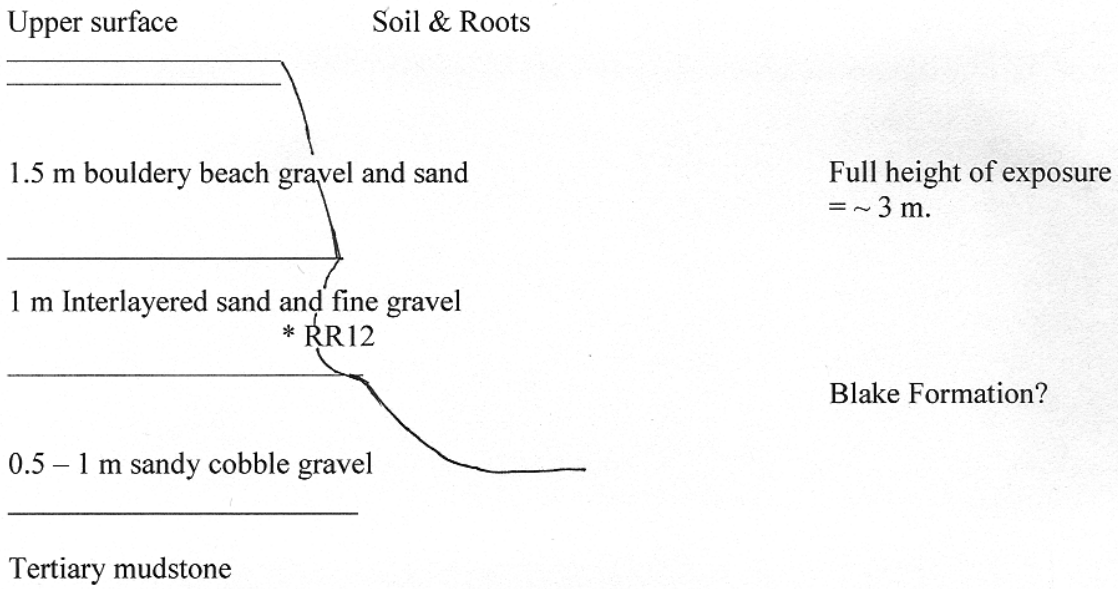

Exposed in an old gold mine (< 150 years) on a marine terrace a few hundred metres SE of Point Elizabeth. The site is about 10 to 12 m back from the top of the cliff overlooking Rapahoe Beach and is immediately alongside the Point Elizabeth Track. It is also about 15 to 20 m east of a relatively young fault trace. The fault displaces the marine terrace by about 2 m and is visible in the adjacent cliff face. RR12 is from a thin layer of medium sand situated between granule beds.

This site is at a significantly significantly lower elevation than that of RR11.

Photo: RR12. In the photo Dr J Shulmeister and Dr U Rieser are in the process of taking the IRSL sample.

Sample RR13, Lab Code WLL150

Sampled by: RV Rose, J Shulmeister, U Rieser on 2/3 February 2002
Location: Caledonian Formation, Darkies Terrace, Point Elizabeth
Elevation: ~ 115 to 120 metres a. m. s. l.
Map & Grid Ref: NZMS 260 J31 N 586690 E 236345
Formation: Caledonian
Material: Clean friable marine beachsand
Depth of Burial: ~ 5 to 7 m
IRSL age 87.1 ± 8.3 ka (silt in marine sand).
Outcrop: Exposure in an old mine tunnel adjacent to the historic access track on Darkies Terrace near Point Elizabeth.

Stratigraphic Relationships at Sample Sites RR13a and RR13b

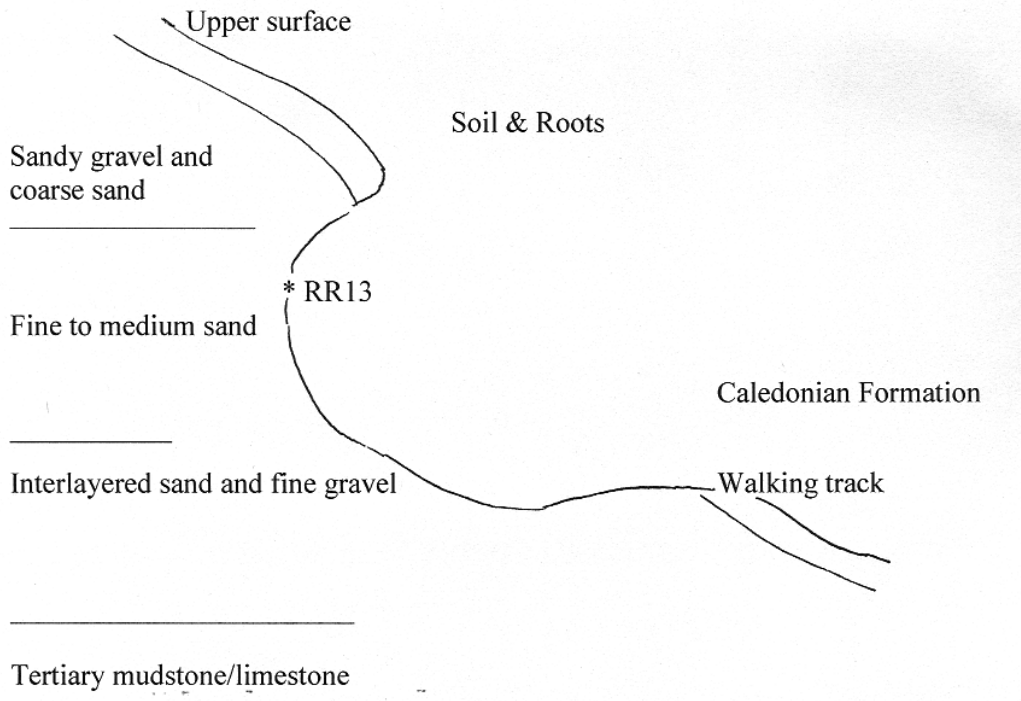

The sampled outcrop is in a small tunnel adjacent to the old goldminer's trail along this discontinuous 120 m high terrace. The site is about 1.5 km SSE of Point Elizabeth. The sampled material is a tan coloured fine-medium sand.

Photo: In the photo Dr J Shulmeister and Dr U Rieser are in the process of taking the IRSL sample.

Samples RR14, RR15 & RR16. Lab codes WLL277, WLL297 & WLL2278

Sampled by: RV Rose, J Shulmeister, U Rieser on 2/3 February 2002
Location: Road to new residential subdivision south of Mill Creek, South Beach, Greymouth
Map/Grid Ref: NZMS 260 J32; N 585520 E 236060 for RR14; N 585530 E 236060 for RR15 & RR16
Elevation: ~ 56 to 60 metres a.m.s.l. for RR14; ~52 to 56 metres a.m.s.l. for RR15 and RR16
Formation: Rutherglen
Material: The samples are friable grey fine to medium sand. The sand is free from obvious staining by water borne iron or manganese.
Depth of Burial: RR14 1-2 m; RR15 ~7-8 m; RR16 ~8-9 m
IRSL Age: RR14: No age as sand sized quartz unsuitable, insufficient silt in the sample.
RR15: 65.9 ± 5.4 ka (silt from marine sand)
RR16: No age as sand unsuitable and there was insufficient silt in the sample.
Outcrop: Cutting adjacent to the main access road to the subdivision.
Photo: Dr U Rieser taking sample RR14, an IRSL sample from the Rutherglen formation at the Tasman View Subdivision, South Beach, Greymouth.

The site of samples RR14, RR15, and RR16 is located at the western edge of a raised marine terrace (Rutherglen Formation) that overlooks South Beach, Paroa and Mill Creek. The upper surface at this site had been excavated to create a logging skid site for the harvesting of a *pinus radiata* plantation, and has since been converted to a residential section. Along the edge of the skid-site a cutting had been created alongside the main access road onto the terrace and the samples were obtained from this cutting. For RR14 the sampled material was no more than 2 m below the original terrace surface.

The sampled material is a soft friable laminated, planar bedded, fine-medium grey marine sand. The sample was taken about 1.5 m below the sand/overlying soil contact. The sand contains a high % of biotite mica and abundant quartz. There is no visible bioturbation and no shell material. The low heavy mineral content in this profile indicates a near-shore rather than a beach depositional environment.

Stratigraphic Relationships at Sample Sites RR15 and RR16

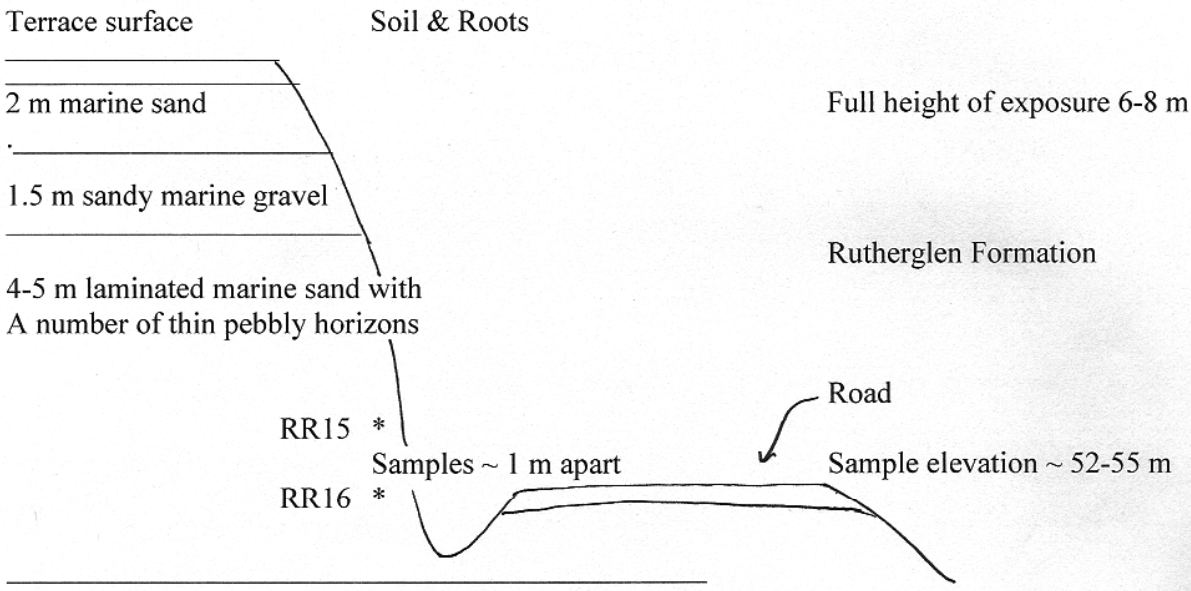

The material sampled for RR15 is a silty/muddy marine sand
The material sampled for RR16 is a relatively clean fine to medium sand.

The sample location is a road cutting alongside the main access road to the terrace. At the time of sampling the area was being prepared for subdivision. In 2009 the area has been developed for housing. This site overlooks South Beach and Paroa.

The samples were buried by at least 3 metres prior to the creation of the road cutting. The maximum depth of cover below the terrace surface is 7 to 8 m.

Samples RR17 & RR18, Lab Codes WLL172 & WLL151

Sampled by: RV Rose, J Shulmeister, U Rieser on 2/3 February 2002
Location: Private driveway (Mackley Ferguson) off Power Road, Karoro, Greymouth
Elevation: ~ 72 metres a. m. s. l. (72 m by aneroid – P Suggate 9/2/03)
Map & Grid Ref: NZMS 260 J32 N 5857000 E 2361300 (300?)
Formation: Rutherglen
Material: Ancient friable grey marine sand
Depth of Burial: RR17 ~3 m; RR18 ~4 m
IRSL Age: RR17: 63.6 ± 10.5 ka (4-11 micron feldspars from the laminated mud/silt).
RR18: No age, insufficient silt in the sample, quartz sand not suitable
Outcrop: Cutting adjacent to the side of the driveway where the driveway emerges onto the terrace.

Stratigraphic Relationships at Sample Sites RR17 and RR18

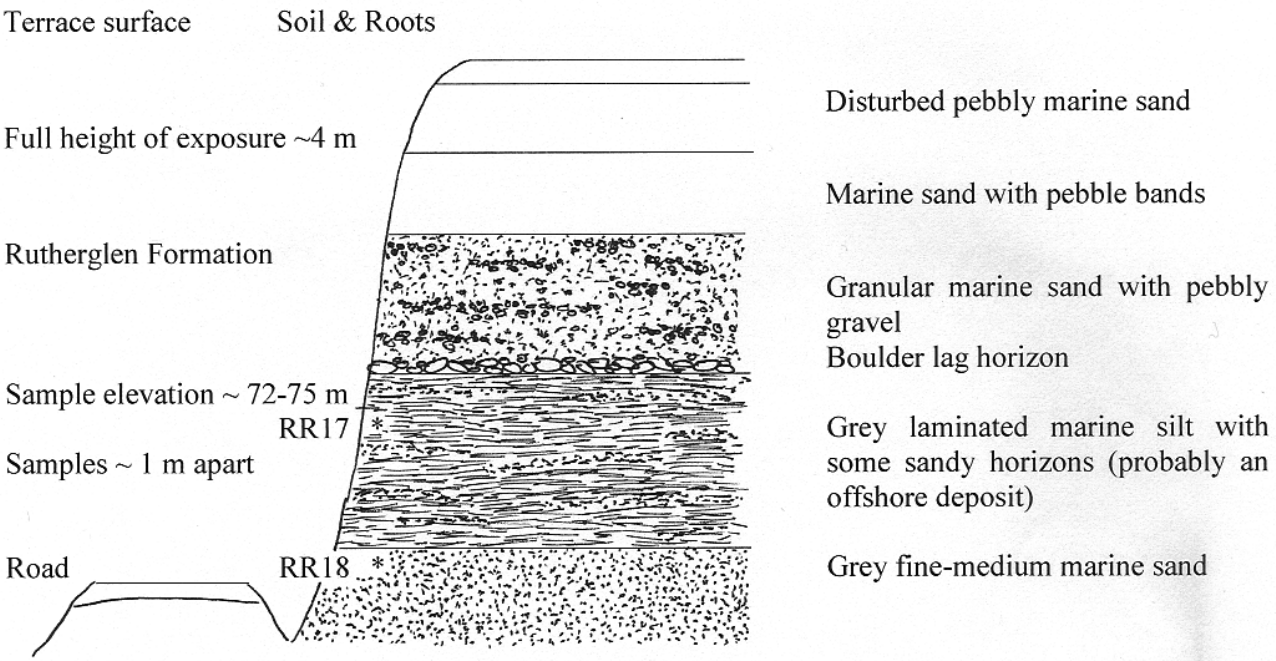

The sample location is a road cutting in a long driveway up onto the raised marine terrace immediately to the north of Power Road, South Beach/Karoro. The samples were buried by at least 3 metres prior to the creation of the road cutting. The maximum depth of cover below the terrace surface is 4 m. The site is situated about 50 - 100 m to the west of the strandline which separates the Rutherglen and Karoro strandlines. The strandline is situated at a subdued terrace riser that has an elevation difference of about 2 to 3 metres.

Photo: RR17, RR18

Sample RR19, Lab Code WLL173

Sampled by: RV Rose, J Shulmeister, U Rieser on 2/3 February 2002
Location: Older part of the Holocene (raised strandline deposits) at Rapahoe Beach
Map & Grid Ref: NZMS 260 J31 N 586845 E 236480
Elevation: ~ 6 to 8 metres a. m. s. l.
Formation: Nine Mile
Material: Clean quartz rich grey beach sand
Depth of Burial: 3 m
IRSL Age: No age obtained due to insufficient silt in the sample, quartz sand unsuitable
Outcrop: Exposure in a cutting adjacent to a vehicle access track.

Stratigraphic Relationships at Sample Site RR19

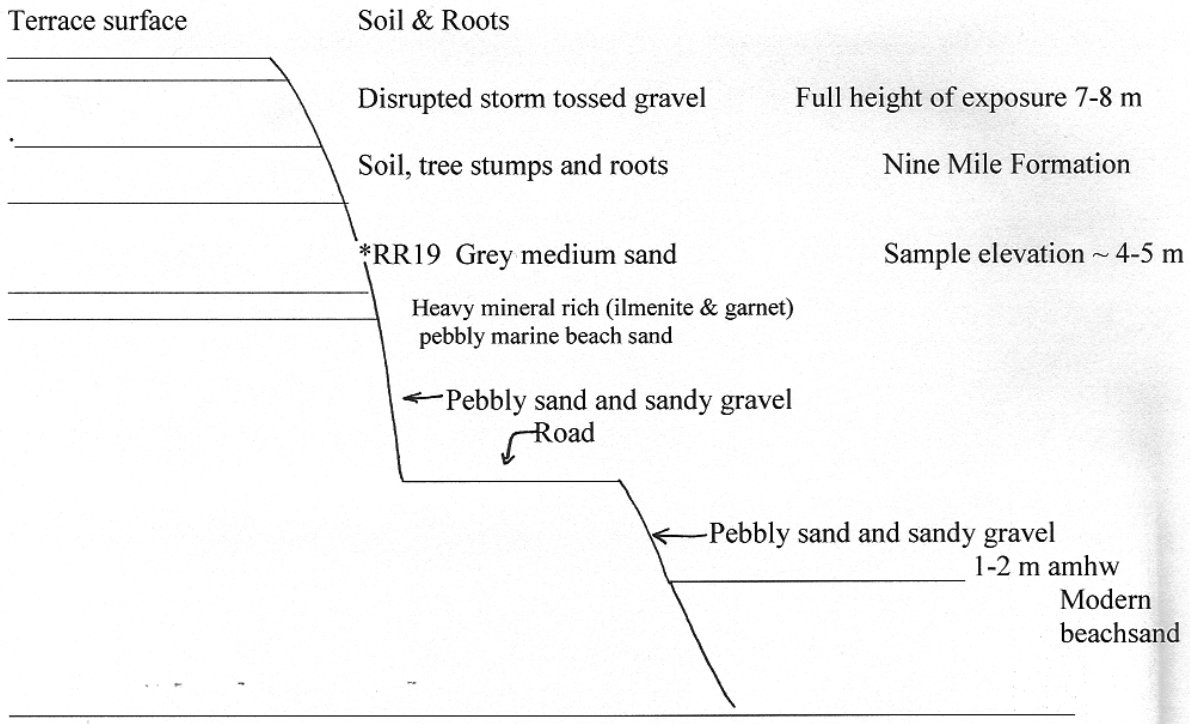

The sample site is situated at Rapahoe Beach about 7 km NNE of Greymouth. The coverbeds above the sample are about 1.5 to 2 m thick. This "beach-cliff" has been subject to active erosion so the sample was originally (prior to about 100 yrs ago) well back into the face. The vehicle track was excavated in the 1990's. The site is situated adjacent to the much higher cliff leading up to the Awatuna Formation.

Sample RR20, Lab Code WLL524

Sampled by: RV Rose on 11 July 2004
Location: Road cutting (about 5 m high) adjacent to SH 6, no more than 0.5 m above the level of the road.
Elevation: ~ 45 m
Map & Grid Ref: NZMS 260 J31 N 7425 E 6730
Formation: Awatuna Formation?
Material: Light brown clayey soil
Depth of Burial: 4.5 to 5 m
Correlation: Previously MIS 5e or MIS 5c
IRSL Age RR 20: 42.5±6.8 ka (silt from organic soil)
Outcrop: The outcrop is in a road cutting adjacent to SH 6. It is approximately opposite the opening in the cliff face from which Schulz Creek emerges (opposite side of SH 6). The position is approximately the same as that illustrated in Burrows (1997). When the IRSL sample was taken there was a "Children Walking" road sign about 2 metres from the sample point.

Sample profile RR20

----------		Surface
3.5 to 4.5 m		Interlayered soil and silty fluvial gravel
----------		
45 cm		Sandy light to medium brown organic-rich soil, some wood fragments with a few small pebbles
----------		
20 cm		Medium to dark brown organic soil , numerous wood fragments
----------		
35 cm	*	Sample RR20 in middle of this interval. Light brown clayey soil at base grading up to brown organic-rich soil
----------		
4 m+		Beach pebbles and beach sand

Centre of sample 16 cm above the clay/gravel contact

Stratigraphic Relationships at Sample Site RR20

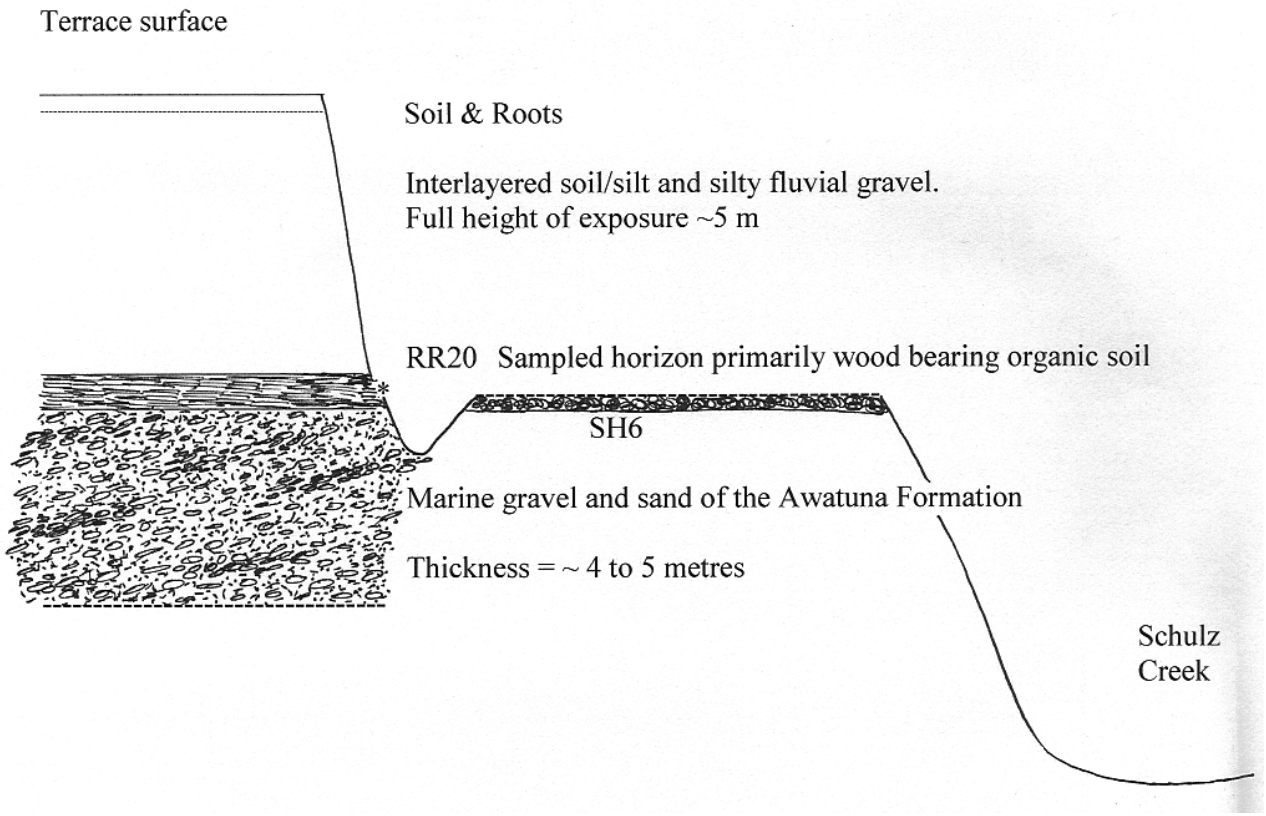


Photos: RR20

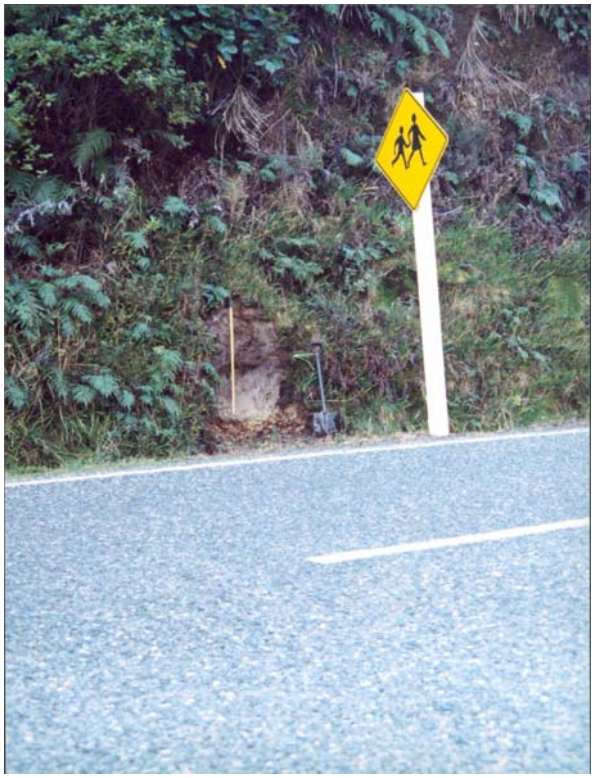

Photos: RR20

Sample RR 21, Lab Code WLL526

Sampled by: RV Rose on 11 July 2004
Location: Road cutting, SH 7, Kamaka, Grey Valley
Elevation: 30 m approximately
Map & Grid Ref: NZMS 260 K31 N 6305 E 7760
Formation: Larrikins Formation
Material: Silt/Very fine sand
Depth of Burial: 4 to 5 m
Correlation: Previously MIS 2
IRSL Age: 35.3 ± 3.2 ka (silt)
Outcrop: IRSL sample taken from a silt / v.fine sand horizon. This outcrop was dated by ^{14}C by Denton et al (1999). The outcrop is situated on the south side of State Highway 7 about 5 metres above the road.

Photos: RR21

Sample Profile RR21

3 m+ Fluvial gravel, top not exposed
---------- Contact not exposed
30 cm+ Laminated silt and fine sand
----
45 cm Light brow organic rich silt, numerous small (3 cm diameter) cores taken previously by another investigator.
* RR22 taken 18 cm above the brown silt/grey silt contact
----
70 cm Grey silt and very fine silty sand,

----
1 m+ Inter-bedded medium to coarse sand and silty sand

Samples RR 22 and RR 23, Lab Codes WLL527 and WLL528

Sampled by: RV Rose on 12 July 2004
Location: "Fergusons Pond", South Beach, Greymouth
Elevation: ~ 75 metres
Map & Grid Ref: NZMS 260 J32 N 5450 E 6110
Formation: Karoro Formation (previously mapped and Rutherglen Formation)
Material: Organic rich soil
Depth of Burial: RR22- 3 m; RR23- 4.5 m
IRSL Age: RR 22 84.3 ± 8.7 ka (feldspar from silt in organic rich soil)
RR 23 65.7 ± 5.7 ka (feldspar from silt in soil)
Photos:

Outcrop: The outcrop is part of a face created during 2002/03 for a logging skid site (where harvested logs are hauled for de-limbing and loading out). The exposure was steep and fresh. The site

was sampled for AAR dating in the 1980's by Soons & Lee. At that time there was a "Forestry water supply pond" at the site that was destroyed when the plantation was logged.
Sample RR22 was taken just above the orange banded clay in the top-left photo.

Above: Image of the Fergusons Pond locality

Above: Karoro Formation under discontinuous soil and fluvial gravel at Blue Spur Road. Grid Reference NZMS260 J33 N2920 E4835

Stratigraphic Relationships at Sample Sites RR22, RR23

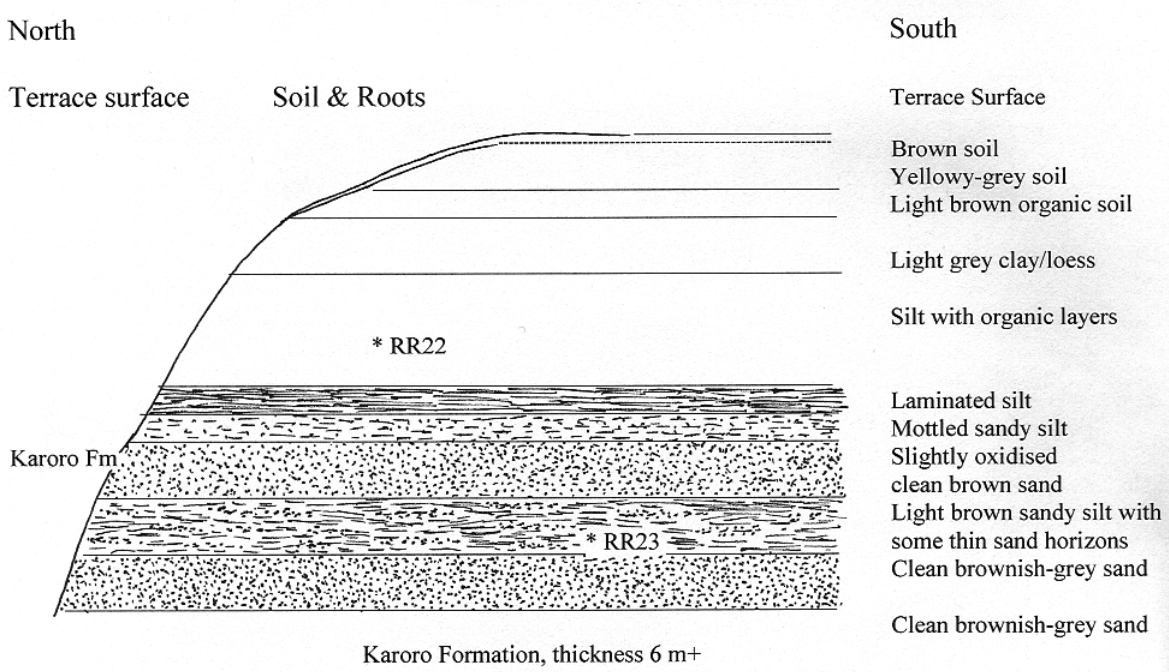

Karoro Formation, thickness 6 m+

Photos above: Sampled Profile RR22, RR23; Karoro Formation coverbeds, Ferguson's Pond. RR23 was taken from the level of the handpiece (top of handle) of the spade in the photo on the lower right.

Profile 1: "Fergusons Pond" at the north (left hand side) end of the face shown in the above photos

Upper 1.5 m not recorded
---
50 cm Light grey silt/clay

---
15 cm Grey silt/clay
25 cm Dark brownish grey silt, organic rich with wood

---
15 cm Grey silt/clay
* RR22 25 cm Dark brownish-grey organic rich soil with wood, darkening towards base
---
---
15 cm Grey silt
30 cm Banded orange/cream clay with minor sand partings
---
25 cm Mottled sandy light brown silty soil
---

45 cm Clean brown slightly oxidized and stained sand
---

* RR23 50 cm Light brown sandy soil
---
20 cm Clean brown sand

---
9 cm Sandy clay
20 cm Clean brownish grey sand

---
7 cm Sandy clay

20 cm+ Grey sand
Base not exposed

Profile 2: Karoro Formation coverbeds, Ferguson's Pond, south end (left side of photos) of the face

Surface
======= Litter
15 cm Organic soil Holocene
---
25 cm Orange-mottled yellowish-brown soil
---
30 cm Organic-rich soil
---

50 cm Light grey soil/silt, loessic, some wood (mainly roots)
---
30 cm Medium grey loessic silt, some wood
---
20 cm Dark grey loessic silt, more wood than immediately above
---
60 cm Medium grey loessic silt, minor wood

--- 13 cm Dark greyish-brown soil/peat, abundant wood
30 cm Grey organic rich silt, some wood
======= 6 cm Dark brownish-grey soil/peat, abundant wood
20 cm Grey organic-rich silt, some wood
---
30 cm Orange, brown & creamy coloured laminated silt/clay (same band as in profile 1)
---
25 cm Mottled silty soil
---
30 cm+ Stained heavy mineral (ilmenite, garnet) bearing sand, probably marine
Base not exposed

Total thickness of exposure ~ 4m

Sample RR 24, Lab Code WLL529

Location: The site is situated immediately adjacent to Chesterfield Road approximately 130 metres SE of the Chesterfield Road EA Road intersection.
Sampled by: RV Rose on 13 July 2004
Elevation: 65 m
Map and Grid Ref: NZMS 260 J32 N 4070 E 5525
Formation: Mapped as Loopline Formation by Suggate & Waight (1999)
Material: The sample is from a hard silt bed situated below the lower organic soil/peat bed and above the fluvioglacial gravel.
Depth of Burial: 0.9 to 1.0 m
Correlation: Previously MIS 4 for the fluvioglacial outwash gravel
IRSL age: 53.8 ± 4.3 ka (feldspar from silt)

Outcrop: The outcrop consists of a cutting into the soil cover on the terrace surface. It is located immediately adjacent to Chesterfield Road.

Photograph:

Sample profile RR24

----------	Holocene soil obscured by bulldozed debris from road widening
----------	
30 cm	Grey loessic silt (Contains Kawakawa tephra at a nearby site described by Mew et al (1986)). Brownish and somewhat organic at the base but decreasingly organic upward
----------	
18 cm	Organic-rich silty soil
----------	6 cm blackish-brown peat
========	2-4 cm very hard iron cement
10-12 cm *	RR24 Brownish sandy silt
----------	
10 m+	Granular sand and sandy gravel

Sample RR 25, Lab Code WLL530

Location: The site is a gravel quarry overlooking the valley of Sunday Creek
Sampled by: RV Rose on 12 July 2004
Elevation: 100 metres
Map & Grid Ref: NZMS 260 J32 N 3890 E 5555
Photo: Yes / No
Formation: Waimea Formation
Material: Silt
Depth of Burial: 3.5 m
Correlation: Previously MIS 6
IRSL Age RR 25: 75.9 ± 7.6 ka (feldspar from silt)
Outcrop: The outcrop is situated in a gravel quarry. Quarrying has produced extensive exposures of the full thickness of the cover beds on the Waimea Formation at this locality.
Profile: Total depth of coverbeds = ~3.6 to 3.8 m

Upper Surface

30 cm	Holocene soil & peat
30 cm	Grey loessic silt
20 cm	Wood bearing brown organic soil, stumps in growth position piercing up into the overlying loess.
30 cm	Brown fluvial gravel, organic rich silty sand in the interstices.
88 cm	Sandy silt/loess, light grey at the base, grading up to light greyish-brown at the top
50 cm	Silty sand with pebble bands grading laterally into cobble gravel
75 cm	Light grey silt/loess
==========	6-8 cm Strongly oxidised silt, vivid reddish, orange and brown colours
30 cm	Carbonaceous silty soil, RR25 taken from the centre of this bed
12 cm	Light-brown silty sand
6 m+	Orange-red oxide stained fluvial gravel, Waimea Formation

Sample RR 26, Lab Code WLL531

Location: Candle Light Gold Workings, Bundi Road, Camerons
Sampled by: RV Rose on 18 July 2004
Elevation: ~ 62 m
Map & Grid Ref: NZMS 260 J32 N 4700 E 5950
Photo: No
Formation: Rutherglen Formation
Material: Laminated silt/clay
Correlation: Previously MIS 5e
Depth of Burial: Now 5 m but originally thicker (8 m) but some cover beds subsequently eroded by fluvial action.
IRSL Age: RR26: 71.7 ± 8.8 ka (feldspar from laminated silt)
Outcrop: In an old sluice face on the western side of an area of 19th century gold workings. The Mined area is a 30 m wide linear trench running NNE-SSW. The trench is situated on the Rutherglen marine strandline (sedimentary environment ideal for concentrating alluvial gold). Situated about 20 m SSW along the sluice face from RR27.

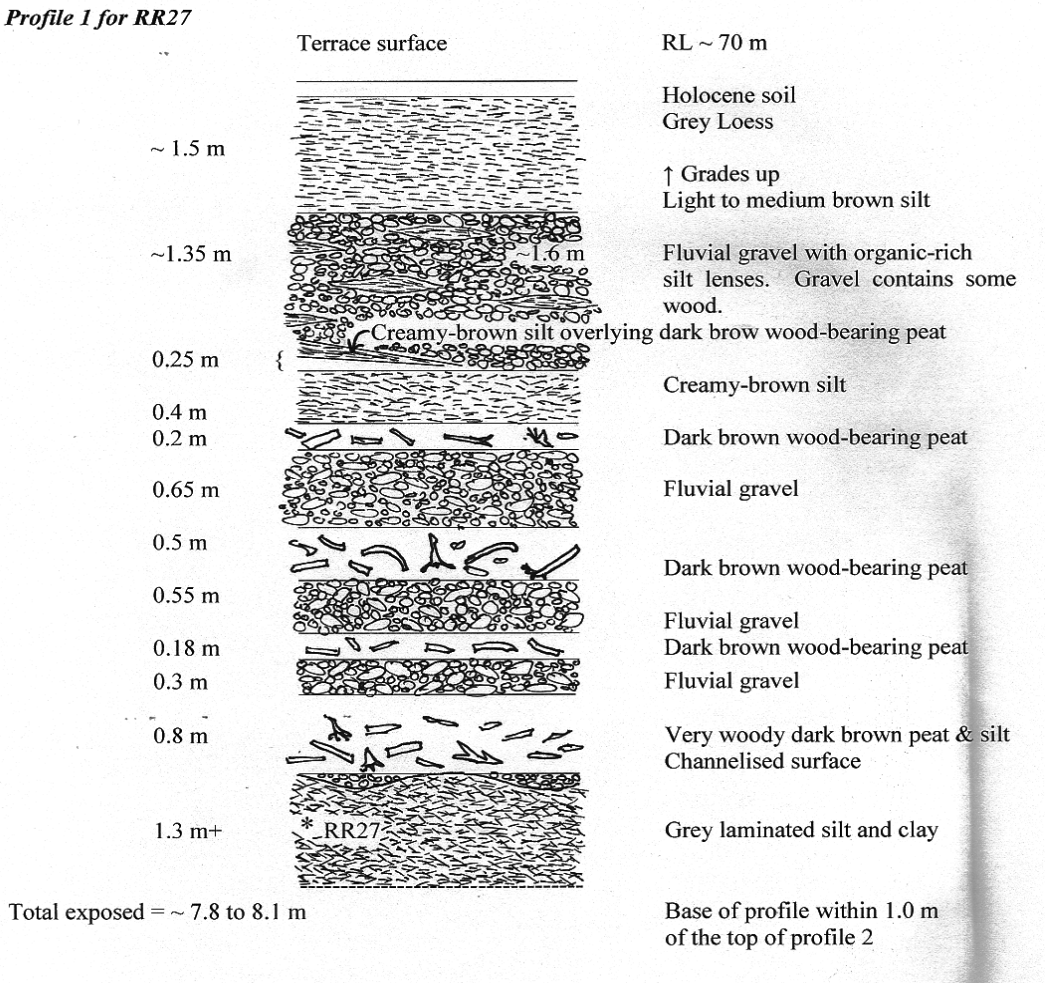

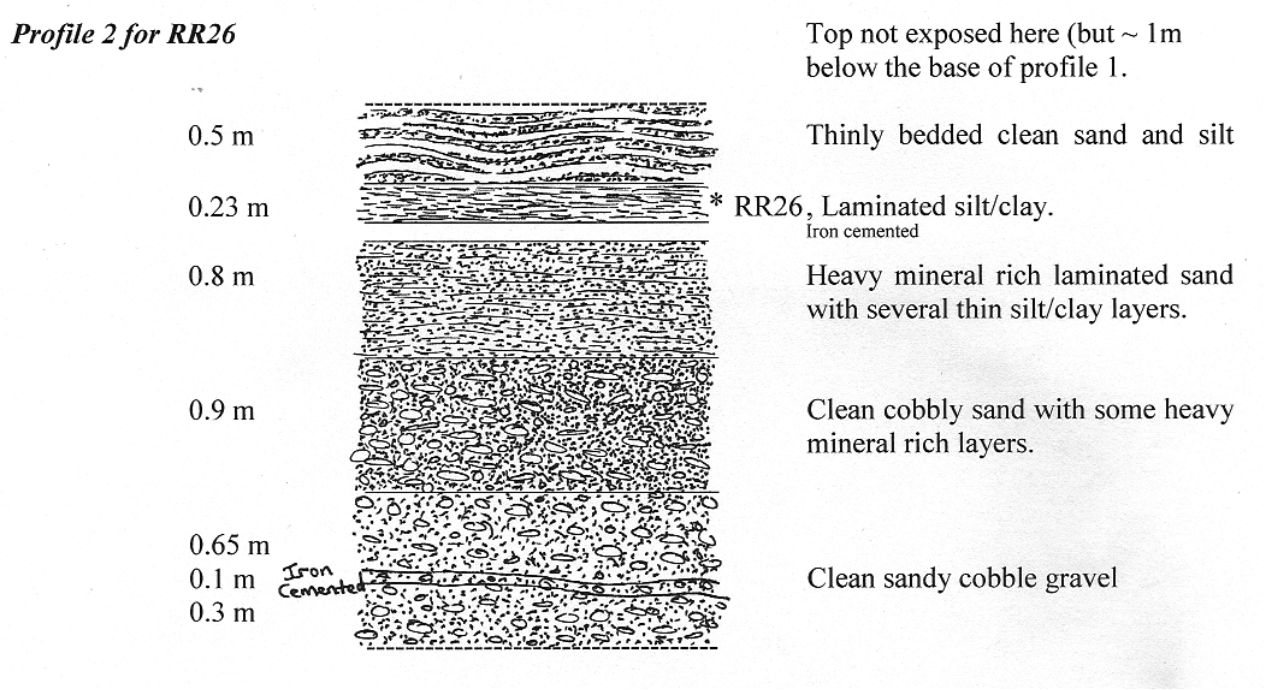

Sample RR 27, Lab Code WLL532

Location: Candle Light gold workings, Bundi Road, Camerons
Sample by: RV Rose on 18 July 2004
Elevation: ~ 62 to 64 m
Map & Grid Ref: NZMS 260 J32 N 4710 E 5950
Photo: No
Formation: Rutherglen Formation
Material: Laminated silt/clay
Depth of Burial: 6.5 – 7.5 m
Correlation: Previously MIS 5e
IRSL Age: RR27: 96.5 ± 10.2 (silt)
Outcrop: In an old sluice face on the western side of the old gold workings. The workings are in a linear trench running NNE-SSW. The trench is about 30 m wide and is situated on the Rutherglen marine strandline (ideal alluvial gold concentrating sedimentary environment). RR27 is stratigraphically above RR26.

Profile 1 for RR27

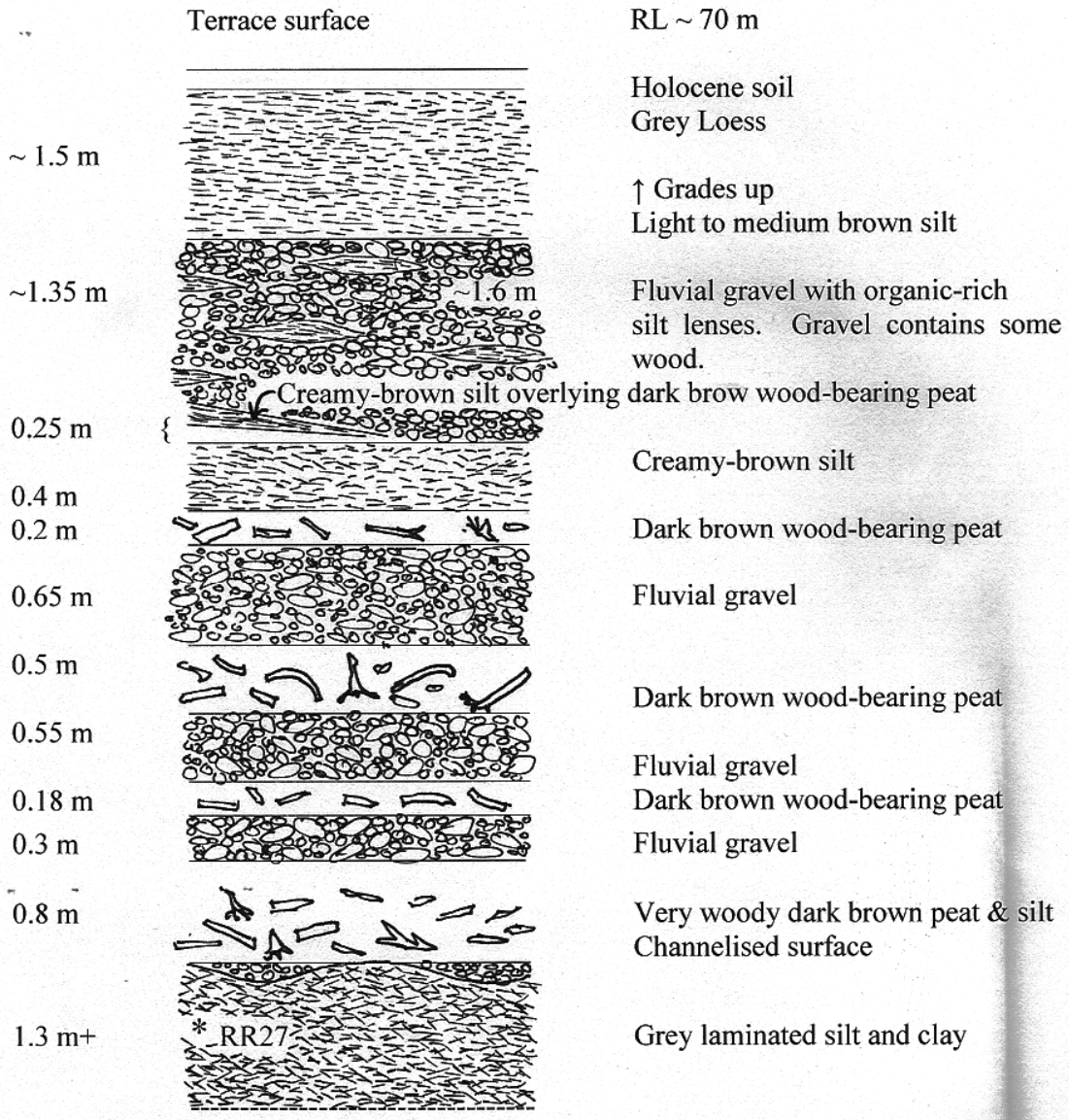

Stratigraphic Relationships at Sample Sites RR26 & RR27

The two IRSL samples were taken from an upright face in an old alluvial goldmine at Candlelight. Samples have been taken for pollen analysis from essentially the same mine and the results are reported in Moar & Suggate (1996). The results are summarised in figure 6.12 (Chapter 6). The stratigraphy reported by Moar & Suggate is somewhat oversimplified. In their figure 3 they illustrate a coverbed sequence over the Rutherglen Formation marine sand that is composed entirely of silt/clay, peat, and

loess. RR26 and RR27 come from what is essentially the same part of the mine face. These two samples are separated by about 20 m. In each case the maximum accessible depth of the face was cleaned back to reveal the Quaternary strata within.

The marine portion of the Rutherglen Formation commences just beneath RR26. The immediately overlying silt and clay is likely the same age as the heavy mineral bearing marine sand and gravel. From the nature of the old gold workings, the base of which are full of bouldery tailings and exotic forestry spoil, the marine sequence extends several metres below the base of this profile. RR26 is situated about 1.5 m below the base of profile 1, and about 2.5 m below RR27.

Sample RR 28, Lab Code WLL533

Location: On a vehicle track (access to electricity transmission lines) off Loopline Road, near above Kapitea Reservoir. The site is about 250 metres north of Loopline Road along the track.
Sampled by: RV Rose on 19 September 2004
Elevation: ~ 165 metres
Map Ref: NZMS 260 J32 N 3370 E 6165
Photo: No
Formation: Loopline Formation
Material: Laminated silt of proximal glacial origin taken from immediately below a buried peat bed and immediately above coarse glacial till.
Depth of Burial: < 2 m
Correlation: Previously MIS 4
IRSL Age: RR28: 78.1 ± 6.8 ka (silt)

Outcrop: The outcrop is a road cutting adjacent to a 4wd vehicle track. The track was formed in the late 1990's to service what was then a new electricity transmission line. The locality contains numerous exposures of glacial till and surficial fluvioglacial deposits. The exposure that was sampled was selected on the basis of the presence of a well defined peat layer and the clear stratigraphic relations between the peat and the other strata at the site. The coverbed sequence is situated on till mapped as Loopline Formation adjacent to the Kapitea Reservoir. Cosmogenic isotope dating (this project) from nearby indicates that this site was probably over-riden by glacial ice during deposition of the Larrikins(1) Formation at c. 22 ka. The profile is situated a few hundred metres to the north of Loopline Road. The sample site is located about 10 m below the crest of the "Loopline/Larrikins" moraine on the up-valley side overlooking Kapitea Reservoir.

The coverbed sequence at the site of RR28 is:

	Surface
----------	
40 cm	Humus/peat
----------	
20 cm	Grey loessic silt

10-30 cm	Rich-brown peat/organic silt containing tree stumps in growth position
----------	iron pan variably developed at this contact
30 cm	Clean sand grading laterally to fluvial gravel
----------	iron pan variably developed at this contact
30 cm	Very hard light-brown laminated silt/loess RR28 was taken from centre of this unit Grades laterally to fluvial gravel
----------	
$1m^{+}$	Grey glacial till of unknown age
	Total coverbed thickness = 1.4 m

The IRSL age for RR28 is 78.1 ± 6.8 ka (silt). This is significantly older than expected which raises the possibility that the very hard laminated silt and underlying glacial till could be a remnant of the Waimea Formation rather than of the Loopline Formation. The sample age is not clearly distinguishable from that of RR25 (75.9 ± 7.6 ka) from the Waimea Formation near Sunday Creek and or from that of RR29 (84.9 ± 7.2 ka) taken at Blakes Terrace.

Stratigraphic Relationships at Sample Site RR28

East sloping surface leading down from a moraine crest to the shore of the Kapitea Reservoir

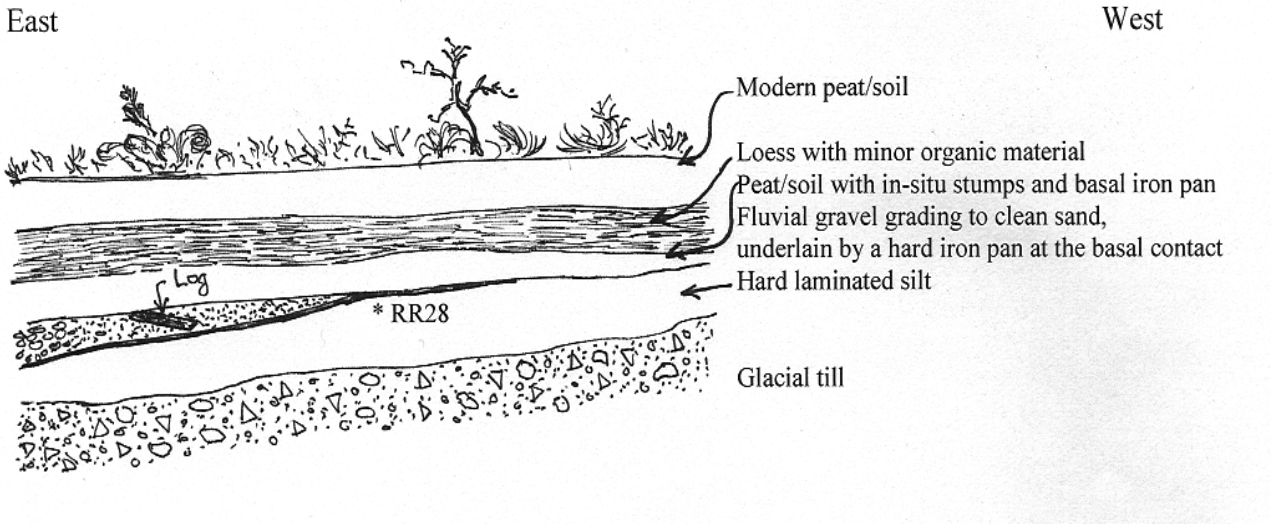

Sample RR 29, Lab Code WLL534

Location: Blakes Terrace, Awatuna
Sampled by: RV Rose on 10 October 2004
Elevation: ~18-22 metres a.m.s.l.
Map & Grid Ref: NZMS 260 J32 N 4005 E 5220
Photo: No
Formation: Buried Pre-Loopline fine grained unit
Material: Silty fine to medium sand
Depth of Burial: ~ 10 m
Correlation: Previously MIS 4
IRSL Age: RR 29: 84.9 ± 7.2 ka (feldspar from soil / loess)
Outcrop: Thick (1.3 to 2 m) bed of fine fluvial silty sand exposed in a road cutting. The cutting is adjacent to a steep metaled road situated on the Holocene sea cliff near Awatuna. The road leads from the innermost Holocene strandline to the surface of a terrace underlain by the Loopline Formation at an elevation of ~ 35 metres. The location is near to and just northeast of Awatuna, on the east side of SH6 and the Greymouth-Hokitika Railway. The sampled material is situated approximately 15 -18 m below the surface of the terrace. The silty bed is situated immediately above a 0.3 to 0.5 m thick bouldery lag deposit that has an erosional base on finer-grained gravel. The silt is overlain and underlain by fluvial gravel.
Profile:

	Terrace surface at ~ 35 m elevation

15-18 m	Fluvial cobble to boulder gravel, cobbles generally 10-20 cm diameter
=======	Iron cemented erosional contact
	Grey, largely massive silty sand with occasional pebble bands
130 cm	
----------*	RR29 15 cm above contact
	Fluvial cobble gravel, most of the cobbles < 10 cm diameter

Stratigraphic Relationships at Sample Site RR29

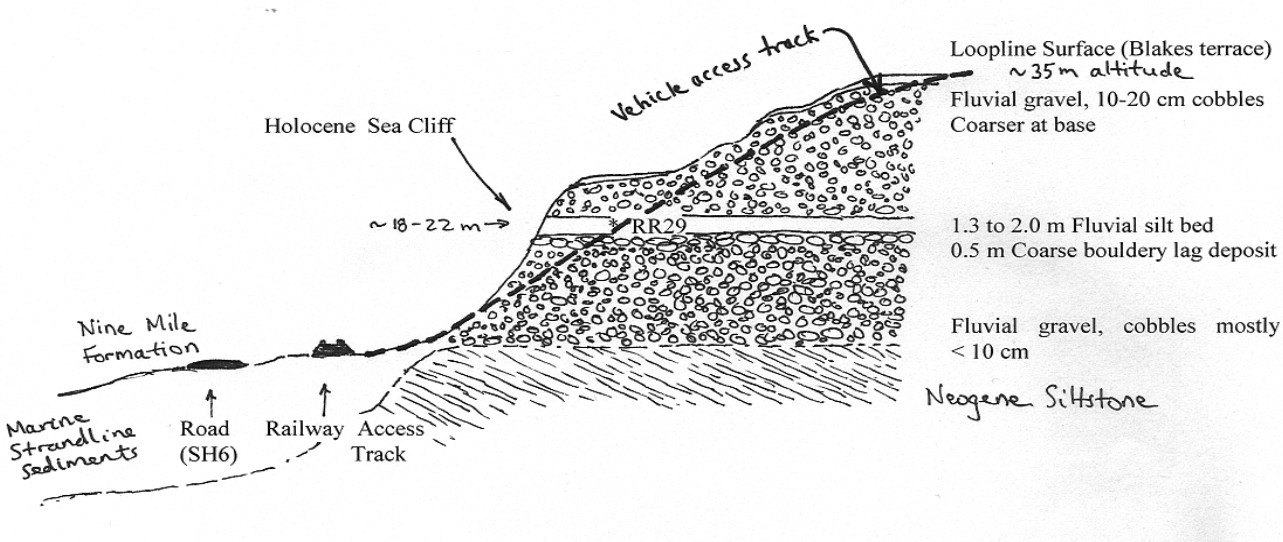

Sample RR 30, Lab Code WLL535

Location: Blakes Terrace (Blake Formation)
Sampled by: RV Rose on 10 October 2004
Elevation: ~ 44 metres a.m.s.l.
Map & Grid Ref: NZMS 260 J32 N 4005 E 5275
Formation: Blake Formation
Material: Soil on marine sand
Depth of Burial: < 2 m
Correlation: Previously MIS 4 when the terrace was though to be fluvial
IRSL Age: RR30: 63.6 ± 7.4 ka (feldspar from soil / loess)
Outcrop: Sampled from near the base of a soil outcrop of the edge of a bulldozed track across the terrace surface. Track dozed to the full depth of the soil but not below.

Profiles at the RR30 sample site on Blakes Terrace

Three profiles were measured at this locality, two on the Blake Formation (profiles 1 and 2) and one on the Loopline Formation (profile 3). Profiles one and two were taken from exposures either side of a bulldozed track on top of the terrace. Profile three was taken from the side of the same track about 50 metres to the north.

The cover-bed sequence at **profile 1** which is situated on the Blake Formation is:

	Surface	

	Spoil (from dozer blade). Surficial Holocene organic deposits removed during formation of track.	
---		
30 cm	Medium grey loessic silt	Larrikins?
---		
30 cm	Light greyish-brown silt, abundant wood and roots	
---		
25 cm	Dark-brown organic silt, abundant woo d and roots	Pre Larrikins
---		
13 cm * RR30	Peat and very-dark brown organic silt. RR30 (63.6±7.4)	Pre Larrikins
---		
13 cm	Grey silty sand	
---		
40 cm^{+}	Fine-Medium ilmenite bearing grey-brown sand. No stones, pebbles, or granules	Blake

Cover-bed thickness at profile 1 = ~ 1.1 m. This excludes any Holocene peat or organic silt that may have been present. The dating method for sample RR30 is IRSL.

The cover-bed sequence at **profile 2** (opposite side of track to profile 1 and also on the Blake Formation) is:

	Surface	
10 to 20 cm	Peat	Holocene
10 cm	Brown organic silt	Holocene?
30 cm	Light-grey loessic silt	Larrikins?
15 cm	Light brown silt	Loopline?
30 cm	Mixed peat and brown organic rich silt, wood bearing	Pre-Loopline?
	~~? abrupt contact defined by thin iron oxide zone	
10 cm	Grey coarse fluvial sand.	
	~~?	
40 cm+	Very hard orange-brown iron-oxide-cemented sand	Blake

Cover-bed thickness at profile 2 = ~ 1.0 m.

The cover-bed sequence at **profile 3** situated on fluvioglacial gravel assumed to be Loopline Formation is:

	Surface	
50^{+} cm	Debris churned by dozer blade	
33^{+} cm	Peat and wood bearing silt	Holocene
15-20 cm	Grey to brownish-grey loessic silt, some small wood fragments	Larrikins?
20 cm	Woody peat and dark brown organic silt	
15 cm	Light brown silt	
20 to 25 cm	Wood bearing brown organic silt Abundant wood at base	
0 to 15 cm	Coarse to granular sand with a few pebbles (lensoidal sandy pockets, potential unconformity)	
26 cm	Brown organic silt, some wood, alternating sandy and less sandy layers	
3 to 7 cm	Grey loessic silt	
6 to 7 cm	Very woody dark brown peat and organic silt	
15 cm	Brownish-grey sandy silt, some wood	

c. 2 metres	Fluvial gravel	Loopline
> 2 metres	Marine sand	Blake

Cover-bed thickness at profile 3 = ~ 1.7 m.

The marine sand was not observed at this profile. It is interpreted from nearby exposures that indicate a shallowing in the thickness of the Loopline gravel between this site and profiles 1 and 2 about 50 metres to the south.

The cover-beds at profile 3 include 4 peaty layers, which is more than is typically observed on the Loopline Formation. In addition the total thickness of the cover-beds is greater than is normally observed on the Loopline Formation. The Loopline Formation has an unconformable contact with the Blake Formation at this locality. The relationship is exposed in the base of the bulldozer track at a point between profiles 1 and 3.

The cover bed sequence at profile 3 significantly thicker than that at profiles 1 &2. The alluvial sand bed in profile 2 almost certainly represents an erosional unconformity. So it can not be assumed that the coverbeds on the Blake Formation at profiles 1 & 2 represent the full depositional history for the locality.

Profile 3 contains a coverbed sequence that is much thicker than at any Loopline site previously sampled for pollen analysis. It represents a potential opportunity for gaining a much more detailed climate history than that revealed from other Otiran sites.

Stratigraphic Relationships at Sample Sites RR30 & RR31

RR30 Profile 1

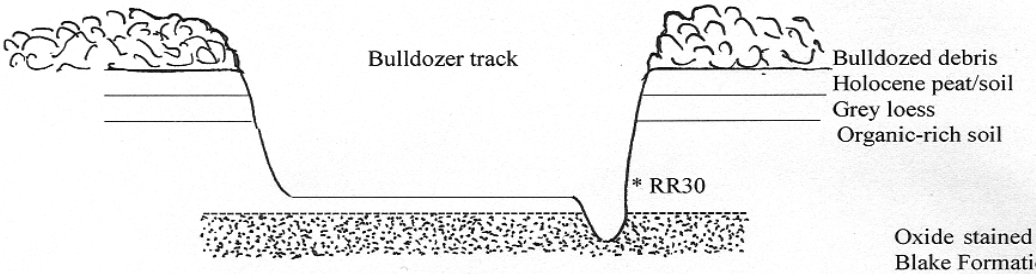

Total soil thickness approx 1.15 m

RR30 Profile 2 *(~ 50 m north of profile 1)*

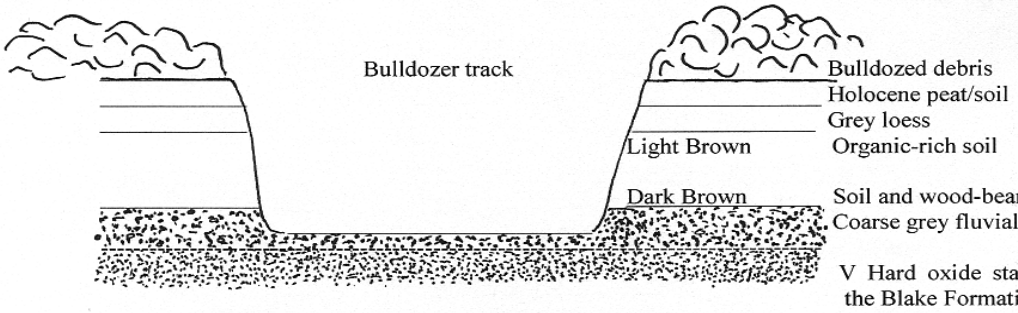

Total soil & fluvial sand thickness approx 1.0 m

RR30 Profile 3 *(~ 100 m north of profile 1)*

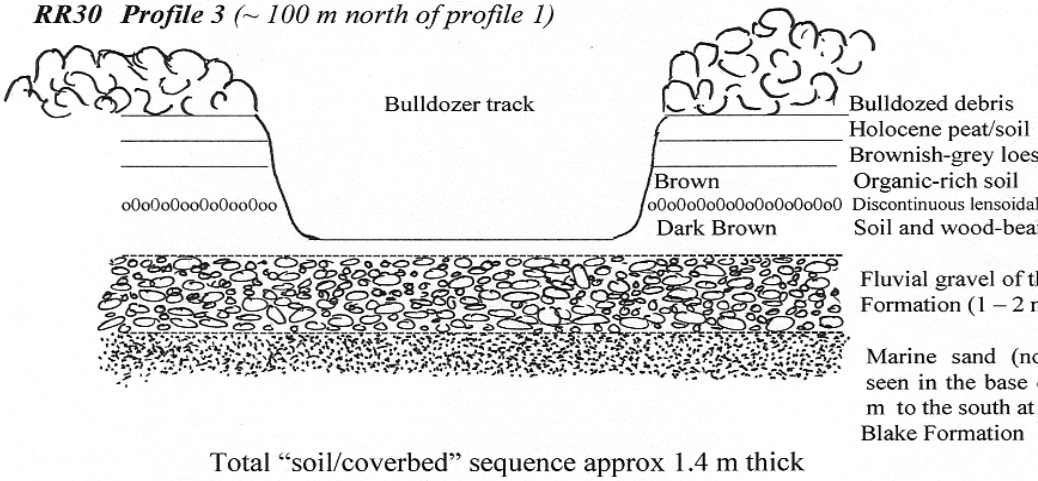

Total "soil/coverbed" sequence approx 1.4 m thick

Sample RR 33, Lab Code WLL536

Location: Tasman View Subdivision, South Beach, Greymouth
Sampled by: RV Rose
Date: 24 July 2005
Elevation: Surface ~ 65-68 metres a.m.s.l.
Map & Grid Ref: NZMS 260 J32 N 5490 E 6065
Formation: Rutherglen Formation
Material: Organic rich soil
Depth of Burial: 1 to 1.2 metres
Correlation: Previously MIS 5e
IRSL Age: RR33: 56.3 ± 7.1 ka (feldspar from soil / loess)
Outcrop: Full profile through the soil that overlies the marine sand of the Rutherglen Formation. Outcrop in a drain along side the Subdivision access road.

Photo of RR33:

Profile at RR33:

----------	Surface
60 cm	Brown soil, increasingly organic towards the surface
----------	
35 cm	Grey loessic soil, minimal organic content
----------	
20 to 30 cm	Dark-brown organic soil/peat

----------	15 cm Brown sand, substantial organic content
25 cm	Clean light-brown medium sand
=======	2-3 cm iron cemented sand

35 cm+ Clean light greyish-brown medium sand

Sample RR 34, Lab Code WLL537

Location: Tasman View Subdivision
Sampled by: RV Rose on 24 July 2005
Elevation: Surface ~ 72-75 metres a.m.s.l.
Map & Gris Ref: NZMS 260 J32 N 5490 E 6095
Formation: Karoro Formation
Material: Organic rich soil
Depth of Burial: 1 to 1.2 metres
Correlation: Previously MIS 7/5e
IRSL Age: RR34: 92.5 ± 9.4 ka (feldspar from soil / loess)
Outcrop: Full profile through the soil that overlies marine sand of the Rutherglen Formation. Outcrop in a drain beside the road through the Tasman View Subdivision. On downsteam side of culvert, in drain oriented normal to the road.
Photo:

Profile at RR34

	Surface
========	
100 cm	Brown peaty soil with abundant wood

30-40 cm	Yellow-grey loessic silt with occasional wood

15-20 cm	Friable dark-brown peat
----------	
50 cm	Grey loessic silt with occasional wood
----------	
30 cm *RR34	Dark brownish-grey organic soil

	Clean brownish-grey marine sand, some stained and cemented horizons
	Base not exposed

APPENDIX TWO: LOCATION OF LUMINESCENCE SAMPLE SITES AND OTHER KEY SITES IN NORTH WESTLAND

Satellite Image One: Phelps Mine and Pine Creek, Southside, Hokitika

Luminescence Samples RR1, RR2, RR3, RR4, RR5

Satellite Image Two: Chesterfield Road, Chesterfield

Luminescence Samples RR7, RR8, RR9, RR24

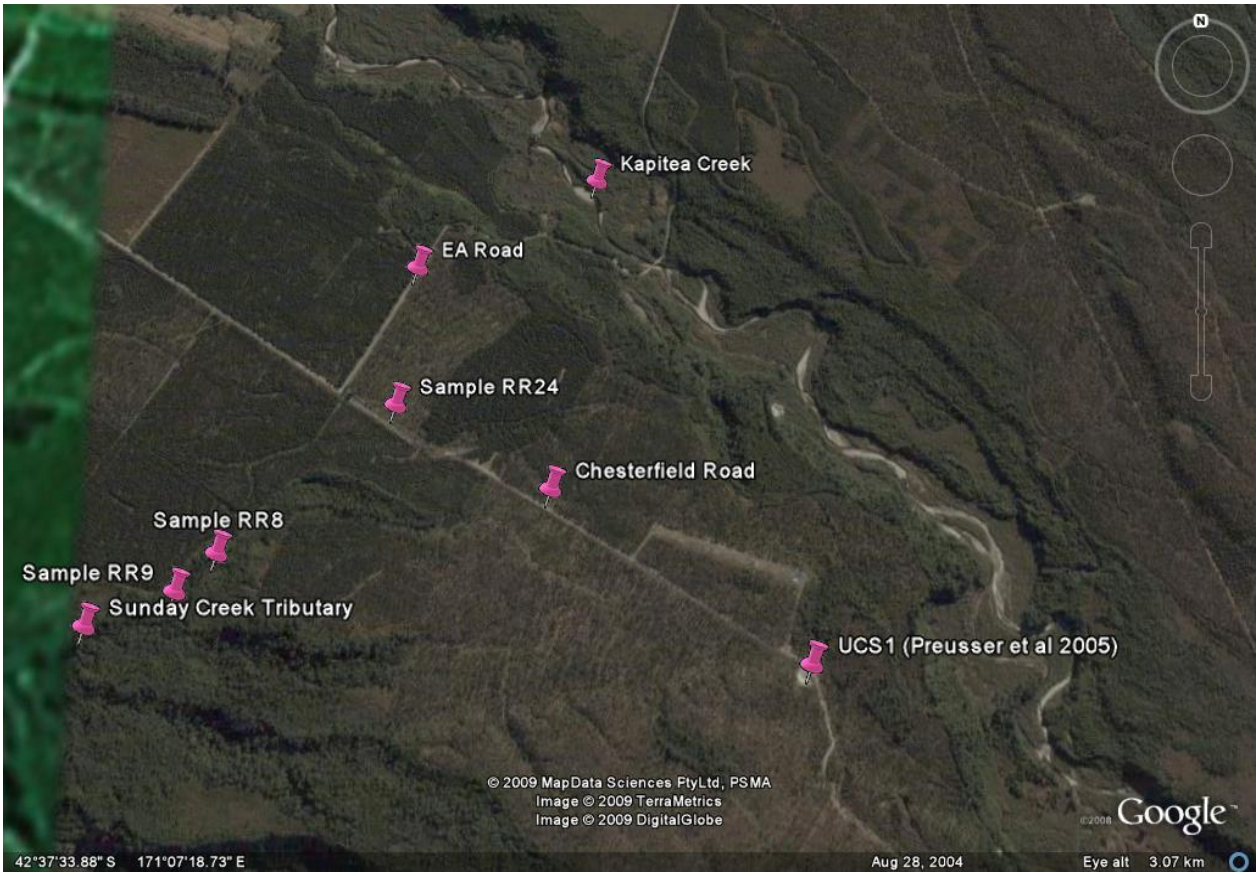

Satellite Image 3: North Beach-Point Elizabeth Area

Luminescence Samples RR10, RR11, RR12, RR13, RR19

Satellite Image 4: Tasman View Subdivision and Ferguson's Pond Area

Luminescence Samples RR14, RR15, RR16, RR22, RR23, RR33, RR34

Satellite Image 5: Power Road & Ferguson's Driveway, Karoro

Luminescence Samples RR17, RR18

Satellite Image 6: Schulz Creek area, State Highway 6, Greigs

Luminescence Sample RR20

Satellite Image 7: State Highway 7, Kamaka, Grey Valley

Luminescence Sample RR21

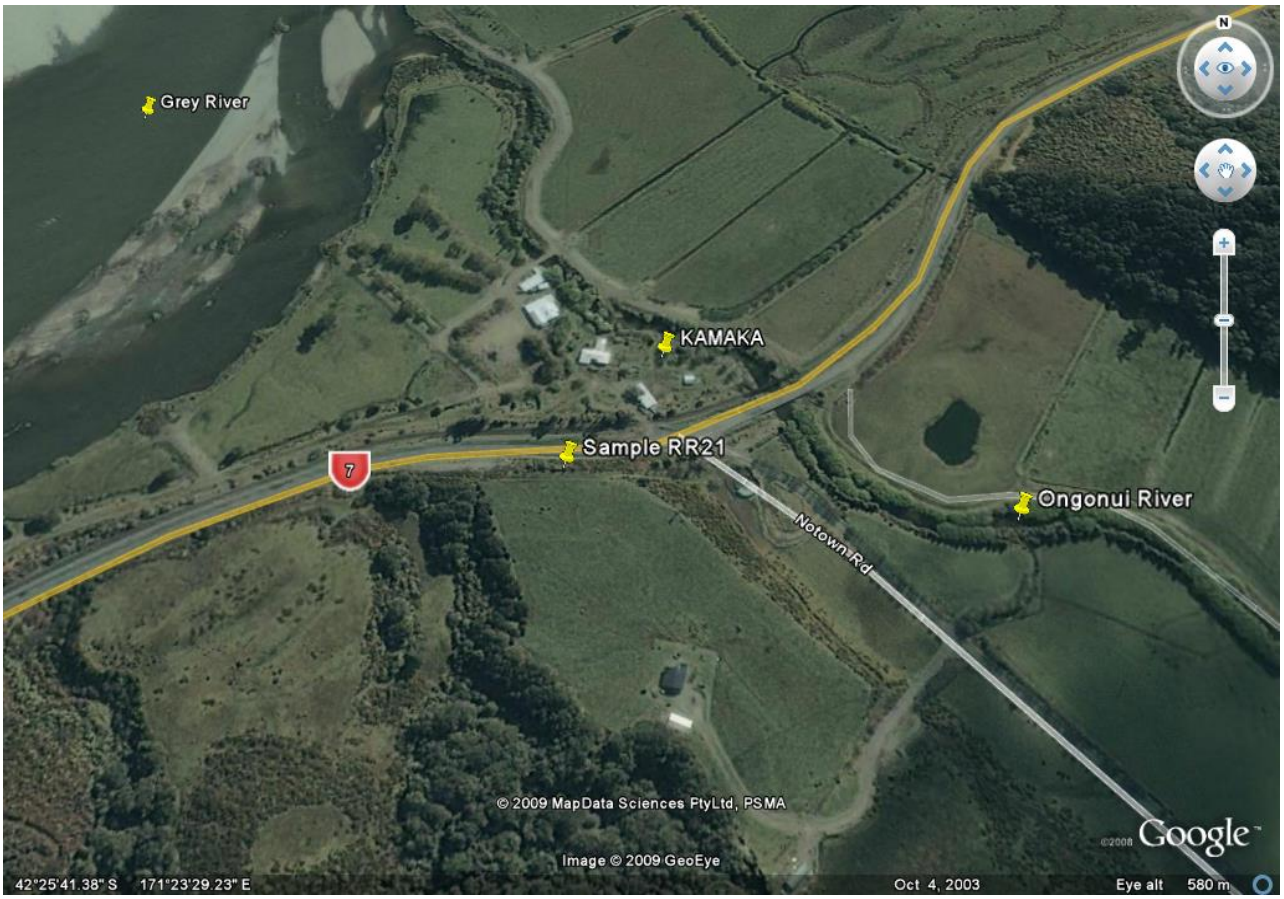

Satellite Image 8: Sunday Creek, Awatuna

Luminescence Sample RR25 (Waimea Formation)

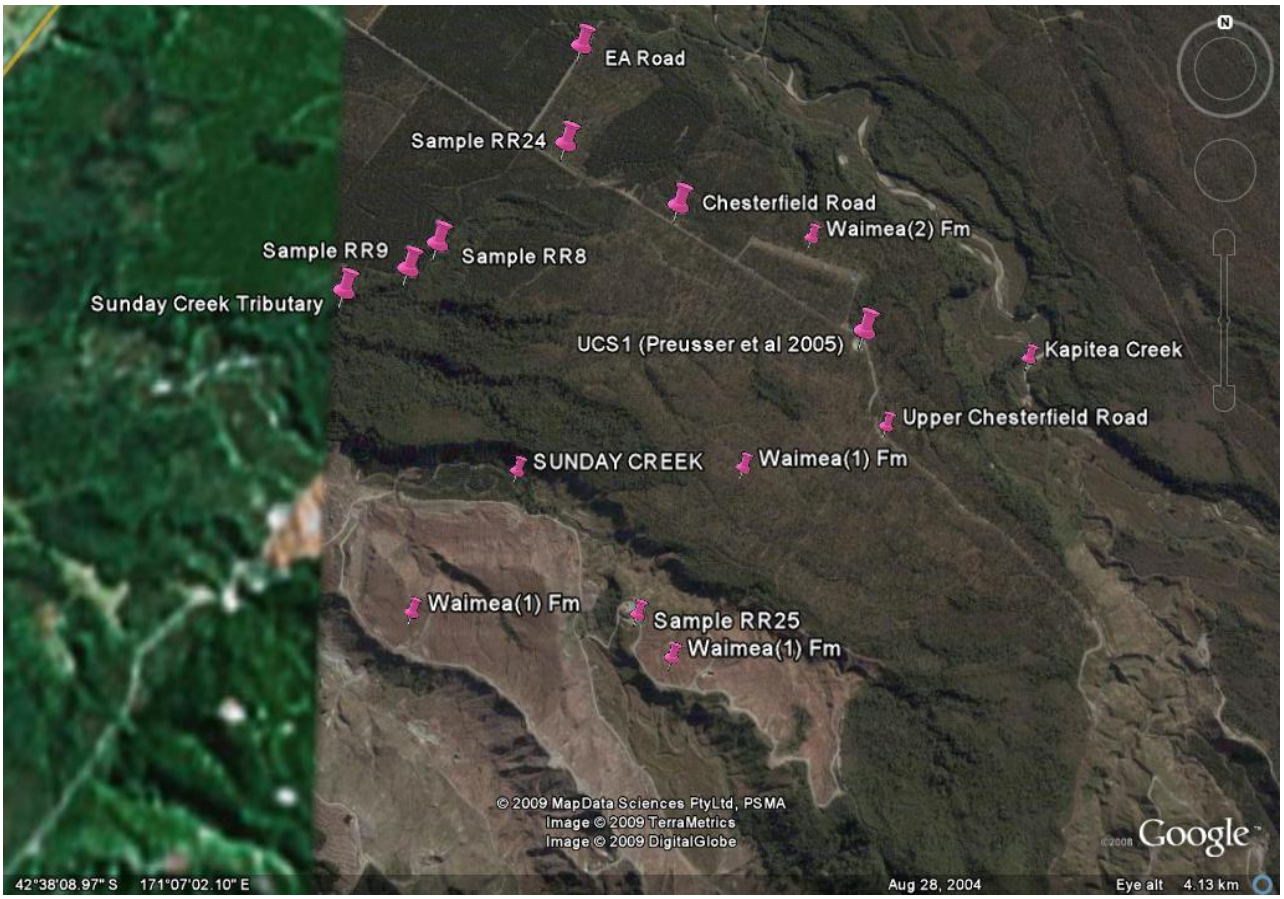

Satellite Image 9: Candle Light Area, Camerons.

Luminescence Samples RR27, RR27

Satellite Image 10: Kapitea Reservoir- Stafford Loop Road- Dillmanstown Area

Luminescence Sample RR28

Satellite Image 11: Awatuna and Blakes Terrace Areas

Luminescence Samples RR29, RR30

Satellite Image 12: Hokitika Gravel Quarry and Blue Spur Area

Satellite Image 13: Nelson Creek Quarry and Grahams Terrace Areas

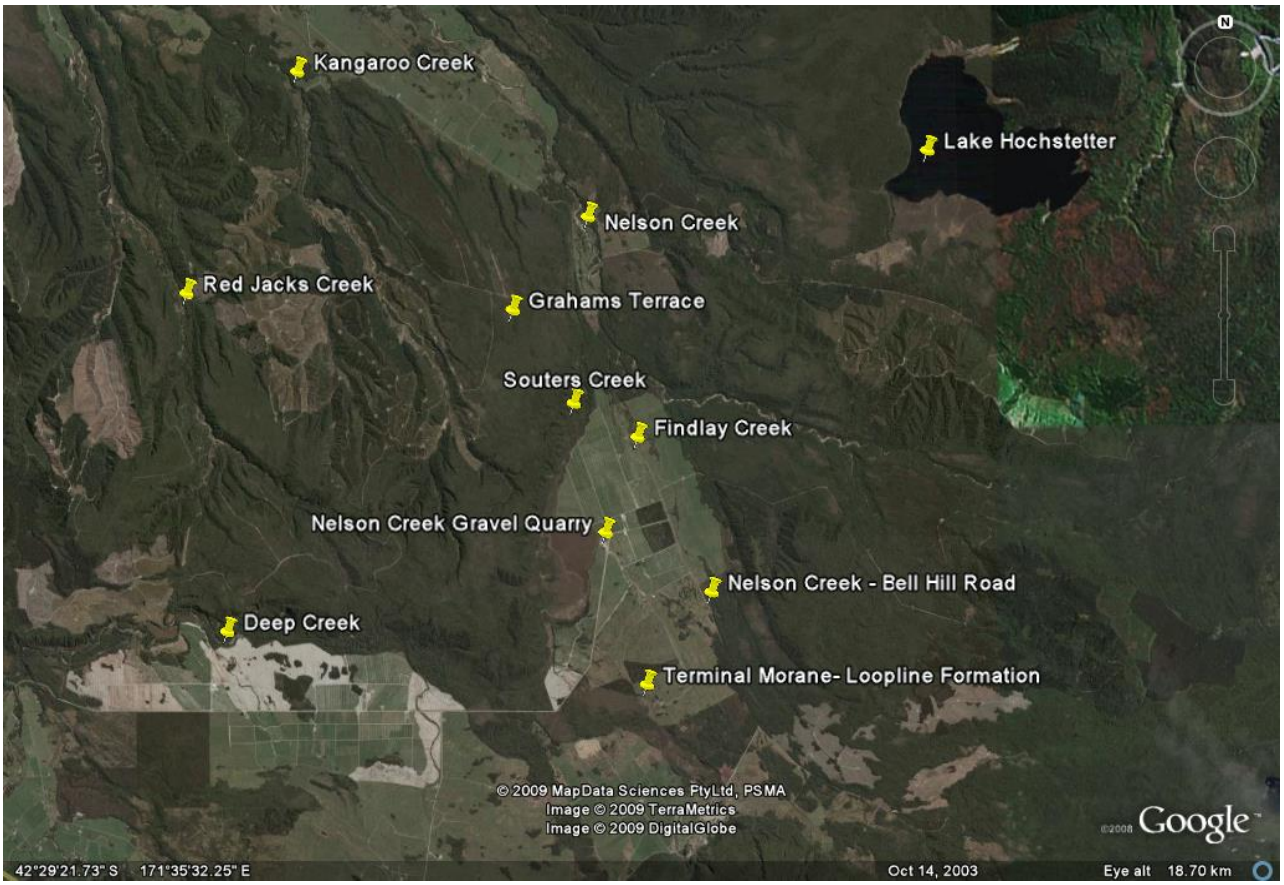

Satellite Image 14: Raupo Gravel Quarry, State Highway 7, Grey Valley.

APPENDIX THREE: SELECTED SOIL PROFILES

Profile A: Soil Sequence, Access Track / Historic Gold Sluicing Claim, adjacent to Callaghans Road.
Profile B: Soil Sequence, Active Opencast Goldmine adjacent to Callaghans Road.
Profile C: Gravel Quarry, Adjacent to the Stafford Loop Road / Callaghans Road Intersection.
Profile D: Exotic Forestry Track off Stafford Loop Road
Profile E: Kumara Cemetery Road
Profile F: Kumara Cemetery Road
Profile G: Electricity Transmission Track, Kapitea Reservoir
Profile H: Gravel Quarry close to Stafford Loop Road/Loopline Road Intersection
Profile I: Blakes Terrace, Awatuna

Profile A: Soil Sequence, Access Track / Historic Gold Sluicing Claim, adjacent to Callaghans Road.

Grid ref J32 3440 N 5850 E

Measured: 24/5/09

Numerical age: No samples at this site.

Correlation: Waimea(2) Formation.

The site is mapped as Waimean terminal moraine by Suggate & Waight (1999). The area had just been logged (pinus radiata) and replanted prior to inspection of the soil profile. The geomorphology is suggestive of the site being a fluvial terrace. The terrace is situated about 10-12 m lower than that at Profile B (also adjacent to Callaghans Road). Given that the profile is at the top of a face originally created by historic opencast gold-sluicing. Given the nature of the uppermost 5 m of gravel in the face this terrace is almost certainly composed of bouldery fluvioglacial outwash rather than till (glacial till has never been a mining target here unless it rests on older gold bearing fluvial gravel). So the uppermost gravel is fluvial and the surface is not a moraine.

The site is in an old opencast mine excavated below the surface of the Waimea(2) Formation. Soil is present at the ground surface. This soil rests on coarse bouldery granite-rich iron-stained gravel. The terrace surface has a significant slope eastward toward Kapitea Creek. So it might not be ideal for the long-term preservation of soil deposits.

The exposure is in a cutting on the side of a 4WD track that leads down off Callaghans Road into an old opencast gold sluicing claim.

The soil sequence is:

Spoil	Upper portion disturbed by forestry activity

> 20 cm	Organic silt, roots, stumps
---	
50 cm	Grey loessic silt

10-15 cm	Dark brown organic-rich slit
---	
15 cm	Light-medium brown silt
---	
5 m+	Iron cemented bouldery fluvial gavel
	Total coverbed thickness = 1 m

Profile B: Soil Sequence, Active Opencast Goldmine adjacent to Callaghans Road.

Grid ref J32 3600 N 5975 E

Measured: 24/5/09

Numerical age: No samples at this site.

Correlation: Waimea(1) Formation.

Probably situated close to the glacial terminus. No glacial till was observed at the site even though this site is at the terminal position mapped by Suggate & Waight (1999). The site is a dissected fluvial terrace rather than a moraine.

The sample site was part of an opencast alluvial goldmine. When sampled the active mine pit was situated about 50 to 70 metres east of Callaghans Road. The soil profile will be destroyed as part of the mining operation before the PhD thesis is accepted. This deep exposure is only available as a result of the activity of the mining permit holder. An opportunity was taken to measure the profile at one of the opencut faces in the goldmine before the soil stripping process was undertaken to expose the next block of gold bearing fluvial gravel.

The highly organic soil sequence is unusually deep at this site. The site appears to have been favourable to rapid soil formation and preservation. It is situated near the foot of Italians Hill and may have received substantial fluvial sediment input from streams draining eastward off the hill. The fluvioglacial gravel under the soil sequence is extremely bouldery. Several boulders were noted with dimensions of up to 1.5 x 1.5 x 1 m. The gravel is fluvioglacial outwash transported by a large vigorous meltwater flow.

In the active mine pit the soil profile was exposed over a length of about 30 to 40 metres. Some of the horizons were continuous over the length of the face. The sequence includes beds of pebble and cobble conglomerate that represent old stream beds. There are channels backfilled by silt as well.

Measurement of the full profile required that it be split into 3 parts (B1, B2, B3) as the face was too high and steep to record the details in one continuous segment. The total thickness of the cover beds at this location is from 6 to 7 metres. This is much thicker than at any site previously sampled for pollen

analysis and represents a potential opportunity for gaining a much more detailed climate history than that revealed from other Waimean sites.

Profile B1, total thickness ~ 4 m.

----------	Surface
20 cm	Organic soil

10-20 cm	Grey Silt
----------	
30 cm	Brown sandy silt

0-20 cm	Grey silt

20-30 cm	Brown peat with roots and stumps, rather gravelly

1.2 m	Sandy pebble conglomerate

----------	5 cm grey silt
----------	15 cm med-brown silt
20 cm	Dark brown silt

15-20 cm	Gravel
----------	
50 cm	Dark brown silt
----------	
20 cm	Roots and stumps (old forest floor)

	Bouldery gravel

Profile B2, total thickness ~ 4.3 m about 15 m along the mine face from profile B1.

----------	Surface
50 cm	Brown organic silt

----------	20 cm Highly organic pebbly conglomerate
50 cm	Light brown sandy silt
----------	
50 cm	Light to medium grey silt
----------	
50 cm	Brown silt with fine roots

----------	15 cm Banded grey and brown silt
45 cm	Light to medium grey silt
---------	
20 cm	Brown silty peat, abundant fine roots
---------	
60 cm	Greyish-brown silt
=====	10 cm blackish-brown peat
60 cm	Bouldery gravel with a matrix of brown sand and soil, abundant roots up to 3 cm thick
----------	
6 m+	Coarse bouldery gold-bearing gravel with no significant organic content

Profile B3

Profile B3 is situated about 10 m further along the mine face from profile B2. Profile B3 represents a lateral variation of the highly organic bouldery gravel near the base of profile B2.

=======	Black peat
0.5 m	Dark-brown organic rich sandy pebble conglomerate

0.6 m	Medium-brown organic rich pebbly silt
----------	
6 m+	Coarse bouldery gold-bearing gravel

Profile C: Gravel Quarry, Adjacent to the Stafford Loop Road / Callaghans Road Intersection.

Grid ref J32 3410 N 5990 E

Measured: 24/5/09

Numerical age: No samples at this site.

Correlation: The site is assumed to be Loopline Formation as mapped by Suggate and Waight (1999). There is no evidence that this site has been overwhelmed by fluvioglacial outwash of the Larrikins Formation (which distinguishes this site from Profile D and from Profile H).
The site is in a gravel quarry excavated below the surface of the Loopline Formation. The site is situated between the two upper branches of Kapitea Creek. At this site there is no cover of Larrikins gravel across the Loopline surface. The Loopline soil is present at the ground surface. This soil rests on coarse bouldery granite rich iron stained gravel. The upper 2 to 3 metres of the gravel appears to be a lag deposit, iron stained in the upper half to two thirds. It overlies 3 m^+ of grey granite rich cobble gravel.

The soil sequence is:

Spoil		
----------		
20 cm	Dark brown organic silt with abundant roots (Larrikins Soil?)	

5-10 cm	Grey silt	(Larrikins loess?)

35-40 cm	Medium brown silt	(Loopline Soil?)
----------		
20 cm	Grey silt	
----------		
5 cm	Heavily iron cemented pan	

0.6 m^+	Heavily iron stained bouldery granite-rich gravel	(Loopline gravel?)

Total coverbeds = 0.95 m

If the stratigraphic correlation is correct then the medium brown silt at about 0.3 to 0.7 m depth is probably equivalent to the Chesterfield interstadial.

Profile D: Exotic Forestry Track off Stafford Loop Road

Grid ref J32 3600 N 6050 E

Measured: 24/5/09

Numerical age: No samples at this site.

Correlation: The site is mapped as Loopline Formation by Suggate and Waight (1999). However the uppermost pebble conglomerate and overlying soil is probably Larrikins Formation, overlying Loopline soil and gravel.

This soil sequence is preserved in a shallow cutting adjacent to an exotic forestry track. The site is at the end of the track where is track widens out to a logging skid site. This site is about 700 m down the track from the starting point at Stafford Loop Road. The sequence is:

Spoil	(disturbed by earth-moving machinery)	
25 cm	Brown organic soil, abundant roots and stumps	Holocene
20 cm	Reddish-brown greywacke pebble conglomerate	Larrikins(1) Gravel
10 cm	Light brown greywacke pebble conglomerate	
30-35 cm	Grey laminated sandy silt and silty sand	Early Larrikins loess?
5-10 cm	Light brown silt	
30 cm	Medium to dark brown organic silt	Chesterfield-Interstadial?
0-10 cm	Grey silt	Loopline Loess
50 cm plus	Light brown sandy granite-rich bouldery gravel (base not exposed)	Loopline Gravel

Total coverbed thickness = 1.35 m

The greywacke pebble conglomerate near the top of the profile contains only a minor granite pebble component. This is quite different to the bouldery gravel at the base of the profile, which contains a mixture of about 50% granite and 50% greywacke.

If the stratigraphic correlation is correct then the medium to dark brown organic silt at about 1 m depth is probably equivalent to the Chesterfield interstadial.

Profile E: Kumara Cemetery Road

Grid Ref J32 N 3620 E 6085

Measured: 2003

Numerical age: No samples at this site.

Correlation: The site is mapped as Loopline Formation by Suggate and Waight (1999).

Outcrop: The cover-bed sequence is situated on the Loopline Formation immediately adjacent to an incised valley/floodplain. The valley was formerly a meltwater flow-path during the Larrikins(1) and Larrikins(2) glacial maxima. This shallow valley acts as the spill-way for the Kapitea Reservoir near Dillmanstown. Two profiles were recorded from the same face, which is a road cutting in the terrace riser between the floodplain and the Loopline surface. The site is located on the south side of the incised channel a few hundred metres from the intersection of the Kumara Cemetery Road and Stafford Loop Road.

The sequence for **Profile E1** is:

Top 50 cm	Humus/peat	Holocene
	Gradational contact	
20 cm	Hard rich-brown organic silt	Holocene
25 cm	Hard rich-brown sandy silt with a few pebbles	Larrikins(1)
~~	Unconformable contact	
0-15 cm	Light-grey loessic silt	Loess?
10 cm	Hard light-brown silt	Chesterfield Interstadial?
50 cm	Hard light-grey silt	Loopline Loess?
15 cm	Hard light-brown silt	
20 cm	Hard Light brownish-grey silt	Loopline Loess?
20 cm	Hard grey silt	" " ?
20cm	Hard sandy silt	
6 m^{+}	Coarse fluvial gravel	Loopline Gravel

Total coverbed thickness = 2.45 m

Profile E1 is situated about 6 metres from profile E2. Both are on the east side of the road. E1 and E2 are situated either side of a channel structure in the underlying gravel, the lower 0.6 m of the coverbeds constituting channel fill.

The sequence for **Profile E2** is:

30 to 70 cm	Humus/peat	Holocene
	Gradational contact	
20 cm	Hard rich-brown soil	Holocene?
0 to 10 cm	Pale grey loess	Larrikins
20 cm	Hard light-brown soil	
35 cm	Pale-grey silt	Loess?
8 cm	Pebbly sand	
10 cm	Light brown soil	Chesterfield Interstadial?
10 cm	Pale grey silt	Loess?
6 m^{+}	Coarse fluvial gravel	Loopline Gravel

Profile F: Kumara Cemetery Road

Grid ref J32 N 3670 E 6070

Measured: 2003

Numerical age: No samples at this site.

Correlation: The site is mapped as Loopline Formation by Suggate and Waight (1999).

Outcrop: The coverbed sequence is situated on the Loopline Formation immediately adjacent to an incised valley/floodplain. The valley was formerly a meltwater flow-path during the Larrikins(1) and Larrikins(2) glacial maxima. This shallow valley acts as the spill-way for the Kapitea Reservoir near Dillmanstown. One profile was recorded from a road cutting in the terrace riser between the floodplain and the Loopline surface. The site is located on the north side of the incised channel a few hundred metres from the intersection of the Kumara Cemetery Road and Stafford Loop Road.

The coverbed sequence at profile F is:

----------	Surface	
30 cm	Humus/peat	Holocene
----------	Some stones on the contact	
20 cm	Soft rich-brown organic silt	Holocene?
----------		
30 cm	Hard light-brown silt/loess with some fossil wood and roots	Larrikins(1)
----------	Gradational contact	
20 cm	Hard brown peaty silt, abundant wood	Chesterfield Interstadial?
----------		
30 cm	Hard light-brown silt/loess, minor fossil wood and roots	Loopline Loess?
----------		
6 m^{+}	Coarse fluvioglacial gravel and roots	Loopline Gravel
	Total coverbed thickness = 1.6 m	

Here the Loopline gravel is dominated by Torlesse Greywacke with lesser granite and schist. The matrix is dominantly greywacke derived. The gravel at Profile E on the opposite side of the meltwater channel is similar in character.

Profile G: Electricity Transmission Track, Kapitea Reservoir

Grid ref J32 N 3370 E 6165

Measured: September 2004

Numerical age: RR28 sampled from this site gave an $IRSL_{blue}$ age of 78.1 ± 6.8 ka (silt fraction)

Correlation: The site is mapped as Loopline Formation by Suggate and Waight (1999).

Outcrop: The coverbed sequence is situated on till mapped as Loopline Formation adjacent to the Kapitea Reservoir. Cosmogenic isotope dating from nearby indicates that this site was probably over-riden by glacial ice during the Larrikins(1) event. The profile is situated in a road cutting. The road/track is a 4WD access route for maintenance of electricity transmission lines. It is situated a few hundred metres to the north of Loopline Road. The sample site is located about 10 m below the crest of the "Loopline/Larrikins" moraine on the up-valley side overlooking Kapitea Reservoir.

The coverbed sequence at this site is:

	Surface
----------	
40 cm	Humus/peat
----------	
20 cm	Grey loessic silt

10-30 cm	Rich-brown peat/organic silt
----------	iron pan variably developed at this contact
30 cm	Clean sand grading laterally to fluvial gravel
----------	iron pan variably developed at this contact
30 cm	Very hard light-brown laminated silt/loess RR28 taken from centre of this unit Grades laterally to fluvial gravel
----------	
$1m^{+}$	Grey glacial till of unknown age
	Total coverbed thickness = 1.4 m

Profile H: Gravel Quarry close to Stafford Loop Road/Loopline Road Intersection

This locality is a gravel quarry immediately adjacent to and on the SE side of Stafford Loop Road about 200 m SW of the intersection with Loopline Road. The profile described here is in an excavated face on the SE side of the quarry opposite to Stafford Loop Road. The site was not sampled for luminescence dating as part of this project but was sampled by Preusser et al (2005). The description they provide does not permit the sample to be assigned to any particular level in the profile. It is assumed that the dated sample comes form the lower (granite-rich) gravel.

----------	Surface
30 to 100 cm	Complex deposit of loess, soil and peat with abundant wood
----------	
20 to 70 cm	Complex deposit of soil, gravel, peat and wood. Some of the stumps are in growth position, but entirely within the gravel
----------	
3 to 4 m	Larrikins Formation. Fluvioglacial outwash gravel composed of subangular greywacke gravel with minor schist and granite
----------	
~ 1.5 m	Complex deposit of organic soil, silt, loess, sand and fine gravel Wood-bearing
----------	
3 m+	Loopline Formation? Sub-rounded to rounded fluvioglacial gravel. Granite dominated, minor schist and greywacke, but more schist than the Loopline gravel above.

There is a major provenance change between the two main gravel units. There is almost certainly a major depositional hiatus between the two gravels. The intervening unit is not present everywhere in the quarry face and has subsequently been buried by quarry waste. This unit contains an organic soil/peat layer up to 40 cm thick

Profile I: Blakes Terrace, Awatuna

Grid ref J32 N 4005 E 5275 (for Profiles 1 & 2, Profile 3 situated on the same bulldozer track but about 50 m to the north)

Measured: Nov 2004

Numerical age: $IRSL_{blue}$ sample RR30 was taken profile 1 at this locality. The age is 63.6±7.4 ka.

Correlation: The site is mapped as Loopline Formation by Suggate and Waight (1999). Closer inspection reveals that although the terrace surface is more-or-less level overall, part of it is a fluvioglacial outwash terrace and part is a raised marine terrace. The fluvioglacial portion is Loopline Formation. For the purposes of this study the marine portion is defined informally as Blake Formation.

Outcrop: Three profiles were measured at this locality, two on the Blake Formation (profiles 1 and 2) and one on the Loopline Formation (profile 3). Profiles one and two were taken from exposures either side of a track on top of the terrace created by a bulldozer. Profile three was taken from the side of the same track about 50 metres to the north.

The cover-bed sequence at **profile 1** which is situated on the Blake Formation is:

----------	Surface Spoil (from dozer blade). Surficial Holocene organic deposits removed during formation of track.	
----------		
30 cm	Medium grey loessic silt	Larrikins?
----------		
30 cm	Light greyish-brown silt, abundant wood and roots	
----------		
25 cm	Dark-brown organic silt, abundant wood and roots	
----------		
13 cm	Peat and very-dark brown organic silt. RR30 (63.6±7.4) taken here	
----------		
13 cm	Grey silty sand	
----------		
40 cm^{+}	Fine-Medium ilmenite bearing grey-brown sand. No stones, pebbles, or granules	Blake

Cover-bed thickness at profile 1 = ~ 1.1 m. This excludes any Holocene peat or organic silt that may have been present. The dating method for sample RR30 is IRSL.

The cover-bed sequence at **profile 2** (opposite side of track to profile 1 and also on the Blake Formation) is:

----------	Surface	
10 to 20 cm	Peat	Holocene
----------		
10 cm	Brown organic silt	Holocene?
----------		
30 cm	Light-grey loessic silt	Larrikins?
----------		
15 cm	Light brown silt	Loopline?
----------		
30 cm	Mixed peat and brown organic rich silt, wood bearing	Pre-Loopline?
----------	~~~~? abrupt contact defined by thin iron oxide zone	
10 cm	Grey coarse fluvial sand.	
----------	~~~~?	
40 cm+	Very hard orange-brown iron-oxide-cemented sand	Blake

Cover-bed thickness at profile 2 = ~ 1.0 m.

The cover-bed sequence at **profile 3** situated on fluvioglacial gravel assumed to be Loopline Formation is:

----------	Surface	
50^{+} cm	Debris churned by dozer blade	

33^{+} cm	Peat and wood bearing silt	Holocene

15-20 cm	Grey to brownish-grey loessic silt, some small wood fragments	Larrikins?
----------		
20 cm	Woody peat and dark brown organic silt	
----------		
15 cm	Light brown silt	
----------		
20 to 25 cm	Wood bearing brown organic silt Abundant wood at base	
----------		
0 to 15 cm	Coarse to granular sand with a few pebbles (lensoidal sandy pockets, potential unconformity)	
----------		
26 cm	Brown organic silt, some wood, alternating sandy and less sandy layers	
----------		
3 to 7 cm	Grey loessic silt	
----------		
6 to 7 cm	Very woody dark brown peat and organic silt	
----------		
15 cm	Brownish-grey sandy silt, some wood	
----------		
c. 2 metres	Fluvial gravel	Loopline

> 2 metres	Marine sand	Blake

Cover-bed thickness at profile 3 = ~ 1.7 m.

The marine sand was not observed at the profile. It is interpreted from nearby exposures that indicate a shallowing in the thickness of the Loopline gravel between this site and profiles 1 and 2 about 50 metres to the south.

The cover-beds at profile 3 include 4 peaty layers, which is more than is typically observed on the Loopline Formation. In addition the total thickness of the cover-beds is greater than is normally observed on the Loopline Formation. The Loopline Formation has an unconformable contact with the Blake Formation at this locality. The relationship is exposed in the base of the bulldozer track at a point between profiles 1 and 3.

The cover bed sequence at profile 3 significantly thicker than that at profiles 1 &2. The alluvial sand bed in profile 2 almost certainly represents an erosional unconformity. So it can not be assumed that the coverbeds on the Blake Formation at profiles 1 & 2 represent the full depositional history for the locality.

Profile 3 contains a coverbed sequence that is much thicker than at any Loopline site previously sampled for pollen analysis. It represents a potential opportunity for gaining a much more detailed climate history than that revealed from other Otiran sites.

APPENDIX FOUR: LUMINESCENCE MEASUREMENTS

A4.1: INTRODUCTION

The following data have been supplied by the luminescence dating laboratory at Victoria University of Wellington. The data are displayed in graphical format. The underlying digital data is archived at the dating laboratory. During the dating process a very large quantity of data is produced. It is not particularly informative or practical to present all of the data. In terms of this data the writer is not directly accountable for its production and played no part in the laboratory analysis. The analysis was done independently at the laboratory which minimises the chance that prior expectations might influence the resulting ages.

The measurements produced by the dating laboratory and by the National Radiation Laboratory (the NZ Government National Standards agency) are correct within the error margins given. The spectrometers are calibrated against the international standards, (International Atomic Agency in Vienna) and so would only be faulty if these standards are faulty.

For this project data from five (RR15, RR21, RR25, RR28, and RR33) of the thirty two individual luminescence samples have been selected for display. These samples are representative of the general range of depositional environments from which material was collected.

Samples RR15 and RR33 come from the same raised terrace at South Beach. RR15 is from a shallow marine sand. RR33 is from the base of a soil profile situated on the marine strandline immediately east (inland) from RR15. On geological grounds the two samples should produce similar ages, with RR33 expected to be slightly younger than RR15. Both samples are from depositional environments that should ensure full bleaching of the luminescence signal prior to burial.

Sample RR25 is from the base of the thick coverbed sequence situated on fluvioglacial outwash gravel of the Waimea Formation. So the sample age should reflect the commencement of accumulation of the coverbeds. The sample is a brown-coloured silt that is not conspicuously organic. The overlying coverbeds contain lenses of fluvial gravel. So the general depositional environment in which the sampled material was deposited is fluvial. The sampled material could be an “overbank” silt, in which case accumulation could have been quite rapid (potentially hours to weeks).

Sample RR21 is a light brown fluvial silt from Kamaka. The silt is underlain and overlain by fluvial gravel. Samples collected from the same unit by Preusser et al (2005) have been shown to be affected by partial bleaching. There is no doubt silt in this unit could have accumulated quickly from river water that was almost completely opaque to sunlight. So for RR21 the potential for incomplete bleaching is high.

Sample RR26 is from a fluvioglacial silt unit that is immediately underlain by glacial till and which is situated immediately below a fluvial sand/gravel bed. As indicated in chapter five the environment of deposition (proximal fluvioglacial) is one in which one would expect samples to suffer from partial bleaching issues.

A4.2 SHINEDOWN CURVES

In each case the shinecurves shown below are representative for the sample. For each sample results are displayed for an unirradiated disc ('natural') and a disc irradiated with the highest dose [N.B.: overall, a MAAD age is based on 48 shinedown curves, plus 58 normalisation measurements, plus 10 shinedown curves for the fading test]. Note that sample WLL297 (RR15) was measured by SAR (not MAAD) because it was very close to saturation, so 'highest dose' means a regenerated dose on the same aliquot as the 'natural', not a different disc as with MAAD.

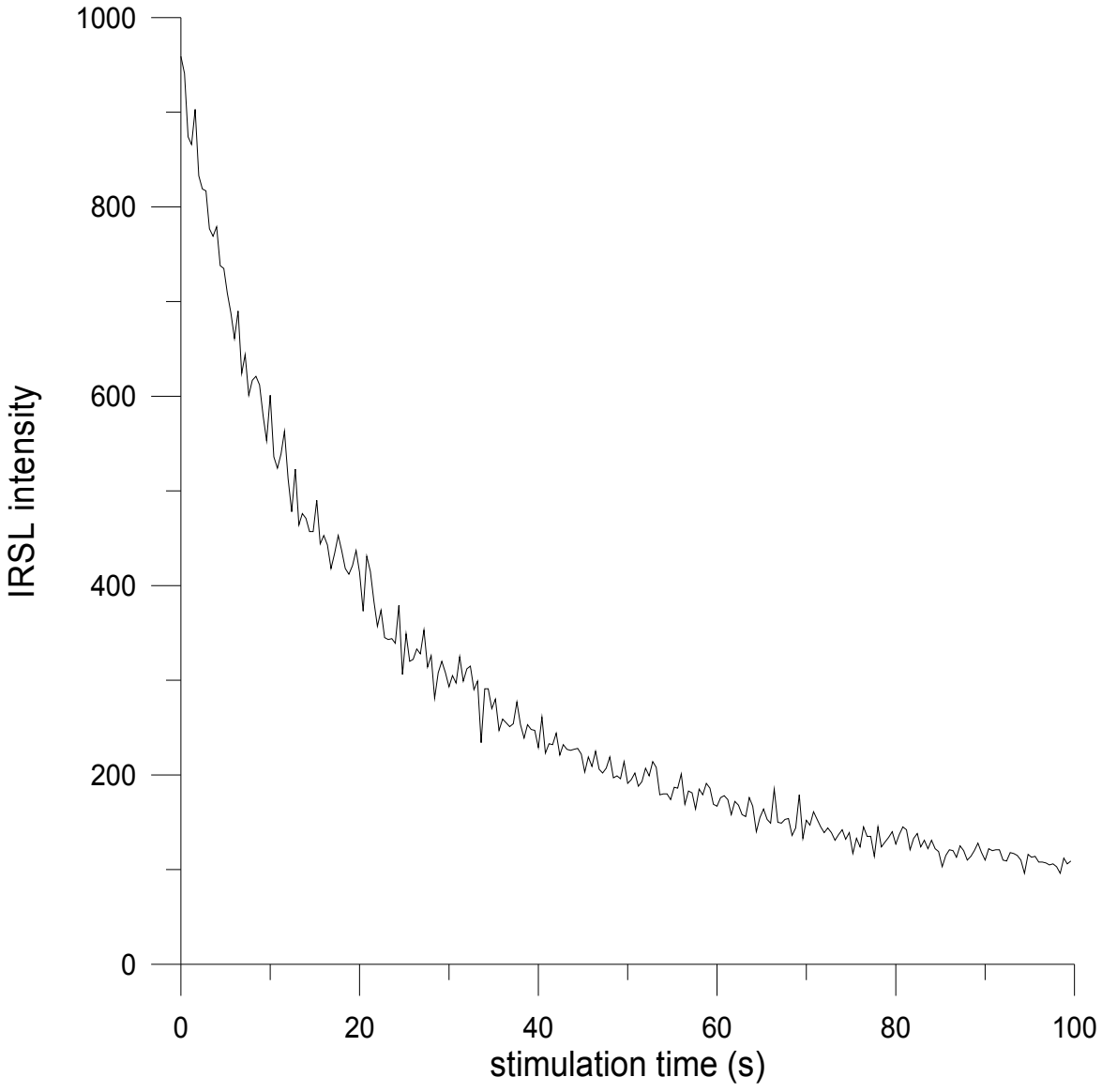

A4.2.1a: WLL536 (RR33) natural (0Gy additive) of MAAD protocol, disc1, IRSL(blue)

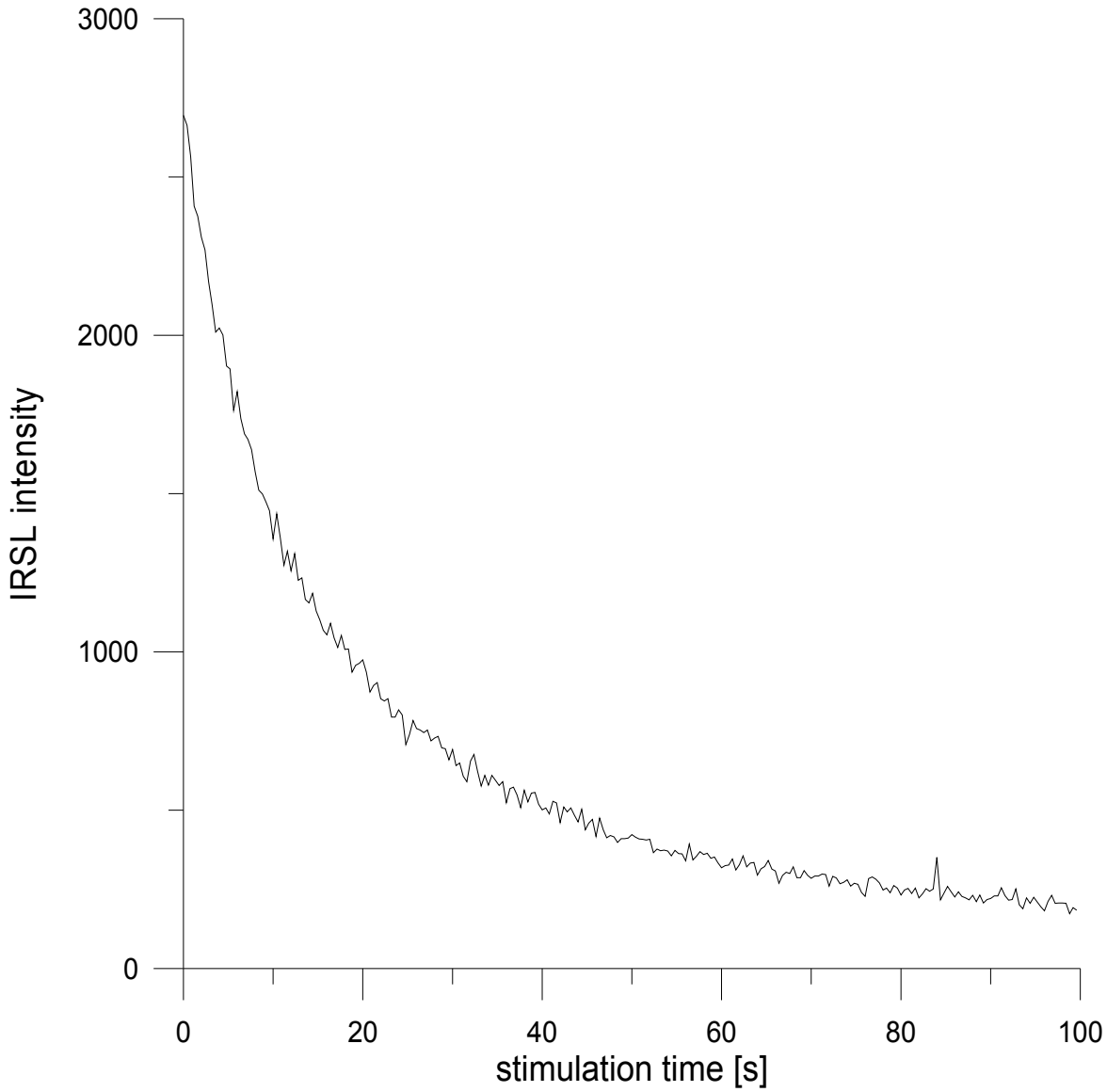

A4.2.1b: WLL536 (RR33) highest dose (660Gy additive) of MAAD protocol, disc39, IRSL(blue)

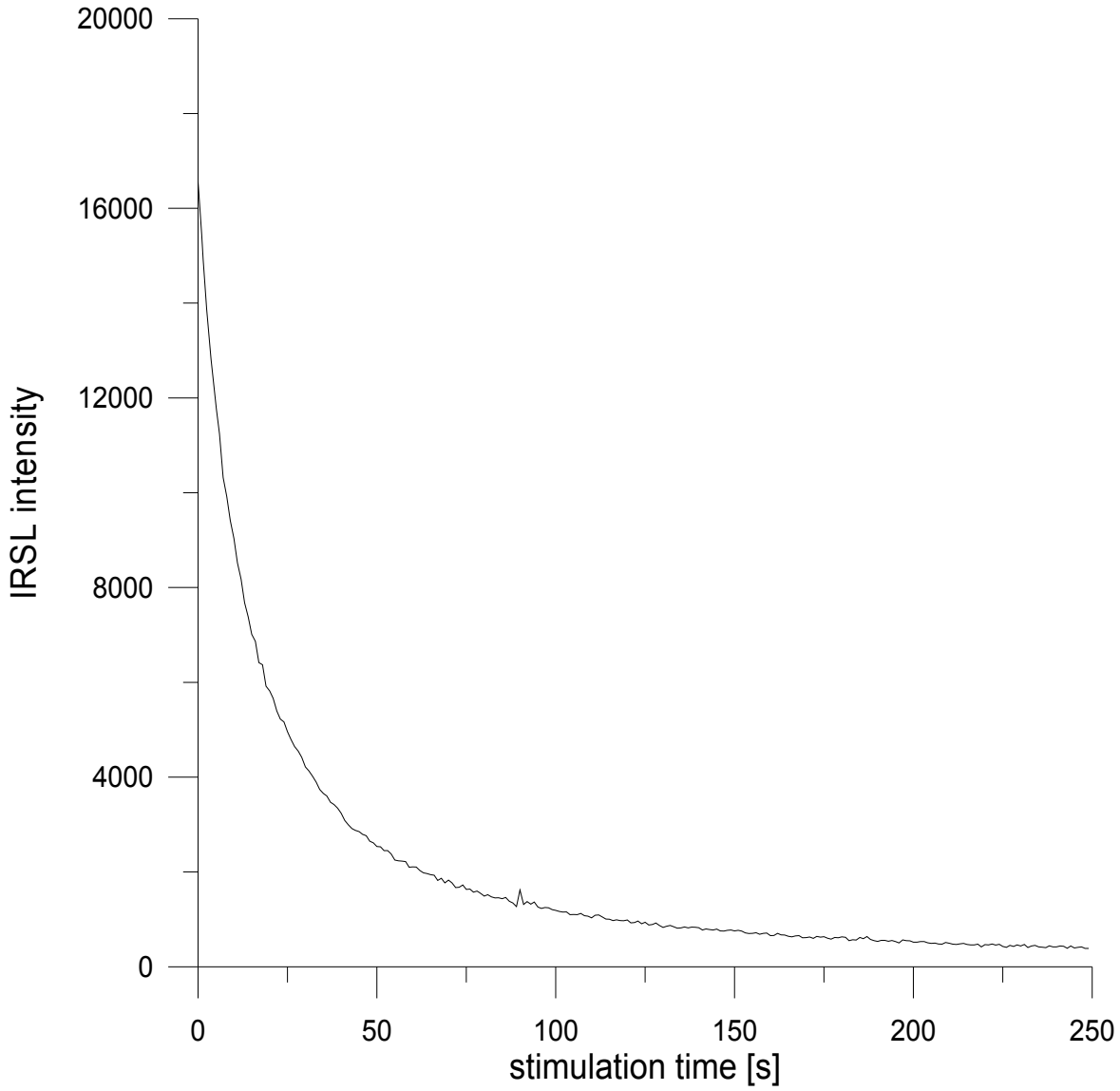

A4.2.2a: WLL297 (RR15) natural dose of SAR protocol, disc1, IRSL(blue)

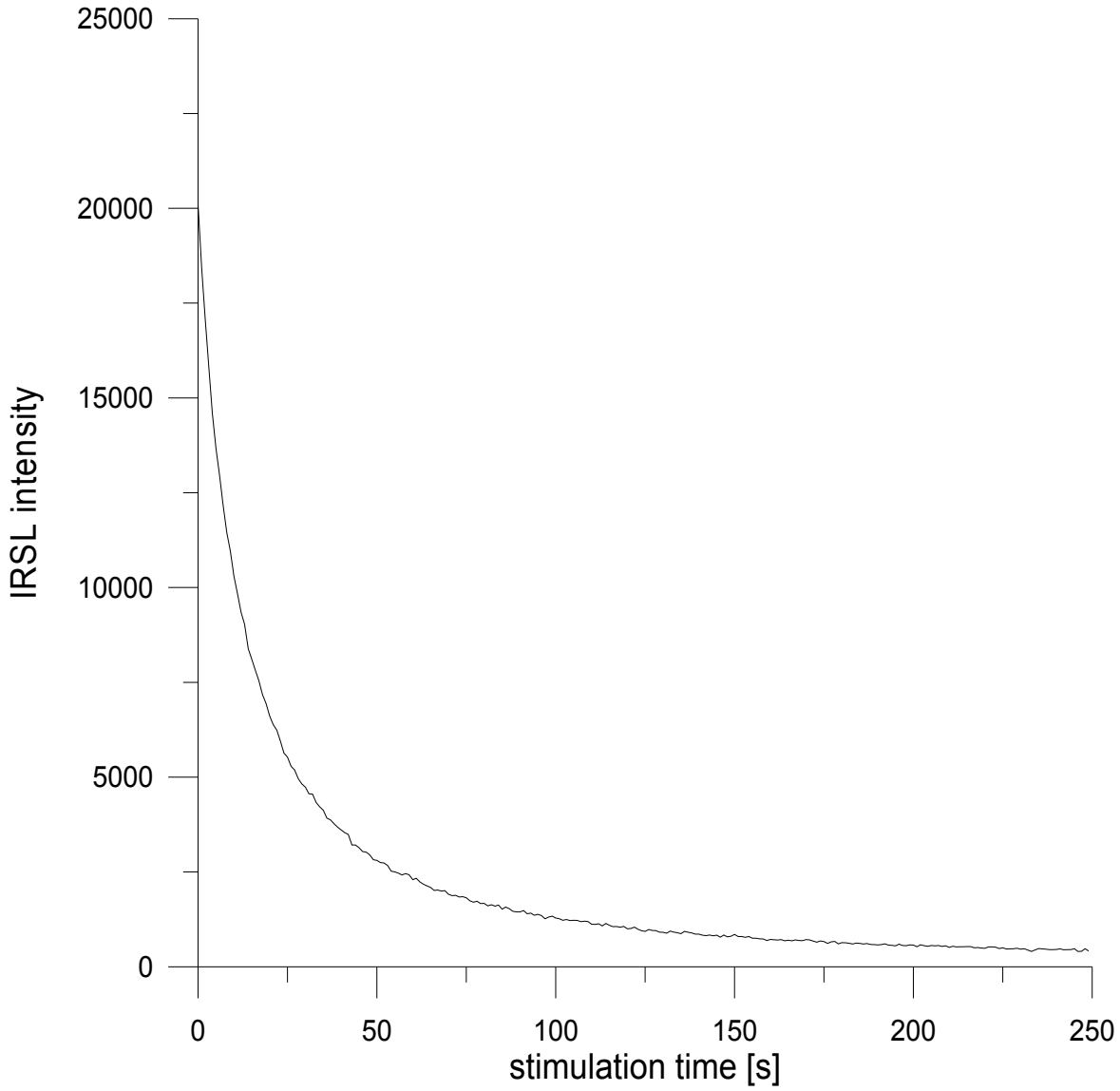

A4.2.2b: WLL297 (RR15) highest dose of SAR protocol (560Gy), disc1, IRSL(blue)

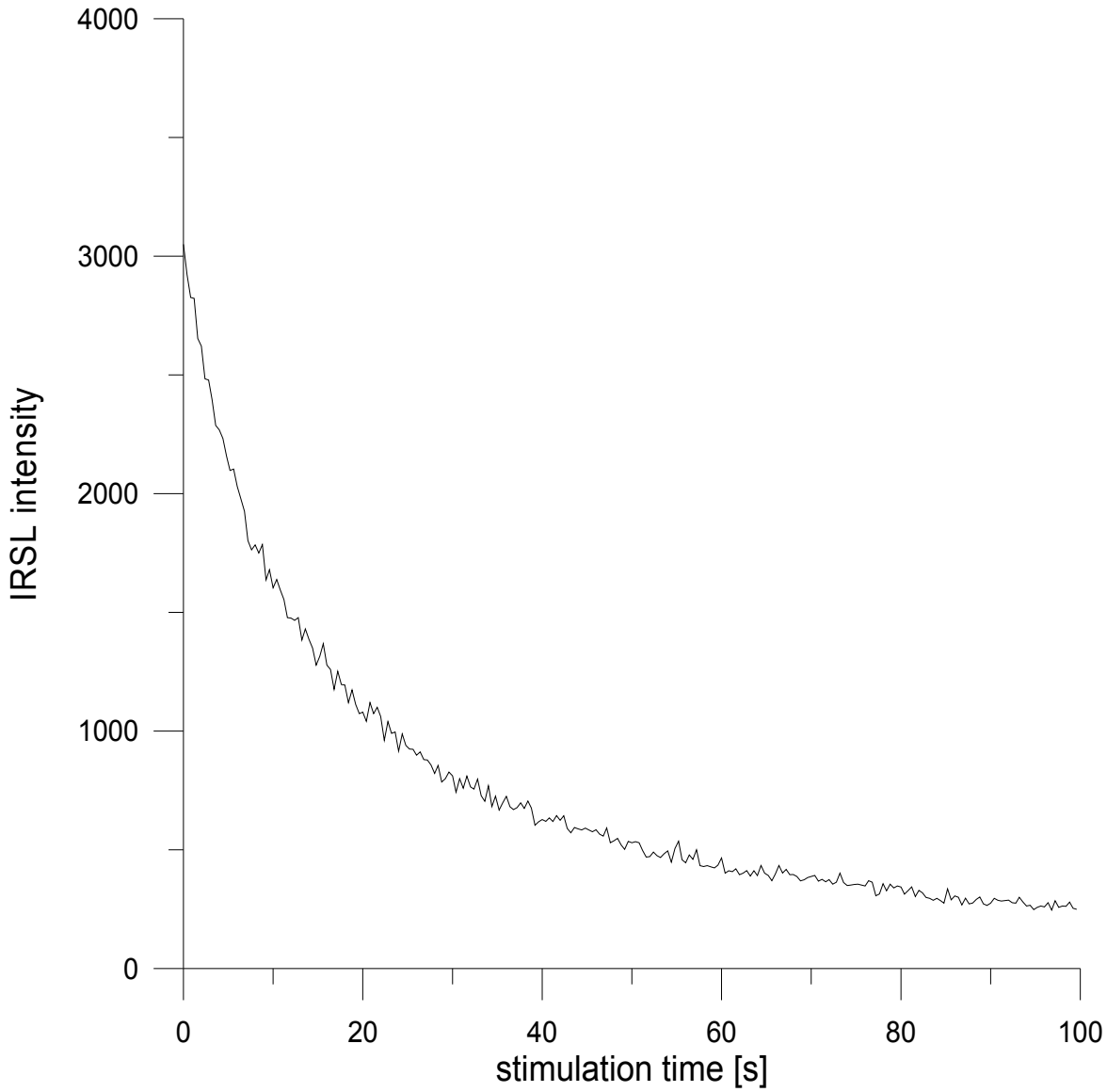

A4.2.3a: WLL526 (RR21) natural (0Gy additive) of MAAD protocol, disc1, IRSL(blue)

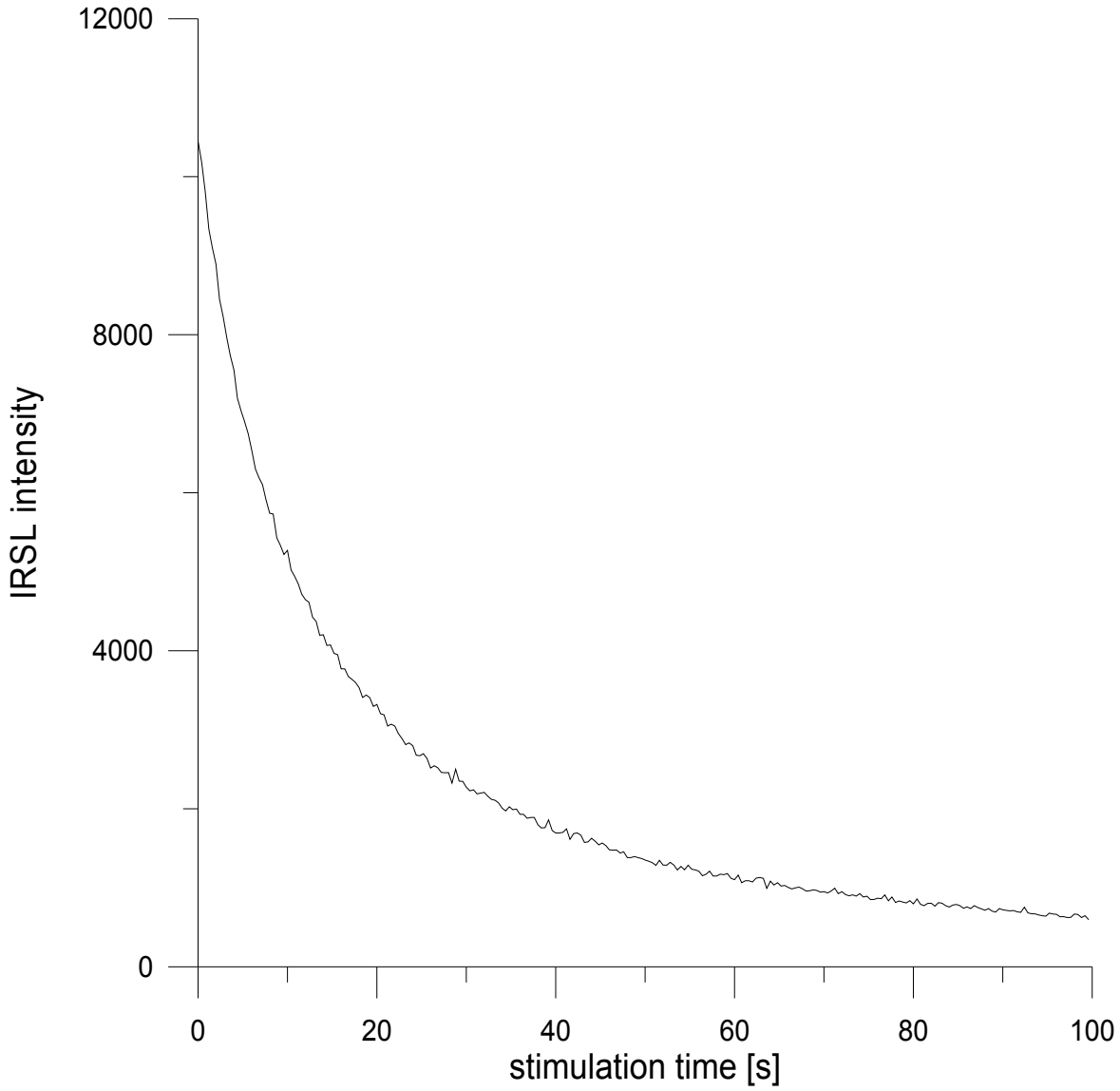

A4.2.3b: WLL526 (RR21) highest dose (700Gy additive) of MAAD protocol, disc39, IRSL(blue)

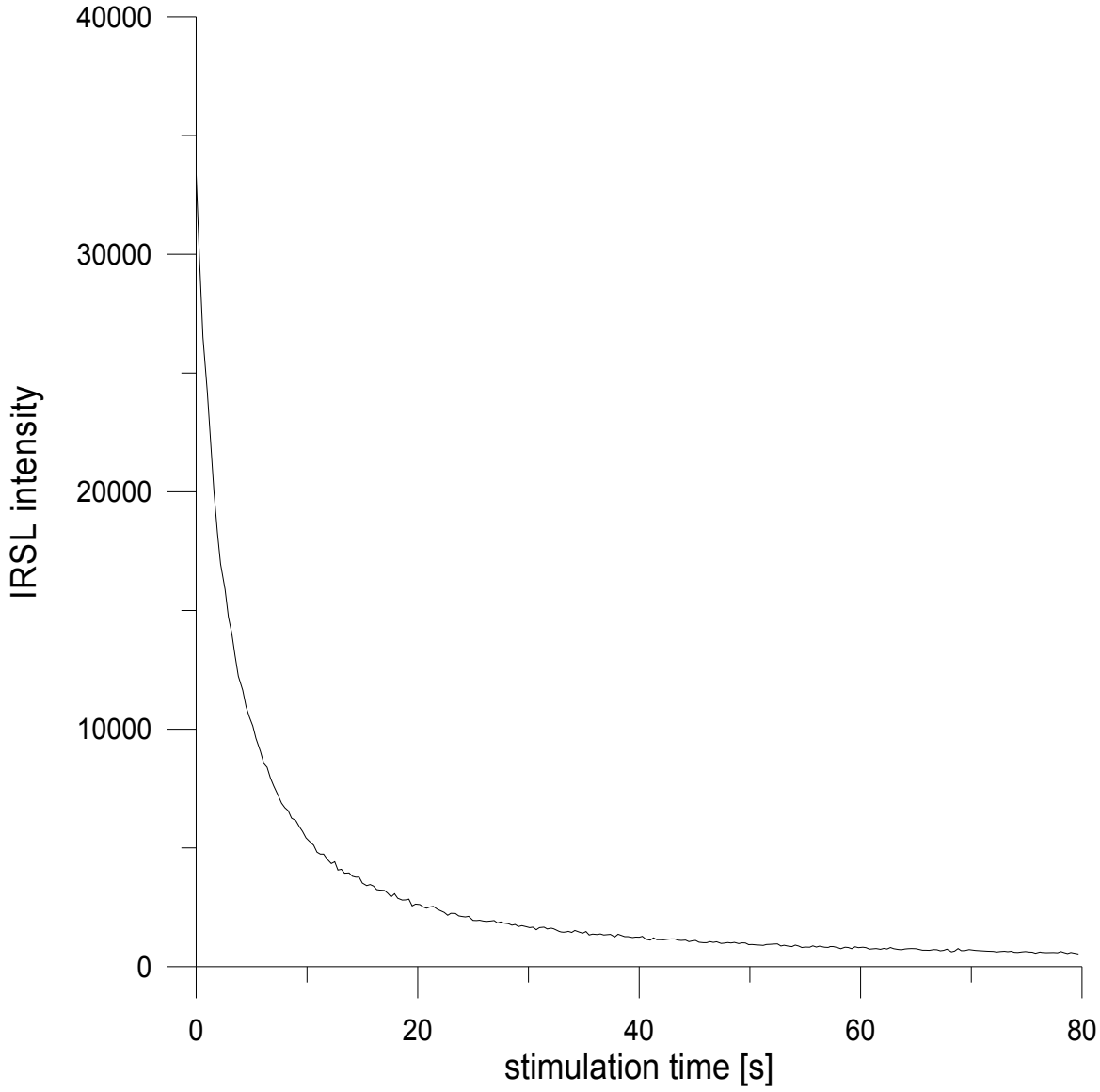

A4.2.4a: WLL533 (RR28) natural (0Gy additive) of MAAD protocol, disc1, IRSL(blue)

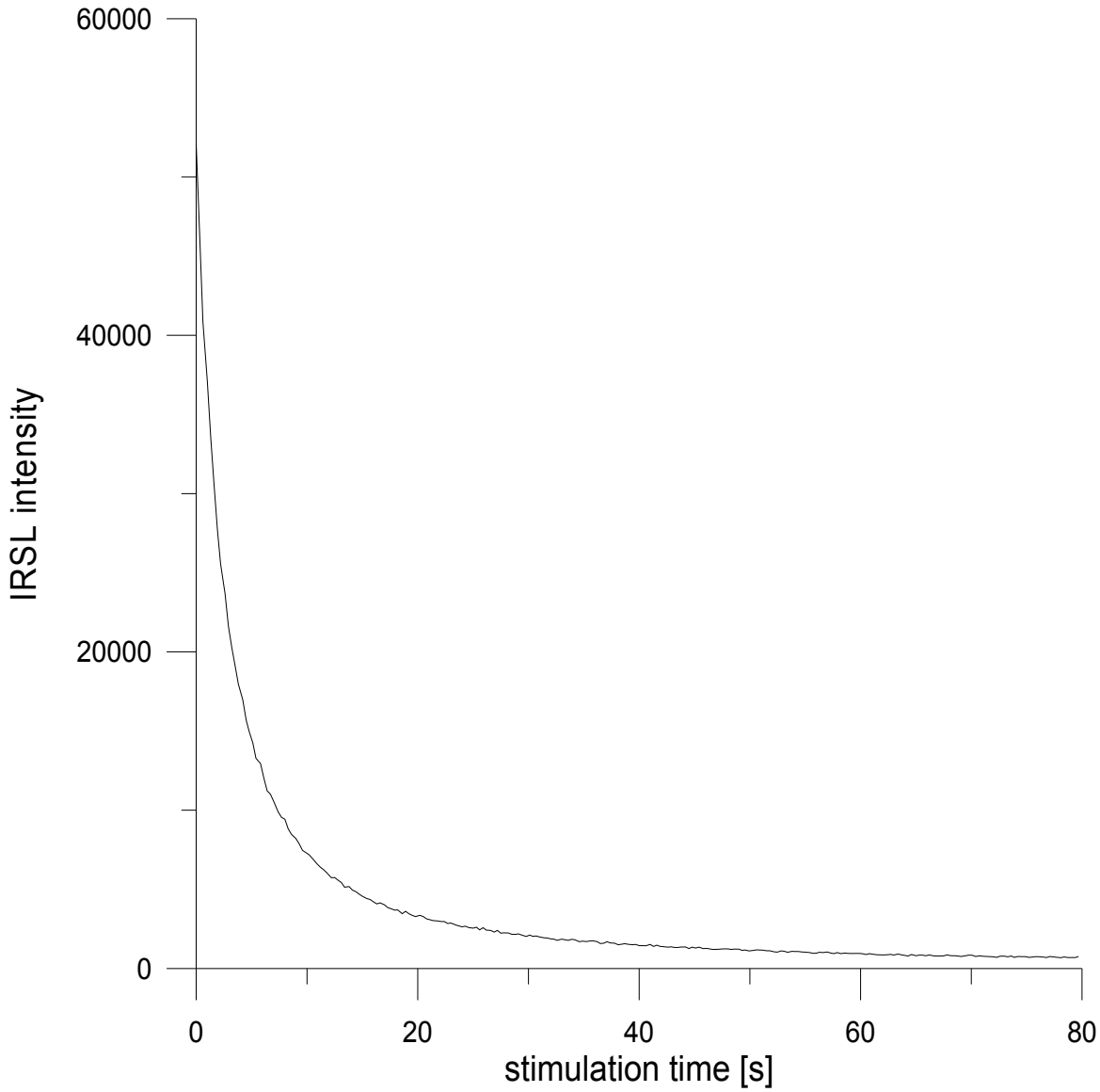

A4.2.4b: WLL533 (RR28) highest dose (1400Gy additive) of MAAD protocol, disc39, IRSL(blue)

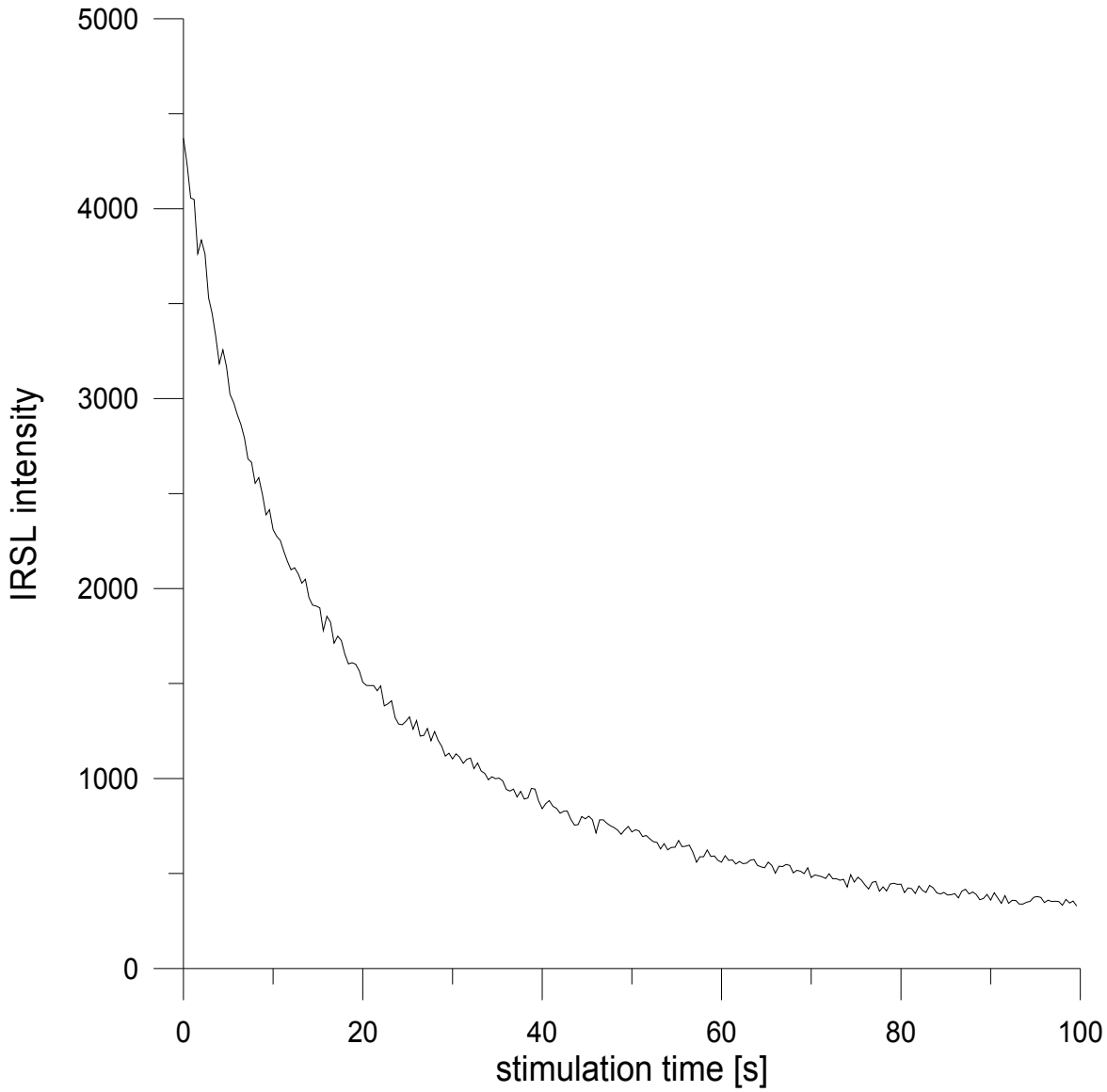

A4.2.5a: WLL530 (RR25) natural (0Gy additive) of MAAD protocol, disc1, IRSL(blue)

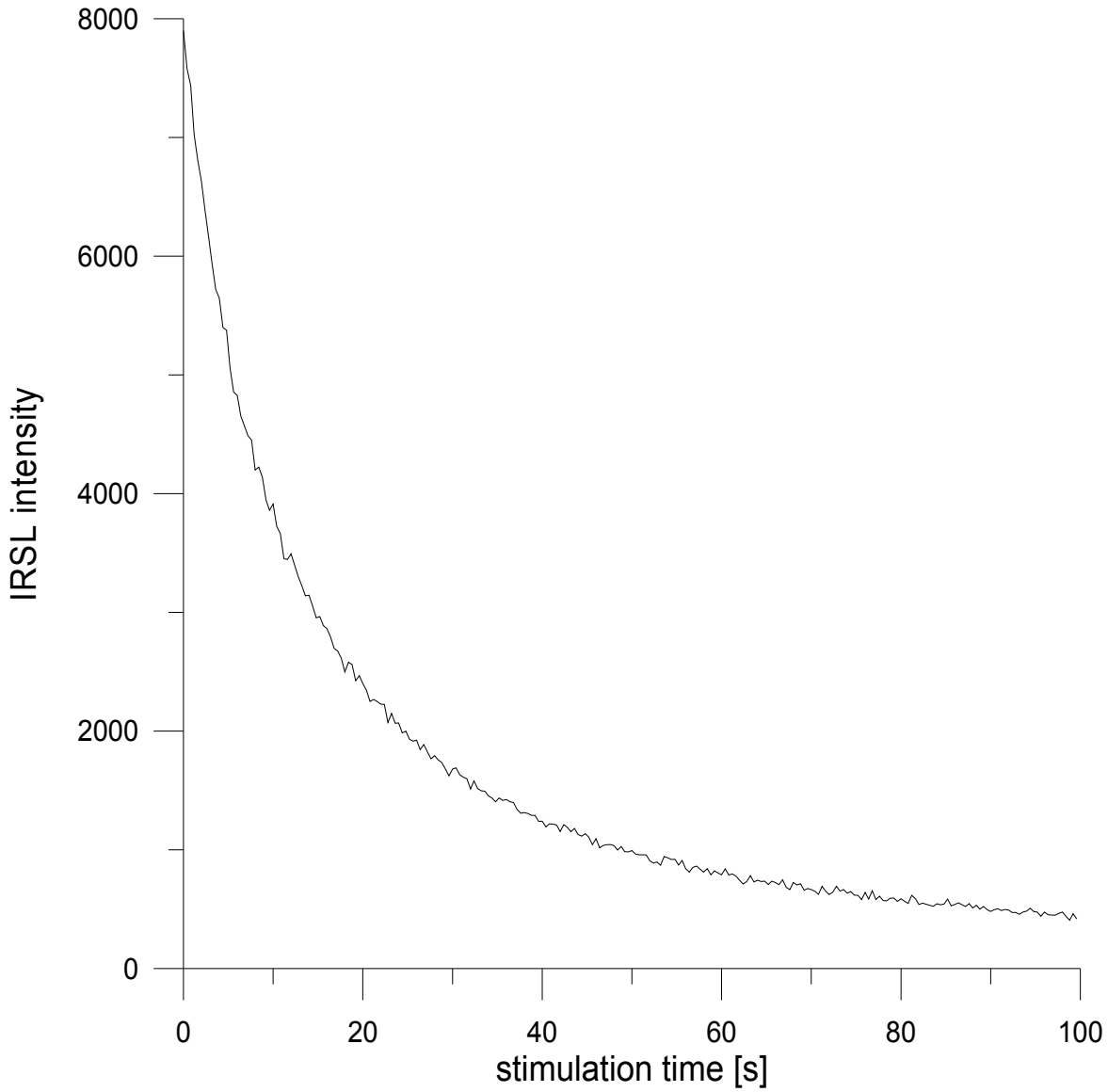

A4.2.5b: WLL530 (RR25) highest dose (1680Gy additive) of MAAD protocol, disc39, IRSL(blue)

A4.3 GROWTH CURVE ANALYSIS

A4.3.1 WLL536 (RR33)

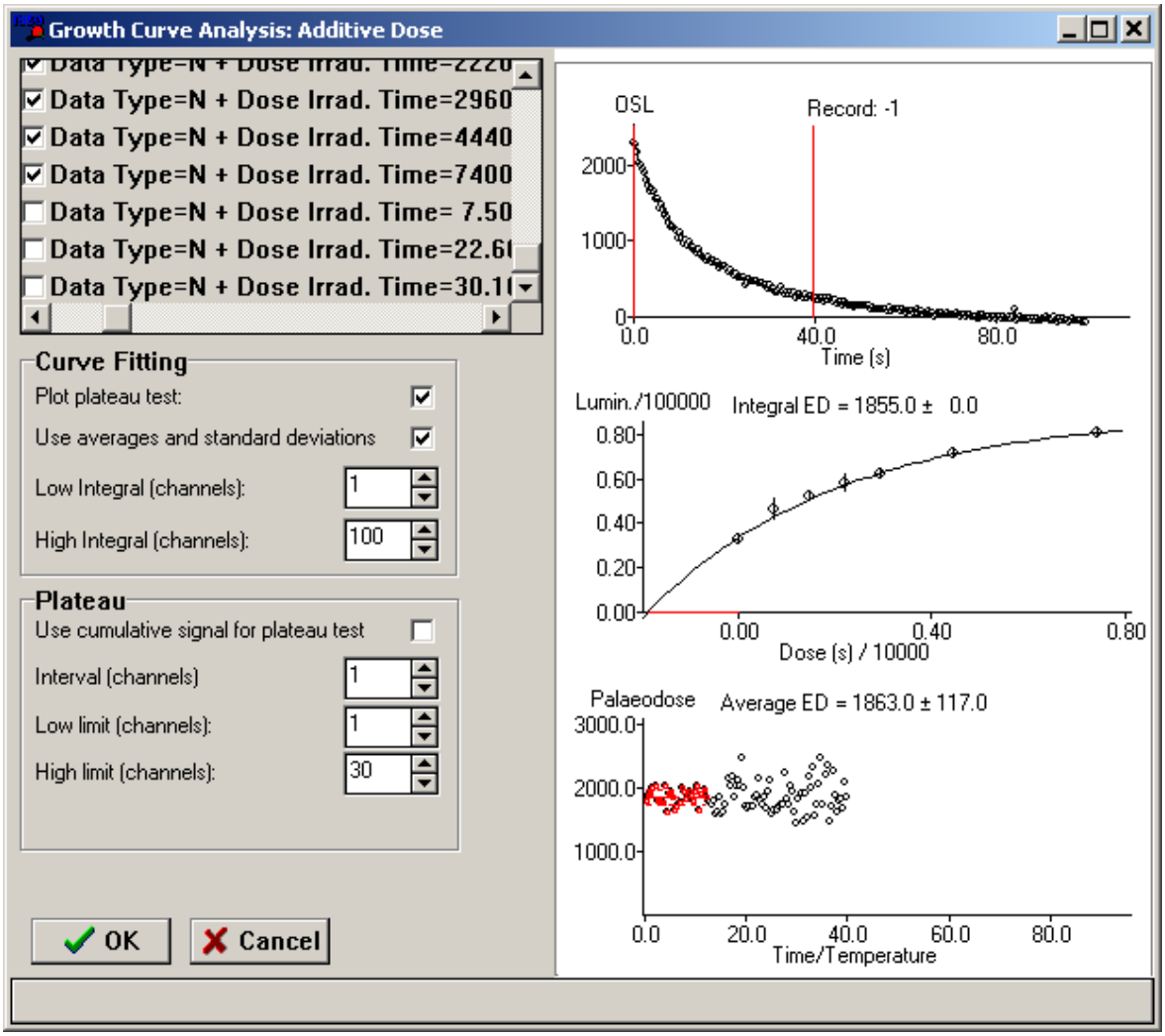

Graph (middle): Growth curve, saturating exponential
Graph (bottom): Plateau test. The perfectly flat plateau indicates there's no problem with partial bleaching (though that alone is no proof)

A4.3.2 WLL297 (RR15, measured by SAR)

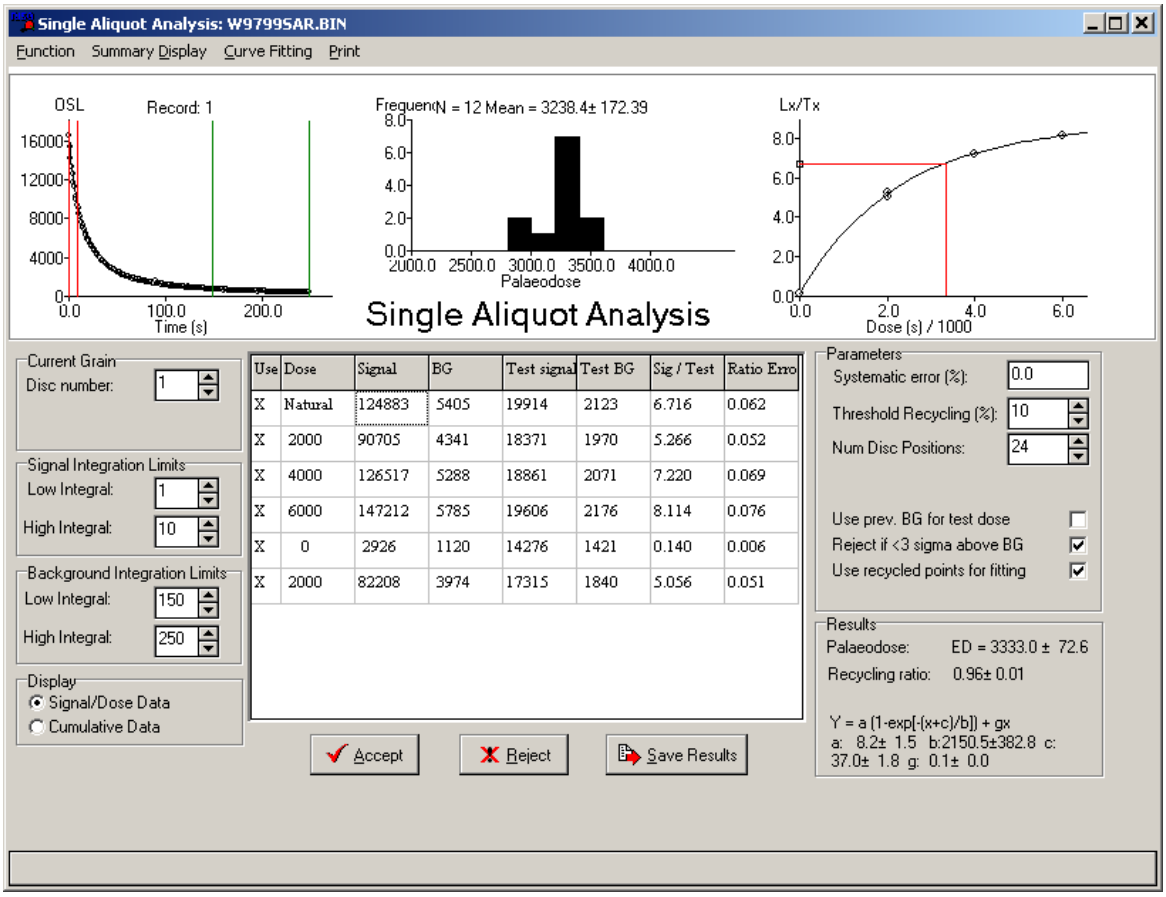

Graph (middle): Dose distribution for the 12 discs measured. As this is done on millions of fine grains, nothing should be read into the exact shape of the distribution, its simply a narrow Gaussian.

Graph (right): Growth curve of disc #1 (the other 11 discs look very similar)

A4.3.3 WLL526 (RR21)

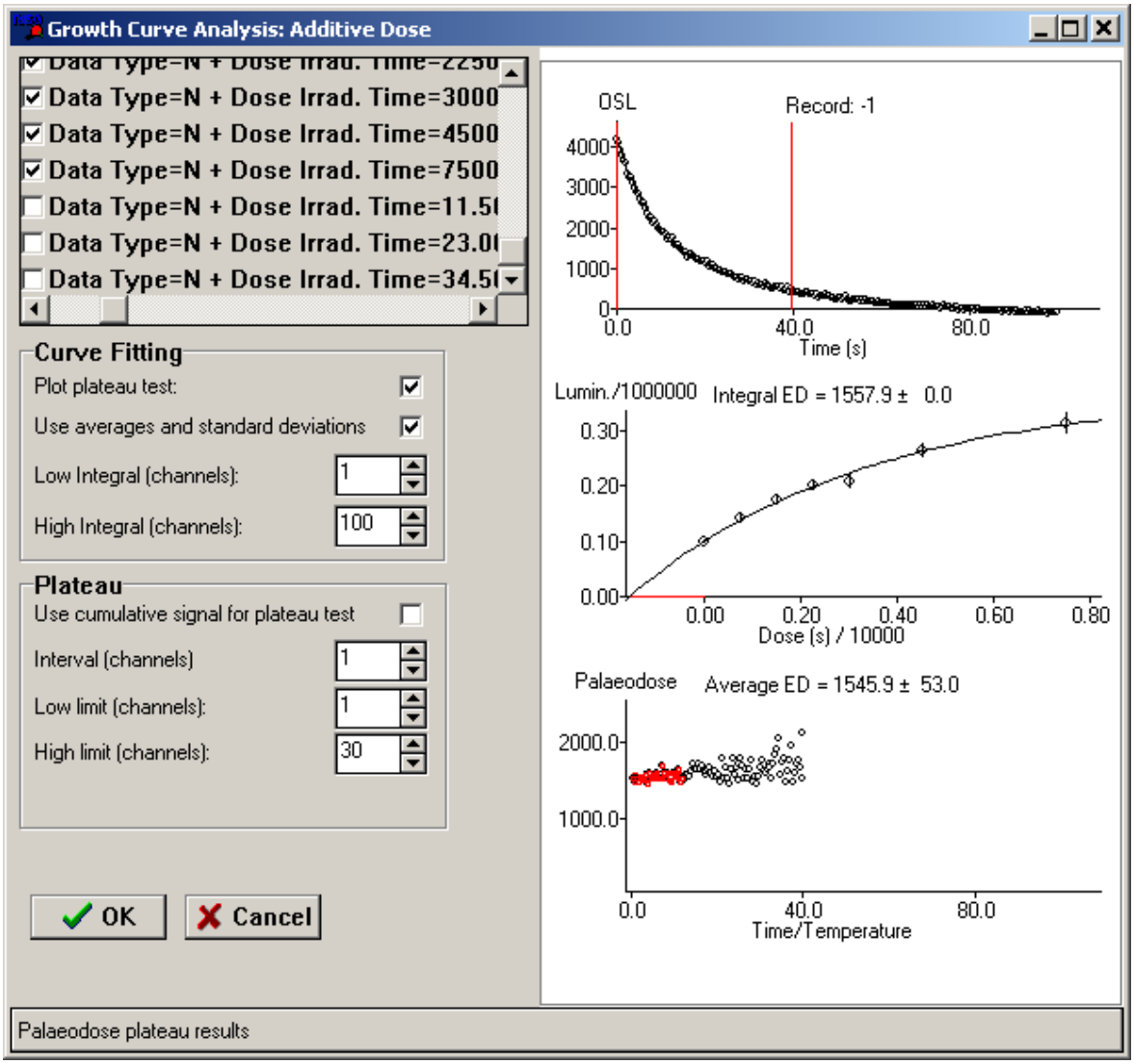

Graph (middle): Growth curve, saturating exponential
Graph (bottom): Plateau test. The plateau is not exactly flat, as for WLL536. The very slight rise could indicate a problem with partial bleaching, but as it is a very small effect.

A4.3.4 WLL533 (RR28)

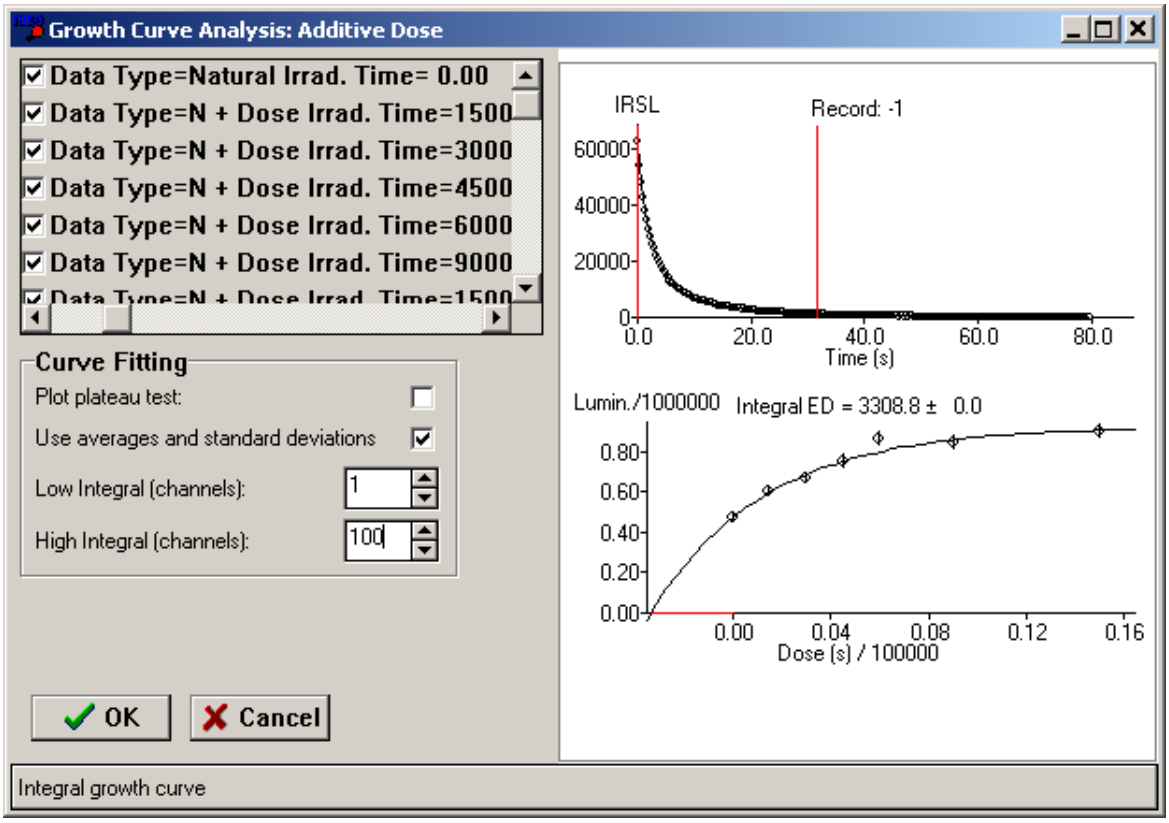

Graph (bottom): Growth curve, saturating exponential
Comment: Plateau test failed because the software produced mathematically unstable fits. That occasionally happens for high dose (old) samples, and indicates nothing apart from difficulties in mathematically determination of the optimum fit.

A4.3.5 WLL530 (RR25)

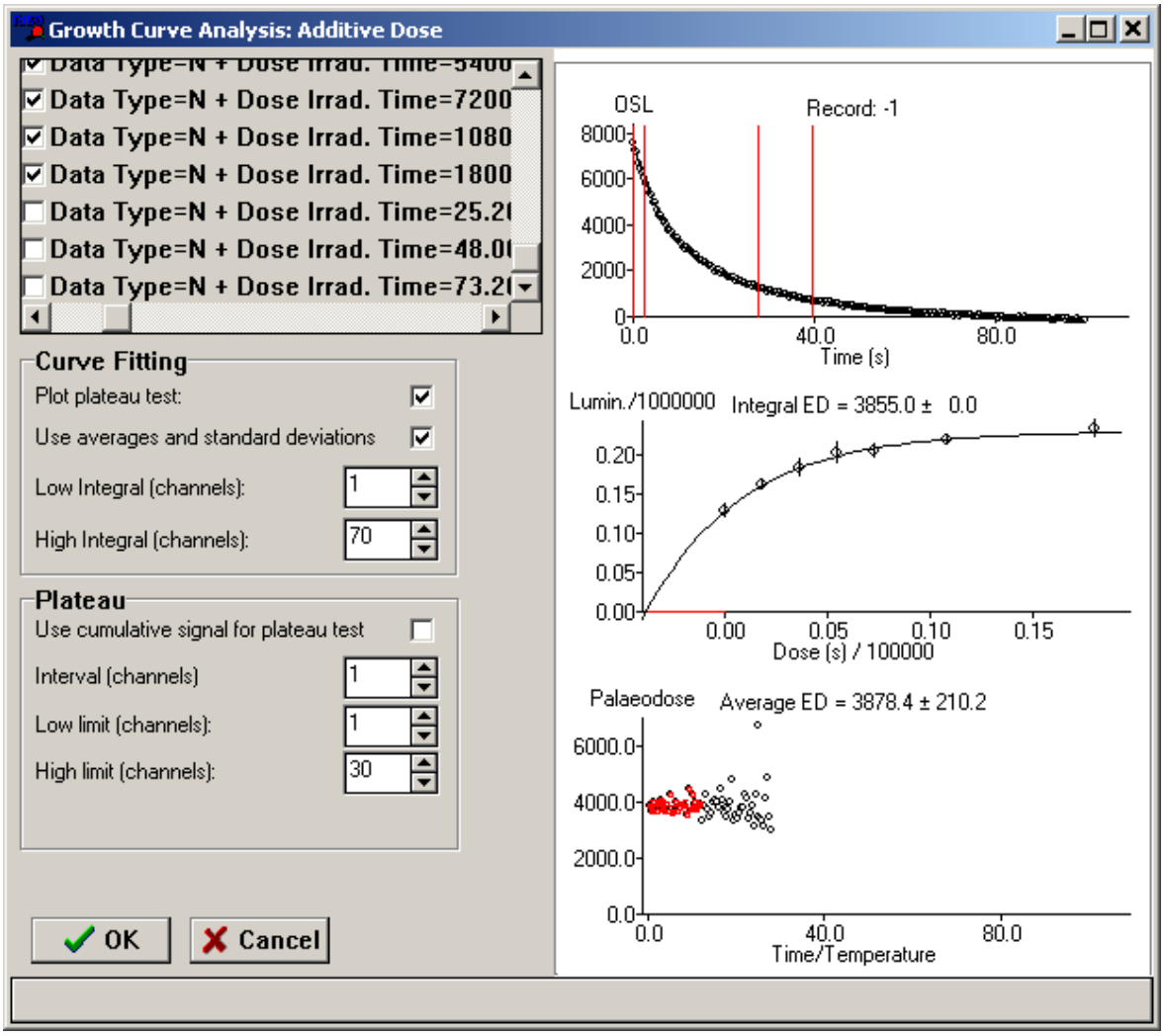

Graph (middle): Growth curve, saturating exponential
Graph (bottom): Plateau test. The perfectly flat plateau indicates there's no problem with partial bleaching (though that alone is no proof). Above channel 70 the mathematical fit was unstable, but channels 1-70 are sufficient for a plateau.

A4.4: LUMINESCENCE MEASUREMENTS FROM PROJECTS UNDERTAKEN IN WESTLAND

Table A4.1 Published luminescence ages from Westland

Luminescence ages by Preusser et al (2005) from North Westland

Radiation measurements all equivalent dose, Ages in kyr BP.

Location	Sample Code	IRSL(blue age (kyr)	TL(blue) age	OSL(UV) age	TL(UV) age	IRSL(UV) age	ED(post-IR-OSL) age
Pine Ck Quarry (Southside, Hokitika)	PIC 1	74±15	87±10	66 ± 5	68 ± 15		
"	PIC2	78±14	70±10	63 ± 9	66 ± 11		
"	PIC3	76±11	114±17	80 ± 13	78 ± 12		
Phelps Goldmine (Southside)	PGM1	67±8	72±9	72 ± 12	70 ± 12		
"	PGM2	76±18	204±40	65 ± 12	107 ± 13		
"	PGM3	66±8	67±10	84 ± 9	89 ± 17		
"	PGM4	74±8	261±48	101 ± 25			
"	PGM5					63±6	102±10
"	PGM6					58±5	69±7
"	PGM7					69±6	103±10
"	PGM8					61±6	83±8
"	PGM9					76±8	85±8
"	PGM10					22.4±2.3	21.5±2.1
"	PGM11					19.3±2.5	17.1±1.5
Sunday Creek	SDC1	118±28					
"	SDC2	81±11					
"	SDC3	64±5					
"	SDC4	71±10	77±10	86 ± 9	86 ± 17		
"	SDC5	58±8	94±14	64 ± 10	66 ±10		
"	SDC6	71±8					
"	SDC7	61±8	81±9	66 ± 11	89 ± 4		
"	SDC8	58±7	78±9				
Kamaka	KMK1	20.2±2.1	17.3±4				
"	KMK2	41±5	84±35	38 ± 5	84 ± 8		
"	KMK3	45±4	83±16	29 ± 4	35 ± 4		
"	KMK4	39±5	75±13	35 ± 6	36 ± 10		
"	KMK5a	24.3±1.5					
"	KMK5b	21.8±2.1					
"	KMK6	23.4±3.6	26.1±2.9	38 ± 4	25.8 ± 2.6		
"	KMK7	28.5±3.2	71±20				
"	KMK8a	25.8±2.4					
"	KMK8b	24.4±1.5					
Hokitika Gravel Pit	BSG4					22.0 ± 2.2	25.1 ± 2.8
"	BSG5					21.9 ± 2.1	27.2 ± 2.8
Nelson Creek	NCL3					15.6 ± 1.7	15.5 ± 1.5
"	NCL4					14.1 ± 1.5	13.9 ± 1.5
Raupo	RPO1/1					17.9 ± 2.3	20.6 ± 2.2
"	RPO1/2					22.5 ± 2.4	23.5 ± 2.2
"	RPO2/1					20.3 ± 1.9	22.8 ± 2.2
"	RPO2/2					16.8 ± 1.7	18.4 ± 1.8

Upper Chesterfield Road	UCS2		27 ± 3	36 ± 3
“	UCS3		39 ± 4	57 ± 6
Stafford Loop Road	LOL1	64 ± 5		
Nelson Creek	NCL1	109 ± 8		
“	NCL2	113 ± 8		
Upper Chesterfield Road	UCS1	81 ± 7		
Raupo Upper Gravel	RUG1	16.1 ± 0.7		
“	RUG2	18.8 ± 1.6		
“	RUG3	10.1 ± 1.1		
Raupo Lower Gravel	RGL1	31 ± 2		
“	RGL2	33 ± 4		
Hokitika Gravel Pit	BSG1	82 8		
“	BSG2	85 6		
“	BSG3	88 8		

Luminescence ages by Hormes et al 2003 from Raupo in the Grey Valley

Location	Sample	IRSL(blue) Age (kyr)	GLSL Age (kyr)	TL (kyr)
Raupo	RPO1/1 IR	26 ± 3.8		44.5±7.7
“	RPO1/1 GL		23.4±4.6	53.4±9.7
“	RPO1/2 IR	25.2±31		55.6±10
“	RPO1/2 GL		22.8±2.5	46.2±4.2
“	RPO2/1 IR	20.2±2.7		35.2±5.1
“	RPO2/1GL		18.7±2.2	35.7±5.2
“	RPO2/2 IR	22.6±2.7		38.5±5.9
“	RPO2/2GL		20±2.6	44.7±6.8

Luminescence ages by Vandergoes et al (2005) from Okarito, South Westland

Radiation measurements all equivalent dose, Ages in Kyr BP

Core	Sample	Age $_{IRSL\ (blue)}$ (kyr)	Age $_{TL(UV)}$ & Post-IR-OSL (kyr)	Horizon
0212	OBC-1	13.3 ± 1.3	11.7 ± 1.3	Upper organic silt/peat
0113	OKA 6	17 ± 3		Upper grey silt
0113	OKA 5	17 ± 3		Upper grey silt
0004	BPB 1	28 ± 3	24 ± 3	Upper grey silt
0212	OBC-2	12.6 ± 1.2	12.5 ± 1.2	Upper grey silt
0212	OBC-3	16.0 ± 1.4	15.6 ± 1.3	Upper grey silt
0212	OBC-4	15.2 ± 1.2	15.6 ± 1.5	Upper grey silt
0212	OBC-5	22.7 ± 1.9	21.3 ± 1.9	Upper grey silt
0212b	OBD-1	13.2 ± 1.1	13.1 ± 1.2	Upper grey silt
0212b	OBD-2	13.3 ± 1.2	12.4 ± 1.3	Upper grey silt
0212b	OBD-3	16.2 ± 1.4	15.8 ± 1.4	Upper grey silt
0212b	OBD-4	18.4 ± 1.6	16.8 ± 1.4	Upper grey silt
0212b	OBD-5	24.4 ± 2.1	24.3 ± 2.2	Upper grey silt
0212b	OBD-6	30.6 ± 2.5	32.3 ± 2.7	Upper grey silt
0212b	OBD-7	25.5 ± 2.1	25.6 ± 2.2	Upper grey silt
0212b	OBD-8	34.1 ± 2.8	34.5 ± 2.9	Upper grey silt
0212b	OBD-9	33.7 ± 2.9	34.3 ± 3.1	Upper grey silt
0212b	OBD-10	31.8 ± 2.8	34.3 ± 3.2	Upper grey silt
0212b	OBD-11	34.7 ± 2.9	37.0 ± 3.2	Upper grey silt

0212b	OBD-12	31.9 ± 2.6	32.6 ± 2.7	Upper grey silt
0212b	OBD-13	44.9 ± 3.8	46.3 ± 4.3	Upper grey silt
0212b	OBD-14	43.2 ± 3.7	42.4 ± 3.6	Upper grey silt
0212b	OBD-15	48.4 ± 4.2	51.8 ± 5.0	Upper grey silt
0212b	OBD-16	50.1 ± 4.3	53.0 ± 4.6	Upper grey silt
0212b	OBD-17	54.6 ± 4.6	59.3 ± 5.7	Lower organic silt/peat
0212b	OBD-18	66.4 ± 5.4	68.5 ± 5.8	Lower organic silt/peat
0112b	OKA 4	107 ± 30		Lower organic silt/peat
0004	BPB 2	97 ± 12	208 ± 58	Lower grey silt
0004	BPB 3	57 ± 12	60 ± 20	Lower grey silt
0004	BPB 4	48 ± 6	48 ± 6	Lower grey silt
0004	BPB 5	75 ± 10	75 ± 10	Lower grey silt
0112b	OKA 3	177 ± 49		Lower grey silt
0112b	OKA 2	(Saturation)		Lower grey silt
0112b	OKA 1	133 ± 64		Lower grey silt

Luminescence ages by Berger et al (2001) from Saltwater Forest (South Westland) and (Blue Spur) North Westland

Location	Sample	Age $_{IRSL\ (blue)}$ (kyr)	Age $_{TL(UV)}$ (kyr)
Blue Spur	BSR91-5		46.9±7.3
Blue Spur	BSR91-9		53±16
Blue Spur	BSR91-1	44±17	
Saltwater Forest	HR191-5		36.2±3.4
Saltwater Forest	HR191-1	89±15	324±55
Saltwater Forest	HR191-16	66±16	244±35
Saltwater Forest	HR191-12	145±36	87±30
Saltwater Forest	HR191-8	36±5.7	26±7

The luminescence methods used in the published studies listed above are:

IRSL(blue): Infrared stimulated luminescence (blue light) in all four studies.
TL(UV): Thermoluminescence (ultraviolet light) in all four studies.
IRSL(UV): Infrared stimulated luminescence (ultraviolet light) by Preusser et al (2005).
OSL(UV): Optically stimulated luminescence (ultraviolet light) by Preusser et al (2005).
TL(blue): Thermoluminescence (blue light) by Preusser et al (2005).
Post IR-OSL: Preusser et al (2005).
GLSL: Green light stimulated luminescence by Hormes et al (2005).

In table A5.1 the samples from Okarito are classified in terms of the stratigraphy. This interpretation of the stratigraphy, which is discussed in chapter 5, section 5.9, that is unique to this thesis rather than that of the originators of the data (being Vandergoes et al 2005).

Table A4.4a Dosimetry for luminescence dating (1st sampling round, this PhD project) of silt in samples from North Westland

Sample no.	Field code	Grain-size (µm) & Sed.	Depth below surface (m)	dD_e/dt (Gy/ka)[1] (Cosmic radiation)	Water content	U (µg/g) from ^{234}Th	U (µg/g)[2] from ^{226}Ra, ^{214}Pb, ^{214}Bi	U (µg/g) from ^{210}Pb	Th (µg/g)[2] from ^{208}Tl, ^{212}Pb, ^{228}Ac	K (%)	*a*-value	D_e (Gy) (IRSL(blue)	dD/dt (Gy/ka)	OSL-age (ka) ($IRSL_{blue}$)	Location
WLL216	RR-1	Sand	22.5	0.0239±0.0012	1.139	1.86±0.44	2.43±0.13	2.83±0.44	10.4±0.4	1.37±0.05	N/A		2.44±0.13		Phelps Goldmine
WLL169	RR-2	4-11 silt	22.5	0.0239±0.0012	1.296	3.64±0.40	4.10±0.34	3.80±0.49	16.2±0.7	1.25±0.05	0.052±0.011	116.6±5.8	3.47±0.32	33.6±3.6	Phelps Goldmine
WLL170	RR-3	4-11 Silt	10	0.0633±0.0032	1.305	3.74±0.39	3.21±0.14	3.40±0.49	11.6±0.5	1.89±0.11	0.061±0.005	196.3±10.3	3.46±0.31	56.8±5.9	Phelps Goldmine
WLL217	RR-4	Sand	17.5	0.0337±0.0017	1.182	2.26±0.49	2.73±0.08	2.67±0.44	10.8±0.4	1.83±0.07	N/A		2.83±0.19		Phelps Goldmine
WLL147	RR-5	Sand	20	0.0282±0.0014	1.201	4.93±0.53	4.79±0.24	4.37±0.61	26.4±0.7	1.93±0.11	N/A		4.23±0.31		Phelps Goldmine
WLL218	RR-6	4-11 Silt	8	0.0774±0.0039	1.297	2.83±0.53	3.67±0.10	3.24±0.53	12.0±0.5	2.29±0.08	0.051±0.013	477.0±20.7	3.87±0.36	123.3± 12.7	Scandinavian Hill
WLL148	RR-7	Sand	8	0.0774±0.0039	1.177	2.73±0.39	3.26±0.26	2.83±0.49	15.4±0.5	2.11±0.11	N/A		3.53±0.24		Scandinavian Hill
WLL219	RR-8	4-11 Silt	15	0.0408±0.0020	1.383	2.59±0.77	3.30±0.09	3.64±0.49	8.2±0.4	1.27±0.05	0.084±0.007	93.6±2.0	2.69±0.27	34.8±3.5	Sunday Creek Tributary
WLL220	RR-9 [MA] RR-9 [SA]	4-11 Sand	17	0.0350±0.0017	1.215	5.10±0.81	6.97±0.15	5.74±0.69	28.4±0.8	0.86±0.04	N/A	229.6±13.8 259.4±29.2	3.84±0.28	47.8±6.6 54.0±7.3	Sunday Creek Tributary
WLL149	RR-10	Sand	5	0.1082±0.0054	1.183	2.79±0.36	3.05±0.30	3.88±0.49	11.0±0.4	1.92±0.07	N/A		3.06±0.21		North Beach, Greymouth
[1]WLL171	RR-11	4-11 Silt	3.5	0.1300±0.0065	1.602	2.82±0.37	4.07±0.39	4.61±0.53	9.79±0.42	1.46±0.10	0.076±0.007	140.3±4.7	2.60±0.35 (2.73±0.35)	53.9±7.6 (51.5±6.9)	North Beach, Greymouth
[1]WLL296	RR-12	4-11 Sand	2	0.1581±0.0079	1.141	3.00±0.34	2.22±0.04	2.52±0.33	8.22±0.12	1.56±0.03	0.037±0.005	120.4±3.6	3.05±0.15 (2.97±0.15)	39.5±2.4 (40.6±2.4)	Point Elizabeth, Greymouth
WLL150	RR-13 [MA] RR-13 [SA]	4-11 Sand	6	0.0963±0.0048	1.196	2.80±0.35	2.62±0.26	2.35±0.44	10.8±0.4	2.25±0.11	N/A	331.5±8.3 375.2±87.5	3.19±0.23	87±8.3 98.6±24.4	Point Elizabeth, Greymouth
WLL277	RR-14	Sand	1.5	0.1692±0.0085	1.067						N/A				South Beach, Greymouth
WLL297	RR-15	4-11 Sand	7.5	0.0816±0.0041	1.208	4.43±0.46	3.75±0.06	4.44±0.44	15.7±0.2	1.64±0.04	0.058±0.015	270.1±4.0	4.10±0.33	65.9±5.4	South Beach, Greymouth
WLL278	RR-16	Sand	8.5	0.0735±0.0037	1.148						N/A				South Beach, Greymouth
WLL172	RR-17	4-11 Silt	3	0.1386±0.0069	1.336	3.80±0.44	4.23±0.27	4.77±0.61	15.2±0.5	3.26±0.14	0.057±0.008	319.3±43.0	5.02±0.48	63.6±10.5	Power Road, Karoro

WLL151	RR-18	Sand	4	0.1221±0.0061	1.175	2.79±0.37	3.08±0.21	3.40±0.49	12.1±0.5	1.97±0.12	N/A		3.21±0.22		Power Road, Karoro
WLL173	RR-19	Sand	1.5	0.1692±0.0085	1.198	6.71±0.65	6.74±0.24	6.23±0.73	45.0±1.0	1.38±0.11	N/A		5.47±0.37		Rapahoe Beach
Mean		Silt Sand All		0.0904			3.76 3.79 3.78±0.19		12.16 17.65 15.72	1.90 1.56 1.78	0.0635 0.048 0.0595		3.52 3.54 3.53		

Table A4.4b Dosimetry for luminescence dating of silt samples from North Westland (2nd sampling round, this PhD project)

Sample no.	**Field code**	**Grain-size (µm)**	**Depth below surface (m)**	**dD_e/dt (Gy/ka)[1] (Cosmic radiation)**	**Water content**	**U (µg/g) from ^{234}Th**	**U (µg/g)[2] from ^{226}Ra, ^{214}Pb, ^{214}Bi**	**U (µg/g) from ^{210}Pb**	**Th (µg/g)[2] from ^{208}Tl, ^{212}Pb, ^{228}Ac**	**K (%)**	***a*-value**	**D_e (Gy) (IRSL(blue)**	**dD/dt (Gy/ka)**	**OSL-age (ka) ($IRSL_{blue}$)**	**Location**
WLL524	RR20	4 to 11	4.75	0.1104±0.0055	1.306	3.34±0.24	3.16±0.16	3.70±0.23	11.29±0.14	1.67±0.04	0.123±0.021	165.4±21.0	3.89±0.38	**42.5±6.8**	Schulz Creek, SH6, 12 Mile
WLL526	RR21	"	4.5	0.1138±0.0057	1.307	3.70±0.24	3.63±0.17	3.95±0.23	14.18±0.16	2.09±0.04	0.090±0.007	152.9±5.3	4.34±0.37	**35.3±3.2**	SH7, Kamaka, Grey Valley
WLL527	RR22	"	3	0.1373±0.0069	1.375	2.65±0.25	2.73±0.17	2.99±0.24	10.06±0.14	2.90±0.06	0.154±0.011	384.8±11.9	4.56±0.45	**84.3±8.7**	South Beach, Greymouth
WLL528	RR23	"	4.5	0.1138±0.0057	1.257	3.08±0.24	3.21±0.16	3.43±0.22	14.08±0.17	2.01±0.04	0.096±0.010	288.4±11.8	4.39±0.34	**65.7±5.7**	South Beach, Greymouth
WLL529	RR24	"	0.95	0.1807±0.0090	1.215	3.27±0.20	3.03±0.13	3.48±0.18	13.45±0.14	1.82±0.04	0.086±0.012	227.2±8.4	4.22±0.30	**53.8±4.3**	Chesterfield Rd, Chesterfield
WLL530	RR25	"	3.5	0.1288±0.0064	1.306	4.08±0.32	4.02±0.21	4.19±0.29	13.72±0.18	1.97±0.04	0.095±0.008	334.2±18.1	4.41±0.37	**75.9±7.6**	Upper Sunday Creek
WLL531	RR26	"	5	0.1072±0.0054	1.229	4.35±0.29	3.72±0.18	4.11±0.25	15.08±0.18	2.05±0.04	0.081±0.034	332.0±11.0	4.63±0.55	**71.7±8.8**	Candle Light, Camerons
WLL532	RR27	"	7.5	0.0808±0.0040	1.307	4.13±0.28	3.20±0.18	3.66±0.25	13.11±0.16	2.58±0.05	0.08±0.02*	418.5±15.5	4.34±0.43	**96.5±10.2**	Candle Light, Camerons
WLL533	RR28	"	1.2	0.1746±0.0087	1.299	3.95±0.26	3.71±0.17	3.92±0.24	12.27±0.15	1.60±0.03	0.062±0.004	278.7±9.7	3.57±0.29	**78.1±6.8**	Kapitea Reservoir
WLL534	RR29	"	14.5	0.0421±0.0021	1.183	3.34±0.34	3.10±0.25	3.73±0.30	12.85±0.19	1.96±0.05	0.076±0.020	355.3±8.6	4.18±0.34	**84.9±7.2**	Blakes Terrace, Awatuna
WLL535	RR30	"	1.3	0.1722±0.0086	1.259	3.53±0.35	3.13±0.23	3.29±0.30	21.75±0.27	0.80±0.02	0.069±0.011	243.5±19.8	3.83±0.31	**63.6±7.4**	Blakes Terrace, Awatuna
WLL536	RR33	"	1.1	0.1770±0.0089	1.392	3.92±0.28	2.88±0.17	3.28±0.24	13.43±0.17	1.39±0.03	0.087±0.019	183.6±12.1	3.26±0.35	**56.3±7.1**	South Beach, Greymouth
WLL537	RR34	"	2.2	0.1525±0.0076	1.3	3.77±0.33	3.20±0.21	3.17±0.27	17.21±0.22	1.59±0.04	0.048±0.006	337.2±19.8	3.64±0.30	**92.5±9.4**	South Beach, Greymouth
Mean		**4 to 11 µm**			**1.29**	**3.62±0.28**	**3.29±0.18**	**3.6±0.25**	**14.04±0.17**	**1.88±0.04**	**0.088±0.14**		**4.097±0.37**		

Table A4.4c Dosimetry for luminescence dating of silt in samples from Westport (PhD project, Burge 2007)

Sample no.	Field code	Grain-size (µm)	Depth below surface (m)	dD_e/dt (Gy/ka)[1] (Cosmic radiation)	Water content	U (µg/g) from ^{234}Th	U (µg/g)[2] from ^{226}Ra, ^{214}Pb, ^{214}Bi	U (µg/g) from ^{210}Pb	Th (µg/g)[2] from ^{208}Tl, ^{212}Pb, ^{228}Ac	K (%)	*a*-value	D_e (Gy) (IRSL(blue)	dD/dt (Gy/ka)	OSL-age (ka) ($IRSL_{blue}$)	Location
WLL451	KR-B2		3.5	0.1300± 0.0065	1.357	5.23± 0.33	3.98± 0.06	5.29±0.3	14.91± 0.17	2.15± 0.05	0.069± 0.005	126±3.3	4.46±0.38 (4.11±0.38)	28.4±2.9 (30.6±2.9)	Keoghans Road, Westport
WLL452	KR-A3		4.7	0.114± 0.0056	1.252	6.57± 0.46	4.7±0.07	5.49± 0.39	16.68± 0.21	3.21± 0.07	0.076± 0.008	226±23.5	6.25±0.45 (5.9±0.45)	36.2±4.9 38.4±4.9	"

Table A4.4d Dosimetry for luminescence dating of silt in samples from North Westland by Preusser et al (2005)

Sample No.	Grain-size (µm)	Depth below surface (m)	Water content in age calculation (%)	U (ppm)	Th (ppm)	K (%)	De (TL methods) (Gy)	De IRSL (blue) (Gy)	dD/dt (Gy/ka) Optical methods	dD/dt (Gy/ka) TL methods	IRSL (blue) age (ka)	TL age (ka)	Location
BSG5	4 to 11	0.9	25±5	3.17±0.11	12.56±0.58	1.07±0.02	73.2±2.2 UV		3.3±0.3			22.0±2.2 UV	Hokitika Gravel Quarry
BSG4	"	1	25±5	3.14±0.11	12.69±0.58	1.09±0.02	73.2±1.4 UV		3.3±0.3			21.9±2.1 UV	Hokitika Gravel Quarry
KMK7	"	13	25±5	3.12±0.09	12.04±0.36	1.40±0.05	250±69 blue	96.7±6.1	3.4±0.3	3.5±0.3	**28.5±3.2**	71±20 blue	SH7, Kamaka
KMK6	"	14	25±5	3.28±0.10	12.33±0.37	1.68±0.05	93±6.9 blue	80.6±10	3.4±0.3	3.6±0.3	**23.4±3.6**	26.1±2.9 blue	SH7, Kamaka
KMK4	"	14	35±5	3.03±0.09	13.12±0.39	1.69±0.05	258±40 blue	130±13	3.3±0.3	3.4±0.3	**39±5**	75±13 blue	SH7, Kamaka
KMK3	"	14	35±5	3.09±0.09	12.51±0.38	1.72±0.05	288±51 blue	151±5	3.4±0.3	3.5±0.3	**45±4**	83±16 blue	SH7, Kamaka
KMK2	"	14	35±5	3.38±0.10	12.50±0.37	1.69±0.05	302±122 blue	142±12	3.5±0.3	3.6±0.3	**41±5**	84±35 blue	SH7, Kamaka
KMK1	"	14	35±5	2.94±0.09	13.18±0.40	1.48±0.05	56.5±12 blue	64±4	3.2±0.3	3.3±0.3	**20.2±2.1**	17.3±4.0 blue	SH7, Kamaka
NCL4	"	0.8	25±5	3.05±0.10	13.42±0.62	1.26±0.03	49.9±2.5 UV		3.5±0.3			14.1±1.5 UV	Nelson Creek/Bell Hill
NCL3	"	0.6	25±5	3.03±0.10	13.47±0.62	1.21±0.03	54.5±3.0 UV		3.5±0.3			15.6±1.7 UV	Nelson Creek/Bell Hill
PGM11	"	0.3	25±5	2.23±0.08	7.15±0.33	0.70±0.01	43.6±4.0 UV		2.3±0.2			19.3±2.5 UV	Phelps Gold Mine, Southside
PGM10	"	0.1	25±5	2.76±0.09	11.37±0.52	1.07±0.02	69.5±3.6 UV		3.1±0.3			22.4±2.3 UV	Phelps Gold Mine, Southside
PGM9	"	10	25±5	2.90±0.10	11.56±0.53	1.39±0.03	247±14 UV		3.3±0.3			76±8 UV	Phelps Gold Mine, Southside

PGM8	"	10	25±5	3.01±0.10	12.49±0.57	1.48±0.03	213±10 UV		3.5±0.3			61±6 UV	Phelps Gold Mine, Southside
PGM7	"	10	25±5	1.89±0.06	7.94±0.33	0.97±0.02	156±5 UV		2.2±0.2			69±6 UV	Phelps Gold Mine, Southside
PGM6	"	10	25±5	2.95±0.10	11.57±0.53	1.35±0.03	189±4 UV		3.3±0.3			58±6 UV	Phelps Gold Mine, Southside
PGM5	"	22	25±5	2.37±0.09	10.49±0.48	1.21±0.03	181±5 UV		2.9±0.3			63±6 UV	Phelps Gold Mine, Southside
PGM4	"	22	25±5	2.57±0.09	12.50±0.37	1.72±0.05	988±122 blue	272±15	3.6±0.3	3.8±0.3	**74±8**	261±49 blue	Phelps Gold Mine, Southside
PGM3	"	22	25±5	3.38±0.10	13.18±0.40	1.69±0.05	264±30 blue	252±21	3.8±0.3	3.9±0.3	**66±8**	67±10 blue	Phelps Gold Mine, Southside
PGM2	"	22	25±5	2.94±0.09	12.72±0.38	1.48±0.05	726±127 blue	259±57	3.4±0.3	3.6±0.3	**76±18**	204±40 blue	Phelps Gold Mine, Southside
PGM1	"	22	25±5	2.40±0.07	9.76±0.29	0.79±0.02	188±12 blue	169±11	2.4±0.2	2.5±0.2	**67±8**	75±9 blue	Phelps Gold Mine, Southside
PIC1	"	10	25±5	2.75±0.14	10.08±0.50	1.00±0.05	252±19 blue	204±36	2.8±0.3	2.9±0.3	**74±15**	87±10 blue	Pine Creek, Southside
PIC2	"	10	25±5	2.80±0.08	10.85±0.33	1.30±0.04	225±24 blue	243±36	3.1±0.3	3.2±0.3	**78±14**	70±10 blue	Pine Creek, Southside
PIC3	"	22	15±5	2.62±0.08	11.61±0.35	1.77±0.05	369±43 blue	237±25	3.1±0.3	3.2±0.3	**76±11**	114±17 blue	Pine Creek, Southside
RPO1	"	8.5	25±5	3.80±0.19	13.93±0.70	2.09±0.10			4.4±0.4				Raupo, upper gravel
RPO2	"	8.5	30±5	4.27±0.10	15.66±0.71	1.77±0.08			4.3±0.4				Raupo, upper gravel
RUG2	"	3.5	25±5	1.90±0.06	15.39±0.71	1.88±0.04		70.8±1.8	3.7±0.3		**18.9±1.6**		Raupo, lower gravel
SDC8	"	14	35±5	3.10±0.09	11.27±0.34	1.17±0.04	230±19 blue	165±12	2.9±0.3	3.0±0.3	**58±7**	78±9 blue	Sunday Creek
SDC7	"	14	30±5	2.70±0.08	9.09±0.27	1.24±0.03	226±16 blue	166±16	2.7±0.2	2.8±0.2	**61±8**	81±9 blue	Sunday Creek
SDC5	"	14	80±20	2.44±0.07	10.03±0.30	0.98±0.03	167±14 blue	102±5	1.8±0.2	1.9±0.2	**58±8**	94±14 blue	Sunday Creek
SDC4	"	14	40±5	1.96±0.06	7.97±0.24	0.72±0.02	150±14 blue	133±14	1.9±0.2	2.0±0.2	**71±10**	77±1 blue	Sunday Creek
UCS3	"	0.3	25±5	3.01±0.10	10.10±0.46	0.94±0.02			3.0±0.3				Upper Chesterfield Road
UCS2	"	0.5	25±5	2.80±0.08	8.56±0.39	0.67±0.01			2.5±0.3				Upper Chesterfield Road
Mean			**29**	**2.87**	**11.61±0.43**	**1.32±0.04**			**3.145±0.3**	**3.16±0.3**			

Table A4.4e Dosimetry for luminescence dating of sand in samples from North Westland by Preusser et al (2005)

Sample	Water Content in age calc (%)	Depth (m)	K Feldspar Internal dose due to 40K &87Rb	Grainsize (µm)	Total U (ppm)	Th (ppm)	K (%)	dD/dt (Gy/ka) Optical methods	Dose (Gy)	IRSL (blue) Age (ka)	Location
BSG3	15±5	2.6	0.6±0.1	150-200	2.54±0.09	11.52±0.53	1.72±0.04	3.5±0.2	305±23	**88±8**	Hokitika Gravel Quarry
BSG2	15±5	2.6	0.6±0.1	150-200	2.70±0.09	12.05±0.55	1.77±0.04	3.6±0.2	305±18	**85±6**	Hokitika Gravel Quarry
BSG1	15±5	2.6	0.8±0.1	200-250	2.44±0.08	11.21±0.52	1.84±0.04	3.6±0.2	300±27	**82±8**	Hokitika Gravel Quarry
KMK8	25±5	13	0.5±0.2	100-200	2.90±0.09	12.04±0.36	1.49±0.05	3.0±0.2	73.2±2.7, 77.4±5.7	**24±1.5, 25.8±2.4**	SH7, Kamaka
KMK5	25±5	14	0.5±0.2	100-200	2.24±0.07	9.14±0.27	1.69±0.05	2.8±0.2	68.9±2.0, 62.0±4.9	**24.3±1.5, 21.8±2.1**	SH7, Kamaka
LOL1	15±5	2	0.6±0.1	150-200	2.21±0.08	9.21±0.42	1.84±0.04	3.3±0.1	214±15	**64±5**	Stafford Loop Road Gravel Quarry
NCL2	15±5	2.8	0.9±0.1	250-300	2.02±0.07	8.84±0.41	1.67±0.04	3.6±0.1	400±24	**113±8**	Nelson Creek Gavel Quarry
NCL1	25±5	2.8	0.9±0.1	150-200	1.99±0.07	9.36±0.43	1.75±0.04	3.4±0.1	372± 23	**109±8**	Nelson Creek Gavel Quarry
RGL2	15±5	16	0.8±0.1	200-250	1.94±0.07	9.36±0.43	1.80±0.04	3.3±0.1	100±7	**31±2**	Raupo lower gravel
RGL1	15±5	16	0.8±0.1	200-250	1.8±0.06	8.05±0.37	1.92±0.04	3.3±0.1	109±12	**33±4**	Raupo lower gravel
RUG3	15±5	3.5		100-150	5.69±0.19	25.21±1.16	1.92±0.04	5.2±0.3	52.6±2.0	**10.1±0.7**	Raupo upper gravel
RUG1	15±5	1	0.8±0.1	200-250	1.34±0.05	6.00±0.28	1.74±0.04	3.0±0.1	70.8±1.8	**16.1±1.1**	Raupo upper Gravel
SDC6	30±5	15		100-200	5.22±1.16?	32.98±0.99	0.96±0.03	4.2±0.2	297±29	**71±±8**	Sunday Creek, Chesterfield
SDC3	30±5	15	0.5±0.2	100-200	4.00±0.12	24.76±0.74	0.71±0.03	3.3±0.2	209±14	**65±5**	Sunday Creek, Chesterfield
SDC2	30±5	15	0.5±0.2	100-200	4.16±0.12	25.14±0.75	0.89±0.03	3.5±0.2	282±52	**81±11**	Sunday Creek, Chesterfield
SDC1	30±5	15	0.5±0.2	100-200	2.78±0.08	16.55±0.50	1.11±0.03	2.9±0.2	338±79	**118±18**	Sunday Creek, Chesterfield
UCS1	15±5	1.1	0.8±0.1	200-250	2.03±0.07	8.35±0.38	1.76±0.04	3.3±0.1	271±20	**81±7**	Upper Chesterfield Road
			0.71		**2.82±0.15**	**14.14±0.53**	**1.56±0.035**	**3.46±0.18**			
						10.84±0.47 excluding SDC1, SDC2, SDC3, & SDC6					

Table A4.4f Dosimetry for luminescence dating of samples from Okarito by Vandergoes et al (2005)

Core	Sample No.	Depth below surface (cm)	Water content in age calculation (%)	U (ppm)	Th (ppm)	K (%)	De (Gy) (TL & Post-IR-OSL methods)	De (Gy) (IRSL (blue)	dD/dt (Gy/ka) Optical methods	dD/dt (Gy/ka) TL methods	IRSL (blue) age (ka)	TL(UV) & Post-IR-OSL age (ka)	Location
OOO4	BPB 1	210-220	34.5	1.21 ± 0.02	5.78 ± 0.12	0.55 ± 0.01	30 ± 1	34 ± 2	1.2 ± 0.1	1.2 ± 0.1	**28 ± 3**	24 ± 3	Okarito
	BPB 2	307-317	32.6	1.31 ± 0.03	7.10 ± 0.14	0.52 ± 0.01	281 ± 72	126 ± 6	1.3 ± 0.1	1.4 ± 0.1	**97 ± 12**	208 ± 58	Okarito
	BPB 3	327-337	28.5	1.59 ± 0.03	8.08 ± 0.16	0.55 ± 0.01	91 ± 29	84 ± 15	1.5 ± 0.2	1.5 ± 0.2	**57 ± 12**	60 ± 20	Okarito
	BPB 4	342-352	31.5	1.69 ± 0.05	8.37 ± 0.17	0.71 ± 0.01	80 ± 4	77 ± 6	1.6 ± 0.2	1.7 ± 0.2	**48 ± 6**	48 ± 6	Okarito
	BPB 5	362-372	37.8	2.19 ± 0.04	8.76 ± 0.18	0.87 ± 0.02	144 ± 12	139 ± 10	1.8 ± 0.2	1.9 ± 0.2	**75 ± 10**	75 ± 10	Okarito
O113	OKA 6	288-297	32.1	2.25 ± 0.10	10.92 ± 0.22	1.47 ± 0.13		40 ± 4	2.4 ± 0.3		**17 ± 3**		Okarito
	OKA 5	300-307	36.2	2.22 ± 0.10	10.33 ± 0.22	1.51 ± 0.13		40 ± 4	2.3 ± 0.3		**17 ± 3**		Okarito
0112b	OKA 4	761-765	29.8	2.40 ± 0.11	10.16 ± 0.21	2.33 ± 0.21		306 ± 80	2.9 ± 0.3		**107 ± 30**		Okarito
	OKA 3	780-794	27.8	2.27 ± 0.10	10.81 ± 0.23	4.64 ± 0.41		744 ± 195	4.2 ± 0.4		**177 ± 49**		Okarito
	OKA 2	806-816	31.2	2.54 ± 0.11	11.29 ± 0.24	3.91 ± 0.35		saturation	3.9 ± 0.4		**-**		Okarito
	OKA 1	821-828	27.8	2.49 ± 0.11	11.85 ± 0.25	3.98 ± 0.35		528 ± 247	4.0 ± 0.4		**133 ± 64**		Okarito
O212	OBC-1	245-253	52.4	1.55 ± 0.07	6.09 ± 0.13	0.47 ± 0.04	15.9 ± 1.0	18.1 ± 0.8	1.4 ± 0.1		**13.3 ± 1.3**	11.7 ± 1.3	Okarito
	OBC-2	253-258	55.9	1.52 ± 0.07	7.59 ± 0.16	0.57 ± 0.05	19.2 ± 0.8	19.3 ± 0.6	1.5 ± 0.1		**12.6 ± 1.2**	12.5 ± 1.2	Okarito
	OBC-3	283-287	26.8	1.91 ± 0.08	9.13 ± 0.19	0.93 ± 0.08	37.1 ± 1.1	37.9 ± 1.1	2.4 ± 0.2		**16.0 ± 1.4**	15.6 ± 1.3	Okarito
	OBC-4	287-291	27	2.07 ± 0.09	10.87 ± 0.23	1.15 ± 0.10	42.9 ± 2.2	41.8 ± 0.5	2.8 ± 0.2		**15.2 ± 1.2**	15.6 ± 1.5	Okarito
	OBC-5	291-302	36.4	1.92 ± 0.08	7.78 ± 0.13	1.09 ± 0.10	46.7 ± 2.0	49.7 ± 1.9	2.2 ± 0.2		**22.7 ± 1.9**	21.3 ± 1.9	Okarito
0212b	OBD-1	285-290	50.2	2.63 ± 0.12	9.80 ± 0.21	1.27 ± 0.11	32.1 ± 0.9	32.3 ± 0.4	2.5 ± 0.2		**13.2 ± 1.1**	13.1 ± 1.2	Okarito
	OBD-2	296-300	24.8	2.61 ± 0.11	11.92 ± 0.25	1.04 ± 0.10	37.2 ± 2.1	40.2 ± 1.0	3.0 ± 0.3		**13.3 ± 1.2**	12.4 ± 1.3	Okarito
	OBD-3	306-311	21.4	2.56 ± 0.11	10.29 ± 0.22	1.14 ± 0.10	47.5 ± 1.5	48.7 ± 1.5	3.0 ± 0.3		**16.2 ± 1.4**	15.8 ± 1.4	Okarito
	OBD-4	316-321	20.1	2.47 ± 0.11	8.88 ± 0.19	1.13 ± 0.10	48.1 ± 0.8	52.6 ± 1.8	2.9 ± 0.2		**18.4 ± 1.6**	16.8 ± 1.4	Okarito
	OBD-5	329-333	20.9	2.37 ± 0.10	9.56 ± 0.20	0.88 ± 0.08	64.7 ± 1.8	65.0 ± 1.6	2.7 ± 0.2		**24.4 ± 2.1**	24.3 ± 2.2	Okarito
	OBD-6	339-343	21.3	2.21 ± 0.10	7.93 ± 0.17	0.94 ± 0.08	80.1 ± 1.6	75.8 ± 1.0	2.5 ± 0.2		**30.6 ± 2.5**	32.3 ± 2.7	Okarito
	OBD-7	350-354	24.9	2.73 ± 0.12	11.80 ± 0.25	1.19 ± 0.10	80.6 ± 2.4	80.2 ± 0.6	3.2 ± 0.3		**25.5 ± 2.1**	25.6 ± 2.2	Okarito
	OBD-8	359-363	22.3	2.29 ± 0.10	7.72 ± 0.16	1.04 ± 0.10	87.6 ± 1.7	86.7 ± 1.2	2.5 ± 0.2		**34.1 ± 2.8**	34.5 ± 2.9	Okarito
	OBD-9	368-372	17.8	2.17 ± 0.10	9.21 ± 0.19	0.87 ± 0.08	90.0 ± 3.9	88.3 ± 2.8	2.6 ± 0.2		**33.7 ± 2.9**	34.3 ± 3.1	Okarito
	OBD-10	381-385	16.9	2.41 ± 0.11	8.89 ± 0.19	0.89 ± 0.08	93.1 ± 3.4	86.2 ± 2.3	2.7 ± 0.2		**31.8 ± 2.8**	34.3 ± 3.2	Okarito
	OBD-11	385-389	18.1	2.15 ± 0.09	8.45 ± 0.18	0.87 ± 0.08	93.2 ± 2.1	87.5 ± 1.3	2.5 ± 0.2		**34.7 ± 2.9**	37.0 ± 3.2	Okarito
	OBD-12	389-393	22.2	2.35 ± 0.10	9.07 ± 0.19	1.15 ± 0.10	90.8 ± 1.8	88.9 ± 1.5	2.8 ± 0.2		**31.9 ± 2.6**	32.6 ± 2.7	Okarito
	OBD-13	421-425	43.1	2.79 ± 0.12	8.26 ± 0.17	1.26 ± 0.11	114.6 ± 5.6	111.1 ± 3.6	2.5 ± 0.2		**44.9 ± 3.8**	46.3 ± 4.3	Okarito
	OBD-14	445-450	29.7	3.05 ± 0.13	11.67 ± 0.25	1.34 ± 0.12	136.2 ± 2.6	138.7 ± 3.7	3.2 ± 0.3		**43.2 ± 3.7**	42.4 ± 3.6	Okarito
	OBD-15	450-453	23.9	3.00 ± 0.13	7.16 ± 0.15	1.27 ± 0.11	148.6 ± 7.9	138.7 ± 4.8	2.9 ± 0.2		**48.4 ± 4.2**	51.8 ± 5.0	Okarito
	OBD-16	456-461	20	2.24 ± 0.10	8.59 ± 0.18	0.85 ± 0.08	132.3 ± 3.0	125.0 ± 2.4	2.5 ± 0.2		**50.1 ± 4.3**	53.0 ± 4.6	Okarito
	OBD-17	485-489	77.4	2.30 ± 0.10	10.95 ± 0.23	1.29 ± 0.11	121.0 ± 6.7	111.6 ± 3.5	2.0 ± 0.2		**54.6 ± 4.6**	59.3 ± 5.7	Okarito
	OBD-18	489-492	51.2	2.30 ± 0.10	6.35 ± 0.13	1.10 ± 0.10	132.7 ± 4.5	128.6 ± 3.4	1.9 ± 0.2		**66.4 ± 5.4**	68.5 ± 5.8	Okarito
Mean				**2.23±0.09 ppm**	**9.16±0.19 ppm**	**1.32±0.10 %**			**2.51±0.2**	**1.54±0.16**			

Table A4.4g Dosimetry for luminescence dating of silt in samples from Westland by Berger et al (2001)

Sample No.	Grain-size (µm)	Method	Water content used in age calculation	U (ppm)	Th (ppm)	K_2O (%) (±0.05)	De (TL &IRSL methods) (Gy)	dD/dt (Gy/ka) TL& IRSL methods	b value (pGy/m^2)	IRSL (blue) age (ka)	TL age (ka)	Location
BSR91-5	4-11	TL/E	0.17±0.03	2.40±0.25	5.10±0.8	0.52	105±15	2.24±0.11	0.69±		46.9±7.3	Blue Spur
	4-11		0.27±0.03	3.62±0.41	11.4±1.3	1.25						"
BSR91-9	4-11	TL/E+L	0.25±0.05	3.5±0.44	11.4±1.4	1.13	129±45	2.75±0.20	0.61±		53±16	"
	4-11	TL/E+L		3.44±0.43	9.2±1.7	1.00	147±43					"
BSR91-1	4-11	IRSL/E	0.18±0.05	3.85±0.48	11.2±1.6	2.92	214±83	4.82±0.31	1.0±	44±17		"
HR191-5	4-11	TL/E	0.39±0.04	3.71±0.43	11.5±1.4	1.48	107±9	2.96±0.12	0.732± 0.086		36.2±3.4	Saltwater Forest
HR191-1	4-11	TL/Q-SL	0.46±0.02	3.65±0.44	13.0±1.5	1.69	990±160	3.04±0.17	1.0±0.2		324±55	"
	4-11	IRSL/E	0.39±0.03	3.47±0.38	8.9±1.2	1.22	271±46			89±15		"
HR191-16	4-11	TL/Q-SL	0.38±0.03	3.48±0.35	13.9±1.2	1.68	770±110	3.15±0.13	1.0.±0.2		244±35	"
	4-11	IRSL/E	0.47±0.05	3.97±0.39	9.8±1.3	1.54	205±49			66±16		"
HR191-12	4-11	TL/E+L	0.37±0.03	4.03±0.44	10.4±1.4	1.75	288±90	3.31±0.18	1.0±0.2		87±30	"
	4-11	IRSL/E	0.32±0.03	3.48±0.40	10.7±1.3	1.48	480±120			145±36		"
HR191-8	4-11	TL/E+L	0.36±0.03	3.76±0.45	12.5±1.5	1.35	80±20	3.08±0.20	1.0±0.2		26±7	"
	4-11	IRSL/E	0.32±0.03	2.81±0.38	9.9±1.5	1.34	111±16			36±5.7		"
Mean	**4-11**			**3.25±0.41**	**10.64±1.3**	**1.45±0.05**		**3.17±0.18**				

Cooper & Kostro 2006 NZJGG 49: 203-216. Samples from a raised marine terrace, Knights Point, South Westland

Field Code	Laboratory code	Depth	dD_c/dt (Gy/ka)[1]	K (%)	Th (ppm)	U (ppm)	Total dose rate (mGy/a)	Equivalent dose (Gy)	Age (ka)
KP-01-TL	WLL287	1	0.1863	0.073±0.002	2.59±0.17	0.48±0.02	0.844±0.041	103.8±3.1	123.0±7.0
KP-03-TL	WLL288	4	0.1256	0.052±0.002	2.58±0.25	0.47±0.02	0.713±0.035	104.1±3.1	146.0±8.4

1 Contribution of cosmic radiation to the total dose rate, calculated as proposed by Prescott & Hutton (1995).
2 Ratio wet sample to dry sample weight. Errors assumed 50% of (δ–1).
3 U and Th-content is calculated from the error weighed mean of the isotope equivalent contents.
4 Errors are 1σ.

Table A4.4h: Site data for exposure ages

Sample	Longitude (°E)	Latitude (°S)[1]	Altitude (m)	Scaling factor	Scaling factor	Horizon correction	Thickness correction[2]
Loopline Formation (Loop Line Road, Kumara)							
LL-01	171.1911	42.6976	150	1.108	1.033	1.0	0.9710/1.299/0.9725
LL-02	171.1924	42.6990	150	1.102	1.028	1.0	0.9916
LL-04	171.1870	42.6919	165	1.117	1.035	1.0	0.9850
LL-05	171.1868	42.6914	165	1.117	1.035	1.0	0.9670
LL-06	171.1892	42.6899	165				
Loopline Formation (Arnold River valley)							
LPL-01	171.4305		148	1.103	1.030	1.0	0.9894/1.107/1.013
LPL-02	171.4344		156	1.106	1.029	1.0	0.9941
LPL-03	171.4275		145	1.100	1.029	1.0	0.9889/1.102/1.026
LPL-04	171.4204		142	1.091	1.022	1.0	0.9791
LPL-05	171.4252		150	1.100	1.026	1.0	0.9606
Loopline Formation (Molloys Lookout)							
LPL-06	171.4690		235	1.189	1.069	1.0	0.9804
LPL-07	171.4694		229	1.182	1.066	1.0	0.9797
Loopline Formation (Bell Hill Farm)							
LPL-08	171.5981		264	1.221	1.085	1.0	0.9787
LPL-09			253	1.215	1.084	1.0	0.9751/1.254/0.9935
LPL-11	171.6026		253				
Moana Formation (Lake Brunner)							
MNA-01	171.4652	42.5760	107	1.062	1.011	1.0	0.9843/1.144/1.032
MNA-02	171.4660	42.5756	103	1.058	1.009	1.0	0.9590/1.356/1.030
MNA-03	171.4647	42.5763	106	1.056	1.005	1.0	0.9727
MNA-04	171.5068	42.5850	111	1.061	1.008	1.0	0.9874
MNA-05	171.5154	42.5940	149	Not run			
MNA-06	171.5172	42.5923	167	1.118	1.035	1.0	0.9661
MNA-07	171.5225	42.5930	153	1.104	1.028	1.0	0.9847
MNA-08	171.5168	42.5920	155	1.106	1.029	1.0	0.9751
MNA-09	171.5419	42.5927	159	1.110	1.031		0.9757
MNA-10	171.5470	42.5939	163	1.114	1.034	1.0	0.9630
LAR-09	171.5625	42.5799	180	1.131	1.042	1.0	0.9804
Larrikins Formation (Lake Brunner)							
LAR-01	171.5442	42.5578	226	1.186	1.071	1.0	0.9874/1.137/0.9986
LAR-02	171.5526	42.5526	233	1.187	1.069	1.0	0.9710

LAR-03	171.5740	42.5752	223	1.177	1.064	1.0	0.9860
LAR-04	171.5682	42.5741	224	1.178	1.064	1.0	0.9802
LAR-05	171.5581	42.5530	232	1.186	1.068	1.0	0.9725
LAR-06	171.5606	42.5532	232	1.186	1.068	1.0	0.9855
LAR-07	171.5355	42.5632	184	1.141	1.049	1.0	0.9808/1.195/1.006
LAR-08	171.5369	42.5638	178	1.129	1.041	1.0	0.9867
LAR-10	171.5573	42.5594	231	1.185	1.068	1.0	0.9730
LAR-11	171.5605	42.5466	220	1.173	1.062	1.0	0.9499
LAR-12	171.5598	42.5382	218	1.171	1.061	1.0	0.9820
LAR-13	171.5683	42.5428	220	1.179	1.067	1.0	0.9737/1.259/0.9926
LAR-14	171.5266	42.5357	229	1.183	1.067	1.0	0.9558
LAR-15	171.5111	42.5370	214	Not run			
LAR-16	171.5110	42.5360	212	1.171	1.063	1.0	0.9790/1.192/1.035
LAR-17	171.4581	42.5222	149	1.099	1.026	1.0	0.9804
LAR-18	171.4447	42.5220	143	1.093	1.023	1.0	0.9788
LAR-19	171.4399	42.5262	147	1.097	1.025	1.0	0.9846
LAR-20	171.4352	42.5222	146	1.096	1.024	1.0	0.9870

ρ = 3.0 g.cm^{-3}; Λ = 160 g.cm;

1 Geomagnetic latitude?.

2 Correction factors for spallation, thermal neutrons, and epithermal neutrons respectively (where applicable for ^{36}Cl sample

APPENDIX FIVE

Alluvial gold adjacent to glacial margins, West Coast, South Island, New Zealand

R.V. Rose

A paper presented at the 2000 New Zealand Minerals & Mining Conference

Wellington, 29-31 October 2000.

Conference Proceedings p 137-162.

Alluvial gold adjacent to glacial margins, West Coast, South Island, New Zealand

R Rose

Resource Management Services, PO Box 354, Greymouth, Telephone 0064-3-768 7137, Email rob&karen@minidata.co.nz

Abstract

A substantial proportion of current and historic West Coast gold production comes from deposits situated around the margins of "ice age" glaciers. Gold has been eroded and transported by glacial ice then deposited in till and outwash gravel. The interplay between fluvial and glacial processes, climate, basement geology, tectonic uplift, sediment supply and sea level dictates many aspects of the development of the West Coast landscape. The way in which the external forcing factors interact is crucial in determining the gold content of placer deposits in this region. The following is an outline of some of the factors that influence the gold distribution in vicinity of glacial margins.

Introduction

The West Coast has contributed around 25% of New Zealand's annual gold production over the last 5 to 10 years. Total reported placer production is around 8.6 million ounces. All of the gold produced in this region since the 1950s has come from placer deposits.

At least 75% (more than 6 million ounces) of the placer gold produced from this region has come from proximal fluvioglacial deposits and "secondary" deposits formed through the erosion of proximal deposits. This environment and these types of deposit have not been described in detail in the mining and economic geology literature. The intent of this paper is to discuss the structure and origin of such deposits. It expands on some of the ideas previously outlined by Jury and Hancock (1989) and Suggate (1996).

Regional geology and climate

Physiography

The West Coast is a long narrow region confined between steep mountain ranges to the east and the Tasman Sea to the west. In between are foothills to the main ranges, terraced river valleys and a narrow, discontinuous coastal plain.

Gold bearing alluvial deposits are situated primarily in the lower lying areas beneath river/stream floodplains, on terraces flanking the floodplains and on raised marine terraces that trend sub-parallel to the modern coastline. Most of the alluvium is derived from the mountainous parts of the region. Sediment transport occurs via one or more of the following: landslides, glaciers, rivers, streams, and marine longshore drift.

Plate tectonics and continental collision

The primary tectonic feature within the region is the Alpine Fault, the single largest fracture zone within the New Zealand section of the Australian-Pacific plate boundary. Most of the displacement within the plate boundary occurs at the Alpine Fault. A lesser proportion is distributed across a wide zone that includes the Southern Alps. The fault divides the region into two areas underlain by basement rock of contrasting character. It also separates the region into contrasting physiographic zones: the Southern Alps (to the east) and the West Coast lowlands & foothills (to the west).

Continental collision within the plate boundary zone produces a combination of horizontal and vertical movement. The Alpine Fault is oriented at an angle such that it dips to the southeast under the Southern Alps. For at least 5 to 6 million years rock on the Southern Alps side of the fault has been continually pushed west-southwest and upward on an oblique angle across the fault plane.

Vertical uplift of basement rock situated between the Alpine Fault and the Main Divide of the Southern Alps amounts to at least 15 km over the last 5-6 million years. In some places uplift could be as great as 20-25 km. This is balanced by a similar amount of surface erosion. The Southern Alps represent the difference between total uplift and total erosion. Presently, uplift is at a maximum in the Mt Cook area where the rate is probably around 10-12 mm per year (~ 1 km per 100,000 years).

The modern rate of horizontal displacement at the Alpine Fault in Westland is around 30 mm per year. The fault has been active for at least 18 million years and is responsible for at least 450 km of horizontal displacement.

A lesser proportion of relative plate motion occurs within the West Coast lowlands and in offshore areas. In the lowlands uplift is much slower than in the Southern Alps but its effects are important with respect to placer geology. At present uplift rates are thought to be no greater than 0.5 mm per year in the lowlands. In the Paparoa and Victoria Ranges rates could be as high as 2 mm per year.

The primary influences of the plate boundary zone on placer geology are:

- Its role over several million years in the uplift and exposure of gold bearing basement rocks (Alpine Schist in the Southern Alps and Greenland group west of the Alpine Fault). This has provided sources for gold bearing coarse clastic sediment that has been deposited in West Coast sedimentary basins.
- Its indirect effect on regional climate by uplifting the Southern Alps which intercept the moist westerly airflow, causing orographic rainfall.
- Its role in the uplift and recycling of relatively young gold bearing clastic deposits resulting in repeated concentration of the alluvial gold.
- During glacial periods the Southern Alps provide a regional-scale source for glacial ice, an efficient means of liberating gold from the bedrock and a conveyor-like transport system. During interglacial periods these mountains provide source catchments for gold transporting rivers in the West Coast region.

For an overview of general gold dispersal patterns resulting from uplift and erosion within the plate boundary zone see Craw et al. (1999).

Primary gold sources

There are two primary bedrock sources for gold in the West Coast Region. These are the Alpine Schist situated east of the Alpine Fault and the Greenland Group greywacke situated west of the Alpine Fault. In both cases the gold is hosted mainly within quartz veins, vein stockworks, zones of hydrothermal alteration and fault crush zones. Other bedrock gold sources include the Haupiri Group (Maruia and Owen valleys) and mineralised granite at a number of localities.

The schists are present along the length of the region in a continuous belt on the west side of the Southern Alps. It is clear that the Alpine Schist is the source for at least some of the gold found in alluvial deposits that are situated on the lowlands. Very young deposits of exclusively schist-derived gold have been mined directly above schist bedrock at a number of localities including the Matakitaki, Taipo and Whataroa valleys. An enormous volume of schist has been eroded from the Southern Alps.

Traditional opinion favours the Greenland Group as the most important source for the gold found in West Coast placers. Although the Greenland Group has a patchy surface distribution it is present intermittently along the length of the region. The Greenland Group has provided a large quantity of gold directly by hard rock mining (particularly in the Reefton area). Some placer deposits have been derived directly and exclusively from the Greenland Group. It is also a potential source for gold in many other deposits.

It is difficult to compare the relative contributions of the Alpine Schist and Greenland Group to gold in placer deposits. Because source areas in the Greenland Group have typically not been glaciated as recently there has been more time for the accumulation of rich localised placer deposits. All major valleys in areas underlain by Alpine Schist have been glaciated within the last 20,000 years so there has been limited time for the build up of new deposits.

Modern climate

Due to the prevailing moist westerly air flow off the Tasman Sea, the West Coast has a relatively wet, mild climate. The main mountain ranges form a barrier to the prevailing winds, forcing weather systems to produce orographic precipitation. The areas that receive the greatest annual precipitation are situated on the western flanks of the main ranges.

High annual precipitation and in particular high intensity rainfall events contribute to the generally high rates of erosion and sediment transport within the region. Sediment production is generally higher in the Southern Alps than elsewhere in the region. Locally, sediment sources other than the Southern Alps are important.

Glacial climate

Changes in the regional climate strongly influence rates of sediment production, and types of erosion and deposition. West Coast climate is known to vary in response to global climatic cycles.

Long term climate fluctuations (over thousands to tens of thousands of years) have caused alternation between temperate (modern) and sub arctic (ice age) extremes in this region. Colder climates lead to accelerated rates of physical weathering, particularly in mountainous areas. During cold climate periods an ice sheet develops on the Southern Alps. It feeds numerous valley glaciers that are generally larger than the biggest of the presently surviving glaciers in the Mt Cook area. The Taramakau Glacier, for instance, reached as far west as Kumara Township as recently as 17,500 years ago. At that time the locality now known as Jackson's was buried by hundreds of metres of glacial ice.

The role of glaciers in placer formation

Economic significance

Expansion of glaciers results in a massive increase in the production and transport of coarse sediment, which is carried

away as outwash from the glaciers by meltwater streams. In times of glaciation, the beds of rivers and streams build up when sediment supply exceeds the erosive power of the meltwater flow. In mining terms glaciers are important because they act as a transport mechanism for heavy minerals that have been liberated from bedrock or from sedimentary deposits. In the West Coast region, glacial sediment is normally gold bearing, though grades are generally low.

The locations of meltwater discharge from glaciers are important because this is where a large proportion of the gold carried by the glacier is released. A number of the largest concentrations of placer gold in the West Coast region are contained within proximal outwash situated immediately adjacent to important glacial moraines. These include the Greenstone, Kumara, Callaghans, Kaniere, Rimu and Ianthe goldfields along with many smaller deposits at other localities.

In addition to materials deposited directly from the glaciers there are numerous "secondary" placer deposits. These have been formed by rivers and streams that have eroded into and re-deposited proximal outwash and moraine. They include deposits in the catchments of the following Creeks: Kapitea, Waimea (near Stafford), Saltwater, 12 Mile (Notown), Redjacks, Blackwater, Nelson, Deadmans, Callaghans, Mossy, Moonlight, and Blackball. Also included are numerous deposits in the catchments of New River, the Ahaura, Snowy, Big Grey, Taramakau, Greenstone, Arahura, Maruia and Matakitaki rivers.

Glaciation

During glacial periods the average annual temperature falls progressively, perhaps by as much as 5 to 6 degrees centigrade, so there is less opportunity for snow to melt. Summers shorten and become cooler. Winters lengthen and become colder. Ice accumulates in the high country eventually spilling into mountain valleys and flowing down towards the lowlands.

As the glaciers advance down-valley they engulf pre-existing fluvial and morainic deposits. Eventually the alluvium is scoured away and incorporated within the ice mass. Loose fractured bedrock from the valley floor and valley sides is also incorporated into the ice. The rock impregnated ice mass grinds the underlying rock, widening and deepening the valley.

In a less confined setting where glaciers have spread onto the lowlands (Piedmont Glaciation) the ice can move forward over older alluvial deposits without destroying them. Older alluvium can be buried by younger glacial deposits and old landscapes can be modified significantly as a result.

Valley glaciers act rather like giant conveyor belts. Debris that is eroded by the glacier or falls or washes onto it is transported by the moving ice and released by melting near the terminus. During an ice age each individual glacier transports a huge quantity of sediment ranging from fine rock powder to huge boulders.

When the glacial terminus retreats up-valley fluvial downcutting normally begins in areas accessible to the meltwater river(s). Glacial retreat usually reduces the number of points of meltwater outflow across the main terminal and lateral moraines.

Moraines and glacial till

Moraines are glacial landforms that are composed of till. Typically, they are recognised as long narrow hills or strings of small hills and patches of hummocky ground. The form of many moraines results from glacial till being mounded/molded by moving ice. Till is ungraded sediment that has been deposited directly from glacial ice, typically in a low energy environment. It is alluvium that has not been sorted by the action of a rapid water flow. Till is normally rather chaotic or structureless in appearance with minimal identifiable layering. The boulders and stones tend to be distributed in a rather random manner, with large stones and small stones lying side by side at any point in the deposit

A regularly observed characteristic of glacial till is that large numbers of stones and boulders are present but not frequently in contact. The large stones and boulders are typically encased in fine "puggy" material that is itself a chaotic mixture of small pebbles, granules, sand, silt and rock flour. Rock flour usually forms a substantial proportion of a morainic deposit and constitutes the matrix that holds the deposit together.

The heavy mineral content of till is normally rather low. Gold and blacksand are present in West Coast till but typically in small quantities. On the West Coast till is almost always stony and normally bouldery. It sometimes contains horizons of laminated stone-free silt that is characterised by a large component of rock flour. This type of material often indicates the former presence of a lake.

Another defining characteristic of glacial till is the shape and texture of the contained stones. The roundness and smoothness of stones may be variable but there are always a large number of angular, sharp edged stones. These stones tend to have very rough surface textures and often exhibit deep scratch marks (striations) that result from stone on stone and stone on bedrock grinding within the glacier.

Till can be distinguished from fluvioglacial outwash gravel and other fluvial and marine deposits by eye. In stream deposits the stones are normally in direct contact with each other. Stream gravel is more rounded (few sharp edges or pointed corners) and contains stones with relatively smooth surfaces. In stream gravel the matrix is normally confined to the interstices between the stones and is generally dominated by sandy material. The fine matrix in West Coast stream gravel contains only small amounts of rock flour or clay. Exceptions occur where the stream is in a catchment with source materials dominated by soft siltstone, fine sandstone or limestone.

Terminal and lateral moraines

Moraines of particular significance to placer geology are those that define the terminal and lateral positions of the major glaciers, particularly those associated with extensive glacial advances.

Terminal moraines form at the lower end of a glacier (at its terminus). Typically, they appear as low ridges or chains of small hummocky hills. Where confined by valley margins they often have an arcuate to semicircular pattern. Where glaciers have advanced into open country without definable valley margins the terminal moraines are usually long sinuous ridges. Some of these features are illustrated in Figures 1 and 2.

Terminal moraines commonly merge into lateral moraines. Lateral moraines are formed along the sides of a glacier rather than at the end of a glacier. They tend to be oriented sub-parallel to the direction of ice flow.

Even at the peak of a major glaciation the position of a glacial terminus can change significantly from time to time. It can advance or retreat along part of its front or along the entire front in response to changes in the ice level (caused by fluctuations of relatively small magnitude in climate or annual precipitation). Changes in the geometry of the basal surface of the ice can affect glacial flow patterns. Continuous construction of moraine at the ice margins can affect glacial flow patterns and meltwater flow patterns. Clearly proximal deposits can have complex histories of accumulation.

For the most part the main terminal and lateral moraines of the most recent glaciation mark the inland limits of economic placer deposits in the West Coast region.

Re-deposition by glaciers

On a purely theoretical basis one would predict that new proximal outwash deposits would contain more gold if the glacier that produced them was eroding into older gold bearing alluvial deposits. One might look for evidence that a glacier had overtopped the terminal moraines and proximal outwash of an older event. Alternatively, one could look for evidence that a glacier has been eroding into some other ancient deposit that is known to be gold bearing (e.g. Old Man Group Conglomerate).

Reconcentration of gold from older deposits appears to have occurred at Kumara. The glacial advance that produced the Larrikins Formation destroyed proximal deposits of the (older) Loopline Formation. Gold originally situated in Loopline Formation gravels was redeposited and additional "new" gold was added from the glacial source areas. The result is an extensive proximal outwash plain containing more gold than might otherwise have been expected. It is also significant that the "Larrikins age" river was confined in a narrower valley than the "Loopline age" (older) river.

After the conclusion of a glaciation it can be thousands to tens of thousands of years before the next glaciation begins. In the interim erosion of gold-bearing source rocks continues within the catchment and new alluvial deposits develop in previously glaciated areas. At the onset of a new ice age a new glacier will push down from the high country sweeping up the existing valley fill as it goes. This material is released and deposited in front of the terminus because, although the ice face is advancing, it is also melting continuously. Heavy minerals and boulders scattered though the proximal sediment are recycled within and in front of the advancing glacier. The process is a little like a person sweeping across a floor with a broom. The old pile is swept forward while new material is also gathered with each successive push. This process continues until the glacier reaches its maximum down-valley extent. Gold freshly derived from hard-rock sources can be added to proximal deposits while the glacier maintains a position near to its down-valley maxima.

Meltwater

The terminal face of a glacier pushes forward when ice accumulation exceeds the rate of melting. Melting (or ablation) occurs near the terminus regardless of whether the terminal face is advancing, retreating or static though the rate is variable depending on the season and on the weather. The zone where melting takes place can extend several kilometres up-valley from the terminus.

It is assumed that melting is most rapid at times when the glaciers are deluged by relatively warm northerly driven rainfall. Heat contained within rainwater causes melting of surface ice. The volume melted can be as large as the volume of rainfall. Melting events can produce major flooding in rivers that discharge from the glaciers.

Upon melting, solid material situated on or contained within the ice is released. If melt water is able to drain quickly from a glacier it will carry away a substantial proportion of the finer sediment. Most of the fine glacial rock flour produced from West Coast glaciers is deposited in the Tasman Sea.

Characteristics of proximal outwash

Material deposited on braided floodplains by energetic meltwater streams is usually referred to as outwash or fluvioglacial outwash. The final surface of the deposit is normally referred to as the outwash plain. Gravel derived from meltwater streams is widespread on the West Coast. Most of the major valleys contain such deposits. The progressive accumulation of fluvioglacial outwash is illustrated in Figures 3a and 3b.

The character of fluvioglacial outwash changes with relative proximity to the glacial terminus. It is influenced by the strength, longevity, and gradient of the meltwater stream. If the flow occupies the same general position for an extended period of time it will produce deposits that resemble ordinary stream gravels. Gravel deposited by meltwater takes on a progressively more fluvial (stream-like) appearance with distance away from the point of discharge. Stones become more rounded as they roll along the bed. They are abraded by fine materials carried by the meltwater flow. Smaller flows that are intermittent or less persistent through time tend to produce deposits that are more till-like in character.

Outwash generally has a finer average grainsize with increasing distance from the glacial terminus. Small stones,

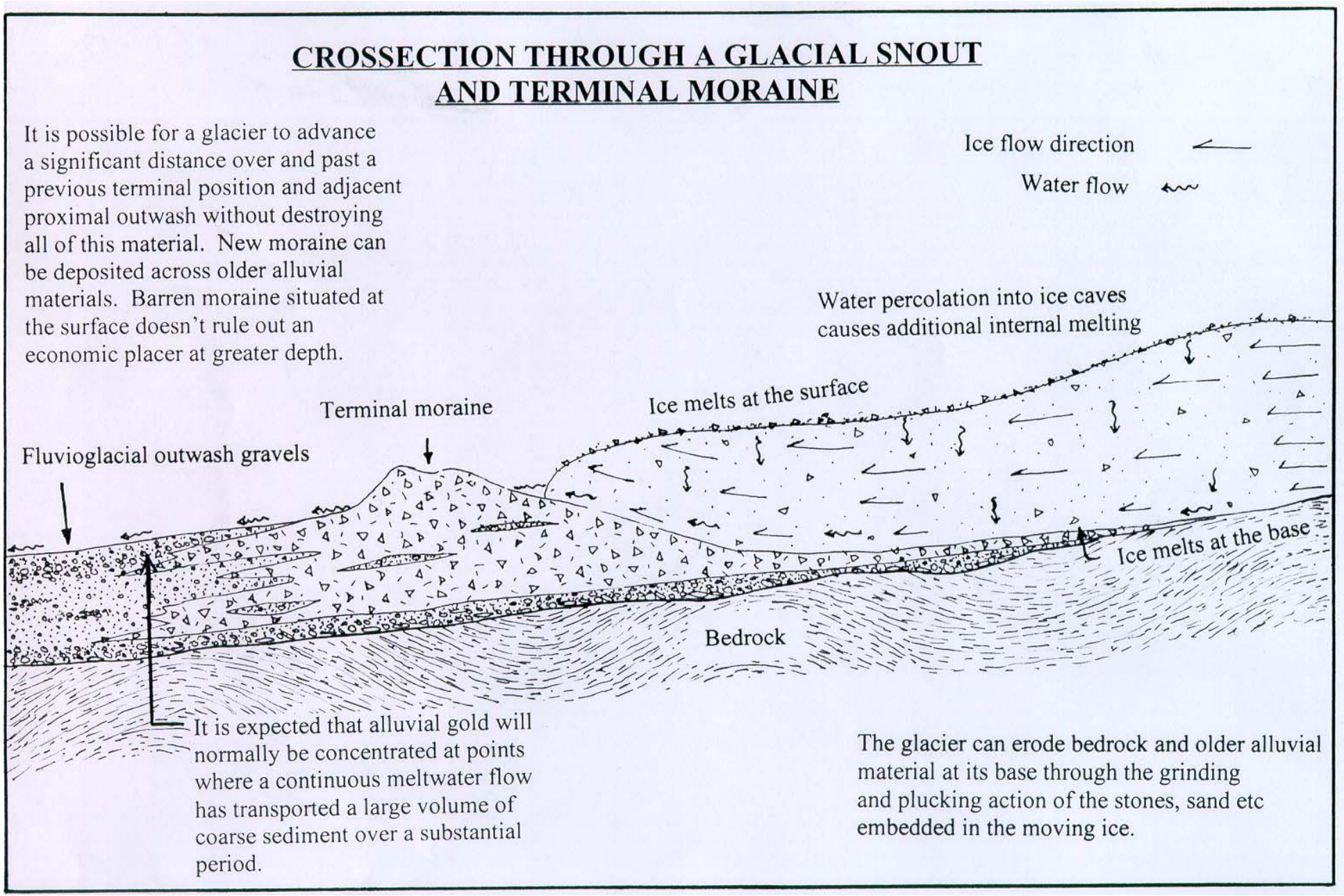
CROSSECTION THROUGH A GLACIAL SNOUT
AND TERMINAL MORAINE
It is possible for a glacier to advance a significant distance over and past a previous terminal position and adjacent proximal outwash without destroying all of this material. New moraine can be deposited across older alluvial materials. Barren moraine situated at the surface doesn't rule out an economic placer at greater depth.
Ice flow direction
Water flow
Water percolation into ice caves causes additional internal melting
Terminal moraine
Ice melts at the surface
Fluvioglacial outwash gravels
Ice melts at the base
Bedrock
It is expected that alluvial gold will normally be concentrated at points where a continuous meltwater flow has transported a large volume of coarse sediment over a substantial period.
The glacier can erode bedrock and older alluvial material at its base through the grinding and plucking action of the stones, sand etc embedded in the moving ice.

Figure 1.

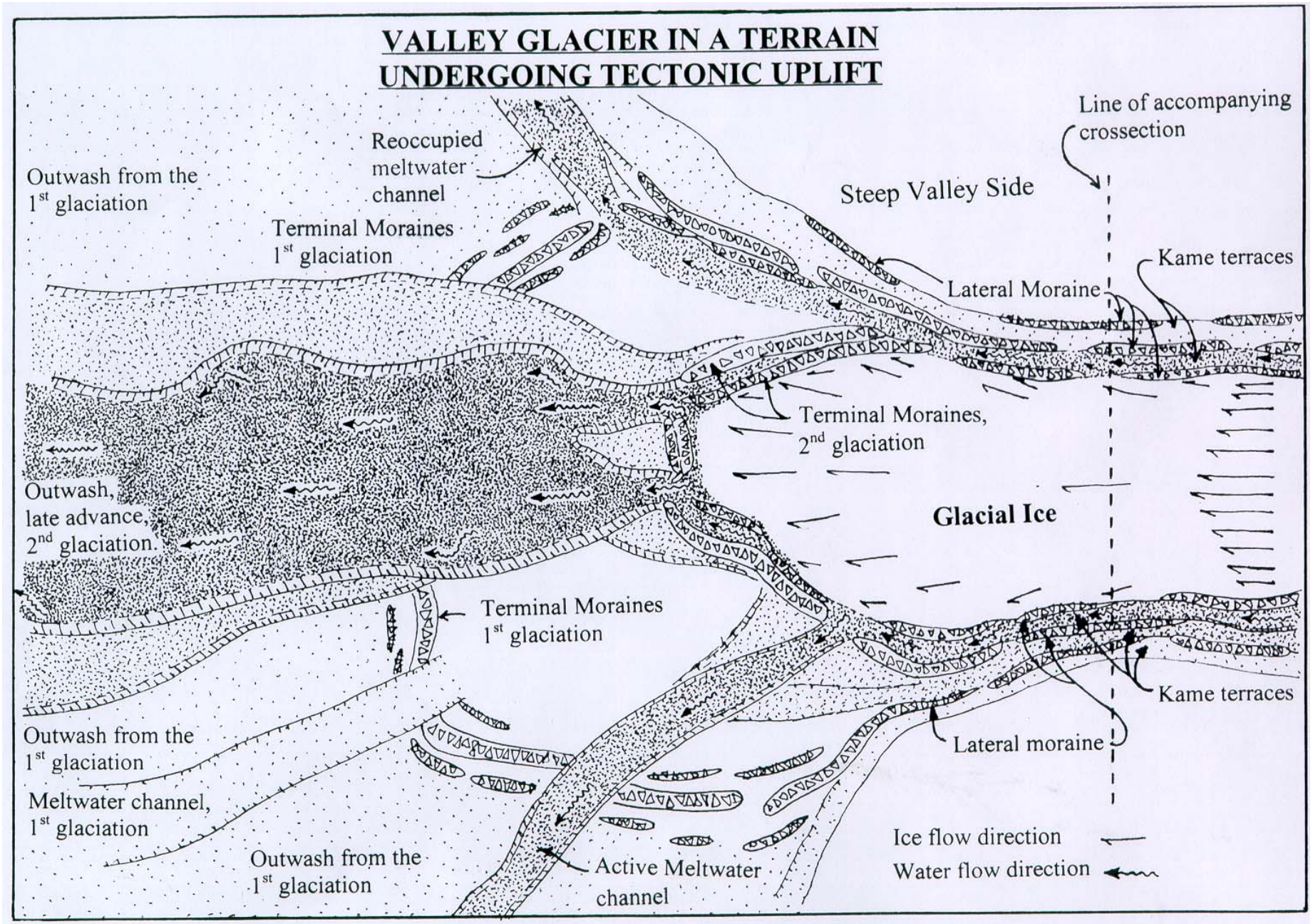
VALLEY GLACIER IN A TERRAIN
UNDERGOING TECTONIC UPLIFT
Line of accompanying crossection
Reoccupied meltwater channel
Outwash from the 1st glaciation
Steep Valley Side
Terminal Moraines 1st glaciation
Kame terraces
Lateral Moraine
Terminal Moraines, 2nd glaciation
Outwash, late advance, 2nd glaciation.
Glacial Ice
Terminal Moraines 1st glaciation
Kame terraces
Outwash from the 1st glaciation
Lateral moraine
Meltwater channel, 1st glaciation
Ice flow direction
Water flow direction
Outwash from the 1st glaciation
Active Meltwater channel

Figure 2.

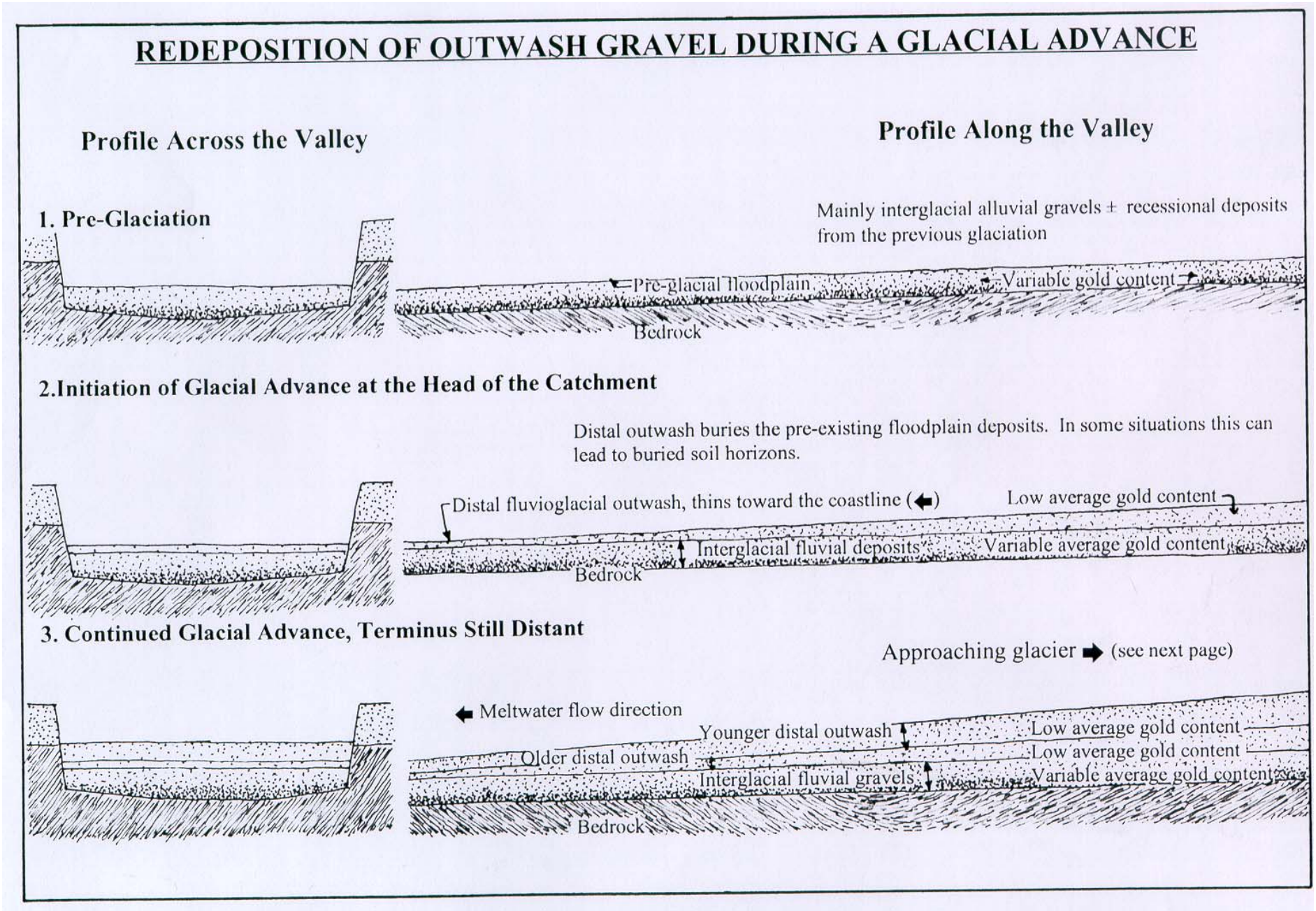
REDEPOSITION OF OUTWASH GRAVEL DURING A GLACIAL ADVANCE
Profile Across the Valley
Profile Along the Valley
1. Pre-Glaciation
Mainly interglacial alluvial gravels ± recessional deposits from the previous glaciation
Pre-glacial floodplain
Variable gold content
Bedrock
2.Initiation of Glacial Advance at the Head of the Catchment
Distal outwash buries the pre-existing floodplain deposits. In some situations this can lead to buried soil horizons.
Distal fluvioglacial outwash, thins toward the coastline (⬅)
Low average gold content
Interglacial fluvial deposits
Variable average gold content
Bedrock
3. Continued Glacial Advance, Terminus Still Distant
Approaching glacier ➡ (see next page)
⬅ Meltwater flow direction
Younger distal outwash
Low average gold content
Older distal outwash
Low average gold content
Interglacial fluvial gravels
Variable average gold content
Bedrock

Figure 3a.

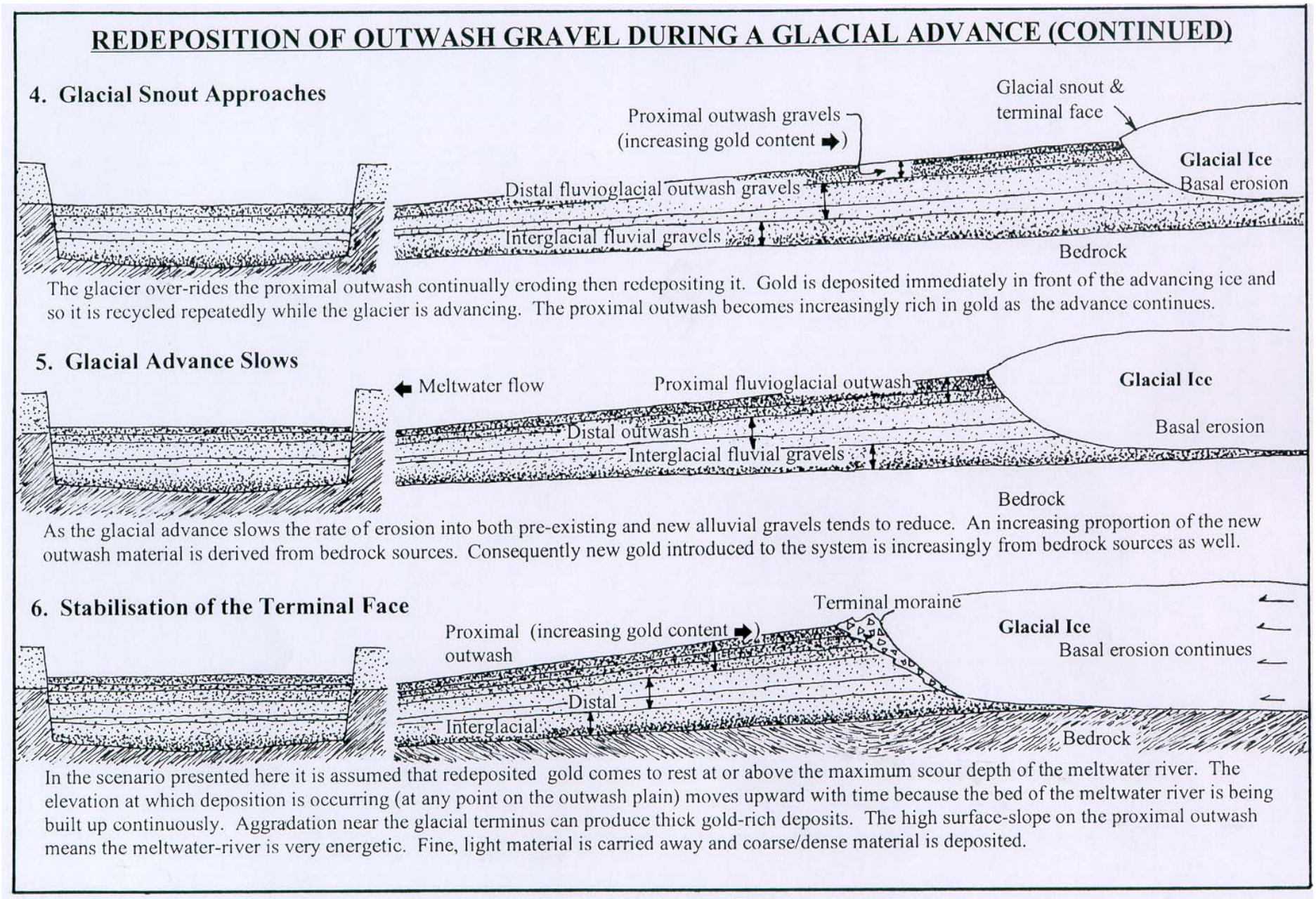
REDEPOSITION OF OUTWASH GRAVEL DURING A GLACIAL ADVANCE (CONTINUED)
4. Glacial Snout Approaches
Glacial snout & terminal face
Proximal outwash gravels (increasing gold content ➡)
Glacial Ice
Basal erosion
Distal fluvioglacial outwash gravels
Interglacial fluvial gravels
Bedrock
The glacier over-rides the proximal outwash continually eroding then redepositing it. Gold is deposited immediately in front of the advancing ice and so it is recycled repeatedly while the glacier is advancing. The proximal outwash becomes increasingly rich in gold as the advance continues.
5. Glacial Advance Slows
⬅ Meltwater flow
Proximal fluvioglacial outwash
Glacial Ice
Basal erosion
Distal outwash
Interglacial fluvial gravels
Bedrock
As the glacial advance slows the rate of erosion into both pre-existing and new alluvial gravels tends to reduce. An increasing proportion of the new outwash material is derived from bedrock sources. Consequently new gold introduced to the system is increasingly from bedrock sources as well.
6. Stabilisation of the Terminal Face
Terminal moraine
Proximal outwash (increasing gold content ➡)
Glacial Ice
Basal erosion continues
AGGRADED
Distal
Interglacial
Bedrock
In the scenario presented here it is assumed that redeposited gold comes to rest at or above the maximum scour depth of the meltwater river. The elevation at which deposition is occurring (at any point on the outwash plain) moves upward with time because the bed of the meltwater river is being built up continuously. Aggradation near the glacial terminus can produce thick gold-rich deposits. The high surface-slope on the proximal outwash means the meltwater-river is very energetic. Fine, light material is carried away and coarse/dense material is deposited.

Figure 3b.

pebbles and sand are much more prone to transport in running water than large boulders. Coarser and heavier material tends to be deposited relatively close to the glacier. The pattern has economic significance for miners because, just like large glacial boulders, alluvial gold resists fluvial transport. One would expect the quantity of large boulders and alluvial gold in proximal outwash in front of an advancing glacier to increase in a systematic manner over time due to recycling and new addition.

Gold grades are likely to be high in shallow proximal outwash immediately in front of the terminal moraine, particularly where a substantial meltwater flow emerged from the terminal area and flowed down a confined outwash plain. Grades will be lower in more distal outwash. The highest grades are often not situated at the bedrock contact. The deeper material is older and can represent a situation in which the glacial terminus was further up valley and gold had further to travel. Prominent deposits that seem to fit this model include the Callaghans, Kumara and Ianthe goldfields. General trends in the gold content of fluvioglacial outwash gravel are illustrated in Figure 4.

If meltwater is constrained between a glacier and an adjacent valley side or moraine then a narrow floodplain or "kame terrace" can develop in that position. It will generally be oriented parallel to the ice margin. This environment is ideal for the concentration of alluvial gold. The internal structure of kame terraces is normally quite complex due to the rather changeable ice margin conditions. Gold grades can be very high but payable zones can be difficult to trace for any distance. The western side of the Hokitika Valley from Back Creek to Seddon Terrace then to Woodstock and Arthurstown contains prominent examples of placer deposits along a lateral glacial margin. These fluvial deposits have been left perched above the floor of the main valley after the glacier retreats. Similar deposits are found in a number of other West Coast valleys. The formation of a kame terrace is illustrated in Figure 5.

Erosion of proximal deposits by meltwater rivers can cause a reconcentration of proximal outwash, effectively increasing the gold grade. Such erosion can also result in gold being spread further downstream. This gold is normally found above a "false bottom", the enriched material lying on older, lower-grade outwash.

Outwash and glacial till cover a large proportion of the West Coast lowlands, and many of the foothills as well. Older deposits tend to be found at higher elevations because the land is being uplifted steadily by mountain building processes. Rivers tend to cut down through the fluvioglacial deposits and bedrock as uplift continues. Therefore, succeedingly younger glacial advances result in the formation of outwash plains that are lower in elevation than the preceding ones.

Gold in the discharge from West Coast glaciers

The crystalline bedrock (primary gold source) contains gold at very low average grades, usually only a few parts per billion. Strong mineralisation is found in isolated zones that constitute a small proportion of the total rock mass. During glacial erosion bedrock is shredded and much of the contained gold is liberated. The detritus is relatively homogenised on release from the glacier. It is normally auriferous but the average gold content is low.

The volumetric bulk of West Coast aggradational outwash gravel is sub-economic after no more than a kilometre or two of fluvial transport. The aggradational section of a most profiles contains less than 85 milligrams of gold per cubic metre after a limited distance of transport from the gold source. Exceptions occur in situations that are proximal to terminal moraines. The exact down valley distance over which such materials are economic depends on a variety of factors and is different in each of the main valleys. Some areas can be identified as being of relatively low prospectivity on the basis that they are dominated by distal outwash. Other areas can be targeted because they fit the profile of a suitable proximal deposit, or because there is potential for finding an older buried lag deposit.

A large amount of sorting is required in order to produce a deposit containing economic grades. It probably takes hundreds of years of continuous sediment release at a stable glacial terminus before a substantial gold placer can accumulate. Continuous supply needs to be accompanied by continuous removal of fine grained and low specific gravity sediment (mostly schist, greywacke and granite detritus). From time to time fluvial erosion may dominate over sediment supply producing extreme gold grades in some layers.

Gold resists transport even in a high-energy environment. Individual gold grains are trapped between the large boulders and don't move again until the boulders are dislodged by a deep scouring event. Near to terminal moraines meltwater rivers tend to have rather steep gradients. Here thick bouldery deposits can build up and gold grades can be very high. Grades inevitably reduce in a downstream direction, as does the average size of the boulders.

Exploration for gold

In the search for gold within glacial outwash deposits several points should be kept in mind:

- Payable gold is rarely found in glacial till but may be found at the contact between till and outwash.
- One should look for bouldery deposits that show clear evidence of deposition in rapidly flowing water. The matrix between the boulders should contain a large proportion of heavy mineral bearing sand, granules and pebbles. The amount of glacial rock flour will be low in comparison to glacial till.
- There will ideally be some indication in the general landscape that a substantial stream or river once flowed through the area. There doesn't need to be such a stream at the present day since the ancient water source (typically glacial) may no longer exist.

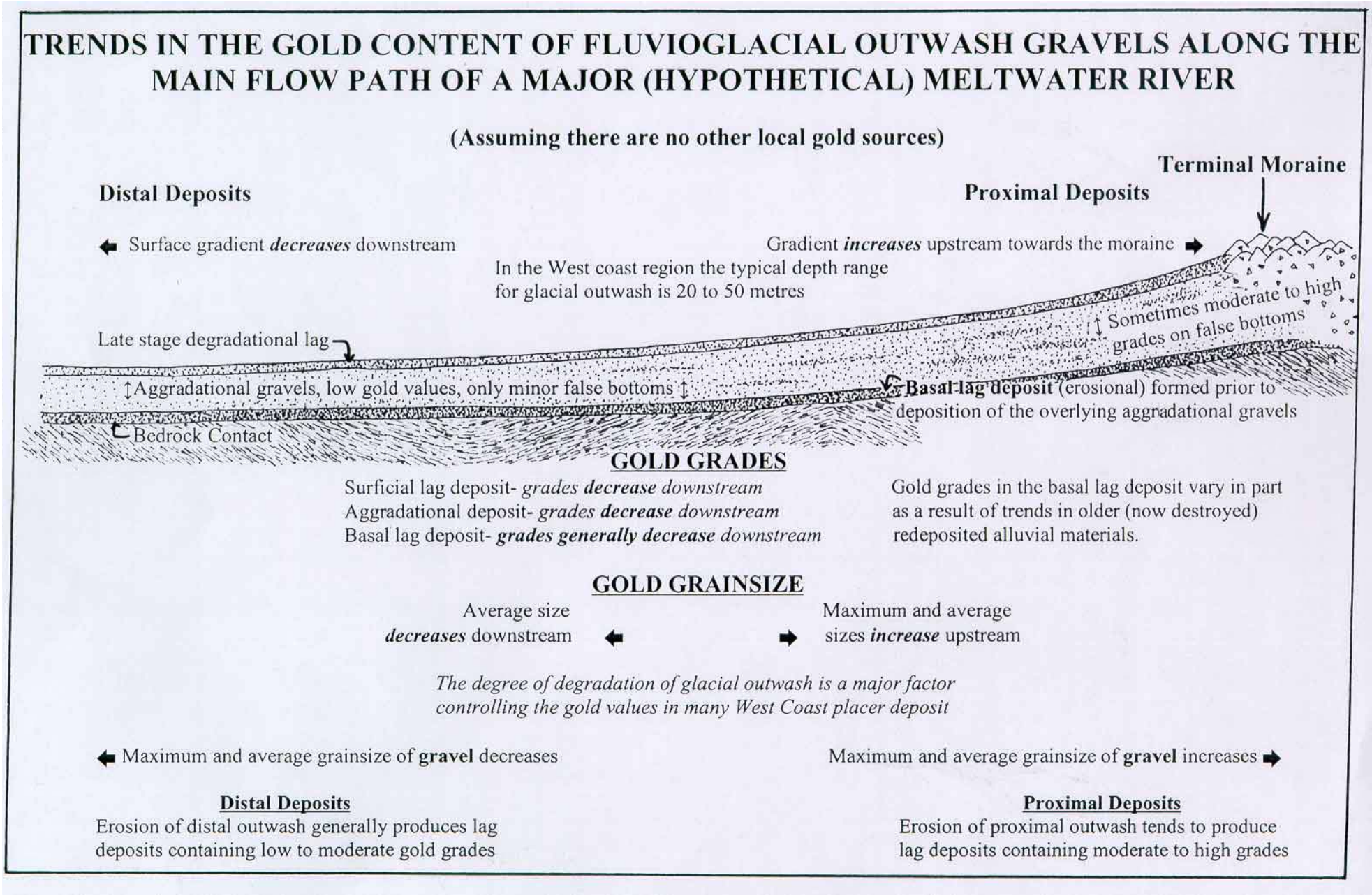
TRENDS IN THE GOLD CONTENT OF FLUVIOGLACIAL OUTWASH GRAVELS ALONG THE MAIN FLOW PATH OF A MAJOR (HYPOTHETICAL) MELTWATER RIVER
(Assuming there are no other local gold sources)
Terminal Moraine
Distal Deposits
Proximal Deposits
Surface gradient decreases downstream
Gradient increases upstream towards the moraine
In the West coast region the typical depth range for glacial outwash is 20 to 50 metres
Late stage degradational lag
Sometimes moderate to high grades on false bottoms
Aggradational gravels, low gold values, only minor false bottoms
Basal lag deposit (erosional) formed prior to deposition of the overlying aggradational gravels
Bedrock Contact
GOLD GRADES
Surficial lag deposit- grades decrease downstream
Aggradational deposit- grades decrease downstream
Basal lag deposit- grades generally decrease downstream
Gold grades in the basal lag deposit vary in part as a result of trends in older (now destroyed) redeposited alluvial materials.
GOLD GRAINSIZE
Average size decreases downstream
Maximum and average sizes increase upstream
The degree of degradation of glacial outwash is a major factor controlling the gold values in many West Coast placer deposit
Maximum and average grainsize of gravel decreases
Maximum and average grainsize of gravel increases
Distal Deposits
Erosion of distal outwash generally produces lag deposits containing low to moderate gold grades
Proximal Deposits
Erosion of proximal outwash tends to produce lag deposits containing moderate to high grades

Figure 4.

VALLEY GLACIER IN A TERRAIN UNDERGOING TECTONIC UPLIFT

Sketch Crossections

1. During Glaciation

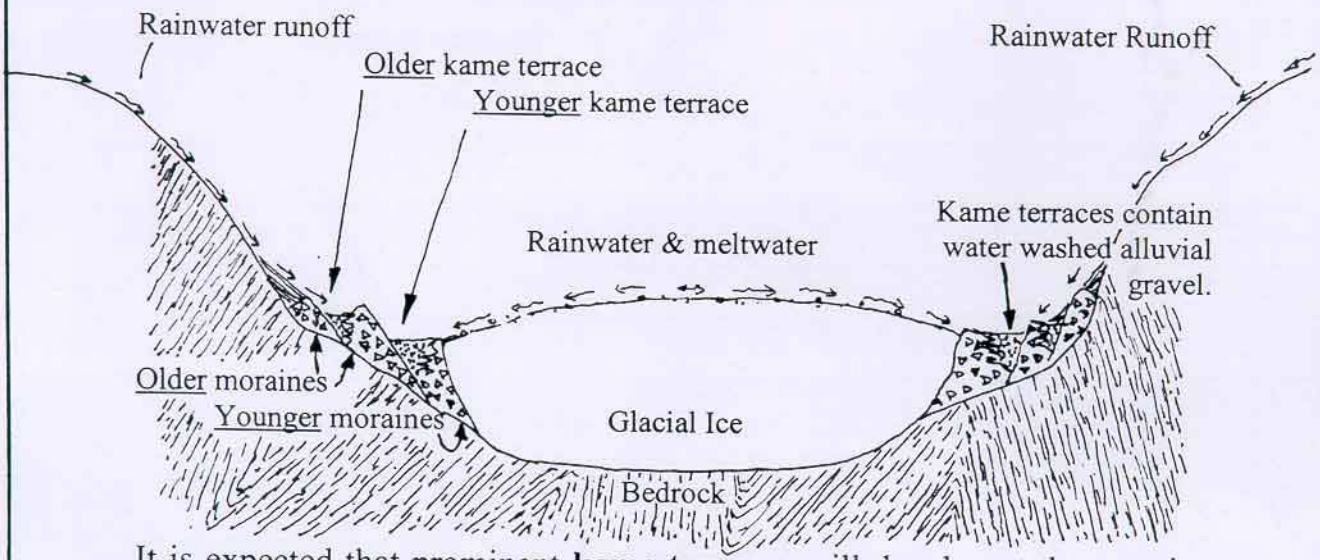

It is expected that prominent **kame terraces** will develop at the margins of the glacier if substantial runoff and meltwater collects and is constrained to flow around the valley margins. These terraces are less likely to develop if most of the runoff and meltwater escapes via ice caves and tunnels situated beneath the surface of the glacier.

2. After Glacial Retreat

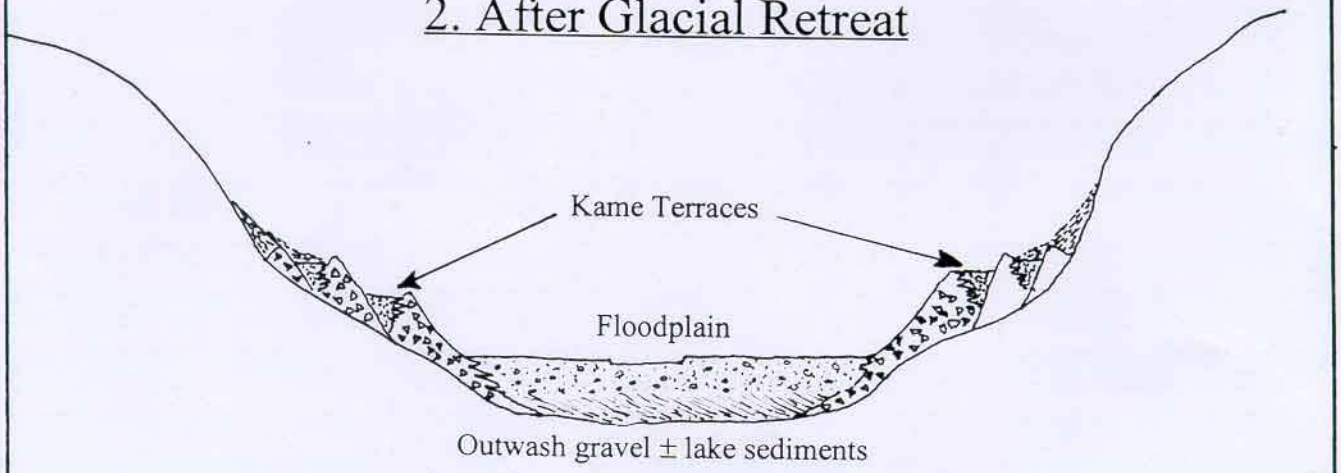

Kame terraces that are situated on steep slopes are prone to erosion and surface modification. The original form isn't always maintained for a long period of time.

Figure 5.

- Preferably, there will be clear evidence of a reasonable surface gradient. In general, the gradient of an outwash surface increases as one nears the terminal moraine.
- It is advisable to explore down slope from a significant terminal or lateral moraine. Explorers should seek sites where there are indications that the glacier stabilised at its terminus for a significant period.
- One would normally look for a site where there is evidence that meltwater had an unimpeded flow away from its site of release from the glacier. The presence of a big volume of outwash down-valley from the prospective area is desirable particularly if there is some indication that a large proportion of it has been washed through the site in question.
- Older unbreached glacial moraines situated on the seaward side of a particular moraine loop can restrict the passage of meltwater derived from younger terminal position. If the surface gradient of the intervening ground is low as the result of the damming effect of the seaward moraine then deposits here can't be expected to be particularly enriched in gold. A low gradient may indicate rapid deposition, minimal sorting and less chance for gold accumulation.
- Drilling is advisable because the richest gold may 10 m or more below the surface. Because of complex depositional histories in the terminal regions of the major glaciers, high gold concentrations can sometimes be found on several levels within a stratigraphic profile. Glaciers can advance over fluvial deposits without destroying them. Consequently, fluvial gravel can be inter-layered with glacial till. Quinns Terrace and Kumara are localities where miners have operated economic mines in outwash gravel overlying deeper, richer gold bearing horizons that were only discovered later.
- One can't assume that a drill hole or excavator pit has been bottomed upon striking glacial till. Glaciers can advance over fluvial deposit without destroying them. Till can be deposited on top of or be found inter-layered with gold bearing outwash gravel.
- The presence of old gold workings nearby is good for confidence but the absence of workings does not rule out the possibility of finding payable gold.

Exploration targets will include areas where there has been a large and vigorous flow of meltwater within a defined channel. In the West Coast region, there are several prominent examples of large placer deposits situated in meltwater channels that have been mined successfully. These include (but are not limited to) the Kumara goldfield, the bed of the Taramakau River downstream of Kumara, the valley of Waimea Creek (Stafford), and the Rimu Channel (Adair Road) near Hokitika. The Rimu Dredging Company which mined within the Rimu Channel from 1921 to 1953 had a declared gold production of 272,000 ounces and an additional (mainly war time) production of at least 20,000 ounces. Other mining activities within the Rimu Channel have probably produced at least 30,000 ounces.

Fluvial degradation

Degradational processes

Degradation is net reduction in the volume and thickness of alluvial materials. During fluvial degradation, erosion dominates over accumulation. Most of the alluvial gold produced from the West Coast region has been derived from degradational material.

Degradation occurs when sediment supply is less than bedload carrying capacity. Having previously built up its bed during an aggradational phase a stream begins to erode the sediment beneath its bed. Over time it swings back and forth across the floodplain repeatedly removing the top surface of the aggradational deposit. This lowers the level of the floodplain. If degradation continues for long enough the stream will eventually scour down to basement and may begin to cut a channel that has banks of solid bedrock.

When streams erode older alluvial deposits, materials of relatively low specific gravity are removed selectively. Clay, mud and silt particles can be transported in suspension for large distances in turbulent water. Sand, pebbles and small stones can be rolled or bounced along the bed in the current. Repeated transport of fine grained and low-density material is one key to formation of degradational deposits.

Bigger, heavier stones and high-density particles of all sizes are difficult for streams to shift and are retained in the degradational lag. Transport distances are shorter and flood events capable of moving them are less frequent. Heavy minerals tend to be deposited in places where it is relatively difficult to remobilise them. Gold grades in lag materials generally increase during degradation of older gold bearing alluvium. The main reason for this is the high density (high specific gravity) of alluvial gold which limits its erodability.

Each time the upper surface of the underlying aggradational material is exposed in the bed of the creek heavy boulders and gold drop down onto it. As soon as it is exposed to scouring, gold that was previously situated in the aggradational material tends become incorporated in the degradational lag. The lag deposit is developed across the entire floodplain.

The speed at which degradation occurs depends on the size and gradient of the stream concerned. Larger streams and rivers can do a lot of work in what is a short time by geological standards. They do so with particular efficiency if the material being degraded is relatively unconsolidated.

Major causes of widespread fluvial degradation

Sea level controls the general base level. Local rivers and streams cannot erode more than a few metres below mean low sea level. At sites that are a long way from the coastline, for instance in the Maruia and Matakitaki valleys, changes in sea level tend to have less effect than in localities near to the

coast. Here the factors determining whether a stream will aggrade or degrade are dominated by the sediment supply rate and by changes in annual precipitation. In the West Coast context river and stream floodplains tend to be degraded (or scoured) under the following circumstances:

- when the average stream gradient is increased, for instance by tectonic uplift, tectonic tilting or by a falling sea level (which has a widespread effect on local base levels);
- when the rate of sediment supply from the local source area declines; or
- when the size (or discharge) of the stream increases significantly.

With the exception of direct effects from tectonic processes, changes from aggradation to degradation are typically driven by climate change.

Description of deposits

Degradational deposits are characterised by the presence of large, heavy stones or boulders, particularly at the base. The boulders tend to be jammed tightly together. Consequently the material can be hard to dig even with earth moving machinery. The matrix between the boulders normally contains less fine sand and silt than the corresponding material in an aggradational deposit. The matrix in a degradational deposit generally contains relatively more and coarser high-density mineral grains than that in nearby aggradational deposits. In contrast aggradational deposits contain boulders and stones of smaller size and these are often not in direct contact.

Degradational deposits are typically floored by a selection of the largest boulders that were available to be rolled by the maximum flood flow of the stream concerned. Sometimes deposits of this type contain boulders that are far too large to have been rolled by the stream concerned. In the West Coast region the main reason for this is the wide distribution of huge boulders originally carried and deposited by glacial ice and subsequently incorporated in fluvial deposits without being moved any significant distance.

Depth of scouring and deposit thickness

In an active river, coarse gold is rarely lifted vertically much further the difference in elevation between the base of the deepest pool and the top of the adjacent river beach/bar. This vertical distance is a function of the energy of the flow during the largest flood events in that river (when the deepest pools are created). It matches the typical thickness of the basal gold bearing lag deposits in drill holes.

The thickness of a degradational deposit is governed by the transport power of the stream that produced it and the rate of sediment supply to the stream. Large rivers are capable of generating relatively thick degradational deposits so long as the bed load remains relatively high. A lesser bed load encourages more rapid scouring and if the scouring continues till local bedrock is reached then the heavy lag material can be scoured away as well. The larger the river the greater the potential depth of scouring. Substantial basal gold enrichment extends generally no more than 6-7 m above the bedrock contact.

In profiles where coarse degradational gravel overlies relatively fine-grained aggradational gravel the contact between the contrasting materials is usually sharp and flat to slightly undulating. The depth of the degradational material can be consistent over large areas. This shows up in drill-logs from gold exploration.

The average stream flow in a catchment can change dramatically over time, sometimes quite abruptly. Examples include abandoned meltwater channels where the stream or river simply disappears as the glacial ice retreats. In such cases the thickness of degradational horizons can't be used to indicate the active scour depth of the modern stream that drains the catchment. Local run off typically supplies only a fraction of the former meltwater flow. The "Rimu Channel" at Adair Road near Hokitika is a good example of an abandoned meltwater channel.

"Bottoms"

In West Coast mining jargon the term "bottom" is used to describe either a well-defined layer containing high gold grades, usually a lag deposit, or the surface on which the gold bearing horizon is resting. Bedrock is considered to be "true bottom". In digging to a "false bottom", you are reaching for the base of a gold bearing horizon that rests on alluvium containing substantially less gold than the target.

The most obvious gold bearing bottom (often the mining target) is normally situated adjacent to bedrock. However, some profiles contain more than one "bottom". The most striking local example is at Ross where at least eight separate horizons were worked by tunnelling in the 19th Century. These were in an uninterrupted stratigraphic sequence and were separated by materials that contained insufficient gold for successful underground mining.

Gold distribution in degradational materials

Gold is usually concentrated preferentially in the coarser portion of layers that have resulted from degradation. Normally the highest grades and the largest flakes are found at or near the base of such layers. However, there are situations where the richest material in a degradational unit is situated above bottom. This is particularly common where the gold has a fine grainsize and flattened shape. Such gold can be moved up from a deep pool onto a gravel bar during flood conditions.

Due to selective transport, gold situated in degradational materials usually has coarser maximum and average grainsize than gold in the parent material from which it was derived.

This is the case regardless of whether the parent material is a hard rock deposit or an older alluvial deposit. The finer grainsize gold is carried downstream further, and more frequently than the coarser gold. On average, fine gold has a lesser tendency to be buried deeply within an active streambed so it is available for erosion and transport on a more regular basis.

Consider a flight of degradational terraces in a valley profile at a right angle to the river (or valley axis). If the gold in the lower terraces is derived by degradation of higher terrace gravels the expectation would be that the average gold grainsize would increase down the terrace sequence. At each stage of degradation, gravel volume is reduced, coarse gold is moved a little further down-valley and fine gold is moved substantially further down-valley. New gold may also be added from other sources within the catchment.

Economic deposits

The overwhelming majority of gold produced from West Coast placer deposits has been derived from degradational layers. These are typically situated in contact with local bedrock (true bottom). The deposits that are of most interest to small scale miners are those where there is minimal overburden. These are relatively easy to mine. Most deposits fitting this description are situated in the valleys of small to medium sized streams. Commonly these are isolated from the huge influxes of glacial outwash that swamp the valleys of the major rivers during glacial periods. In the larger valleys burial of degradational deposits can cause a reduction of the overall gold grade.

Economic deposits are found particularly:

- where the full thickness of the deposit is degradational in character;
- where the gold content of a degradational horizon justifies the stripping of overburden (which often has an aggradational character); or
- where shallow degradational gravels can be mined without disturbing low grade materials that lie beneath the base of degradation.

Tectonic uplift and degradation

In the area north of Ross most of the land surface and a considerable area of sea floor are rising due to uplift that is caused by the crustal stresses associated with deformation in the plate boundary zone. Uplift probably occurs in an abrupt and episodic manner associated with major earthquakes. During earthquakes the landscape is altered by a combination of fault displacement, folding and tilting. Although such activity may be intermittent in the short term, rates tend to even out in the long term (tens of thousands of years).

In geological terms the West Coast landscape is very young. The Southern Alps as we know them have existed for no more than 5 million years. It is probable that the Paparoa, Brunner, Mt William and Victoria Ranges were not recognisable in their modern form prior to 2 million years ago. Uplifted country adjacent to the Southern Alps (for instance Mt Greenland, Mt Camelback, Tuhua, Mt Turiwhate, the Hohonu Range and Bell Hill) probably did not exist in recognisable form prior to 2 million years ago.

As recently as 2 million years ago the entire West Coast lowlands and foothills areas collectively constituted a large alluvial plain rather like the modern Canterbury Plains. Floodplains of the main rivers almost certainly coalesced. The hills that presently occupy the ground between the main rivers did not exist as recently as a few hundred thousand years ago. Virtually all surface features in the lowlands have formed within the last 500,000 years.

The uplift rate varies across the region. It is greatest in mountainous areas that are underlain by hard crystalline rocks such as granite and schist. In lower lying areas the uplift rate is between 0.2 and 0.5 mm per year. Old marine shorelines situated well inland from the modern coast (up to 4 km at Hokitika, 2.5 km at Rutherglen, and 10 km near Westport) are now at elevations up to 270 m above sea level. Many of the earthquakes responsible for the uplift probably occur on large offshore fault lines paralleling the coastline.

The major West Coast rivers are generally able to erode downward at least as fast as tectonic processes are lifting the land up. If the climate were stable over the long term then rivers would settle onto a steady state (constant) down valley profile. In reality this is not possible because the climate changes frequently, altering the rate of sediment supply and the sea level. Changes in sediment supply rate can delay the down-cutting action of rivers in an uplifting terrain. However, incision can't be postponed indefinitely. Uplift eventually causes rivers to adjust floodplain slopes and elevations by cutting lower paths to the sea.

Deepening of the main valleys forces the rivers to abandon the intervening high ground. The terraced and hilly ground situated between the Arahura and Taramakau rivers is an example. The valleys of these two major rivers are very young. The floodplains were formerly much more extensive than at the present day.

The rate of downcutting by small streams is not as fast as that of the larger rivers. On the West Coast elevated areas that are drained by small streams become increasingly hilly because the streams can't erode the entire area at a rate that matches the speed of uplift. They simply don't have the necessary erosive power.

Role of sea-level fluctuation in West Coast placer evolution

Climate and sea level

Sea level can rise or fall depending on whether the global climate is becoming generally warmer or generally colder. A

colder global climate causes the growth of new ice caps and the expansion of existing ones (e.g. Greenland). During the last ice-age the Laurentide ice sheet (covering much of Canada and some of the northern states of the USA) expanded to cover an area as large as the continent of Antarctica. At a thickness of 2 km or more this represents a very large volume of water. Growth of continental ice sheets lowers worldwide sea level because there is a transfer of water storage from the oceans to the continents. When the ice reaches its maximum volume sea level falls by as much as 120 m.

As sea level falls the sea tends to withdraw off shallow continental shelf areas. Shorelines move in a seaward direction changing the length and gradient of West Coast rivers and changing the extent of the "Coastal Plain". Sea level rises when continental ice sheets melt. This causes coastlines to migrate in a landward direction and influences river gradients.

Warming of global climate towards an interglacial (modern) state forces glaciers and continental ice sheets to melt returning water to the oceans and causing the sea level to rise. The rate at which sea level rises can be as fast as 5 cm per year for periods of a few hundred years (5 m per hundred years). In response coastlines migrate in a landward direction. The rate of sea-level rise can be as high as 5 cm per year (5 m per hundred years for periods of a few hundred years). Along the West Coast this can potentially result in coastal migration of up to 500 m per hundred years. Normally the rate of rise is slower but it can still average more than 1 cm per year for periods as long as 11,000 years.

Changes in sea level have a direct influence on fluvial processes and on the formation of placer deposits. This subject is addressed in this paper in connection with fluvial incision. At present we are handicapped by the fact that there is no precise or universally accepted sea-level curve for the Late Pleistocene to Recent period.

Interglacial (high) sea level

At present the sea level is close to the maximum expected during a normal interglacial period. It has been at or near this level for around 6500 years. The previous sustained period when the sea was at this level was about 116,000 to 129,000 BP (years before present). The sea has also approached its modern level briefly (for a few thousand years) at about 78,000 BP; 83,000 BP; 98,000BP; 104,000 BP and perhaps around 50,000 BP.

Glacial (low) sea level

For the most part during the past 150,000 years sea level has been considerably lower than it is today. The most prominent minima occurred at about 17-21,000 BP; 40,000 BP; 60-65,000 BP; 86-90,000 BP; 110,000 BP; and 140-150,000BP. Of these the minima at 21,000, 65,000 and 145,000 were the most severe. For much of the period between 23,000 and 17,000 BP sea level was around –110 to –130 m. In the interval between 24,000 BP and 75,000 BP sea level fluctuated strongly between about –15 and –100 m.

There is an opportunity for valley deepening by rivers at times when sea level is particularly low. The extent to which incision occurs is dependent on sediment supply within the catchment and on the gradient of the river. Incision is particularly likely if a fall in sea level is not accompanied by substantial seaward retreat of the coastline.

Effect of tectonic uplift

In the short term (hundreds to a few thousand years) there is sufficient power in the surf zone for marine erosion to maintain the coastline at a more-or-less constant position (so long as worldwide sea level is reasonably stable). Even if an earthquake causes uplift of the lowlands the position of the coastline usually changes only slightly (generally no more than a few hundred metres).

Abrupt uplift has an almost instantaneous effect on river gradients. Coastal uplift increases the average slope of the lower reaches of rivers. The entire floodplain gains additional elevation above sea level. Consequences include increased average velocity of flood-flow and increased sediment transport capacity. Rivers tend to readjust floodplains back towards the original down valley profile by eroding to a lower level. Floodplain erosion due to tectonic uplift is not restricted to coastal areas. The process quickly spreads up-river. Ultimately it leads to the removal of soil and gravel from the floodplain and to a reduction in the depth of floodplain materials.

Along some parts of the North Westland coastline there has been as much as 5 to 10 m of uplift during the last 6500 years. Holocene marine beach deposits no older than this are situated 5 to 12 m above modern sea level. The entire width of some floodplains has been lowered by a similar amount. There must have been extensive scouring of floodplains since the stabilisation of sea level because the rivers maintain modern profiles that grade down smoothly to modern sea level. Fluvial erosion resulting from uplift causes gravel deposits under floodplains to become shallower. Post-glacial gravel beneath the Grey River at Greymouth is 5 to 10 m shallower than it was 6000 years ago. Formerly the maximum depth must have been about 60 m. The present depth is 50 to 55 m.

Effect of sea-level change on gradients

The coastal plain

One result of sea-level fluctuation is migration of the coastline. The position of the coast moves in a seaward direction if sea level falls and in a landward direction if sea level rises. The rate of retreat or advance depends on the speed of sea level change. If the coastline retreats then rivers must flow further (across a wider coastal plain) to discharge into the sea. During extreme glacial conditions (sea level at –120 m) the extra distance could be as much as 14 to 19 km for rivers situated between Greymouth and Hokitika.

The modern sea floor has a geographically variable gradient as has the glacial coastal plain (Table 1).

River gradients

When the sea level rises or falls there is an immediate impact on the gradient and sediment transport capacity of most West Coast rivers. This is significant because most of the West Coast placer goldfield is situated relatively close to the modern coastline.

The gradient of the shallow portion of the continental shelf (see Table 1) can be compared with the surface gradients of modern West Coast floodplains (Table 2).

The average gradient of the "glacial" coastal plain is greater than that of the modern floodplains of the major rivers in North Westland. Therefore it is concluded that a lowering of sea level and retreat of the coastline should cause a steepening of the average gradient of West Coast rivers. During glacial periods West Coast rivers should have steeper gradients than during interglacial periods. This can be tested by measuring the gradients of glacial (Larrikins and Loopline formations) outwash plains in the lower parts of the main valleys (Tables 3 and 4).

There are substantial differences gradients of glacial (outwash terrace) and interglacial floodplains near to the modern coastline. For surfaces formed during glaciation slopes increase as the terminal moraines are approached. The average gradient of the coastal plain is not the only factor controlling ice age river gradients. The average discharge of the rivers and the quantity of bedload are also important.

Incision as a result of sea-level change

Channel depths

Near the modern coast there are deep deposits of alluvial gravel under the floodplains of the major West Coast rivers (Table 5). How did these deposits originate? The rivers are clearly unable to scour to this depth at the modern day, even during the largest of floods. The existence of such deep deposits is evidence for a much lower sea level in the recent geological past.

Process of channel incision

At several times in the past the main West Coast rivers have cut deep channels that have subsequently been buried by younger alluvial materials. Some of these channels can't have been produced when the sea was near to its present level.

In the Grey Valley channel incision reached at least as far as Maimai near Reefton, about 70 to 75 km from the coast at the time of scouring. Incision affected most of the larger tributaries of the Grey River. Deep gutters grade downstream to the floor of the channel beneath the main river. Prominent examples with good drilling (gold exploration) coverage include Moonlight Creek, Blackball Creek, Nelson Creek, Redjacks Creek, and Twelve Mile Creek (all in the Grey

Shore to 120 m depth	
Between Greymouth and Chesterfield	6.5 m/km
Off Awatuna	6.9 m/km
Off Hokitika	8.3 m/km
Shore to 20 m depth	
Between the Grey and Taramakau River mouths	3.5 m/km steepening in an offshore direction
Between the Hokitika and Arahura River mouths	5.5 m/km steepening in an offshore direction

Table 1. Modern sea floor gradient (data from the Royal N Z Navy hydrographic charts).

Grey River	1.17 m/km for the lower 17 km (0-20 m) 2.16 m/km (20-60 m)
Hokitika River	1.08 m/km for the lower 18.5 km (0-20 m) 2.2 m/km (20-40 m)
Taramakau River	1.95 m/km for the lower 10.25 km (0-20m) 2.2 m/km (20-40m).
New River	2.67 m/km for the lower 7.5 km (to Card Creek confluence).
Arahura River	4.0 m/km for the lower 5 km (0-20 m) 4.4 m/km (20-40 m)

Table 2. Surface gradients of modern West Coast floodplains (Nine Mile Formation).

Grey Valley	4.5 m/km (Kaiata to Dobson)
Taramakau Valley	8.9 m/km (Kumara Junction to Kumara 40-80 m),
	13.0 m/km (upper part Historic Kumara Tailings)
Arahura Valley	8.9 m/km (60-100 m contours, Fox Creek area)
	6.67 m/km (Little Houhou Ck, 20-40 m contours)
	13.3 m/km (100-140 m contours)
Hokitika Valley	8.6 m/km (Hokitika to Tuckers Flat)
Rimu Channel	11.4 m/km (0-60 metre contours)

Table 3. Gradients of glacial outwash plains in the lower parts of the main valleys (Larrikins Formation).

Taramakau Valley	8.0 m/km (South side btw Kumara & Kumara Junction)
Kapitea Creek	8.0 m/km
Arahura Valley	6.67 m/km (Nth side, Flowery Ck area 40-80m) 5.8 m/ km approx (South side)

Table 4. Gradients of glacial outwash plains in the lower parts of the main valleys (Loopline Formation).

Grey River	~49 m below the gravel surface in several metres of water at the Cobden Bridge (about 2 km from the coast), 27.5+ m at the south bank under the Stillwater Bridge, ~30.5 m at confluence with the Arnold River.
Hokitika River	~40 m? (up to 40 m 3.8 km from the coast)
Taramakau River	~34 m 3.75 km from the coast (line UK, Kaniere Gold Dredging Company).
New River	33.8 m ~1.4 – 1.5 km from the coast (drilling by L&M); ~ 23.5 m 4 km from the coastline (drilling by Golden Shamrock)
Mikonui River	38-40 m at the coast (drilling by the Mikonui Gold Dredging Company).
Arahura River	~39 m about 725 m from the coastline (drilling by L&M), 27 m 3 km from the coastline (drilling by the Arahura Dredging Company)
Waimea Creek	~15-20 m? at Awatuna (14.6 m 2.75 km from coast)
Houhou Creek	~29 m 600 m from the coast
Buller River	Probably more than 40 m at Organs Island, 7 km from the coast; more than 30 m in each of 3 drillholes (none of which were bottomed) at the Buller Bridge (Westport).

Table 5. Present depth of incised channels from gold prospecting and bridge pile investigations.

Valley), and the Greenstone River, a tributary of the Taramakau River.

Deeply incised fluvial channels must extend offshore approximately opposite the mouths of the larger West Coast rivers. At this time, there is no data available with regard to the position, dimensions or the gold content of offshore (submerged) river channels. Given that such areas would be difficult to mine using existing technology they will not be considered further here.

West Coast rivers respond very quickly both to changes in sea level and changes in the rate of sediment supply. The materials situated beneath the modern floodplains are relatively unconsolidated and are easily eroded if the relative level of the sea falls. A fall in sea level causes an increase in river gradient and consequently an increase in the ability of rivers to scour alluvium from beds and floodplains.

The incised channels have a basal gradient (Table 6) that is steeper than the modern (interglacial) floodplain but similar

to the glacial (ice age) floodplain. For the Grey, New and Taramakau rivers this suggests that channel incision was completed after sea level began to rise and before it reached the present interglacial maximum.

Gold grades in the basal lag deposits seem to be higher in valleys where there is a steep channel gradient. High gradient channels tend to be situated near major glacial moraines. High gradient channels that have accommodated large meltwater flows and substantial sediment throughput are associated with shorter channel lengths. The moraines at the head of the channel are not a long distance from the glacial age coastline.

In Figure 6 two cycles of incision have been illustrated. Note that the gold-bearing lag deposits are all of similar thickness regardless of the actual gold grade. This is a result of formation by the same river. Even though sediment supply rate has fluctuated the (water) discharge of the river has been relatively constant. The lag deposits form during periods of reduced bed sediment supply and lesser bedload. The aggradational deposits form during periods of increased sediment supply and higher bedload.

Timing of deep incision

The most recent period of widespread incision occurred following the ~18,000 BP peak of the last glaciation. Most of the scouring probably took place before ~10,000 BP when sea level was low but generally rising. Incision was followed by a period of rapid floodplain aggradation that was more or less complete by about 6,000 BP. Aggradation commenced before sea level reached its present interglacial high. This general pattern of events has occurred several times on the West Coast during the late Pleistocene.

The proposed sequence of events is illustrated in a general way in Figures 7a to 7d and is as follows:

1. An interglacial (warm) period occurs, the sea level is high and rivers have aggraded substantially, particularly near to the coastline.
2. Interglacial conditions end with the onset of significant climatic cooling. Sea level begins to fall as the continental ice caps and valley glaciers expand. In the West Coast region glaciers begin to advance down valley as a result of the accumulation of ice in the high country. The production of coarse sediment increases as the glaciers expand. Aggradation commences on river floodplains in front of the advancing glaciers. The rate of aggradation is highest near to the terminus and declines in a downstream direction.
3. Sedimentation rates increase rapidly throughout the entire catchment area with the onset of climatic cooling. There is a rapid aggradational response to glaciation similar to that which has taken place in the Waiho Valley during the 1990s as a result of a minor advance of the Franz Josef glacier.
4. Bed loads increases as glaciers advance, preventing the formation of deeply incised channels as a response to lowering of sea level.
5. Eventually a steady state situation develops whereby floodplain longitudinal profiles stabilise. Rivers respond to small changes in sea level and to minor advance or retreat of the local glaciers but deeply incised channels do not form.
6. When climate enters a substantial warm phase and the glaciers retreat in response then large moraine-dammed lakes form immediately. These act as giant sediment traps that can take thousands of years to fill. The sea level is still very low because the major continental ice caps (that contain massive volumes of water) respond more slowly to climate change than local valley and piedmont glaciers.
7. In response to the abrupt decrease in sediment supply the major rivers immediately cannibalise young unconsolidated sediment from their beds and floodplains. Deep scouring occurs along the full distance between the moraine-dammed lakes and the sea. This erosion progressively deepens the channel and lowers the floodplain. Steep valley sides are developed with exposed bedrock if incision has been deep enough.
8. If the moraine is fully breached by the downcutting river then the lake will empty and will no longer act as a sediment trap. At this stage the sediment supply to the

Grey River	2.8 m/km between the Cobden bridge and the Arnold River confluence (a distance of ~ 15 km).
New River	5.8 m/km between the 5 and 23 metre surface contours (Camerons to Marsden Township – about 6.5 km).
Taramakau River	~4.9 m/km between road-rail bridge at State Highway 6 and the road bridge at Kumara.
Arahura River	~7 - 8 m/km for the 3 km immediately upstream from Kaihinu. This channel may be older than the Grey, New River, and Taramakau examples and is probably a composite of two or more periods of incision.
Rimu Channel	~11 m/km. Age uncertain but probably formed during the last glaciation.
Mikonui River	8.04 m/km from the coastline to the 3 km point. Like the Arahura this channel is a composite of two or more incision events.

Table 6. Gradient of the bedrock contact in deeply incised channels, based mainly on alluvial gold exploration drillholes.

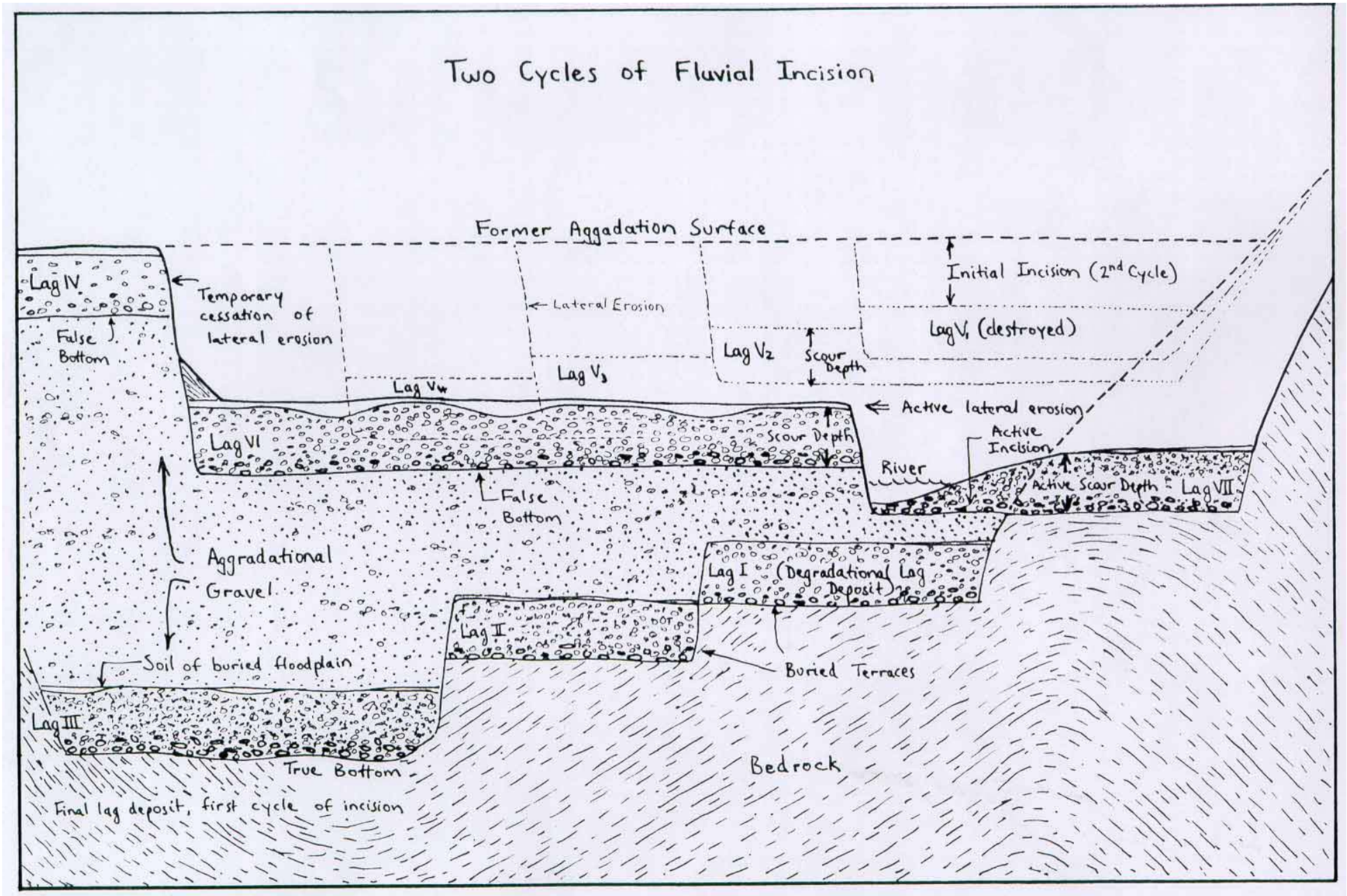
Two Cycles of Fluvial Incision
Former Aggadation Surface
Lag IV
Temporary cessation of lateral erosion
False Bottom
Lateral Erosion
Lag V2
Scour Depth
Lag V3
Lag V1 (destroyed)
Initial Incision (2nd Cycle)
Lag V4
Active lateral erosion
Lag VI
Scour Depth
Active Incision
River
Active Scour Depth
Lag VII
False Bottom
Aggradational Gravel
Lag I (Degradational Lag Deposit)
Lag II
Soil of buried floodplain
Buried Terraces
Lag III
True Bottom
Bedrock
Final lag deposit, first cycle of incision

Figure 6.

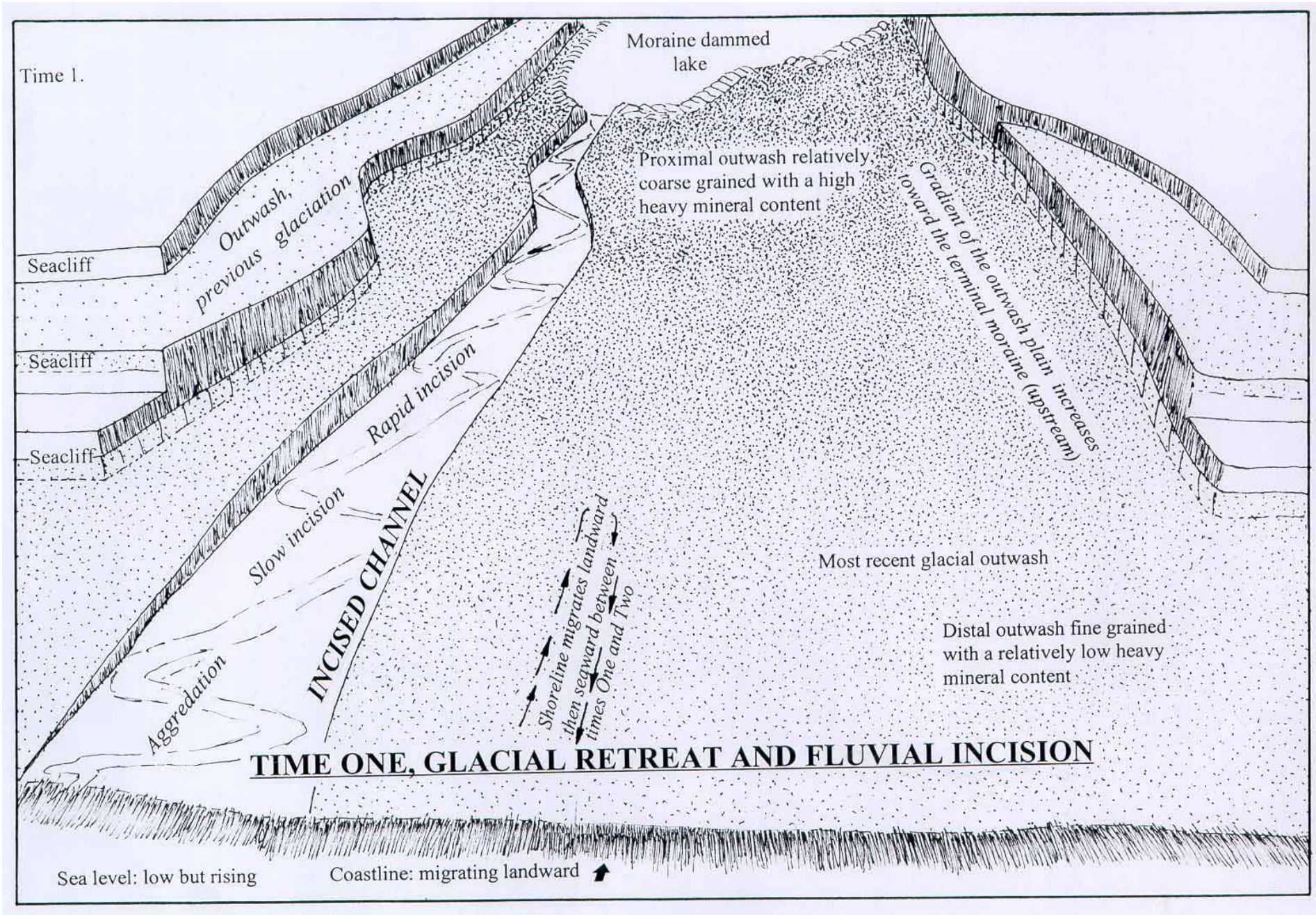
Time 1.
Moraine dammed lake
Proximal outwash relatively coarse grained with a high heavy mineral content
Gradient of the terminal moraine outwash plain increases toward the terminal moraine (upstream)
Outwash, previous glaciation
Seacliff
Seacliff
Seacliff
Rapid incision
Slow incision
INCISED CHANNEL
Shoreline migrates landward then seaward between times One and Two
Most recent glacial outwash
Distal outwash fine grained with a relatively low heavy mineral content
Aggredation
TIME ONE, GLACIAL RETREAT AND FLUVIAL INCISION
Sea level: low but rising
Coastline: migrating landward

Figure 7a.

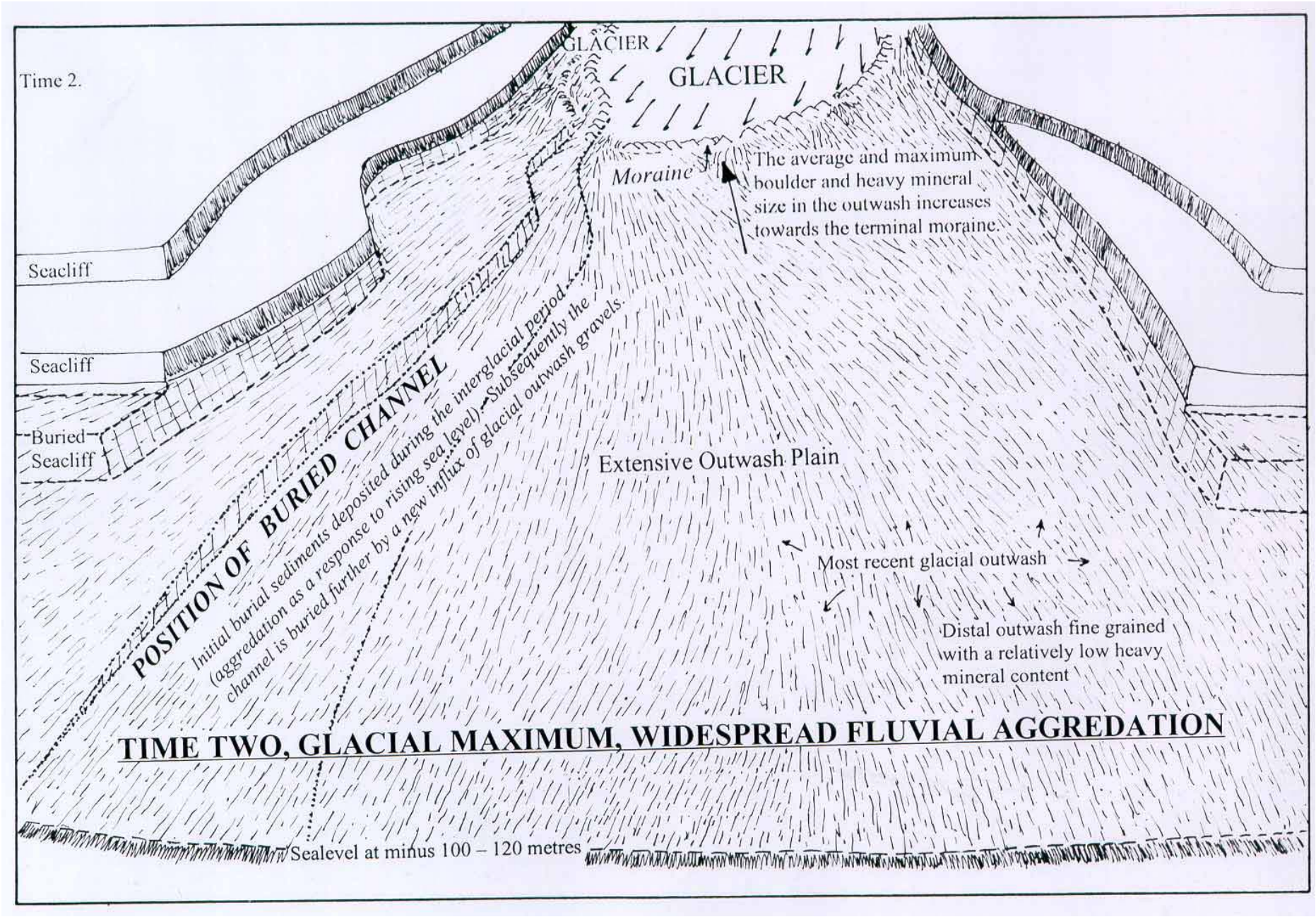
Time 2.
GLACIER
GLACIER
Moraine
The average and maximum boulder and heavy mineral size in the outwash increases towards the terminal moraine.
Seacliff
Seacliff
Buried Seacliff
POSITION OF BURIED CHANNEL
Initial burial sediments deposited during the interglacial period (aggredation as a response to rising sea level). Subsequently the channel is buried further by a new influx of glacial outwash gravels.
Extensive Outwash Plain
Most recent glacial outwash
Distal outwash fine grained with a relatively low heavy mineral content
TIME TWO, GLACIAL MAXIMUM, WIDESPREAD FLUVIAL AGGREDATION
Sealevel at minus 100 – 120 metres

Figure 7b.

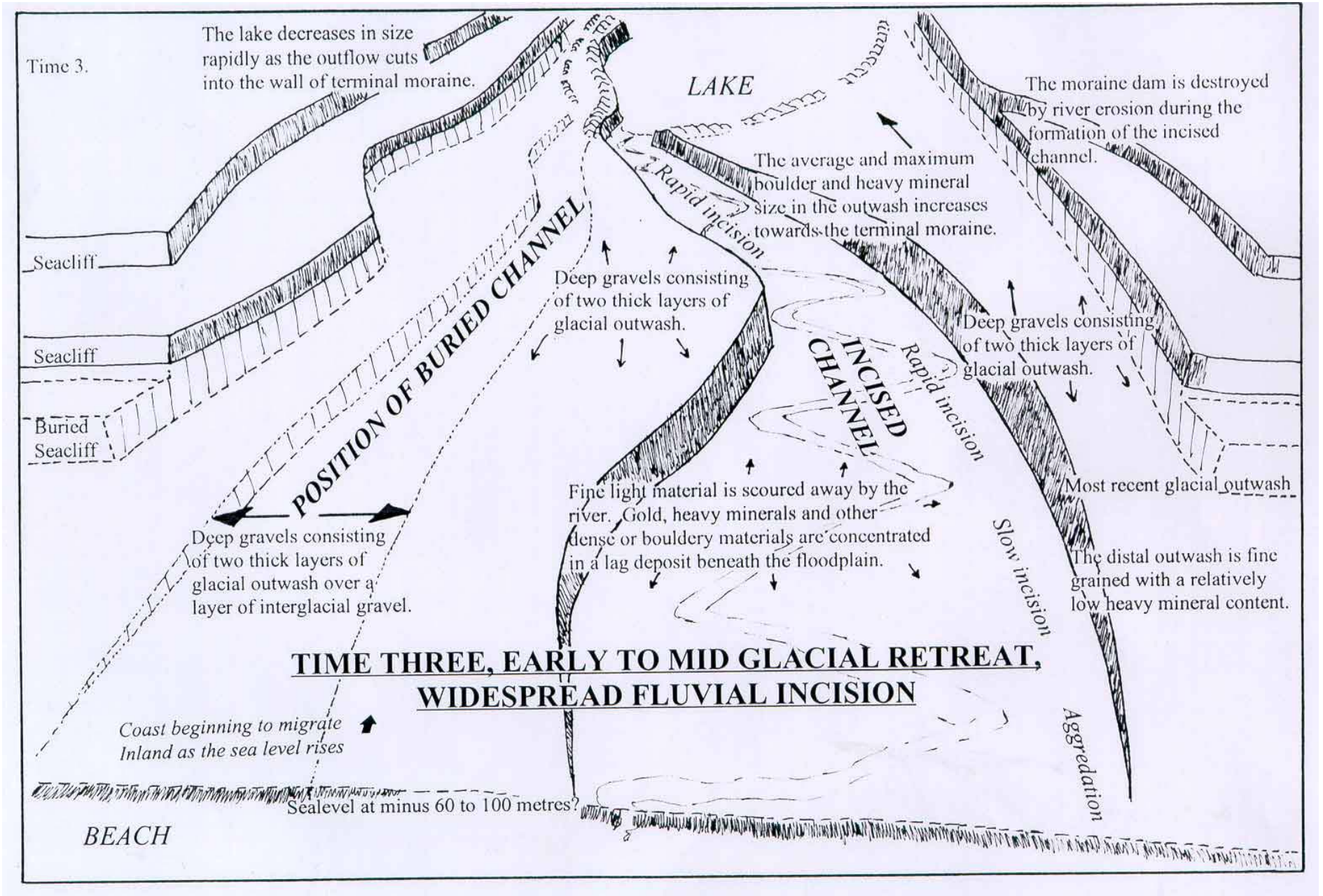
Time 3.
The lake decreases in size rapidly as the outflow cuts into the wall of terminal moraine.
LAKE
The moraine dam is destroyed by river erosion during the formation of the incised channel.
The average and maximum boulder and heavy mineral size in the outwash increases towards the terminal moraine.
Rapid incision
Seacliff
Seacliff
Buried Seacliff
POSITION OF BURIED CHANNEL
Deep gravels consisting of two thick layers of glacial outwash.
INCISED CHANNEL
Rapid incision
Deep gravels consisting of two thick layers of glacial outwash.
Most recent glacial outwash
Fine light material is scoured away by the river. Gold, heavy minerals and other dense or bouldery materials are concentrated in a lag deposit beneath the floodplain.
Slow incision
The distal outwash is fine grained with a relatively low heavy mineral content.
Deep gravels consisting of two thick layers of glacial outwash over a layer of interglacial gravel.
TIME THREE, EARLY TO MID GLACIAL RETREAT, WIDESPREAD FLUVIAL INCISION
Coast beginning to migrate Inland as the sea level rises
Aggredation
Sealevel at minus 60 to 100 metres?
BEACH

Figure 7c.

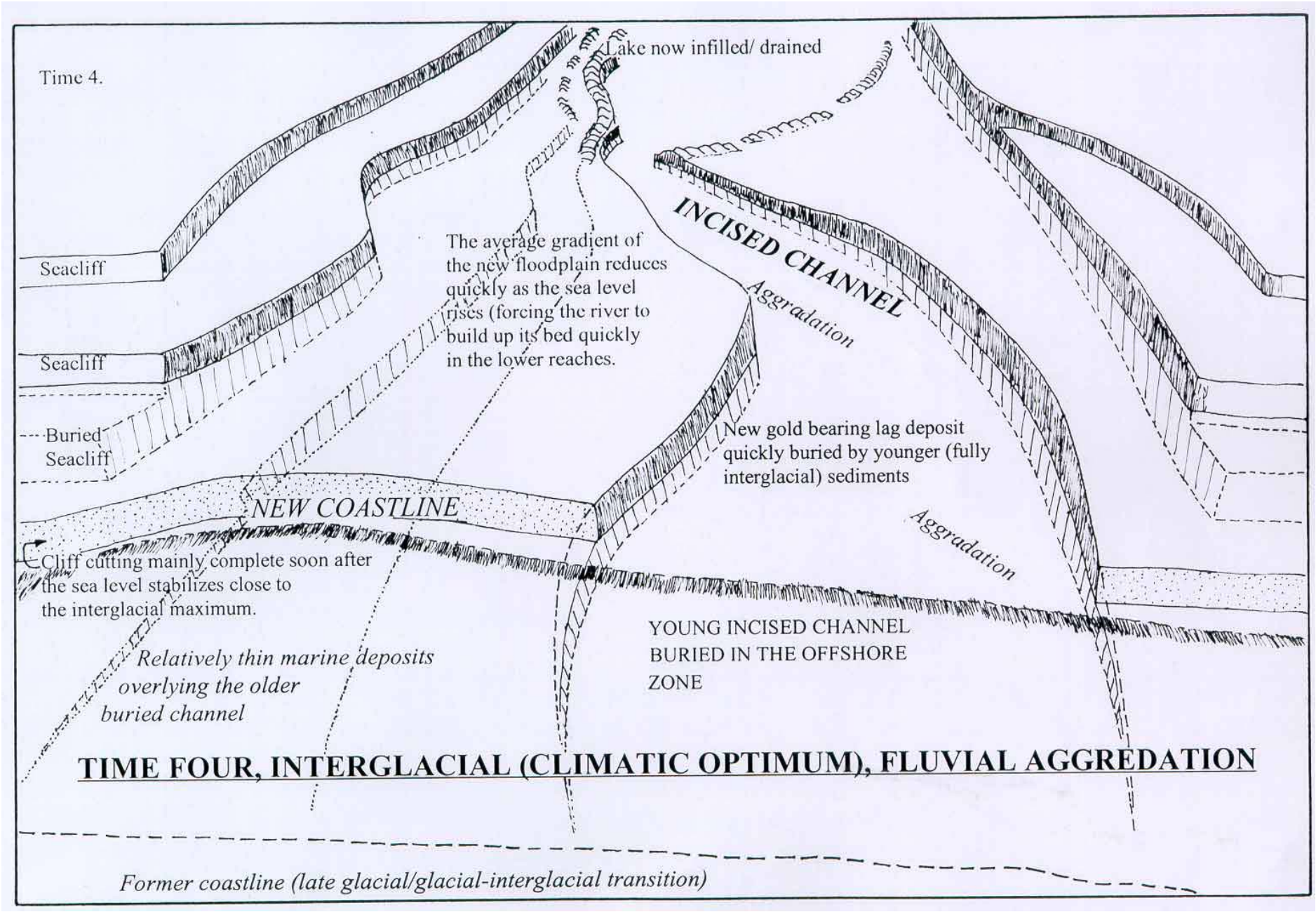
Time 4.
Lake now infilled/ drained
Seacliff
Seacliff
Buried Seacliff
The average gradient of the new floodplain reduces quickly as the sea level rises (forcing the river to build up its bed quickly in the lower reaches.
INCISED CHANNEL
Aggradation
New gold bearing lag deposit quickly buried by younger (fully interglacial) sediments
NEW COASTLINE
Aggradation
Cliff cutting mainly complete soon after the sea level stabilizes close to the interglacial maximum.
YOUNG INCISED CHANNEL BURIED IN THE OFFSHORE ZONE
Relatively thin marine deposits overlying the older buried channel
TIME FOUR, INTERGLACIAL (CLIMATIC OPTIMUM), FLUVIAL AGGREDATION
Former coastline (late glacial/glacial-interglacial transition)

Figure 7d.

river increases and the downcutting process may be arrested. Similarly if the lake is entirely filled with sediment from up valley sources then the sediment trap has been overwhelmed and the rate of sediment supply to the lower part of the valley will increase suddenly.

9. Rivers begin to aggrade near to the coastline in response to rising sea level. Eventually downcutting is reversed in areas further inland as the effect of rising sea level spreads up-valley.

Incision controlled by sea-level fluctuation occurs mainly in short bursts of a few thousand years. The rate of lateral erosion is limited once incision reaches the level of the local bedrock. If a deep channel is backfilled with younger outwash by a subsequent glacial advance the rate of sideways or lateral erosion might increase once more, even if the river is in a generally aggradational phase.

Taramakau River

In terms of historic gold mining the best example of an incised channel is that of the modern Taramakau River. Dredging in this channel between 1955 and 1983 produced more than 250,000 ounces of alluvial gold. The Taramakau is a prime location for testing competing hypotheses because the most recent scour channel is very well explored and nearby terraces have been dated.

At Kumara, immediately adjacent to the terminal moraine from the last glacial maximum (~20,000 BP), the elevation of the surface of the Larrikins Formation is 90 to 95 m above (modern) mean sea level. The elevation of the Taramakau River floodplain at Kumara is 20 m amsl. The maximum depth of alluvial materials beneath the floodplain at the confluence with the Greenstone River is ~20 m, i.e. approximately equal to modern sea level. This means that there has been ~90 m of post-glacial incision of the Taramakau River at Kumara. A substantial proportion of this incision has been through the local bedrock (Stillwater Mudstone).

At Kumara the Moana Formation (outwash of a late-glacial ice readvance) is entirely contained within the incised valley of the Taramakau River. At the Kumara Bridge the elevation of the outwash surface (since destroyed) is projected at around 50 to 60 m. This means that the Taramakau River had incised a minimum of ~30 to 40 m by 14 to 16,000 BP (age of the Moana advance; Suggate & Waight, 1999). It is assumed that a further 50 to 60 m of incision occurred after the Moana advance but prior to the Holocene period.

Post Moana incision must have taken place while the sea level was relatively low. The projected depth of the Taramakau incised channel at the Rail/State Highway bridge is 35 - 40 m. At the time active scouring of bedrock was taking place at this locality the coastline was probably 3 to 4 km northwest of its present position. The river bed would have been above sea level at the bridge meaning that sea level was more than 35 to 40 m below its present level.

We also need to take into account the fact that there has been at least 6 m of tectonic uplift at Camerons (about 1 km from the Rail bridge) since 7000 BP. This is likely to mean 10 m of uplift since 10,000 BP. The scoured surface below the Taramakau River will have been uplifted a similar amount in the last 10,000 BP. I therefore speculate that the base of the scour channel at the Taramakau Rail bridge was formed when the sea surface was 45 to 50 m lower than present mean sea level. Depending isostatic adjustments to glacial retreat and marine transgression it seems probable that maximum incision beneath the Taramakau River occurred at or before 11,000 BP. This was the last time that sea level was sufficiently low to allow fluvial erosion at minus 40-45 m.

Total incision below the Larrikins Formation surface near the Rail bridge is about 70-75 m, given that the Larrikins surface is about 30 m amsl here.

Lateral extent of outwash terraces

Some outwash terraces are very extensive, the Larrikins and Loopline formations being obvious examples. Rivers have been capable of lateral erosion to the extent that older outwash terraces can be completely destroyed in a relatively short period.

West Coast glaciers fluctuate in size as a response to small changes in climate and precipitation. Terminal positions are unstable and consequently the rate of sediment discharge to the meltwater rivers varies significantly. When coupled with a variable base level (sea level) this means the depositional environment in the major rivers is likely to alternate rapidly between degradation and aggradation.

The gravel under some terraces was probably been deposited when the climate is intermediate between full glacial and interglacial conditions. During these periods the sea level is unstable (fluctuating by say ± 20 m) and generally intermediate between glacial maxima (very low) and interglacial/modern (very high) elevations. Such conditions could last thousands to tens of thousands of years, long enough that significant tectonic uplift will take place on the lowlands. If the elevation of the floodplain is quasi-stable for a long period then the river will tend to cut into slightly higher flanking terraces. These terraces are composed mainly of older unconsolidated fluvioglacial outwash. The amount of vertical incision and lateral erosion that results from this combination of circumstances is governed in part by:

- the duration over which these conditions last;
- the timing and cumulative amount of uplift;
- the timing and magnitude of climate change; and
- the degree of sea level fluctuation.

Landforms that are created from a set of circumstances such as these can potentially be overwhelmed and completely buried by outwash from a younger and more extreme glacial event.

Implications for gold distribution

Deeply incised stream channels tend to be floored with bouldery gravel that has a relatively high gold content. Because the stream/river is confined in a well-defined channel for a long period, gold can be spread for a substantial distance down the channel.

It is possible for incised channels to be reburied and entirely obscured by subsequent influxes of sediment. If the stream in a particular catchment then enters a new phase of incision/ downcutting the new channel might not occupy the position of the previous channel. Old incised channels can be preserved under terraces that flank the modern river floodplains. Good examples are present in the valley of New River at Dunganville and Woods Creek, in the Taramakau Valley and in the Arahura Valley.

One example that might fit the pattern is a deep channel situated under the Larrikins Formation between Kumara and Kumara Junction. The Taramakau River formed this channel, probably during the interval between the glacial advances that produced the Loopline and Larrikins Formations. It is only possible to identify the channel because of a scattering of alluvial drillholes across this terrace. The channel occupies only part of the outwash plain. It was subsequently overwhelmed by outwash of the Larrikins Formation which is much more extensive than the buried channel.

Infilling of incised channels as sea level rises

Rapidly rising sea level has a severe impact on sediment transport and deposition along the lower reaches of rivers. The sea can inundate a river valley creating a bay that extends inland for a significant distance. Where there is sufficient long-shore-drift the valley can be dammed by beach material causing the formation of a lake inland from the bar. Lake Mahinapua is one example. Another is that of the Paringa River in South Westland. Here marine sediment (including shellfish remains) is found upstream from State Highway 6 about 10 km from the modern coast. Until relatively recent times (perhaps only a few thousand years ago) this valley was a shallow fiord that has since been filled in.

Moraine-dammed lakes intercept sediment carried by rivers. Outflow from such lakes contains minimal sediment. Lakes have the effect of greatly damping or smoothing peak flood discharge downstream of the outlet. This reduces the scouring and sediment transport capacity of the river downstream of the lake potentially decreasing its ability to concentrate gold and produce economic deposits. In such cases the lower part of the valley is more likely to be inundated or blocked by a barrier bar as sea level rises.

Rising sea level can have an effect on floodplain gradient and sedimentary processes far from the coastline. When the bedload is not intercepted in a lake, a river can build its bed quickly, slowing or preventing the inundation of its floodplain. Floodplain aggradation near the coastline reduces the gradient of the river changing its sediment carrying capacity and erosive power. The effect extends up tributary valleys for a significant distance as well.

In the Grey Valley the gradient of the floodplain has been reduced as far inland as Maimai (more than 50 km from the modern coastline) near Reefton. West Coast examples of valley backfilling resulting from large changes in sea level include the floodplains of the Grey, New and Taramakau rivers. These have been drilled extensively. Most of the post-glacial aggredation probably occurred during a period no longer than 4500 years between 11,000 and 6500 BP. In the Grey Valley at the confluence of Grey River and Stillwater Creek there is a road bridge across the Creek. A drillhole at the bridge abutment recovered wood 19.2 m below the surface. The wood was radiocarbon dated (see Grant-Taylor & Rafter 1971) at 8190 ± 120 years BP (age before 1950). This indicates aggradation of about 19 m within in a period of no more than 2300 years, as the floodplain reached its modern elevation by 6000 BP.

Around the New Zealand the sea surface has been within 2 to 3 m of the modern level for about 6500 years. There has been an approximate balance between erosion and deposition in many West Coast rivers during this period. Exceptions include the Waiho River at Franz Josef, where a recent advance of the Franz Josef glacier has increased the bed load of the river and caused significant aggradation.

Older examples of valley backfilling due to rising sea level have not been described in detail except at Houhou Creek (see Cotton & Stewart 1989). Drill holes into the Loopline Terrace north of Kapitea Creek intersected buried wood and soil at around 16 m. This horizon is at the same level as a nearby exposure of interglacial Awatuna Formation (beach sand) in Sunday Creek and overlies about 10 m of river gravel. The gravel could have an interglacial origin and might be as old as 100,000 years if the stratigraphy of Suggate & Waight (1999) is correct. Old river gravel briefly exposed in recent mine faces in the Arahura Valley opposite Humphries Gully contained a buried soil horizon containing logs that are almost certainly of interglacial origin, probably older than 60,000 years.

Backfill in deeply incised channels

Incised channels of the large rivers in North Westland are invariably backfilled with alluvium dominated aggredational gravel. The backfill contains few, if any soil horizons. These rivers carry sufficient gravel in the regular bedload that they can construct vertically continuous aggradational deposits of that material. This is the case both when aggredation is related to the advance of glaciers (climatic cooling) and when it is caused by rapidly rising sea level (climatic warming).

Smaller streams have lesser erosive and sediment carrying capacity in general than do large rivers. Typically, they lack an active glacial source for coarse sediment. Tributary streams

can generally aggrade incised channels at a similar speed to a dominant river but commonly not exclusively with coarse sediment. In such cases aggradation can produce deposits containing mainly fine sediments. Incised channels are backfilled with interlayered mud, silt, sand, gravel, soil, and swampy vegetation. The lower reaches of Waimea Creek, Houhou Creek and New River are prominent examples. Potentially a rising base level can convert floodplains in smaller catchments into swamps or shallow lakes through blockage of the outlet. When the base level is lowered again accumulated fine-grained sediment can scoured away entirely.

When sea level is rising rapidly the sediment deposited in the lower reaches of the larger West Coast rivers is dominated by material that is relatively fine grained. Similarly, when glaciers are advancing rapidly the distal outwash is relatively fine-grained. These materials are unlikely to contain much gold.

Conclusions

Proximal glacial environments are under-explored in the West Coast and Otago regions. One of the reasons is that past generations of miners did not fully appreciate the significance of the glacial environment and did not recognise the landforms that indicated an area might be prospective. When these deposits were found it was mainly by chance. Explanations for the deposits usually emerged after the fact (when geologists visited the new discoveries). Reports filed by the geologists were not always written in language suited to the layperson or easily accessible to the miners. There is still potential for the discovery of substantial placer deposits in this environment. There is also still potential for the discovery of "secondary" placer deposits that have been produced by reconcentration of proximal fluvioglacial materials.

Acknowledgements

This paper is one of the outcomes of a research project carried out for the West Coast Commercial Gold Miners Association. Support was received from Technology New Zealand, the Ministry of Economic Development, the Grey, Westland, and Buller District Councils and L & M Mining Ltd. Richard Cotton, John Wood, and Tony Jury are thanked for assistance with the report from which this paper is derived.

References

Craw, D.; Youngson, J.H.; Koons, P.O. 1999: Gold dispersal and placer formation in an active oblique collisional mountain belt, Southern Alps, New Zealand. Economic Geology 94: 605-614.

Grant-Taylor, T. L. and Rafter, T.A. 1971: New Zealand radio-carbonmeasurements-6. New Zealand Journal of Geology and Geophysics 14: 364-402.

Cotton, R. J. and Stewart, M. 1989: Alluvial gold resource evaluation, Houhou Creek, Hokitika. In Proceedings 23rd Annual Conference, NZ Branch, Australasian Institute of Mining and Metallurgy pp 13-35.

Jury, A.P. and Hancock, P.M. 1989: Alluvial gold deposits and mining opportunities on the West Coast, South Island, New Zealand. Pp 147-153 in Kear, D (ed): Mineral Deposits of New Zealand. Australasian Institute of Mining and Metallurgy monograph 13.

Suggate, R. P. 1996: Detrital gold in North Westland. In Proceedings 29th Annual Conference, NZ Branch, Australasian Institute of Mining and Metallurgy pp 137-152.

Suggate, R. P. and Waight, T. E. 1999: Geology of the Kumara-Moana area. Sheets J32 and part K32. Institute of geological and Nuclear Sciences Geological Map 24. Institute of Geological and Nuclear Sciences Ltd, Lower Hutt, New Zealand.

Author

ROBERT ROSE has worked in the alluvial gold mining industry for the last 14 years, and as an independent consultant since 1993. Qualifications include a BSc and an MSc from Canterbury University.